CLIMATIC IMPACT ASSESSMENT PROGRAM

PROCEEDINGS
OF THE
SURVEY CONFERENCE
FEBRUARY 15-16, 1972

A.E.Barrington, Editor

SPONSORED BY THE
U.S. DEPARTMENT OF TRANSPORTATION

DOT-TSC-OST-72-13

HELD AT THE TRANSPORTATION SYSTEMS CENTER, 55 BROADWAY, CAMBRIDGE, MA. 02142

TECHNICAL REPORT STANDARD TITLE PAGE

1. Report No.	2. Government Accession No.	3. Recipient's Catalog No.
DOT-TSC-OST-72-13		

4. Title and Subtitle	5. Report Date
CLIMATIC IMPACT ASSESSMENT PROGRAM, PROCEEDINGS OF THE SURVEY CONFERENCE, FEBRUARY 15-16, 1972	September 1972
	6. Performing Organization Code

7. Author(s)	8. Performing Organization Report No.
A. E. Barrington, Editor	DOT-TSC-OST-72-13

9. Performing Organization Name and Address	10. Work Unit No.
Department of Transportation Transportation System Center 55 Broadway Cambridge, MA 02142	R3537
	11. Contract or Grant No. OS-320

12. Sponsoring Agency Name and Address	13. Type of Report and Period Covered
Department of Transportation Office of the Assistant Secretary for Systems Development and Technology Washington, D.C. 20590	Conference Proceedings, February 15-16, 1972
	14. Sponsoring Agency Code

15. Supplementary Notes

16. Abstract

This volume contains the proceedings of a survey conference, held at the DOT Transportation Systems Center, which was the first of the reporting milestones of the Climatic Impact Assessment Program. CIAP, managed within the Office of the Secretary of Transportation, will assess, by report in 1974, the impact of climatic changes which might result from perturbation of the upper atmosphere by the exhaust effluent of a world high-altitude aircraft fleet, as projected to 1990.

The primary objective of this conference was to introduce the objectives and scope of CIAP to domestic and foreign representatives of industry, universities, and government agencies. Nineteen speakers were invited, at very short notice, to prepare informal introductory surveys in their respective disciplines which would be instructive to specialists in other areas and would illustrate the range of activities related to CIAP. These tutorials dealt with the general categories of engine emissions, the natural stratosphere, the physical and biological impact of stratospheric perturbations, and risk/benefit analysis. All but one of the talks are included in this volume, each followed by an abbreviated version of the ensuing open discussion.

17. Key Words	18. Distribution Statement
Climatic Impacts Engine Emissions Stratosphere	DOCUMENT IS AVAILABLE TO THE PUBLIC THROUGH THE NATIONAL TECHNICAL INFORMATION SERVICE, SPRINGFIELD, VIRGINIA 22151.

19. Security Classif. (of this report)	20. Security Classif. (of this page)	21. No. of Pages	22. Price
Unclassified	Unclassified	281	

Form DOT F 1700.7 (8-69)

PREFACE

This volume contains the proceedings of a survey conference, held at the DOT Transportation Systems Center, which was the first of the reporting milestones of the Climatic Impact Assessment Program. CIAP, managed within the Office of the Secretary of Transportation, will assess, by report in 1974, the impact of climatic changes which might result from perturbation of the upper atmosphere by the exhaust effluent of a world high-altitude aircraft fleet, as projected to 1990.

The primary objective of this conference was to introduce the objectives and scope of CIAP to domestic and foreign representatives of industry, universities, and government agencies. Nineteen speakers were invited, at very short notice, to prepare informal introductory surveys in their respective disciplines which would be instructive to specialists in other areas and would illustrate the range of activities related to CIAP. These tutorials dealt with the general categories of engine emissions, the natural stratosphere, the physical and biological impact of stratospheric perturbations, and risk/benefit analysis. All but one of the talks are included in this volume, each followed by an abbreviated version of the ensuing open discussion.

Many of the speakers had to devote considerable time and effort to converting their informal presentations into papers suitable for this publication. Their labors, and those of the editorial staff, are gratefully acknowledged.

A.E. Barrington, Editor
Chief, Environmental Measurements Branch
DOT Transportation Systems Center

Survey Conference

Climatic Impact Assessment Program

February 15-16, 1972

Auditorium, TSC

Cambridge, Massachusetts

Chairman

ALAN J. GROBECKER

Director, Climatic Impact Assessment Program

DOT-OST

Program Chairman

DR. RICHARD L. STROMBOTNE

DOT-OST

U. S. DEPARTMENT OF TRANSPORTATION

Transportation Systems Center
Cambridge, Massachusetts

PROGRAM

TUESDAY **15** FEBRUARY

8:15 A.M.	REGISTRATION	Auditorium, Transportation Systems Center
9:00 A.M.	WELCOME	James C. Elms, Director Transportation Systems Center
9:10 A.M.	INTRODUCTION	Robert H. Cannon, Jr., Assistant Secretary for Systems Development and Technology
9:20 A.M.	OVERVIEW	Alan J. Grobecker, Conference Chairman
10:00 A.M.	I. ENGINE EMISSIONS	A. Kenneth Forney, Chairman of Sessions I. A and B.
10:10 A.M.	A. Physics and Chemistry	J. Grobman National Aeronautics & Space Administration Lewis Research Center Cleveland, Ohio
10:50 A.M.	INTERMISSION	
11:05 A.M.	B. Routes	R. W. Rummel Trans World Airlines New York, New York
11:45 A.M.	II. NATURAL STRATOSPHERE	Richard L. Strombotne, Chairman of Sessions II. A and B.
11:55 A.M.	A. Structure	S. V. Venkateswaran Department of Meteorology University of California at Los Angeles Los Angeles, California
12:35 P.M.	LUNCHEON	
1:35 P.M.	B. Composition and Chemistry General Chemistry of the Stratosphere	M. Nicolet Centre National de Recherches de l'Espace Brussels, Belgium
2:20 P.M.	Gaseous Composition of the Stratosphere	J. P. Friend New York University New York, New York
3:00 P.M.	Chemical Reactions	P. J. Crutzen University of Stockholm Stockholm, Sweden
3:40 P.M.	INTERMISSION	
3:55 P.M.		H. S. Johnston University of California Berkeley, California
4:35 P.M.	Chemical Modeling	F. P. Hudson Sandia Laboratories Albuquerque, New Mexico
5:15 P.M.	Aerosols	R. D. Cadle National Center for Atmospheric Research Boulder, Colorado
7:00 P.M.	SOCIAL HOUR AND BANQUET at the Parker House Hotel, Main Dining Room	

PROGRAM

WEDNESDAY 16 FEBRUARY

9:00 A.M.	C. General Dynamics of the Stratosphere	Robert L. Underwood, Chairman of Session II, C and D
9:10 A.M.	Radiation	Z. Sekera Department of Meteorology University of California at Los Angeles Los Angeles, California
9:50 A.M.	Motion	R. Dickinson National Center for Atmospheric Research Boulder, Colorado
10:30 A.M.	INTERMISSION	
	D. Dynamic Climatology of the Stratosphere and Troposphere	
10:45 A.M.	Observation	R. E. Newell Department of Meteorology Massachusetts Institute of Technology
11:25 A.M.	Simulation of Stratosphere	J. D. Mahlman National Oceanic & Atmospheric Admin. Environmental Research Laboratories Princeton University Princeton, New Jersey
12:10 P.M.	Tropospheric Simulation	Y. Mintz Department of Meteorology University of California Los Angeles, California
12:50 P.M.	LUNCHEON	
1:50 P.M.	E. Instrumentation of the Stratosphere	Samuel C. Coroniti, Chairman of Session II, E
2:00 P.M.	Problems of Vehicles	I. C. Poppoff National Aeronautics & Space Administration Ames Research Center Moffett Field, California
2:40 P.M.	General Concepts	D. Heath National Aeronautics & Space Administration Goddard Space Flight Center Greenbelt, Maryland
3:20 P.M.	INTERMISSION	
3:35 P.M.	III. PHYSICAL AND BIOLOGICAL IMPACT OF STRATOSPHERIC PERTURBATIONS	Richard L. Strombotne, Chairman of Sessions III and IV
3:45 P.M.		K. C. Smith Stanford University School of Medicine Stanford, California
4:20 P.M.	IV. RISK/BENEFIT CONSIDERATIONS	R. Erdmann Department of Engineering University of California at Los Angeles Los Angeles, California
5:00 P.M.	V. RAPPORTEURS AND OPEN DISCUSSION	M. McElroy, Chairman of Session V J. C. McConnell S. Wofsy

PROCEEDINGS
of the Survey Conference

CAMBRIDGE, MASS. FEBRUARY 1972

CONTENTS

Welcome ..... *Robert H. Cannon* 1

Chairman's Address: The DOT Climatic Impact Assessment Program ..... *A.J. Grobecker* 2

Introduction ..... *A.K. Forney* 24

Jet Engine Emissions ..... *Jack Grobman* 25

Supersonic Transport Routes ..... *R.W. Rummel* 34

Aeronomic Chemistry of the Stratosphere ..... *Marcel Nicolet* 44

Trace Material Composition of the Lower Stratosphere ..... *James P. Friend* 71

The Photochemistry of the Stratosphere with Special Attention Given to the Effects of NO_x Emitted by Supersonic Aircraft ..... *Paul J. Crutzen* 80

Laboratory Chemical Kinetics as an Atmospheric Science ..... *Harold Johnston* 90

Modeling the Chemical Kinetics of the Stratosphere ..... *Frank P. Hudson* 115

Composition of the Stratospheric "Sulfate Layer" ..... *Richard D. Cadle* 130

Radiation Scattering in the Stratosphere ..... *Z. Sekera* 140

Motions in the Stratosphere ..... *Robert E. Dickinson* 148

Behavior of CO-Mixing Ratio near the Tropopause and in the Lower Stratosphere ..... *Peter Warneck* 162

Climatology of the Stratosphere from Observations ..... *Reginald E. Newell* 165

Numerical Simulation of the Stratosphere: Implications for Related Climate Change Problems ..... *J.D. Mahlman and S. Manabe* 186

Numerical Simulation of the Seasonally and Inter-Annually Varying Tropospheric Circulation ..... *Y. Mintz, A. Katayama, and A. Arakawa* 194

The Measurement of Minor Stratospheric Constituents Using High-Altitude Aircraft ..... *I.G. Poppoff* 217

Some Experimental Techniques and Problems Associated with Stratospheric Measurements ..... *Donald F. Heath* 226

The Biological Effects of Ultraviolet Radiation on Man, Animals and Plants ..... *Kendric C. Smith* 243

Risk/Benefit Considerations of Stratospheric Flight ..... *R.C. Erdmann and Chauncey Starr* 251

Conference Summary ..... *Michael B. McElroy* 260

List of Participants 270

WELCOME

Hon. Robert H. Cannon, Jr.
Asst. Secretary for System Development and Technology
U.S. Department of Transportation
Washington, D.C. 20590

I can't tell you how pleased I am to see such a turnout of top people from all over the world, in the areas CIAP is addressing. I want to thank each one of you for making the effort to be here with us – in fact, I should probably thank you in direct proportion to the transportation difficulties you've undergone in getting here!

This program reminds me of Charlie Brown's first law: no problem is so big or so complicated that it can't be walked away from. We can't walk away from this one, though. Any time we consider a new transportation system which might have adverse effects on the earth or on the societies in which we live, we have a deep responsibility to determine as accurately as possible what those effects might be. We take that responsibility very seriously.

The Climatic Impact Assessment Program is fully supported by the Administration and by Congress. Our FY 1972 budget plus FY 1971 funds reprogrammed to get us off to a fast start total more than seven million dollars; we are seeking more than five million from Congress for FY 1973. I want to make it clear, though, that we are well aware that we are not doing something brand new, all by ourselves. Most of the work which will give us the results needed for this assessment has been under way for some time. Our job is to focus it, to accelerate it where necessary and supplement it where needed, so that we will have a timely assessment which will reflect the participation and have the support of the full scientific community.

This is why it was so important to us to have you all here today, early in our program, to give us your views: are we going about the job correctly; are we after the right things; can we make the necessary decisions and assessments within Dr. Grobecker's stiff time schedule? We need your help very much, both in planning this program and in assessing its results. Again, thank you very much for being with us.

CHAIRMAN'S ADDRESS: THE DOT CLIMATIC IMPACT ASSESSMENT PROGRAM

A. J. GROBECKER
Office of the Secretary of Transportation
Washington, D. C. 20590

The Department of Transportation's Climatic Impact Assessment Program (CIAP) has as its objective the assessment of the impact of climatic changes resulting from perturbation of the upper atmosphere by the propulsion effluents of a world high-altitude aircraft fleet as projected to 1990.

This study is divided into six steps. The first examines the nature of the stratosphere, including its present distributions of temperature, constituents, motions, and circulation. It will combine actual measurements with studies of chemical dynamics, and perform atmospheric modeling.

A second step, proceeding concurrently with the first, considers the nature of the propulsion effluents which will be entering the atmosphere about 1990. This study takes into account the amount of the engine emission products and projections of air routes and frequency of use, described as upper and lower bounds. Both steps one and two may be to some extent experimentally verified.

The third step is a projection of a perturbed stratosphere, a combination of the results of steps 1 and 2, described in terms of changed height distribution of constituent densities. For this projection more than 30 constituents must be considered, as well as changes in energy transport down and up through the stratosphere.

A fourth step is the consideration of the perturbations of the troposphere which may result from changes in solar radiation because of perturbations in the stratosphere. These may include changes in heating, temperature, latitudinal temperature gradients, winds, and precipitation, as well as changes in ultraviolet flux at the earth's surface.

A fifth step, based on the findings of step 4, is the determination of the physiological, biological, and botanical effects of the tropospheric changes on man, animals, and plants. It is with these impacts that most people are concerned. In addition to the technological description of the biological environmental effects, quantification of them in terms of economic measures is needed. This is undertaken in the sixth step. These economic measures provide a measure for possible comparison with the advantages of flight in the stratosphere.

Figure 1 shows the schedule for the accomplishment of these major steps. The investigation of the geophysical nature of the stratosphere will continue throughout the program and will require the largest part of the funding which is available to DOT. For the accomplishment of the succeeding steps, the most useful results of step 1 and step 2 (the study of the propulsion effluents) are those derived in calendar year 1972. Steps 3, 4, 5, and 6 will show results chiefly in calendar 1973.

A seventh item in the schedule indicates with circles the approximate times for major reporting milestones. These will occur at intervals of about six months and culminate in a final report at the end of 1974.

The DOT Climatic Impact Assessment Program is in large part dependent on work going on as the planned activity of more than 50 Government laboratories. Such work, which is necessary to steps 1 and 2, is being accomplished under the sponsorship of various cooperating agencies – the Atomic Energy Commission, National Aeronautics and Space Administration, National Science Foundation, Department of Commerce, and Department of Defense, to name just a few. While this work in general is necessary to the mission of and has been justified by the sponsoring agencies, none of the other agencies has as its particular goal the realization of a summary report in 1974 of the kind described here as a goal of the DOT CIAP study. Work being done in Europe under the sponsorship of the developers of the Concorde and of the Tupolev 144, and that of other governments, is also required by the CIAP study, and will be a major contribution to it. Ongoing efforts in various universities and in industry will also be

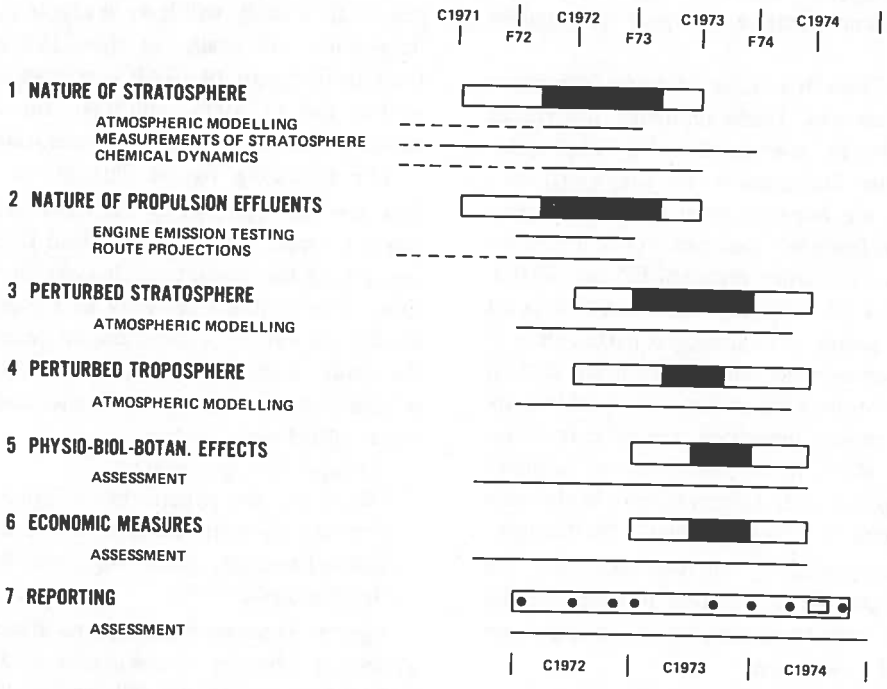

Figure 1. Schedule of Major Steps in the CIAP Program.

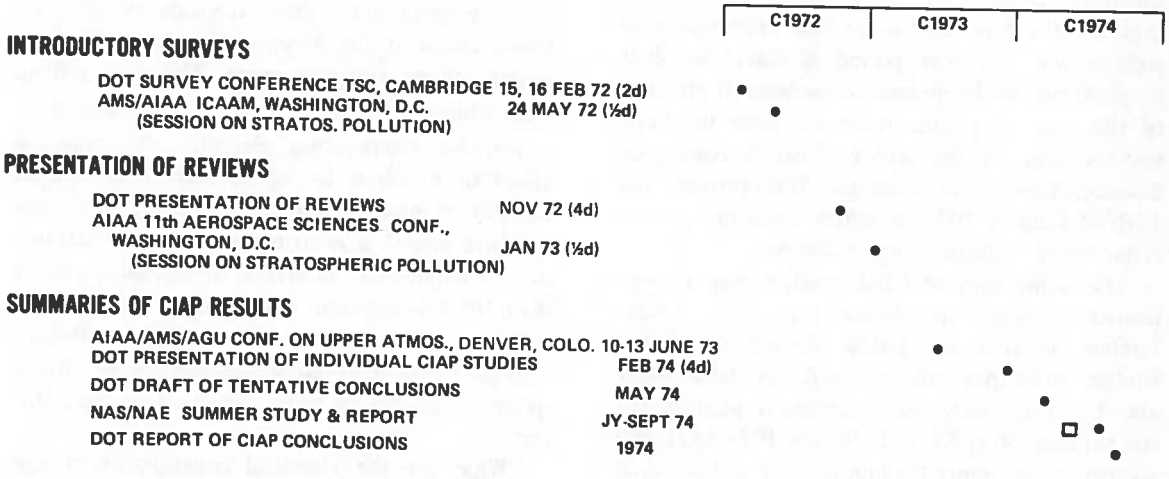

Figure 2. CIAP Reporting Milestones.

exploited. DOT will support, within its budget limitations, contributions to fill the gaps and produce as comprehensive a report as possible in 1974.

Figure 2 shows the dates of some important reporting milestones. These reporting milestones represent activities, some under the direct sponsorship of the Department of Transportation, others which we hope to have under the sponsorship of professional societies. As a follow-up to conferences of earlier years (SCEP and SMIC), this conference of February 1972 constitutes an introductory survey. The principal participants at this conference were invited in recognition of their special contributions in an area of scientific interest. The papers presented are introductions, prepared on short notice, designed to acquaint other participants with different areas of the wide field with which CIAP is concerned – for example, explaining the chemistry to meteorologists, the meteorology and fluid dynamics to chemists, the physiological considerations to both chemists and meteorologists, and so on.

In addition to these survey introductions, it is desirable that comprehensive, completely referenced review papers be prepared to cover topics for which adequate reviews do not currently exist. (Examples of some that do are the critical reviews prepared by Elmar Reiter under AEC sponsorship.) The Department of Transportation plans to organize the presentation of such comprehensive reviews within a time period adequate for their preparation, to be presented perhaps at the end of this year. A public forum for some of these reviews may be the AIAA Eleventh Aerospace Sciences Conference from the 10th through the 12th of January 1973, in which a half-day session is dedicated to atmospheric pollution.

The summaries of CIAP studies may be expected to appear in calendar year 1973. A conference suitable for public discussion of the studies, to be sponsored by the AIAA and possibly also by other technical societies, is planned for the summer of 1973. In February 1974 DOT will sponsor a conference for presentation of individual CIAP studies. These will provide the basis for the first draft of conclusions, to be prepared in May 1974. The Department of Transportation is currently discussing with the National Academies of Science and Engineering the possibility of a 1974 summer study under the Academies' sponsorship, leading to a NAS/NAE report in the fall of 1974 of conclusions as to the impact of climatic changes. Such a study will have available as a primary data source all results of the CIAP effort. The final DOT report of CIAP conclusions, expected at the end of 1974, will take the Academies' summer study report into consideration.

The following figures illustrate a concept of how the various steps of the CIAP problem may relate to each other and may lead to conclusions concerning the impact of climatic changes. I use these data at this stage only as a means of illustrating the nature of questions to be addressed by the study. I defer to the speakers who follow me to give you the best data, with the benefit of their more critical evaluation.

A proper first question is:

"What are the general interrelations of radiation and dynamic control of the stratosphere, photochemistry, climatology, and dynamics of the stratosphere?"

Figure 3 shows temperature-altitude profiles at several latitudes representative of January and mid-latitude spring and fall seasons. Also shown are the names of the atmospheric regions: the troposphere, below about 10 kilometers; the stratosphere, between the temperature minimum at the tropopause and the temperature maximum at the stratopause at about 50 kilometers; the mesosphere, which is the region between the temperature maximum at the stratopause and the minimum above at the mesopause; and the thermosphere, above the mesopause. The stratosphere, with which we are concerned, is characterized by a positive temperature gradient, the principal effect of which is to inhibit vertical convective transfer of material within that zone. The temperature inversion is strongest above the altitude of 30 kilometers. However, at latitudes greater than 30°, the inversion is sufficiently strong above 10 kilometers to seriously affect vertical motions.

Other important questions relating to stratospheric composition to be addressed by the CIAP are:

"What are the chemical constituents of the stratosphere?"

"What are the important chemical reactions of the gases in the stratosphere?"

Figure 4 shows some of the important constituents for the daylight atmosphere. (The data are the work of Bortner and Kummler, 1969.)

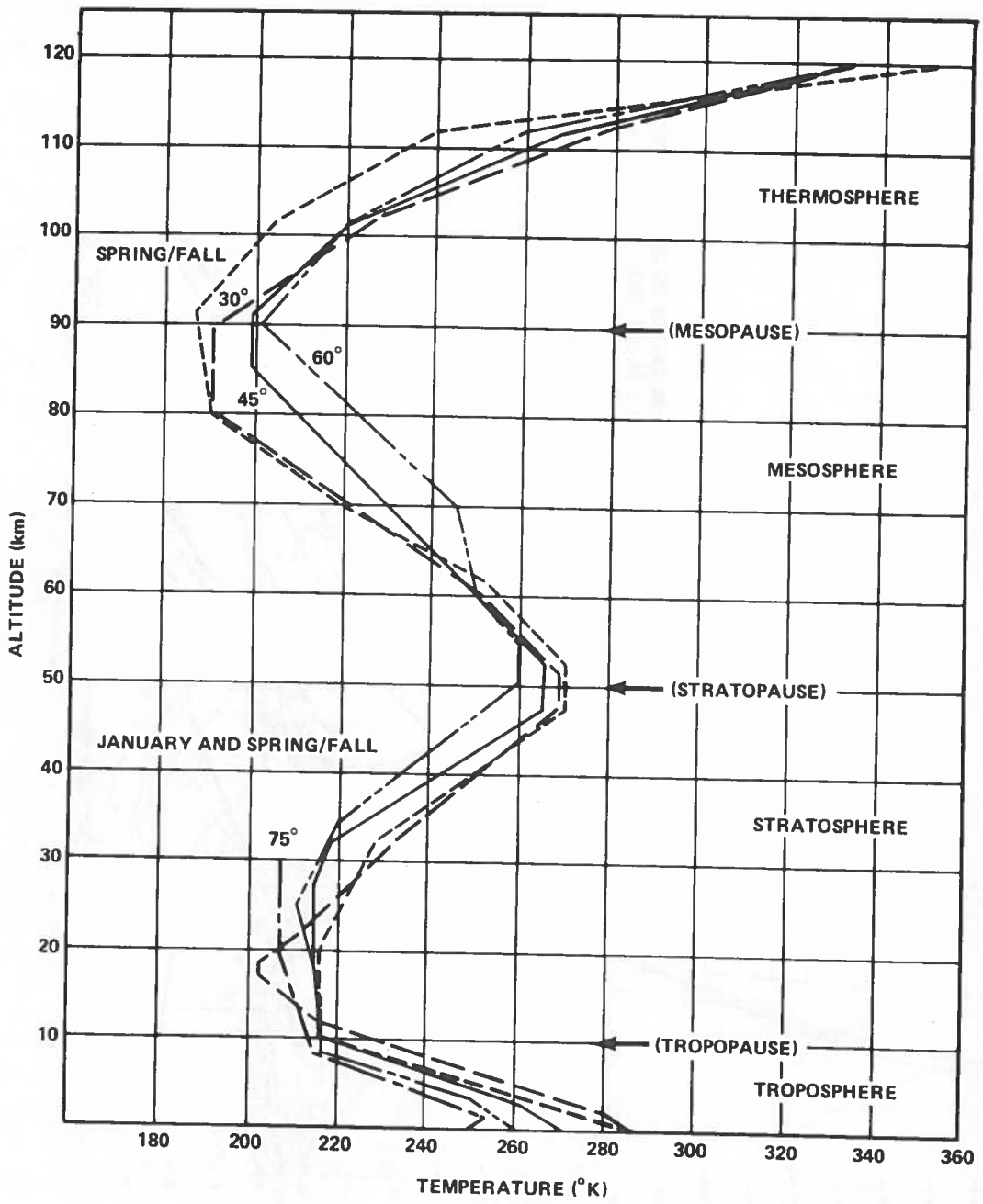

Figure 3. Temperature-Altitude Profiles of the 30°, 45°, 60°, and 75°N January and Mid-Latitude Spring/Fall Supplementary Atmospheres. (USSA Supplement, 1966)

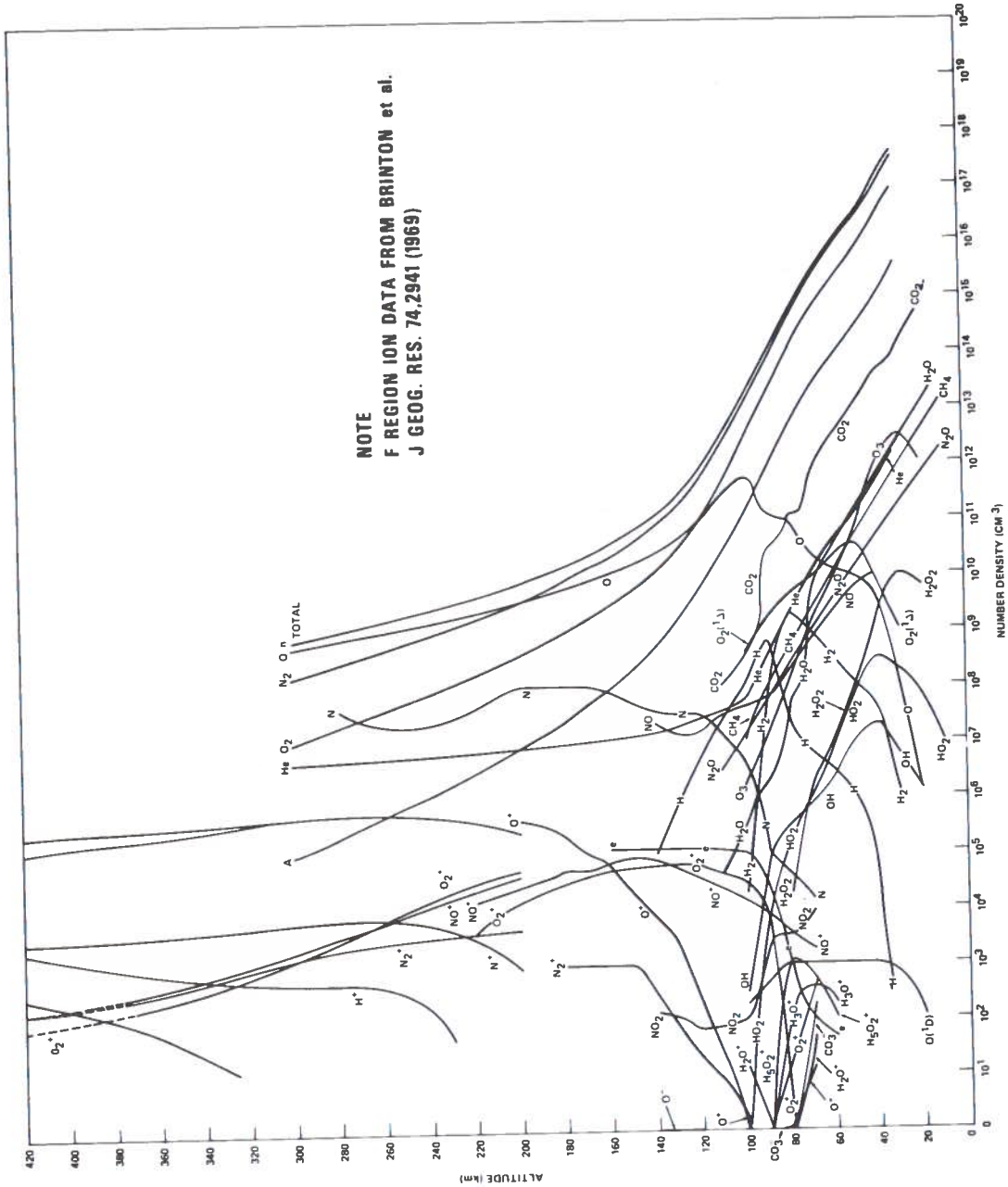

Figure 4. The Daylight Atmosphere - 1969. (After Bortner & Kummler, 1969)

The constituents shown represent only two-thirds of the number of stratospheric constituents which should be considered by CIAP. The region between about 10 and 40 kilometers is particularly interesting, since the constituents vary in mixing ratio from parts per million to parts per billion to one part in 10^{16}.

The concentration of these constituents may vary greatly over the globe. Figure 5 shows the total ozone content above the surface of the earth, expressed in units of .001 cm, at standard temperature and pressure. On one day the variations in total ozone over the earth range from about 0.2 millimeter to more than 0.6 millimeter. Since the radiative flux in the ultraviolet part of the spectrum, which may drive important photochemical reactions, is very sensitive to the vertical column of ozone, this variation may be crucial.

Further questions to be addressed by CIAP include:

"How well known are the chemical rate coefficients and which of these need further study?"

"What naturally resident aerosols need to be introduced into our calculations?"

Part of the CIAP study is concerned with pollutants which may be introduced by 1990 world-wide air fleets. Since these pollutants affect the stratosphere through complicated chemical processes, one must ask:

"What species are emitted, at what mass rate, at optimum power levels of the engines which will be flying at stratospheric altitudes?"

"What are the routes and frequency of travel which are projected for 1990?"

In considering the general dynamics of the natural stratosphere we wish to know:

"How is the height distribution of radiation within the stratosphere determined?"

"How is the radiation affected by the gaseous and aerosol constituents of the atmosphere?"

Figure 6 shows values of cross-sections for ozone absorption in wavebands relevant to the CIAP study. It is necessary to know absorption cross-sections in the UV for about fifteen photochemically sensitive constituents.

Related questions to be addressed by CIAP are:

"What is the radiation within the stratosphere received from the sun, expressed in terms of mean and standard deviations?"

"What is the radiation within the stratosphere received from below?"

These radiations are functions of the absorption cross-sections of constituents above and below the altitude of particular interest. In the case of the solar flux, the flux outside the atmosphere is well known. Examples of values of solar flux outside the atmosphere are given in Figure 7.

With respect to the motions of the natural stratosphere, questions for CIAP include:

"What are the sources of motion within the stratosphere?"

"What is the spectrum of motion energy within the stratosphere, expressed in terms of mean and standard deviations?"

Figure 8 shows a spectrum of wind speed as measured at an altitude of about 100 meters at Caribou, Maine. The peaks are characteristic of the Brunt-Vaisala period of about two minutes, of the 12- and 24-hour tidal motions, of planetary waves of period between 3 and 6 days, and of the periods of the rotation of the sun (30 days) and of the earth about the sun (1 year). The long period waves are amplified more strongly as altitude increases.

The magnitude of the stratospheric motions was estimated by R. E. Newell in 1969. Table 1 shows that at 20 kilometers the large-scale geostrophic motions, on a horizontal scale of about 5000 kilometers, have a horizontal value of about 10 meters per second in periods of about 30 days. Thermal tidal motions at 20 kilometers, on a horizontal scale of about 10,000 kilometers, have a horizontal motion of about 3/10 of a meter per second, and a period of about 12 hours. The internal gravity waves at 20 kilometers, on a scale of about 100 kilometers, have a horizontal velocity of about 5 meters per second and a period of about a half-hour.

An important question involving theoretical dynamics for CIAP to address is:

"What is the inter-relation of gradients of temperature, velocity, and chemical densities?"

Concerning the dynamic climatology of the natural stratosphere, a question for CIAP is:

"What are the mean temperatures and winds in the stratosphere and how do they vary as functions of latitude, longitude, and altitude?"

Newell has shown the meridional cross-section of temperature as a function of altitude and latitude to be as given in Figure 9. In the troposphere, tem-

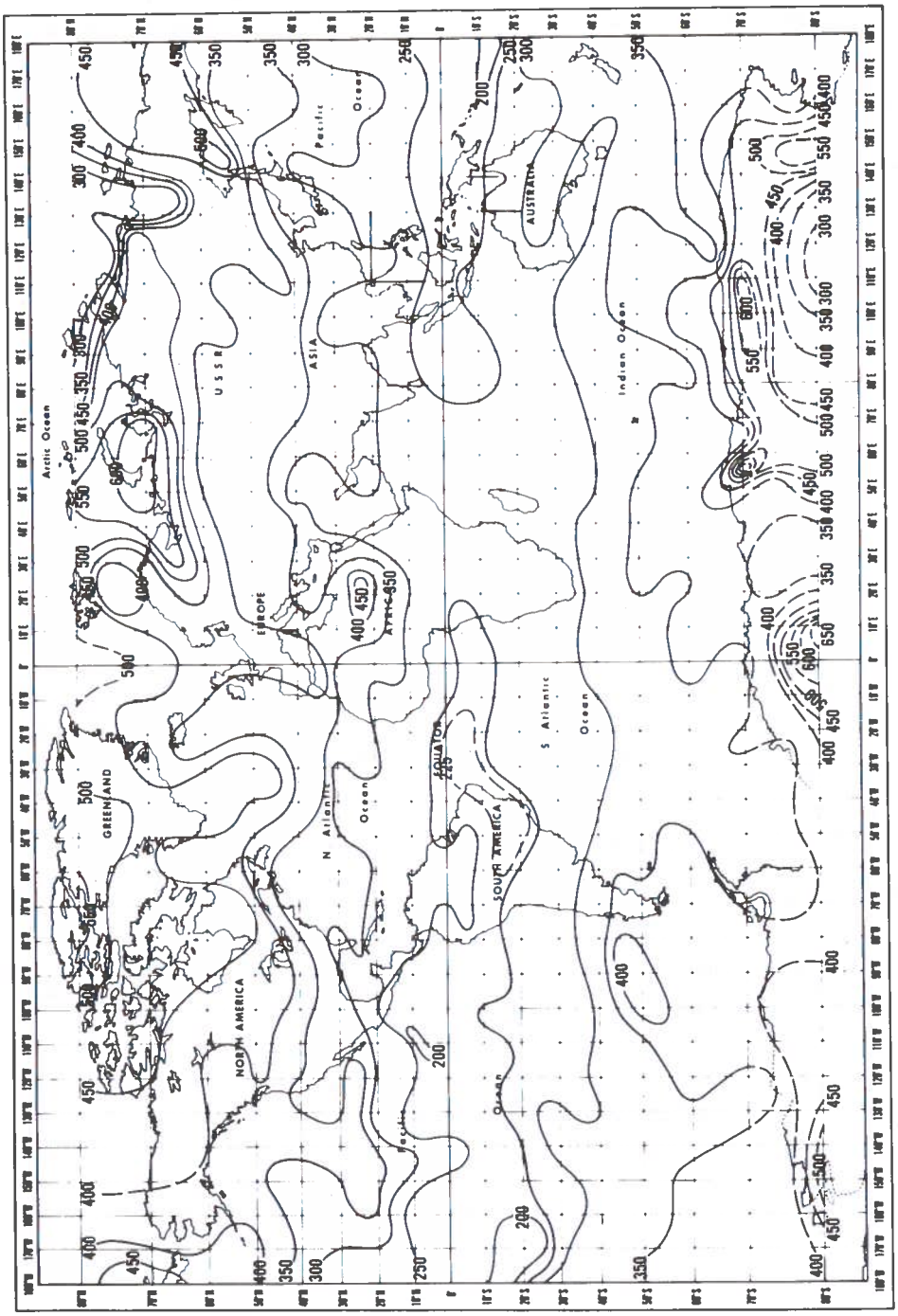

Figure 5. Total Ozone Content (10^{-3} cm STP), April 28, 1969. (C. Prabhakara, NASA GSFC, 17 Nov. 71)

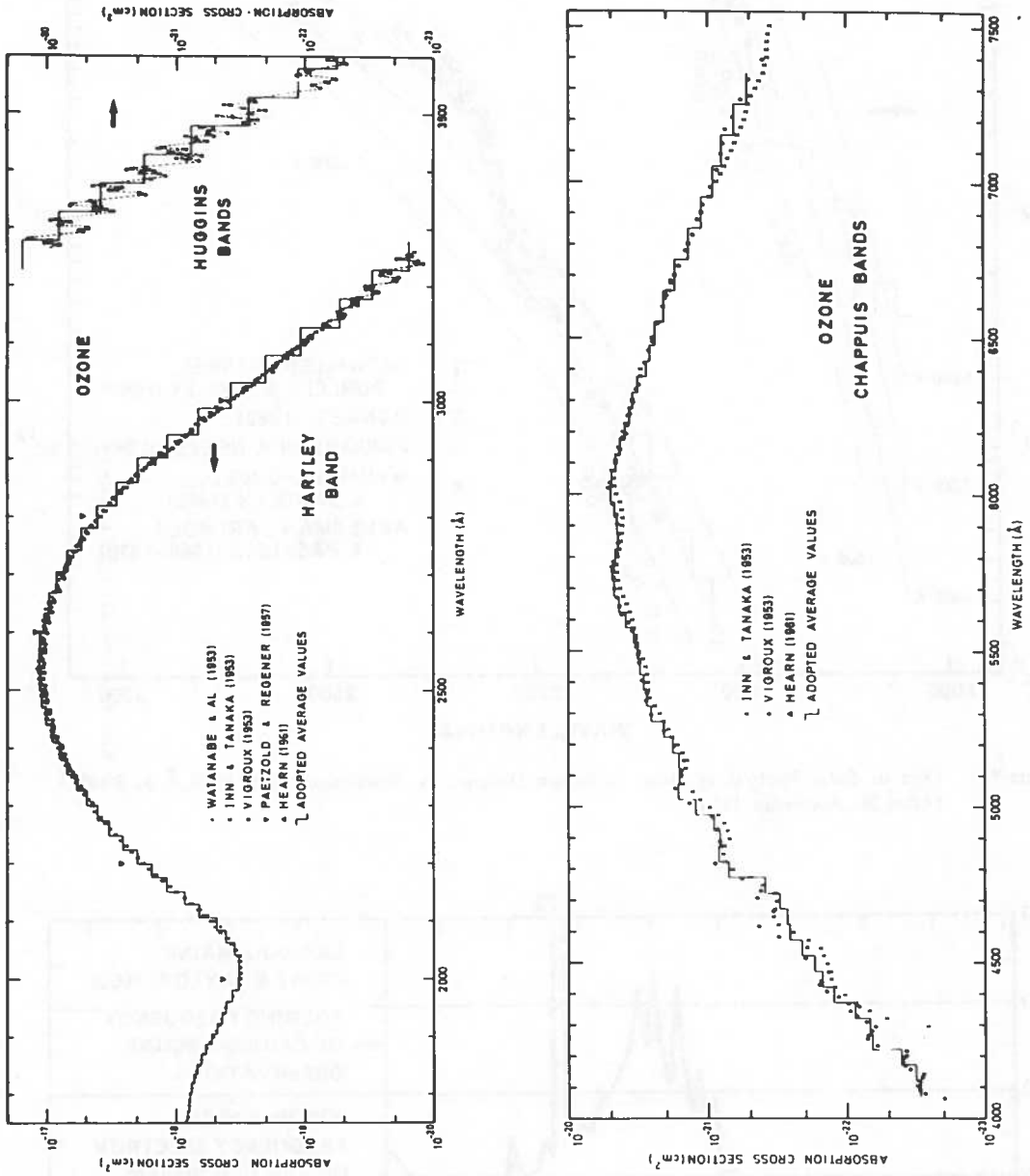

Figure 6. Absorption Cross-Sections of Ozone. (After M. Ackerman 1971)

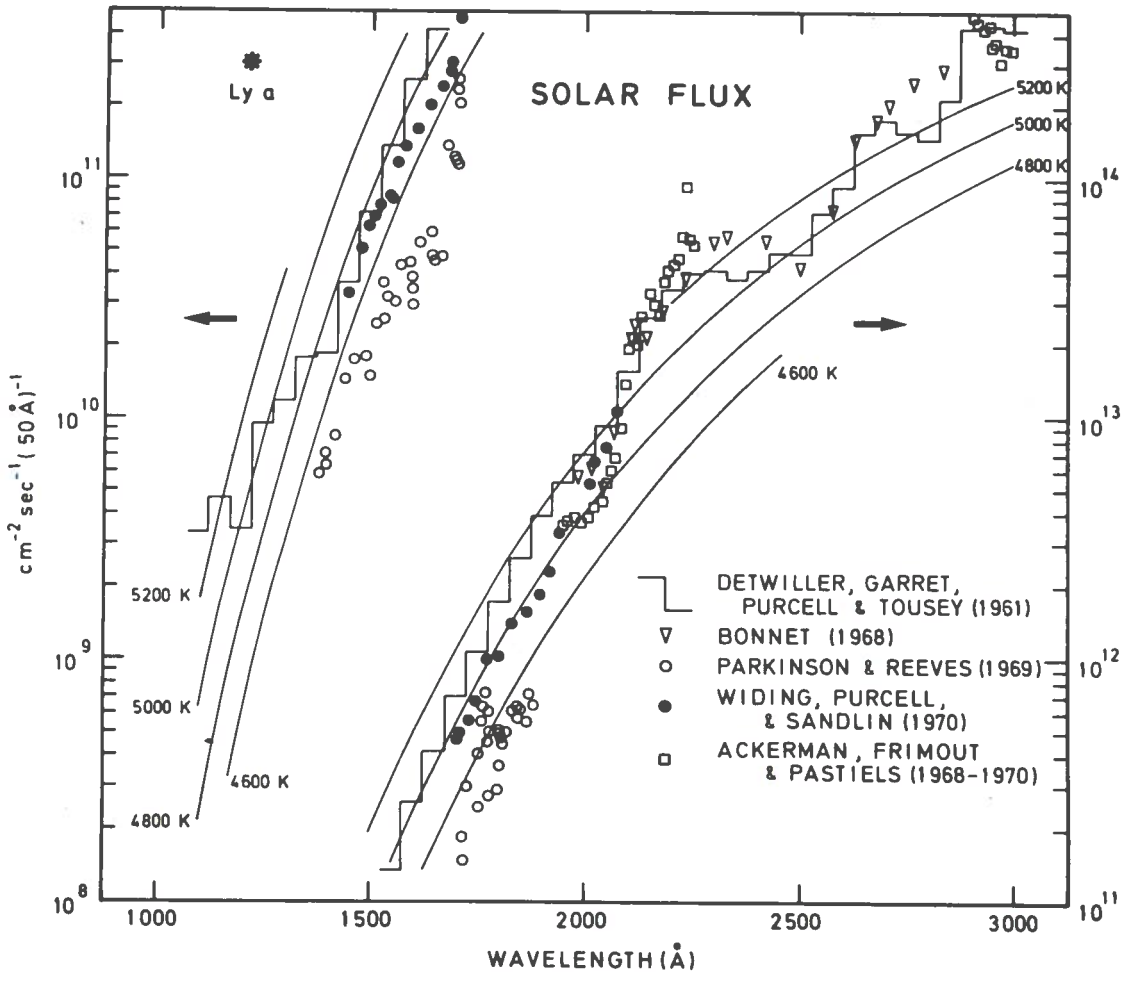

Figure 7. Flux of Solar Photons at Mean Earth-Sun Distance vs. Wavelength from 1000 Å to 3000 Å. (After M. Ackerman 1971)

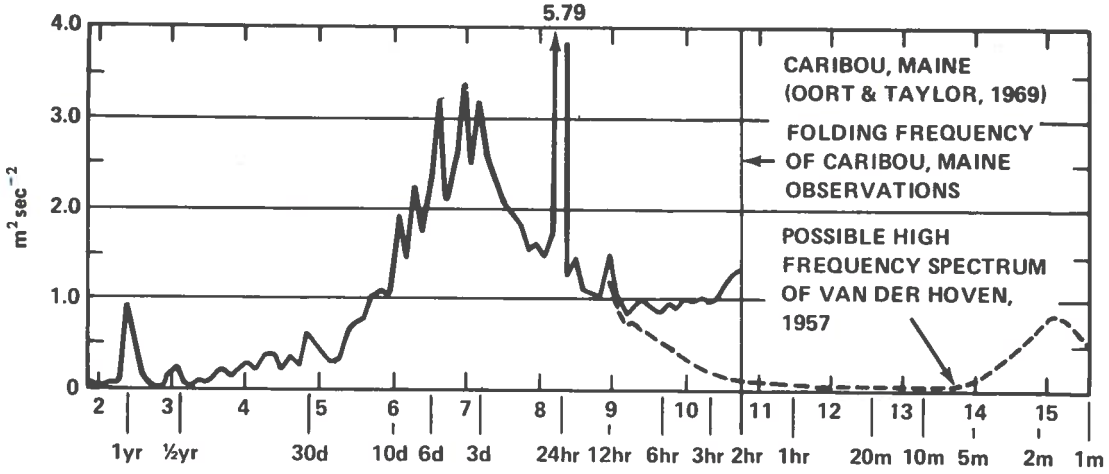

Figure 8. Spectrum of Horizontal Wind Speed at Caribou, Maine. (After Oort and Taylor, 1969)

Table 1. Characteristics of Atmospheric Motions. (After R.E. Newell, 1969)

X, Z, horizontal and vertical dimensions *u, w*, horizontal and vertical velocities *t*, time scale

Layer	Large-scale geostrophic motions					Thermal tidal motions				
	X km	*Z* km	*u* m/sec	*w* cm/sec	*t* sec	*X* km	*Z* km	*u* m/sec	*w* cm/sec	*t* sec
Lower thermosphere 100–120 km	10^4	50	30 (1)	5 (2)	5×10^3	10^4	5–50 (3)	30 (1)	5–50 (2)	10^3
Mesopause, 80 km										
Stratopause, 50 km	5×10^3	50	60	1–2 (7, 8)	5×10^3	10^4	20 (9)	10 (9)		10^3
30 km	5×10^3	30	20		5×10^3	10^4	50	0.5 (11)		10^3
20 km	5×10^3	15	10	1	5×10^3	10^4	50	0.3 (11)		10^3
10 km	10^3	15	20	5	5×10^3	10^4	50	0.3 (11)		10^3

Layer	Internal gravity waves					Other				
	X km	*Z* km	*u* m/sec	*w* cm/sec	*t* sec	*X* km	*Z* km	*u* m/sec	*w* cm/sec	*t* sec
Lower thermosphere 100–120 km	10^3	10	50 (4)	50 (2)	10^4 (5)					
Mesopause, 80 km	10–100 (6)		10–100 (6)							
Stratopause, 50 km		2 (12)	6 (10)		10^4 (10)					
30 km		1 (10)	5 (10)		10^4 (10)					
20 km		2 (12)	5 (12)		2.10^3 (12)					
						Large cumulus clouds				
10 km	20–150 (13)		0.1 (13)		$3–50 \times 10^3$(13)	10	10	20	$1–50 \times 10^3$	10^4

References:
1. Greenhow and Neufeld, 1961.
2. Estimates from $w = uZ/X$ (continuity).
3. Green, 1965.
4. Kochanski, 1966.
5. Hines, 1960.
6. Witt, 1962.
7. Kays and Craig, 1965.
8. Vincent, 1966, private communication.
9. Reed *et al.*, 1966.
10. Newell, Mahoney and Lenhard, 1966.
11. Harris *et al.*, 1962.
12. Weinstein *et al.*, 1966.
13. Gossard, 1962.

peratures at the pole are low with respect to the higher temperatures at the equator. In the stratosphere, by contrast, above 20 kilometers, the high temperatures are at the poles and the low temperatures are near the equator.

In Figure 10, Newell shows the meridional cross-section of mean zonal winds. The troposphere cross-section illustrates the Hadley-cell circulation with hemispheric motions directed by three meridional circulations. In the stratosphere, however, there is a single cell in each of the two hemispheres; meridional circulation moves the heat, as in refrigerator action, from a region of low temperature near the equator to one of higher temperature at the pole.

Figure 11 shows the standard deviation of the meridional wind components and Figure 12 the relative size of the ratio of the standard deviations of the meridional wind to a vertical wind. The vertical winds, greatest at a latitude of about 30 in the troposphere, are approximately 10 times as intense in the stratosphere.

A further question which must be addressed by CIAP is:

"What factors must be included in a computer simulation of the stratosphere?"

Table 2 is significant for its blank spaces. It summarizes what is presently known and what CIAP needs to know about the stratosphere. Shown at the left are 33 constituents involved in the 37 most significant chemical reactions of 175 considered by Frank Hudson. Note that there is about an equal division between hydrogenous, nitrogenous, and carboniferous constituents. The second column lists the logarithm of the density at 30 kilometers for those constituents whose natural vertical distribution of density is known.

The sources and sinks of the several constituents may be many and various. The thunderstorms projecting into the lower stratosphere, the troposphere itself, the oceans, aerosols, and volcanic eruptions will be considered.

At present we plan to measure only a few of these pollution species in engine testing, such as water vapor, nitrogen oxides, carbon oxides, hydro-

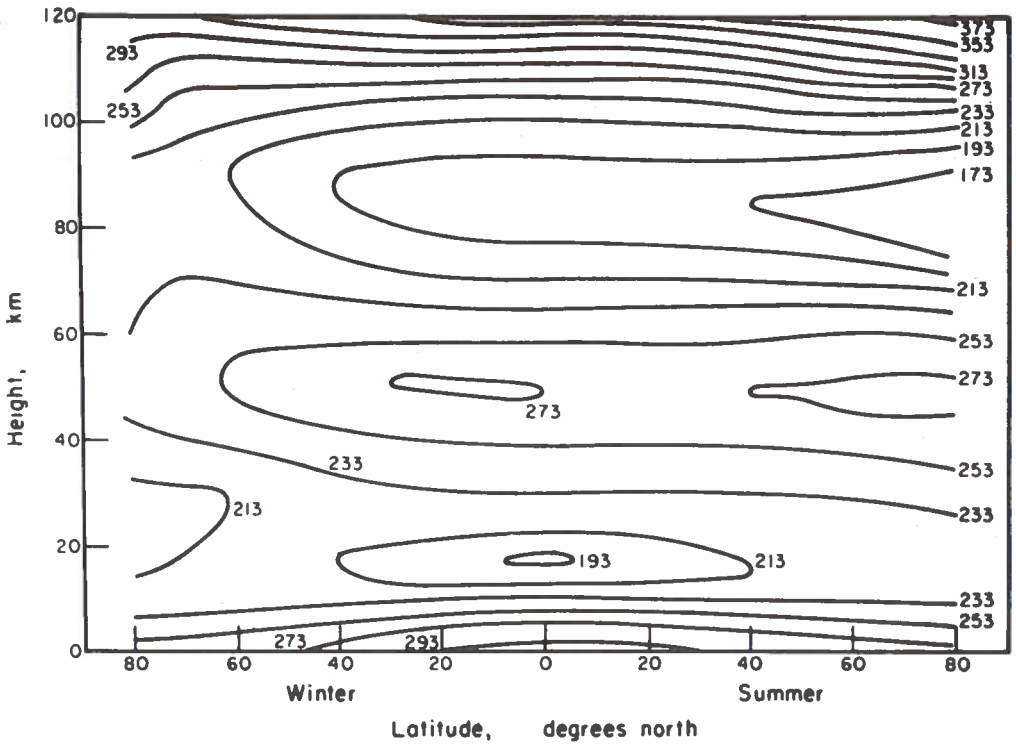

Figure 9. Meridional Cross-Section of Temperature (°K). (After R.E. Newell, 1969)

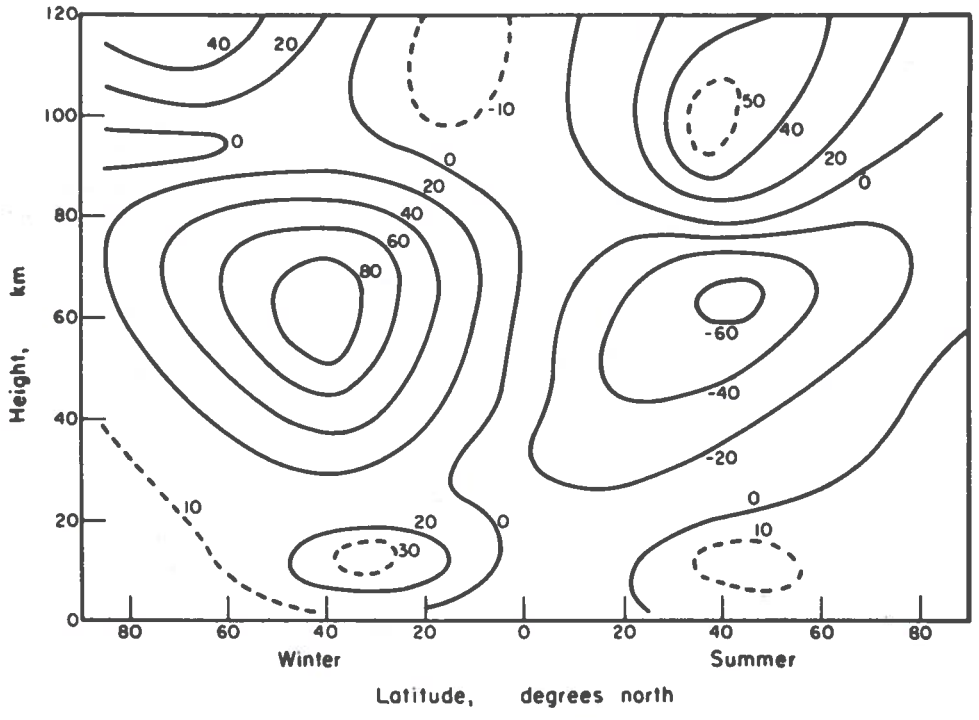

Figure 10. Meridional Cross-Section of Mean Zonal Wind (m/sec). (After R.E. Newell, 1969)

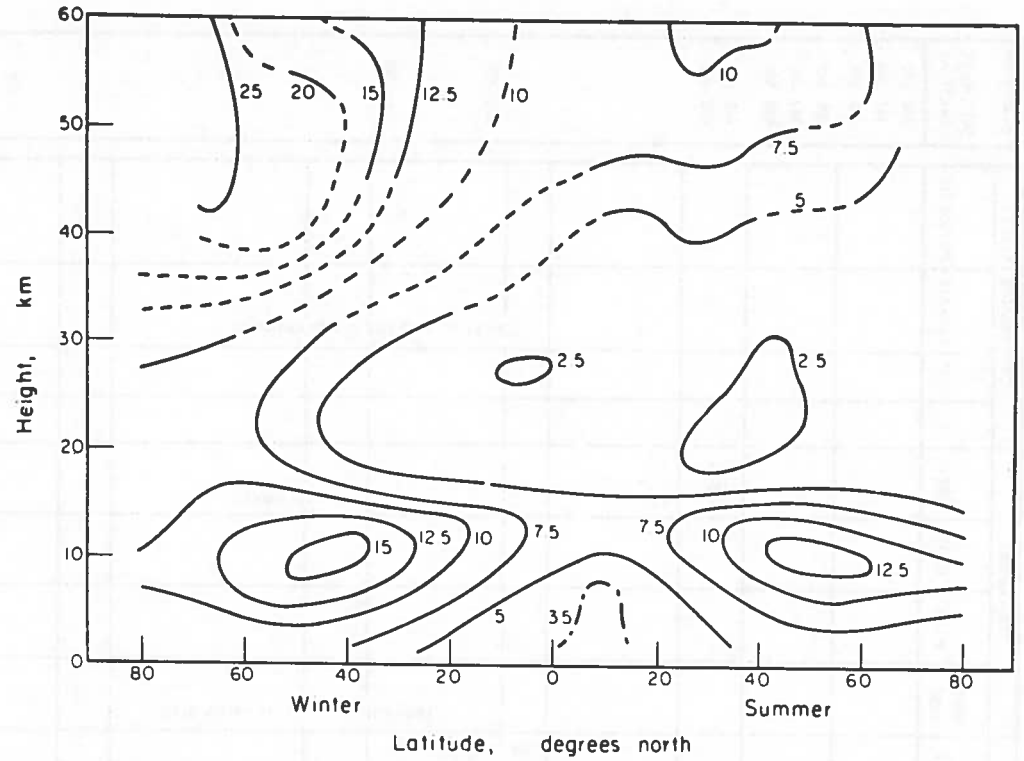

Figure 11. Meridional Cross-Section of Standard Deviation of Meridional Wind Component (v) (m/sec) (After R.E. Newell, 1969)

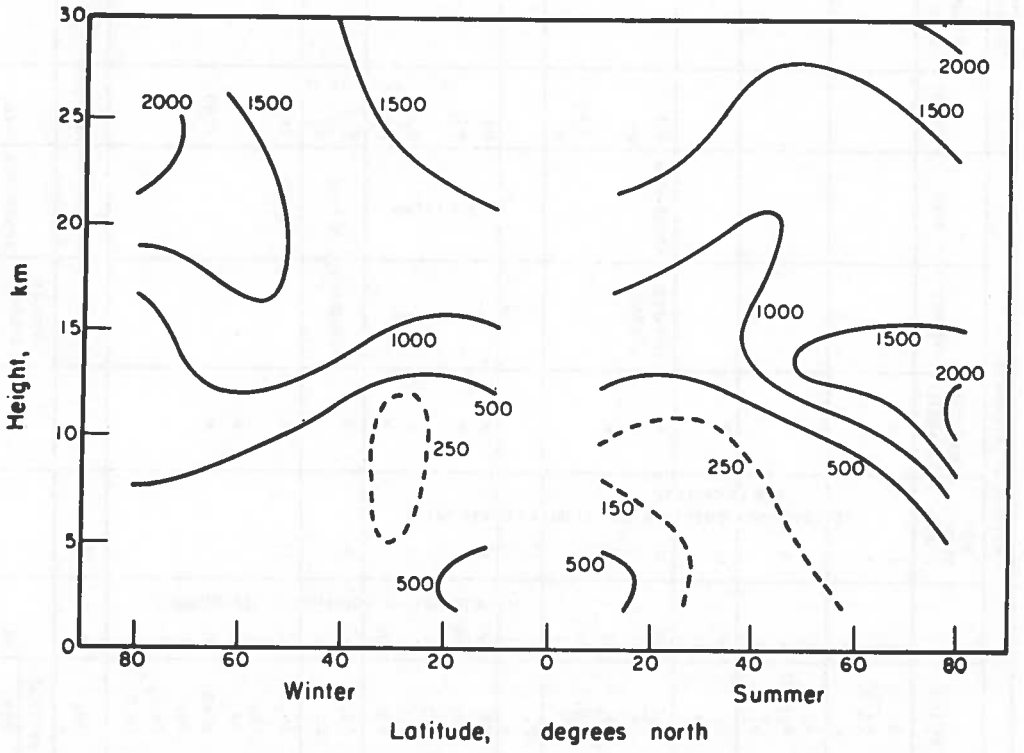

Figure 12. Meridional Cross-Section of the Ratio $\sigma(v)/\sigma(w)$. (After R.E. Newell, 1969)

Table 2. Existing Data on the Most Important Stratospheric Constituents.

NATURAL STRATOSPHERE						POLUTION			TRANSPORT				PERTURBATION EFFECT				RADIATION
SPECIES		LOG DENSITY @ 30 km	MEASURE CAPABILITY	SOURCE	SINK	SPECIES	MEASURE CAPABILITY	RATE	ROUTE/ LINE	WAKE	EDDY	CIRCUL	$\bar{n}$	$\sigma(n)$	CLIMATE	PHYSIO-BIO	CRIT. WAVE LENGTH nm
O	H	8	*														200 - 242
$O(^1D)$	H	3															242 - 300
σ	H																450 - 650
O_2	H	17	*														200 - 242
$O_2(^1\Delta)$	H	9															242 - 300
O_2^*	H																450 - 650
O_3	HJ	12	*									$\overline{n(O_3)v}$					200 - 300
O_3^*	H																450 - 650
H_2O	HJC	12	*	THUNDER STORMS	ABSORPTION	H_2O						$\overline{n(H_2O)v}$					
OH	HJ	7	*			OH											
HO_2	HJ	8	*														
H_2O_2	HJC	10				H_2O_2											
H						H											
N_2	H	17															
N		3															
NO	HJC	10	*	RATE COEFF K_{1m}	RATE COEFF K_{-1}	NO		500 SST IN 1985, (334 x 4) + (166 x 2) ENGINES, $7^{hr}/d$ INFLIGHT, $120^{lb}/hr$ NO									260 - 400
NO_2	HJC		*			NO_2											
NO_3	H																
N_2O		12	*			N_2O J = 93											
N_2O_5	HJC		*			N_2O_5 J = 58											500 - 700
CO_2	H	14	*	TROPOSPHERE	OCEANS	CO_2 J = 85											
CO	HJ					CO											
CH_4	HJ	12	*		PLANTS	CH_4											
CH_3	H																
CH_2	H		*														
HCHO	H		*			HCHO											
CHO	H																
CH_3O_2	H																
CH_3O	H																
SO_2	H				ADSORPTION	SO_2											
PARTICLES	I			THUNDER STORMS	ADSORPTION	HNO_3											<300
HNO_3	HC			VOLCANO													
HNO_2	J																

2/3 IN NO HEMI, 1/3 SO HEMISPHERE

STARR 1968

CHANGES IN T, $\bar{V}$, PRE C.I.P. UV FLUX

TOTAL DENSITY 4 (10) 17 REF BORTNER & KUMMLAR 1969 (PLOTTED BY BTL)

C = CRUTZEN 1971

J = JOHNSTON 1971

H = HUDSON 1971

1.42 $(10)^6$ lb/hr NO

carbons, sulfur oxides, and particulates. I suspect that this list of pollution constituents should be enlarged.

The mass of the pollution species introduced into the stratosphere will depend upon route projections, frequency of travel on the routes, and the engines' emission rates. One prediction, which assumes a fleet of 500 SST's traveling seven hours per day, emitting at the Concorde rate of about 120 pounds of NO per hour, indicates that the deposition into the stratosphere would be on the order of 0.4 million pounds of NO per day. In considering the transport processes, one begins with route projections (about two-thirds in the Northern Hemisphere and one-third in the Southern Hemisphere for 1990); the pollutants will be laid down along the vehicle trajectories. This line of effluents is dispersed by the dynamics of the wake, by diffusion due to atmospheric turbulence caused by wind shear, and finally by the general circulation of the stratosphere, which moves air masses from one part of the globe to another. The perturbation effects will be estimated by machine. In the last column are listed the critical wavebands, expressed in nanometers, of the photochemically active radiation affecting the distribution of the constituents.

The equilibrium of the species at each altitude can be established by simultaneously integrating differential equations for the 33 species. Figure 13 presents the basic equation. Note the large differences in the relative contributions of the various terms. If typical values for reactions involving NO and O_3 at 20 kilometers are substituted, the first term of the contribution (that is, the photochemical term) has a value of approximately 10^9. The reactive chemistry term (the product of the rate coefficient and the contributing mean densities) has a value of about 10. Clearly, in the daytime the photochemistry dominates the reactive chemistry. The chemical loss terms are comparable in size and form with the chemical production terms.

The advection term, involving the wind velocity and the gradient of density, is seen in this instance to have a value of about 10^6. Although in the daytime this term is swamped by the photochemistry, at nighttime it swamps the chemical reactivity. A third term for diffusion, which is important principally for transport in the vertical dimension, has a value of about 10. The ratio of standard deviation to mean value for these terms is also indicated in the second row. The photochemical term uncertainty is about 10 if the solar flux activating the photochemistry is measured *in situ,* but is about 10^3 or more if the flux is estimated from an out-of-the-atmosphere measurement diminished by an exponential factor dependent upon the integrated densities in vertical column of the absorbing constituents. If Prabhakara's ozone column variation is used, the value of the photochemically active solar flux at 20 kilometers may be uncertain by a factor of 10^3 to 10^5. The uncertainty of the chemical rate coefficient in some instances is 10^3; in most instances, however, rate coefficients are known within a factor of 10. Contributing to the uncertainty of the advection term are the uncertainties of winds and of the gradients, each about 10^3. The uncertainty of the diffusion term has contributions from the Laplacian of the density (representing the sources and sinks) and from the diffusion coefficient. The diffusion term uncertainty is likely to be on the order of 10^6.

This over-simplified expression suggests that a sensitivity analysis is needed to determine which sources of uncertainty in computing the density-height distribution of the perturbed stratosphere contribute most to the uncertainty of the final result. Conclusions to be drawn from the example are that (1) the densities of as many of these constituents as possible should be determined simultaneously in space and time, (2) the photochemically reactive solar ultraviolet flux should also be determined at the same time and location, (3) velocities and diffusion transport need to be determined, and (4) the most important determinations are those such as satellite measurements, which yield a field of densities from which gradients and Laplacian values may be determined.

Other questions related to the simulation of the stratosphere by computer include:

"What are the limitations on computer stratospheric simulations done in the next two years?"

"In what ways can a complete model of the stratosphere-troposphere-ocean, as planned for future development at Geophysical Fluid Dynamics Laboratory, be abridged to derive answers desired by CIAP?"

$$\frac{\partial n_i}{\partial t} = \left[\left\{ J_k(z) = \int_{\lambda_1}^{\lambda_2} \sigma(\lambda)\epsilon(\lambda) I(\lambda, z)\, d\lambda = \int_{\lambda_1}^{\lambda_2} \sigma(\lambda)\epsilon(\lambda) I(\lambda, \infty)\, e^{-\sum_i \sigma_i(\lambda) \int_z^\infty n_i \sec x\, dz}\, d\lambda \right\} \bar{n}_k + k_{jk} \left\{ \bar{n}_j \bar{n}_k + \overline{n_j' n_k'} \right\}\right] - [\text{Loss}] - \bar{V} \cdot \nabla n_i - D\nabla^2 n_i$$

Mean Value: $\underbrace{10^{-18} \cdot 1 \cdot 10^{15} \cdot 10^{12}}_{10^9}$ $\underbrace{10^{-23} \cdot 10^{12} \cdot 10^{12}}_{10}$ $\underbrace{\underbrace{10^4 \cdot 10^2}_{10^6}\ \underbrace{}_{10}}$

S.D./Mean $\underbrace{10 + 10 + 10}_{10}$ in situ $\underbrace{10 + 10 + 10 \quad + 10^3}_{10^3}$ computed $\underbrace{10^3 + 10 + 10}_{10^3}$ $\underbrace{\underbrace{10^3 + 10^3}_{10^3}\ \underbrace{10'}_{10^6}}$

(j) + (k) → (i) + (m)

n_i	Density distribution, for each altitude, determined by integrating simultaneously 37 equations of the form above, relating 33 different species
σ	Absorption cross section
ϵ	Quantum yield
I	Solar flux, of wavelength λ and at altitude z
x	Solar zenith angle
k	Reaction rate coefficient
$\bar{V}$	Mean wind velocity
∇n_i	Gradient of the density
D	Diffusion coefficient
$\nabla^2 n_i$	Laplacian of density, representing a source or sink
$\overline{n_j' n_k'}$	Cross correlation of density fluctuations

Figure 13. Equation for Determining Species Equilibrium in a Perturbed Stratosphere.

With respect to instrumenting the measurement of constituents and of transport within the natural stratosphere, a questinn for CIAP is:

"What concepts and techniques for remote and *in situ* measurements are presently available and most applicable to measure water vapor, ozone, the trace gases important to CIAP, and particulates?"

Some of the experimental methods used in exploring the atmosphere were described by Difedele in 1968, and are shown in Figure 14. It can be seen that in the 20-to-40-kilometers region the principal means are aircraft and balloons doing meteorologic sounding, ground-based lidar, and various methods of determining absorption of sunlight and the infrared thermal emission.

In examining tropospheric changes which may result from stratospheric perturbations, CIAP must address these questions:

"What direct observations of the climatology of the troposphere can be of assistance in exploring troposphere-stratosphere relations?"

"How may the effects of changes in radiation heating of the troposphere, which result from changes in constituent-density distribution within the stratosphere, be interpreted in terms of altitudes and directions of mean winds (at 500 millibars, say) and of precipitation in the short term and in the long term?"

Some suggestions as to the form of the answers were suggested by a study made ten years ago by Professor Y. Mintz using a very simple two-layer tropospheric model. It should be noted, however, that this model does not take into account the important influence of geography.

First of all, Figure 15 shows the cellular meridional circulation on a rotating earth, according to a picture attributed to G.C. Rossby in 1945. In this figure are represented the three Hadley cells, which produce low-level easterly winds in the lower tropics, westerly winds in the mid-latitudes, and easterly winds in the polar regions. The bonndaries between the oppositely directed winds are the source of inertial waves which give a roughly sinusoidal form to the zonal wind trajectories as they circle the earth. Mintz found in his study that this waveform was necessary for the transport of heat in the troposphere from the high temperatures of the equator to the low temperatures of the poles.

Figure 16 shows a polar view of how the zonal wave motion enhances the meridional heat transport, and also the relations of the underlying high- and low-pressure areas. The circulation in the northern hemisphere is counter-clockwise around the low-pressure areas and clockwise around the high-pressure areas. The number of the nodes of this wave motion of circulation is a function of the heating and temperature gradient.

Figure 17 shows the model Mintz used to describe the radiation budget for the planet Earth. It depends on infrared emission from carbon dioxide within the troposphere, and on the solarization as it is affected by the tropospheric albedo. There is a net differential heating (ΔQ) which is the difference between these values. Employing this model, Mintz derived a change in heating (expressed in kilojoules per second) between summer and winter of 2×10^{12} to 8×10^{12}. The planetary wave number, that is, the representative number of nodes of the mid-latitude zonal trajectory around the earth, is described as a function inversely proportional to the heating of the upper troposphere. He found the nodes to number from 7 to 8 in the summer and 5 to 6 in the winter. Mintz suggested the root mean square velocity of the mean hemispheric wind to be a function of the heating differential divided by the temperature in the upper troposphere, and by this method of estimation calculated that the wind speeds in the winter are approximately twice those in the summer, as has been observed.

I have suggested some implications with a sketch of my own, Figure 18. W indicates a schematic trajectory near the polar front in the wintertime; the shape is assumed to be positioned largely by the persistent high-pressure region of continental Siberia. S indicates the summer winds trajectory with a slight shift of phase within the continental United States in the summertime. Both the summer and winter winds, from the standpoint of the United States, seem to originate in Alberta, bringing dry polar air down through the West to a southernmost extreme at about Oklahoma. The zonal trajectory there turns north, carrying with it masses of moist tropical air dragged out of the gulfstream, alternating with masses of dry polar air. As a consequence, the United States west of the Mississippi is generally dry by contrast with the territory east of the Mississippi.

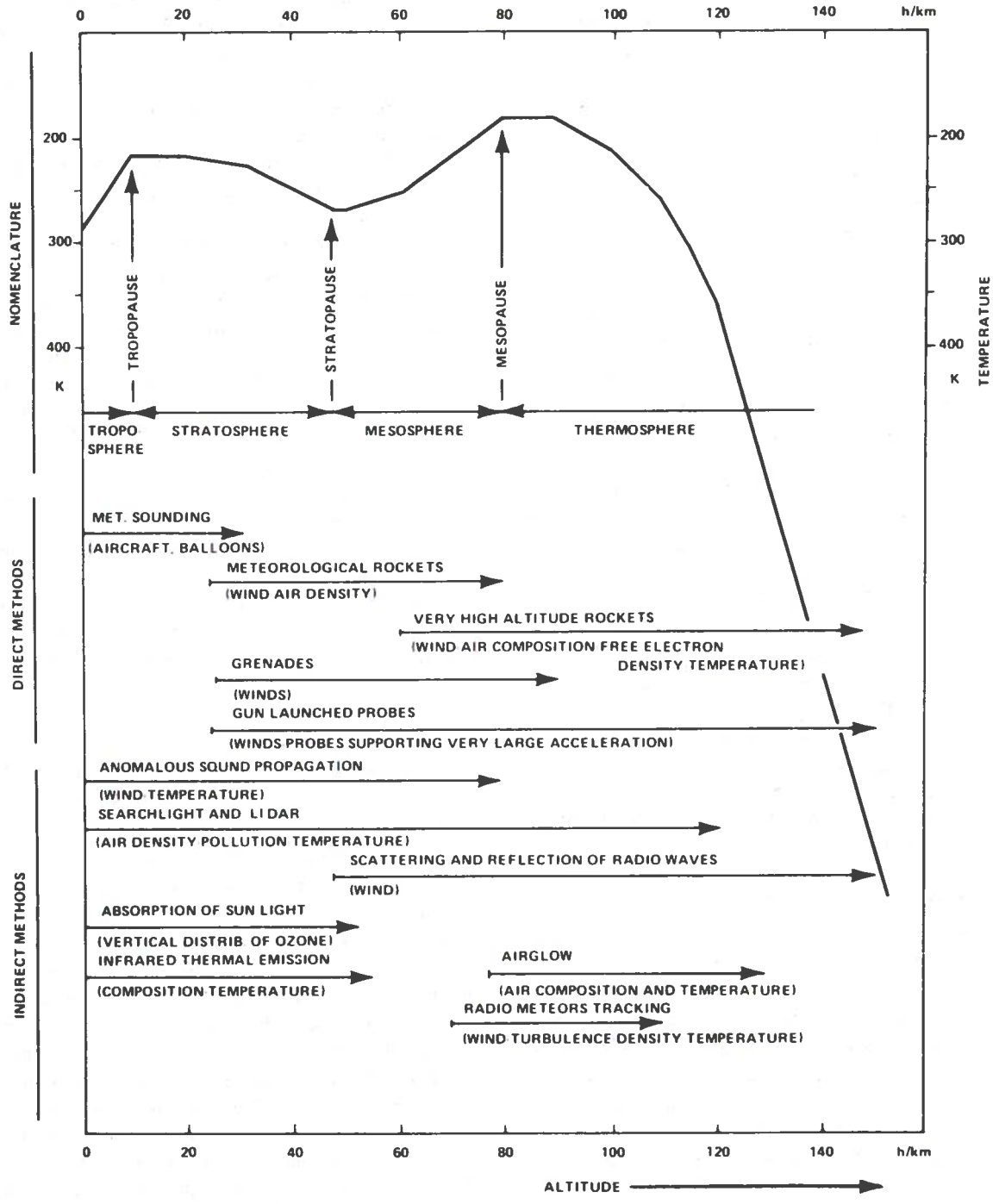

Figure 14. Experimental Methods in Exploring the Atmosphere. (After Difedele, 1968)

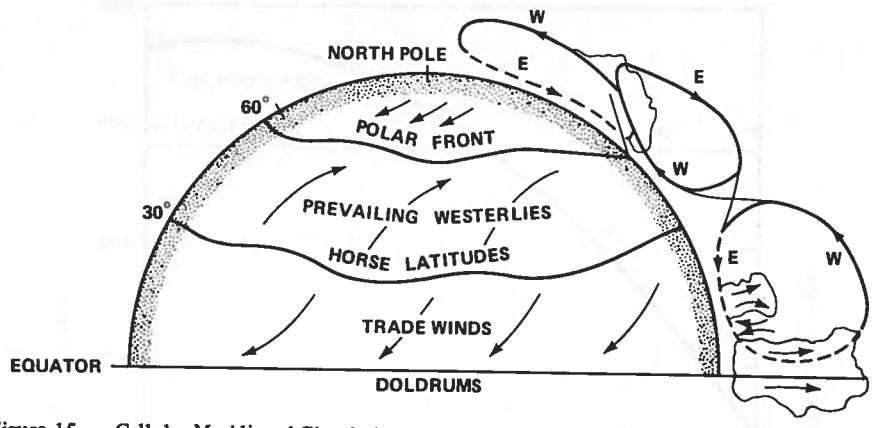

Figure 15. Cellular Meridional Circulation on a Rotating Earth. (After G.C. Rossby, 1945)

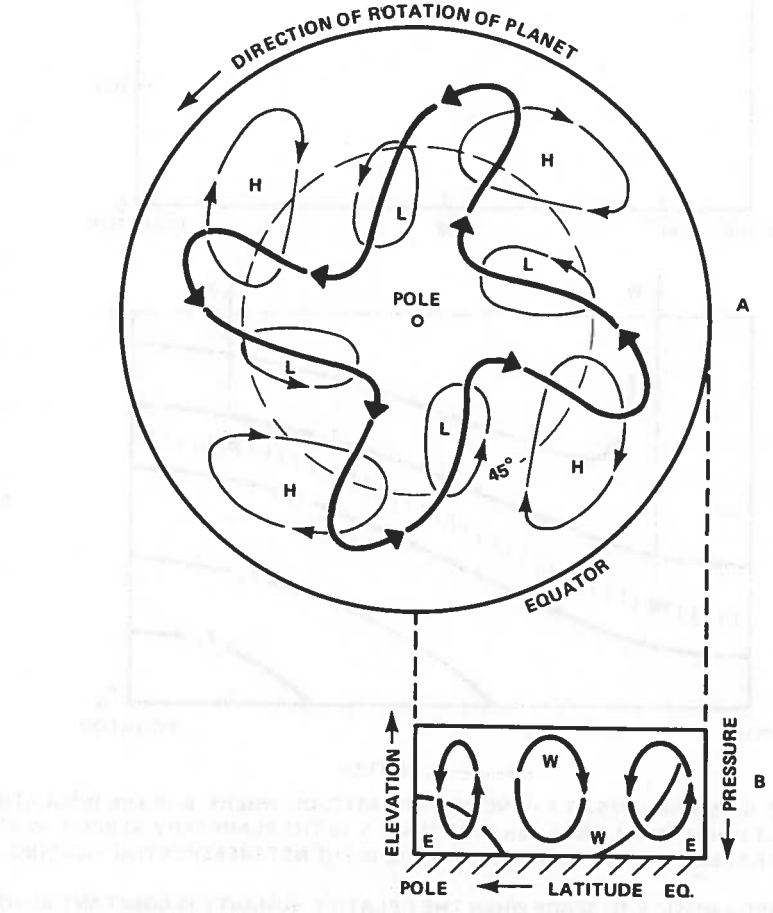

A) STREAMLINES OF THE FLOW AT THE MIDDLE AND UPPER LEVELS (HEAVY LINE) AND NEAR THE GROUND (THIN LINE). L = LOW PRESSURE, H = HIGH PRESSURE.

B) CROSS SECTION SHOWING THE ZONALLY-AVERAGED MERIDIONAL CIRCULATION; AND THE ZONALLY-AVERAGED ZONAL WIND, WHERE W = WESTERLY WIND, E = EASTERLY WIND.

Figure 16. A Wave Regime of General Circulation. (After Mintz, 1961)

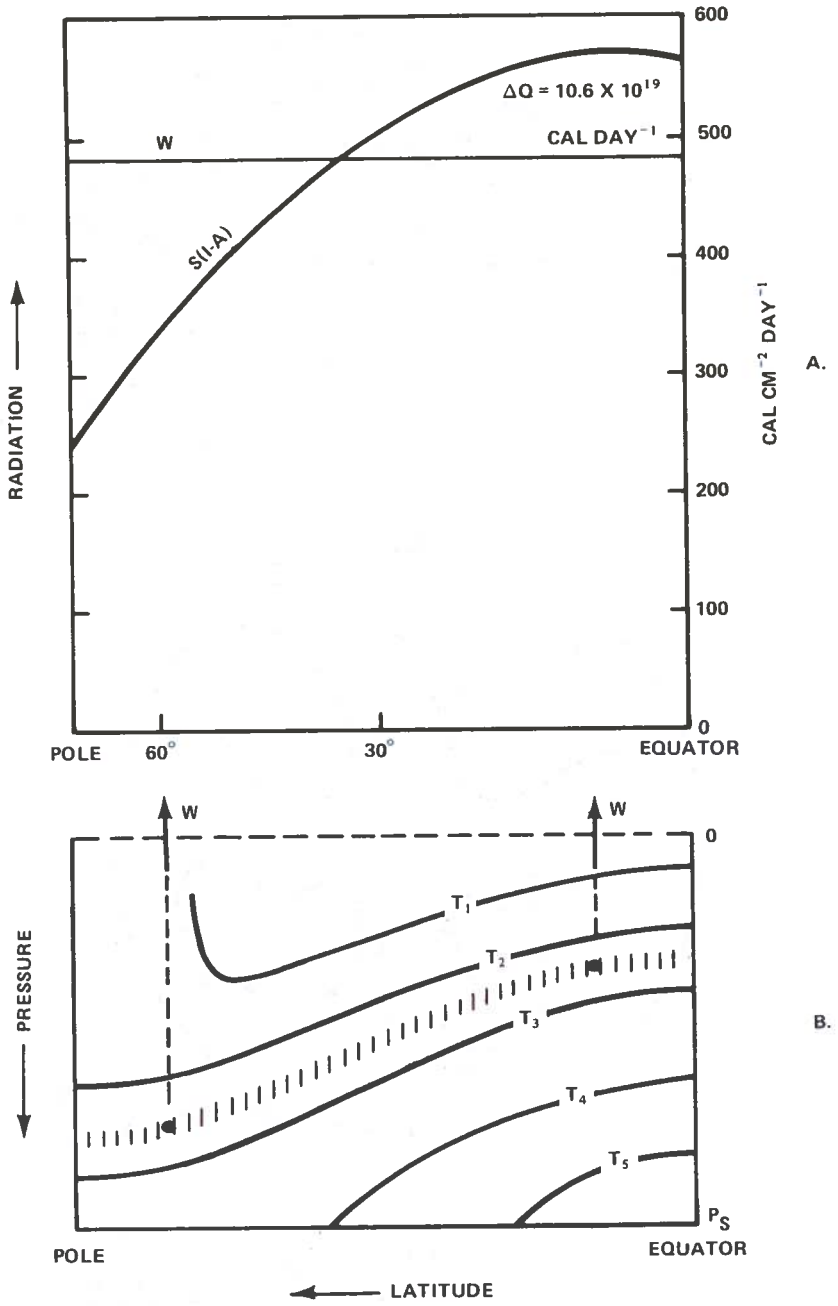

A. ENERGY GAIN AND LOSS AS A FUNCTION OF LATITUDE, WHERE S IS THE INSOLATION PER UNIT HORIZONTAL AREA PER UNIT TIME, A IS THE PLANETARY ALBEDO, W IS THE INFRARED EMISSION TO SPACE, AND ΔQ IS THE NET DIFFERENTIAL HEATING.

B. INFRARED EMISSION TO SPACE WHEN THE RELATIVE HUMIDITY IS CONSTANT ALONG THE ISOTHERMAL SURFACES T. THE SHADED BAND REPRESENTS A LAYER OF WATER VAPOR, OF CONSTANT OPTICAL THICKNESS, WHICH CONTRIBUTES TO THE TOTAL INFRARED EMISSION W.

Figure 17. Assumed Radiation Budget for Earth. (Mintz, 1961)

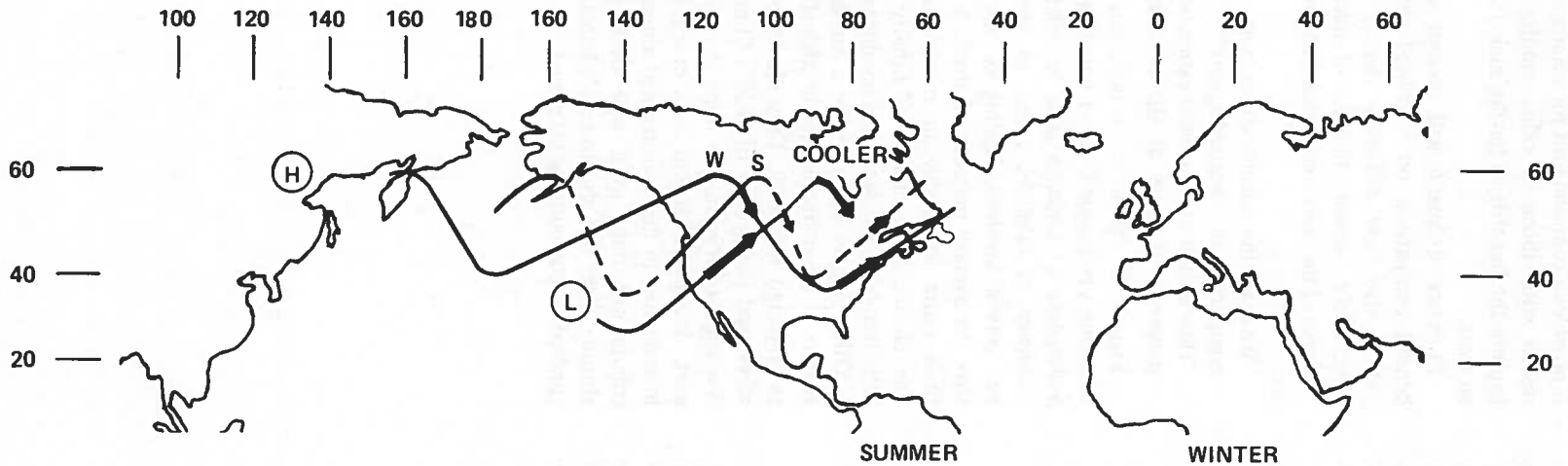

	SUMMER	WINTER
CHANGE IN HEATING ΔQ (KJ sec^{-1})	$2(10)^{12}$	$8(10)^{12}$
PLANETARY WAVE NUMBER $n_d = \frac{a\,\Omega\,m}{R}\,2^{1/4}\left(\frac{C_p}{T_z\,s}\right)^{1/2}$	7-8	5-6
MEAN SQUARE VELOCITY $(\overline{V_z^2})^{1/2} \cong \left[\frac{q\,m\;\;2^{1/4}\;\;\Delta Q}{\pi\,a\,p_s \sin 30\;\;(C_p T_z S)^{1/2}}\right]^{1/2}$	X 1	X 2

Figure 18. Implications of Climatic Change. (After Mintz, 1961)

Let us speculate as to a possible effect of a markedly reduced solarization of the stratosphere resulting from changes in the stratosphere. Pursuing the suggestion drawn from Mintz' study, the winds would be stronger, and there might be a phase shift of the zonal wave. This might bring, as this sketch suggests, warm moist air onto the shores of the Pacific Northwest, while the polar dry air came down into the eastern part of the United States. Such an effect would sensationally alter our local climate. All these suggestions are speculations, of course; they might perhaps be tested by climatological simulation.

Later in this conference Professor Smith discusses the effect of the ultraviolet radiation in the troposphere on man, animals, and plants. Increased penetration of UV radiation into the atmosphere is a possible effect of diminution of the ozone column within the stratosphere. Certainly questions for CIAP are:

"What wavebands of radiation are particularly damaging?"

"What are the effects of ultraviolet radiation, at various levels of intensity, on living tissue?"

As a final conclusion of the study, it is desirable that these adverse physiological-biological-botanical effects, as those which affect people most directly, be expressed where possible in terms of economic measures. Expression by economic measure is advisable both because it is an additional index by which the significance of a technical statistic may be appreciated, and because it provides a common unit for comparison of CIAP results with those of other studies which may explore the benefits of having such a high-altitude air fleet.

Professor Erdmann will present such a risk-benefit comparison on a related subject which people also have difficulty viewing other than subjectively, namely, the use of nuclear power.

Some of the questions which CIAP must address are:

"What are the considerations in any risk/benefit comparison of climatic impacts?"

"How should one go about estimating economic measures of costs of the climatic impacts?"

Figure 19 shows a comparison made by Erdmann's colleague C. Starr which plots people's willingness to undergo risks in relation to the incidence of fatalities versus an annual benefit per person involved, leading to the conclusion that the average member of the U.S. population finds quite acceptable in many walks of life one chance in a million of fatality due to his activities, both voluntary and involuntary.

Other papers will examine a number of other aspects of the consequences of high-altitude flight as projected for 1990. They illustrate in part the scope and perspective of DOT's Climatic Impact Assessment Program. We hope that our 1974 report, drawing as it will on a broad spectrum of investigators in this country and abroad, will contribute not only to a wise decision on high-altitude flight but also to man's knowledge of the atmosphere surrounding his planet.

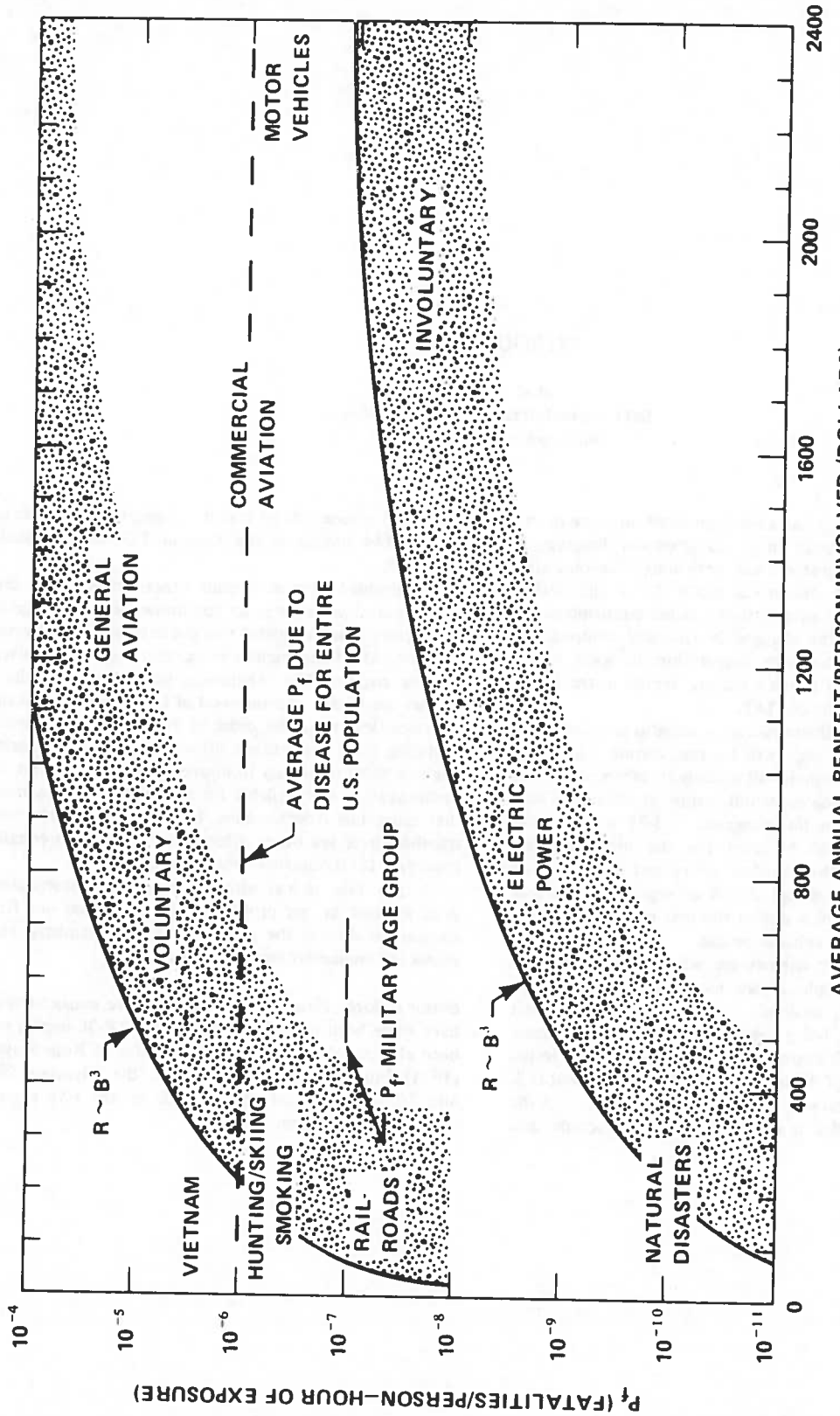

Figure 19. Risk (R) Plotted Relative to Benefit (B) for Various Kinds of Voluntary and Involuntary Exposure. (C. Starr, Science *165*, 1232-1238)

INTRODUCTION

A.K. Forney
DOT Federal Aviation Administration
Washington, D.C. 20591

As Dr. Grobecker has already pointed out, one of the parts of the Climatic Impact Assessment Program is examination of engine exhaust emissions. The objective of this part is to develop a model for a chemically-reacting wake of an aircraft flying in the stratosphere, in order to predict the changes in chemical composition occurring in the exhaust product within the wake, to the extent necessary to provide realistic inputs to the atmospheric modeling part of CIAP.

In order to have this model as meaningful as practicable, a series of engine tests will be run, during which the engine exhaust emissions will actually be measured, under conditions simulating supersonic cruise at altitude. There are four engines in this program. A J-85 afterburning turbojet engine will be used for the most detailed measurements at the broadest set of test conditions to determine what products are in an engine exhaust and what happens to them during the first twenty diameters downstream of the exhaust nozzle.

The three other engines are what we call SST-like engines. By that phrase we mean that they are the U.S.-built engines available to us that are the most like the engines being used in the three supersonic transports. A J-93 engine is the one that will be tested as representative of the no-longer-under-development U.S. SST. A J-58 engine will be tested as representative of the Olympus 593 engine in the Anglo-French Concorde, and the TF-30 engine will be tested as being representative of the NK-144 engine in the Russian TU-144 supersonic airplane.*

We decided that we would benefit most from this symposium if we were to let you know some of our problems rather than just giving you the details of our planned program. All of the engines in our test program are afterburning engines. The exhaust-gas temperatures of these engines are in the neighborhood of 1900^{o} Kelvin, and the gas velocities are on the order of 900 meters per second. Sampling these gases in an altitude chamber is not easy, nor is it going to be easy to insure low scatter of our data. Instrumentation is available for measuring the substances that cause Los Angeles smog, but we need to determine whether there are other substances that may be equally important for the upper-atmosphere studies.

At any rate, it was with the objective of stimulating your interest in our problems that we invited our first speaker to discuss the problems in the chemistry and physics of engine exhaust emissions.

Editor's Note: Plans for the CIAP engine emission tests have since been revised. Testing of the TF-30 engine has been eliminated; as a result of the offer of Rolls Royce (1971) Ltd. to supply test data on the Olympus 593 Mk. 602 (production) engine, tests of the J-58 engine have also been eliminated.

JET ENGINE EMISSIONS

JACK GROBMAN
NASA Lewis Research Center
Cleveland, Ohio 44135

ABSTRACT: The sources and concentrations of the various constituents in the engine exhaust and the influence of engine operating conditions on emissions are discussed. Cruise emissions to be expected from supersonic and subsonic engines are predicted on the basis of existing data relating emissions to combustor operating conditions. The basic operating principles and performance criteria that determine the design of gas turbine combustors are briefly reviewed. Recent reports that consider combustor design techniques that may be used to reduce emissions are surveyed.

INTRODUCTION

This paper is a brief tutorial review of the emission characteristics of jet engines, particularly during high-altitude cruising. Many recent reports [1-3] have discussed the relative contribution of jet aircraft emissions from ground and low-altitude maneuvers to urban pollution. Even though the overall contribution of aircraft to urban pollution is small, the air quality in the vicinity of commercial airports is considered to be significantly affected by jet aircraft emissions. During idling and taxiing, the principal pollutants are unburned hydrocarbons and carbon monoxide; during landing and take-off, they are oxides of nitrogen and smoke. Emission data for a number of commercial jet engines for subsonic aircraft have been documented in Reference 4. These data apply mainly to operating modes below an altitude of 900 meters (3000 feet), which include idle, takeoff, climbout, descent, and landing. These data were obtained by ground-based sampling of the exhaust from jet engines operating over a range of engine speeds to simulate the various operating modes. No similar data are yet available on the emissions of either subsonic or supersonic aircraft at cruise conditions. The constituents of the engine exhaust are mainly a function of the combustor operating conditions, including combustor inlet total temperature and pressure, combustor reference velocity or reaction dwell time, and fuel-air ratio. Cruise emissions from either subsonic or supersonic jet aircraft may be predicted from their combustor operating conditions during cruise by using typical emission data correlations obtained over a range of combustor operating conditions.

The constituents in the exhaust may be divided into five categories: the unreacted constituents in the air, the products of complete combustion, the products of incomplete combustion, oxides of nitrogen, and constituents due to trace elements in the fuel. During cruise the products of incomplete combustion (carbon monoxide and hydrocarbons) are relatively low in concentration, because gas turbine combustors operate at a combustion efficiency near 100 percent at cruise conditions. (The concentrations of these products would be slightly higher in the exhaust of an afterburning turbine engine than in that of an unaugmented engine, since afterburners tend to burn less efficiently than main combustors.)

Nitric oxide is considered to be the most significant emission product formed during altitude cruise. The quantity of nitric oxide formed in the combustor is a strong function of flame temperature, which increases with increasing combustor-inlet total temperature. Combustor-inlet total temperature increases with increases in either compressor pressure ratio or flight Mach number. Altering gas turbine combustor designs to make substantial reductions in oxides of nitrogen will be an extremely difficult task. Research is in progress to develop and evaluate experimental combustors that reduce NO_x without compromising on engine performance. Combustor design techniques which can reduce pollutant emissions are presented in References 5 through 9.

CONSTITUENTS IN JET ENGINE EXHAUST

The various constituents in jet engine exhaust under typical takeoff or cruise conditions are

tabulated in Figure 1. The constituents have been grouped by source into five different categories. These include (1) inert substances and unreacted oxygen from air, (2) products of complete combustion of fuel, (3) products of incomplete combustion, (4) oxides of nitrogen formed during the heating of air, and (5) elements or compounds derived from sulfur and trace metals present in kerosene fuel. The concentration of the components in the air and products of complete combustion were determined for an overall fuel-air ratio of 0.014 using commercial Jet A-1 kerosene fuel. This ratio generally has a range of 0.01 - 0.03 during cruise. The products of incomplete combustion include carbon monoxide; unburned fuel; partially oxidized hydrocarbons (such as aldehydes); hydrogen; and particulates (soot), consisting mainly of carbon. Combustors for gas turbine engines are designed to operate with maximum performance during cruise; the estimated concentrations of the products of incomplete combustion shown in Figure 1 are equivalent to an overall combustion inefficiency of about one percent or less. Afterburners for gas turbine engines tend to be less efficient than the main combustor, so the concentrations of the products of incomplete combustion are generally several times greater for such augmented engines.

CONSTITUENTS	SOURCE	ESTIMATED CONCENTRATION
N_2	AIR	77% (VOL)
O_2	AIR	16.6% (VOL)
A	AIR	0.9% (VOL)
H_2O	EFF COMBUSTION	2.7% (VOL)
CO_2	EFF COMBUSTION	2.8% (VOL)
CO	INEFF COMBUSTION	10-50 PPM
UNBURNED HC	INEFF COMBUSTION	5-25 PPMC
PARTIALLY OXIDIZED HC	INEFF COMBUSTION	
H_2	INEFF COMBUSTION	5-50 PPM
SMOKE (PARTICULATES)	INEFF COMBUSTION	0.4-50 PPM (MASS)
NO, NO_2	HEATING OF AIR	50-400 PPM
SO_2, SO_3	FUEL	1-10 PPM
TRACE METALS	FUEL	5-20 PPB

Figure 1. Engine Exhaust Constituents. Fuel is commercial Jet A-1 kerosene; the overall fuel-air ratio is 0.014.

Oxides of nitrogen are formed from the reactions of oxygen and nitrogen at the elevated temperatures in the reaction zone of the combustor. These oxides of nitrogen (NO_x) generally consist of 90 to 95 percent nitric oxide (NO) and the remainder nitrogen dioxide (NO_2). The quantity of nitric oxide formed is affected by a number of factors, including engine compressor pressure ratio, flight Mach number, fuel-air ratio, and combustor design.

Commercial specifications for Jet A-1 kerosene require that the sulfur concentration in the fuel not exceed a value of 0.3 percent by weight. In practice, the sulfur concentration is generally less than 25 percent of this value. The sulfur in the fuel is mostly converted into sulfur dioxide (SO_2), with lesser amounts of sulfur trioxide (SO_3). A variety of trace metals are present in the fuel, such as aluminum, iron, manganese, nickel, sodium, potassium, and vanadium. The total concentration of the trace metals in jet engine exhaust is estimated to be about 5-20 parts per billion.

TYPICAL JET ENGINE EMISSION CHARACTERISTICS

Figure 2 illustrates the carbon monoxide (CO), total hydrocarbon, and oxides of nitrogen (NO_x) emissions over a range of engine speeds for a typical subsonic-aircraft gas-turbine engine with a compressor pressure ratio of 13.4 using JP-5 fuel (similar to Jet A-1). The term "emission index" (grams of pollutant per kilogram of fuel burned) is used instead of the more familiar volumetric concentration term, parts per million, in order to normalize emissions on the basis of fuel flow. At a fuel-air ratio of 0.015, an emission index of unity is equivalent to either 15 ppmCO, 30 ppmC total hydrocarbons, or 10 ppmNO_x. The NO_x emission index is calculated by expressing all oxides of nitrogen as NO_2. At low engine speeds corresponding to idle operation, the CO and hydrocarbon emissions are at their highest, whereas oxides-of-nitrogen emissions are at their lowest. At an engine speed of 100 percent, corresponding to takeoff conditions, the NO_x emissions are

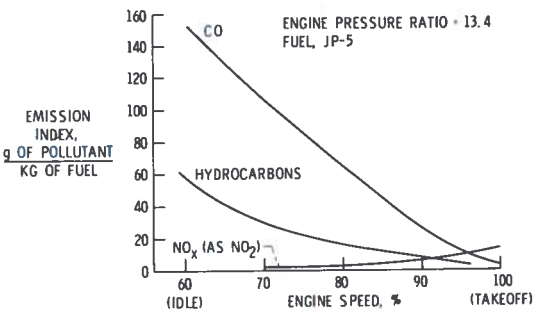

Figure 2. Typical Engine Exhaust Emission Characteristics

highest, whereas CO and hydrocarbon emissions approach their minimum. For a subsonic aircraft, CO and hydrocarbon emission levels at cruise would be expected to be similar to the levels during takeoff, but NO_x emissions would be lower than at takeoff.

Figure 3 tabulates the main emission products, together with their major causes. A range of emissions at either idle or takeoff is shown for typical subsonic commercial engines. High hydrocarbon and CO emissions that occur only during idle are due to inefficient combustion. Inefficient combustion is caused by a combination of poor fuel atomization at low fuel-flow rates, lean reaction-zone fuel-air ratios, and low combustor-inlet pressure and temperatures. Higher NO_x emissions during takeoff are caused by the increased reaction rates of oxygen and nitrogen at higher flame temperatures caused by high combustor inlet temperatures. Smoke density is high at takeoff because of high combustor pressures and rich reaction-zone fuel-air ratios. Only nitric oxide is formed in any significant quantities during subsonic cruise, but the NO_x emission index during cruise is less than that during takeoff because the combustor-inlet temperature and pressure are lower.

POLLUTANT	CRITICAL OPERATING CONDITION	TYPICAL EMISSION LEVELS, g/KG FUEL	MAJOR CAUSES
HYDROCARBONS	IDLE	7-75	POOR FUEL ATOMIZATION LEAN FUEL-AIR RATIOS LOW COMBUSTOR PRESSURE AND TEMPERATURE
CARBON MONOXIDE	IDLE	30-77	
OXIDES OF NITROGEN	TAKEOFF	13-40	HIGH FLAME TEMPERATURE
SMOKE	TAKEOFF	SAE SMOKE NUMBER 20-65	HIGH PRESSURE RICH FUEL-AIR RATIOS

Figure 3. Jet Aircraft Emissions. (The SAE smoke number is a commonly accepted measure of smoke density in a gas-turbine exhaust.)

COMPARISON OF SUBSONIC AND SUPERSONIC ENGINES

Figure 4 shows a typical turbofan engine used on subsonic aircraft. The main engine components include a fan, compressor, combustor, and turbine. A portion of the air passing through the fan enters the compressor, while the remaining air is bypassed around the core engine to provide additional thrust. The flow rate and the total temperature and pressure of the air entering the combustor from the compressor discharge are established by the overall fan and compressor pressure ratio, flight altitude, and flight speed. The fuel-air ratio is determined by the combustor temperature rise required to obtain the designed turbine inlet temperature. The frontal area of the combustor generally does not exceed the required frontal area of the compressor or turbine, in order to avoid unnecessary engine drag. The overall length of the combustor is kept as short as practical to minimize engine shaft length and bearing requirements. The combustor shown in the drawing is of the can-annular type, in which a number of tubular combustion liners are arranged within a common annular housing. Most recent engines use an annular combustor, with a continuous combustion liner installed within an annular housing.

A schematic drawing of a conventional annular combustor is shown in Figure 5. The combustor consists of three main parts: a diffuser, the primary (reaction) zone, and the secondary (dilution) zone. The diffuser is used to slow the relatively high-velocity airflow discharging from the compressor to produce a high static pressure. Lower combustor velocities are necessary to obtain stable combustion and to avoid excessive combustor pressure loss. Fuel is generally injected by pressure-atomizing nozzles, and combustion is initiated and stabilized in the primary zone. Enough air is introduced into the primary zone through swirlers around the fuel nozzles or through openings in the liner wall to maintain a near-stoichiometric mixture of fuel and air. Air bypassing the primary zone is injected into the secondary zone through additional openings in the liner and is mixed with the hot gases from the primary zone to achieve the desired turbine inlet temperature distribution. The remaining airflow is used to film-cool the walls of the chamber. Most of the chemical reactions

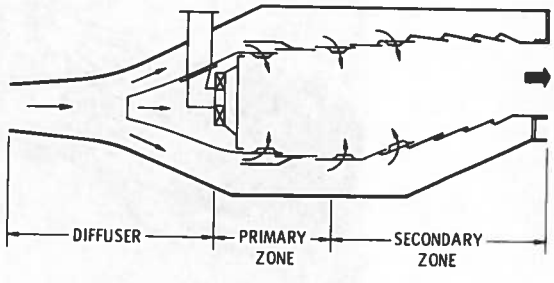

Figure 5. Conventional Annular Combustor

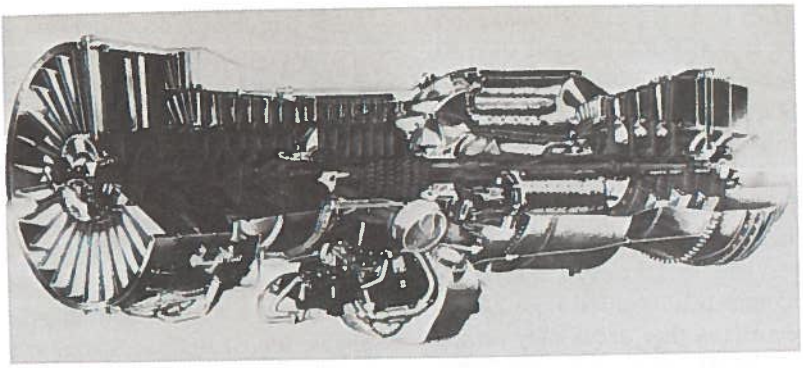

Figure 4. Turbofan Engine

are completed prior to dilution in the secondary zone. Consequently, the chemistry of the emission products is essentially frozen near the exit of the combustor.

Figure 6 shows a drawing of one type of engine suitable for powering a supersonic aircraft. The main differences between the afterburning turbojet shown in this figure and the turbofan engine shown in Figure 4 are: (1) incorporation of an inlet diffuser (not shown) to slow the air to subsonic speeds before it enters the engine, (2) omission of a fan and bypass duct, (3) addition of an afterburner to provide thrust augmentation, and (4) installation of a supersonic exhaust nozzle. Afterburning turbojet engines similar to that shown in Figure 6 are used on the Concorde SST and were to be used on the Boeing SST. Other engine types could be considered for future SST designs. Recent studies [10] have shown that an afterburning turbofan engine may offer advantages in reducing jet noise.

The afterburner consists of an inlet diffuser, to slow down the turbine discharge gases; an array of fuel-spray bars followed by an array of flameholders; and a combustion chamber that is air-cooled and acoustically damped to prevent screech. From a combustion point of view, the operating conditions in an afterburner are generally more severe than in the main combustor, and therefore the afterburner combustion efficiency tends to be lower.

A comparison of the cruise operating conditions of representative subsonic turbofan and supersonic afterburning (AB) turbojet engines is shown in Figure 7. The flight conditions chosen for the supersonic engine were taken from the GE-4/Boeing SST flight envelope. A combustion efficiency of nearly 100 percent is achieved during cruise for either of these engines, so minimum quantities of hydrocarbons and CO are formed. The afterburner combustion efficiency would be expected to be several percent less than that of the main com-

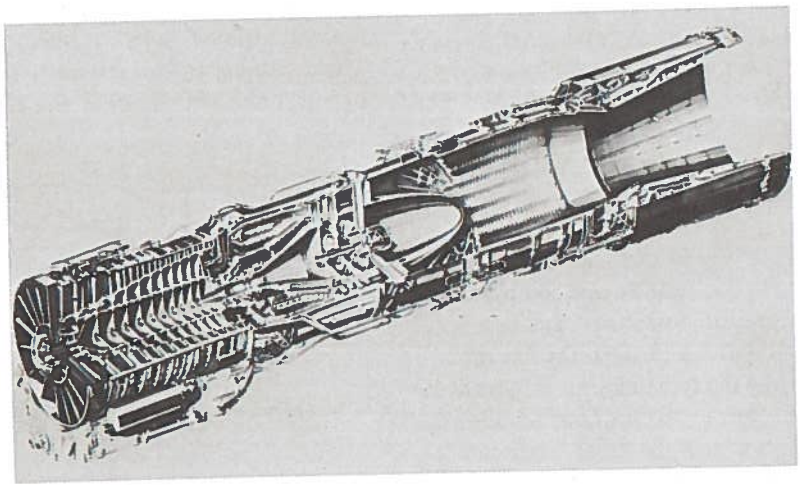

Figure 6. Turbojet Engine with Afterburner

bustor; however, the quantity of fuel burned in the afterburner during cruise amounts to only about 22 percent of the total fuel burned in the engine. The main factor affecting the formation of nitric oxide in either engine is the combustor inlet total temperature. Increasing either the compressor pressure ratio or the flight speed results in an increase in combustor inlet total temperature. Preliminary data [11] indicate that afterburning does not significantly add to NO_x emissions from supersonic aircraft.

	TURBOFAN	AB TURBOJET
CRUISE MACH NO.	0.85	2.7
CRUISE ALTITUDE, FT	35 000	65 000
COMBUSTOR INLET TEMP, °F	820	1100
COMBUSTOR INLET PRESSURE, PSIA	150	90
COMBUSTOR REF VELOCITY, FT/SEC	70	140
COMBUSTOR FUEL-AIR RATIO	0.02	0.018
AB INLET TEMP, °F	------	1600
AB INLET PRESSURE, PSIA	------	25
AB INLET VELOCITY, FT/SEC	------	500
AB FUEL-AIR RATIO	------	0.005
TOTAL FUEL FLOW, LB/HR (PER ENGINE)	5100	22 000

Figure 7. Cruise Operating Conditions

EFFECT OF OPERATING VARIABLES ON EMISSIONS

Hydrocarbons and Carbon Monoxide. Combustion efficiency can be defined as the ratio of the actual enthalpy rise to the theoretical enthalpy rise attainable for the amount of fuel used. The theoretical enthalpy rise assumes that the combustion reaction proceeds to completion to form gaseous products of combustion in equilibrium at the combustor exit temperature. Previous studies [12] have correlated combustion efficiency against a combustion parameter composed of inlet total pressure (P_{inlet} or P_3), multiplied by inlet total temperature (T_{inlet} or T_3), and divided by reference velocity (V_R), where reference velocity is equal to the combustor airflow rate divided by the product of the air density at the combustor inlet and the maximum cross-sectional flow area of the combustor.

A typical combustion efficiency correlation plotted in Figure 8 shows that combustion efficiency increases as inlet pressure and inlet temperature increase, and decreases as combustor velocity increases. Typical values of the correlation parameter for takeoff and cruise fall far to the

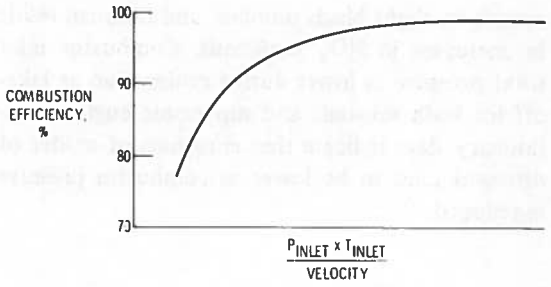

Figure 8. Combustion Efficiency Correlation

right of the bend in the curve, so there are no significant problems in obtaining good combustion efficiency for these conditions. At engine idle, the value for the correlation parameter is low and, in addition, fuel flow is low; for this condition, obtaining good combustion efficiency is difficult. As expected, the emission indices for CO and total hydrocarbons decrease with increasing values of the correlation parameter. A plot of the CO emission index against the correlation parameter for a typical combustor obtained from Reference 13 is shown in Figure 9. The correlation plot for the hydrocarbon emission index follows a similar trend.

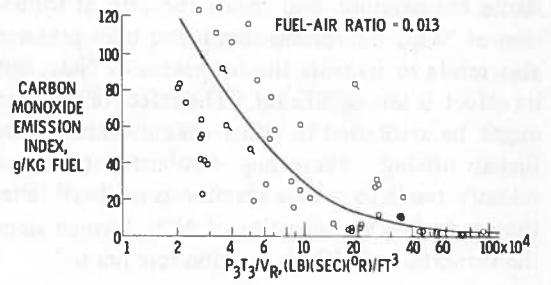

Figure 9. Effect of Correlation Parameter P_3T_3/V_R on CO Emissions

Oxides of Nitrogen. Figure 10 (obtained from Reference 2) shows the effect of engine pressure ratio on NO_x emissions at takeoff. The increase in the NO_x emission index with increasing engine pressure ratio is due principally to increasing combustor inlet temperature. For a given subsonic engine, the combustor inlet temperature during cruise is less than at takeoff because the ambient temperature is lower at the cruise altitude and because corrected engine speed is lower; therefore, NO_x emissions at cruise are less than at take-

creases in flight Mach number, and thus can result in increases in NO_x emissions. Combustor inlet total pressure is lower during cruise than at takeoff for both subsonic and supersonic engines. Preliminary data indicate that emissions of oxides of nitrogen tend to be lower as combustor pressure is reduced.

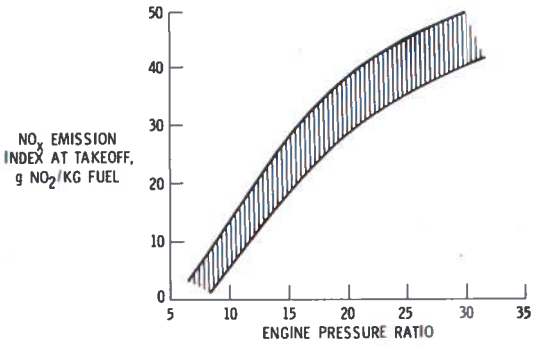

Figure 10. Effect of Engine Pressure Ratio on NO_x Emissions

The effect of combustor operating variables on NO_x formation is summarized in Figure 11. Increasing combustor inlet temperature increases the flame temperature, and hence the rate of formation of NO_x. Increasing combustor inlet pressure also tends to increase the formation of NO_x, but its effect is less significant. The effect of pressure might be attributed to either chemical kinetics or fuel-air mixing. Increasing combustor reference velocity tends to reduce reaction-zone dwell time, thus reducing the quantity of NO_x formed since the formation of NO_x is reaction-rate limited.

INCREASES IN PARAMETER	EFFECT ON NO_x
COMBUSTOR-INLET TEMP	GREAT INCREASE
COMBUSTOR-INLET PRESSURE	INCREASE
COMBUSTOR REFERENCE VELOCITY	DECREASE
FUEL-AIR RATIO	INCREASE

Figure 11. Effect of Combustor-Inlet Conditions on NO_x Formation

In general, increasing the over-all fuel-air ratio has been observed to increase NO_x formation. Theoretically, the local fuel-air ratio in the primary (reaction) zone should have a very significant effect on NO_x formation by its effect on flame temperature. Flame temperature should be near a maximum at stoichiometric conditions and should be lower for fuel-air mixtures that are either leaner or richer than stoichiometric. Gas turbine combustors are generally designed so that the primary-zone fuel-air ratio is near stoichiometric in order to optimize combustion performance. Operating with a primary zone that is fuel-lean leads to unstable combustion, while operating on the fuel-rich side causes excessive carbon formation. Even if the reaction zone were operated either leaner or richer than stoichiometric, factors that affect the homogeneity of the reactants, such as the fuel-air mixing intensity, fuel droplet size distribution, and fuel evaporation rate, are as important to NO_x formation as the average local fuel-air ratio in the reaction zone.

COMBUSTOR DESIGN TECHNIQUES TO REDUCE EMISSIONS

Combustor operating variables, such as combustor inlet total pressure and temperature, and over-all fuel-air ratio, are fixed by the engine design. Factors affecting engine design are discussed in Reference 10. Combustor reference velocity must be limited to prevent excessive pressure losses. Thus, the only means readily available to the combustor designer to control emissions are the method of fuel atomization, the mixing of fuel and air, and the general geometry of the combustor. Preliminary research on the subject of emission reductions in gas turbine combustors is discussed in References 5-9. Hydrocarbon and CO emissions were shown to be a problem mainly during idle, and smoke mainly a takeoff problem; since this paper is concerned mostly with emissions in the upper atmosphere, the discussion in this section will be limited to methods for reducing NO_x emissions.

The two principal methods for reducing nitric oxide emissions are reducing the reaction-zone temperature (flame temperature) and reducing the reaction-zone dwell time. The reaction-zone temperature may be reduced by either (1) operating

with either a fuel-rich or fuel-lean reaction zone, (2) operating with a more homogeneous fuel-air mixture, or (3) introducing inert substances into the reaction zone. The reaction zone fuel-air ratio may be shifted by altering the combustor airflow distribution. However, rich reaction zones tend to form excessive amounts of carbon monoxide, hydrocarbons, and smoke, while lean reaction zones present severe combustion stability problems. If this approach is to be used, variable geometry might be required to continuously control combustor airflow distribution to avoid poor combustion efficiency and minimize the emission products due to incomplete combustion.

The fuel-air mixture could be made more homogeneous either by increasing mixing intensity, by premixing the fuel and air before they enter the reaction zone, by prevaporizing the fuel before it enters the reaction zone, or by increasing the number of fuel injection points. Inert substances that might be used to reduce flame temperature include water or recirculated combustion products. Water injection would be impractical during cruise because of payload penalties. A significant increase in the amount of combustion products recirculated in the reaction zone might require excessive pressure losses.

The reaction-zone dwell time could be reduced either by shortening the length of the reaction zone or by increasing the number of local burning zones in order to reduce the recirculation path length. One experimental combustor being studied at NASA-Lewis that incorporates many of the above approaches is shown in Figure 12. This annular combustor, shown in cross-section in Figure 13, is about 30 percent shorter than conventional combustors. It incorporates 120 small individual burners, referred to as swirl-cans, into a modular array arranged in three concentric annular rows. The modular combustor has no well-defined primary or secondary zone like the conventional combustor. Nearly all the airflow, except for that required to cool the liner, passes directly through or around the modules. The details of each swirl-can element are illustrated in Figure 14. Each swirl-can, which is about 5 cm (2 inches) in diameter, consists of a carburetor, swirler, and flame stabilizer. The carburetor premixes the fuel with a portion of air entering an orifice in the upstream end of the chamber. The swirler acts to further mix the fuel and air and to impart a swirl to the mixture. Combustion is initiated and maintained at the flame stabilizer. The air flowing around the outside of the module

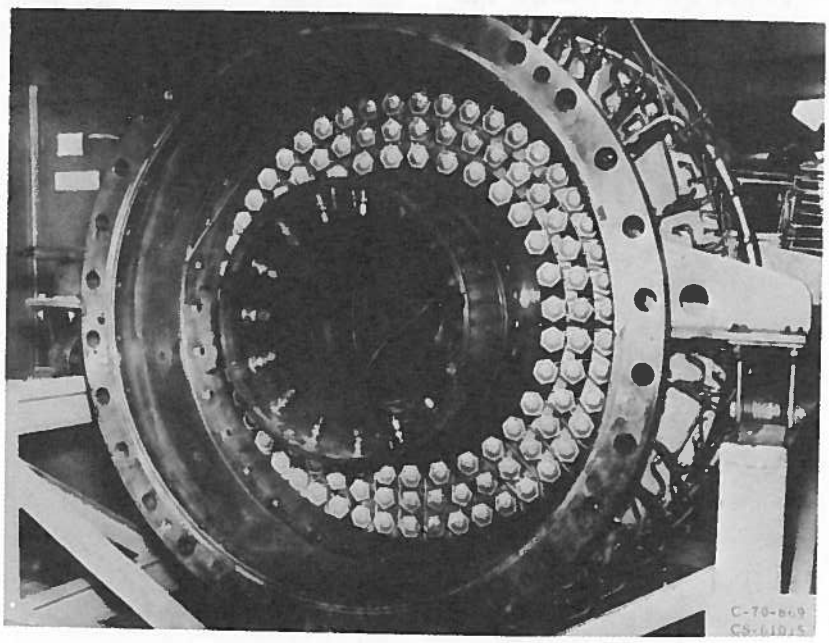

Figure 12. Photograph of Experimental Swirl-Can Combustor (Looking Upstream)

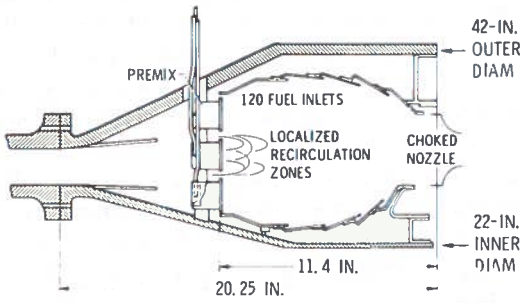

Figure 13. Cross-Sectional Sketch of High-Temperature Swirl-Can Combustor

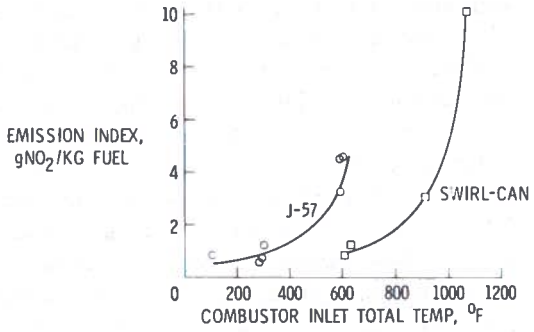

Figure 15. Effect of Inlet Total Temperature on Emission Index for Oxides of Nitrogen

mixes with the hot combustion gases in the wake of each module. There the combustion reaction is completed and the gases are mixed to the desired turbine inlet temperature distribution. Further details on the operation and performance of the swirl-can combustor are described in References 14-15.

The main advantages of this type of combustor are that fuel and air are partially premixed prior to burning and that burning and mixing downstream of each module is very rapid. Nitrogen-oxides emission data for the experimental swirl-can combustor are compared to those for a more conventional combustor in Figure 15. The NO_x emission index is plotted against combustor inlet total temperature. Even though these results are quite preliminary, and there are a number of problems remaining to be solved before such a combustor may be incorporated into an actual engine, the swirl-can concept appears to be a promising approach for obtaining reduced NO_x emissions.

CONCLUDING REMARKS

Oxides of nitrogen appear to be the only pollutant emission products that are formed during high-altitude cruise in significant concentration. A great deal of research is currently in progress to develop methods of reducing NO_x emissions from gas turbine combustors. Other research being performed to determine the ambient concentration of gaseous constituents and associated chemical-reaction cycles in the upper atmosphere may provide a clearer answer to whether or not reduc-

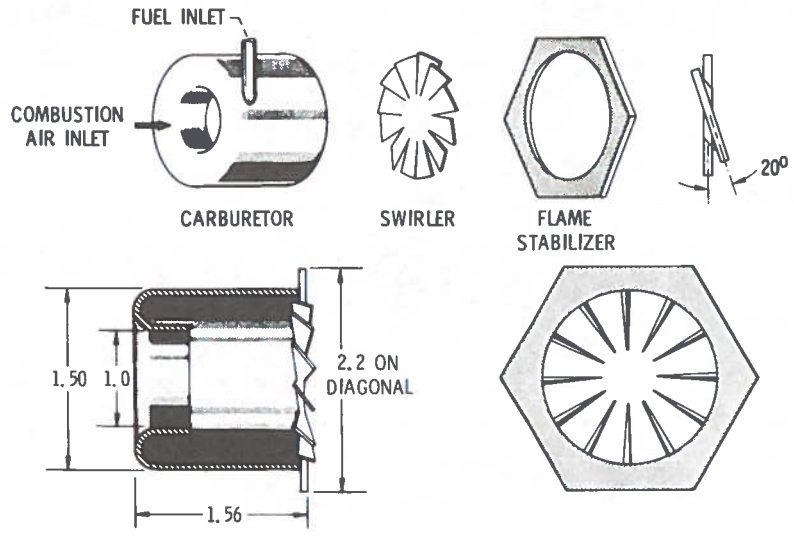

Figure 14. Combustor Module Details

tions in cruise emissions are required, and, if so, how large. It is fairly clear, however, that whether the approaches described herein or some similar approach is required to reduce NO_x emissions, a significant modification to conventional gas turbine combustors will be required. Furthermore, a considerable effort will be required to accomplish these emission reductions without compromising on other combustor performance requirements.

REFERENCES

1. Platt, M., Baker, R.C., Bastress, E.K., Chng, K.M., and Siegel, R.D., "The Potential Impact of Aircraft Emissions Upon Air Quality," Northern Research and Engineering Corporation, Report No. 1167-1, 1971.

2. Anon., "A Study of Aircraft Gas Turbine Engine Exhaust Emissions," Aerospace Industries Association of America, 1971.

3. Sawyer, R.F., "Atmospheric Pollution by Aircraft Engines and Fuels," NATO Advisory Group for Aerospace Research and Development, AGARD-AR-40, 1972.

4. Bogdan, L., and McAdams, H.T., "Analysis of Aircraft Exhaust Emission Measurements," Cornell Aeronautical Laboratory, CAL No. NA-5007-K-1, October, 1971.

5. Butze, F., "Methods for Reducing Pollutant Emissions from Jet Aircraft," NASA TM-X-68000, 1971.

6. Bastress, E.K., et al., "Assessment of Aircraft Emission Control Technology," Northern Research and Engineering Corporation, Report No. 1168-1, 1971.

7. Norster, E.R., and Lefebvre, A.H., "Effects of Fuel Injection Methods on Gas Turbine Combustor Emissions," Cranfield Inst. of Technology, England. Presented at 1971 General Motors Research Lab Symposium, September 27-28, 1971.

8. Bahr, D.W., "Control and Reduction of Aircraft Exhaust Emissions from Aircraft Turbine Engines." Presented at 1971 General Motors Research Lab Symposium, September 27-28, 1971.

9. Grobman, J., "Effect of Operating Variables on Pollutant Emissions from Aircraft Turbine Engine Combustors," NASA TM X-67887, 1971.

10. Beheim, M.A., et al., "Subsonic and Supersonic Propulsion," *Vehicle Technology for Civil Aviation,* NASA SP-292.

11. Diehl, A., "Preliminary Investigation of Gaseous Emissions from Jet Engine Afterburners," NASA TM X-2323, 1971.

12. Childs, J., Reynolds, W., and Graves, C., "Relation of Turbojet and Ramjet Combustion Efficiency to Second-Order Reaction Kinetics and Fundamental Flame Speed," National Advisory Committee for Aeronautics (now NASA), Rep. 1334, 1957.

13. Briehl, D., Papathakos, L., and Strancar, J., "Effect of Operating Conditions on the Exhaust Emissions from a Gas Turbine Combustor," NASA TN D-6661, 1972.

14. Niedzwiecki, R.W., Juhasz, J., and Anderson, D.N., "Performance of a Swirl-Can Primary Combustor to Outlet Temperatures of 3600°F (2256K)," NASA TM X-52902, 1970.

15. Grobman, J., Jones, R.E., Marek, J., and Niddzwiecki, R. W., "Combustion," *Aircraft Propulsion,* NASA SP-259, 1971.

DISCUSSION

J. Kaplan asked for a definition of NO_x. Grobman replied that in the combustion chamber NO_x was about 95% NO and 5% NO_2, and that after emission the NO was eventually converted to NO_2, so that the emission index was expressed as pounds of NO_2 per thousand pounds of fuel.

A. Ferri asked why engines not suitable for supersonic transport were being used for NO measurements. He suggested that Concorde measurements and laboratory simulations would both be preferable. K. Forney admitted the validity of the point, but explained that truly low-emission engines were not yet operational even for the Concorde. The engines tested were a) available and b) representative of present-day engine technology, and he was more concerned with lack of data on behavior at altitude.

H. Levine asked about kinetics calculations of the combustion-chamber reactions. Grobman cited a number of current combustion-modeling efforts: Northern Research and Engineering (FAA, EPA), Pratt & Whitney (AF), General Applied Science Laboratory (NASA), Purdue, and Imperial College in London.

SUPERSONIC TRANSPORT ROUTES

R. W. RUMMEL
Trans World Airlines
New York, New York 10016

ABSTRACT: The following three questions relating to future supersonic transport operations are answered in order to define suitable parameters for determining the impact of such operations on the environment.

1. What are the routes and frequency of travel thereon which are projected for 1990?
2. What are the techniques for such projections to the future?
3. What is the expected range of uncertainty of such projections?

Some definition of the probable scope and character of future SST operations world-wide is needed for reasonably realistic calculations of the global distribution of SST emission products. Obviously when predictions of any future transportation systems are so dependent on evolving political, social, and economic factors, they are subject to appreciable error. This is especially true of SST predictions, since supersonic transportation is a new, untried mode for which no historical traffic or public acceptance data exists. Although good work has been done in this field, it is important that the fragility of current SST forecasts be understood by those who would use them. The following are some of the significant variables which affect predictions of future SST levels of operations and route applications.

1. *State of the World's Economies.* First, the rate of growth and the character of future air transportation systems are directly dependent upon the degree of economic health enjoyed by the world's economies, as well as on the specific gross national products of nations. Certainly future flight patterns will reflect changes in national wealth, the degree of industrialization attained, international community interests, and so on.
   The size of future SST fleets will probably be more affected by national economies than subsonic-type aircraft have been, because of the inherently high operating costs of supersonic-type aircraft, which, in turn, will require fare differentials unknown at present.

2. *International Political Situations.* Second, international political situations, including the difference between war and peace, extended national crises, and desires to dominate will influence of shape the emerging air transportation system.

3. *Government Policies/Regulations.* Sonic-boom overpressure legislation which prohibits flights or induces unfavorable flight routings would inhibit growth. Also, widespread significant over-water sonic-boom restrictions, combined with overland flight prohibitions, would nearly eliminate SST prospects.

4. *Economic Health of Air Transportation Interests.* The degree of economic health of the airlines will substantially determine their collective ability to procure fleets and expand services. This could prove to be a serious limitation on implementing any forward-looking, technologically ambitious program.

5. *Operational Characteristics of the SST's.* Such factors as payload-range, operating costs, ATC system compatibility, airport location and suitability, and the like, may limit SST route segment applications. In this regard, the emergence of either improved or entirely new SST's as time passes is likely to affect SST route applications. For example, a true polar route might be used if SST flight range capability increases sufficiently.

6. *Marketing Requirements.* Until tested, marketing aspects have to be considered problematical. Passenger acceptance of fares and services is an open issue because fare differentials have not been defined. They may be substantial. Indeed, the division of passenger traffic between subsonic and supersonic flights may prove to depend more on fare differential than on any other single factor.
7. *Environmental Acceptability.* The pervasive question of environmental acceptability obviousvly seriously affects SST usage. It is very difficult to resolve in the absence of adequate scientific data, and given complicated political structures in the U. S. and elsewhere which involve a wide range of interests, any of which can establish acceptability rules. These include airport operators; city, county, state, and federal governments; and international organizations. Even if further research should establish the total environmental acceptability of widespread SST operations, it would take an appreciable period to convince the authorities and the public that this is so. At present, no special flight prohibitions exist except as related to noise. However, since the SST route and level-of-operations projections presented herein are for the purpose of assisting in the determination of environmental acceptability, all this is partially moot.
8. *Evolution of Competing Transportation Modes.* Subsonic aircraft services will unquestionably evolve and improve. The split of business between the subsonic and supersonic modes is not apt to be fixed.

It is clear, then, that predictions of future SST routes and levels of operations, like most long-range projections that involve socioeconomic factors, must be viewed as speculative. Nonetheless, route patterns must be postulated to permit the prediction of the global distribution of SST effluents in order to explore their effect on the environment. Two such cases are presented here, both appropriate for use as models for calculating the worldwide distribution of SST emission products, as long as all the variables noted above are kept in mind.

The first case is for the Concorde only, and assumes no U. S. SST. The other case assumes the existence of both the Concorde and the U. S. SST or its equivalent, notwithstanding termination of the U. S. program.[1] A 1990 peak for SST operations was assumed on the theory that improved, different modes would produced about then. Of course, the year is not nearly so important as the peak itself. The likelihood that improved and perhaps more economical versions of SST's currently being developed will appear before 1990 seems to justify the inclusion of the U. S. SST as a representative type. Please refer to Figure 1.

Figure 1, a Mercator projection, shows anticipated weekly round-trip flights for the Concorde assuming no U. S. SST.[2] Routes appear as lines. The small numbers denote the number of round-trip flights anticipated for each segment by the European Aerospace Corporation. The dashed lines indicate subsonic flights with SST's. The large numbers show the same round-trip flight frequency by principal routing areas. Clearly, the North Atlantic with 582 round-trip frequencies per week is the most densely populated route, the North American West Coast to Hawaii second, and the Caribbean area an easy third.

The routes shown are not intended to be precise flight tracks. For example, the route from Perth to Sydney, Australia is shown as a straight line, whereas it is more apt to lie over the South Australian Basin so as to avoid overland sonic overpressure problems. The same is true elsewhere - - for example, in Europe, where some of the segments shown would most likely have to be flown subsonically to coastal areas. Similarly, the South American route from São Paolo, Brazil to Lima, Peru and from Buenos Aires, Argentina to Santiago, Chile may need to be operated in the subsonic mode.

---

[1] Equivalent data for the TU-144 are not available.

[2] These anticipated flight routes, frequencies, and flight profile characteristics for the Concorde-only fleet were furnished by the French Aerospace Corporation (now called the European Aerospace Corporation) in two letters to Trans World Airlines, Inc. The first, dated March 4, 1971, referenced FAC-NY-8165, contained flight profile information, the second, dated April 8, 1971, referenced FAC-NY-8283, contained anticipated routes and frequencies for 1990.

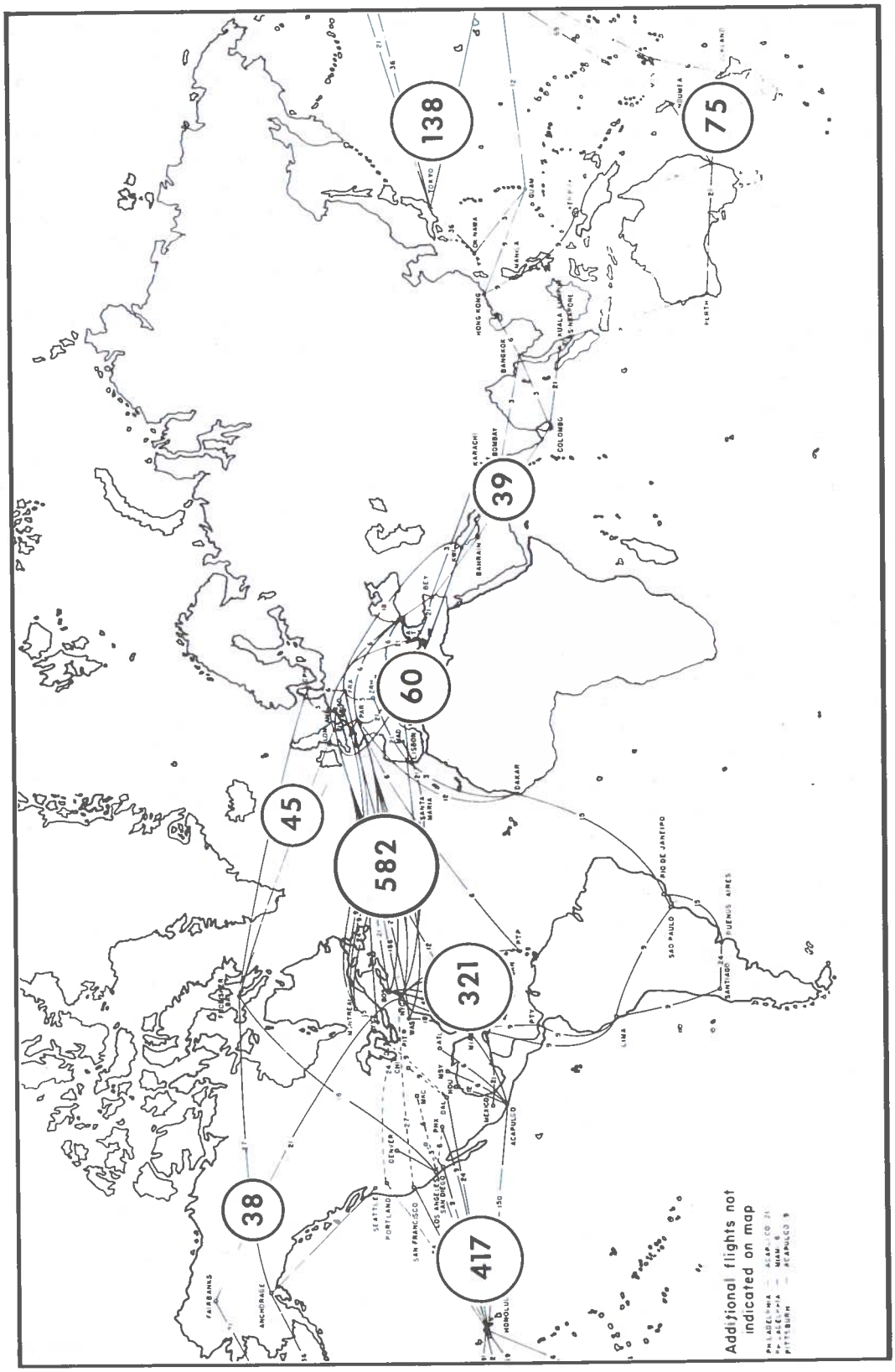

Figure 1. Anticipated Weekly Round Trips for the Concorde by 1990, Assuming No SST.

I should perhaps also point out that subsonic operations with supersonic transports will be exceedingly expensive. For this reason, the operators will seek to avoid such operations. In this regard, please note that 38 weekly round trips are shown over the Northwest Territories of Canada. Such flights may not be permissible for political reasons, because of sonic booms. However, perhaps they could be flown supersonically over the Hudson Bay region and on tracks that lie roughly between the Gulf of Boothia and the Beaufort Sea. Such tracks would not depart seriously from great-circle routes.

Figure 2, the second case or model, shows the anticipated routes and frequencies for Concorde and U. S. SST fleets as published in *Aviation Week and Space Technology*, January 5, 1970, pp. 47-9. It represents a vast background effort and is considered to be the best available from this country. Daily rather than weekly round-trip flight frequencies are presented. As in the case of the Concorde only, the route patterns generally reflect historical subsonic trends, except for the exclusion of overland supersonic operations (dashed lines) and more Arctic-area activity.

The large encircled figures represent estimated daily round-trip flight frequencies by principal routing areas. Note that flight frequencies are appreciably greater than in the previous case and the need for flying supersonically over water is more clearly illustrated.

An extremely vivid imagination is required to visualize the tremendous volume of SST flights that Figure 2 portrays, especially considering the highly probable continuance of a fair number of subsonic flight schedules over the same routes. Figure 2 shows 351 daily round-trip North Atlantic SST flights in 1990. This compares to 128 subsonic flights during peak 1971. The Figure 2 estimate assumed that 90% of the 1990 air-carrier passenger traffic would be supersonic! I think history will prove this to be unrealistically high, especially considering that when the 90% figure was assumed it was believed that very little or no fare differential between supersonic and subsonic activity would be required. High fare differentials are now in prospect, which will undoubtedly limit the SST market. Major (and currently unanticipated) technological breakthroughs would be required to change this prospect. In addition, when the background for this chart was developed, a continuance of successive high-traffic growth years was expected. Unfortunately, that has not happened. As an example, I.A.T.A. world-wide scheduled airlines figures show that in 1967 there was a 16.5% growth over 1966; in 1968 it 12.5%; 1970, 10.7%; and in 1971 only 5.9%. In the U.S. domestic trunk services, which is perhaps somewhat less indicative, in 1967 the airlines and the public enjoyed a 25% increase in traffic; 1968 over the preceding year was 15%; 1969, 17.2%; 1970, 0.3% - - a real debacle; and in 1971, 1.8%, which was not much better. I doubt that anyone expects the poor growth experienced in the past two years to continue indefinitely, but there is good reason to seriously question high growth rates like 15 or 20% per year, one year after the other.

Furthermore, the very high costs associated with advanced aircraft developments and the resulting very high predicted SST sales prices, coupled with the historic profit level of the air carrier industry, lead to the conclusion that purchase of the large fleets envisioned earlier and presented in these figures is not apt to occur.

However, since environmental considerations suggest that it is desirable to overestimate rather than underestimate SST emission products, both cases appear to be appropriate for consideration.

Figure 3 shows estimated relative flight density by 1990 for the Boeing and Concorde fleets with an arbitrary value of 1.00 assigned to the North Atlantic. It is based on the same flight frequencies and routes as the previous figure. It shows, for example, that the Honolulu - North America West Coast will enjoy 37% of the number of North Atlantic flights, Tokyo - West 30%, the central Caribbean area 13%, etc.

Insufficient information makes it impossible to project TU-144 operations; hence the question mark. Also, if political circumstances permit, trans-Siberian flights from Japan and possibly China via Russia to Europe appear inviting from a mileage point of view, provided adequate airports and other essential facilities would be made available. If these develop to any significant extent, some of the traffic shown passing over the South China Sea and the Indian Ocean would probably be diverted northward.

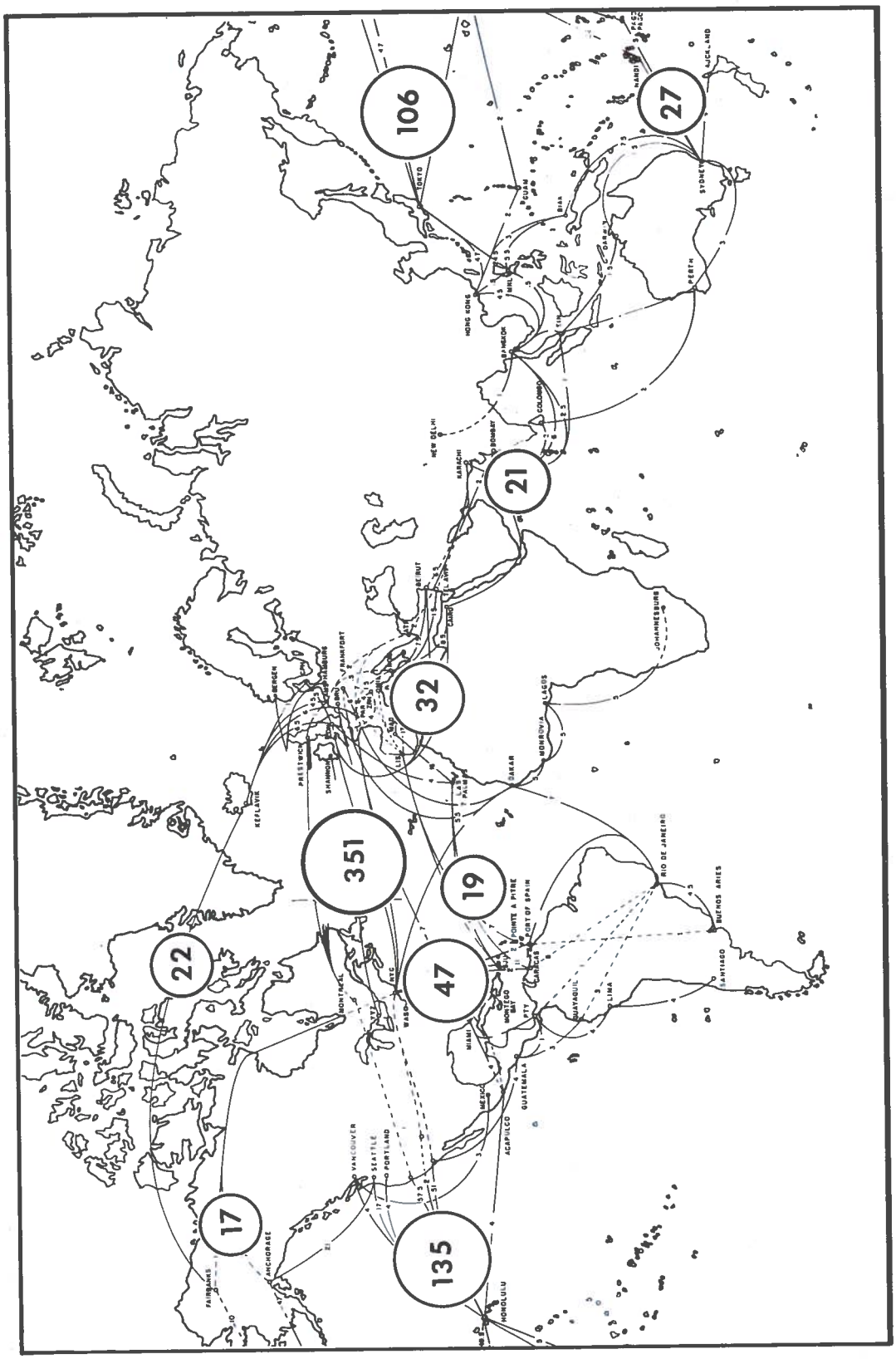

Figure 2. Proposed Daily Round-Trip Flights for the Boeing and Concorde SST Fleet by 1990.

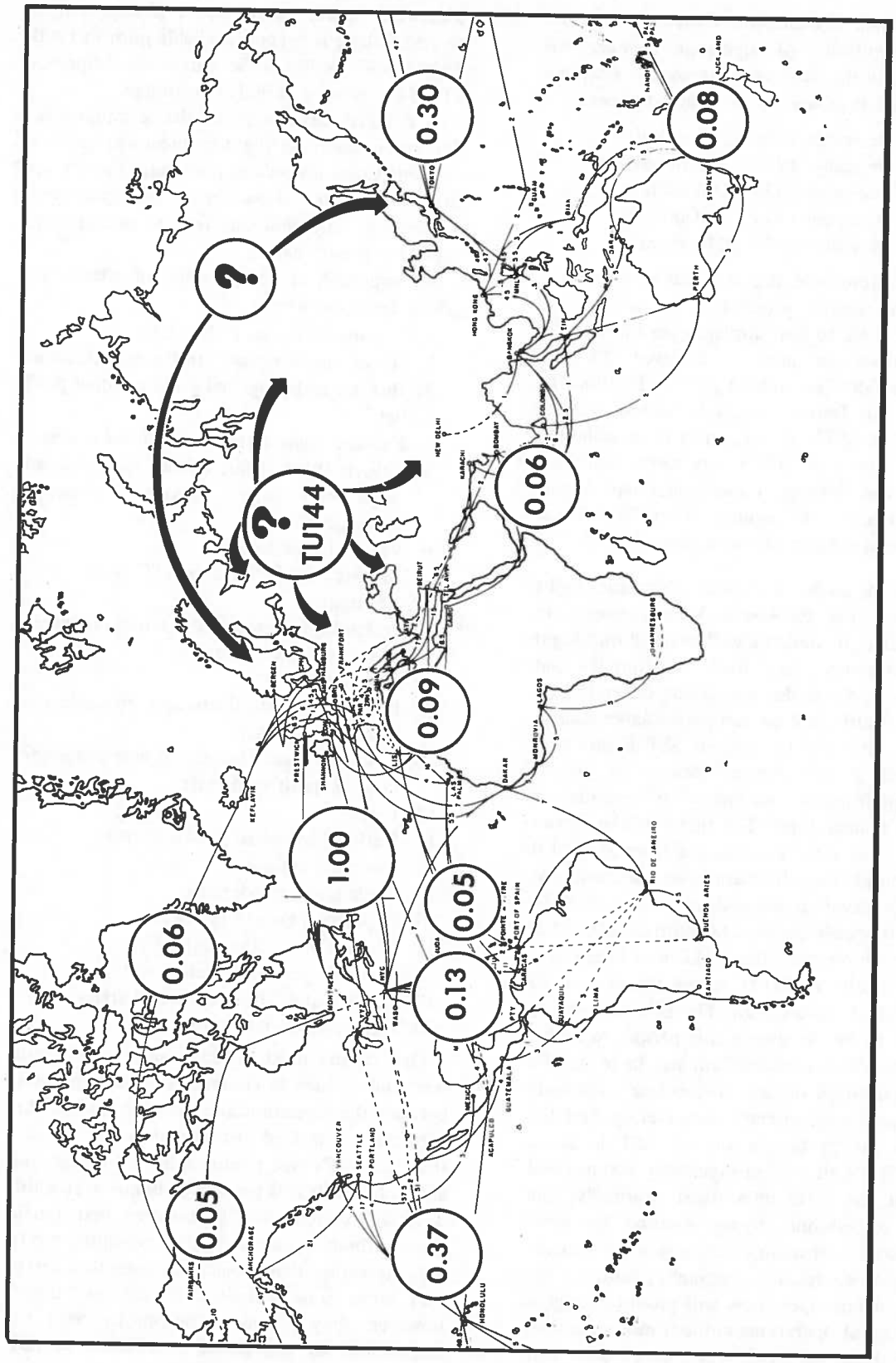

Figure 3. SST Estimated Relative Flight Density by 1990 (Concorde Plus U. S. SST).

To give you an indication of the estimated rate of implementation of supersonic services, the following is the European Aerospace Corporation's estimate of worldwide Concorde fleets:

December 1976	65 aircraft
December 1977	95 aircraft
December 1978	140 aircraft
December 1979	180 aircraft
December 1970	240 aircraft

European Aerospace also said that if the market exists, the aircraft production rate after 1980 could be three to four airplanes per month. If a rate of three per month is achieved, the total would be 600 Concordes by 1990. In 1966 the Institute for Defense Analysis forecast a total fleet of 500 SST's. Boeing, prior to cancellation, forecast a total of 543. A very recent report by the National Planning Association, dated August 1971, forecasts the equivalent of 762. These forecasts agree quite well with case two.

Figure 4 shows a typical Concorde flight profile on the Paris-New York segment. In looking at it, it would be well to recall that flight tracks currently vary both horizontally and vertically in day-to-day operations, depending on weather, traffic, and aircraft performance characteristics. This will be true of SST flights to a somewhat greater degree because of greater aircraft-performance sensitivity to variations in ambient temperatures. The flight profile shown assumes that sonic acceleration from Mach 1.0 speeds with engine afterburners on commences at 25,000 ft elevation and ends at about 44,000 ft. Mach 2.0 speeds are maintained from 50,000 ft elevation throughout the cruise to a final elevation of nearly 60,000 ft, where the descent to destination is undertaken. The afterburners are assumed to be off during this period. Nonetheless, some thrust augmentation may be required a small percentage of time, depending on outside air temperatures, aircraft maneuvering, and the like. In the profile shown the SST is above 44,000 ft for all but approximately 300 nautical miles of the 3,100-mile flight. Naturally, the extent of subsonic flying imposed by sonic overpressure restrictions will vary somewhat depending on routes and geography; thus, on the average, actual operations will produce a higher percentage of operations in the troposphere than implied. Looking ahead, it is quite possible that cruising to altitudes of around 70,000 ft or somewhat higher would occur if improved or new SST designs become available prior to 1990. They could be Concorde derivatives, improved TU-144's, or some entirely new design.

A detailed description of the techniques for developing the route/flight frequency projections contained herein would require much more space than is available. However, a bibliography is attached for any who may wish to examine this subject in greater depth.

In summary, these are some of the factors which were considered:

1. Historic air carrier traffic data
2. Historic and projected traffic growth trends
3. Historic and projected gross national product
4. Existing flight patterns and airline routes
5. Vehicle flight characteristics such as speed, range (minimum and maximum), passenger appeal, etc.
6. Value of time saved
7. Airport availability and ATC system capacity limits
8. Probable passenger load factors on average and on specific routes
9. Operating costs
10. Existing aircraft fleets and probable new fleet procurements
11. Probable characteristics of new contemporary competitive aircraft
12. Fares
13. National industrial growth factors
14. Emerging nations
15. Sonic boom restrictions
16. Population growth factors
17. Aircraft production capability
18. Probable passenger preferences
19. Political stability in the world arena
20. National policies.

One of the most difficult areas to estimate was, and is, how to compute the passenger split between the supersonic and subsonic modes. This is because of lack of historical data and the fact that the SST's will require a fare surcharge, the amount of which is presently unknown. It is this question, combined with concern that traffic growth forecasts are high, that prompted me to indicate earlier that projections presented herein may prove to be optimistic. By the same token, however, they provide a pessimistic basis for calculations of the global distribution of SST emission products.

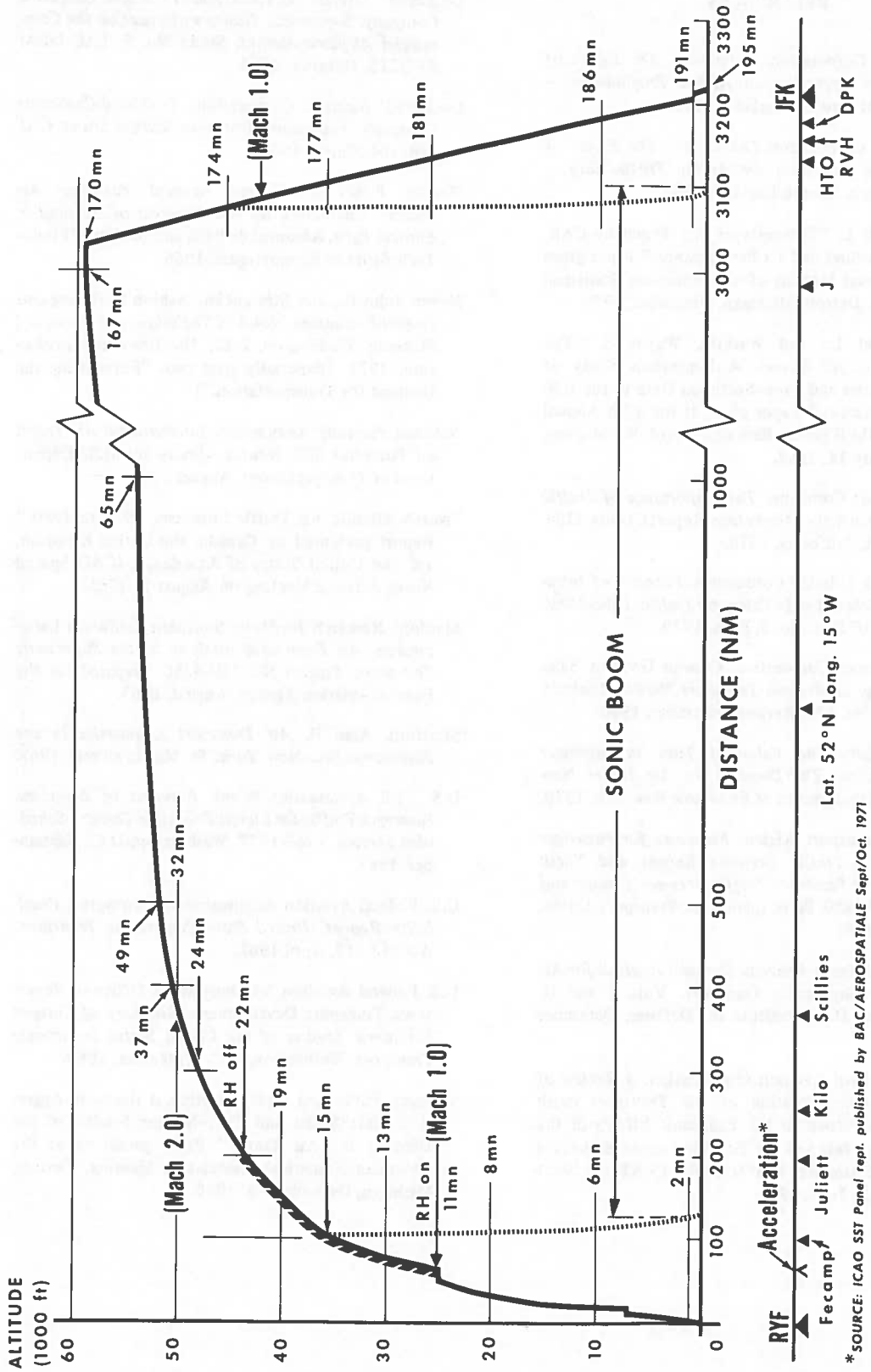

Figure 4. Typical Concorde Flight Profile Paris - New York.

REFERENCES

British Airline Corporation. *Concorde– The Effect of Single Class Operation on Airline Profitability – International.* Bristol, England; 1969.

British Airline Corporation. *Concorde– The Effect of Single Class Operation on Airline Profitability – U.S. Domestic.* Bristol, England, 1969.

Brown, Samuel L. "Forecasts of Air Travel by CAB Staff: A Method and Its Performance." Paper given at the Annual Meetingsof the American Statistical Association, Detroit, Michigan, December, 1970.

Brown, Samuel L., and Watkins, Wayne S. "The Demand for Air Travel: A Regression Study of Time – Series and Cross-Sectional Data in the U.S. Domestic Market." Paper given at the 47th Annual Meeting of the Highway Research Board, Washington, D.C., January 16, 1968.

Douglas Aircraft Company. *The Importance of Traffic Forecasting in Airline Marketing.* ReportC1-804-2164, Long Beach, California, 1970.

European Civil Aviation Conference. *Forecast of Intra-European Scheduled Air Passenger Traffic, 1968-1980.* ECAC, CEAC Doc. No. 3, Paris, 1970.

General Dynamics Corporation. Convair Division. Sales Engineering. *Supersonic Transport Market Analysis.* Report SE No. 476, Revised December, 1960.

Gronau, Reuben. *The Value of Time in Passenger Transportation: The Demand for Air Travel.* New York, National Bureau of Economic Research, 1970.

Institut du Transport Aérien. *Forecasts for Passenger and Freight Traffic Between Europe and North America and Passenger Traffic Between Europe and Asia, 1970-1980.* Paris, Institut du Transport Aerien, October 1968.

Institute for Defense Analysis. *Demand Analysis for Air Travel by Supersonic Transport.* Vols. I and II. Washington, D.C., Institute for Defense, December 1966.

International Civil Aviation Organization. *A Review of the Economic Situation of Air Transport* (with Special Reference to the Economic Effects of the Long-Range Jets and the Possible Future Market for Supersonic Aircraft). ICAO Circular 73-AT/10. Montreal, Canada, June, 1965.

Lockheed Aircraft Corporation. Lockheed-California Company. *Supersonic Transport Impact on the Commercial Airplane Market.* Study No. 5, LAC OEA/SST/225, October, 1966.

Lockheed Aircraft Corporation. Lockheed-California Company. *Supersonic Transport Market Study.* CA/MR/104, March, 1964.

Marche, Roger and Flaven, Bernard. *Passenger Air Travel - Characteristics and Forecast of Demand in Europe.* Paris, Aéroport de Paris and Société d'Etudes Techniques et Economiques, 1966.

Meyer, John R., and Straszheim, Mahlon R. *Pricing and Project Evaluation.* Vol. I of *Techniques of Transport Planning.* Washington, D.C., The Brookings Institution, 1971. (Especially part two, "Forecasting the Demand for Transportation.")

National Planning Association. *International Air Travel on Potential SST Routes.* (Study for U.S. Department of Transportation), August 1971.

"North Atlantic Air Traffic Forecasts, 1971 to 1980." Report presented by Canada, the United Kingdom, and the United States of America at ICAO Special North Atlantic Meeting on August 9, 1965.

Stanford Research Institute. Southern California Laboratories. *An Economic Analysis of the Supersonic Transport.* Project No. ISU-4266. Prepared for the Federal Aviation Agency, August, 1963.

Stratford, Alan H. *Air Transport Economics in the Supersonic Era.* New York, St. Martin's Press, 1967.

U.S. Civil Aeronautics Board. *Forecast of Domestic Passenger Traffic for Eleven Trunkline Carriers Scheduled Service, 1968-1977.* Washington, D.C., September, 1967.

U.S. Federal Aviation Administration. *Economic Feasibility Report, United States Supersonic Transport.* AD 652 313, April 1967.

U.S. Federal Aviation Administration. Office of Supersonic Transport Development. *Summary of Current Economic Studies of the United States Supersonic Transport.* Washington, D.C. September, 1969.

Verleger, Philip and Eads. "Statistical Biases in Aggregate Time Series and Cross-Section Studies of the Demand for Air Travel." Paper presented at the American Statistical Association Meeting, Detroit, Michigan, December 28, 1970.

DISCUSSION

M. Wurtele questioned the assumption that growth would continue as before, noting that the change to SST's could make as significant a difference to air traffic as the introduction of subsonic jets. Rummel presented the expansion factors used for some of the various geographical areas, and noted that he considered this approach reasonable but not the only possibility. K. Forney took the opportunity to emphasize CIAP's concern with all stratospheric flight, not just SST's.

Dr. S.V. Venkateswaran's presentation was not available in publishable form when these *Proceedings* went to press.

AERONOMIC CHEMISTRY OF THE STRATOSPHERE

MARCEL NICOLET
Institut d'Aéronomie Spatiale
Brussels, Belgium

ABSTRACT: In the stratosphere, dissociation of H_2O, CH_4, and H_2 is brought about mainly by reactions with excited oxygen atoms produced by the photodissociation of ozone. A discrepancy noted between theoretical and observational concentrations of O_3 in the upper stratosphere suggests two possible explanations: the observed solar radiation fluxes for O_2 photodissociation are larger than the actual ones, with too-large rate coefficients and absorption cross-sections, or ozone is reduced by the effect of hydrogen compounds or of nitrogen oxides.

The reaction of the excited oxygen atom with methane and nitrous oxide leads to a destruction of these two molecules in the stratosphere which corresponds to the production of carbon monoxide with water vapor and that of nitric oxide, respectively. The vertical distribution of water vapor is not affected by its dissociation in the stratosphere, since its re-formation is rapid.

The fact that the ratio of hydroxyl and hydroperoxyl radical concentrations cannot be determined with adequate precision complicates the calculation of the destruction of ozone which occurs through reactions of OH and HO_2, not only with atomic oxygen in the upper stratosphere, but also with CO and NO in the lower stratosphere, respectively. The same difficulty arises in connection with the dissociation of nitric acid molecules formed by the reaction of OH and NO_2; the processes of destruction by photodissociation or by reaction with OH are not yet known with precision. Another difficulty, of a different kind, is that the nitric oxide concentration is not certain at the stratopause.

INTRODUCTION

Theories of the ozone distribution in the terrestrial atmosphere were first formulated by Chapman (1930, 1943). He considered the balance between the formation and destruction of ozone in relation to its regular daily and annual variations. The atmosphere was regarded as static, without horizontal or vertical transfer of ozone. Any reactions with nitrogen or other atmospheric constituents were ignored.

The introduction of hydrogen compounds into the photochemical treatment of the ozone problem by Bates and Nicolet (1950) led to the first indication of a possible action of hydroxyl and hydroperoxyl radicals on the ozone distribution, especially in the mesosphere where the photodissociation of water vapor and methane occur. Furthermore, in the stratosphere, the reaction of H_2O with electronically excited atomic oxygen in the ^1D state (Cadle, 1964; Hampson, 1964) suggests that H_2O may be dissociated in the stratosphere. The concentrations of $O(^1D)$ produced by ozone photolysis in the stratosphere and troposphere are sufficiently large to produce OH radicals (and H atoms) not only from water vapor but also from methane and molecular hydrogen. Finally, the action of nitrogen oxides on ozone (Crutzen, 1970; Johnston, 1971) may be considered in the atmospheric ozone equilibrium. However, the formation of nitric acid (Nicolet, 1965, 1970b; Johnston, 1971) seems to be the mechanism responsible for the removal of nitrogen oxides.

THE OZONE FORMATION

The equations governing the rates of change in the concentration of ozone and atomic oxygen, $n(O_3)$ and $n(O)$, are

$$\frac{dn(O)}{dt} + 2k_1\, n(M)\, n^2(O) + k_2\, n(M)\, n(O_2)\, n(O) + k_3\, n(O_3)\, n(O) = 2n(O_2)\, J_2 + n(O_3)\, J_3 \quad (1)$$

and

$$\frac{dn(O_3)}{dt} + n(O_3)\, J_3 + k_3\, n(O)\, n(O_3) = k_2\, n(M)\, n(O_2)\, n(O) \quad (2)$$

which lead to the general form

$$\frac{dn(O)}{dt} + \frac{dn(O_3)}{dt} + 2k_1\, n(M)\, n^2(O) + 2k_3\, n(O_3)\, n(O) = 2\, n(O_2)\, J_2 \qquad (3)$$

In the above equations, J_2 and J_3 are the photodissociation coefficients of O_2 and O_3, respectively:

$$(J_2)\ O_2 + h\nu \rightarrow O + O \qquad (4)$$

$$(J_3)\ O_3 + h\nu \rightarrow O_2 + O \qquad (5)$$

The rate coefficients are

$$(k_1)\ O + O + M \rightarrow O_2 + M \qquad (6)$$

$$(k_2)\ O + O_2 + M \rightarrow O_3 + M \qquad (7)$$

$$(k_3)\ O + O_3 \rightarrow 2\, O_2. \qquad (8)$$

In the stratosphere, reaction (6) takes place very slowly and can be omitted in all photochemical discussions of stratospheric ozone (Bates and Nicolet, 1950). Furthermore, atomic oxygen is always in photochemical equilibrium with ozone. Therefore, the rate of change of $n(O_3)$ in the stratosphere becomes

$$\frac{dn(O_3)}{dt} + \frac{2k_3\, J_3}{k_2\, n(M)\, n(O_2)}\, n^2(O_3) = 2n(O_2)\, J_2. \qquad (9)$$

Introducing the time $\tau_{eq}\,(O_3)$, necessary to attain 50% of the photochemical value $n_*(O_3)$, the following equation is obtained

$$\tau_{eq}\,(O_3) = 0.275\, n_*(O_3)/n(O_2)\, J_2. \qquad (10)$$

With numerical values (Table 1), it can be shown (see Figure 5a) that photochemical equilibrium can be adopted for $n(O_3)$ at the stratopause. From (9), the following equation

$$n_*^2(O_3) = \frac{k_2}{k_3}\, n(M)\, n^2(O_2)\, \frac{J_2}{J_3} \qquad (11)$$

represents photochemical equilibrium conditions in the stratosphere for a pure oxygen atmosphere. The numerical values of the ozone concentration $n(O_3)$ depend on the ratios k_2/k_3 and J_2/J_3.

The ratio k_2/k_3 is not yet known with sufficient accuracy for aeronomic purposes. According to Clyne et al. (1965) the following expression for k_2 represents their experimental data over the temperature range 188-373°K (if M = N_2, O_2)

$$k_2 = 3.7 \times 10^{-35}\, e^{900/T}\ cm^6\ sec^{-1} \qquad (12a)$$

From Kaufman and Kelso (1967) the result is

$$k_2\,(N_2, O_2) = (5.8 \pm 1.0) \times 10^{-34}\ cm^6\ sec^{-1} \qquad (12b)$$

Table 1. Atmospheric Parameters in the Stratosphere

Altitude (km)	Temperature (°K)	Total Concentration (cm^{-3})	Ozone (Example) (cm^{-3})
15	211	3.9×10^{18}	1.0×10^{12}
20	219	1.7×10^{18}	2.9×10^{12}
25	227	7.7×10^{17}	3.2×10^{12}
30	235	3.6×10^{17}	2.9×10^{12}
35	252	1.7×10^{17}	2.0×10^{12}
40	268	8.1×10^{16}	1.0×10^{12}
45	274	4.3×10^{16}	3.2×10^{11}
50	274	2.3×10^{16}	1.0×10^{11}

for T = 300°K. Other measurements (Hochanadel et al., 1968; Mulcahy and Williams, 1968; Donovan et al.,1970) lead to various values of the same order of magnitude, indicating differences of about a factor of two over the temperature range 200 to 300°K. The value recommended by Johnston (1968) is (see Figure 1a)

$$k_2\,(N_2, O_2) = 1.85 \times 10^{-35}\, e^{1050/T}\ cm^6\ sec^{-1}, \qquad (12c)$$

while a recent measurement by Davis (1972) between 200°K and 346°K leads to (see Figure 1a again)

$$k_2\,(N_2) = (1.1 \pm 0.7) \times 10^{-34}\, e^{+(500 \pm 50)/T}\ cm^6\ sec^{-1} \qquad (12d)$$

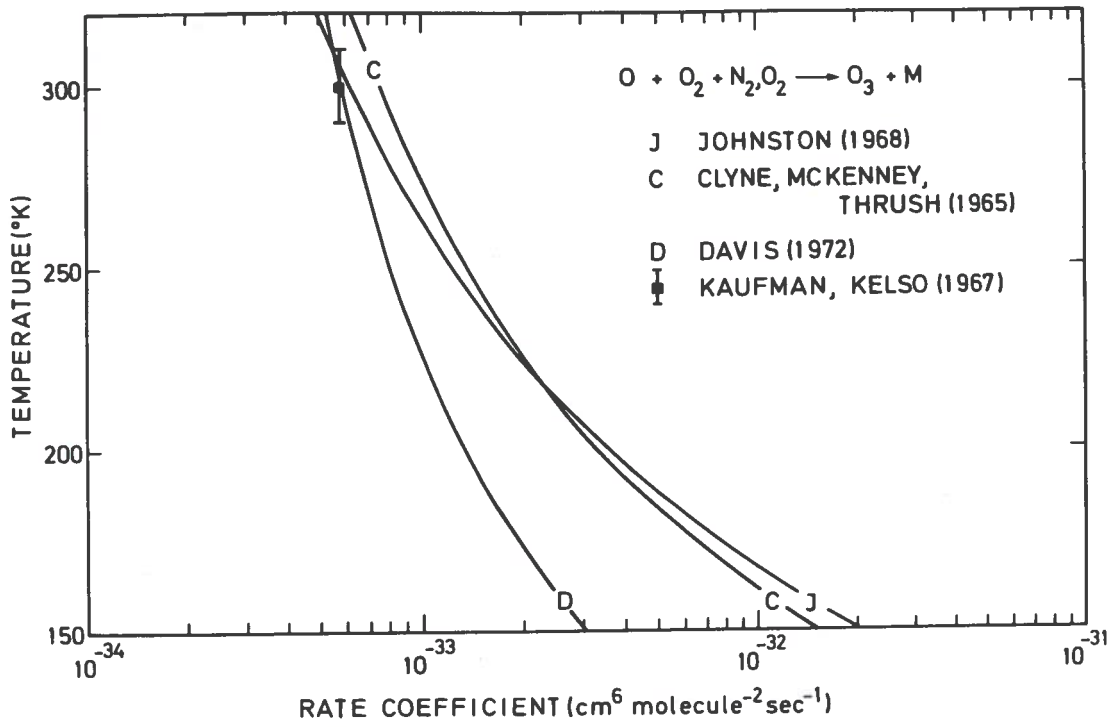

Figure 1a. Experimental values of the rate coefficient k_2 (cm^6 sec^{-1}) of the three-body reaction $O_2 + O + M \rightarrow O_3 + M$ when the third body is N_2 (4/5) and O_2 (1/5).

Figure 1a compares (12a), (12b), (12c), and (12d) over the temperature range 150°K - 300°K. It shows that there is a difference of about a factor of 2 at 225°K, reaching a factor of 4 near 160°K. At 300°K there is good agreement betweent the various measurements (cf. Kaufman's and Kelso's data).

As far as the rate coefficient k_3 is concerned, the value recommended by Johnston (1968) is

$$k_3 = 2 \times 10^{-11} e^{-2411/T} cm^3 sec^{-1} \qquad (13a)$$

Recent measurements over the temperature range 200 to 300°K by Krezenski, Simonaitis, and Heicklen (1971) lead to

$$k_3 = (1.2 \pm 0.2) \times 10^{-11} e^{-(2164 \pm 100)/T} cm^3 sec^{-1} \qquad (13b)$$

and others over the temperature range 269 to 409°K by McCrumb and Kaufman (1972) lead to

$$k_3 = (1.05 \pm 0.18) \times 10^{-11} e^{-(2169 \pm 50)/T} cm^3 sec^{-1} \qquad (13c)$$

Expressions (13b) and (13c) lead to the same numerical values below 200°K, where the difference from (13a) is about a factor of 2 (see Figure 1b).

Therefore, using (12d) with (13b) and (12c) with (13a), the ratio k_2/k_3, which plays an important role in equation (11), can be written

$$\frac{k_2 \text{ (Davis)}}{k_3 \text{ (Heicklen)}} = (1.0 \pm 0.2) \times 10^{-23} e^{(2650 \pm 250)/T} cm^3 \qquad (14a)$$

and

$$\frac{k_2 \text{ (Johnston)}}{k_3 \text{ (Johnston}} = 9.26 \times 10^{-25} e^{3445/T} cm^3 \qquad (14b)$$

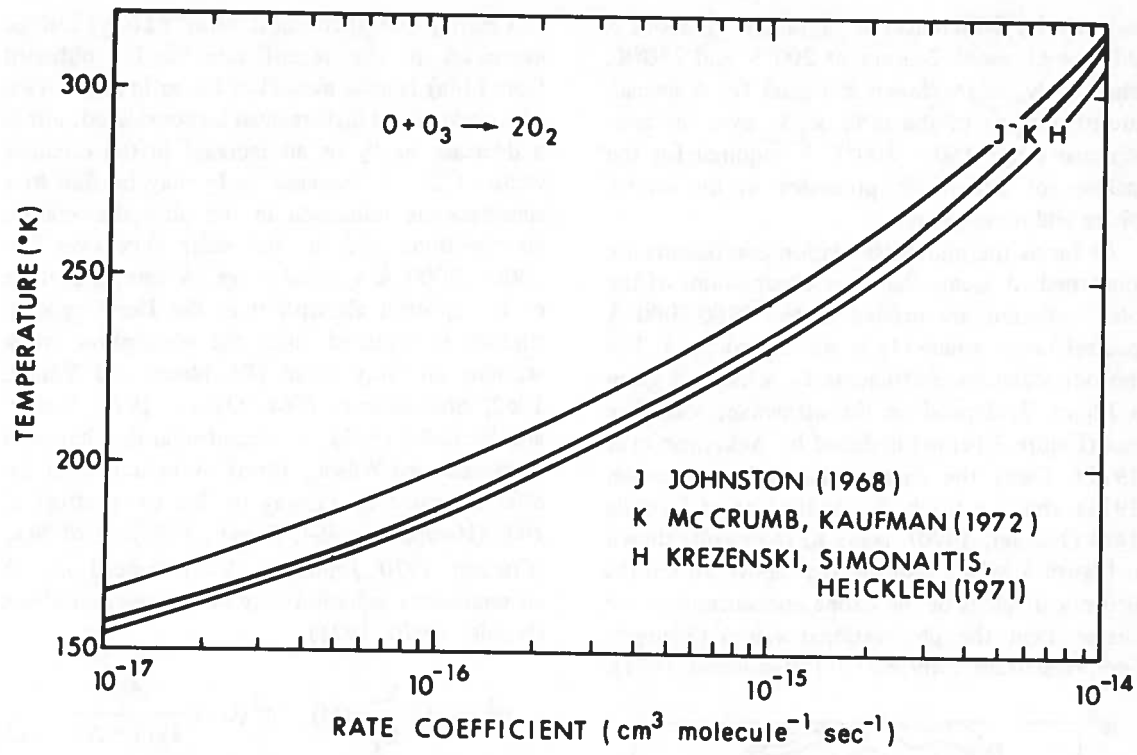

Figure 1b. Experimental values of the rate coefficient k_3 of the reaction $O + O_3 \rightarrow 2\,O_2$.

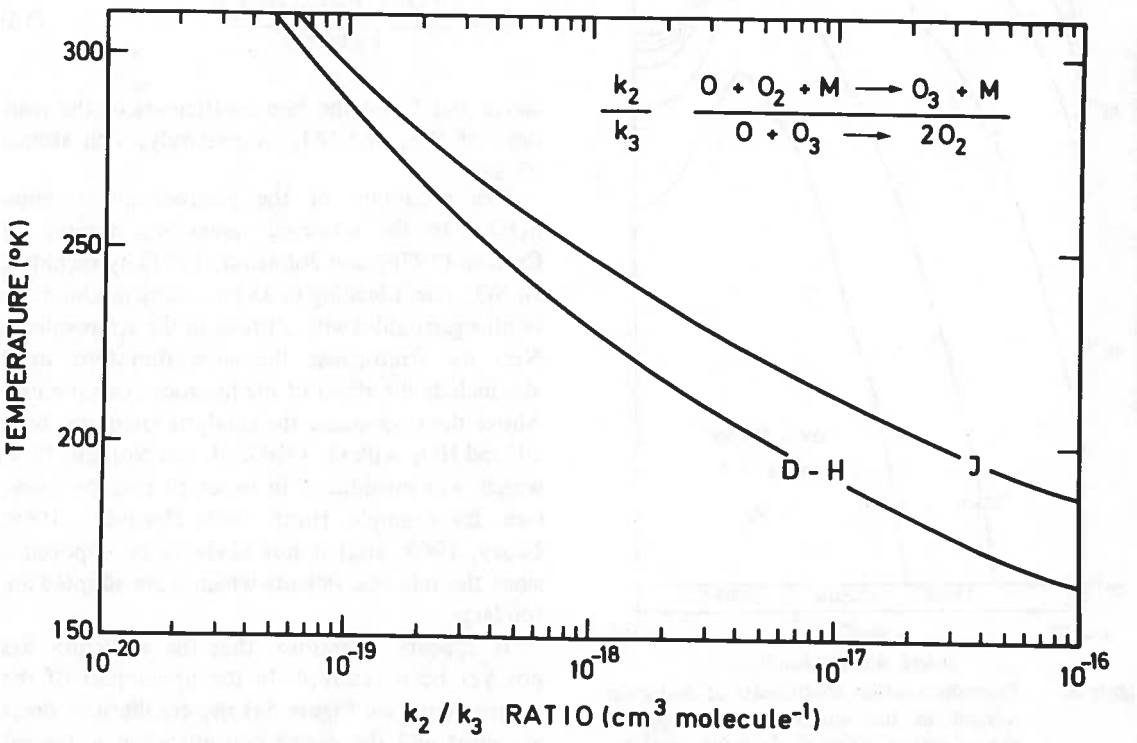

Figure 1c. Experimental values of the ratios of the rate coefficient k_2 and k_3 given in fig. 1a and fig. 1b.

respectively. Differences of a factor of about 5 and one of about 2 occur at 200°K and 270°K, respectively, as are shown in Figure 1c. A special, careful analysis of the ratio k_2/k_3 over the temperature range 150 - 300°K is required for the analysis of aeronomic processes in the stratosphere and mesosphere.

As far as the photodissociation coefficients are concerned, it seems that new observations of the solar radiation are needed in the 2300-2000 Å spectral range, where O_2 is photodissociated. The photodissociation coefficients J_2, which are given in Figure 2, depend on the ultraviolet solar-flux data (Figure 3 below) deduced by Ackerman et al. (1971). Using the data tabulated by Ackerman (1971) and a ratio k_2/k_3 equivalent to formula (14b) (Nicolet, 1970) leads to the results shown in Figure 4, which indicate that above 30 km the theoretical values of the ozone concentrations are greater than the observational values (Krueger, 1969; Hilsenrath, 1969 and 1971; Randhawa, 1971).

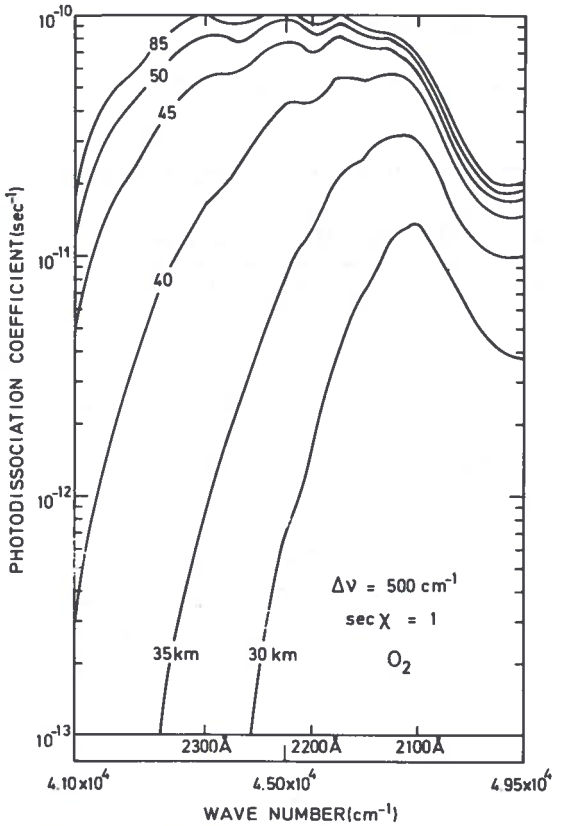

Figure 3. Photodissociation coefficients of molecular oxygen in the stratosphere for spectral ranges corresponding to $\Delta\nu = 500$ cm^{-1} between 2400 A and 2000 Å.

Clearly, the theoretical value $n_*(O_3)$ can be decreased if the recent ratio k_2/k_3 obtained from (14a) is used instead of the ratio (14b). Two other additional factors must be considered: either a decrease in J_2 or an increase in the effective value of J_3. A decrease in J_2 may be due to a simultaneous reduction in the photodissociation cross-sections and in the solar flux over the 2300 - 2000 Å spectral range. A careful analysis of the spectral absorption in the Herzberg continuum is required since the absorption cross-sections are very small (Ditchburn and Young, 1962; Shardanand, 1969; Ogawa, 1971; Hasson and Nicholls, 1971). A reduced solar flux has been suggested (see Wilson, 1966). A reduction in the effective value of J_3 may be due to an effect of HO_x (Hampson, 1964, Roney, 1965) or of NO_x (Crutzen, 1970; Johnston, 1971). Instead of (11) an equivalent equation may be written as follows (Nicolet, 1970, 1971).

$$n_*^2(O_3) = \frac{k_2}{k_3}\, n(M) \quad n^2(O_2)\, \frac{J_2}{J_3(1+A)} \qquad (15)$$

where A is a correction term of the form

$$A = \frac{a\, n(HO_x) + b\, n(NO_x)}{k_3\, n(O_3)} \qquad (16)$$

and a and b are the rate coefficients of the reactions of HO_x and NO_x, respectively, with atomic oxygen.

The reduction of the photochemical values $n_*(O_3)$ to the observed values was treated by Crutzen (1970) and Johnston (1971) by including an NO_x effect leading to an increasing mixing ratio of nitrogen oxides with altitude in the stratosphere. Near the stratopause the correction term must also include the effect of the hydrogen compounds. Above the tropopause the catalytic chain involving OH and HO_2 with O_3 (McGrath and Norrish, 1958) which was introduced in order to remove ozone (see, for example, Hunt, 1966; Hesstvedt, 1968; Leovy, 1969; etc.) is not likely to be important, since the rate coefficients which were adopted are too large.

It appears, therefore, that the difficulty has not yet been resolved. In the upper part of the stratosphere (see Figure 5a) the equilibrium times are short and the ozone concentration is insensitive to atmospheric transport. In the lower strato-

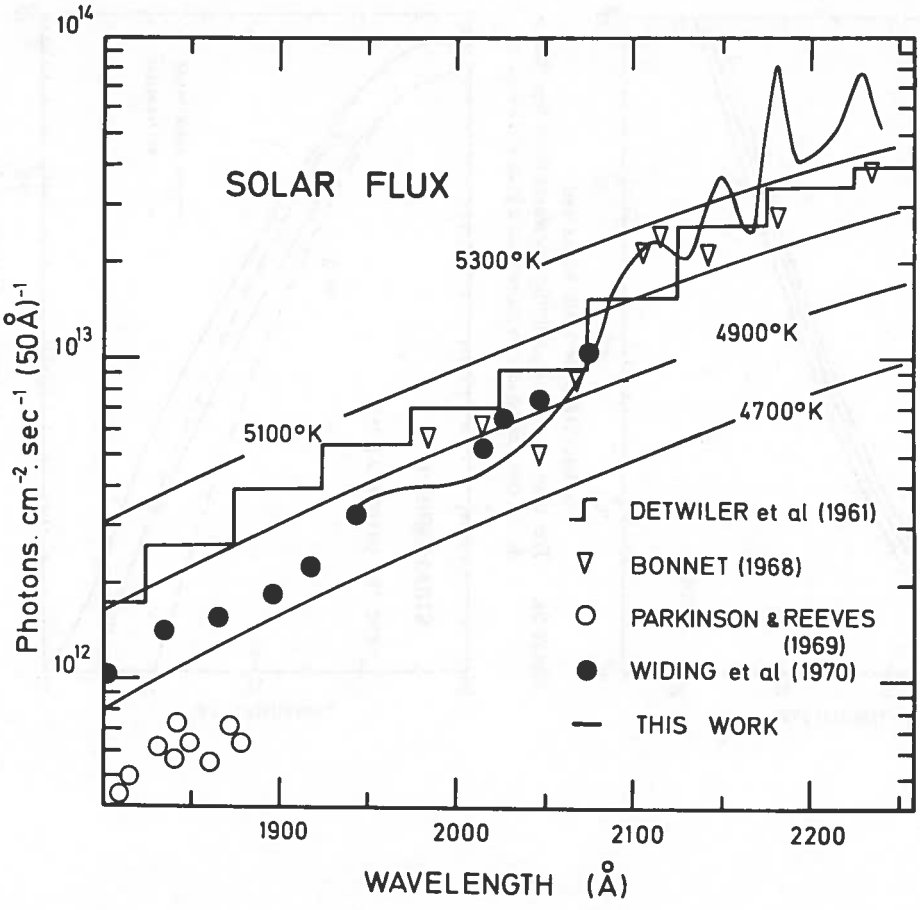

Figure 2. Observational data of solar radiation in the 1800-2250 Å spectral range, according to Ackerman, Frimout, and Pastiels (1971).

sphere (Figure 5b) the equilibrium ozone concentration depends strongly on zenith angle and the O_3 concentration is controlled by downward transport. There is a complete departure from photochemical equilibrium conditions, since equilibrium times are greater than 1 year and dynamic considerations must be introduced. Thus, instead of (9), the general equation becomes (16)

$$\frac{\partial n(O_3)}{\partial t} + \text{div}\,[n(O_3)\, w_{O_3}] + \frac{2 k_3 J_3}{k_2 n(M)\, n(O_2)} \left\{ n^2(O_3) + a\, n(HO_x) + b\, n(NO_x) \right\} = 2\, n(O_2)\, J_2 \qquad (17)$$

where w_{O_3} is the transport velocity of O_3.

THE HYDROGEN-OXYGEN ATMOSPHERE

The production of $O(^1D)$ atoms by the photolysis of the stratospheric ozone is important. A precise determination depends on the exact efficiency of $O^1D)$ production in the processes

$$O_3 + h\nu\,(\lambda < 3100\text{Å}) \rightarrow O_2\,(^1\Delta_g) + O(^1D) \qquad (18a)$$

$$O_3 + h\nu\,(\lambda < 4000\ \text{Å}) \rightarrow O_2\,(^3\Sigma_g) + O(^1D) \qquad (18b)$$

According to DeMore and Raper (1966), all oxygen atoms are $O(^1D)$ at $\lambda \leqslant 3100$ Å; for $\lambda > 3100$ Å, there is a drop in the efficiency leading to $O(^3P)$ atoms at 3340 Å (Jones and Wayne, 1969).

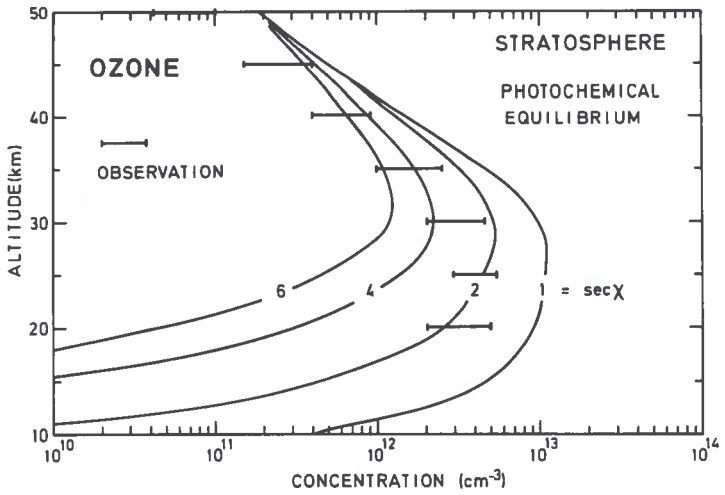

Figure 4. Ozone concentrations for photochemical equilibrium conditions compared with observational data. χ is the solar zenith angle.

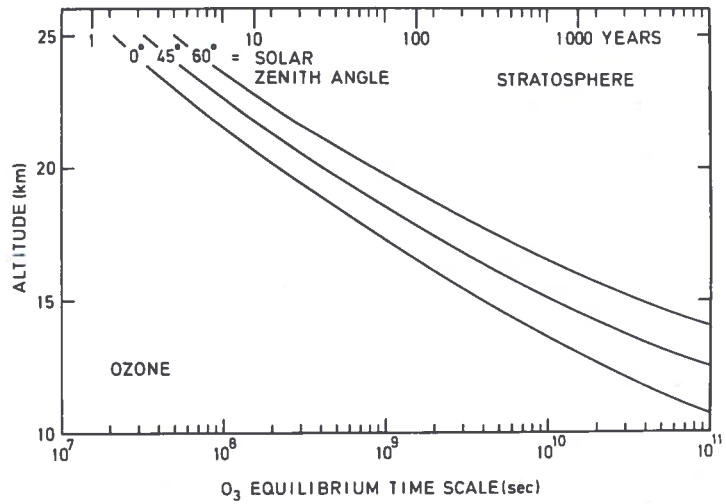

Figure 5a. The time to reach equilibrium increases from less than a day at the stratopause to more than a year at 25 km.

Figure 5b. There is a departure from photochemical equilibrium conditions in the lower stratosphere, since O_3 equilibrium times increase from 1 year at 25 km to more than 100 years at 15 km.

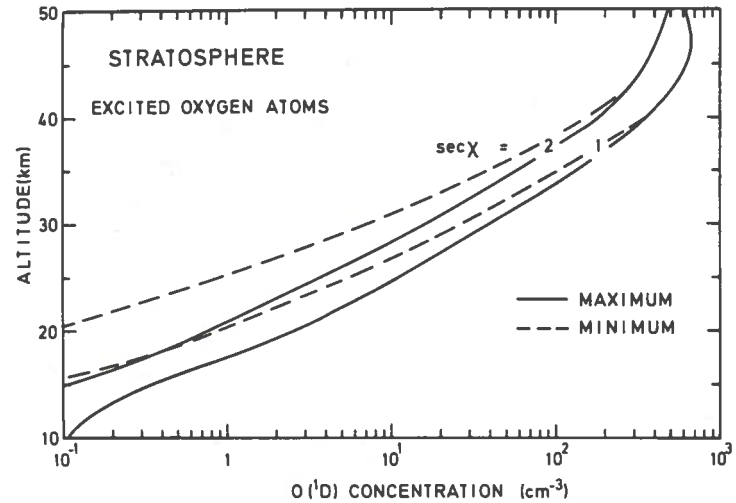

Figure 6. Concentration of excited oxygen atoms for two solar zenith angles and two different (minimum and maximum) productions.

Two extreme values of the $O(^1D)$ production have been adopted; considering the following working value for the quenching rate coefficient

$$k_Q(^1D) = 5 \times 10^{-11} \text{ cm}^3 \text{ sec}^{-1} \quad (19)$$

due to N_2 and O_2 (see, for example, Young et al., 1968; Paraskevopoulos and Cvetanović, 1969; DeMore, 1970; Noxon, 1970), one finds the photoequilibrium values of $O(^1D)$ concentrations for various solar zenith angles illustrated in Figure 6. At the stratopause the variation is small, but in the lower stratosphere the values depend significantly on zenith angle and are sensitive to the spectral efficiency of $O(^1D)$ production which is chosen from the experimental data.

The study of the reaction of $O(^1D)$ with H_2O, CH_4, and H_2 is an important step in the analysis of the aeronomic behavior in the stratosphere. The following reactions occur:

$$O(^1D) + H_2O \rightarrow OH + OH^* (v \leqslant 2) + 28.8 \text{ kcal} \quad (20)$$

$$O(^1D) + CH_4 \rightarrow CH_3 + OH^* (v \leqslant 4) + 43.5 \text{ kcal} \quad (21)$$

$$O(^1D) + H_2 \rightarrow H + OH^* (v \leqslant 4) + 43.5 \text{ kcal} \quad (22)$$

Thus the presence of $O(^1D)$ atoms leads to the possibility of the production of H atoms and OH radicals by H_2O, H_2, and CH_4 in the stratosphere. With the fractional volume considerations that can be adopted (see Nicolet, 1971 for references and explanation) as conventional values at the tropopause for H_2 (0.5×10^{-6}), for CH_4 (1.5×10^{-6}), and for H_2O (3×10^{-6}), the total production $P(HO_x)$ of HO_x radicals at the bottom of the stratosphere is

$$P(HO_x) = 13 \times 10^{-6} \, n(M) \;\; n^*(O) \, a^* \quad (23)$$

where a* is the rate coefficient for (20), (21), and (22). Such a coefficient has a value greater than 10^{-10} cm^3 sec^{-1} (Nicolet, 1970, 1971). Recent experimental analysis (Young et al., 1968; Donovan et al., 1970; Paraskevopoulos and Cvetanović, 1971; Heicklen et al., 1971) leads to

$$a^* = (3 \pm 1) \times 10^{-10} \text{ cm}^3 \text{ sec}^{-1} \quad (24)$$

Thus the production of HO_x in the stratosphere near the tropopause may attain

$$P(HO_x) \simeq 10^{-4} \, n(O_3) \, J_3^* \quad (25)$$

where J_3^* is the photodissociation rate coefficient leading to $O(^1D)$ atoms. Numerical results lead to a production of OH radicals from the H_2O dissociation of not less than 10^4 cm^{-3} sec^{-1} above 20 km for an overhead sun, reaching 7×10^4 cm^{-3} sec^{-1} in the upper stratosphere.

Inspection of the reactions introduced by Bates and Nicolet (1950) indicates that, in the stratosphere (Nicolet, 1971), a large number of them can be ignored when the rate coefficients are sufficiently well known.

At the stratopause level, a three-body reaction involving atomic hydrogen and molecular oxygen leads to a hydroperoxyl radical

$$(a_1) \quad H + O_2 + M \rightarrow HO_2 + M + 46 \text{ kcal.} \quad (26)$$

The rate coefficient based on measurements made at low temperature by Clyne and Thrush (1963b) and Larkin and Thrush (1964) has a negative temperature coefficient

$$a_1 \, n(M) = 3.3 \times 10^{-33} \, e^{800/T} \, n(N_2, O_2) \text{ cm}^3 \text{sec}^{-1} \quad (27)$$

At the stratopause, and in the upper part of the stratosphere, the reaction of H with O_3 cannot be neglected

$$(a_2) \quad H + O_3 \rightarrow O_2 + OH^*_{v \leqslant 9} + 77 \text{ kcal} \quad (28)$$

has practically no activation energy (Kaufman, 1964), and

$$a_2 = 1.5 \times 10^{-12} \, T^{1/2} \text{ cm}^3 \text{ sec}^{-1} \quad (29)$$

corresponding to the experimental value of $(2.6 \pm 0.5) \times 10^{-11}$ cm^3 sec^{-1} at 300°K (Phillips and Schiff, 1962). The dependence on temperature

indicated by a plus one-half power in (29), and other reactions, shows that the activation energy must be small and that a measurement over the 150 - 300°K temperature range is required. Such a form also shows that there is a certain steric hindrance factor, as can be seen when (29) is compared with the conventional value, relevant to the present reactions, of $1.5 \times 10^{-11} T^{1/2}$ given by the elementary kinetic theory of elastic spheres.

Thus, it may be concluded that hydrogen atoms are immediately transformed into hydroperoxyl radicals in the stratosphere, since reaction (26) is rapid (see Table 2). However, at and in the neighborhood of the stratopause, reaction (28), which leads to OH, cannot be forgotten.

Table 2. Aeronomic Rate Coefficients in the Stratosphere

Altitude (km)	$a_1\, n(M)\, n(O_2)$ (sec^{-1})	$a_2\, n(O_3)$ (sec^{-1})	$a_5\, n(O)$ (sec^{-1})
15	4.7×10^5	2.4×10^1	2.4×10^{-6}
20	7.7×10^4	6.4×10^1	4.2×10^{-5}
25	1.4×10^4	7.3×10^1	3.0×10^{-4}
30	2.6×10^3	6.7×10^1	1.8×10^{-3}
35	4.6×10^2	4.8×10^1	1.1×10^{-2}
40	1.2×10^2	2.5×10^1	6.0×10^{-2}
45	2.3×10^1	7.9	1.8×10^{-1}
50	6.8	2.5	3.3×10^{-1}

An important reaction which forms a chain leading to the re-formation of oxygen molecules with the production of hydrogen atoms, in conjunction with reaction (28), is the bimolecular process

$$(a_5) \quad OH + O \rightarrow H + O_2 + 16.6 \text{ kcal} \qquad (30)$$

Laboratory data (Clyne and Thrush, 1963a; Kaufman, 1964, 1969; Breen and Glass, 1970) lead to values of a_5 from $(5 \pm 2) \times 10^{-11}$ cm^3 sec^{-1} between 265°K and 293°K to $(4.3 \pm 1.3) \times 10^{-11}$ cm^3 sec^{-1} at 300°K. A working value

$$a_5 = 3 \times 10^{-12} T^{1/2} \text{ cm}^3 \text{ sec}^{-1} \qquad (31)$$

is adopted, with a possible error of 50%. When the conventional value of the ozone concentration is adopted (see Table 1), the loss coefficient of OH is as given in Table 2.

It is clear that reaction (30), even if it is rapid in the major part of the stratosphere, is relatively slow in the lower stratosphere, where other processes may be more important. The chain reaction introduced by McGrath and Norrish (1958)

$$(a_6) \quad OH + O_3 \rightarrow HO_2 + O_2 \qquad (32)$$

and

$$(a_{6b}) \quad HO_2 + O_3 \rightarrow OH + 2O_2 \qquad (33)$$

as the potent ozone-destroying mechanism can be neglected. No direct measurement has been reported. An upper limit $a_6 \geqslant 5 \times 10^{-13}$ cm^3 sec^{-1} at room temperature (Kaufman, 1964, 1969) was adopted (Hampson, 1966; Hunt, 1966; Dütsch, 1968; Hesstvedt, 1968; Leovy, 1969; Shimazaki and Laird, 1970) as the actual value in the stratosphere and mesosphere. A recent analysis by Langley and McGrath (1971) shows that a_6 should be less than 10^{-16} cm^3 sec^{-1} at room temperature. With a steric hindrance factor of the order of 10^{-2} and an activation energy of about 6 kcal, a_6 should be not more than

$$a_6 = 1.5 \times 10^{-13} T^{1/2} e^{-3000/T} \qquad (34)$$

leading to $a_6\, n(O_3) < a_5\, n(O)$ in the entire stratosphere. Furthermore, reaction (33), which was introduced with a rate coefficient

$$a_{6b} = 5 \times 10^{-14} \text{ cm}^3 \text{ sec}^{-1} \qquad (35)$$

must be rejected (DeMore, 1967; Nicolet, 1970). Measurements of reactions (32) and (33) are required at 200°K, the temperature of the lower stratosphere.

The reaction leading to OH does not occur as in (33), but involves atomic oxygen (Kaufman, 1964)

$$(a_7) \quad O + HO_2 \rightarrow O_2 + OH^*_{v \leqslant 6} + 55 \text{ kcal} \qquad (36)$$

Reaction (36) has not been measured. Considering the work of Foner and Hudson (1962), Kaufman (1964) suggests that $a_7 \geqslant 10^{-11}$ cm^3 sec^{-1}. Reactions (36) and (30) must be compared, since they represent, in the major part of the stratosphere and mesosphere, the chain reaction which destroys ozone through the direct attack of oxygen atoms and re-formation of oxygen molecules.

The values of the rate coefficients a_5 and a_7 which are generally adopted (Hampson, 1966; Hunt, 1966; Hesstvedt, 1968; Dütsch, 1968; Crutzen, 1969; Leovy, 1969) give

$$a_5/a_7 = 5 \times 10^{-11}/10^{-11} = 5. \quad (37)$$

Since no direct measurement of reaction (36) has been reported, the ratio $a_5/a_7 = 5$ cannot be invoked to explain the aeronomic behavior of OH and HO_2. The following value is adopted here for a_7 (see remark for a_2),

$$a_7 = 1.5 \times 10^{-12}\, T^{1/2}\ \text{cm}^3\ \text{sec}^{-1} \quad (38)$$

with the qualification that the ratio a_5/a_7 is not known with sufficient precision and may be between 10 and 1. According to a recent analysis of the HO_2 reactions by Hochanadel et al. (1972), their experimental results can be simulated if a value of the order of 7×10^{-11} cm^3 sec^{-1} is used for a_7. There is, therefore, a possibility that $a_5/a_7 \simeq 1$. In any case, experimental data are needed in order to determine the ratio a_5/a_7, which must be known exactly to calculate the ratio $n(HO_2)/n(OH)$ in the stratosphere and mesosphere.

Expressions for the equilibrium ratios of $n(OH)/n(H)$ and $n(HO_2)/n(H)$ can be easily obtained if it is assumed, as a first approximation, that only reactions (26) to (36) are involved. Thus

$$\frac{n(OH)}{n(H)} = \frac{a_1\, n(M)\, n(O_2) + a_2\, n(O_3)}{a_5\, n(O)} \quad (39)$$

$$\frac{n(HO_2)}{n(H)} = \frac{a_1\, n(M)\, n(O_2)}{a_7\, n(O)} \quad (40)$$

and

$$\frac{n(OH)}{n(HO_2)} = \frac{a_1\, n(M)\, n(O_2) + a_2\, n(O_3)}{a_1\, n(M)\, n(O_2)} \cdot \frac{a_7}{a_5} \quad (41a)$$

The ratio given by (41a) must be used at the stratopause (see Table 2), but below 40 km it becomes

$$\frac{n(OH)}{n(HO_2)} \simeq \frac{a_7}{a_5}. \quad (41b)$$

In the lower stratosphere, hydroxyl and hydroperoxyl radicals are involved in other important reactions with minor constituents which do not belong to the hydrogen-oxygen atmosphere. CO and NO must be considered, since they can react with OH and HO_2, respectively. Among all possible reactions (Nicolet, 1971; Levy, 1971; McConnell et al., 1971) it seems that these two reactions are the most important processes at and above the tropopause.

A simplified reaction scheme is illustrated in Figure 7 for the hydroxyl radical. The radical OH is produced by reactions (20), (21), and (22) of $O(^1D)$ atoms with H_2O, CH_4, and H_2 molecules.

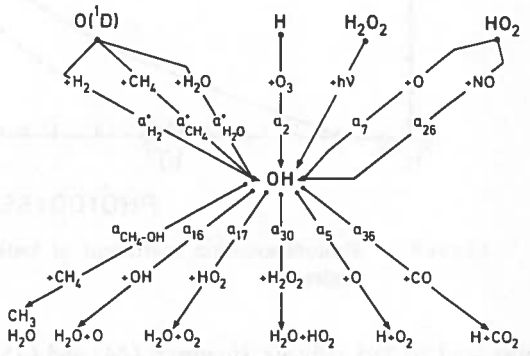

Figure 7. Reaction scheme of the hydroxyl radical in a hydrogen-oxygen atmosphere.

Reactions of ozone (28) and of atomic oxygen (36) with H atoms and HO_2 radicals, respectively, lead also to OH radicals. The photodissociation of hydrogen peroxide cannot be excluded; the process is

$$(J_{H_2O_2}) \quad H_2O_2 + h\nu \rightarrow 2\,OH \quad (42)$$

with a photodissociation rate coefficient (Figure 8) which is not less than 10^{-6} sec^{-1} in the stratosphere. The following reactions (Nicolet, 1965, 1970), in which nitrogen oxides are involved,

$$(a_{26}) \quad NO + HO_2 \rightarrow NO_2 + OH + 9\ \text{kcal} \quad (43)$$

$$(a_{32}) \quad NO + H_2O_2 \rightarrow HNO_2 + OH + 11\ \text{kcal} \quad (44)$$

$$(a_{33}) \quad NO_2 + H_2O_2 \rightarrow HNO_3 + OH + 11\ \text{kcal} \quad (45)$$

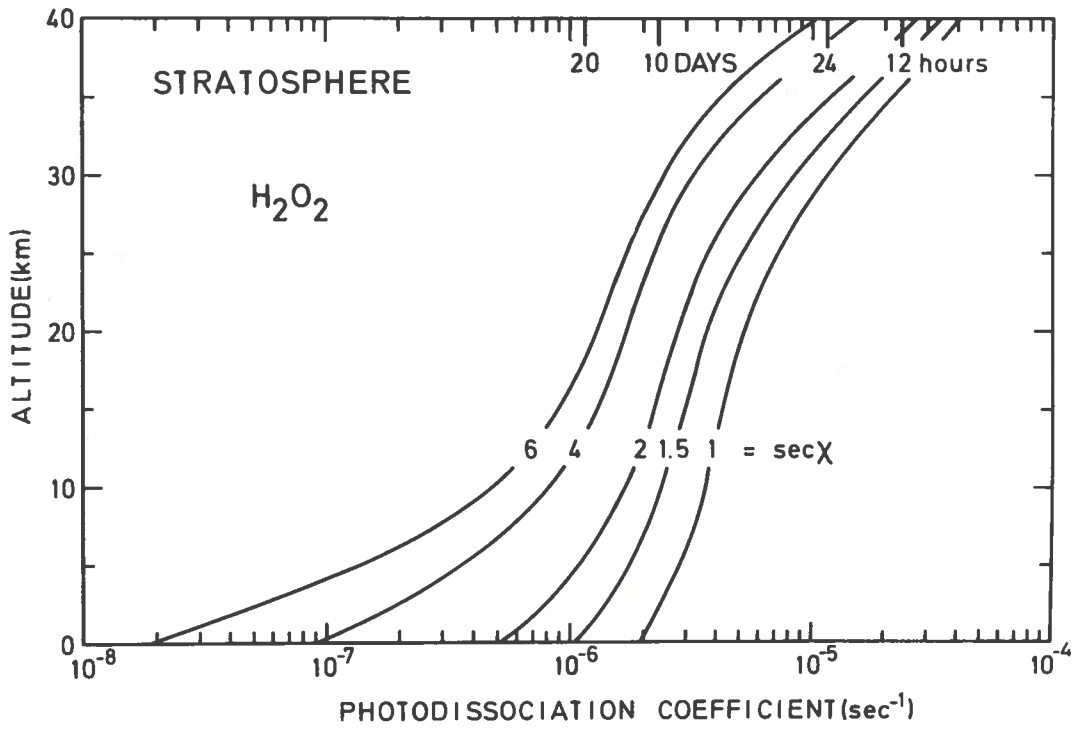

Figure 8. Photodissociation coefficient of hydrogen peroxide in the stratosphere for various solar zenith angles χ .

also lead to OH radicals. However, (44) and (45) are very slow reactions ($< 5 \times 10^{-20}$ cm^3 sec^{-1}) which cannot play a role in the stratosphere, according to recent measurements made by Gray, Lissi, and Heicklen (1972). The rate coefficient a_{26} is not well known; nevertheless, it seems that working values of the order of 5×10^{-13} cm^3 sec^{-1} are needed (Levy, 1971) at ground level, and it is certain that such a reaction must play a role in the lower stratosphere where a_7 n(O) is less than 10^{-5} sec^{-1}. A precise experimental determination of the rate coefficient is needed for the analysis of the exact action of nitric oxide on the ratio $n(HO_2)/n(OH)$ in the lower stratosphere.

On the other hand, the radical OH, if it reacts rapidly with atomic oxygen (reaction 30) in the stratosphere, also has a role when H_2O_2, H_2, CO, and CH_4 are present. The processes (46), (48), (50), and (52), shown below, have been observed:

$$(a_{30})\ OH + H_2O_2 \rightarrow H_2O + HO_2 + 30\ kcal \quad (46)$$

with the rate coefficient (Greiner, 1968)

$$a_{30} = 4.1 \times 10^{-13}\, T^{1/2}\, e^{-600/T} \quad (47)$$

which leads to a rate coefficient of about 3×10^{-13} cm^3 sec^{-1} at 200°K.

$$(a_{19})\ OH + H_2 \rightarrow H_2O + H + 15\ kcal \quad (48)$$

with the rate coefficient (Greiner, 1968)

$$a_{19} = 7 \times 10^{-12}\, e^{-2000/T} \quad (49a)$$

or

$$a_{19} = 2 \times 10^{-13}\, T^{1/2}\, e^{-1800/T} \quad (49b)$$

which leads to about 5×10^{-16} cm^3 sec^{-1} at 200°K;

$$(a_{36})\ OH + CO \rightarrow CO_2 + H + 24\ kcal \quad (50)$$

with the rate coefficient (Greiner, 1969)

$$a_{36} = (1.25 \pm 0.25) \times 10^{-13}\ cm^3\ sec^{-1} \quad (51)$$

for temperatures of the lower stratosphere;

$$(a_{38})\ OH + CH_4 \rightarrow H_2O + CH_3 + 15\ kcal \quad (52)$$

with the rate coefficient (Greiner, 1970)

$$a_{38} = 5 \times 10^{-12} e^{-1900/T} \text{ cm}^3 \text{ sec}^{-1} \quad (53a)$$

or

$$a_{38} = 2 \times 10^{-13} T^{1/2} e^{-1750/T} \text{ cm}^3 \text{ sec}^{-1} \quad (53b)$$

which leads to about 5×10^{-16} cm^3 sec^{-1} at 200°K. It must be pointed out that reactions (46), (48), and (52) lead to the formation of water vapor. Very precise rate coefficients are required for these reactions involving OH, since they play a role in the lower stratosphere where the temperature is not far from 200°K. In addition, the following loss processes of OH lead to the reformation of H_2O

$$(a_{16}) \quad OH + OH \rightarrow H_2O + O + 17 \text{ kcal} \quad (54)$$

$$(a_{17}) \quad OH + HO_2 \rightarrow H_2O + O_2 + 71 \text{ kcal} \quad (55)$$

Several measurements of reaction (54) have been made (Kaufman, 1964, 1969; Westenberg and deHaas, 1965; Dixon-Lewis et al., 1966; Wilson and O'Donovan, 1967; Mulcahy and Smith, 1971). Experimental values are well represented by a value of about 2×10^{-12} at 300°K. With a working value of 1 kcal for the activation energy, a_{16} can be written

$$a_{16} = 7.5 \times 10^{-13} T^{1/2} e^{-500/T} \quad (56)$$

leading to about 9×10^{-13} cm^3 sec^{-1} at 200°K. However, at sufficiently high pressures (lower stratosphere, for example) reaction (54) is replaced by

$$(a_{16M}) \quad OH + OH + M \rightarrow H_2O_2 + M \quad (57)$$

with a rate coefficient (Caldwell and Back, 1965)

$$a_{16M} = 4 \times 10^{-30} \text{ cm}^6 \text{ sec}^{-1} \quad (58)$$

leading to 8×10^{-12} cm^3 sec^{-1} at 20 km.

Reaction (55) is extremely important in the stratosphere and mesosphere, since it must be used to determine n(OH) n(HO_2) before determining the OH and HO_2 concentrations. In 1964, Kaufman suggested that $a_{17} \geqslant 10^{-11}$ cm^3 sec^{-1}. Almost all aeronomic studies treated this as an exact value, but such an assumption was risky for the analysis of the ozone problem in the stratosphere. Recent measurements by Hochanadel et al. (1972) indicate that the rate coefficient

$$a_{17} = 2 \times 10^{-10} \text{ cm}^3 \text{ sec}^{-1} \quad (59a)$$

i.e., an extremely rapid reaction.

With such a high value of the rate coefficient, it is possible to consider reaction (55) the principal process leading to the re-formation of water vapor in the mesosphere. In the upper stratosphere a constant mixing ratio of H_2O corresponding to 3 ppmv leads to n(OH) n(HO_2) $> 10^{14}$ cm^{-6}. The values of the hydroxyl and hydroperoxyl concentrations depend on the various reactions which are involved between OH and HO_2. Calculated OH concentrations are given in Table 3a for two arbitrary constant ratios n(HO_2)/n(OH) = 9 and 1, assuming that only H_2O is involved in the production of OH radicals and that reaction (55) between OH and HO_2 is the re-formation process of H_2O. (Such examples are introduced here to show that important errors may occur in the aeronomic analysis, and that experimental data are urgently needed in order to determine the exact ratio n(HO_2)/n(OH).

Table 3a. Examples of Hydroxyl Radical Concentrations [n(H_2O) = 3 ppm; n(HO_2)/n(OH) = 9 or 1; solar conditions: between sec χ = 1 and 2]

Altitude (km)	n(HO_2)/n(OH) = 9	n(HO_2)/n(OH) = 1
15	$(1.1 \pm 0.3) \times 10^6$	$(3 \pm 1) \times 10^6$
20	$(2.0 \pm 0.5) \times 10^6$	$(6 \pm 2) \times 10^6$
25	$(2.8 \pm 0.6) \times 10^6$	$(8 \pm 2) \times 10^6$
30	$(3.5 \pm 0.7) \times 10^6$	$(1 \pm 0.2) \times 10^7$
35	$(4.5 \pm 0.9) \times 10^6$	$(1.4 \pm 0.2) \times 10^7$
40	$(5.4 \pm 0.8) \times 10^6$	$(1.6 \pm 0.3) \times 10^7$
45	$(5.2 \pm 0.8) \times 10^6$	$(1.6 \pm 0.2) \times 10^7$
50	$(4.1 \pm 0.3) \times 10^6$	$(1.2 \pm 0.1) \times 10^7$

Before this discussion of the hydroxyl and hydroperoxyl radicals ends, the following two-body process must be considered:

$$(a_{27})\quad HO_2 + HO_2 \rightarrow H_2O_2 + O_2 + 42\ \text{kcal.} \quad (60)$$

If it is assumed that the rate coefficient a_{27} cannot be too different from a_{16}, as was indicated by indirect laboratory measurements (Foner and Hudson, 1962; Dixon-Lewis and Williams, 1962; Kaufman, 1964), the following value should be estimated:

$$a_{27} = 7.5 \times 10^{-13}\, T^{1/2}\, e^{-500/T}\ \text{cm}^3\ \text{sec}^{-1} \quad (61a)$$

However, recent measurements by Hochanadel et al.(1972) lead to almost 4 times the value given by (61a); the laboratory results at 298°K give

$$a_{27} = (9.5 \pm 0.8) \times 10^{-12}\ \text{cm}^3\ \text{sec}^{-1} \quad (61b)$$

This value is higher than an estimate made by Paukert in 1969.

An idea of the behavior of hydrogen peroxide can be obtained with a simplified equation, based only on (42) and (60):

$$\frac{dn(H_2O_2)}{dt} + n(H_2O_2)\, J_{H_2O_2} = a_{27}\, n^2(HO_2) \quad (62)$$

The relation $n(HO_2) \leqslant n(H_2O_2)$ is valid at the stratopause if $n(HO_2) \geqslant 10^7\ \text{cm}^{-3}$, and in the lower stratosphere (about 20 km) if $n(HO_2) \geqslant 10^6\ \text{cm}^{-3}$, when photoequilibrium conditions are used for (62).

Finally, considering equilibrium conditions for HO_2 and OH, the following equations are obtained (cf. Figure 9):

$$n(HO_2)\,[a_7\, n(O) + a_{26}\, n(NO) + a_{17}\, n(OH) + 2\, a_{27}\, n(HO_2)] = n(OH)\,[a_5\, n(O) + a_{36}\, n(CO) + a_{30}\, n(H_2O_2)] \quad (63)$$

and (Figure 7)

$$a^* n^*(O)\,[n(H_2O) + n(CH_4) + n(H_2)] = n(OH)\,[\tfrac{1}{2} a_{38}\, n(CH_4) + a_{17}\, n(HO_2) + a_{16}\, n(OH)] \quad (64a)$$

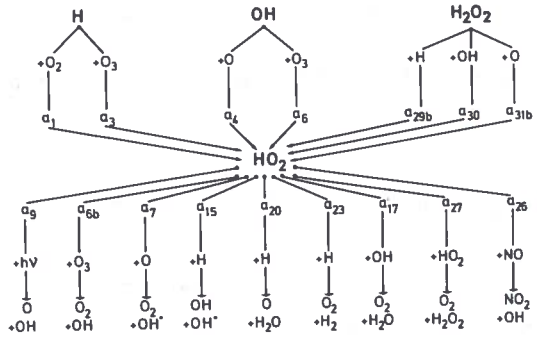

Figure 9. Reaction scheme of the hydroperoxyl radical in a hydrogen-oxygen atmosphere.

In the upper stratosphere (63) and (64)* are written as follows:

$$\frac{n(OH)}{n(HO_2)} = \frac{a_7}{a_5} \quad (41b)$$

and

$$[n(CH_4) + n(H_2) + n(H_2O)]\, a^*\, n^*(O) = a_{17}\, n(HO_2)\, n(OH). \quad (65)$$

Numerical results based on equation (65) are given in Table 3b. However, in the lower stratosphere for daytime conditions

$$\frac{n(OH)}{n(HO_2)} = \frac{a_7\, n(O) + a_{26}\, n(NO)}{a_5\, n(O) + a_{36}\, n(CO)} \quad (66a)$$

and at the tropopause for daytime conditions

$$\frac{n(OH)}{n(HO_2)} = \frac{a_{26}\, n(NO)}{a_{36}\, n(CO)}. \quad (66b)$$

Table 3b. Examples of Hydroxyl Radical Concentrations [$n(H_2O)$ = 3 ppm; $n(CH_4)$ = 1.5 ppm; $n(H_2)$ = 0.5 ppm; CH_4 Effect]

Altitude (km)	sec χ = 1 (overhead sun)	= 1.4 χ = 45°	= 2 χ = 60°
15	1.1×10^6	6.3×10^5	3.1×10^5
20	6.0×10^6	3.5×10^6	2.0×10^6
25	1.6×10^7	4.8×10^6	5.8×10^6

As far as (64) is concerned, in the lower stratosphere and particularly near the tropopause level, it may be assumed that

$$[n(CH_4) + n(H_2) + n(H_2O)]\ a^*\ n^*(O)$$

$$\geqslant a_{38}\ n(OH)\ n(CH_4)/2 \qquad (64b)$$

which leads to a determination of the concentration of hydroxyl radicals

$$n(OH) \leqslant \frac{a^*\ n^*(O)\ [n(CH_4) + n(H_2) + n(H_2O)]}{n(CH_4)\ a_{38}\ /2} \qquad (67a)$$

With numerical values (see Table 3b) corresponding to mixing ratios 0.5 ppmv for H_2, 1.5 ppmv for CH_4, and 3 ppmv for H_2O, $n(OH) = (6 \pm 3) \times 10^5$ cm^{-3} at 15 km for solar conditions varying from an overhead sun to a zenith angle of 60°, $n(OH) = (3 \pm 2) \times 10^6$ at 20 km, and $n(OH) = (10 \pm 3) \times 10^6$ cm^{-3} at 25 km. Thus, the OH concentrations in the lower stratosphere decrease when methane is present and the values given in Table 3a below 25 km are too high.

After sunset, instead of (67a), we must write

$$\frac{1}{n(OH)}\ \frac{dn(OH)}{dt} = -\ a_{38}\ n(CH_4) \qquad (67b)$$

which shows that OH is rapidly transformed into H_2O, since the lifetime of OH radicals is relatively short in the lower stratosphere. With a loss coefficient of the order of 3×10^{-3} sec^{-1} at 20 km, the initial concentration of hydroxyl radicals is reduced to 10^{-5} in a very short time, of the order of 3 hours. Furthermore, equation (66a) cannot be applied, since atomic oxygen is present only in the daytime atmosphere. Finally, NO is transformed into NO_2 in the nighttime stratosphere, and equation (66b) cannot be used.

If the mixing ratios of NO and CO in the lower stratosphere are taken as 4 ppbv and 40 ppbv, respectively, equations (66a) and (66b) indicate that the ratio $n(HO_2)/n(OH)$ depends on the carbon monoxide and nitric oxide concentrations. With $a_{26} \simeq 10\ a_{36}$, $n(HO_2)/n(OH) \simeq 1$. Near 30 km the role of oxygen atoms is important.

Thus, the importance of reactions with hydrogen compounds in the photochemistry of ozone and atomic oxygen in the lower stratosphere depends strongly on the actions of carbon monoxide and of nitric oxide. The action of methane must be introduced in the process of H_2O re-formation above the tropopause level.

Finally, instead of as in (9), the rate of change of O_3 in the stratosphere must be written (Nicolet, 1966, 1970)

$$\frac{dn(O_3)}{dt} + \frac{J_3}{k_2\ n(M)\ n(O_2)}\ n(O_3)\ [2\ k\ n(O_3)$$

$$+ a_5\ n(OH) + a_7\ n(HO_2)] = 2n(O_2)\ J_2 \qquad (68a)$$

In the upper stratosphere (68a) becomes, using (41b),

$$n(O_3) = \frac{k_2}{k_3}\ n(M)\ n(O_2)\ \frac{n(O_2)\ J_2}{n(O_3)\ J_3 + a_5\ n(OH)} \qquad (68b)$$

NITROGEN-OXYGEN ATMOSPHERE

In a pure oxygen atmosphere the photochemical destruction of ozone is given by reaction (8)

$$O_3 + O \rightarrow O_2 + O_2 \qquad (69)$$

and in a hydrogen-oxygen atmosphere by a catalytic cycle of an $HO\text{-}HO_2$ system involving reactions (30) and (36) in the stratosphere,

$$O + OH \rightarrow H + O_2 \qquad (70)$$

$$O + HO_2 \rightarrow OH + O_2. \qquad (71)$$

In a nitrogen-oxygen atmosphere the catalytic cycle involves NO and NO_2 (Crutzen, 1970; Johnston, 1971; Nicolet, 1971). Nitric oxide reacts with ozone as follows

$$(b_4)\quad NO + O_3 \rightarrow NO_2 + O_2 + 48\ \text{kcal} \qquad (72)$$

with a rate coefficient which is sufficiently certain (Johnston and Crosby, 1954; Clyne, Thrush, and Wayne, 1964)

$$b_4 = 1 \times 10^{-12}\ e^{-1250/T}. \qquad (73)$$

NO_2 is subject to photodissociation

$$(J_{NO_2}) \quad NO_2 + h\nu\ (\lambda < 3975\ A) \rightarrow NO + O \qquad (74)$$

The photodissociation rate coefficient is about 4×10^{-3} sec^{-1} at 50 km, and not less than 3×10^{-3} sec^{-1} at 15 km. An average value of $(3.4 \pm 0.5) \times 10^{-3}$ may be adopted in the stratosphere.

However, the following reaction plays a role in the upper stratosphere:

$$(b_3) \quad O + NO_2 \rightarrow NO + O_2 + 46\ kcal \qquad (75)$$

It is a relatively rapid reaction (Schiff, 1964; Klein and Herron, 1964; Westenberg and deHaas, 1969). At 200°K, the extrapolation of such experimental data leads to 2 and to 7×10^{-12} $cm^3\ sec^{-1}$, which may be given either by

$$b_{3a} = 5 \times 10^{-13}\ T^{1/2}\ cm^3\ sec^{-1} \qquad (76a)$$

or by

$$b_{3b} = 1 \times 10^{-12}\ T^{1/2}\ e^{-350/T}\ cm^3\ sec^{-1} \qquad (76b)$$

An unpublished result (Davis, 1972) gives

$$b_{3c} = 9.2 \times 10^{-12}\ cm^3\ sec^{-1} \qquad (76c)$$

over the 235 - 350°K temperature range.

Thus, this again clearly shows that the experimental values of many rate coefficients must be known with greater accuracy for the study of aeronomic processes in the stratosphere.

Considering that (72), (74), and (75) are the principal reactions in the stratosphere (Nicolet, 1965)

$$\frac{dn(NO_2)}{dt} + n(NO_2)\ [J_{NO_2} + b_3\ n(O)] = b_4\ n(NO)\ n(O_3) \qquad (77a)$$

and, for daytime conditions, since $1/J_{NO_2} \leqslant 3 \times 10^2$ sec,

$$\frac{n(NO_2)}{n(NO)} = \frac{b_4\ n(O_3)}{J_{NO_2} + b_3\ n(O)}. \qquad (77b)$$

With the numerical values adopted in (73) and (76c), the $n(NO_2)/n(NO)$ ratio is given in Table 4 at various altitudes and for two values of the zenith angle. The ratio increases from about 1 at 15 km to nearly 4 at 30 km, and decreases above 35 km to about 2×10^{-2} at 50 km. Thus, the daytime ratio $n(NO_2)/n(NO)$ should be of the order of 1 in the lower stratosphere, but is related to the ozone variation.

Table 4. Ratio $n(NO_2)/n(NO)$ in the Stratosphere

Altitude (km)	Solar Zenith Angle sec χ = 1	sec χ = 2
15	0.9(1)	0.95(1)
20	2.7	2.9
25	3.6	3.8
30	3.6(2)	3.7(2)
35	2.7	2.7
40	0.6	0.9
45	8.9×10^{-2}	1.4×10^{-1}
50	1.6×10^{-2}	2.1×10^{-2}

(1) effect of J_{NO_2} alone

(2) effect of $b_3\ n(O)$ also

Thus, if we introduce the effect of nitrogen oxides (NO and NO_2) into the ozone equation (9), from (72), (74), and (75) we must write

$$\frac{dn(O_3)}{dt} + \frac{J_3\ n(O_3)}{k_2\ n(M)\ n(O_2)}\ [2k_3\ n(O_3) + b_4\ n(NO) + b_3\ n(NO_2)] = 2n(O_2)\ J_2 + n(NO_2)\ J_{NO_2} \qquad (78)$$

which becomes, with (77),

$$\frac{dn(O_3)}{dt} + \frac{2\ J_3\ n(O_3)}{k_2\ n(M)\ n(O_2)}\ [k_3\ n(O_3) + b_3\ n(NO_2)] = 2n(O_2)\ J_2 \qquad (78b)$$

Comparing (78) with (68), which involves the effect of hydroxyl and hydroperoxyl radicals, the ozone concentration in the upper stratosphere is given by

$$n(O_3) = \frac{k_2}{k_3} n(M)\, n(O_2) \times \frac{n(O_2)\, J_2}{n(O_3)\, J_3 + a_5\, n(OH) + b_3\, n(NO_2)} \qquad (78c)$$

which shows that the correction term to J_3 (see (15) and (16) can be written

$$A = \frac{a_5\, n(OH) + b_3\, n(NO_2)}{k_3\, n(O_3)} \qquad (79)$$

Table 5 shows that the same effect is obtained for a ratio $n(OH)/n(NO_2)$ of the order of 10^{-1}. For example, if between 35 km and 40 km the ozone concentration is of the order of 10^{12} cm^{-3}, then from 5×10^7 to about 10^8 OH molecules have the same effect as from 5×10^8 to about 10^9 NO_2 molecules.

Table 5. Numerical values of $\frac{a_5}{k_3}\frac{n(OH)}{n(O_3)} + \frac{b_{3b}}{k_3}\frac{n(NO_2)}{n(O_3)}$

Altitude (km)	a_5/k_3	b_{3b}/k_3
15	9.6×10^4	6.1×10^3
20	6.8	4.6
25	4.9	3.5
30	3.6	2.7
35	2.0	1.7
40	1.2	1.1
45	1.0	1.0
50	1.0	1.0

In the ozonosphere, various reactions with nitrogen oxides may be considered (see Nicolet, 1965, 1971; Johnston, 1971). Among the possible reactions, a three-body association leading to nitrous and nitric acids,

$$(b_{22}) \quad OH + NO_2 + M \rightarrow HNO_3 + M + 53\ \text{kcal} \qquad (80)$$

is an important process for which the rate coefficient for T = 300°K is (Simonaitis and Heicklen, 1971)

$$b_{22} = 1.3 \times 10^{-30}\ \text{cm}^6\ \text{sec}^{-1} \qquad (81a)$$

for M = He, or

$$b_{22} = 1.1 \times 10^{-29}\ \text{cm}^3\ \text{sec}^{-1} \qquad (81b)$$

if $M = H_2O$.

With $b_{22} = 5 \times 10^{-30}$ cm^6 sec^{-1} for O_2 and N_2, it can be seen that the lifetime of OH is very short in the lower stratosphere if there is no re-formation process of OH. In fact,

$$(b_{27}) \quad OH + HNO_3 \rightarrow H_2O + NO_3 + 15\ \text{kcal} \qquad (82)$$

with a coefficient which, according to Husain and Norrish (1963), should be of the order of

$$b_{26} = 1.5 \times 10^{-13}\ \text{cm}^3\ \text{sec}^{-1} \qquad (83)$$

A possible reformation process for OH from HNO_3 is photodissociation (see Leighton, 1961):

$$(J_{HNO_3}) \quad HNO_3 + h\nu \rightarrow OH + NO_2 \qquad (84)$$

Another reaction

$$(b_{28}) \quad O + HNO_3 \rightarrow OH + NO_3 \qquad (85)$$

is slow, and according to Morris and Niki (1971) its rate coefficient is less than 2×10^{-14} cm^3 sec^{-1}. It seems, therefore, that the relevant differential equation for the HNO_3 concentration is

$$\frac{dn(HNO_3)}{dt} + n(HNO_3)\,[J_{HNO_3} + b_{27}\, n(OH) + b_{28}\, n(O)] = b_{22}\, n(OH)\, n(NO_2)\, n(M) \qquad (86)$$

Nighttime equilibrium conditions would lead to

$$\frac{n(HNO_3)}{n(NO_2)} < \frac{b_{22}\, n(M)}{b_{27}} \simeq 10^2 \qquad (87a)$$

at 15-20 km. However, according to computations based on equation (67b), the hydroxyl radicals disappear in the lower thermosphere after sunset, and, consequently, a nighttime equilibrium cannot be attained for the ratio $n(HNO_3)/n(NO_2)$. Thus, the photodissociation process (84) cannot be eliminated as an effective loss process of HNO_3 in the lower stratosphere, since J_{HNO_3} could be greater than 10^{-7} sec^{-1}. Photoequilibrium conditions, which may or may not exist in the lower stratosphere, lead to

$$\frac{n(HNO_3)}{n(NO_2)} = \frac{n(OH)\, b_{22}\, n(M)}{J_{HNO_3} + b_{27}\, n(OH)} \qquad (87b)$$

Once again, exact values of the parameters are needed for a determination of the theoretical ratio $n(HNO_3)/n(NO_2)$. Observational results indicate that the HNO_3 mixing ratio in the lower stratosphere is not less than 10^{-9} (Murcray et al., 1969; Rhine et al., 1969) and that the NO_2 mixing ratio is less than 3×10^{-8} (Ackerman and Frimout, 1969).

Thus, it seems that the OH radicals are not only subject to reactions with hydrogen compounds (Figure 7), but also depend on nitrogen compounds. The equilibrium value in the lower stratosphere would be, to a first approximation (Figure 10),

$$n(OH) = \left\{ a^* n^*(O) \left[n(CH_4) + n(H_2O) + n(H_2) \right] + n(HNO_3) J_{HNO_3} \right\} \div \left\{ a_{38}\, n(CH_4) + b_{22}\, n(M)\, n(NO_2) + a_{17}\, n(HO_2) \right\} \qquad (88a)$$

If the photodissociation of nitric acid is inefficient, (88a) can be reduced to the oversimplified form

$$n(OH) \equiv \frac{a^* n^*(O) \left[n(CH_4) + n(H_2O) + n(H_2) \right]}{b_{22}\, n(M)\, n(NO_2)} \qquad (88b)$$

over the 15-25 km stratospheric region. From equation (88b), one determines that, with $n(NO_2) = 4 \times 10^{-9}\, n(M)$, the OH concentration would be only between 10^4 cm^{-3} and 10^5 cm^{-3} in the lower

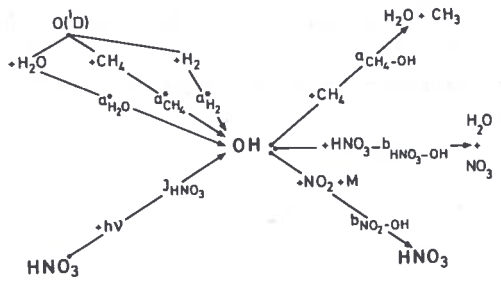

Figure 10. Scheme of the principal reactions of hydroxyl radicals above the tropopause in the lower stratosphere.

part (15-20 km) of the stratosphere. Table 6 shows the various concentrations of OH molecules which are obtained according to which loss process is involved; a factor of about 100 can be involved at 15 km which is reduced to less than 10 at 25 km.

Table 6. Examples of Hydroxyl Radical Concentrations (cm^{-3}) in the Lower Stratosphere

Altitude (km)	Table 3a (HO_2)	Table 3b (CH_4)	Effect of HNO_3
15	(1 ± 0.3) to $(3\pm1) \times 10^6$	$(6\pm3) \times 10^5$	$(4\pm2) \times 10^4$
20	(2 ± 0.5) to $(6\pm2) \times 10^6$	$(3\pm2) \times 10^6$	$(1\pm0.5) \times 10^5$
25	(3 ± 0.6) to $(8\pm2) \times 10^6$	$(10\pm3) \times 10^6$	$(1\pm0.6) \times 10^6$

Consequently, if there is no active photodissociation of nitric acid between 15 and 20 km, the OH concentrations are relatively low. Results given in Table 6 indicate differences from the results of McConnell et al. (1971); their computed OH profile indicates an almost constant value of its concentration between the ground level and 20 km. Such different values show that a careful analysis of all aeronomic processes in the lower stratosphere is required before a final conclusion can be reached.

The presence of nitrogen oxides in the stratosphere may be related to the downward transport of NO molecules from the mesosphere. In the mesosphere the nitric oxide concentration depends on the photodissociation rate J_{NO}, which is related to a predissociation process. For zero optical depth, $J_{NO} = 5 \times 10^{-6}$ sec^{-1}; its value decreases rapidly in the mesosphere, since the absorption depends on the structure of the (10-0) and (9-0) Schumann-Runge bands of molecular oxygen and of the (1-0) δ bands of nitric oxide (Figure 11).

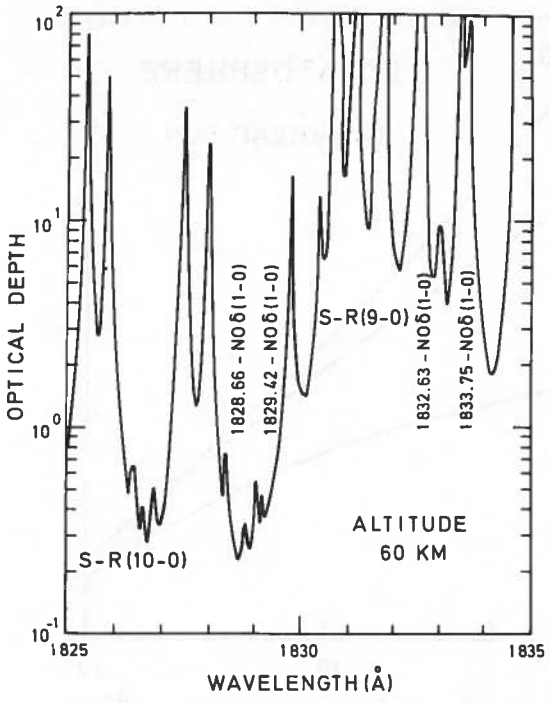

Figure 11. The δ bands of nitric oxide are shielded in the mesosphere by the Schumann-Runge bands of molecular oxygen and determine the photodissociation coefficient.

The differential equation pertaining to the variation of the nitric oxide concentration in the mesosphere

$$\frac{\partial n(NO)}{\partial t} + n(NO)\, J_{NO} + \frac{\partial}{\partial z}\left[n(NO)\, w_{NO}\right] = 0 \tag{89}$$

becomes

$$\frac{\partial n(NO)}{\partial t} + \frac{\partial}{\partial z}\left[n(NO)\, w_{NO}\right] = 0 \tag{90}$$

at the stratopause, since J_{NO} is very small at that level. Observational values of the NO concentration (Pontano and Hale, 1970) of the order of 10^9 cm^{-3} at the stratopause are larger than the theoretical values deduced by Strobel (1972) [$10^6 < n(NO) < 10^7$ cm^{-3}] and also more than a mixing distribution [$n(NO) \simeq 10^8$ cm^3] if $[n(NO_2) + n(NO)]/n(M) = 3 \times 10^{-9}$ at the tropopause (Nicolet, 1965).

Nitric oxide is produced in the stratosphere by a reaction between nitrous oxide and the excited oxygen atom in the O(1D) state (Nicolet, 1970)

$$(b_{38})\quad O(^1D) + N_2O \rightarrow N_2 + O_2 \tag{91a}$$

$$(b_{39})\quad O(^1D) + N_2O \rightarrow 2\,NO \tag{91b}$$

with a global rate coefficient of the order of 2×10^{-10} cm^3 sec^{-1} (Young et al., 1968) and a ratio $b_{38}/b_{39} \simeq 1$ according to Greenberg and Heicklen (1970). Thus the production of NO molecules is given by

$$\frac{dn(NO)}{dt} = 2 \times 10^{-10}\, n(N_2O)\, n[O(^1D)]\ \text{cm}^{-3}\ \text{sec}^{-1} \tag{92}$$

Since N_2O is photodissociated by $\lambda < 3400$ A (Bates and Hayes, 1967) leading only to (Nicolet, 1970; Nicolet and Vergison, 1971)

$$N_2O + h\nu\ (\lambda < 3400\ \text{A}) \rightarrow N_2(X^1\Sigma) + O(^1D) \tag{93}$$

in the *stratosphere*, the vertical distribution of nitrous oxide, which does not produce NO by photodissociation, decreases rapidly with height according to the differential equation

$$\frac{\partial n(N_2O)}{\partial t} + \text{div}\left[n(N_2O)\, w_{N_2O}\right] + n(N_2O)\, J_{N_2O} = 0 \tag{94}$$

Examples of the vertical distribution of nitrous oxide with a mixing ratio of 2.5×10^{-7} at the tropopause are illustrated in Figure 12. It is clear that the distribution depends on what eddy diffusion coefficients are adopted (Nicolet and Vergison, 1971; McElroy and McConnell, 1971). The measurements in the stratosphere by Schutz et al. (1970) and Goldman et al. (1970) indicate that more observations are needed in order to determine the stratospheric distribution of N_2O with latitude and altitude.

Nevertheless, it is possible to consider (Nicolet and Vergison, 1970) the stratospheric production of nitric oxide P_n to be of the order of

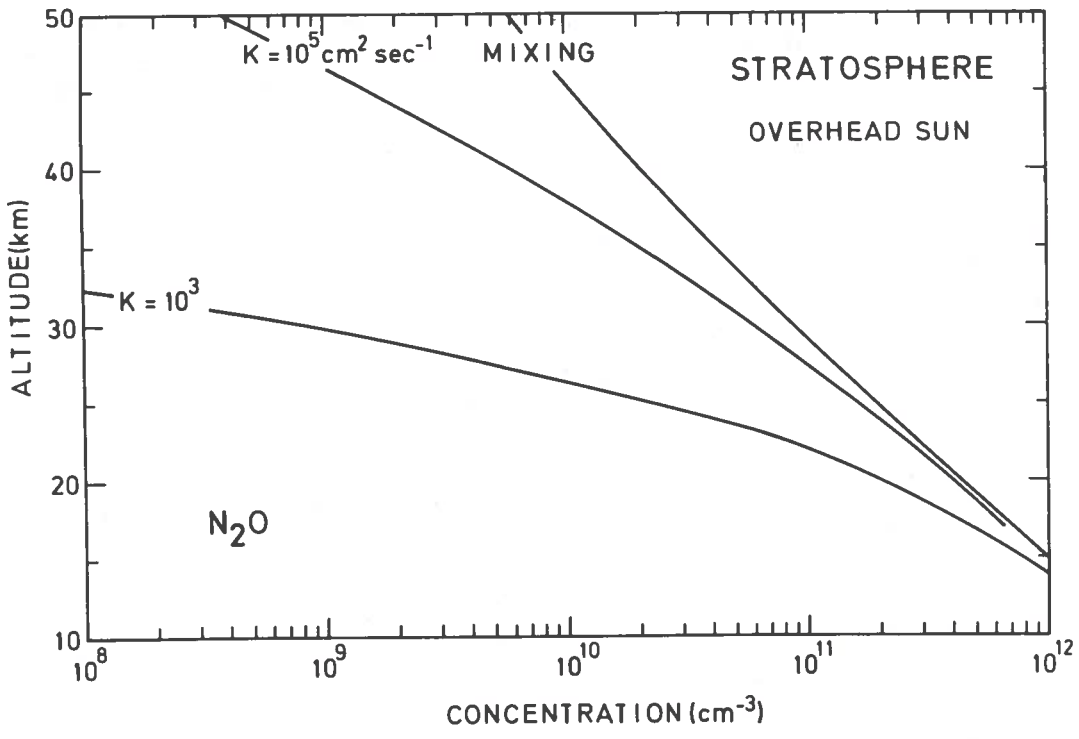

Figure 12. Vertical distributions of the nitrous oxide concentration in the stratosphere related to various eddy diffusion coefficients $K = 10^3$ cm^2 sec^{-1}, $K = 10^5$ cm^2 sec^{-1}, and mixing.

$$P_n(NO) = (1.5 \pm 1) \times 10^8 \text{ cm}^{-2} \text{ sec}^{-1} \qquad (95)$$

which is of the same order of magnitude as the artificial injection by 500 supersonic-transport aircraft.

Finally, the differential equation pertaining to the variation of nitric oxide in the stratosphere is

$$\frac{\partial n(NO)}{\partial t} + \text{div}\,[n(NO)\, w_{NO}] +$$

$$+ \text{div}\,[n(HNO_3)\, w_{HNO_3}] = P(NO) \qquad (96)$$

where P(NO) is given by (92). The downward transport of nitric acid from the stratosphere into the troposphere may be considered as a destruction process of stratospheric nitrogen oxides. Thus, special attention should be given to atmospheric conditions relating to the tropopause and its multiple structure. The exchange between troposphere and stratosphere must be studied at various latitudes.

THE CO AND CH_4 PROBLEM IN THE STRATOSPHERE

Methane, which has been found as a permanent constituent of the troposphere, has continuous sources at ground level. It is dissociated by ultraviolet radiation in the mesosphere and by oxidation processes in the stratosphere (Nicolet, 1971).

The dissociative reactions in the stratosphere are

$$(a^*_{CH_4}) \quad O(^1D) + CH_4 \rightarrow CH_3 + OH + 43.5 \text{ kcal} \qquad (21)$$

and

$$(a_{38}) \quad OH + CH_4 \rightarrow CH_3 + H_2O + 15 \text{ kcal} \qquad (52)$$

In the upper stratosphere the photodissociation of CO_2 produces at least 10^3 CO molecules cm^{-3} sec^{-1}. In the lower stratosphere CO_2 is photodissociated at a very low rate. In the

lower stratosphere the photodissociation process is less important than the oxidation process (21), which can be considered as follows:

$$O(^1D) + CH_4 \rightarrow CO + 4\ H \qquad (97)$$

as far as the CO production is concerned. Methyl radicals which are produced by reactions (21) and (52) react with molecular oxygen

$$CH_3 + O_2 + M \rightarrow CH_3O_2 + M + 26\,kcal \qquad (98)$$

with a rate coefficient of the order of 10^{-31} cm^6 sec^{-1} at room temperature (Heicklen, 1968; Spicer et al., 1972).

Methylperoxyl radicals react with oxides of nitrogen via

$$(b_{31a})\ CH_3O_2 + NO \rightarrow CH_3O_2NO \qquad (99a)$$

or

$$(b_{31b})\ CH_3O_2 + NO \rightarrow H_2CO + HNO_2 \qquad (99b)$$

as regards NO. The production of methyl peroxynitrite is about 1.5 times the simultaneous production of formaldehyde and nitrous acid. In the same way the reactions with NO_2 are

$$(b_{32a})\ CH_3O_2 + NO_2 \rightarrow CH_3O_2NO_2 \qquad (100a)$$

or

$$(b_{32b})\ CH_3O_2 + NO_2 \rightarrow H_2CO + HNO_3 \qquad (100b)$$

Here the production of formaldehyde and nitric acid is about 3 times the production of methylperoxynitrate. There is no evidence that the reaction between CH_3O_2 and NO produces CH_3O + NO_2 (Spicer et al., 1972).

Finally the photochemistry of formaldehyde (McQuigg and Calvert, 1969) indicates that two distinct primary photodissociation processes occur, leading to HCO and CO:

$$H_2CO + h\nu \rightarrow H + HCO \qquad (101a)$$

and

$$H_2CO + h\nu \rightarrow H_2 + CO \qquad (102a)$$

It should be noted that the photodissociation of formaldehyde leads to the production of molecular hydrogen in the stratosphere.

The photodissociation coefficients of H_2CO, based on recently published cross-sections (Calvert et al., 1972), can be determined. For the production of hydrogen atoms and formyl radicals, the photodissociation coefficient $J_{H\text{-}HCO}$ is

$$J_{H\text{-}HCO} = 9.4 \times 10^{-5}\ sec^{-1} \qquad (101b)$$

at zero optical depth; the simultaneous production of molecular hydrogen and carbon monoxide leads to the photodissociation coefficient $J_{H_2\text{-}CO}$

$$J_{H_2CO} = 1.3 \times 10^{-4}\ sec^{-1} \qquad (102b)$$

The photodissociation coefficients are given in Table 7 at three altitudes in the lower stratosphere and for solar zenith angles between 0° and 60°. Thus, the total photodissociation coefficient of H_2CO is $(1.3 \pm 0.2) \times 10^{-4}$ sec^{-1} in the lower stratosphere.

A rapid reaction such as

$$H_2CO + OH \rightarrow HCO + H_2O + 36\,kcal \qquad (103a)$$

Table 7. Photodissociation Coefficients of Formaldehyde

Altitude (km)	H-HCO and H_2-CO (sec^{-1})	H - HCO (sec^{-1})	H_2 - CO (sec^{-1})
15	$(1.2 \pm 0.1) \times 10^{-4}$	$(3.3 \pm 0.6) \times 10^{-5}$	$(8.5 \pm 0.7) \times 10^{-5}$
20	$(1.3 \pm 0.1) \times 10^{-4}$	$(3.8 \pm 0.5) \times 10^{-5}$	$(9.5 \pm 0.6) \times 10^{-5}$
25	$(1.4 \pm 0.1) \times 10^{-4}$	$(4.3 \pm 0.5) \times 10^{-5}$	$(1.0 \pm 0.5) \times 10^{-4}$

with a rate coefficient (Morris and Niki, 1971)

$$a_{OH\text{-}CH_2O} = 1.5 \times 10^{-11}\ cm^3\ sec^{-1} \qquad (103b)$$

seems to be a less important process in the lower stratosphere than the direct photodissociation process; it requires OH concentrations greater than 10^7 cm^{-3} to compete with the photodissociation, whose coefficient J_{H_2CO} is of the order of 1.3×10^{-4} sec^{-1} in the lower stratosphere.

Thus, equations (98) to (101) indicate that the oxidation of methane leads to the production of carbon monoxide (97) and to the simultaneous production of formaldehyde and nitric acid. The production of formaldehyde $P(CH_2O)$ is given by

$$P(CH_2O) = \frac{0.4\, b_{31}\, n(NO) + 0.75\, b_{32}\, n(NO_2)}{b_{31}\, n(NO) + b_{32}\, n(NO_2)}$$

$$\times\, [a^*_{CH_4}\, n^*(O) + a_{38}\, n(OH)]\, n(CH_4) \qquad (103c)$$

$$\simeq \frac{1}{2}\, [a^*_{CH_4}\, n^*(O) + a_{38}\, n(OH)]\, n(CH_4). \qquad (103d)$$

From (101), (102), and (103), we may write

$$n(CH_2O)\ \frac{[a^*\, n^*(O) + a_{38}\, n(OH)]\, n(CH_4)}{2[J_{H\text{-}HCO} + J_{H_2\text{-}CO} + 1.5 \times 10^{-11}\, n(OH)]} \qquad (104a)$$

and in the lower stratosphere an oversimplified equation

$$n(CH_2O) \leqslant \frac{a^*\, n^*(O)\, n(CH_4)}{2J_{H_2CO}} \qquad (104b)$$

since $a_{38}\, n(OH)$ may be of the same order of magnitude as $a^*\, n^*(O)$.

With a mixing ratio of CH_4 of the order of 1.5 ppmv between 15 and 25 km, the CH_2O concentrations could reach the following photochemical equilibrium values: $(2 \pm 1) \times 10^6$ cm^{-3} at 15 km, $(9 \pm 5) \times 10^6$ cm^{-3} at 20 km, and $(1 \pm 0.5) \times 10^7$ at 25 km. Such concentrations should lead to productions of H_2 molecules of the order of 10^3 cm^{-3} sec^{-1} near 20 km. Reaction (101a) would lead also to the production of hydrogen atoms of about 10^3 cm^{-3} sec^{-1} near 20 km, which corresponds to an indirect production of HO_2 radicals. In the same way the formyl radical also leads directly by reaction with O_2 or indirectly by photodissociation to hydroperoxyl radicals in the stratosphere. An additional source of nitric acid, not previously considered, is given by

$$P(HNO_3) = \frac{0.75\, b_{32}\, n(NO_2)}{b_{31}\, n(NO) + b_{32}\, n(NO_2)}$$

$$[a^*_{CH_4}\, n^*(O) + a_{38}\, n(OH)]\, n(CH_4) \qquad (105)$$

Such a source increases when the NO_2 and O_3 concentrations increase.

In order to determine the importance of reaction (97) in leading to the production of CO, it is necessary to know the vertical distribution of CH_4 in the entire stratosphere. Measurements made in the stratosphere by Bainbridge and Heidt (1966) indicate that the transport of methane $F_K(CH_4)$ across the tropopause is given by

$$F_K CH_4) = n(CH_4)\, K\ \frac{1}{H_{CH_4}} + \frac{1}{H_M} \qquad (106)$$

where K is the eddy diffusion coefficient, and H_{CH_4} and H_M are the scale heights of CH_4 and of the atmosphere respectively; it corresponds to an eddy diffusion flux of about 5×10^9 molecules CH_4 cm^{-2} sec^{-1}. Such a transport is equivalent to a stratospheric production of 5×10^9 carbon monoxide molecules cm^{-2} sec^{-1}; it also results in an addition of 10^{10} water vapor molecules cm^{-2} sec^{-1} in the stratosphere. Such an addition does not differ greatly from artificial injection by 500 SST aircraft.

However, a vertical flow of about 5×10^9 CH_4 molecules cm^{-2} sec^{-1} corresponds to an average eddy diffusion coefficient of 2×10^3 cm^2 sec^{-1}, which would lead to a decrease of about a factor of 1000 in the mixing ratio of methane from the tropopause to the stratopause. The examples (Figure 13) of the vertical distribution of methane of the stratosphere show the important differences for two typical values of the average eddy diffusion coefficient K = 10^3 and 10^4 cm^2 sec^{-1}. The first observational result (Scholz et al., 1970) leading

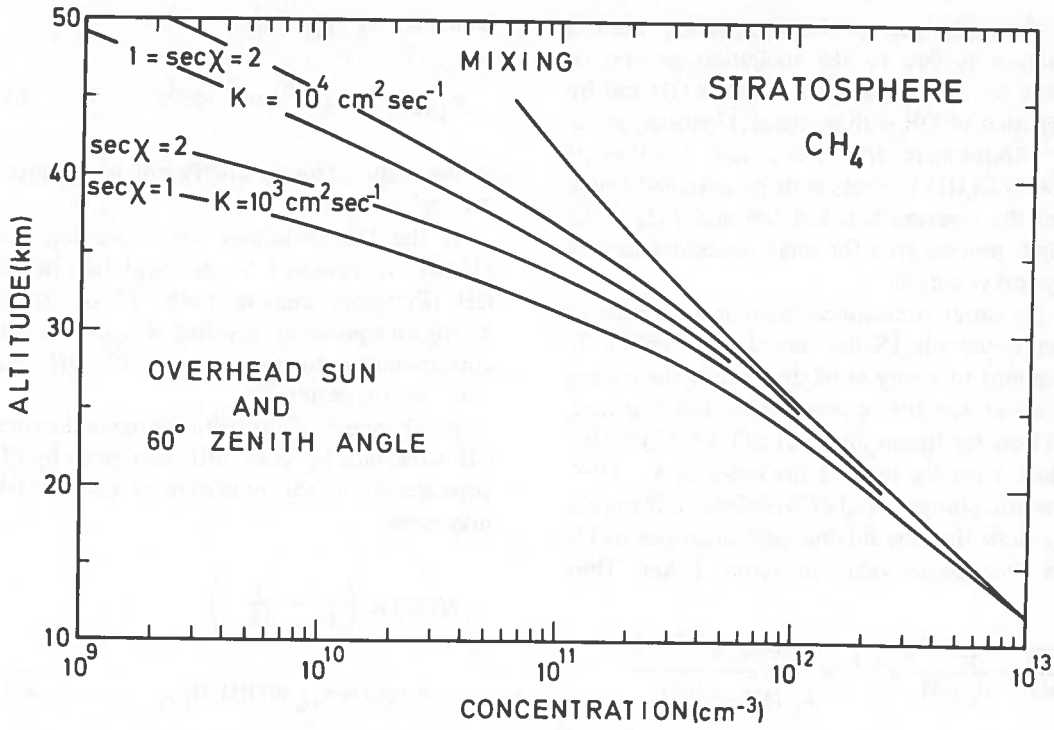

Figure 13. Vertical distribution of the methane concentration in the stratosphere for 2 solar zenith distances (0° and 60°) and 2 eddy diffusion coefficients ($K = 10^3$ cm^2 sec^{-1} and 10^4 cm^2 sec^{-1}) compared with mixing.

to $\leqslant 5 \times 10^{-8}$ for the CH_4 mixing ratio at the tropopause corresponds to $K < 10^4$ cm^2 sec^{-1}, but a second analysis (Ehhalt et al., 1972) leading to a CH_4 mixing ratio of 2.5×10^{-7} requires an eddy diffusion coefficient of about 2×10^4 cm^2 sec^{-1}.

If we accept this last result, we must assume that the scale height h of the CH_4 mixing ratio is not less than 20 km. In other words (see equation 106), if

$$\frac{1}{h} = \frac{1}{H_{CH_4}} - \frac{1}{H_M} = \frac{1}{2.2 \times 10^6} \qquad (107)$$

as given by Bainbridge and Heidt (1966) for their second profile between 15 to 24 km, is extended up to 50 km, the CH_4 mixing ratio decreases from 15 km to 50 km to 20% of its tropopause value as given by Ehhalt et al.(1972). But such a relatively high mixing ratio at the stratopause requires an average eddy diffusion coefficient for the total stratosphere greater than 10^4 cm^2 sec^{-1}. Such a high value indicates that new observational results are needed.

As far as carbon monoxide is concerned, the general equation for its vertical distribution in the stratosphere must be written as follows:

$$\frac{\partial n(CO)}{\partial t} + \text{div}\,[n(CO)\, w_{CO}] + a_{36}\, n(OH)\, n(CO) = n(CO_2)\, J_{CO_2} + n(CH_4)\,[a^*\, n^*(O) + a_{38}\, n(OH)] \qquad (108a)$$

At the stratopause, there is a photochemical equilibrium (Hays and Olivero, 1970); the principal process for the production of carbon monoxide is the photodissociation of carbon dioxide, and the principal loss process is the reaction of CO with OH radicals, since the transport is too slow. Instead of (108a), the photochemical conditions may be considered as follows

$$n(CO_2)\, J_{CO_2} = a_{36}\, n(OH)\, n(CO) \qquad (108b)$$

In the major part of the stratosphere the CO production is due to the oxidation process of methane by excited oxygen atoms $O(^1D)$ and by the reaction of OH with methane. However, in the lower stratosphere the dissociative reaction of CH_4 with $O(^1D)$ is a very slow process, and below 25 km the reaction between OH and CH_4 is the principal process even for small concentrations of the hydroxyl radical.

In the lower stratosphere there is a decrease of carbon monoxide (Seiler and Junge, 1969). It corresponds to a very rapid decrease of the mixing ratio above the tropopause (Seiler and Warneck, 1972) from the tropospheric ratio $(1.4 \pm 0.2) \times 10^{-7}$ to another mixing ratio of the order of 4×10^{-8}. Such results (Junge et al., 1970); Seiler and Warneck, 1972) show that the mixing ratio decreases to 1/e of its tropopause value in about 1 km. Thus

$$\frac{n(CO)}{n(M)} = \frac{n_{tr}(CO)}{n_{tr}(M)}\, e^{-z/h} \equiv \frac{n_{tr}(CO)\, e^{-z/H_{CO}}}{n_{tr}(M)\, e^{-z/H_M}} \tag{109}$$

with

$$\frac{1}{h} = \frac{1}{H_{CO}} - \frac{1}{H_M} = \frac{1}{10^5} \tag{110}$$

In this transition region the transport leads to

$$F_{CO} = n_{tr}(CO)\, w_{CO} = n(CO)\, K \frac{1}{H_{CO}} - \frac{1}{H_M} \tag{111a}$$

and with (110)

$$F_{CO} = n_{tr}(CO)\, K/10^5 \text{ cm}^{-2} \text{ sec}^{-1} \tag{111b}$$

With $n_{tr}(CO) = 1.5 \times 10^{12}$ cm^{-3} at the tropopause ($\leqslant 9$ km), the vertical flux of CO molecules above the tropopause is

$$F_{CO} = 1.5 \times 10^7 \text{ K cm}^{-2} \text{ sec}^{-1} \tag{111c}$$

which is very important;

$$F_{CO} \geqslant 5 \times 10^{10} \text{ cm}^{-2} \text{ sec}^{-1} \tag{111d}$$

if the eddy diffusion coefficient is not less than 3×10^3 cm^2 sec^{-1}.

If the CO molecules which are injected by (111d) are removed by the oxidation of CO by OH (Pressman and Warneck, 1970; Hesstvedt, 1970), an equivalent recycling of hydroxyl radicals corresponding to more than 10^5 OH radicals cm^{-3} sec^{-1} is required.

Furthermore, if the diffusive upward current of CO molecules by eddy diffusion given by (111a) corresponds to the oxidation of CO by OH, we may write

$$n(CO)\, K \left(\frac{1}{H_{CO}} - \frac{1}{H_M} \right) = n(CO)\, a_{36}\, n(OH)\, H_{CO} \tag{112}$$

Equation (112), with $K = 3 \times 10^3$ and $H \simeq 1$ km, leads to $n(OH) > 10^6$ cm^{-3} (Seiler and Warneck, 1972). Such a value is very high when the reaction between OH and CH_4 is considered. With a concentration of about 10^{-2} $O(^1D)$ atoms at 10 km, as given by McConnell et al. (1971), it is difficult to produce more than 5×10^2 OH molecules cm^{-3} sec^{-1} and to reach a concentration of 10^6 OH molecules cm^{-3} at 10 km. The loss process by the reaction between OH and CH_4 reaches about 1.5×10^{-2} sec^{-1}.

In conclusion, the aeronomic conditions (Figure 14) are different in the lower and upper stratosphere. The ratio of the hydroxyl and hydroperoxyl radical concentrations depends on reactions with oxygen atoms in the upper stratosphere, but is related to the carbon monoxide and nitric oxide concentrations in the lower stratosphere. Furthermore, the dissociation and reformation of water vapor are related to the presence of CH_4 and H_2 and their vertical distribution in the lower stratosphere. On the other hand, the NO_x concentrations depend not only on the vertical transport from or to the stratosphere of NO and NO_2, but also on the formation of nitric acid, its dissociation, and finally its downward transport to the troposphere.

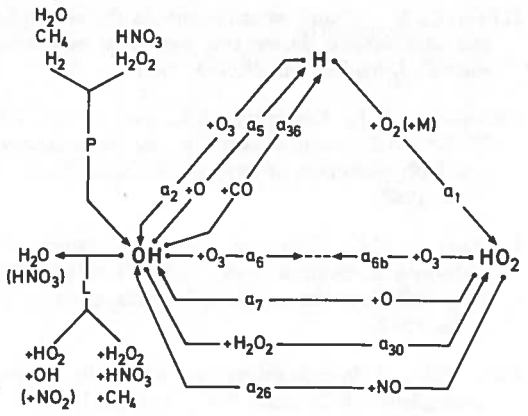

Figure 14. Reaction scheme showing the water vapor cycle in the stratosphere.

REFERENCES

Ackerman, M., "Ultraviolet solar radiation related to mesospheric processes", in *Mesospheric Models and Related Experiments*, Reidel Publ. Cy., Dordrecht, pp. 149-159, 1971.

Ackerman, M., and Frimout, D., "Mesure de l'absorption stratosphérique du rayonnement solaire de 3,05 a 3,70 microns", Bull. Acad. Roy. Belgique, Cl. Sc., *55*, 948, 1969.

Ackerman, M., Frimout, D., and Pastiels, R., "New ultraviolet solar flux measurements at 2000 A using a balloon borne instrument", in *New Techniques in Space Astronomy*, Reidel Publ. Cy., Dordrecht, pp. 251-253, 1971.

Bainbridge, A.E., and Heidt, L.E., "Measurements of methane in the troposphere and lower stratosphere", Tellus, *18*, 221, 1966.

Bates, D.R., and Hays, P.B., "Atmospheric nitrous oxide", Planet. Space Sci., *15*, 189, 1967.

Bates, D.R., and Nicolet, M., "Photochemistry of water vapor", J. Geophys. Res., *55*, 301, 1950.

Breen, J.E., and Glass, G.P., "Rates of some hydroxyl radical reactions", J. Chem. Phys., *52*, 1082, 1970.

Cadle, R.D., "Daytime atmospheric O(^{1}D)", Disc. Faraday Soc., *37*, 66, 1964.

Caldwell, J., and Back, R.A., "Combination reactions of hydroxyl radicals in the flash photolysis of water vapor," Trans. Faraday Soc., *61*, 1939, 1965.

Calvert, J.G., Alistair Kerr, J., Demerjian, K.L., and McQuigg, R.D., "Photolysis of formaldehyde as a hydrogen source in the lower atmosphere", Science, *175*, 751, 1972.

Chapman, S., "A theory of upper atmospheric ozone", Memoirs Roy. Met. Soc., *3*, 103, 1930.

Chapman, S., "Photochemistry of atmospheric oxygen", Reports Prog. Phys., *9*, 92, 1943.

Clyne, M.A.A., and Thrush, B.A., "Rates of elementary processes in the chain reaction between hydrogen and oxygen: I. Reactions of oxygen atoms", Proc. Roy. Soc., *A275*, 544, 1963a.

Clyne, M.A.A., and Thrush, B.A., "Kinetics of the reaction of hydrogen atoms with molecular oxygen", Proc. Roy. Soc., *A275*, 559, 1963b.

Clyne, M.A.A., McKenney, D.J., and Thrush, B.A., "Rate of combination of oxygen atoms with oxygen molecules", Trans. Faraday Soc., *61*, 2701, 1965.

Clyne, M.A.A., Thrush, B.A., and Wayne, R.P., "Kinetics of the chemiluminescent reaction between nitric oxide and ozone", Trans. Faraday Soc., *60*, 359, 1964.

Crutzen, P.J., "The influence of nitrogen oxides on the atmospheric ozone content", Quart. J. Roy. Met. Soc., *96*, 320, 1970.

Davis, D.D., Private communication (1972).

Dixon-Lewis, G., and Williams, A., "Role of hydroperoxyl in hydrogen oxygen flames", Nature, *196*, 1309, 1962.

Dixon-Lewis, G., Wilson, W.E., and Westenberg, A.A., "Studies of hydroxyl radical kinetics by quantitative ESR", J. Chem. Phys., *44*, 2877, 1966.

Demore, W.D., "New mechanism for OH catalyzed chain decomposition of ozone", J. Chem. Phys., *46*, 813, 1967.

Demore, W.D., "O(^{1}D) quenching efficiency of O_2 relative to other gases", J. Chem. Phys., *52*, 4309, 1970.

Demore, W.D., and Raper, O.F., "Primary processes in ozone photolysis", J. Chem. Phys., *44*, 1780, 1966.

Ditchburn, R.W., and Young, P.A., "The absorption of molecular oxygen between 1850 and 2500 Å", J. Atm. Terr. Phys., *24*, 127, 1962.

Donovan, R.J., Husain, D., and Kirsch, L.J., "Reactions of oxygen atoms: Part II. Relative rate data for the quenching of O($^1D_2$) using the OH radical as a spectroscopic marker", Chem. Phys. Letters, *6*, 488, 1970.

Donovan, R.J., Husain, D., and Kirsch, L.J., "The rate of the reaction $O + O_2 + M \rightarrow O_3 + M$ (M = He, Ar and Kr)", Trans. Faraday Soc., *66*, 2551, 1970.

Dütsch, H.U., "The photochemistry of stratospheric ozone", Quart. J. Roy. Met. Soc., *94*, 483, 1968.

Ehhalt, D.H., Heidt, L.E., and Martell, E.A., "The concentration of atmospheric methane between 44 and 62 kilometers altitude", J. Geophys. Res. *77,* 2193, 1972.

Foner, S.N., and Hudson, R.L., "Mass spectrometry of the HO_2 free radical", J. Chem. Phys., *36,* 2681, 1962.

Goldman, A., Murcray, D.G., Murcray, F.H., Williams, W.J., Kyle, T.G., and Brooks, J.N., "Abundance of N_2O in the atmosphere between 4.5 and 13.5 km", J. Opt. Soc. Amer., *60,* 1466, 1970.

Gray, D., Lissi, E., and Heicklen, J., "The reaction of H_2O_2 with NO_2 and NO", to be published, 1972.

Greenberg, R.I., and Heicklen, J., "Reaction of $O(^1D)$ with N_2O", Int. J. Chem. Kinet., *2,* 185, 1970.

Greiner, N.R., "Hydroxyl radical kinetics by kinetic spectroscopy: III. Reactions with H_2O_2 in the range 300-450°K", J. Phys. Chem., *72,* 406, 1968.

Greiner, N.R., "Hydroxyl radical kinetics by kinetic spectroscopy: V. Reactions with H_2 and CO in the range 300-500°K", J. Chem. Phys., *51,* 5049, 1969.

Greiner, N.R., "Hydroxyl radical kinetics by kinetic spectroscopy: VI. Reactions with alkanes in the range 300-500°K", J. Chem. Phys., *53,* 1070, 1970.

Hampson, J., Photochemical behavior of the ozone layer, Technical Note 1627, Canadian Arm. Res. and Dev. Establishment, 1964.

Hasson, V. and Nicholls, R.W., "Absolute spectral measurements on molecular oxygen from 2640-1920 A: II. Continuum measurements, 2430-1920 Å", J. Phys., *B4,* 1789, 1971.

Hays, P.B., and Olivero, J.J., "Carbon dioxide and monoxide above the troposphere", Planet. Space Sci., *18,* 1729, 1970.

Heicklen, J., "Gas-phase reactions of alkylperoxy and and alkoxy radicals", Advances in Chemistry Series, No. 76, p. 23, 1968.

Heicklen, J., Simonaitis, R., Greenberg, R., Krezenski, D., Goldman, R., and Lissi, E., "Reaction of oxygen atoms $O(^1D)$", to be published, 1971.

Hesstvedt, E., On the photochemistry of ozone in the ozone layer, Geof. Publik., *27,* 1968.

Hesstvedt, E., "Vertical distribution of CO near the stratopause", Nature, *225,* 50, 1970.

Hilsenrath, E., "An ozone measurement in the mesosphere and stratosphere by means of a rocket sonde", J. Geophys. Res., *74,* 6873, 1969.

Hilsenrath, E., "Ozone measurements in the mesosphere and stratosphere during two significant geophysical events", J. Atmos. Sci., *28,* 295, 1971.

Hochanadel, C.J., Ghormley, J.A., and Boyle, J.W., "Vibrationally excited ozone in the pulse radiolysis and flash photolysis of oxygen", J. Chem. Phys., *48,* 2416, 1968.

Hochanadel, C.J., Ghormley, J.A.. and Ogren, P.J., "Absorption spectrum and reaction kinetics of the HO_2 radical in the gas phase", J. Chem. Phys., *56,* 4426, 1972.

Hunt, B.G., "Photochemistry of ozone in a moist atmosphere", J. Geophys. Res., *71,* 1385, 1966.

Husain, D., and Norrish, R.G.W., "The production of NO_3 in the photolysis of nitrogen dioxide and of nitric acid vapour under isothermal conditions", Proc. Roy. Soc., *273A,* 165, 1963.

Johnston, H., "Gas phase reaction kinetics of neutral oxygen species", National Standard Reference Data Series, NBS 20, 1968.

Johnston, H., "Reduction of stratospheric ozone by nitrogen oxide catalysts from SST exhaust", Science, *173,* 517, 1972.

Johnston, H.S., and Crosby, H.J., "Kinetics of the fast gas phase reaction between ozone and nitric oxide", J. Chem. Phys., *22,* 689, 1954.

Jones, I.T.N., and Wayne, R.P., "Photolysis of ozone by 254-, 313-, and 334-nm radiation", J. Chem. Phys., *51,* 3617, 1969.

Junge, C.E., Seiler, W., and Warneck, P., "The atmospheric ^{12}CO and ^{14}CO budget", J. Geophys. Res., *76,* 2866, 1971.

Kaufman, F., "Aeronomic reactions involving hydrogen: A review of recent laboratory studies", Ann. Geophys., *20,* 106, 1964.

Kaufman, F., "Neutral reactions involving hydrogen and other minor constituents", Canad. J. Chem., *47,* 1917, 1969.

Kaufman, F., and Kelso, J.R., "M effect in the gas-phase recombination of O with O_2", J. Chem. Phys., *46,* 4541, 1967.

Klein, F.S., and Herron, J.T., "Mass-spectrometry study of the reactions of O atoms with NO and NO_2", J. Chem. Phys., *41,* 1285, 1964.

Krezenski, D.C., Simonaitis, R., and Heicklen, J., "The reactions of $O(^3P)$ with ozone and carbonyl sulfide", Int. J. Chem. Kinetics, *3,* 467, 1971.

Krueger, A.J., "Rocket measurements of ozone over Hawaii", Ann. Geophys., *25,* 307, 1969.

Langley, K.F., and McGrath, W.D., "The ultraviolet photolysis of ozone in the presence of water vapor", Planet. Space Sci., *19*, 413, 1971.

Larkin, F.S., and Thrush, B.A., "Recombination of hydrogen atoms in the presence of atmospheric gases", Disc. Faraday Soc., *37*, 112, 1964.

Leighton, P.A., *Photochemistry of Air Pollution*, Academic Press, New York, 1961.

Levy, H. II, "Normal atmosphere: Large radical and formaldehyde concentrations predicted", Science, *173*, 141, 1971.

Leovy, C.B., "Atmospheric ozone: An analytic model for photochemistry in the presence of water vapor", J. Geophys. Res., *74*, 417, 1969.

McConnell, J.C., McElroy, M.B., and Wofsy, S.C., "Natural sources of CO", Nature, *233*, 187, 1971.

McCrumb, J.L., and Kaufman, F., "Kinetics of the O + O_3 reaction", J. Chem. Phys, in press, 1972.

McElroy, M.B., and McConnell, J.C., "Nitrous oxide: A natural source of stratospheric NO", J. Atmos. Sc., *28*, 1095, 1971.

McGrath, W.D., and Norrish, R.G.W., "Influence of water on the photolytic decomposition of ozone", Nature, *182*, 235, 1958.

McQuigg, R.D., and Calvert, J.G., "The photodecomposition of CH_2O, CD_2O, CHDO and CH_2O-CD_2O mixtures at Xenon flash lamp intensities", J. Amer. Chem. Soc., *91*, 1590, 1969.

Morris, E.D., and Niki, H., "Mass spectrometric study of the reactions of nitric acid with O atoms and H atoms", J. Phys. Chem., *75*, 3193, 1971.

Morris, E.D., and Niki, H., "Mass spectrometric study of the reaction of hydroxyl radical with formaldehyde", J. Chem. Phys., *55*, 1991, 1971.

Morris, E.D., and Niki, H., "Reactivity of hydroxyl radicals with olefins", J. Phys. Chem., *75*, 3640, 1971.

Mulcahy, M.F.R., and Williams, D.J., "Kinetics of combination of oxygen atoms with oxygen molecules", Trans. Faraday Soc., *64*, 59, 1968.

Mulcahy, M.F.R., and Smith, R.H., "Reactions of OH radicals in the H - NO_2 and H - NO_2 - CO systems", J. Chem. Phys., *54*, 5215, 1971.

Murcray, D.R., Kyle, T.G., Murcray, F.H., and Williams, W.J., "Presence of HNO_3 in the upper atmosphere", J. Opt. Soc. Amer., *59*, 1131, 1969.

Nicolet, M., "Nitrogen oxides in the chemosphere", J. Geophys. Res., *70*, 679, 1965.

Nicolet, M., "Ozone and hydrogen reactions", Ann. Geophys., *26*, 531, 1970a.

Nicolet, M., "Aeronomic reactions of hydrogen and ozone", Aeronomica Acta, *A-79*, 1970b and in *Mesospheric Models and Related Experiments*, Reidel Publ. Cy. Dordrecht, pp. 1-51, 1971.

Nicolet, M., "Photochimie de l'ozone dans la stratosphère sous l'action des oxydes d'azote et des composés de l'hydrogène", Bull. Acad. Roy. Belgique, Cl. Sc., *57*, 935, 1971.

Nicolet, M. "Un regard sur la stratosphère", Aeronomica Acta, *A-91*, 1971.

Nicolet, M. et Vergison, E., "L'oxyde azoteux dans la stratosphère", Aeronomica Acta, *A-90*, 1971.

Niki, H., "Reaction of $O(^3P)$ atoms with formaldehyde", J. Chem. Phys., *45*, 2330, 1966.

Niki, H., Daby, E., and Weinstock, B., "Reaction of atomic oxygen with methyl radicals", J. Chem. Phys., *48*, 5729, 1969.

Noxon, J.F., "Optical emission from $O(^1D)$ and $O_2(b^1\Sigma g)$ in ultraviolet photolysis of O_2 and CO_2", J. Chem. Phys., *52*, 1852, 1970.

Ogawa, M., "Absorption cross sections of O_2 and CO_2 continua and far uv regions", J. Chem. Phys., *54*, 2550, 1971.

Paraskevopoulos, G., and Cvetanović, R.J., "Competitive reactions of the excited oxygen atoms, $O(^1D)$", J. Amer. Chem. Soc., *91*, 7572, 1969.

Paraskevopoulos, G., and Cvetanović, R.J., "Relative rate of reaction of $O(^1D_2)$ with H_2O", Chem. Phys. Letters, *9*, 603, 1971.

Paukert, T.T., "Spectra and kinetics of the hydroperoxyl free radical in the gas phase", University of California, Berkeley, UCRL-19109, 1969.

Phillips, L.F., and Schiff, H.I., "Reactions of hydrogen atoms with nitrogen dioxide and with ozone", J. Chem. Phys., *37*, 1233, 1962.

Pontano, B.A., and Hale, L.C., "Measurements of an ionizable constituent of the low ionosphere using a Lyman- α source and blunt probe", Space Research, *10*, 208, 1970.

Pressman, J.A., and Warneck, P., "The stratosphere as chemical sink for carbon monoxide", J. Atmos. Sci., *27*, 155, 1970.

Randhawa, J.S., "The vertical distribution of ozone near the equator", J. Geophys. Res., *76*, 8139, 1971.

Rhine, P.E., Tubbs, L.D., and Williams, D., "Nitric acid vapor above 19 km in the earth's atmosphere", Applied Optics, *8*, 1500, 1969.

Roney, P.L., "On the influence of water vapour on the distribution of stratospheric ozone", J. Atmos. Terr. Phys., *27,* 1177, 1965.

"SCEP" *Man's Impact on the Global Environment: Assessment and Recommendations for Action.* Report of the study of critical environmental problems (SCEP), MIT Press, Cambridge, Mass., 1970.

Schiff, H.I., "Reactions involving nitrogen and oxygen", Ann. Geophys., *20,* 115, 1964.

Scholz, T.G., Ehhalt, D.H., Heidt, L.E., and Martell, E.A., "Water vapor, molecular hydrogen, methane and tritium concentrations near the stratopause", J. Geophys. Res., *75,* 3049, 1970.

Schutz, K., Junge, C., Beck, B., and Albrecht, B., "Studies of atmospheric N_2O", J. Geophys. Res., *75,* 2230, 1970.

Seiler, W., and Junge, C., "Decrease of carbon monoxide mixing ratio above the polar tropopause", Tellus, *21,* 447, 1969.

Seiler, W., and Warneck, P., "Decrease of CO mixing ratio at the tropopause", J. Geophys. Res., *77,* 1972, to be published.

Shardanand, "Absorption cross sections of O_2 and O_4 between 2000 and 2800 Å, Phys. Rev., *186,* 5, 1969.

Shimazaki, T., and Laird, A.R., "A model calculation of the diurnal variation in minor neutral constituents in the mesosphere and lower thermosphere including transport effects", J. Geophys. Res., *75,* 3221, 1970.

Singer, S.F., "Stratospheric water vapour increase due to human activities", Nature, *233,* 543, 1971.

Simonaitis, R., and Heicklen, J., "The kinetics of the reaction of OH with NO_2", EOS, *52,* 835, 1971.

"SMIC" *Inadvertent Climate Modification: Report of the Study of Man's Impact on Climate* (SMIC), MIT Press, Cambridge, Mass., 1971.

Spicer, C.W., Villa, A., Wiebe, H.A., and Heicklen, J. "The reactions of methylperoxy radicals with NO and NO_2", to be published, 1972.

Strobel, D.F., "Odd nitrogen in the mesosphere", J. Geophys. Res., *76,* 8384, 1971 and "Nitric oxide in the D region", 1972, to be published.

Westenberg, A.A. and deHaas, N., "Atom-molecule kinetics using ESR detection: Results for O + OCS, O+CS_2, O + NO_2 and H + C_2H_4", J. Chem. Phys., *50,* 707, 1969.

Wilson, A.W., "Ozone production in the stratosphere", in *Les problèmes météorologiques de la stratosphère et de la mésosphère,* Presses Universitaires, Paris, pp. 383-392, 1966.

Wilson, W.E., and O'Donovan, J.T., "Mass-spectrometry study of the reaction rate of OH with itself and with CO", J. Chem. Phys., *47,* 5455, 1967.

Young, R.A., Black, G., and Slanger, T.G., "Reaction and deactivation of $O(^1D)$", J. Chem. Phys., *49,* 4758, 1968.

DISCUSSION

H. Dütsch noted that some photodissociation of HNO_3 must be assumed to account for its observed distribution, with a maximum at about 25 km. Nicolet replied that the HNO_3 absorption was being studied in the laboratory, and that some photodissociation might exist; a photodissociation coefficient of 10^{-7} would still be important for OH concentrations of 10^4 or 10^5 per cc. Dutsch asked how important the NO + HO_2 reaction is, pointing out that it might improve the agreement of the HNO_3 model with the observed distribution. Nicolet replied that there had been no direct measurement of that reaction, but smog chemists were using a working value of 5×10^{-14} cm^3 sec^{-1}, and it might have a value of the order of 10^{-12} cm^3 sec^{-1}. He added that photodissociation of HO_2 had not been introduced into his analysis, but its dissociation coefficient in the gas phase might be 10^{-4} sec^{-1}. H. Johnston offered recent absorption-spectrum information on both reactions: nitric acid has an absorption cross-section of 10^{-17} at 2000 Å; HO_2 has about the same absorption coefficient in the gas phase as in liquid solution, but its peak absorption wavelength is about 200 Å shorter in the gas phase. He noted that Wayne had suggested that nitric acid might photolyze to give H + NO_3 instead of OH + NO_2 at short wavelengths.

A. Goldburg asked on what basis Nicolet identified certain concentrations as being equivalent to SST emissions. Nicolet cited Table 1.4 of the SCEP report for H_2O and NO, and said he had divided the latter by a factor of 4. Goldburg said the SCEP report's NO emission rate was high by more than a factor of 10, according to GE calculations. Nicolet replied that the difference was less than a factor of 2.

J. McConnell added comments on HO_2 and OH.

TRACE MATERIAL COMPOSITION OF THE LOWER STRATOSPHERE

JAMES P. FRIEND
Department of Meteorology and Oceanography
New York University
Bronx, N.Y. 10453

ABSTRACT: Recent investigations suggest that the global natural distributions in the atmosphere of ozone, methane, carbon monoxide, and oxides of nitrogen are linked together through a photochemical system. This system operates as follows: ozone photolysis produces $O(^1D)$, which oxidizes N_2O to NO and also reacts with H_2O to give OH; OH attacks CH_4, giving rise to a chain that ultimately produces CO and OH; NO and subsequent NO_2 react with O_3 and O to regulate odd oxygen. The system appears to prevail in the lower stratosphere.

Review of known aspects of global sources, sinks, and concentrations of various trace substances of importance in the lower stratosphere reveals the following:

a. *H_2O vapor.* Temporal and spatial variations of concentrations are not well enough known to resolve the controversy between "dry sky" advocates and those who think water-vapor mixing ratios are non-uniform in the vertical. Also, more data are necessary to establish trends in lower stratospheric water-vapor concentrations. It is important to start a proper global-scale measurement program at the earliest possible time because increasing use of the lower stratosphere by commercial jet aircraft will preclude obtaining data on natural water vapor in that region.
b. *Methane.* Estimates of global sources are quite crude. Model calculations based on an oxidation of methane by OH attack followed by several other steps seem to agree with the relatively few available concentration measurements. The residence time of methane resulting from the model calculations is 0.3 yr.
c. *Carbon monoxide.* Since oxidation of methane seems to be a principal source of CO, natural sources are now thought to outweigh polluting sources by a factor of about 15. CO may be removed from the atmosphere largely by reaction with OH radicals. However, soil bacteria may contribute to removal at the earth's surface. Crude models suggest a residence time of 0.20 yr for CO.
d. *Ozone.* The photochemistry of stratospheric ozone appears to be affected by natural background concentrations of NO and NO_2. Enough information on stratospheric concentrations of O_3 exists so that it can be stated that transport by atmospheric general circulations, as well as photochemistry, is important in the global distribution of ozone.
e. *Sulfate aerosol.* Stratospheric sulfate aerosols may be formed by the gas-phase oxidation of SO_2 by O-atoms. Much of the SO_2 that enters the stratosphere may be of volcanic origin. Comparison of sulfate concentrations with those of the other trace materials considered in the paper shows the aerosol to be relatively much less abundant.

INTRODUCTION

It is necessary to understand the behavior of naturally occurring trace materials in the stratosphere if we are to assess the impact of pollutants on that region, and if we are to estimate the possible ensuing climatic changes. The paper reviews the broad atmospheric chemical aspects of the "major" trace constituents of the stratosphere (H_2O, O_3, CH_4, and $SO_4^=$ aerosol), and points out the areas in which further "background" knowledge is needed.

While the paper deals primarily with chemical aspects, it should be kept in mind that atmospheric dynamics plays a major role in regulating the magnitudes of the various chemical effects. It seems clear that the goal of the Climatic Impact Assessment Program will be accomplished only after a suitable melding of the appropriate chemistry and atmospheric dynamics has been formulated, tested, and verified. The desired product of such melding is, of course, a model that will represent the chemistry and meteorology of the lower stratosphere and atmospheric phenomena in adjacent regions, such as transfer to and removal in the troposphere of ozone and aerosols. Without "baseline" data on the concentrations of the various trace materials, the models cannot be tested and

verified. Thus this paper focuses on baseline information concerning global-scale distributions of important trace constituents and potential pollutants in the stratosphere.

A GLOBAL-SCALE ATMOSPHERIC CHEMICAL SYSTEM

A decade or so ago, when Junge [1] wrote his pioneering book on atmospheric chemistry, the trace gaseous substances water vapor, ozone, carbon monoxide, and methane were considered to be virtually independent and non-interacting in the lower atmosphere, and even in the lower stratosphere. The oxides of nitrogen, NO and NO_2, were recognized as playing complex roles in the formation of photochemical smog [2], but were considered of little importance elsewhere because their concentrations in nature are so small. Nitrous oxide, N_2O, was known to be produced by soil bacteria participating in nitrogen fixation, but was considered to be virtually inert and of little significance in the atmosphere.

A body of knowledge is currently developing which seems to present a picture in quite remarkable contrast to the above-described situation. A summary discussion of the picture is given below. Detailed presentation with references is foregone; however, the basic material is contained in the works of Westberg, Cohen, and Wilson [3]; Levy [4]; Johnston [5,6]; McConnell, McElroy, and Wofsy [7]; McElroy and McConnell [8]; Singer [9]; Calvert et al. [10]; and Weinstock and Niki [11]. Many other important investigations have contributed to the present knowledge; these works are cited in the above-listed references.

While considering the chemical reactions given below the reader should keep in mind these natural global sources:

Table 1. Natural Global Sources of Atmospheric Trace Gases

Substance	Global Source
Ozone, O_3	Stratospheric photochemical reactions
Methane, CH_4	Decay of vegetation in swamps and paddy fields, and enteric fermentation
Nitrous oxide, N_2O	Nitrogen-fixing bacteria in soils

The reactions

$$O_3 + h\upsilon(\lambda < 3100\ \text{Å}) \rightarrow O(^1D) + O_2 \qquad (1a)$$

$$O_3 + h\upsilon(\lambda < 3100\ \text{Å}) \rightarrow O(^3P) + O_2 \qquad (1b)$$

$$O + O_2 + M \rightarrow O_3 + M \qquad (2)$$

illustrate the "all-oxygen" system that would exist in the lower stratosphere below the elevation (about 25 km) of maximum ozone concentration created by photochemical equilibrium in a hypothetical stagnant atmosphere. Reaction (1a) creates $O(^1D)$, which, in effect, is the starting point for all the subsequent reactions. Note that reaction (1a) could occur in natural atmospheres close to the earth's surface where measurable amounts of ozone of stratospheric origin have been found [12]. The reaction

$$N_2O + O(^1D) \rightarrow 2\ NO \qquad (3)$$

has been studied for its importance in the lower atmosphere [8], and it has been concluded that it is the source of a natural background of NO in the lower stratosphere. McElroy and McConnell [8] estimate that the rate of production of NO in the lower stratosphere is approximately the same as the estimated rates of NO production in the stratosphere by routine operation of 500 SST's. The reactions:

$$NO + O_3 \rightarrow NO_2 + O_2 \qquad (4)$$

$$NO_2 + O \rightarrow NO + O_2 \qquad (5)$$

and other pairs involving NO_x (NO and/or NO_2) have been recognized by Johnston [5] to constitute a catalytic system for the destruction of odd oxygen (O and O_3). Consequently, the presence of NO_x in the stratosphere limits the amounts of odd oxygen. It now appears that the *natural* concentrations of ozone in the stratosphere are regulated by an interlinking of the all-oxygen system and the NO_x catalytic system in which reaction (3) forms the critical bridge. For accurate descriptions of the above and subsequent systems several other reactions must be taken into account. Such reactions are the photolysis of NO_2, quenching of $O(^1D)$, and radical-radical combinations. The reactions presented in this section illustrate the main interconnections of the various chemical systems; they are not to be construed as a complete mechanism.

Another important reaction of $O(^1D)$ is

$$O(^1D) + H_2O \rightarrow 2\,OH \qquad (6)$$

This appears to be the principal source of OH radicals in natural and polluted atmospheres, with more $O(^1D)$ being supplied by photolysis of NO_2 in polluted atmospheres.

The reaction of OH with O_3 to form HO_2 and the reaction of HO_2 with O-atoms to form OH (along with other reactions of OH, HO_2, O, and O_3) constitute another catalytic system for the removal of odd oxygen in the stratosphere. Johnston [5] has pointed out that such cycles would have a trivial effect on odd oxygen in the presence of NO_x at mixing ratios in excess of 10^{-9}. In view of McElroy and McConnell's [8] work, as mentioned above, it appears that cycles involving the radical species derived from H_2O are not important in regulating natural concentrations of odd oxygen.

Johnston [6] has shown that nitric acid can be created in the stratosphere by the reaction

$$NO_2 + OH + M \rightarrow HNO_3 + M \qquad (7)$$

He indicates that any NO_2 created in the mesosphere would probably be converted to HNO_3 before reaching the lower stratosphere. If this is the case, reaction (7) would be applicable to NO_2 generated originally from reactions (3) and (4) occurring in the lower stratosphere.

The further importance of OH appears to lie in its ability to attack CH_4 and CO in chemical cycles that involve HO_2. The oxidation of methane could proceed, according to Levy [4], by the following reactions:

$$CH_4 + OH \rightarrow CH_3 + H_2O \qquad (8)$$

$$CH_3 + O_2 \rightarrow CH_3O_2 \qquad (9)$$

$$CH_3O_2 + NO \rightarrow CH_3O + NO_2 \qquad (10)$$

$$CH_3O + O_2 \rightarrow H_2CO + HO_2 \qquad (11)$$

$$HO_2 + NO \rightarrow NO_2 + OH \qquad (12)$$

$$H_2CO + h\upsilon \rightarrow HCO + H \ (\phi_a > 0.5 \text{ for } \lambda < 3150\,\text{Å})^* \qquad (13a)$$

$$H_2CO + h\upsilon \rightarrow CO + H_2 \ (\phi_b > 0.5 \text{ for } \lambda < 3150\,\text{Å}) \qquad (13b)$$

$$HCO + O_2 \rightarrow HO_2 + CO \qquad (14)$$

$$CO + OH \rightarrow CO_2 + H \qquad (15)$$

$$H + O_2 + M \rightarrow HO_2 + M \qquad (16)$$

Reactions (8) through (12) can be seen to be a cycle regenerating OH through HO_2. Furthermore, from reactions (13) and (14) it is apparent that CO is a natural product of the oxidation of CH_4; this has been estimated by Weinstock and Niki [11] to account for global background concentrations of CO. Carbon monoxide is readily oxidized by OH as in reaction (15). The resultant H-atom forms HO_2 through reaction (16). Thus in polluted atmospheres reactions (6), (15), (16), and (12) can form a cycle wherein CO is oxidized to CO_2; the free-radical species are interconverted among OH, HO_2, and H; and NO is oxidized to NO_2 [3], This mechanism may account for the hitherto unexplained rapid conversion of NO to NO_2 in photochemical smog. Ultraviolet radiation from the sun ($\lambda < 3200$ Å) is important in the whole system through the photolytic reactions of ozone (reactions (1a,b)), NO_2, and formaldehyde (reactions (13a,b)).

In summary, the above set of reactions, though not complete and not usable as a mechanism in modeling studies, illustrates the relationships of the naturally occurring trace substances CH_4, CO, O_3, H_2O, N_2O, NO and NO_2. The connecting links are short-lived free radicals, the most important of which are $O(^1D)$, $O(^3P)$, OH, HO_2, and H. In particular, the natural atmospheric chemical system described can be thought to have three main interconnected subsystems as in Figure 1. ing scheme:

The system also operates in polluted atmospheres where photochemical smog is prevalent.

* ϕ is the quantum yield

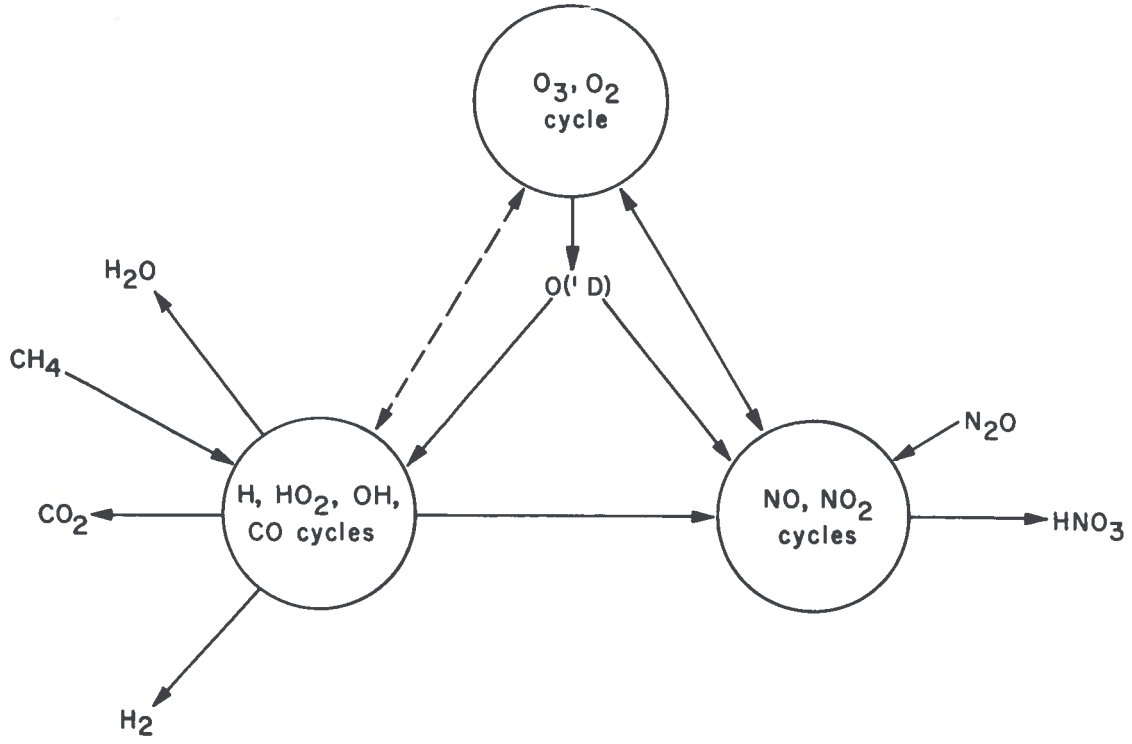

Figure 1. Relationship of cycles in the natural atmospheric chemical system. (The dashed line connecting the oxygen system to the hydrogen-water system indicates its lesser importance compared to the other linkages.)

In these polluted atmospheres, however, it is necessary to consider the involvement of olefinic and other hydrocarbons besides CH_4. The role of N_2O is probably quite negligible, since NO_x is present in urban atmospheres in relatively great abundance.

THE GLOBAL-SCALE CHEMICAL ASPECTS OF TRACE MATERIALS IN THE LOWER STRATOSPHERE

This section presents brief summaries of sources, sinks, concentrations, and major features of trace substances in the lower stratosphere.

1. *Water Vapor*
   a. Sources. The primary source of water vapor in the lower stratosphere is thought to be the hydrologic cycle operative at the surface of the earth and in the troposphere. An additional possible source is the oxidation of methane of terrestrial origin in the lower stratosphere (cf. reference 9 and reactions (8) - (16) in the previous section).

   b. Concentrations. The concentrations of water vapor are generally found to be in the range of (1 to 8) x 10^{-6} g H_2O/g air throughout most of the lower stratosphere. An average value of 2 x 10^{-6} g/g = 3.2 ppm (by volume) would be representative for 20 km altitude. (See the remarks below.)

   c. Sinks. Most of the water vapor in the lower stratosphere is ultimately transported into the troposphere by the dynamic processes of turbulent diffusion, large-scale mean circulations, and mesoscale extrusions at mid-latitudes of stratospheric air into the troposphere. Another sink of lesser intensity is photolytic decomposition at high altitudes, which leads eventually to production of H_2 and escape of H-atoms into space.

d. Remarks. A fair degree of controversy has arisen over the relatively sparse data on stratospheric water vapor concentrations. The work of Mastenbrook [13] appears to support a "dry sky", that is, a low mixing ratio constant with height (2×10^{-6} g/g). The works of others, most recently Sissenwine et al. [14], indicate a vertical profile that is in substantial agreement with Mastenbrook's up to about 21 km, where increasing mixing ratio with height then occurs up to at least about 32 km. The controversy has not been resolved. The subject suffers from lack of adequate spatial and temporal coverage in the data. It is a difficult task to provide this adequate data. However, in view of the role of water vapor in climate regulation, and in view of the increasing use of the lower stratosphere by jet aircraft, I feel that a proper program to measure stratospheric water vapor on a global scale is of prime importance. Natural distributions of water vapor will be quite obscured by projected SST operations, so time is an important factor in obtaining the needed measurements.

As was mentioned in the previous section, it is now thought that free radical species derived from water vapor do not play a significant role in regulating ozone concentrations in the lower stratosphere.

2. *Methane*

a. Sources. The main sources and the associated production rates of methane on a global scale are:

Source	Production Rate ($Tg\ yr^{-1}$)*	
Decaying vegetation in paddy fields and swamps	1450	(ref 15)
Enteric fermentation (mostly in cattle)	45	(ref 9)
Coal fields, grasslands, forests	30	(ref 15)
Total production rate	1500 $Tg\ yr^{-1}$	

*Tg = teragram = 10^{12} grams (IUPAP international standard nomenclature)

Singer [9] pointed out that raising cattle constitutes a potentially important human-controlled source of methane. In his paper he quoted a production rate of 270 Tg yr^{-1} (taken from a work by Koyama) for decaying vegetation in swamps and paddies. Robinson and Robbins [15] revised upward this earlier quoted estimate by a factor of about 5. In the present listing the proportion from enteric fermentation is thus considerably smaller than that discussed by Singer.

b. Concentrations. From the work of Bainbridge and Heidt [16] and Ehhalt [7] the following can be put forth as estimates of global average concentrations of methane:

Surface (clean air)	0.7 - 1.7 ppm (1.2 ppm average)
Tropopause	1.1 ppm
20 km	1 ppm

c. Sinks. The sink in the troposphere is large and may be due to the oxidation scheme discussed previously [11,17]. The model study by McConnell et al. [7] is consistent with reaction (8) being the primary sink of methane in the troposphere and the stratosphere.

d. Remarks. The residence time for methane calculated by McConnell et al. [7] from their model is 0.3 yr. Oxidation of CH_4 by O-atoms may be a source of OH in the stratosphere [18]. Oxidation of methane may be a source of H_2 above 20 km altitude [19].

3. *Carbon Monoxide*

a. Sources. The sources of carbon monoxide and estimated production rates are:

	Production Rate ($Tg\ yr^{-1}$)	
Fuel combustion	270	SCEP [20]
Oxidation of CH_4	2500	ref 7
Forest fires	10	ref 15
Terpene oxidation	11	ref 15
Oceans	(9)	ref 21
Total production rate	2800+ $Tg\ yr^{-1}$	

Swinnerton et al. [21] reported finding concentrations of CO in surface ocean waters that are in excess of those expected for equilibrium with the air above the ocean. The table shows their rough estimate of the strength of this source of CO.

As noted before, the oxidation of methane apparently accounts for most of the background concentrations of CO in clean surface air. The large production rate from this source calculated by McConnell et al. [7] reflects this concept.

b. Concentrations. Background surface air concentrations measured in the early 1950's and again in the late 1960's have shown relatively constant average values of the order of 0.1 ppm with a range of 0.03 - 0.2 ppm. Seiler and Junge [22] reviewed the background measurements and estimated a global average tropospheric value in the range of 0.10 - 0.15 ppm. Seiler and Junge [22] also reported on measurements made in the vicinity of the tropopause: concentrations are of the order of 0.1 ppm at the tropopause, decreasing rapidly with height to less than 0.01 ppm within a few kilometers of the tropopause.

c. Sinks. The tropospheric sink is large and unknown in specific detail. The study of Inman et al. [23] has shown that soil bacteria may constitute a strong, globally distributed sink. Pressman and Warneck [24] have shown that the stratospheric sink of CO is probably the reaction

$$CO + OH \rightarrow CO_2 + H \qquad (15)$$

It appears now that, if the source from CH_4-oxidation is as large as that given in the table above, the stratospheric sink only removes a small fraction of all CO produced. Weinstock and Niki [11] suggest that OH concentration in the troposphere may be sufficient to account for most of the sink with reaction (15).

d. Remarks. Using an average tropospheric concentration of 0.1 ppm (which gives a total amount of CO in the atmosphere of 560 Tg), the average lifetime, τ, relative to the above-listed sources is:

$$\tau = \frac{560\ \text{Tg}}{2800\ \text{Tg yr}^{-1}} = 0.20\ \text{yr.}$$

This result is similar to those of Levy [4] and McConnell et al. [7], who obtained 0.2 yr and 0.3 yr respectively. The latter assumed a global background concentration of 0.15 ppm instead of 0.1 ppm as used above.

Given the widespread but non-uniform distribution of sources and sinks, the "cycle" of CO in the atmosphere is indeed quite complex.

4. *Ozone*

a. Sources. Ozone is created in the stratosphere by the reactions

$$O_2 + h\upsilon\ (\lambda < 2420\ \text{Å}) \rightarrow O + O$$

$$O_2 + O + M \rightarrow O_3 + M$$

Because solar radiation with a wavelength of less than 2420 Å does not effectively penetrate to lower levels, the region of O_3 production is limited to altitudes above 25 km, with the maximum rate of formation occurring at about 35 km (solar elevation of 45^{o}). Ozone can be created in polluted atmospheres in which the O-atoms are derived from photolysis of NO_2.

b. Concentrations. Because of the importance of photochemical processes, ozone concentrations vary with solar elevation and altitude. Additional variation with season occurs beyond that which might be expected from the dependency of photochemistry on solar elevation. A time-averaged meridional cross-section of stratospheric ozone shows a range of concentrations of 0.5 - 10 ppm by volume. In such cross-sections the tropical regions have peak concentrations of mixing ratio at 35 km and peak concentrations of density or partial pressure at 25 km. In the polar regions peak concentrations in density occur at 16 km. The polar latitude peak (spatially defined) attains a maximum in late winter or early spring. At 20 km altitude in mid-latitudes the O_3 concentrations vary in the range 3-5 ppm by volume (volumetric mixing ratio) with a maximum in the late winter or early spring. The foregoing description of O_3 concentrations in the stratosphere corresponds to that given by several authors. It is sufficient, however, to refer to the recent review by Dütsch [25].

c. Sinks. In the region above about 25 km, ozone is destroyed by photolysis (reactions (1a,b)). It is also destroyed in the stratosphere by catalytic reactions involving oxides of nitrogen, such as reactions (4) and (5) [5], if, as stated earlier, the oxidation of N_2O by $O(^1D)$ produces sufficient natural background concentrations of NO [8]. In the absence of NO_x, reactions of O_3 and O-atoms with OH and HO_2 would constitute a sink for O_3. If the mixing ratios of NO_x are in excess of about 10^{-9}, the effects of OH and HO_2 on odd-oxygen removal are insignificant compared to the catalytic destruction by NO_x [5]. A small portion, perhaps about 2%, of the ozone that is created in the stratosphere is transported to the troposphere, where it is destroyed at or near the surface of the earth.

d. Remarks. Consideration of the distributions of O_3 concentrations has led many investigators [26] to conclude that chemical reactions alone cannot account for the major features observed. For example, the occurrence of high concentrations of ozone at low altitudes (16 km) and high latitudes in late winter clearly must result from transport from the source region near the equator at elevations at or above 25 km.

The heating of the middle and upper stratosphere by absorption of radiation by ozone is important to the dynamics of that region. The dynamics of the atmosphere is important in transporting ozone. Thus ozone (with its attendant chemistry) and the atmospheric dynamics are intimately coupled in a complex system, and the detailed understanding of this system still eludes us.

5. *Sulfate Aerosol*

The stratospheric aerosol, which consists mainly of $(NH_4)_2SO_4$ and/or H_2SO_4, is considered briefly here because it is thought to be formed in the stratosphere by gas-phase reactions. Detailed considerations are given by Cadle [27] in this volume.

a. Sources. The oxidation of SO_2 from volcanos, pollution sources, and decay of vegetation (originally emitted as sulfide gases and subsequently oxidized to SO_2) leads to the formation of sulfates. In the stratosphere the reaction

$$SO_2 + O + M \rightarrow SO_3 + M$$

is likely to be the oxidation mechanism.

b. Concentrations. The sulfate aerosol concentrations are quite variable in time and space. Concentrations have been measured in the range of 10^{-2} to 10^{-1} pg cm^{-3} in the region of 20 km altitude. A broad maximum in the vertical profile of concentration exists in the vicinity of 20 km.

c. Sinks. The sulfate aerosol is removed from the stratosphere by transport to the troposphere, from which it is removed by dry deposition or by precipitation.

d. Comments. The median particle radius of the aerosol is about 0.3 μm. The means by which NH_4^+ gets into the aerosol is uncertain, although it seems likely that it originates as NH_3 from the troposphere.

Large volcanic eruptions can cause enhanced stratospheric aerosol concentrations, which would change the albedo and possibly the local heating rate.

6. *Other Materials*

The following substances of interest occur in the stratosphere but have poorly known or unknown concentrations: NO, NO_2, HNO_3, N_2O, SO_2, NH_3, H_2CO. Their respective roles in the stratosphere have been discussed above.

Aitken nuclei (or condensation nuclei) exist in the lower stratosphere in concentrations of the order of 1 cm^{-3} at altitudes up to about 30 km (and perhaps above). No measurements have been made since those of Junge [28] in 1959.

7. *Comparison of Concentrations*

As a final note, the following table makes it possible to compare the concentrations of the various compounds discussed on a molecular basis.

Table 2. Comparison of Concentrations of Trace Substances in the Lower Stratosphere (20 km)

Ozone: 1.5 μg/g = 2.8 x 10^{-12} mole cm^{-3}
Water vapor: 2 μg/g = 1.0 x 10^{-11} mole cm^{-3}
Methane: 1 ppmv = 3.1 x 10^{-12} mole cm^{-3}
Sulfate (NH_4) SO_4: 10^{-1} pg cm^{-3}
= 7.5 x 10^{-16} mole cm^{-3}
Sulfur dioxide (SO_2) = 0.2 ppbv
= 6 x 10^{-16} mole cm^{-3} (extrapolated from troposphere)

Clearly sulfate is in very small abundance in the lower stratosphere compared to O_3, H_2O, and CH_4.

ACKNOWLEDGMENT

This work was supported in part by National Science Foundation Grant No. 24358 GA.

REFERENCES

1. Junge, C.E., *Air Chemistry and Radioactivity,* Academic Press, New York, 1963.

2. Leighton, P.A., *Photochemistry of Air Pollution,* Academic Press, New York, 1961.

3. Westberg, K., Cohen, N., and Wilson, K.W., "Carbon monoxide: its role in photochemical smog formation," Science, *171,* 1013-15, 1971.

4. Levy, H. II, "Normal atmosphere: large radical and formaldehyde concentrations predicted," Science, *173,* 141-3, 1971.

5. Johnston, H., "Reduction of stratospheric ozone by nitrogen oxide catalysts from supersonic transport exhaust," Science, *173,* 517-22, 1971.

6. Johnston, H., "Formation and stability of nitric acid in the stratosphere," submitted to J. Atmos. Sci.

7. McConnell, J.C., McElroy, M.B., and Wofsy, S.C., "Natural sources of atmospheric CO," Nature, *233,* 187-8, 1971.

8. McElroy, M.B., and McConnell, J.C., "Nitrous oxide: a natural source of stratospheric NO," J. Atmos. Sci., *28,* 1095-8, 1971.

9. Singer, S.F., "Stratospheric water vapor increase due to human activities," Nature, *233,* 544-5, 1971.

10. Calvert, J.G., Kerr, J.A., Demerjian, K.L., and McQuigg, R.D., "Photolysis of formaldehyde as a hydrogen atom source in the lower atmosphere," Science, *175,* 751-2, 1972.

11. Weinstock, B., and Niki, H., "Carbon monoxide balance in nature," Science, *176,* 290-2, 1972.

12. Fabian, P., and Junge, C.E., "Global rate of ozone destruction at the earth's surface," Arch. Meteorol., Geophys. Bioklimatol., Series A., *19* (2), 161-72, 1970.

13. Mastenbrook, H.J., "Water vapor distribution in the stratosphere and high troposphere," J. Atmos. Sci., *25,* 299-311, 1968.

14. Sissenwine, N., Grantham, D.D., and Salmela, H.A. "Mid-latitude humidity up to 32 km," J. Atmos. Sci., *25,* 1129-40, 1968.

15. Robinson, E., and Robbins, R.C., "Sources, abundance, and fate of gaseous atmospheric pollutants," Stanford Research Institute Project Report PR-6755. Prepared for the American Petroleum Institute, New York, 1967.

16. Bainbridge, A.E., and Heidt, L.E., "Measurements of methane in the troposphere and lower stratosphere," Tellus, *18,* 221-5, 1966.

17. Ehhalt, D., Private communication.

18. Cadle, R.D., and Powers, J.W., "Some aspects of atmospheric chemical reactions of atomic oxygen," Tellus, *18,* 176-185, 1966.

19. Scholz, T.G., Ehhalt, D.H., Heidt, L.E., and Martell, E.A., "Water vapor, molecular hydrogen, methane, and tritium concentrations near the stratopause," J. Geophys. Res., *75,* 3049-54, 1970.

20. *Man's Impact on the Global Environment: Assessment and Recommendations for Action.* Report of the Study of Critical Environmental Problems (SCEP), M.I.T. Press, Cambridge, Mass., 1970.

21. Swinnerton, J.W., Linnenbom, V.J., and Lamontagne, R.A., "The ocean: a natural source of carbon monoxide," Science, *167,* 984-6, 1970.

22. Seiler, W., and Junge, C.E., "Carbon monoxide in the atmosphere," J. Geophys. Res., *75,* 2217-26, 1970.

23. Inman, R.E., Ingersoll, R.B., and Levy, E.A., "Soil: a natural sink for carbon monoxide," Science, *172,* 1229-31, 1971.

24. Pressman, J., and Warneck, P., "The stratosphere as a chemical sink for carbon monoxide," J. Atmos. Sci., *27,* 155-163, 1970.

25. Dütsch, H.U., "Atmospheric ozone - a short review," J. Geophys. Res., *75,* 1707-12, 1970.

26. See the review in Reiter, E., *Atmospheric Transport Processes,* Part II: Chemical Tracers, USAEC Report TID-25314, 1971.

27. Cadle, R.D., Paper in this volume.

28. Junge, C.E., "Vertical profiles of condensation nuclei in the stratosphere," J. Meteor., *18,* 501, 1961.

DISCUSSION

N. Sissenwine took issue with Friend's water-vapor value. He said he would accept 2 ppm if the only source of water vapor were that in the Hadley cell; he suggested 3 ppm on the theory that the cold trap, which is the governing factor, has heated up over the last few years enough to support 3 ppm. Working with 2 ppm, though, one can easily compute the residence time of water vapor in the stratosphere from the rate and aerial extent of the air ascending through the tropical tropopause, since this is its only source. Sissenwine said he and his associates had decided to accept a velocity value of .03 cm sec^{-1} for this ascending air, with a 2 ppm mixing ratio, over a lateral extent of 17.5^{o} in each hemisphere. (He noted that this is a compromise value, based on an average of the range of values resulting from the studies of Murgatroyd and Singleton, Manabe and Hunt, and Newell.) With these values, one gets a residence time of 760 days.

Sissenwine continued with a survey of other possible sources of water vapor in the stratosphere. Coon and Lodgko recently published measurements which suggest that cumulonimbus clouds are such a source. Six years of weather-radar echoes at AFCRL have led to an estimate for an average of 40.6 million tons of water a day entering the stratosphere as clouds, mostly ice. If 1% of this vaporizes, it would raise the equilibrium mixing ratio one ppm, and so on. (This assumes the same residence time as before, and deals with the stratosphere between 30 and 60 km.) This agrees with Coon and Lodgko, and with an extrapolation over Oklahoma; Roach's WB-57 measurements indicate 5 ppm.

J. McConnell pointed out that recent work on the lifetime of CO indicated that it is a few tenths of a year, not several years, and is removed by a hydroxyl radical. Since the source of the CO is CH_4 in the troposphere and stratosphere, and CH_4 produces water vapor when destroyed, it suggests that the methane in the stratosphere could produce the observed mixing ratio of water, assuming the observed residence time of about two years is correct. Friend agreed, and advocated further measurements.

F. Singer noted that an argument based on any given water-vapor lifetime could rapidly become circular. D. Davis asked whether there was a good reason for excluding formaldehyde as an important stratospheric species. Friend said no, nor hydrogen either, but as far as he knew it had not yet been observed.

THE PHOTOCHEMISTRY OF THE STRATOSPHERE WITH SPECIAL ATTENTION GIVEN TO THE EFFECTS OF NO_x EMITTED BY SUPERSONIC AIRCRAFT

PAUL J. CRUTZEN
Institute of Meteorology
University of Stockholm
Stockholm, Sweden

ABSTRACT: Photodissociation of molecular oxygen in the stratosphere by ultraviolet radiation leads to the production of ozone. Downward transport of some of this ozone explains its natural background in the unpolluted troposphere. Unfortunately, the exact photodissociation rate is uncertain by a factor of almost 3, due to inadequate knowledge of the ultraviolet solar irradiance. Also, the chemical processes that lead to destruction of stratospheric ozone are not well known. Considerable attention has been given recently to the effect of catalytic chains of reactions in which HO_x and NO_x molecules are preserved while ozone and atomic oxygen are converted to molecular oxygen. There are indications that NO_x plays an important role in controlling the amount of ozone in the atmosphere. The concentrations of both HO_x and NO_x can be increased by exhaust effluents from the proposed fleet of stratospheric supersonic aircraft. A simple comparison of the estimated increase of stratospheric NO_x from such effluents with the amount of NO_x required to influence the ozone budget clearly shows that an observable decrease of atmospheric ozone, and hence a reduced protection from hazardous UV radiation, may occur. The problem will probably become most serious locally in summer, when ground-level UV irradiation is at a maximum and exhaust gases disperse slowly in the stratosphere. The exact ozone decrease is hard to predict because of several uncertainties, including those mentioned above. Nevertheless, some results are presented for different choices of parameters. Interactions between HO_x and NO_x may reduce the above effects of SST operation, but will lead to the formation of nitric acid. The possible importance of intermediate steps in the oxidation of methane is briefly discussed.

INTRODUCTION

It was already established in 1930 [1] that the production of ozone in the upper atmosphere takes place via the photodissociation of molecular oxygen

$$\text{R1} \qquad O_2 + h\nu \rightarrow 2O \quad \lambda < 2420\text{Å}$$

and the three-body reaction

$$\text{R2} \qquad O + O_2 + M \rightarrow O_3 + M$$

Ozone, having a peak concentration at altitudes between 15 and 30 km, is a very efficient absorber of solar ultraviolet radiation at wavelengths below about 3100 Å via the process

$$\text{R3a} \qquad O_3 + h\nu \rightarrow O(^1D) + O_2(^1\Delta_g)$$

which leads to the formation of electronically excited atomic and molecular oxygen. Due to this absorption, life at ground levels is protected from the hazardous effect of solar ultraviolet radiation. This protection, so essential to life on our planet, is accomplished by a total mass of ozone equivalent to a 2 to 4.5-mm-thin layer at the earth's surface. The absorption process R3a also provides the dominant energy source for the stratosphere and mesosphere.

The deactivation of $O(^1D)$ is very fast

$$\text{R4} \qquad O(^1D) + M \rightarrow O + M,\ M = O_2, N_2$$

leading to low concentrations of $O(^1D)$ in the atmosphere. Nevertheless $O(^1D)$ plays a crucial role in the chemistry of the upper atmosphere.

The weak absorption of solar radiation via the reaction

$$\text{R3b} \qquad O_3 + h\nu \rightarrow O + O_2 \qquad 3100\text{Å} < \lambda < 11400\text{Å}$$

is the main process responsible for the production of atomic oxygen below about 30 km.

As reactions R2, R3a, and R3b do not lead to a net reduction of odd oxygen, by which term we refer to the sum of atomic oxygen and ozone, it

is necessary to introduce additional reactions in order to balance the odd-oxygen production by process R1. The Chapman reaction [1]

R5 $O + O_3 \rightarrow 2O_2$

is important near the stratopause (50 km), leading to an odd-oxygen destruction rate equal to about 70% of its production rate by process R1. However, in the cold stratosphere below 40 km, its action is greatly reduced due to the large activation energy of R5. Consequently, additional reactions must be considered, and large attention has been given to the catalytic action of H, OH, and HO_2 particles (HO_x) via chains of reactions of the type [2]

R6	$OH+O$	→	$H+O_2$
R7	$H+O_3$	→	$OH+O_2$
Net:	$O+O_3$	→	$2O_2$
R6	$OH+O$	→	$H+O_2$
R8	$H+O_2+M$	→	HO_2+M
R9	HO_2+O	→	$OH+O_2$
Net:	$O+O$	→	O_2
R10	$OH+O_3$	→	HO_2+O_2
R10	$OH+O_3$	→	HO_2+O_2
R13	HO_2+HO_2	→	$H_2O_2+O_2$
R14	H_2O_2+h	→	$2OH$
Net:	$2O_3$	→	$3O_2$
R10	$OH+O_3$	→	HO_2+O_2
R11	HO_2+O	→	$OH+O_2$
Net:	$O+O_3$	→	$2O_2$

In these and other chains for the lower stratosphere, H, OH, HO_2, H_2O_2, and HNO_3 are recycled and a close internal equilibrium is established by R6-R14 and R39-R42.

The production of odd hydrogen particles, by which term we denote H, OH, HO_2, H_2O_2, and HNO_3 together, is accomplished via the reactions

R15	$H_2O+h\nu$	→	$H+OH$ $\lambda<2240$Å
R16	$H_2O+O(^1D)$	→	$2OH$

and maybe in the upper stratosphere and mesosphere by the chain

R17	$H_2O+h\nu$	→	H_2O^{**} $\lambda\approx1.4\mu$m
R18	$H_2O^{**}+O$	→	$2OH$

where H_2O^{**} denotes vibrationally excited water vapour in the $(2\nu_1)$ or $(\nu_1 + \nu_3)$ vibrational modes.

Removal of odd hydrogen in the upper stratosphere and mesosphere takes place by

R19	$OH+OH$	→	H_2O+O
R20	$OH+HO_2$	→	H_2O+O_2
R21	H_2O_2+OH	→	HO_2+H_2O

In the upper stratosphere and mesosphere a close internal equilibrium is established between H, OH, HO_2 and H_2O_2 particles by means of reactions R6-R9.

It is easy to derive the following equations for the concentrations of O (^{1}D) and O:

$$[O(^1D)] = \frac{\mathcal{J}_{3a}\,[O_3]}{k_4\,[M]} \qquad (1)$$

$$[O] = \frac{\{\mathcal{J}_{3a} + \mathcal{J}_{3b}\}\,[O_3]}{k_2\,[O_2]\,[M]} \qquad (2)$$

In the stratosphere, $[O] \ll [O_3]$, and because of the existence of a close chemical equilibrium between atomic oxygen and ozone, any change in the odd-oxygen concentration essentially denotes a change in the ozone concentration. Consequently,

$$\frac{\partial}{\partial t}[O_3] = 2\mathcal{J}_1[O_2] - 2k_5[O]\,[O_3] - 2k_7[H]\,[O_3] - 2k_9[O]\,[HO_2] - 2\mathcal{J}_{14}[H_2O_2] \qquad (3)$$

The last three terms in this expression sum up the catalytic effect of the HO_x particles [3].

For the stratosphere above 30 km, the equation expressing equilibrium between odd-hydrogen production and destruction rates can therefore be written as follows:

$$\{\mathcal{J}_{15} + k_{16}[O^*]\}\,[H_2O] = [OH]\{k_{19}[OH] + k_{20}[HO_2] + k_{21}[H_2O_2]\} \qquad (4)$$

and it is possible to derive approximate values for the concentration of OH at the stratopause level. With the recommended reaction coefficients listed in Table 1, and assuming that

$$\left[\frac{[H_2O]}{[M]} = 5 \times 10^{-6}, \text{ we find } [OH] \approx 3 \times 10^7\right]$$

molecules cm^{-3}.

The above value of [OH] is at least a factor of 3 larger than that experimentally determined [4]. Furthermore, applying this theoretical estimate it follows that the rate of destruction of odd oxygen by the HO_x cycles.

$$D_H \approx -2\, k_6 [O]\ [OH]$$

is equal to 2×10^7 molecules $cm^{-3}sec^{-1}$, which alone is almost twice the production rate of odd oxygen by process R1; to this the effect of reaction R5 must still be added. It seems therefore that some of the applied photochemical parameters given in Table 1 still need some further revision.

The importance of HO_x particles in catalyzing the destruction of odd oxygen decreases rapidly below 45 km; for this very important region in which about 90% of all atmospheric ozone is stored, it is still necessary to consider additional reactions [3, 5].

Table 1. Reactions and Reaction Coefficients

R1	$O_2+h\nu$	→	$O+O$	$\lambda<2420$Å [13], $\mathcal{J}_1 < 10^{-9}$ [3]
R2	$O+O_2+M$	→	O_3+M	$k_2 = 2.04\times10^{-35}\exp(1050/T)$ [9]
R3a	$O_3+h\nu$	→	$O(^1D)+O_2(^1\Delta_g)$	$\lambda \leq 3100$Å [13], $\mathcal{J}_{3a} < 5\times10^{-3}$
R3b	$O_3+h\nu$	→	$O+O_2$	3100Å $\leq \lambda \leq$ 10400Å [3]
R4	$O(^1D)+M$	→	$O+M$	$k_4 = 5\times10^{-11}$ [24]
R5	$O+O_3$	→	$2O_2$	$k_5 = 1.33\times10^{-11}\exp(-2100/T)$ [6]
R6	$O+OH$	→	$H+O_2$	$k_6 = 5\times10^{-11}$ [24]
R7	$H+O_3$	→	OH^*+O_2	$k_7 = 2.6\times10^{-11}$ [24]
R8	$H+O_2+M$	→	HO_2+M	$k_8 = 4\times10^{-32}$ [24]
R9	HO_2+O	→	$OH+O_2$	$k_9 = 2\times10^{-11}$ [24]
R10	$OH+O_3$	→	HO_2+O_2	$k_{10} \leq 10^{-16}$ [31]
R11	$OH+CO$	→	$H+CO_2$	$k_{11} = 10^{-13}$ [19]
R12	HO_2+NO	→	$OH+NO_2$	
R13	HO_2+HO_2	→	$H_2O_2+O_2$	$k_{13} = 8\times10^{-11}\exp(-1000/T)$ [19]
R14	$H_2O_2+h\nu$	→	$2OH$	$\lambda < 5650$Å $J_{14} \geq 5\times10^{-6}$ [3]
R15	$H_2O+h\nu$	→	$H+OH$	$\lambda <$ 2240Å; $J_{15} < 10^{-8}$ [3]
R16	$H_2O+O(^1D)$	→	$2OH$	$k_{14} = 3\times10^{-10}$ [33]
R17	$H_2O+h\nu$	→	H_2O^{**}	$\lambda \approx 1.4\ \mu$m
R18	$H_2O^{**}+O$	→	$2OH$	
R19	$OH+OH$	→	H_2O+O	$k_{19} \approx k_{13}$ [3]
R20	$OH+HO_2$	→	H_2O+O_2	$k_{20} \geq 10^{-11}$ [24]
R21	$OH+H_2O_2$	→	HO_2+H_2O	$k_{21} = 6\times10^{-12}\exp(-600/T)$ [19]
R22	$NO+O_3$	→	NO_2+O_2	$k_{22} = 1.33\times10^{-12}\exp(-1250/T)$ [6]
R23	NO_2+O	→	$NO+O_2$	$k_{23} = 1.67\times10^{-11}\exp(-300/T)$ [6]
R24	NO_2+O_3	→	NO_3+O_2	$k_{24} = 10^{-11}\exp(-3500/T)$ [6]
R25a	$NO_3+h\nu$	→	$NO+O_2$	$J_{25a} \approx 10^{-2}$ (?) [6]
R25b	$NO_3+h\nu$	→	NO_2+O	$J_{25b} \approx 10^{-2}$, $\lambda <$ 5710Å [3]
R26	$NO_2+h\nu$	→	$NO+O$	$J_{26} \approx 5\times10^{-3}$, $\lambda <$ 4000Å [7]
R27	NO_3+NO	→	$2NO_2$	$k_{27} \approx 10^{-11}$ [7]
R28	$NO+h\nu$	→	$N+O$	$J_{28} < 5\times10^{-6}$ [17]
R29	$N+NO$	→	N_2+O	$k_{29} = 2\times10^{-11}$ [25]
R30	$N+O_2$	→	$NO+O$	$k_{30} = 1.2\times10^{-11}\exp(-3525/T)$ [7]
R31	$N+O_3$	→	$NO+O_2$	$k_{31} = 3\times10^{-11}\exp(-1200/T)$ [7]
R32	$N+OH$	→	$NO+H$	$k_{32} = 7\times10^{-11}$ [17]
R33a	$N_2O+O(^1D)$	→	$2NO$	$k_{33a} = 1\times10^{-10}$ [3]
R33b	$N_2O+O(^1D)$	→	N_2+O_2	$k_{33b} = 1\times10^{-10}$ [3]
R34	$N_2O+h\nu$	→	N_2+O	$J_{34} < 5\times10^{-7}$ [3], $\lambda <$ 3370Å

Table 1. Reactions and Reaction Coefficients (Continued)

R35	NO_3+NO_2	→	N_2O_5*	$k_{35} = 7\times10^{-12}$ [26]
R36	N_2O_5*	→	NO_2+NO_3	$k_{36} = 2\times10^{8}$ [26]
R37	N_2O_5*+M	→	N_2O_5+M	$k_{37} = 1.7\times10^{-10}$ [26]
R38a	N_2O_5+M	→	N_2O_5*+M	$k_{38a} = 2\times10^{-5}\exp(-9650/T)$ [26]
R38b	$N_2O_5+h\nu$	→	$2NO_2+O$, NO_2+NO_3	$\mathcal{J}_{38b} \leq 1.7\times10^{-4}$, $\lambda < 8000$ Å
R39	$OH+NO_2$	→	HNO_3*	$k_{39} = 1.05\times10^{-11}\exp(-170/T)$ [27]
R40	HNO_3*+M	→	HNO_3+M	$k_{40} = 2.2\times10^{-10}$ M = H_2O [27] $k_{40} = 2.8\times10^{-11}$, M = He
R41	HNO_3*	→	$OH+NO_2$	$k_{41} = 10^{8}$ [27]
R42	$HNO_3+h\nu$	→	$OH+NO_2$	$J_{42} \geq 5\times10^{-6}$(?) [3]
R43	HNO_3+OH	→	H_2O+NO_3	$k_{43} \overset{?}{\approx} 1.7\times10^{-11}\exp(-1650/T)$ [3]
R44	$CH_4+O(^1D)$	→	CH_3+OH	$k_{44} = 1\times10^{-10}$ [19]
R45	CH_4+OH	→	CH_3+H_2O	$k_{45} = 3.0\times10^{-12}\exp(-1750/T)$ [19]
R46	CH_3+O_2+M	→	CH_3O_2+M	$k_{46} = 6\times10^{-31}$ [21]
R47a	$CH_3O_2+NO_2$	→	$CH_3O_2NO_2$	Reference [28]
R47b	$CH_3O_2+NO_2$	→	CH_2O+HNO_3	Reference [28]
R48	CH_2O+OH	→	$CHO+H_2O$	$k_{48} \geq 7\times10^{-12}$ [29]
R49a	$CH_2O+h\nu$	→	H+CHO	$\lambda < 3200$Å $J_{49a} \overset{?}{\approx} 10^{-5}$ [30]
R49b	$CH_2O+h\nu$	→	$CO+H_2$	$\lambda < 3500$ Å $J_{49b} \overset{?}{\approx} 10^{-5}$ [30]
R50	CHO+O_2	→	$CO+HO_2$	

All reaction rates are expressed in cm-molecule-second units.

CATALYTIC DESTRUCTION OF ODD OXYGEN BY NO_x BELOW 45 KM

The following simple catalytic chain involving NO and NO_2 (NO_x) is important [3, 5, 6].

R22	NO+O_3	→	NO_2+O_2
R23	NO_2+O	→	NO+O_2
Net:	O+O_3	→	$2O_2$

In addition, below 25 km (including the troposphere) some effect may come from the chain

R22	NO+O_3	→	NO_2+O_2
R24	NO_2+O_3	→	NO_3+O_2
R25a	$NO_3+h\nu$ ($\lambda < 11\,\mu$m)	→	NO+O_2
Net:	$2O_3$	→	$3O_2$

provided reaction R25a occurs [3, 6].

Other reactions which do not participate in chains but which are important in defining the equilibrium concentrations of NO, NO_2 and NO_3 are [7]:

R26	$NO_2+h\nu$	→	NO+O ($\lambda < 5710$Å)
R25b	$NO_3+h\nu$	→	NO_2+O
R27	NO_3+NO	→	$2NO_2$

The equilibrium concentrations of NO_2 and NO_3 can then be written as

$$[NO_2] = \frac{k_{22}[O_3]\,[NO_x]}{k_{22}[O_3] + k_{23}[O] + \mathcal{J}_{26}} \qquad (5)$$

where

$$[NO_x] = [NO] + [NO_2] \qquad (6)$$

and

$$[NO_3] = \frac{k_{24}[O_3]\,[NO_2]}{\mathcal{J}_{25a} + \mathcal{J}_{25b} + k_{27}[NO]} \qquad (7)$$

For the rate of change of odd oxygen particles we can approximately write:

$$\frac{\partial}{\partial t}[O_3] = 2\mathcal{J}_1[O_2] - 2k_{23}[O]\,[NO_2] - 2k_{24}[O_3]\,[NO_2] \times \frac{\mathcal{J}_{25a}}{\mathcal{J}_{25a} + \mathcal{J}_{25b} + k_{27}[NO]} \qquad (8)$$

With the aid of equations (5) and (8) it is easy to estimate what mixing ratios of NO_x are required to give satisfactory balance between the production and destruction rates of ozone. Above 30 km the state of photochemical equilibrum is reasonably well approached (although deviations are interesting in defining source regions for ozone), and for the region 25-35 km NO_x mixing ratios can be estimated from relations (5), (2) and the following approximation to (8)

$$\mathcal{J}_1[O_2] \approx k_{23}[O][NO_2] \quad (9)$$

Using the observed concentrations of ozone and molecular oxygen, and the rate coefficients and photochemical parameters from Table 1, this yields upper limits for the mixing ratios of NO_x of about 5×10^{-8} in the main production region of ozone, around 30 km. Although no measurements of NO_x mixing ratios in the stratosphere have been reported, such high mixing ratios seem unlikely at this level. However, lower estimates would be obtained if the rate coefficient k_2 or the solar irradiance below 2500 Å were smaller than listed in Table 1 [8-13]. A reduction by a factor of two and three in these functions is well within the variation limits of available experimental data. The presence of NO_2 near 30 km has been established [14] and an upper limit of 3×10^{-8} for the mixing ratio of NO_2 at about 16 km has been proposed [15]. Mesospheric observations [16] indicate mixing ratios near 4×10^{-8}. However, it should not be assumed without further proof that the NO produced at high altitudes can penetrate down into the stratosphere [17], since NO is photodissociated in sunlight [18].

R28 $NO+h\nu \rightarrow N+O \quad \lambda < 1925$ Å

which is followed by the removal process

R29 $N+NO \rightarrow N_2+O$

or by reactions leading to the reestablishment of NO [17]

R30 $N+O_2 \rightarrow NO+O$
R31 $N+O_3 \rightarrow NO+O_2$
R32 $N+OH \rightarrow NO+H$

An important additional source of NO_x in the stratosphere is provided by the attack of $O(^1D)$ on N_2O [19, 3]

R33a $N_2O+O(^1D) \rightarrow 2NO$

which must be considered together with the reactions

R33b $N_2O+O(^1D) \rightarrow N_2+O_2$
R34 $N_2O+h\nu \rightarrow N_2+O \quad \lambda < 3370$Å

Although there are still uncertainties about the penetration of UV radiation in the very discrete Schumann-Runge band system of molecular oxygen between 1750 and 2000Å, affecting reaction R34, estimates of NO_x mixing ratios due to this source are of the order of 2×10^{-8} in the ozone layer, which clearly is of significance for the atmospheric ozone budget.

THE INFLUENCE OF THE SST ACTIVITY ON THE OZONE LAYER

According to later corrected predictions published in SCEP [20], the proposed action of 500 U.S. SST's could lead to an increase in the global NO_x mixing ratio by about 2.4×10^{-9}. A corresponding number for the British-French Concorde would be 10^{-9}. The emission of NO_x per passenger is not lower for this aircraft, however, which carries 120 passengers against 300 in the American SST. A simple comparison with the mixing ratios which are required in the natural stratosphere to give a satisfactory ozone profile around 30 km clearly indicates that the catalytic action of NO_x can be enhanced to such a degree that an observable decrease of the protecting ozone layer can result [3, 6]. The problem may become particularly serious in regions of high traffic densities in the 30°-50° latitude belt in the Northern Hemisphere, especially in summer when the atmospheric dispersion of gaseous emissions is a minimum, and the transmission to the ground of ultraviolet solar radiation is a maximum due to minimum amounts of protecting ozone. It was suggested in the SCEP report that the local artificial increase in the NO_x mixing ratios could be ten times larger than the global increases. It is therefore imperative to study in detail the dispersive properties of the summer stratosphere.

At the present state of scientific knowledge it is not possible to make reliable quantitative estimates of the effects of NO_x emissions into the stratosphere. The main uncertainties are in our knowledge of

a) the natural stratospheric NO_x content
b) reaction coefficients, particularly k_2 and k_{23}
c) the solar irradiance in the wavelength region below 2400Å
d) chemical loss processes of NO_x, as discussed in more detail in the next section
e) dynamic processes in the stratosphere.

Nevertheless, it is important to give indications of the size of possible decreases in the total atmospheric ozone amount resulting from the NO_x injections, with consideration of the uncertainties mentioned above. The influence of the atmospheric motions on the vertical distribution of the ozone concentration, which becomes very important below 30 km, is taken into account in a very approximate way by the introduction of the well-known concept of vertical eddy diffusion. Consequently, equilibrium concentrations for ozone were calculated with the aid of equation (5) and the following modifications of equations (2) and (8).

$$2\,k_{23}[O]\,[NO_2] + 2\,k_5\,[O]\,[O_3] = 2\,\mathcal{J}_1[O_2] + \frac{d}{dz}\left\{K[M]\,\frac{d}{dz}\left\{\frac{[O_3]}{[M]}\right\}\right\} \qquad (10)$$

$$[O] = \left\{\frac{\mathcal{J}_{3a} + \mathcal{J}_{3b}}{k_2[O_2]\,[M]}\right\}[O_3] + \frac{\mathcal{J}_{26}[NO_2]}{} \qquad (11)$$

(In (10), K denotes the eddy diffusion coefficient, which was taken to be 10^4 cm^2 sec^{-1}.)

At the lower boundary, which was assumed to be at a height of about 10 km in this study, the concentration of ozone was fixed at 5×10^{11} molecules cm^{-3} for all calculations presented. As an upper boundary condition, photochemical equilibrium was assumed to prevail at 45 km [3]. Calculations were performed over ranges of the most uncertain parameters; some results are presented in Table 2. A realistic ozone distribution in the unpolluted atmosphere was obtained by choosing an appropriate background mixing ratio, μ_0, of NO_x. It is this background situation which was then perturbed with additional mixing ratios

Table 2. Calculated percentage decreases in ozone number concentrations and in the total number of ozone molecules per cm^2 above 10 km as caused by additions $\Delta\mu$ to the assumed natural stratospheric NO_x mixing ratios μ_0, which are given in column 4. For each altitude the upper numbers refer to assumptions and results calculated with the values for J_1 calculated from reference [13]; the numbers below correspond to those for a two-times smaller $\mathcal{J}_1$. The observed mean ozone concentrations for the 40° latitude circle are shown in column 2, and the calculated background concentrations, compatible with the adopted background mixing ratios μ_0 for NO_x, in column 3. The last four columns were calculated for peak NO_x mixing ratios $\Delta\mu'$ determined with the formula $\Delta\mu' = \Delta\mu\left\{1 + 9\exp\left(-\frac{|z - z_m|}{3}\right)\right\}$, with z_m = 20 and 17 km, where z is the altitude in km.

The last two lines give the percentage increases in sunburn risk, which were calculated with information given in the SMIC report [22, 23]. Assumed secant of the solar zenith angle = 1.5.

HEIGHT IN KM	$[O_3]$ OBS.	$[O_3]$ CALC.	μ_0	GLOBAL, $\Delta\mu$			PEAK AT 20 KM, $\Delta\mu'$			17 KM
				1(-9)	2(-9)	4(-9)	1(-9)	2(-9)	4(-9)	1(-9)
35	1.5(12)	2.2(12)	5.0(-8)	-1.0	-2.0	-3.8	-1.1	-2.1	-4.1	
			2.5(-8)	-1.9	-3.7	-7.0	-2.1	-4.0	-7.6	-2.0
30	2.7(12)	3.6(12)	4.0(-8)	-0.9	-1.7	-3.2	-1.3	-2.8	-5.5	
			2.0(-8)	-1.3	-2.8	-5.5	-2.5	-5.3	-9.9	-1.6
25	4.4(12)	4.6(12)	1.5(-8)	-1.6	-3.0	-5.6	-6.9	-12.7	-21.7	
			7.5(-9)	-2.4	-5.0	-9.4	-12.3	-20.8	-32.2	-5.7
20	3.8(12)	3.5(12)	1.0(-8)	-2.7	-5.2	-9.8	-18.3	-31.9	-50.2	
			5.0(-9)	-4.6	-9.0	-16.5	-30.0	-46.9	-64.8	-17.0
15	1.8(12)	2.5(12)	1.0(-8)	-3.2	-6.2	-11.7	-20.1	-34.7	-53.7	
			5.0(-9)	-5.5	-10.7	-19.4	-32.4	-49.8	-67.2	-25.6
TOTAL MOLEC./CM^2 ⩾10	7.4(18)	8.9(18)		-1.7	-3.4	-6.5	-8.8	-15.6	-25.2	
				-2.9	-5.9	-10.9	-14.7	-23.6	-34.2	-9.3
SUNBURN RISK				+3.0	+5.0	+11.0	+14.0	+28.0	+51.0	
				+4.0	+9.0	+18.0	+26.0	+47.0	+80.0	+15.0

$\Delta\mu$ of NO_x. It is evident from these results that significant changes in the total ozone content, and thus in the protection from solar ultraviolet radiation, can result from proposed supersonic air transport, thus confirming previous work [3, 6]. The results in the last four columns of Table 2 are calculated according to the recommendation in the SCEP report that the local increase of the NO_x mixing ratios near the flight paths could be ten times larger than the expected global increase. With peak NO_x mixing ratios of the order of 1.5×10^{-8}, the photochemical lifetime of ozone at 17 km is about 1.5 years. Consequently, the steady-state solutions, presented here and obtained by applying equation (11), may be somewhat unrealistic, and a much more detailed study is of course necessary. Another important conclusion which we draw from the results presented in Table 2 is that an accurate knowledge of photochemical parameters is required This is demonstrated here for $\mathcal{J}_1$. Larger changes in the ozone amounts were found, but not presented here, using smaller values for k_2.

Also the inclusion of the chain reactions R22 + R24 + R25a leads to somewhat larger changes in ozone. However, it is also important to investigate whether there are chemical processes which lead to a loss of NO_x into gases which do not participating in any catalytic chains of reactions destroying odd oxygen.

CHEMICAL LOSS PROCESSES FOR NO_x

Up to about 40% of the emitted NO_x may be converted to N_2O_5 by the reactions [3]

R24	NO_2+O_3	→	NO_3+O_2
R35	NO_3+NO_2	→	$N_2O_5^*$
R36	$N_2O_5^*$	→	NO_2+NO_3
R37	$N_2O_5^* + M$	→	N_2O_5+M
R38a	N_2O_5+M	→	$N_2O_5^*+M$
R38b	$N_2O_5+h\nu$	→	$2NO_2+O$
			$\lambda<8000$ Å

Other important loss processes involve the conversion of NO_x into nitric acid via

R39	$OH+NO_2$	→	HNO_3^*
R40	HNO_3^*+M	→	HNO_3+M
R41	HNO_3^*	→	$OH+NO_2$

The main loss of nitric acid is probably by the photodissociation process

R42 $HNO_3+h\nu \rightarrow OH+NO_2$

Unfortunately, the lack of precise knowledge of the rate coefficients k_{39} - k_{41}, especially with M = air in R40, and of the photodissociation process R42, makes a precise quantitative analysis impossible. However, it is clear that there may be a very efficient loss of NO_x into HNO_3, when we write

$$\frac{[HNO_3]}{[NO_2]} = \frac{k_{39}\,[OH]}{\mathcal{J}_{42}} \qquad \frac{k_{40}\,[M]}{k_{40}\,[M] + k_{41}}$$

and adopt the rate coefficients given in Table 1 for M = He, assuming that $[OH] = 10^6$ cm^{-3} at 20 km:

$$[HNO_3] = 0.4\,[NO_2]$$

It is therefore important, but not possible at this stage, to estimate the concentrations of HO_x particles in the lower stratosphere. This is also necessary in order to know the speed with which this conversion from catalytic NO_x to nitric acid takes place. In the lower stratosphere the internal equilibrium between the several forms of odd hydrogen particles is determined mainly by reactions R6-R14 [19], of which the rate coefficients for R10 and R12 are unknown. Also, there is appreciable uncertainty about the loss processes for HO_x particles. The reaction

R43 $HNO_3+OH \rightarrow H_2O+NO_3$

is perhaps the main process leading to loss of HO_x. Unfortunately, its temperature dependence is not well known. Methane is lost via

R44 $O(^1D)+CH_4 \rightarrow CH_3+OH$

but a potentially more important loss mechanism is

R45 $OH+CH_4 \rightarrow H_2O+CH_3$

which initially also leads to an efficient loss of

$\dot{OH}$. However, it is important to follow the subsequent reactions of the methyl radicals to determine whether HO_x particles are restored.

Some laboratory work suggests that the following reactions, which will be taken for illustration (21, 28), are important in the lower stratosphere

R46 $CH_3+O_2+M \rightarrow CH_3O_2+M$

R47a $CH_3O_2+NO_2 \rightarrow CH_3O_2NO_2$

The fate of $CH_3O_2NO_2$ in the stratosphere is not known. An alternative route for reaction of CH_3O_2 may proceed via (21, 28)

R47b $CH_3O_2+NO_2 \rightarrow CH_2O+HNO_3$

leading to the formation of nitric acid and formaldehyde. This reaction should be checked, as considerable rearrangement in the reaction products would have to take place. Nitric acid is mainly destroyed in reaction R42, but some of it is also lost in R43.

Formaldehyde reacts very quickly with OH

R48 $CH_2O+OH \rightarrow CHO+H_2O$

or is photolyzed according to

R49a $CH_2O+h\nu \rightarrow H+CHO$

R49b $CH_2O+h\nu \rightarrow CO+H_2$

CHO is probably removed by

R50 $CHO+O_2 \rightarrow CO+HO_2$

Finally the oxidation of methane is completed by

R11 $CO+OH \rightarrow CO_2+H$

The preferred path of reactions which lead to the oxidation of CH_4 into CO_2 and H_2O determines whether there is net production or destruction of odd hydrogen. For example, the path R45 + R46 + R47b + R42 + R48 + R50 does not affect the odd hydrogen content, while R45 + R46 + R47b + R43 + R48 + R50 leads to net destruction and R45 + R46 + R47b + R42 + R49a + R50 to net production of odd hydrogen.

CONCLUSIONS

The previous discussion has shown that present knowledge does not allow us to disregard the possibility of a serious decrease in the stratospheric ozone level due to the action of NO_x in the exhaust of commercial supersonic air transport. The author stands therefore strongly behind the recommendation expressed in SMIC [23] that it must be shown that the environmental consequences of future SST's are negligible before extensive use of them can take place. In order to be able to show that no ozone depletion takes place, it is necessary to improve our knowledge of

a) reaction coefficients, of which several have been indicated in this lecture
b) the solar irradiance in the ultraviolet below 2500 Å
c) the details of the stratospheric wind systems
d) chemical loss reactions of NO_x particles; accurate knowledge of this requires the knowledge of the stratospheric HO_x content, which in turn may require knowledge of the processes involved in the oxidation of CH_4 to CO_2 in the stratosphere.
e) the gaseous content of the stratosphere.

It is also important to investigate to what degree penetration of tropospheric gases into the stratosphere may affect the ozone layer [23]. For example, if NO_x molecules are of major importance for the atmospheric ozone budget, and if they are mainly removed by reactions with methane or water vapor reaction products, one can speculate about the possibility that a moderate increase in stratospheric H_2O or CH_4 content will result in an increase in the ozone content.

REFERENCES

1. Chapman, S., "A theory of upper atmospheric ozone," Quart. J.Roy. Met Soc., *3*, 103, 1930:

2. Bates, D.R., and Nicolet, M., "The photochemistry of atmospheric water vapour," J. Geoph. Res., *55*, 301, 1950.

3. Crutzen, P.J., "Ozone production rates in an oxygen-hydrogen-nitrogen oxide atmosphere," J. Geophys. Res., *76*, 7311, 1971.

4. Anderson, J.G., "Rocket measurement of OH in the mesosphere," J. Geoph. Res., *76*, 7820, 1971.
5. Crutzen, P.J., "The influence of nitrogen oxides on the atmospheric ozone content," Quart. J. Roy. Met. Soc., *96*, 320, 1970.
6. Johnston, H.S., "Reduction of stratospheric ozone by nitrogen oxide catalysts from supersonic transport exhaust," Science, *173*, 517, 1971.
7. Nicolet, M., "Nitrogen oxides in the chemosphere," J. Geophys. Res., *70*, 679, 1965.
8. Schiff, H.I., "Laboratory measurements of reactions related to ozone photochemistry," paper presented at the IUGG Conference, Moscow, August 1971.
9. Johnston, H.S., "Gas phase reaction kinetics of neutral oxygen species," NSRDS-NBS 20, National Bureau of Standards, 1968.
10. Detwiler, C.R., Garrett, D.L., Purcell, J.D., and Tousey, R., "The intensity distribution in the ultraviolet solar spectrum", Ann. Geophys., *17*, 263, 1961.
11. Brewer, A.W., and Wilson, A.W., "Measurements of solar ultraviolet radiation in the stratosphere," Quart. J. Roy. Met. Soc., *91*, 452, 1965.
12. Hinteregger, H.E., "The extreme ultraviolet solar spectrum and its variation during the solar cycle," Ann. Geophy., *26*, 547, 1970.
13. Ackerman, M., "Ultraviolet solar radiation related to mesospheric processes", in *Mesospheric Models and Related Experiments* (G. Fiocco, Ed.), Reidel Publ. Cy., Holland, 1971.
14. Murcray, D.G., Kyle, T.G., Murcray, F.H., and Williams, W.J., "Nitric acid and nitric oxide in the lower stratosphere," Nature, *218*, 78, 1968.
15. Ackerman, M., and Frimout, D., "Mesure de l'absorption stratosphérique du rayonnement solaire de 3,05 à 3,70 microns," Bull. Acad. Roy. Belgique, Classe Science, *55*, 948, 1969.
16. Meira, L.G., Jr., "Rocket measurements of upper atmospheric nitric oxide and their consequences to the lower ionosphere," J. Geophys. Res., *76*, 202, 1971.
17. Strobel, D.F., "Odd nitrogen in the mesosphere," J. Geophys. Res., *76*, 8384, 1971.
18. Callear, A.B., and Smith, I.W.M., "Fluorescence of nitric oxide: 3, Determination of the rate constants for predissociation, collisional quenching, and spontaneous radiation of NO $C^2\pi (v = 0)$," Disc. Far. Soc., *37*, 96, 1964.
19. Nicolet, M., "Aeronomic reactions of hydrogen and ozone," in *Mesospheric Models and Related Experiments* (G. Fiocco, Ed.), D. Reidel Publ. Cy, Dordrecht, Holland, pp 1-51, 1971.
20. *Man's Impact on the Global Environment: Assessment and Recommendations for Action,"* (Wilson, C.L. and Matthews, W.H., eds), M.I.T. Press, Cambridge, Mass., 1970 (SCEP Report).
21. Van den Bergh, H.E., and Callear, A.B., "Spectroscopic measurement of the rate of the gas-phase combination of methyl radicals with nitric oxide and oxygen at 295 K," Trans. Far. Soc., *67*, 2017, 1971.
22. Urbach, F., "Geographic pathology of skin cancer," in *The Biologic Effects of Ultraviolet Radiation*, Oxford Pergamon Press, 635, 1969.
23. *Inadvertent Climate Modification: Report of the Study of Man's Impact on Climate (SMIC)*, (Wilson, C.L., and Mathews, W.H., Eds.), M.I.T. Press, Cambridge, Mass., 1971.
24. Kaufman, F., "Neutral reactions involving hydrogen and other minor constituents," Can. J. Chem., *47*, 1917, 1969.
25. Schiff, H.I., "Neutral reactions involving oxygen and nitrogen," Can. J. Chem., *47*, 1903, 1969.
26. Johnston, H.S., "Four mechanisms involving nitrogen pentoxide," J. Am. Chem. Soc., *73*, 4542, 1951.
27. Simonaitis, R., and Heicklen, J., "The reaction of OH with NO_2," publication from the Dept. of Chemistry, The Pennsylvania State University, 1972.
28. Spicer, C.W., Villa, A., Wiebe, H.A., and Heicklen, J., "The reactions of methylperoxy radicals with NO and NO_2," CAES Rept. No. 223-71, Dept. of Chemistry and Center for Air Environment Studies, The Pennsylvania State University, 1972.
29. Herron, J.T., and Penzhorn, R.D., "Mass spectrometric study of the reactions of atomic oxygen with ethylene and formaldehyde," J. Phys. Chem. *73*, 191, 1969.
30. Calvert, J.G., and Pitts, J.N., Jr., *Photochemistry*, John Wiley and Sons Ltd, New York, 1966.
31. Langley, K.F., and McGrath, W.D., "The ultraviolet photolysis of ozone in the presence of water vapour," Planet. Sp. Sci., *19*, 413, 1971.

DISCUSSION

A. Ferri emphasized the difference between the OH and NO effects, and noted that while the NO could probably be reduced to acceptable levels by engine redesign, the water could not. F. Urbach questioned Crutzen's 3% increased sunburn effect from ozone reduction; he said Bernard and Klein of the Smithsonian calculated that a 5% decrease in ozone layer would mean an irradiation increase of 30% at wavelengths of 297 nm at the equator and an increase of about six times at 40^{o} latitude. R. Schoen asked whether Urbach was considering only 2975 Å, while Crutzen had integrated over the entire erythermal region; Urbach said no. D. Davis presented some recent rate measurements on $O + O_2 + M$ at 200 - 350°K and $O + NO_2 + M$ at 200 - 350°K. The rate constant for the first at 220°K was 1.3×10^{-33}, a factor of 2 lower than Crutzen's; for the second, also at 220°K, it was 9×10^{-12}, a factor of 2 higher. Crutzen pointed out that this would lower the NO_2 concentrations required to explain the observed ozone profile, and would therefore increase the expected ozone depletion due to NO_x from aircraft.

D. Garvin announced that the National Bureau of Standards has begun a Chemical Kinetics Data Survey in support of CIAP. Data sheets for twenty-seven gas-phase reactions of stratospheric interest have been issued as NBS Reports 10692 and 10828, and more are forthcoming.

LABORATORY CHEMICAL KINETICS AS AN ATMOSPHERIC SCIENCE

HAROLD JOHNSTON
Department of Chemistry
University of California
Berkeley, California

ABSTRACT: As a demonstration of the predictive power of the science of laboratory chemical kinetics, it is shown that one laboratory reaction (the N_2O_5 catalyzed decomposition of ozone) can be precisely predicted from other laboratory reactions: also, a non-controversial atmospheric quantity (the vertical profile of singlet delta oxygen molecules) can be predicted quite satisfactorily from chemical rate constants obtained in the laboratory. The chemical and photochemical constants of the pure air substances, O, O_2, and O_3, are fairly well known, and these constants predict about twice as much stratospheric ozone in clean air as that observed, implying the presence of some other natural ozone-destroying agents. Neither transport to the troposphere nor the water reactions are adequate (by about a factor of 50) to explain the ozone deficit. A natural source of NO_x in the stratosphere is the reaction of nitrous oxide, N_2O, with singlet oxygen $O(^1D)$: the source strength has been calculated by three different investigators to lie in the range of 0.25 to 2.5 x 10^8 molecules cm^{-2} sec^{-1}. The NO_x inventory built up by this natural flux (in the face of all the complexities of atmospheric motions and photochemistry) is sufficient to explain the ozone deficit. The source strength of NO_x from 500 SST's is equal to or several times greater than the natural NO_x source strength. NO_x already exerts the dominant influence on reducing stratospheric ozone to its natural level; if its natural source strength is increased artificially by a factor of two or more, only a remarkable cancellation of effects could prevent a major reduction in stratospheric ozone.

INTRODUCTION

During the last year I presented a series of papers [1, 2, 3] which focused on the question of the important variables in stratospheric chemistry. These papers emphasize, in agreement with Crutzen [4, 5, 6], that the oxides of nitrogen (NO, NO_2, NO_3) are among the most important photochemical variables, and that the water reactions are negligible by comparison. Furthermore, the increase in NO_x which would result from SST flights would be sufficient to significantly reduce stratospheric ozone.

Those papers include calculations based on laboratory studies of chemical kinetics and photochemistry, and on a standard model of the atmosphere. This more general paper looks at photochemistry as a science and explores its validity for predicting stratosphere chemistry.

My research in photochemistry and chemical kinetics has been guided by an interest in the extent to which laboratory measurements such as rate constants, cross-sections, and quantum yields can be extrapolated to different environments, like the stratosphere. Three of my publications [7, 8, 9] present conclusions on the current status of this question.

The first part of this article gives examples of the transferability of rate constants from one environment to another. The second part uses rate constants measured in the laboratory to identify the important variables in the problem of stratospheric ozone, both for the natural stratosphere and for the stratosphere as it might be perturbed by 500 supersonic transport planes (SST's).

LABORATORY PHOTOCHEMISTRY AND REACTION KINETICS

Apparatus [7]. In laboratory studies of chemical and photochemical reaction rates, a wide variety of chemical and physical methods are used. The range of quantities sought to be measured is illustrated in Figure 1 by a highly schematic drawing of a crossed molecular beam and of a constant-volume, constant-temperature reaction vessel. In the crossed molecular beam experiment, the ideal is to select the internal quantum states of the reactants and to measure the reaction cross-sections to produce specific product states as a function of relative velocity. In the bulk reaction flask, the object is to measure the rate of disappearance of all reactants

and the rate of appearance of all products; if there are intermediate species the ideal is to measure their build-up and decay with time.

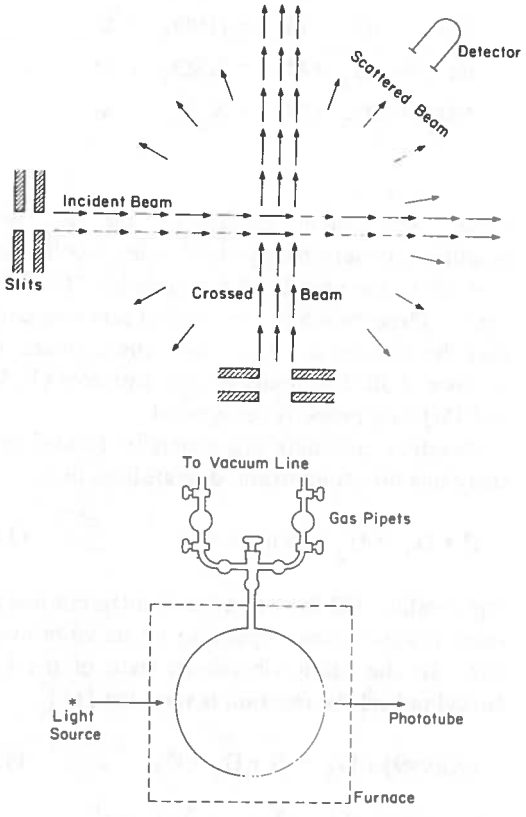

Figure 1. Schematic diagram of a crossed molecular-beam apparatus and a constant-volume reaction flask, illustrating the range of quantities observed in gas-phase reaction kinetics.

General Consideration [9]. The cross-sections observed by molecular beam techniques and also by a number of spectroscopic methods are strictly mechanical quantities. Such cross-sections can be transferred without limit to other environments. However, for even the simplest chemical reaction there are a vast number of parallel reaction paths in terms of the purely mechanical cross-sections, and in general the full lists of such quantities have not yet been evaluated. Although full use should be made of these sharp quantities where they are available, at this time few practical atmospheric problems can be solved completely in terms of such data.

Phenomenological rates measured in the laboratory reaction flask are sums over a large number of elementary physical processes. These sums involve the cross-sections σ and probability distributions P for every quantum process. If the reactants have an equilibrium distribution over all states (internal as well as translational), then every element of the distribution P is specified by one parameter, the temperature, T. The sum of the strictly mechanical cross-sections over the equilibrium distribution of reactants is thus also a single-valued function of the temperature. These words can be compactly expressed by the relations

$$A + B \rightarrow C + D$$

$$\underbrace{A_i + B_j}_{g_l} \xrightarrow{k_{ijlmnp}} \underbrace{C_m + D_n}_{g_p} \qquad (1)$$

$$\text{Rate} = [A]\ [B] \quad \sum_i \sum_j \int_g \sigma_{ij}(g)\, g P_i P_j P_g\, dg \qquad (2)$$

$$= k[A]\ [B]$$

$k = k(T)$ if P_i, P_j, P_g are equilibrium distributions (3)

where square brackets indicate total concentration. This description is readily generalized [10] to reactions of first or third order

$$A \rightarrow \text{products} \qquad (4)$$

$$k' = \text{rate}/[A] \qquad (5)$$

$$A + B + C \rightarrow \text{products} \qquad (6)$$

$$k'' = \text{rate}/[A]\ [B]\ [C] \qquad (7)$$

In a large number of readily identified situations, the reactants have a grossly non-equilibrium distribution over internal quantum states, in particular the vibrational states. In some of these situations there are good grounds to believe that the translational degrees of freedom have an equilibrium distribution and thus a temperature

T, but the vibrational degrees of freedom are strongly non-equilibrium. Figure 2 gives data for the unimolecular decomposition of N_2O_5. The departure from the dashed line, k_{eq}, is all due to the non-equilibrium distribution of the vibrational degrees of freedom of N_2O_5. Consider the situation at 0.1 torr. The rate is not particularly fast; the half-time is 700 seconds; and yet the rate is a factor of 300 slower than the value that would obtain at equilibrium over vibrational states. The reaction is neither first-order nor second-order, but it displays the complex rate function

$$k = \sum_i \frac{a_{Mi}\, c_i[M]}{b_{Mi}[M]+c_i} \qquad (8)$$

The reaction cross-sections reside in the c_i terms, and the non-equilibrium distribution function is

$$P_i = a_{Mi}[M] \,/\, (b_{Mi}[M]+c_i) \qquad (9)$$

In this instance the distribution function depends reproducibly on three macroscopic variables: T, the identity of gas M, and [M], the concentration of gas. Thus the non-equilibrium rate "constant" can be characterized and reproduced by statement of the three variables: T, M, [M].

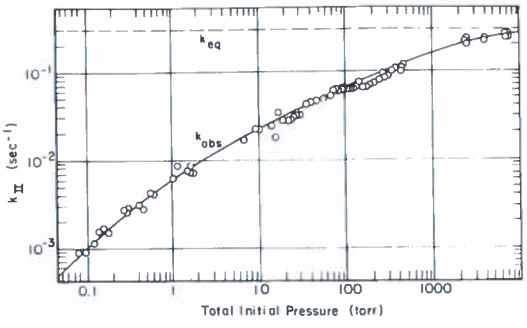

Figure 2. Experimental data for the unimolecular decomposition of nitrogen pentoxide, N_2O_5, showing the large effect of the non-equilibrium distribution of N_2O_5 over its vibrational states when reaction occurs.

This phenomenon of reproducible, non-equilibrium distribution, with its effects of non-integral, variable-reaction order, occurs for a large number of atmospheric reactions, such as:

$$\begin{aligned}
O + O_2 + M &\rightarrow O_3 + M \qquad (10)\\
O + NO + M &\rightarrow NO_2 + M\\
O + NO_2 + M &\rightarrow NO_3 + M\\
HO + HO + M &\rightarrow H_2O_2 + M\\
HO + NO + M &\rightarrow HNO_2 + M\\
HO + NO_2 + M &\rightarrow HNO_3 + M\\
NO_2 + NO_3 + M &\rightarrow N_2O_5 + M
\end{aligned}$$

Under stratospheric conditions, the first two reactions are very nearly third-order, but the last two are in the middle of the complex "fall off" region. These variable, non-integral rate constants may be transferred from one environment to another if all three macroscopic variables (T, M, and [M]) are properly recognized.

Reaction products are generally formed initially in a non-equilibrium distribution, like

$$H + O_3 \rightarrow O_2 + HO(v \leq 9) \qquad (11)$$

The product HO has remarkably different reactivities toward ozone depending on its vibrational state. In the ninth vibrational state of the hydroxyl radical the reaction is very fast [11]:

$$HO(v=9) + O_3 \rightarrow H + O_2 + O_2 \qquad (12)$$

$$k = 7.7\times10^{-12}\ \text{cm}^3\ \text{molecule}^{-1}\ \text{sec}^{-1}$$

In the ground vibrational state of the hydroxyl radical, the reaction is vanishingly slow [12]:

$$HO + O_3 \rightarrow \text{products} \qquad (13)$$

$$k < 10^{-16}\ \text{cm}^3\ \text{molecule}^{-1}\ \text{sec}^{-1}$$

If we knew the rate constant as a function of vibrational state of HO, these constants could be transferred reliably from the laboratory to another environment. However, in the new environment we require a great deal of additional information about the distribution of HO over its vibrational states under the actual conditions. In principle, this problem could be solved in terms of the distribution of HO over its vibrational states in the reaction of H with O_3, and in terms of the rate constants for deactivation of HO by all major atmospheric species. In the absence of

such detailed data, these rates must be regarded as non-transferable from one set of conditions to another, and the reaction must be studied under realistic conditions.

Reactions measured in the laboratory are subject to another kind of complexity. The thermal decomposition of ozone[8] follows the balanced chemical equation

$$2O_3 \rightarrow 3O_2 \qquad (14)$$

However, the reaction occurs as a sequence of three elementary chemical reactions

$$\begin{aligned} &(R1)\ O_3 + M \rightarrow O_2 + O + M \qquad (15)\\ &(R2)\ O + O_2 + M \rightarrow O_3 + M\\ &(R3)\ O + O_3 \rightarrow O_2 + O_2 \end{aligned}$$

The general definition of the rate is based on Equation 14

$$R = -\frac{1}{2}\frac{d[O_3]}{dt} = \frac{1}{3}\frac{d[O_2]}{dt} \qquad (16)$$

and the rate expression derived from (15) is

$$R = \frac{k_1\, k_3[O_3]^2[M]}{k_2[M]\,[O_2] + k_3[O_3]} \qquad (17)$$

Empirical rates based on (14) are of no value in transferring data from one environment to another. The quantities suitable for prediction of new situations are the elementary chemical rate constants: $k_1(T,M,[M])$, $k_2(T,M,[M])$, and $k_3(T)$.

This section can be summarized by a quotation from the preface of reference 8.

> "Now that chemical kinetics is approaching a certain level of maturity, with some of the field passing from frontline research to established applied science, its quantitative data should be tabulated in handbooks. Decisions must be made as to what to tabulate; suggestions have included: empirical rate constants with defined order and regardless of mechanism, parameters of the Arrhenius equation or parameters of activated-complex theory, nothing but molecular transition probabilities or cross sections for identified changes of quantum states. The position taken in this review is that we should tabulate individual rate constants for elementary chemical reactions. I oppose basing handbooks on the other proposals listed above for the following reasons: Empirical rate data for an unanalyzed complex reaction are analogous to empirical thermodynamic data for an impure unanalyzed substance; the data may be useful for the case in hand but of no general interest. The bare reporting of parameters of the Arrhenius equation or activated-complex theory equation conceals the source of the numbers, the probable error, the relationship to other investigations. In tables of data of this sort one entry may represent an average of several hundred observed points as obtained by a dozen different investigators over a wide temperature range, and another entry may be a wild guess by an amateur in the field or the unsupported prediction of a crude theory. A refusal to tabulate any kinetic data except fundamental, quantum-state transitions is analogous to a refusal to tabulate any thermodynamic data until they are obtained by statistical mechanics from molecular parameters."

Prediction of a laboratory result.[7] The decomposition of ozone is strongly catalyzed by dinitrogen pentoxide, N_2O_5. Experimental data are given in Figure 3. Over a wide range of conditions the observed[13] reaction rate is given by

$$\frac{-d[O_3]}{dt} = k_{IV}[N_2O_5]^{2/3}\,[O_3]^{2/3} \qquad (18)$$

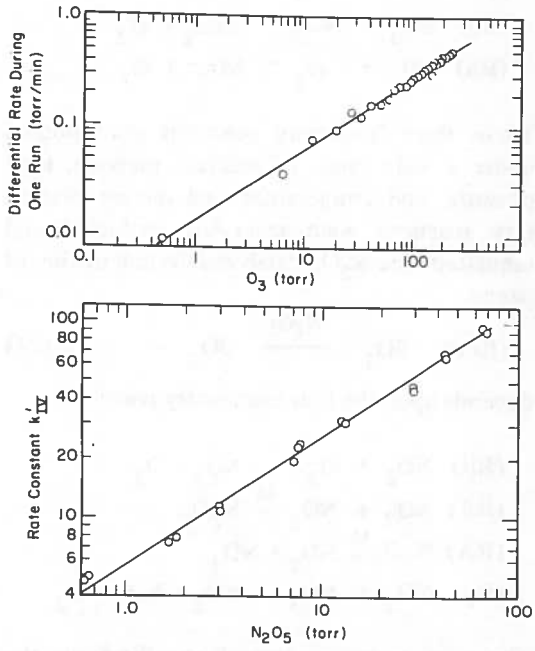

Figure 3. Experimental data and calculated lines for the N_2O_5 catalyzed decomposition of ozone. The prediction of the rate of one laboratory reaction from laboratory measurements made on other reactions. Note the unusual rate law: $k[N_2O_5]^{2/3}[O_3]^{2/3}$

The rate is precisely two-thirds order in N_2O_5 and two-thirds order in ozone. The overall order is thus 4/3.

The points entered in Figure 3 are based on the observed rates of this magnificently strange, four-thirds order reaction. The lines are not based on these observed points; they are predicted on the basis of other laboratory studies.

There are three other complex reactions involving N_2O_5:

$$\begin{aligned} &\text{(RI)} && 2N_2O_5 = 4NO_2 + O_2 && (19)\\ &\text{(RII)} && NO + N_2O_5 = 3NO_2 &&\\ &\text{(RIII)} && 2NO_2 + O_3 = N_2O_5 + O_2 &&\end{aligned}$$

These three reactions represent different special cases of the effect of six elementary chemical reactions.

$$\begin{aligned} &\text{(RA)} && N_2O_5 \overset{M}{\rightarrow} NO_2 + NO_3 && (20)\\ &\text{(RB)} && NO_2 + NO_3 \overset{M}{\rightarrow} N_2O_5 &&\\ &\text{(Re)} && NO_2 + NO_3 \rightarrow NO + O_2 + NO_2 &&\\ &\text{(Rf)} && NO + NO_3 \rightarrow 2NO_2 &&\\ &\text{(Rg)} && NO_3 + NO_3 \rightarrow 2NO_2 + O_2 &&\\ &\text{(Rh)} && NO_2 + O_3 \rightarrow NO_3 + O_2 &&\end{aligned}$$

These three laboratory reactions were studied under a wide range of reactant pressure, total pressure, and temperature, and the six elementary reactions were separately evaluated and tabulated. The N_2O_5 catalyzed decomposition of ozone

$$\text{(RIV)} \quad 2O_3 \xrightarrow{N_2O_5} 3O_2 \qquad (21)$$

depends upon the four elementary reactions

$$\begin{aligned} &\text{(Rh)} && NO_2 + O_3 \rightarrow NO_3 + O_2 &&\\ &\text{(RB)} && NO_2 + NO_3 \overset{M}{\rightarrow} N_2O_5 &&\\ &\text{(RA)} && N_2O_5 \overset{M}{\rightarrow} NO_2 + NO_3 &&\\ &\text{(Rg)} && NO_3 + NO_3 \rightarrow NO_2 + NO_2 + O_2 &&\end{aligned}$$

The rate equation derived exactly from this mechanism is

$$R_{IV} = \tfrac{1}{2}(k_A k_h / k_B)^{\frac{2}{3}} (2k_g)^{\frac{1}{3}} [N_2O_5]^{\frac{2}{3}} [O_3]^{\frac{2}{3}} \qquad (22)$$

Thus, the strange 4/3 order is predicted. The rate constants for A, B, g, and h as derived from the complex reactions I, II, and III were used to calculate the lines in Figure 3, and there is excellent agreement between calculated and observed rate.

We may conclude, then, that the rate of one laboratory reaction can be accurately predicted from the rates of other laboratory reactions.

LABORATORY KINETICS APPLIED TO THE ATMOSPHERE

Prediction of an atmospheric result. In a stratosphere of pure air, the formation and natural balancing of ozone is given by the Chapman reactions [14, 8, 1-6].

$$\begin{aligned} &\text{(Ra)} && O_2 + h\nu \rightarrow O + O && (23)\\ &\text{(Rc)} && O_3 + h\nu \rightarrow O_2 + O &&\\ &\text{(R2)} && O_2 + O + M \rightarrow O_3 + M &&\\ &\text{(R3)} && O_3 + O \rightarrow O_2 + O_2 &&\end{aligned}$$

The photochemical steady state set up by these reactions gives

$$\frac{[O_3]_{ss}}{[O_2]} = \left[\frac{J_a}{J_c}\left(\frac{k_2[M]}{k_3}\right)\right]^{1/2} \qquad (24)$$

"Odd oxygen" (O and O_3) is formed by Ra and destroyed by R3. The processes Rc and R2 interconvert O and O_3 but do not increase or decrease them. The net effect of Rc and R2 is to convert solar energy to heat in the stratosphere, which is the source of the temperature inversion and great stability against vertical mixing of the stratosphere. The steady-state concentration of ozone depends on the ratio of J_a to J_c and of $k_2[M]$ to k_3.

Many other reactions involve excited electronic states of oxygen atoms and molecules. This field, reviewed recently by Wayne [15], continues to be an active one for current research. In addition to the Chapman reactions, we must consider the following (where O and O_2 represent the stable species and a fuller statement of excited species is $^1\Delta_g$ and $^1\Sigma_g^+$) [16]:

(i) Formation of excited species (25)

$$O_3 + h\nu\,(450\text{–}650\ nm) \rightarrow O_2 + O$$
$$(310\text{–}340\ nm) \rightarrow O_2(^1\Delta) + O$$
$$(below\ 310\ nm) \rightarrow O_2(^1\Delta) + O(^1D)$$
$$O(^1D) + O_2 \rightarrow O + O_2(^1\Sigma)$$

(ii) Deactivation of excited species (26)

$$O(^1D) + M \rightarrow O + M$$
$$O_2(^1\Delta) + M \rightarrow O_2 + M$$
$$O_2(^1\Sigma) + M \rightarrow O_2 + M$$

(iii) Light emission by excited species (27)

$$O(^1D) \rightarrow O + h\nu\ (630\ nm)$$
$$O_2(^1\Sigma) \rightarrow O_2 + h\nu\ (760\ nm)$$
$$O_2(^1\Delta) \rightarrow O_2 + h\nu\ (1270\ nm)$$

(iv) Reaction with ozone (28)

$$O(^1D) + O_3 \rightarrow O_2 + O_2$$
$$O + O_3 \rightarrow O_2 + O_2$$
$$O_2(^1\Delta) + O_3 \rightarrow O_2 + O_2 + O$$
$$O_2(^1\Sigma) + O_3 \rightarrow O_2 + O_2 + O$$

Under stratospheric conditions the deactivation processes (ii) predominate over the ozone destruction processes (iv), and loss of odd oxygen to electronically excited species is very small (a few percent) compared to the loss by the Chapman reactions.

The formation and quenching of $O_2(^1\Delta)$ lead to a fairly large concentration of this species in the stratosphere. It signals its presence by the airglow radiation at 1.27 μm. The rate constants for reactions (25) through (28) have been measured in the laboratory and reviewed by Wayne [15]. The vertical profile of $O_2(^1\Delta)$ was deduced from a rocket sounding, and the result as quoted by Wayne [15] is plotted in Figure 4. Wayne emphasized that the calculated curve in Figure 4 involves no adjustable parameters; it is based exclusively on rate constants as measured in the laboratory and the ozone vertical profile as measured by a rocket sounding. The observed $O_2(^1\Delta)$ is based on the radiation intensity at 1.27 μm as observed in another rocket sounding of the upper atmosphere. The agreement between calculated and observed curves is quite satisfactory.

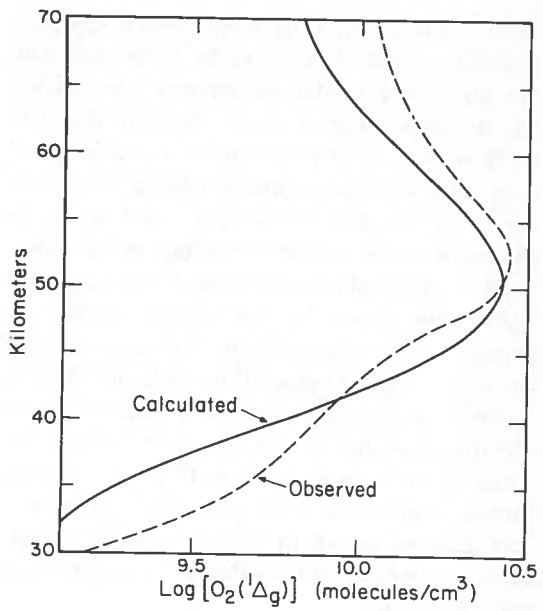

Figure 4. The observed vertical profile of $O_2(^1\Delta_g)$ and the profile calculated on the basis of photochemical constants observed in the laboratory.

In conclusion, for a non-controversial quantity such as the $O_2(^1\Delta)$ air-glow, rate constants as measured in the laboratory are capable of predicting a concentration profile in the upper atmosphere.

Pure air rate constants. Before the effects of trace components in the stratosphere are considered, it is important to understand the effect of the major component—namely, oxygen. In pure air, the ozone steady state depends on the ratio of k_2 and k_3 (Equations 23 and 24). The status of laboratory studies of reactions 1, 2, and 3 (Equations 23 and 15) will be reviewed in detail.

During 1966 and 1967, I spent all the time I had available for research in preparing a book for the National Bureau of Standards (NSRDS-NBS-20) giving a critical review of all published data on the reaction rates of O, O_2, and O_3 [8]. All available kinetic data published in English, German, and French since 1900 were reviewed. Tabulated rate constants were recomputed into common units. Data that appeared only as points on a graph were read off the graph and combined with other data. These oxygen reactions were extensively studied in the 1920's and early 1930's, and again after about

1955. Some of the early work showed very poor precision; these data could be associated with reaction vessels containing surfaces that catalyze the decomposition of ozone. Some of the early work showed good precision for a given series of runs but very poor reproducibility from one series to another; these data could often be shown to involve oxides of nitrogen in the ozone. Studies of the photolysis of ozone by ultraviolet light were shown by the original authors to involve ozone destruction by free radicals based on water. Studies before 1964 of k_3 in fast flow systems with oxygen atoms produced by an electric discharge are known to be invalid because of the large amounts of $O_2(^1\Delta)$ in the gas stream, which also decompose ozone (Equation 28). Studies shown to involve catalysis by surfaces, water, or the oxides of nitrogen were rejected *in toto*.

After this screening of all available data, there remained a large quantity of apparently valid data. A consistency test for the validity of the data was to compare the ratio of k_1 and k_2 as determined strictly from kinetics with the equilibrium constant obtained from thermodynamic data in the JANAF tables[17]

$$\frac{k_1 \text{ (kinetic)}}{k_2 \text{ (kinetic)}} \text{ compared with } K_1 \text{ (thermo.)} \qquad (29)$$

This comparison is reproduced in Figure 5. It can be seen that k_1/k_2 is in excellent agreement with the thermodynamic equilibrium constant. By virtue of this test, the constant for reaction 2 may be obtained more reliably from

$$k_2 = k_1/K_1 \qquad (30)$$

than from direct observation in certain regions of pressure and temperature. Likewise the value of k_1 can be extended by adding to it the values of

$$k_1 = K_1 k_2 \qquad (31)$$

The observed values of k_2 are given as points in Figure 6. Observations were made at temperatures typical of the stratosphere. The best estimate of the rate constant k_2 is based on the extended data for k_1 reflected through the equilibrium constant (Equation 30); the line in Figure 6 was evaluated in this way. It can be seen

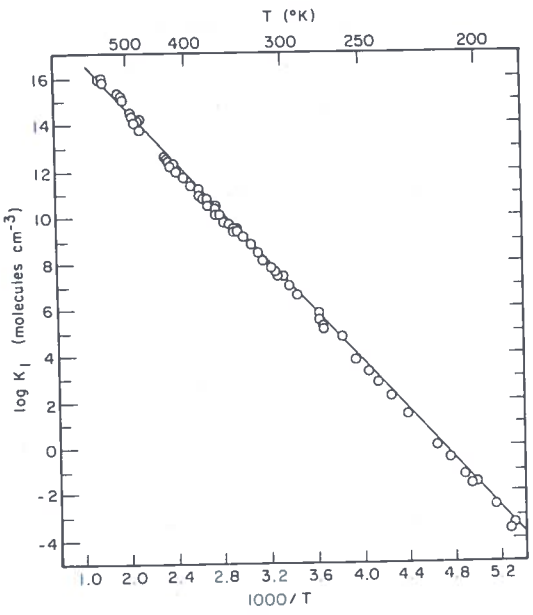

Figure 5. Consistency test for quality of data. The ratio of rate constants k_1/k_2 as observed in the laboratory and analyzed by NSRDS-NBS-20 compared to the equilibrum constant K_1, obtained from JANAF thermochemical tables

$$\left.\begin{array}{ll} k_1 & O_3 + M \rightarrow O_2 + O + M \\ k_2 & O + O_2 + M \rightarrow O_3 + M \\ k_3 & O + O_3 \rightarrow O_2 + O_2 \end{array}\right\} \text{chem. kinet.}$$

$$K_1 = [O_2][O]/[O_3] \qquad \text{thermodynamics}$$

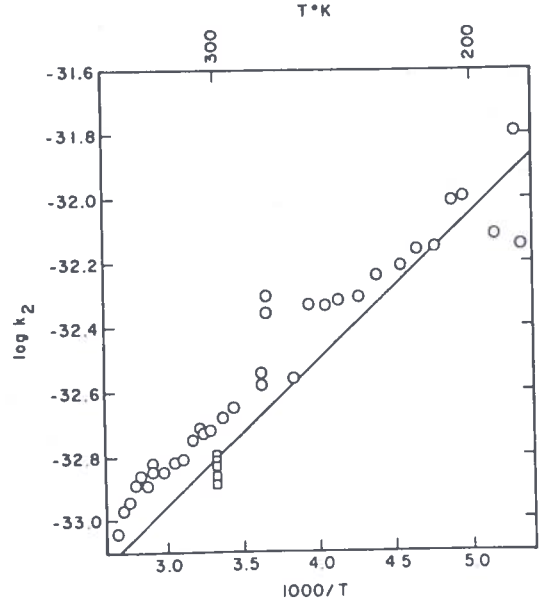

Figure 6. Observed and calculated values of k_2. Points are observed; the line is calculated from $k_2 = k_1/K_1$.

that this rate constant is still uncertain by perhaps ± 50%. Care must be taken to consider the correct M-gas, since k_2 depends on T, identity of M, and concentration of M (Equation 10). The data in Figure 6 are based on equivalent ozone as M-gas, and air is about 0.4 as effective as ozone in this respect. Several laboratory studies were carried out with argon as M-gas, which is 0.25 as effective as ozone.

All data points regarded as valid in 1968 were listed in tables in NBS-20, to permit easy extension of that study as new data on these reactions were obtained. Such an extension was carried out by Krezenski, Simonaitis, and Heicklen (1971) [20]. They measured the rate of reaction 3 from room temperature down to 196°K, whereas the lowest temperature previously investigated was 273°K. Figure 7 shows all data included in NBS-20, the new low-temperature points, and the curve previously used in stratospheric calculations [1, 2]. As this example illustrates, a "most recent" study should be added to the basic background of 50 years of experience embodied in NBS-20, not used to displace the full body of previously established data.

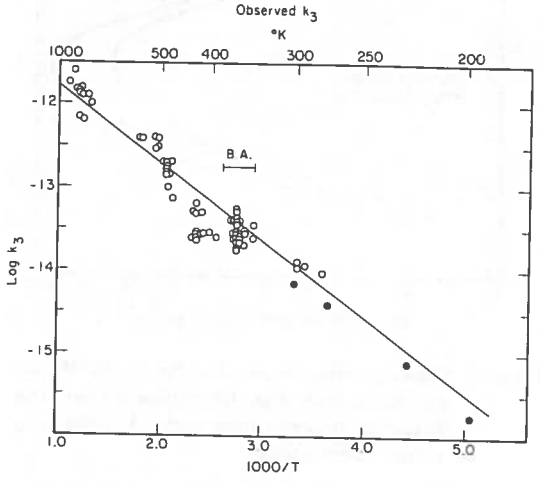

Figure 7. The collective data for k_3 (1906-1966) as reviewed in NBS-20, o; data recently observed [20] at low temperatures, ●; rate expression used by references 1 and 2, solid line.

In the early 1950's Benson and Axworthy [18] re-evaluated the experimental data of Glissman and Schumacher [19]. The temperature range of these data, indicated by the bar in Figure 7, is very narrow compared to the full range now available. All of Benson and Axworthy's points were included in this study, so their study is superseded by NBS-20.

In summary, the full body of laboratory data in Figures 6 and 7 probably give the ratio $(k_2/k_3)^{1/2}$ with an accuracy of ±50 percent under stratospheric conditions.

Photolysis rates. The rate of photolysis of oxygen is written as $J_a[O_2]$, and the rate of photolysis of ozone as $J_c[O_3]$. The parameters J_a and J_c are not rate constants; rather, they depend on the summation over wavelength of light absorption cross-section σ, quantum yield Φ, and local light intensity I. The local light intensity depends on the intensity of incoming solar radiation and on all species that absorb that radiation above the point in question. Both ozone and oxygen absorb below 242 nm, so the light intensity depends on the optical path L of both O_2 and O_3 between the sun and the region of interest. If x represents O_3 and z represents O_2, the functional dependence of the photolysis factors is

$$J_a = \sum_{\Delta\lambda} \sigma_z(\lambda,T,P,)\Phi_z(\lambda)\, I\,(I_{0\lambda},L_x,L_z)$$

$$J_c = \sum_{\Delta\lambda} \sigma_x(\lambda)\Phi_x(\lambda)\, I\,(I_{0\lambda},L_x,L_z) \quad (32)$$

In the stratosphere oxygen absorbs radiation between 190 and 242 nm in the Herzberg continuum, a highly "forbidden" transition. This absorption is enhanced by the perturbation of molecular collisions, and thus the cross-section for absorption by oxygen is a weak function of pressure P and temperature T.

Both old and recent data on the cross-sections σ and solar intensities I_0 have been reviewed by Ackerman [21]. Before Ackerman's review was published, the solar intensities I_0 were most conveniently obtained from a review by Brinkman et al. [22], and the cross-sections were obtainable from several journal articles [23, 24].

The calculations which appeared in my two reports [1, 2] of the summer of 1971 were based on references 22-24. Recently I have made calculations with the data as summarized by Ackerman [21]. For the case of pure, dry air, the photolysis parameters given by Ackerman predict 15 percent less ozone (total vertical column, steady-state calculation) than is predicted by the constants based on references 22-24.

Calculation of the absolute concentration of ozone in pure air. In the stratosphere, the steady-state concentration of ozone is given by Equation 24. The laboratory quantities needed are k_2/k_3, which are available [8, 20] at temperatures between 200 and 1000°K, and J_a/J_c, which can be calculated from photochemical data [21, 22-24]. From pressure and temperature as a function of elevation, the chemical kinetic ratio $k_2[M]/k_3$ can be calculated in a straightforward way. The calculation of the photochemical ratio J_a/J_c poses certain problems. The earth rotates every 24 hours and the seasons undergo annual cycles. As is well known from the theory of photochemical rotating sectors [25], there is a difference between a given light intensity half the time and half the light intensity all the time. If the period (light on and light off) is long compared to the time needed for a substance to reach the steady state, the calculation should be done in terms of full light intensity on for half the time. If the period (light on and light off) is short compared to the lifetime of a substance, then the calculation should be done in terms of half light intensity for all the time. The active ultraviolet radiation is so rapidly attenuated as one moves down from 50 kilometers to 15 kilometers in the stratosphere that there is a profound gradient [26, 1] of half-times required for ozone to reach the steady state: about a day at 45 km, about two weeks at 35 km, about 3 months at 25 km, and several years at 15 km. In terms of photochemical sector theory, it is appropriate at and below 40 km to use the average intensity for all times. In my calculations [1-3], I have averaged the solar intensity for each nanometer of wave length over every 5 degrees of solar angle for the 24-hour day. In this way, I have evaluated steady-state ozone profiles between the equator and 75° latitude at the solar equinox.

Recently Randhawa (1971) published two ozone profiles [27] obtained from rocket soundings at Panama, 9° north, November 1970. These profiles are replotted in Figure 8, where some fine structure of the original data is lost. The calculated curves [1, 2] for pure air at the equator and at 30° latitude are also given in Figure 8; these calculated curves follow directly from the two ratios discussed above and vary as $(k_2[M]/k_3)^{1/2}(J_a/J_c)^{1/2}$. The curves calculated on the basis of pure air indicate far more ozone than is actually observed.

The calculated curves in Figure 8 are drawn with a heavy line above 27 kilometers and a light line below that elevation. This distinguishes between the regions in which the photochemical half-time for ozone is less than three months (above 27 km) and greater than three months (below 27 km). Vertical eddy diffusion and transport (equatorial to polar) may modify a vertical profile in times longer than three months, but probably such modification is small for times less than three months in the lower temperate and tropical regions considered in Figure 8. The calculated curve is far greater than the observed profiles at all elevations, including the high elevations where photochemical reactions are fast.

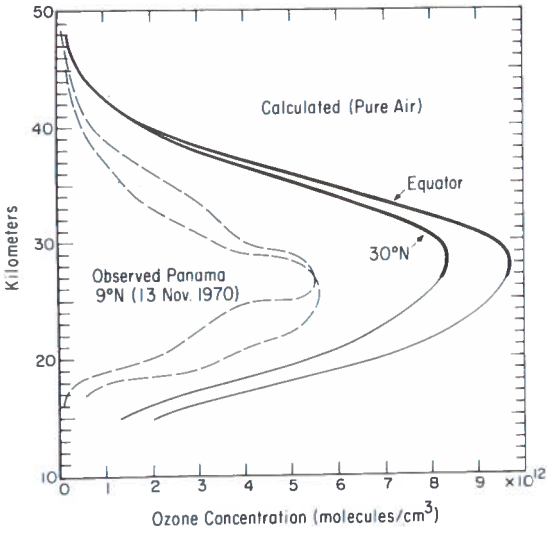

Figure 8. Ozone profiles, observed at Panama (9°N) and calculated from a model of pure dry air. The difference between these curves is referred to as the "ozone deficit".

In short, ozone in the stratosphere is destroyed by some process other than pure air reactions. In tropical regions above 25 kilometers (the ozone factory of the world) there is an ozone deficit of a factor between 2 and 3. Something else is very active in destroying ozone in the natural stratosphere (compare reference 4).

Other loss processes. Various proposals have been made to explain this stratospheric ozone deficit: (1) Loss of ozone by eddy diffusion to the troposphere; (2) loss of ozone to the troposphere by the spring polar overturn; (3) catalytic destruction of ozone by free radicals based on water, the HO_x system; and (4) catalytic destruction of ozone by the oxides of nitrogen, the NO_x system.

Loss of ozone from the stratosphere by air motions. It has been suggested by London[28] that the "ozone deficit" is an artifact of the steady-state calculation. In a large-scale computation considering day and night variation and global circulation, he found little or no ozone deficit for a model simulating the month of January. On the other hand, I find an ozone deficit of a factor of almost three in the tropics and a factor of about 1-3/4 on a global basis. The difference between my results and those of London probably lies more in the values used for rate constants than in steady-state versus global circulation. In a list circulated in April 1971, London gave as his rate constants $k_2 = 5.5 \times 10^{-34}(300/T)^{2.6}$ and $k_3 = 1.86 \times 10^{-11}\exp(-2130/T)$. The values I used[1,2] were $k_2 = 2.4 \times 10^{-35}\exp(1080/T)$ and $k_3 = 1.33 \times 10^{-11}\exp(-2120/T)$. The significant quantity is the ratio k_2/k_3. For three representative stratospheric temperatures, these ratios are related as follows:

	220°K	237°K	260°K
$\frac{k_2/k_3 \text{ Johnston}}{k_2/k_3 \text{ London}}$	2.7	2.3	2.0

To be sure, there is uncertainty as to the values of these rate constants, especially k_2, at low temperatures in air. However, London and Johnston's ozone-deficit differences seem to depend principally on the rate constants.

It is agreed that air motions are dominant in controlling the distribution of stratospheric ozone at low elevations at all latitudes and at all elevations at very high latitudes. The transport of ozone from 30 to 20 km or from 30° to 70° latitude at 30 km does not remove ozone from the stratosphere; it merely displaces it from one part of the stratosphere to another. This section examines the magnitude of the processes which transport ozone from the stratosphere to the troposphere.

Consider a volume element of fixed coordinates in the stratosphere—for example, a cubic meter. For a short interval of time (say, a few minutes) the change of ozone in this volume may be factored into three vectors, each one of which has multiple components. These three vectors are: (A) *The gross rate of formation of ozone from the photolysis of oxygen.* This photochemical reaction is brought about by two processes:

$$\begin{aligned} O_2 + h\nu &\rightarrow O + O \\ 2(O + O_2 + M &\rightarrow O_3 + M) \end{aligned} \qquad (33)$$

$$\text{net: } 3O_2 + h\nu \rightarrow 2O_3$$

The rate of this reaction can be calculated from the local intensity of sunlight and the concentration of oxygen. If one takes the ozone concentration to be the observed average value appropriate for the given elevation, latitude, and season, then one can calculate the local intensity of sunlight as a function of wavelength and evaluate the rate vector A. This calculation is very straightforward, and it makes no assumptions about photochemical steady state or the magnitude of the other rate vectors B and C. (B) *Chemical destruction of ozone.* Odd oxygen is destroyed by three families of reactions: O_x (O_3, O_2, O), NO_x (NO, NO_2), and HO_x (H, HO, HOO). These reactions are discussed in some detail later. These chemical reactions are driven by photochemically produced reactive species, O, HO, etc. (C) *Net transport of ozone by air motions.* Eddy diffusion or a wind component could bring ozone into any of the six faces of the cubic volume element. The air brought in has itself been subject to photochemical and chemical reactions in a nearby region of space, and in general its ozone concentration will not differ greatly from that of the reference volume element. If winds come in through some faces of the cube, they go out through other faces, transporting with them the ozone concentration currently in the volume element. Depending on the instantaneous gradients of the mole fraction of ozone, these air motions will remove more, less, or no ozone from the reference volume element. The net difference between transport in and transport out of the volume element is the vector C.

Three cases of these three rate vectors, A, B, and C, are given in Figure 9. Case I illustrates the situation in which there is a net transport of ozone out of the reference volume element, by virtue of the directions of the winds and the gradients. In this case the photochemical formation rate A is larger than the chemical destruction rate B. Case II represents a photochemical "steady state". (Chemists reserve the word "equilibrium" for the situation in which the balancing forward and reverse processes are the exact reverse; the photochemical process A and the chemical reactions B are not exact mirror images, and chemists call such a balance a "steady state". Meteorologists usually refer to this as photochemical "equilibrium". Of course, either name is satisfactory so long as it is clearly defined.) In this photochemical steady state, the rate of formation of ozone from photolysis of oxygen is exactly balanced by the various chemical reactions that destroy odd oxygen. This situation can come about if the absolute value of the rates A or B is very much larger than the net transport processes C. It can also happen if the transport of ozone into the volume element is equal to the transport out, that is, zero gradients in the direction of the wind, etc. Case III represents a net transport of ozone into the volume element. Air transport and photochemistry add ozone; chemical reactions destroy it.

For Cases I, II, and III in Figure 9 the combinations of photochemistry, chemistry, and transport give a steady state; the concentration of ozone in the volume element is not changing with time. Cases IV, V, and VI parallel Cases I, II, and III, except that the gain processes exceed the loss processes, and so the concentration of ozone increases with time. Of course, there are also processes VII, VIII, and IX, not shown, in which the loss processes exceed the gain processes, and the concentration of ozone in the volume element decreases.

Consider a smoothed, average, actual distribution of ozone over latitude and elevation at the fall equinox. At each nm of wavelength between 190 and 400 nm, consider the solar intensity averaged over a 5° angular grid for the 24-hour day. With an elevation grid of one kilometer and a latitude grid of 15°, the integral of the gross rate of formation of ozone (vector A), over the stratosphere from 15 to 45 kilometers in the

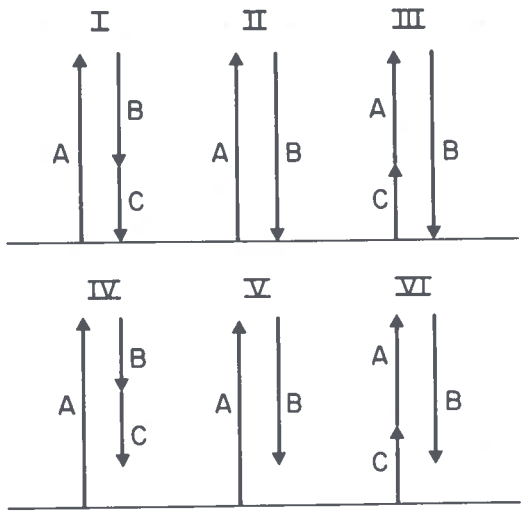

Figure 9. Rate vectors in the ozone balance. A – gross rate of formation of ozone from photolysis of oxygen; B – rate of destruction of odd oxygen (ozone) by chemical reactions; C – net rate of transfer of ozone by air motions. Cases I, II, III: local steady-state considering photochemistry, chemistry, and air transport. Cases IV, V, VI: unbalanced A, B, C leading to net increase in local ozone concentration.

northern hemisphere, is 8×10^{10} tons of ozone per year (the solar flux for the year is approximated as that for the solar equinox). This calculation, of course, involves no assumption about a photochemical steady state.

The transport of ozone from one part of the stratosphere to another does not represent ozone destruction or removal. To estimate the loss of ozone from the stratosphere to the troposphere, one must integrate vector C over the boundary between the stratosphere and troposphere. Vertical eddy diffusion brings large amounts of ozone from the photochemically active region above 25 kilometers down into the photochemically sluggish region between 15 and 20 kilometers. Further vertical eddy diffusion brings ozone down into the troposphere. Paetzold [29] has calculated the average loss from this process to be about 10^{11} molecules of O_3 cm^{-2} sec^{-1} Such a loss integrated over the northern hemisphere is 7×10^{8} tons per year. Horizontal transport and diffusion move large amounts of ozone from tropical regions toward polar ones. Further horizontal transport and subsidences during the winter months build up a thick column of ozone

in polar regions, which is broken up and scattered into the troposphere[30a] in the "spring overturn". It is assumed that this loss is equal to the full difference between the spring maximum and late summer minimum[30b] integrated over all latitudes. Such a loss of ozone to the troposphere is 4×10^8 tons per year for the northern hemisphere [3]. Junge [31a] made a similar calculation, finding the difference of total ozone in the northern hemisphere between spring maximum and fall minimum to be 3.5×10^8 metric tons per year. Ascribing all of this difference to the ozone loss at the "spring overturn" is probably accurate within a factor of two. The sum of these two effects gives 1.1×10^9 tons per year as an estimate of the loss of ozone to the troposphere as a result of air motions. This is regarded as the integral of rate C over the boundary of the stratosphere.

For the entire stratosphere of the northern hemisphere, the integral of rate A, the gross rate of formation of ozone from sunlight, is 8×10^{10} tons per year. The integrated losses due to transport at the boundaries, rate C, are 1.1×10^9 tons per year, or between 1 and 2 percent of the total of rate A. The total ozone inventory of the stratosphere is very nearly in a steady state on a long-term, year-to-year basis. Thus the difference in the gross rate of formation of ozone, A, and the transport of ozone from the stratosphere, C, must be ascribed to chemical destruction by the reaction systems O_x, HO_x, and NO_x. These chemical destruction rates, over the entire stratosphere and entire year, must account for 98 to 99 percent of the balancing of ozone production. Thus the long-term global ozone balance is approximately given by A = 100%, C = 2%, and B = 98%.

At 45°N at the fall solar equinox, the instantaneous (one-day average) rate of A integrated over the vertical column is 90×10^{11} molecules cm^{-2} sec^{-1}, and loss to the troposphere by eddy diffusion (according to Paetzold[29]) is 1×10^{11}.

These considerations make it clear that the ozone deficit as illustrated by Figure 8 cannot be explained in terms of mechanical transport.

In summary, although atmospheric motions are dominant in determing the vertical distribution of ozone in the lower stratosphere and its world-wide distribution at high latitudes, mechanical transport of ozone from the stratosphere to the troposphere balances out less than 2 percent of the gross rate of ozone formation. Therefore, at least 98 percent of natural ozone destruction is brought about by processes in the stratosphere, probably photochemical reactions.

Loss of ozone by water reactions. The free radicals based on water are indicated by the symbol HO_x (H, HO, HOO). These free radicals are formed from singlet D oxygen atoms, which are produced by the photolysis of ozone below 310 nm.

$$
\begin{aligned}
&O_3 + h\nu(\text{below } 310 \text{ nm}) \rightarrow O_2 + O(^1D)\\
&O(^1D) + M \rightarrow O + M \qquad (34)\\
&O(^1D) + H_2O \rightarrow 2HO\\
&O(^1D) + CH_4 \rightarrow HO + CH_3
\end{aligned}
$$

$$
\left(
\begin{aligned}
&CH_3 + O_2 \xrightarrow[M]{} H_2CO + HO\\
&\qquad\qquad \rightarrow CH_3OO\\
&H_2CO + h\nu \xrightarrow{} H_2 + CO\\
&\qquad\qquad \rightarrow H + HCO\\
&H + O_2 + M \rightarrow HOO + M\\
&HCO + O_2 \rightarrow HOO + CO
\end{aligned}
\right)
$$

From laboratory studies a number of reactions have been demonstrated and rate constants evaluated for HO_x reactions. The known reactions in this system include

$$
\begin{aligned}
&(H)\quad H + O_3 \rightarrow HO + O_2 \qquad (35)\\
&\qquad H + O_2 + M \rightarrow HOO + M
\end{aligned}
$$

$$
\begin{aligned}
&(HO)\quad HO + O \rightarrow H + O_2 \qquad (36)\\
&\qquad HO + HO \rightarrow H_2O + O\\
&\qquad HO + HO + M \rightarrow H_2O_2 + M\\
&\qquad HO + HOO \rightarrow H_2O + O_2
\end{aligned}
$$

$$
\begin{aligned}
&(HOO)\quad HOO + O \rightarrow HO + O_2 \qquad (37)\\
&\qquad HOO + HOO \rightarrow H_2O_2 + O_2
\end{aligned}
$$

$$
\begin{aligned}
&(H_2O_2)\quad H_2O_2 + O \rightarrow HO + HOO \qquad (38)\\
&\qquad H_2O_2 + h\nu \rightarrow HO + HO\\
&\qquad H_2O_2 + HO \rightarrow H_2O + HOO
\end{aligned}
$$

$$
(v^*)\quad HO\,(v \geq 3) + O_3 \rightarrow H + O_2 + O_2 \qquad (39)
$$

The rate constants for these reactions are given in references 32-35, 5, 12, and their references. There has been a great deal of activity in this field during the immediate past, and some of the recent estimates have varied rather widely; for example, the ratio of rate constants k_4/k_5 for the reactions

$$\begin{aligned} &(R4)\ O(^1D) + H_2O \rightarrow 2HO \\ &(R5)\ O(^1D) + O_2 \rightarrow O + O_2 \end{aligned} \qquad (40)$$

has been reported as 10.7 [ref. 33a, 1971], 4.2 [ref. 33b, 1971], and 0.12 [ref. 33c, 1970]. In the stratosphere, the important quantity is the ratio of the constants of $O(^1D)$ reactions with water and with air, since this determines the fraction of $O(^1D)$ that goes to form two hydroxyl radicals. It appears that this important ratio is not yet satisfactorily known, although the current active interest will probably remedy the situation very soon.

The reaction of $O(^1D)$ with water to form hydroxyl radicals was discovered [36] by McGrath and Norrish in 1960. They then speculated that the chain decomposition of wet ozone by ultraviolet light was brought about by the reactions

$$\begin{aligned} &(R6)\ HO + O_3 \rightarrow HOO + O_2 \\ &(R7)\ HOO + O_3 \rightarrow HO + O_2 + O_2 \\ &\text{net:}\quad 2O_3 \rightarrow 3O_2 \end{aligned} \qquad (41)$$

Kaufman (1964)[37] attempted to measure the first of these reactions, but did not observe it to occur. He was able to set a limit on its rate:

$$k_6 < 5 \times 10^{-13}\ \text{cm}^3\ \text{molecule}^{-1}\ \text{sec}^{-1}$$

Many unsuccessful attempts have been made to measure the rates of these reactions. Recently Langley and McGrath[12] have looked for this reaction in a situation where it would produce a large effect if it were present. They showed that reaction 6 is 5000 times slower than the limit set by Kaufman, that is,

$$k_6 < 10^{-16}\ \text{cm}^3\ \text{molecule}^{-1}\ \text{sec}^{-1}. \qquad (42)$$

With this very low limit, the thermal chain reaction based on HO and HOO is ruled out as an important process in the stratosphere.

Hunt [38, 39] discussed the need to consider loss processes for ozone other than those based on pure air, and he adopted McGrath and Norrish's hypothetical [36] reaction chain for model calculations. He replaced Kaufman's[37] inequality, $k_6 < 5\times10^{-13}$, by an equality

$$k_6 = 5\times10^{-13}.$$

Hunt said "A rather arbitrary assignment of 10^{-14} was made for the value of k_7, but the reaction must be rather slow as the rate has not been measured yet. . . The ozone profile was. . . sensitive to the value of k_7. . . varying k_7 from 10^{-13} to 10^{-15} changed the total O_3 amount from 0.1 to 0.35 cm STP". Thus by adjusting the rate constant of this hypothetical reaction, one can calculate any desired reduction of the total ozone column. In his article, Hunt[39] made model calculations in which he demonstrated that water reactions would be sufficient to explain the ozone deficit if the rate constants were as big as $k_6 = 5\times10^{-13}$ and $k_7 = 10^{-14}$. The demonstration by Langley and McGrath[12] that k_6 is less than 10^{-16} shows that these water reactions are *not* sufficient to explain the ozone deficit. There is no longer any justification for using these hypothetical reactions in stratospheric photochemical models.

In terms of known chemical reactions, there are several catalytic cycles involving the HO_x system, but their effects are very minor below 45 km. Examples[8] of such cycles are

$$\begin{aligned} &HO + O \rightarrow H + O_2 \\ &H + O_3 \rightarrow HO + O_2 \\ &\text{net: } O + O_3 \rightarrow O_2 + O_2 \end{aligned} \qquad (43)$$

$$\begin{aligned} &HO + O \rightarrow H + O_2 \\ &H + O_2 + M \rightarrow HOO + M \\ &HOO + O \rightarrow HO + O_2 \\ &\text{net: } O + O \rightarrow O_2 \end{aligned} \qquad (44)$$

At high pressures (laboratory conditions) of water and ozone, an energy chain involving vibrationally excited hydroxyl radicals may occur [12]:

$$H + O_3 \rightarrow HO\ (v \leqslant 9) + O_2 \qquad (45)$$
$$HO\ (v \geqslant 3) + O_3 \rightarrow H + O_2 + O_2$$
$$\text{net:} \quad 2O_3 \rightarrow 3O_2$$

Recently two key rate constants in the HO_x system have been found to be much larger than previously supposed.

$$O(^1D) + H_2O \rightarrow 2HO \qquad (46)$$

may be as much as 10 times faster than the deactivation of $O(^1D)$ by air [33a], whereas previous estimates indicated these rate constants to be about the same size. The reaction

$$HO + HOO \rightarrow H_2O + O_2 \qquad (47)$$

has been directly observed for the first time [40], and its rate constant is 20 times larger than Kaufman's estimate [35]. This large rate constant, 2×10^{-10}, for an HO_x termination step has the effect of reducing the calculated HO_x below previous estimates. Also, it is so much larger than the rate constants for $2HOO \rightarrow H_2O_2$ and $2HO \rightarrow H_2O + O$ that Nicolet's ingenious method [32] of calculating the sum of HO and HOO cannot be used. However, the large increases of these two rate constants over their previously presumed values tend to offset each other, and the total HO + HOO is probably not greatly different from Nicolet's 1970 estimate.

In the summer of 1970, the reactions R6 and R7 were believed [41] to occur with large rate constants, and these reactions were the primary basis of the "water model" of stratospheric ozone. At that time the rate constants for deactivation of $O(^1D)$ by air and for the reaction of $O(^1D)$ with water were not known; the rate constant for HO + HOO was presumed to be 20 times lower than it has now been found to be. Recall, however, a quotation [41] from the SCEP report (page 69): "Both carbon monoxide and nitrogen in its various oxide forms can also play a role in stratospheric photochemistry, but despite greater uncertainties in the reaction rates of CO and NO_x than for water vapor, these contaminants would be much less significant than the added water vapor and may be neglected". The statement about uncertainties is backwards. Laboratory chemical kinetics is a predictive atmospheric science only if one sticks to known reactions with measured and re-measured and thoroughly verified rate constants. *The use of rate constants of hypothetical reactions as adjustable parameters must be excluded.* We have an example, Hunt (1966) through SCEP (1970), where the hypothetical water reactions were promoted from an arbitrary artificial model [39] to the basis for dismissing reactions of the oxides of nitrogen [41]!

The other water reactions (Equations 43 and 44) can account for about one percent of the gross destruction rate of ozone, which is about the same as the effect of the reaction $O(^1D) + O_3 \rightarrow 2O_2$. The full family of water reactions is not sufficient to account for the ozone deficit demonstrated by Figure 8.

We may sum up this section by saying that not only are the HO_x reactions inadequate to explain the ozone deficit in the stratosphere, but they are negligible in the ozone budget.

Loss of ozone by catalytic reactions with the oxides of nitrogen. Anyone who has worked extensively with ozone in the laboratory is aware that oxides of nitrogen in very small amounts greatly reduce the yield of an ozonizer and increase the decomposition rate of ozone in any experiment. At room temperature and with relatively high concentrations of ozone, the dominant process is the thermal catalytic reaction already discussed at length [7] (Equations 18-22). Under conditions of the stratosphere (low temperature, low mole fraction of ozone, and powerful ultraviolet radiation field), the dominant process whereby NO_x (NO, NO_2, NO_3) destroys ozone is the simple catalytic cycle

$$(R8)\ NO + O_3 \rightarrow NO_2 + O_2 \qquad (48)$$
$$(R9)\ NO_2 + O \rightarrow NO + O_2$$
$$\text{net:}\ O + O_3 \rightarrow O_2 + O_2$$

Both ozone and oxygen atoms are destroyed, but nitric oxide and nitrogen dioxide are not destroyed. The cycle can be repeated indefinitely,

limited by the rate of the second step. This catalytic cycle occurs in competition with another, "do nothing" cycle

$$\begin{aligned} &(R8)\ NO + O_3 \rightarrow NO_2 + O_2 \qquad (49)\\ &(R10)\ NO_2 + h\nu(300\text{-}400\ nm) \rightarrow NO + O\\ &(R3)\ O + O_2 + M \rightarrow O_3 + M \end{aligned}$$

net: no reaction

Thus reaction (R9) is the rate-determining step in the catalytic cycle.

In the lower stratosphere the steady-state concentration of oxygen atoms is very low, and reactions involving it become slow. Another catalytic cycle becomes very important in the lowest stratosphere:

$$\begin{aligned} &NO_2 + O_3 \rightarrow NO_3 + O_2 \qquad (50)\\ &NO_3 + h\nu\ (VISIBLE) \rightarrow NO + O_2\ (DAY)\\ &NO + O_3 \rightarrow NO_2 + O_2 \end{aligned}$$

net: $2O_3 + h\nu(VISIBLE) \rightarrow 3O_2$

This reaction is driven by visible light, which is abundant at low elevations (unlike the radiation required to produce oxygen atoms). This catalytic cycle, too, may involve a non-catalytic competing reaction

$$\begin{aligned} &NO_2 + O_3 \rightarrow NO_3 + O_2 \qquad (51)\\ &NO_3 + h\nu\ (\text{below } 560\ nm) \rightarrow NO_2 + O\\ &O + O_2 + M \rightarrow O_3 + M \end{aligned}$$

net: no reaction

Most light absorption and photodissociation of NO_3 occurs at wavelengths longer than 500 nm. At night NO_3 combines with NO_2 to form N_2O_5. The next day N_2O_5 is destroyed by both oxygen atoms and photolysis, one of which destroys ozone and the other is neutral.

$$\begin{aligned} &NO_2 + O_3 \rightarrow NO_3 + O_2 \qquad (52)\\ &NO_3 + NO_2 \xrightarrow{M} N_2O_5 \qquad (night)\\ &N_2O_5 + O \rightarrow 2NO_2 + O_2\ (next\ day) \end{aligned}$$

net: $O_3 + O = O_2 + O_2$

$$\begin{aligned} &NO_2 + O_3 \rightarrow NO_3 + O_2 \qquad (53)\\ &NO_3 + NO_2 \rightarrow N_2O_5 \qquad (night)\\ &N_2O_5 + h\nu \rightarrow 2NO_2 + O\ (next\ day)\\ &O + O_2 + M \rightarrow O_3 + M \end{aligned}$$

net: no reaction

The rate constants for the following reactions,

$$\begin{aligned} &NO_2 + O \rightarrow NO + O_2 \qquad (54)\\ &NO + O_2 \rightarrow NO_2 + O\\ &NO_2 + M \rightarrow NO + O + M\\ &NO + O + M \rightarrow NO_2 + M\\ &NO + NO + O_2 \rightarrow NO_2 + NO_2\\ &NO_2 + NO_2 \rightarrow NO + NO + O_2 \end{aligned}$$

have been critically evaluated and summarized by Baulch and co-workers at Leeds University [42]. This volume should be used in the same way as that of reference 8: new data should be added to this critical compilation and the status of each reaction should be based on the sum of new data and old.

The following reactions

$$\begin{aligned} &NO_2 + O_3 \rightarrow NO_3 + O_2 \qquad (55)\\ &NO_3 + NO_3 \rightarrow 2NO_2 + O_2\\ &NO_3 + NO_2 \xrightarrow{M} N_2O_5\\ &NO_3 + NO \rightarrow NO_2 + O_2 + NO\\ &NO_3 + NO \rightarrow NO_2 + NO_2\\ &N_2O_5 \xrightarrow{M} NO_2 + NO_3 \end{aligned}$$

have been critically reviewed and tabulated in reference 7. The primary photochemical processes in the photolysis of nitrogen dioxide have been reviewed in detail by Leighton [43]:

$$NO_2 + h\nu(\text{below } 400\ nm) \rightarrow NO + O \qquad (56)$$

The reaction of nitric oxide with ozone has been studied over a range of temperature in three cases [44]:

$$(R8)\ NO + O_3 \rightarrow NO_2 + O_2$$

One interesting feature of this reaction is that a fraction (depending on pressure) of the product NO_2 molecules emit chemiluminescent light, which can be used as a sensitive analytical method for either NO or O_3. The values of the rate constants in units of cm^3 $molecule^{-1}$ sec^{-1}, as found by three investigators, are:

$1.33 \times 10^{-12} \exp(-2.5/RT)$ [Ref. 44a]
$0.95 \times 10^{-12} \exp(-2.46/RT)$ [Ref. 44b]
$1.97 \times 10^{-12} \exp(-2.55/RT)$ [Ref. 44c]

These three investigations cover a wide range of reactant pressure and temperature, 198 to 345°K, and they agree quite satisfactorily with each other and with values observed at room temperature [44d].

The rates of photolysis of NO_3 and N_2O_5 and the rates of reaction of oxygen atoms with N_2O_5 are not known. Whether the reaction $NO_2 + O_3$ during the day leads to ozone destruction or not depends on whether NO_3 is dissociated as $NO + O_2$ or $NO_2 + O$. During the night the reaction $NO_2 + O_3$ leads to N_2O_5, and whether this leads to ozone destruction or not depends on the relative rates (during the next day) of the reactions

$$N_2O_5 + O \rightarrow 2NO_2 + O_2$$

or

$$N_2O_5 + h\nu \rightarrow 2NO_2 + O.$$

In summary, the rate constants for the key NO_x catalytic cycle ($NO + O_3 \rightarrow NO_2 + O_2$, $NO_2 + O \rightarrow NO + O_2$) are fairly well known, but some of the reactions of the secondary cycle initiated by $NO_2 + O_3$ have not yet been adequately determined in the laboratory.

Apparently there are no measurements of the oxides of nitrogen in the stratosphere. The concentration of nitric oxide at 70 km has been observed to be about 50 parts per billion [45] (ppb, parts in 10^9). Nitrogen dioxide has been demonstrated to be present in the lower stratosphere by infrared absorption [46, 47], but quantitative data have not been obtained. In the troposphere [48] the oxides of nitrogen are about one to four ppb; soil bacteria are the principal source, and rainfall is the principal mechanism for removal (in the form of nitric acid or dissolved nitrates). With a ground source and upper tropospheric sink (dissolved nitrates), the gradient of NO_x is a decrease with increasing elevation in the troposphere. The boundary value of NO_x at the tropopause must be about 1 ppb. The boundary value at the stratopause must be about 50 ppb [45]. The direction of the diffusion flux is downward throughout the stratosphere, and its mole fraction surely lies within the range of one to 50 ppb. These general considerations suggest that we arbitrarily assume the natural stratosphere to contain 10 ppb and 100 ppb for model calculations of the effect of NO_x on the ozone profile.

One of the observed ozone curves in Figure 8 is reproduced and given in Figure 10. The ozone profiles calculated for uniform backgrounds of NO_x at 10 ppb and at 100 ppb are also given in Figure 10. It is immediately obvious that uniform distributions of NO_x between 10 and 100 ppb are sufficient to account for the ozone deficit shown by Figure 8. Crutzen [4] and Johnston [1, 2] have shown that non-uniform distributions of NO_x, averaging respectively 12 and 6.6 ppb, account very well for the actual ozone profile in the upper, photochemically active stratosphere.

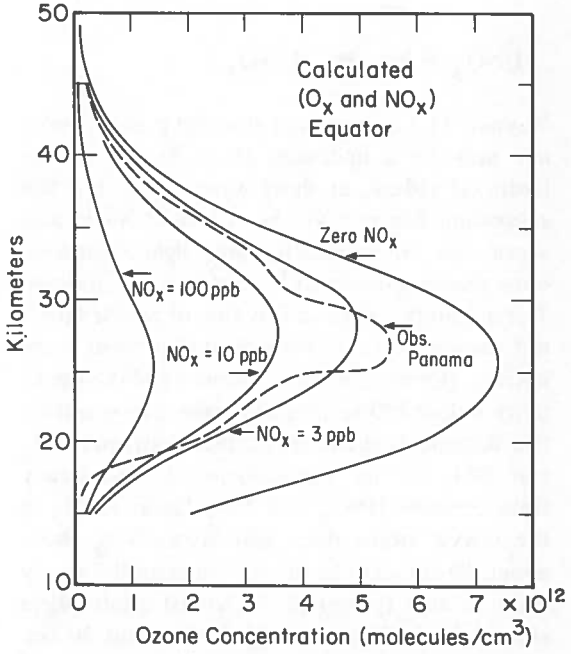

Figure 10. An ozone profile observed at Panama (9°N) and ozone profiles calculated for the equator with uniform NO_x mole fractions of 10 ppb and 100 ppb. NO_x is sufficient to account for the ozone deficit.

In short, the oxides of nitrogen (NO and NO_2) at an average mole fraction of about 10^{-8} in the stratosphere are indeed sufficient to account for the ozone deficit shown by Figure 8.

Nitric acid. From its infrared absorption spectrum, nitric acid has been detected in the lower stratosphere [47, 49]. It is formed [50] by the bimolecular association

$$HO + NO_2 \xrightarrow{M} HNO_3 \qquad (58)$$

which is in its transition region between third-order and second-order kinetics. (The rate constant is neither second-order nor third-order, but variable between these limits.) This rate constant under stratospheric conditions is uncertain by a factor of three or so. Nitric acid is both formed and destroyed by hydroxyl radicals:

$$HO + HNO_3 \rightarrow H_2O + NO_3 \qquad (59)$$

The rate constant for this reaction is known. Nitric acid is photolyzed by ultraviolet radiation

$$HNO_3 + h\nu \rightarrow HO + NO_2 \qquad (60)$$

or

$$HNO_3 + h\nu \rightarrow H + NO_3$$

Wayne[51] has suggested that the primary product may be a hydrogen atom, instead of the hydroxyl radical, at short wavelengths, but this suggestion has not yet been tested. Nitric acid vapor has an extremely large light-absorption cross-section (about 10^{-17} cm^2) around 200 nm. The quantum yield as a function of wavelength is not known, and thus the rate of photolysis is not known. However, if the quantum yield is close to unity below 250 nm, we can make semi-quantitative statements about the balance between HNO_3 and NO_2 in the stratosphere: (1) The steady state between HNO_3 and NO_2 favors HNO_3 in the lowest stratosphere and favors NO_2 above about 30 km. (2) The rate of attaining the steady state is slow (years) in the lowest stratosphere and relatively fast (months) above about 30 km. There is a great need to establish the values of the rate constants in this system.

A number of other reactions in the mixed HO_x, NO_x system have been discussed, but the rate constants have not been measured, such as

$$HO + NO \xrightarrow{M} HNO_2 \qquad (61)$$

$$HO + HNO_2 \rightarrow H_2O + NO_2$$

$$HNO_2 + h\nu\ (300 - 400\ nm) \rightarrow HO + NO$$

$$HOO + NO \xrightarrow{M} HNO_3$$

$$HOO + NO_2 \xrightarrow{M} HOONO_2$$

$$HOO + NO \rightarrow HO + NO_2$$

SOURCES OF NO_x

Sources of natural NO_x. Up to this point it has been argued that the ozone deficit is a real problem, that atmospheric motions, excited neutral oxygen, O_2 ($^1\Delta$), O_2 ($^1\Sigma$), and $O(^1D)$, and the HO_x reactions are insufficient to account for the ozone deficit, but that the NO_x reactions are sufficient to explain the ozone deficit if the natural NO_x background is on the order of 10^{-8} mole fraction. Now, we shall consider the natural sources of NO_x in the stratosphere.

If there were no sources or sinks of NO_x in the stratosphere, the flux and background concentration of NO_x could be calculated by means of the eddy diffusion equation from the boundary values of 50 ppb at the stratopause and about 1 ppb at the tropopause. Such a background is given by one of the curves in Figure 11.

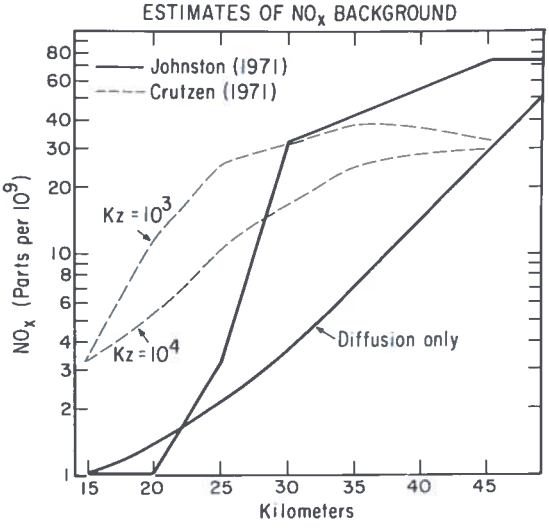

Figure 11. Natural background of NO_x as deduced from various models and methods. Crutzen's models derived from the reaction of N_2O and $O(^1D)$ in the stratosphere. Diffusion model based on boundary values of 50 ppb NO_x at stratopause and one ppb at tropopause. Johnston's model is reference 1, Table 17, entry 5, or reference 2, Table 1, entry 27.

In terms of this model the average NO_x background (that is, the total column of stratospheric NO_x divided by the total column of all stratospheric gases) is 2.3 ppb, and this is the minimum value, consistent with the boundary conditions. The flux for this model is 0.015×10^8 molecules cm^{-2} sec^{-1} if the diffusion constant K_z is 10^3 cm^2 sec^{-1}, and it is 0.15×10^8 if K_z is 10^4, presumed to be the range in the stratosphere [31b].

There is a recently-recognized natural source of NO_x inside the stratosphere: see Crutzen[5], McElroy[51], and Nicolet[52]. Bacteria in the soil and perhaps in surface ocean waters produce a small amount of nitrous oxide N_2O as a part of the nitrogen cycle. Nitrous oxide resembles carbon dioxide in many respects. It is virtually inert in the troposphere, and it has a natural background value of 0.25 parts per million, ppm. It diffuses up into the stratosphere where it is photolyzed

$$N_2O + h\nu \begin{pmatrix} 250 \text{ to } 320, \text{ weak} \\ 180 \text{ to } 220, \text{ moderate} \end{pmatrix} \rightarrow N_2 + O \qquad (62)$$

and where it reacts with singlet oxygen atoms[53]

$$N_2O + O(^1D) \rightarrow N_2 + O_2 \quad 50\% \qquad (63)$$
$$\rightarrow NO + NO \quad 50\%$$

The flux of NO into the stratosphere from this source, according to Crutzen, is between 0.29×10^8 molecules cm^{-2} ($K_z = 10^3$, $k_5 = 8 \times 10^{-11}$) and 1.5×10^8 ($K_z = 10^4$, $k_5 = 4 \times 10^{-11}$). These sources produce a steady state of NO_x in the troposphere as given by Figure 11. These quantities of NO_x are large enough to cut the clean-air ozone in half and to account for the ozone deficit.

Figure 11 also gives a curve for Johnston [1, 2]. This estimate of the NO_x background was deduced as a result of a systematic exploration of the effect of NO_x on the steady-state ozone profile. Since the HO_x reactions were shown to contribute only one or two percent to ozone destruction, these reactions were omitted. The steady-state calculations were made with a narrow grid of elevation (every kilometer from 15 to 50 km), a narrow grid of solar radiation (every nanometer from 190 to 400 nm), a narrow grid of solar angles (every 5 degrees averaged over 24 hours), and a standard pressure and temperature model for the stratosphere; the standard time was the solar equinox. The rate constants used were based on known reactions with rate constants established in the laboratory. There were no adjustable parameters. Thus the method could be used to explore the effect of one unknown parameter, namely, the NO_x background. Although a uniform NO_x background is a highly improbable distribution, model calculations were made for a wide range of uniform distributions with mole fractions of NO_x varying from 10^{-11} to 10^{-6}. A large number of calculations were made with non-uniform distributions of NO_x, where the distributions were selected with an eye to a 50-ppb boundary value at the stratopause, to a 1-ppb boundary value at the tropopause, to a natural source (such as N_2O) in the body of the stratosphere, and to a natural sink (HNO_3) in the lowest stratosphere. Ozone profiles (calculated on an absolute basis) were compared with observed profiles[54] with respect to shape in the upper half of the stratosphere, the total vertical column, and the elevation of the maximum ozone concentration. The selected background distribution is compared with Crutzen's distributions and the diffusion model in Figure 11. Crutzen included HNO_3 in his inventory of NO_x and I excluded it. This different method of bookkeeping accounts for the large difference between us in the lower stratosphere. In other respects the agreement between Crutzen and Johnston as to the natural background is rather good, although they were derived in considerably different ways. (This background was used in the *Science* article[2] and in the UCRL report[1] to demonstrate that the extent of vertical spread of artificial NO_x in the stratosphere is itself an important variable in this problem. For a given stratospheric load of NO_x added to this natural background, the reduction in ozone, steady-state calculation, varied between 3 percent and 50 percent, depending on the thickness of spread of the artificial NO_x).

Calculations of the diffusion of N_2O into the stratosphere and its degree of conversion to NO there have also been made by Nicolet[52] and by McElroy[51]. Their results and Crutzen's are:

Range of calculated NO_x flux in units of molecules cm^{-2} $sec^{-1} \times 10^8$	Author	Ref.
0.29 to 1.5	Crutzen	5
1.5 ± 1.0	Nicolet	52
0.25 to 0.65	McElroy	51

McElroy compared the limited data on the observed N_2O profile in the stratosphere with the prediction made by different values of the vertical diffusion coefficient K_z. He obtained his best agreement of calculated and observed N_2O profile in the stratosphere with $K_z = 10^3$, for which the associated value of the flux of NO in the stratosphere is the low extreme, 0.25×10^8 molecules cm^{-2} sec^{-1}. The elevation of maximum rate of NO formation was 24 kilometers.

Our conclusions are: (1) The reaction of nitrous oxide with singlet oxygen atoms is the most important known source of NO_x in the natural stratosphere. (2) This source strength is adequate to build up a steady state of NO_x in the stratosphere high enough to account for the observed ozone deficit. (3) Three different investigators obtained comparable estimates for the NO_x source strength.

Comparison of the chemical mechanisms for ozone balance. For the two models of an NO_x background shown in Figure 11 (a diffusion model and Johnston's model in the *Science* article[2]) and for a model for stratospheric water, the relative effects of NO_x, O_x, and HO_x on the integrated column rate of ozone destruction are given in Table 1. It can be seen that in the present natural stratosphere, NO_x is the dominant agent for ozone control. It is more than 50 times as important as the water reactions [12].

Artificial source of NO_x from the SST. The exhaust gases of the SST contain some NO_x. Estimates of this quantity have covered a fairly wide range. A definite way to specify the quantity is in units of grams of NO from the exhaust per kilogram of fuel burned. In these units the SCEP report[41] gave 42 grams of NO per kilogram of fuel. I used the figure [1, 2] of 14.8 grams of NO per kilogram of fuel. A number of calculations have been made based on a fleet of 500 SST's or Concordes[55], but of course the number of craft is another independent variable. Recent measurements reported by McAdams [56] indicate that the SST would have emitted between 20 and 30 grams of NO per kilogram of fuel, which is 5 or 10 times greater than a number of estimates made in the spring of 1971.

Table 1. Column contributions to gross rate of formation of ozone for different models of background oxides of nitrogen (units 10^{11} molecules cm^{-2} sec^{-1}).

Process	ozone rate	
	model 1	model 2
O_2 photolysis	+91	+108
NO_x	-64	-88
O_x	-26	-19
HO_x	-1.4	-1.4

model 1. 1 ppb at 15 km, 50 ppb at 45 km, logarithmic interpolation (similar to diffusion model of Figure 10).

model 2. Reference 2, Table 1, item 27.

If 500 SST's flew regularly in the stratosphere 7 hours per day, a new steady-state distribution of NO_x would eventually develop in the stratosphere. The artificial flux of NO would spread horizontally and vertically to a varying degree. The final NO_x inventory of the stratosphere would depend on numerous complex atmospheric motions and many photochemical reactions. A large problem would be the nitric acid reservoir and vertical distribution. This complex superposition of atmospheric motions and photochemistry constitutes an extremely difficult problem, which eventually should be worked out.

On the other hand, it is not necessary to work out this extremely complex problem to get an estimate of the size of the problem itself. 500 SST's, each burning 66 tons of fuel per hour, each flying 7 hours per day in the stratosphere, and each emitting 15 grams of NO per kilogram of fuel, would constitute a world-wide average NO flux of 1.5×10^8 molecules cm^{-2} sec^{-1}. (If the number of planes, fuel per hour, hours per day, or NO in g/kg are other than the values

given above, this figure can be scaled up or down accordingly.) This artificial flux is equal to Nicolet's estimate of the natural NO_x flux (although he indicated uncertainty by plus or minus 67%). This flux of 1.5×10^8 is equal to Crutzen's estimate of the maximum natural value, and it is over 5 times greater than his minimum estimate of 0.29×10^8 molecules cm^{-2} sec^{-1}. This world-wide average SST flux of NO into the stratosphere is 2.3 times greater than McElroy's maximum estimate of the natural NO flux, and it is 6 times his minimum estimate.

To be sure, the NO_x from the SST encounters all the complexities of stratospheric dynamics and photochemistry, but the natural NO produced from N_2O around 24 kilometers is also subject to these same complexities. The present NO_x flux (subject to all the complexities) builds up to such a point that it seems to be the agent that reduces the otherwise pure air ozone column by about a factor of two on a world-wide basis. If the artificial flux is equal to or up to six times larger than the natural flux, then as a first approximation one can expect stratospheric NO_x to increase by a factor between two and seven. If one measure of NO_x (the natural flux) has reduced the natural worldwide ozone by about a factor of two, then two to seven measures of NO_x (the natural plus the artificial flux) threatens to reduce the ozone shield by another very large amount – a 25 to 50 percent reduction on a world-wide basis appears to be the size of the threat.

The NO_x flux from the natural N_2O mechanism as estimated by Crutzen and by McElroy is indicated by a bar graph in Figure 12, with high and low estimates. The expected fluxes of NO_x from 500 Concordes* and from 500 SST's are also given. It can be easily visualized from this figure that the projected artificial source of NO_x from the SST is equal to or greater than the natural source of NO_x. It is difficult to conceive a model that would lead one to expect the artificial NO_x to behave quite differently from the natural NO_x.

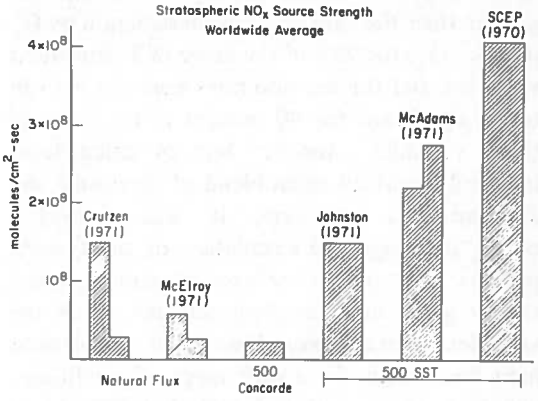

Figure 12. Relative source strengths of NO_x in the stratosphere, including the natural source [$N_2O + O(^1D)$] as calculated by references 5, 51, and 55 and the world-wide average source strength from 500 SST's according to different estimations.

In sum, it is easier to get a grasp on the magnitude of the threat to the ozone shield from artificial NO_x if one compares natural and artificial source strengths of NO_x, instead of trying to compare the stratospheric inventory of NO_x before and after SST flights. In terms of relative source strengths, it appears that 500 SST's will inject NO_x into the stratosphere at a rate equal to or several times greater than the natural source strength. Since the natural NO_x already plays the dominant role in controlling the stratospheric ozone inventory, such an increase in source strength would probably bring about a large reduction in the world's ozone shield.

DISCUSSION

In previous reports [1, 2], I have presented evidence that the oxides of nitrogen, which frequently had been discounted, are an important variable in stratospheric photochemistry, and may *not* "be neglected"[41]. The evidence that NO_x is an important variable took the form of several different model calculations; no attempt was made to solve the problem for all the stratosphere. One calculation (Tables 5 and 6 of reference 1) was based exclusively on chemistry; it showed that for the stratospheric range of

*The Concorde flux of NO was calculated on the following basis: 18,000 pounds of fuel burned per hour by one Concorde, 7 hours flight per day, 15 pounds of NO per thousand pounds of fuel. The Australian Academy of Science report number 15, "Atmospheric Effects of Supersonic Aircraft" gives as 1985 NO_x emission from the Concorde a value twice as large as that shown in Figure 12.

temperature and pressure, and for the amount of NO_x that the SCEP report[41] said would be added to the stratosphere, the rate of destruction of stratospheric ozone by NO_x (NO, NO_2) was greater than the rate of ozone destruction by O_x (O, O_2, O_3) for 95% of the range of independent variables, and the reaction rates were fast enough to be significant for 90 percent of the range of these variables. Another line of calculations involved about an equal blend of chemistry and atmospheric structure; it was shown[1] that: "Although the calculation of steady-state profiles of ozone on the basis of photochemical theory gives an incomplete account of all the variables of the stratosphere, such calculations have been made for a wide range of conditions, and in every case it is found that NO_x has a profound effect in reducing the steady-state ozone column. These calculations over a wide range of conditions give strong evidence for the vulnerability of the stratosphere to added man-made NO_x".

This report specifically illustrates that laboratory chemical kinetics can supply accurate predictions, both in the laboratory and in the atmosphere. However, one must follow strict rules to do so. One must adhere to measured and verified rate constants. Unknown rate constants must never be used as adjustable parameters in atmospheric calculations.

In previous reports[1-6] available rate constants were used to calculate the direction of change of stratospheric ozone upon addition of NO_x. A wide range of NO_x distributions was considered, and in all cases additional NO_x resulted in a decrease in stratospheric ozone. These calculations of the *relative* effect of increased NO_x are fairly insensitive to the absolute value of the pertinent rate constants. In this report an absolute value of the ozone concentration in pure air is calculated, and it is concluded that "something else" besides neutral oxygen species is dominant in reducing stratospheric ozone (compare similar conclusions in reference 4). This calculation depends on the absolute value of two rate constants and is thus sensitive to the accuracy of these quantities. If the ratio k_2/k_3 in conditions of the upper half of the stratosphere should turn out (after further refined laboratory measurement) to be four-fold or more less than the value used here, then the "ozone deficit" argument would be largely eliminated, that is, NO_x would not now be dominant in the stratospheric ozone balance. Even so, the effect of large artificial additions of NO_x is subject to the considerations of the previous reports [1, 2, 6]; large increases of NO and NO_2, as such would have a large effect on ozone, but large increases as HNO_3 would have a smaller effect.

In this problem, laboratory chemical kinetics serves in a role analogous to a grand jury: on the basis of current knowledge, NO_x is an important variable in the stratosphere; it must be "brought to trial", it may not "be neglected". A grand jury does not attempt to prove guilt or innocence; it merely certifies whether a case should be tried. The CIAP program should serve the role of "trial by jury" on this issue. The concentration and distribution of NO_x in the stratosphere, both as it is now and as it would be with SST's operating, must be explored.

ACKNOWLEDGMENT

This work was supported by the U.S. Atomic Energy Commission through the Inorganic Materials Research Division, Lawrence Berkeley Laboratory, University of California, Berkeley.

REFERENCES

1. Johnston, H., "Catalytic Reduction of Stratospheric Ozone by Nitrogen Oxides", Lawrence Radiation Laboratory Report, UCRL-20568, Berkeley, California, June 1971.
2. Johnston, H., Science, *173*, 517 (1971).
3. a. Johnston, H., "The Role of Chemistry and Air Motions on Stratospheric Ozone as Affected by Natural and Artificial Oxides of Nitrogen", paper presented at the Autumn Meeting of the National Academy of Sciences, Washington, D.C., 1971.
   b. Johnston, H., Environmental Affairs, 735(1972).
4. Crutzen, P.J., J. Roy Meteor. Soc. *96*, 320 (1970).
5. Crutzen, P.J., J. Geophys. Res. *76*, 7311 (1971).
6. Crutzen, P.J., "On Some Photochemical and Meteorological Factors Determining the Distribution of Ozone in the Stratosphere: Effects of Contamination by NO_x Emitted from Aircraft", Report AP-6, Institute of Meteorology, University of Stockholm, October 1971.
7. Johnston, H., *Gas Phase Reaction Rate Theory*, The Ronald Press Co., New York, 1966, Chapter 1.
8. Johnston, H., *Kinetics of Neutral Oxygen Species*, U.S. Department of Commerce, National Bureau of Standards, Volume 20 (1968).

9. Johnston, H., Berichte der Bunsengesellschaft für physikalische Chemie, *72*, 959 (1968).

10. Reference 7, chapter 8.

11. Potter, A.E., Jr., Coltharp, R.N., and Worley, S.D., J. Chem. Phys. *54*, 992 (1971).

12. Langley, K.R., and McGrath, W.D., Planet. Sp. Sci. *19*, 413 (1971).

13. Schumacher, H.J., and Sprenger, G., Zeitschrift für physikalische Chemie *B2*, 267 (1929).

14. Chapman, S., Mem. Roy. Meteor. Soc. *3*, 103 (1930); Philosophical Magazine *10*, 369 (1930).

15. Wayne, R.P., "The Photochemistry of Ozone and Singlet Molecular Oxygen in the Atmosphere", in *Mesospheric Models and Related Experiments*, Ed. G. Fiocco, D. Reidel Publishing Company, Dordrecht, Holland, 240-252 (1971).

16. a. Baiamonte, V.D., Hartshorn, L.G., and Bair, E.J., J. Chem. Phys. *55*, 3617 (1971).

b. Findley, F.D., and Snelling, D.R., J. Chem. Phys. *54*, 2750 (1971).

c. Gauthier, M., and Snelling, D.R., J. Chem. Phys. *54*, 4317 (1971).

d. Noxon, J.F., J. Chem. Phys. *52*, 1852 (1970).

e. Von Ellenrieder, G., Castellano, E., and Schumacher, H.J., Chem. Phys. Let. *9*, 152 (1971).

f. Zipf, E.C., Can. J. Chem. *47*, 1863 (1969).

g. Wayne R.P., Advances in Photochemistry *7*, 311 (1969).

h. Gilpin, R., Schiff, H.I., and Welge, K.H., J. Chem. Phys. *55*, 1087 (1971).

17. JANAF Thermochemical Data, The Dow Chemical Company, Midland, Michigan (1961).

18. Benson, S.W., and Axworthy, A.E., Jr., J. Chem. Phys. *26*, 1718 (1957); *42*, 2614 (1965).

19. Glissman, A., and Schumacher, H.J., Zeitschrift für physikalische Chemie, *21B*, 323 (1933).

20. Krezenski, D.C., Simonaitis, R., and Heicklen, J., Int. J. Chem. Kinet. *3*, 467 (1971).

21. Ackerman, M., "Ultraviolet Solar Radiation Related to Mesopheric Processes" in *Mesopheric Models and Related Experiments*, Ed. by G. Fiocco, D. Reidel Publishing Company, Dordrecht, Holland, 149-159 (1971).

22. Brinkman, R.T., Green, A.E.S., and Barth, C.A., "A Digitalized Solar Ultraviolet Spectrum", NASA Technical Report No. 32-951. Jet Propulsion Laboratory, Pasadena, California (1966).

23. Ditchburn, R.W., and Young, P.A., J. Atmos. Terr. Phys. *24*, 127 (1962); Watanabe, K., Inn, E.C.Y., and Zelikoff, M., J. Chem. Phys. *21*, 1026 (1953); Thompson, B.A., Harteck, P., and Reeves, R.R., Jr., J. Geophys. Res. *24*, 6431 (1963); Ogawa, M., J. Chem. Phys. *54*, 2550 (1971).

24. Inn, E.C.Y., and Tanaka, Y., *Ozone, Chemistry and Technology, Advances in Chemistry*, No. 21, American Chemical Society (1959), p. 263.

25. Calvert, J.G., and Pitts, J.N., Jr., *Photochemistry*, John Wiley and Sons, Inc., New York (1966), 651-659.

26. Dütsch, H.U., "Chemical Reactions in the Lower and Upper Atmosphere", International Symposium, Stanford Research Institute (1961).

27. Randhawa, J.S., J. Geophys. Res. *76*, 8139 (1971).

28. London, J., Meeting of the American Meteorological Society, New Orleans, January 1972.

29. Paetzold, H.K., "Vertical Atmospheric Ozone Distribution" in *Ozone, Chemistry and Technology, Advances in Chemistry*, No. 21, American Chemical Society, 1959, 209-220.

30. a. Dobson, G.M.B., *Exploring the Atmosphere*, The Clarendon Press, Oxford (1968), p. 126.

b. Ibid, p. 122.

31. a. Junge, C.E., *Air Chemistry and Radioactivity*, Academic Press, New York and London (1963), p. 57.

b. Ibid, p. 250.

32. Nicolet, M., Annales de Géophysique *26*, 531 (1970); Aeronomica Acta *89* (1971).

33. a. Paraskevopoulos, G., and Cvetanovic, R.J., Chem. Phys. Let. *9*, 603 (1971).

b. Scott, P.M., and Cvetanović, R.J., J. Chem. Phys. *54*, 1440 (1971).

c. Biedenkapp, D., Hartshorn, L.G., and Bair, E.J., Chem. Phys. Let. *5*, 379 (1970).

34. a. Donovan, R.J., Husain, D., and Kirsch, L.J., Chem. Phys. Let. *6*, 488 (1970).

b. Donovan, R.J., and Husain, D., Chem. Rev. *70*, 489 (1970).

35. Kaufman, F., Can.J. Chem. *47*, 1924 (1969).

36. McGrath, W.D., and Norrish, R.G.W., Proc. Roy. Soc. (London) *A254*, 316 (1960).

37. Kaufman, F., Annales de Geophysique *20*, 106 (1964).

38. Hunt, B.G., J. Atmos. Sci. *23*, 88 (1965).

39. Hunt, B.G., J. Geophys. Res. *71*, 1385 (1966).

40. Hochanadel, C.J., Ghormley, J.A., and Ogren, P.J., J. Chem. Phys. *56*, 4426 (1972).

41. *Man's Impact on the Global Environment, Report of the Study of Critical Environmental Problems* (SCEP), M.I.T. Press, Cambridge, Mass. 1970.

42. Baulch, D.L., Drysdale, D.D., and Horne, D.G., *Critical Evaluation of Rate Data for Homogeneous Gas Phase Reactions*, Volume 5, The University, Leeds, England (1970).

43. Leighton, P.A., *Photochemistry of Air Pollution*, Academic Press, New York and London, 1961.

44. a. Johnston, H., and Crosby, H., J. Chem. Phys. *22*, 689 (1954); *19*, 799 (1951).

b. Clyne, M.A.A., Thrush, B.A., and Wayne, R.P., Trans. Faraday Soc. *60*, 359 (1964).

c. Marte, J.E., Tschuikow-Roux, E., and Ford, H.W., J. Chem. Phys. *39*, 3277 (1963).

d. Phillips, L.F., and Schiff, H.I., J. Chem. Phys. *36*, 1509 (1962).

45. Meira, L.G., Jr., J. Geophys. Res. *76*, 202 (1971).

46. Ackerman, M., and Frimout, D., Bull. Roy. Acad. Belg. *55*, 948 (1969).

47. Murcray, D.R., Kyle, T.G., Murcray, F.H., and Williams, W.J., J. Opt. Soc. Amer. *59*, 1131 (1969); Nature *218*, 78 (1968).

48. *Air Quality Criteria for Nitrogen Oxides*, Environmental Protection Agency, Air Pollution Control Office, Washington.

49. Rhine, P.E., Tubbs, L.D., and Williams, D., Applied Optics *8*, 1500 (1969).

50. Johnston, H., submitted to J. Atmos. Sci. (1971).

51. McElroy, M.B., and McConnell, J.C., J. Atmos. Sci. *28*, 1095 (1971).

52. Nicolet, M., and Vergison, E., Aeronomica Acta *90* (1971).

53. Greenberg, R.I., and Heicklen, J., Int. J. Chem. Kinet. *2*, 185 (1970).

54. *Ozone Data for the World*, Meteorological Branch, Department of Transport, in cooperation with the World Meteorological Organization.

55. McAdams, H.T., *Analysis of Aircraft Exhaust Emission Measurement: Statistics*, Cornell Aeronautical Laboratory, Inc. Technical Report NA-5007-K-2, November 1971, p. III-4.

DISCUSSION

Johnston was congratulated on both the substance and the presentation of his talk. A. Goldburg said he was disturbed that Johnston should take a single average ozone profile and look for a concentration of NO_x that reproduces it, since ozone columns vary daily and even hourly; he questioned Johnston's proposal for the main controlling parameter. Johnston replied that he had made several hundred calculations of the total profiles, and plotted detailed ozone observations many hundreds of times, and was not adjusting his figures for the single case he had presented. He referred Goldburg to his detailed UCRL report, which concludes that stratospheric ozone is very sensitive to added NO_x. Goldburg said he was still not convinced that things actually happened that way in the stratosphere. Johnston replied that he had been identifying important variables and there was nothing else to account for the ozone deficit.

F. Singer noted that Johnston's assumption of a constant source of NO_x made this system a steady-state one, without motion and transport. He said he would be interested in data showing the effect of a sudden injection, and wondered whether Johnston had access to data on ozone levels after a volcanic eruption. Johnston answered that he left that to experts in that field; he dealt only with chemistry, and it indicated the need for further research into this supposedly negligible family of reactions. A. Ferri praised Johnston's presentation, but said a one-dimensional model with no cross-gradients or day/night-variations was speculative. More important, he felt, was that the bar in Figure 11 was somewhat misleading: first, disproportion between the Concorde and the U.S. SST was too great, and second, the NO_x could be reduced two orders of magnitude with present technology. The important thing was to understand the chemistry and the diffusion, and he felt the latter was oversimplified because it assumed only molecular diffusion, with no pressure and particularly no thermal diffusion. Johnston agreed that no NO would certainly solve the NO emission problem. He also remarked that chemists and meteorologists tend to concentrate on the importance of their own fields, and that his point – that in the balancing of stratospheric ozone, the transfer to the troposphere is small compared to the gross rate of formation – is by no means the only stratospheric factor that deserves further study.

The following brief presentation was made by F. Kaufman.

FREDERICK KAUFMAN
University of Pittsburgh

I should like to discuss one of the reactions that Dr. Johnston covered in his NSRDS report, $O + O_3$, because it is a key reaction. Dr. McCrumb and I have been measuring the rate of the $O + O_3 \rightarrow 2O_2$ reaction, using chemiluminescence to determine the O atom density. In Figure 7, Dr. Johnston showed you the results of his 1968 review of $O + O_3$. Figure 13 is our latest Arrhenius plot for this reaction, showing some of the earlier measurements but not the results of the 1968 review. Note the work of Krezenski, Simonaitis, and Heicklen at low temperature; the fit is really rather good, though we still get the same clumps of points up and down.

Table 1 shows six determinations of the rate expression for $O + O_3$. There must be a dozen or more in the earlier literature. As Professor Johnston said, they should not be thrown out. It is true, though, that the clumps

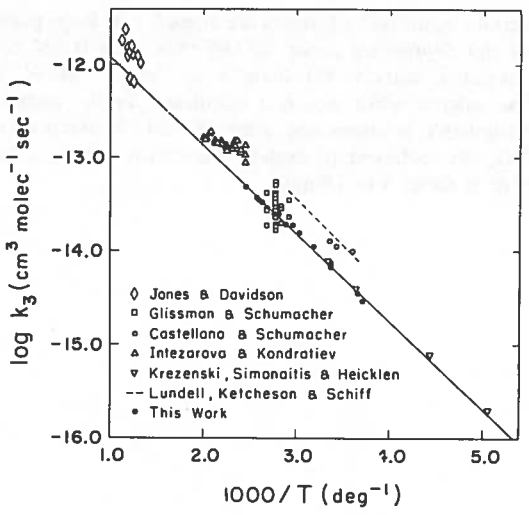

Figure 13. Temperature dependence of the rate coefficient of $O + O_3 \rightarrow 2O_2$ according to McCrumb and Kaufman (*J. Chem. Phys.*, to be published).

should not be taken very seriously, because Benson and Axworthy used mostly early Schumacher data in their work, and the pre-exponential factor A and the activation energy E have been going down since then. At a stratospheric temperature of 220°K, there is almost a factor of 10 between Benson's 0.12 and Schiff's 1.1, whereas the 1968 Johnston review gives 0.35. We think that the last two data groups, Krezenski's and ours, in which the activation energy is about 4.3 and the pre-exponential factor is about 1.1, represent quite believable rates. There are thus errors of a factor of 2 in the old data.

J. Anderson presented the following data.

J.M. ANDERSON
University of Pittsburgh

We are in the midst of a study of the rates of reaction between odd-nitrogen species and OH. Using resonance fluorescence, we have measured OH concentrations as low as 10^{10} cm^{-3}. We have obtained the following rates at 296°K. In the range from 1 to 4 torr, the low-pressure third-order rate of $NO_2 + OH + Ar \rightarrow HNO_3 + Ar$ is $1.0 \pm 0.3 \times 10^{-30}$ cm^6 sec^{-1}. This drops to 0.5×10^{-30} at 20 torr total pressure. The rate of $NO_2 + OH + N_2 \rightarrow HNO_3 + N_2$ is $2.0 \pm 0.5 \times 10^{-30}$, and the rate of $NO + OH + Ar \rightarrow HNO_2 + Ar$ is $3.9 \pm 1.0 \times 10^{-31}$, in the same low-pressure range.

This ended the discussion at the conference. Johnston submitted the following postscript in April to show how his conclusions would be modified by new values presented by D. Davis during the conference.

POSTSCRIPT BY DR. JOHNSTON

During the conference discussion of Dr. Crutzen's paper, Dr. Doug Davis of the University of Maryland announced the first measurements of the following reactions at stratospheric temperatures.

$$O + O_2 + N_2 \rightarrow O_3 + N_2$$

$$k_2 = 1.10 \times 10^{-34} \exp(1.0\,\text{kcal mole}^{-1}/RT)$$

cm^6 $molecule^{-2}$ sec^{-1}

$$O + NO_2 \rightarrow O_2 + NO$$

$$k_9 = (9.2 \pm 0.5) \times 10^{-12}\ cm^3\ molecule^{-1}\ sec^{-1}$$

At temperatures characteristic of the lower stratosphere (about 220°K), Davis' rate of reaction 2 is about one-half as fast, and his rate of reaction 9 is about twice as fast, as the values I used in 1971 and at this conference. In Figure 14 I reproduce the substance of my Figures 8 and 10, with the calculated curves now based on Davis' k_2 and k_9, on Ackerman's solar intensities [21], and on k_3 as deduced from Figure 7, which is essentially the same as that of Krezenski, Simonaitis, and Heicklen [20].

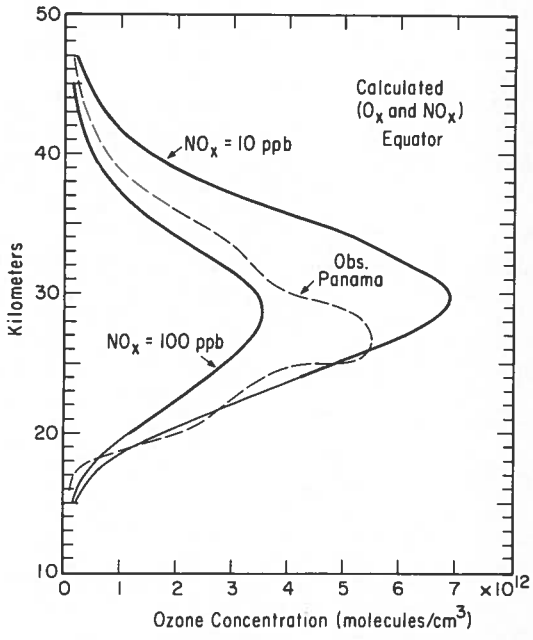

Figure 14. Vertical ozone profiles: —, recalculated using Davis' new rate constants for the reactions of O with O_2 and with NO_2; - - -, observed at 9°N.

The ozone column calculated for zero NO_x at the equator is 0.52 cm, which is 2 to 2½ times the average observed value, and substantially larger than the column

observed by Randhawa [27] at Panama. The equatorial ozone column calculated from the photochemical constants I used in 1971 is 0.67 cm [1]. With Davis' new rate constants, NO_x destroys ozone about four times faster than with my 1971 rate constants. The effect of NO_x on the steady-state profile of ozone for 3, 10, and 100 ppb of NO_x is given in Figure 14. Although certain quantitative features are altered, two main points of my conference paper are still valid with Davis' rate constants, namely, (1) there is an "ozone deficit" at the equator when ozone is calculated on the basis of Chapman's reactions and pure air, and (2) reactions of NO_x are sufficient to explain this deficit if NO_x is present at about 3 to 10 ppb.

MODELING THE CHEMICAL KINETICS OF THE STRATOSPHERE

FRANK P. HUDSON
Sandia Laboratories
Albuquerque, New Mexico 87115

ABSTRACT: A tutorial development of atmospheric processes important to the chemical kinetics of the stratosphere is presented. In parallel, the mathematical simulation of the total interaction of these processes – a chemical kinetics model – is developed. The interaction of the solar flux and the atmosphere is sketched; the energy states of the oxygen molecule are discussed as an example for atmospheric molecules; the build-up of a set of atmospheric species and reactions by steps, and the resultant families of reactions, are shown. The physical-mathematical foundation of the model, coupled continuity equations, is demonstrated, and examples of the types of results obtainable from calculations are given. The sample results are for a model using 33 atmospheric species composed of oxygen, nitrogen, hydrogen, and carbon atoms, with 170 chemical reactions among the species. The paper is a transcription of a lecture presented for the purpose of introducing the physics and chemistry of the stratosphere, and the related mathematical modeling, to scientists of other disciplines.

FOREWORD

This paper is concerned with the methods of assembling the great mass of detailed chemistry presented at this conference into a single mathematical model to allow calculation of atmospheric parameters and behavior to the extent that they are determined by the chemical kinetics.

One of the central purposes of this conference is mutual education among the several disciplines involved in the Climatic Impact Assessment Program. I will try to help those of you whose interest in CIAP is other than the physics and chemistry to gain some perspective on the role that chemical kinetics plays in determining the behavior of the normal and disturbed atmosphere. This background will lead to treatment of the problem of creating a reasonably accurate and complete mathematical simulation of the complex sets of atomic, molecular and photo-processes that determine atmospheric composition in the stratosphere – that is, a chemical kinetics model. The model will be time-dependent, but will incorporate transport of certain chemical species in only a simple fashion. It thus treats only half of the problem of atmospheric modeling. The almost intractable problem of fluid dynamic modeling is presented in later papers, and the means of interfacing the two modes of modeling, a necessary undertaking, must await a future conference.

INTRODUCTION

As Professor Nicolet indicated, chemical reaction models of the atmosphere have been a major method of evaluating and consolidating atmospheric data since the three-species, five-reaction model of Sidney Chapman in 1930. Professor Nicolet has been making significant contributions to this modeling for more than twenty years. The work of Bates, Hunt, Hesstvedt, and others has been vital, and the recent studies of Crutzen and of Johnston presented earlier were very important. The foundation of all models is experimental data, and their validity is only as great as their ability to match atmospheric measurements. The models are a means, however, potentially an excellent means, of bringing together a great deal of disparate atmospheric data, to present a coherent picture of atmospheric processes, and to allow extrapolation and prediction. The availability of large digital computers has made it possible to handle very large chemistry schemes. The major limitation is the availability of data rather than computer capacity or speed.

Instead of presenting the details of a completed computer code – a chemical model – I will show you descriptively the physical processes which must be considered, build up a set of chemical species and reactions, and draw these together through a set of continuity equations, which form

the mathematical simulation of stratospheric chemistry. Finally, I will present some examples of results from a 33-species, 170-reaction model.

The development of a chemical kinetics model could consist of the following steps:

1. Start with the particle densities of the major atmospheric constituents (O_2, N_2) at the altitudes to be considered.
2. Determine the spectrum and amount of solar energy available at these altitudes.
3. Calculate the rate at which the molecules of (1) will absorb the available energy of (2) to produce reactive species such as atoms, radicals, excited states of atoms or molecules, ions, and electrons; and compute the rates of formation of these new species.
4. Determine what chemical reactions occur among the species now present, and the rates at which they occur at the temperatures encountered. Establish what additional new species are formed as a result of these reactions.
5. Incorporate transport processes sufficiently rapid that they compete with the reactions of (4).
6. Include molecular species that are added by transport upward from the earth and the rate at which they are added, as a function of altitude.
7. Do the equivalent of (3) and (4) for the new species, iterating the steps until a sufficient level of detail and complexity is attained.
8. Express the above formation and loss of each species mathematically.
9. Solve these coupled equations simultaneously to determine composition or other characteristics sought under the specified conditions.

The specified conditions include time of day, season of year, latitude, solar activity, and other natural or artificial disturbances.

SOLAR FLUX AND THE ATMOSPHERE

With this introduction, let us start very simply to develop a chemistry model, adding complexity as we go. The detail will be limited to that which demonstrates the points to be considered, and the complexity will also be limited by resorting to graphical simplifications of families of reactions.

To orient the problem, some basic considerations of the solar flux, the earth, and the atmosphere are necessary. In Figure 1, the earth is shown in its elliptic orbit (indicated by the curved vertical arrow) around the sun, constantly bathed in the very broad spectrum of solar energy flux. The earth is also spinning on its own axis (shown flat in the two-dimensional figure, so it must be mentally rotated up 90° out of the plane of the figure). The spin-axis is not normal to the orbital plane, but is at an angle of more than twenty degrees from normal. The earth has, in addition, its own magnetic field which controls the trajectories of impinging charged particles.

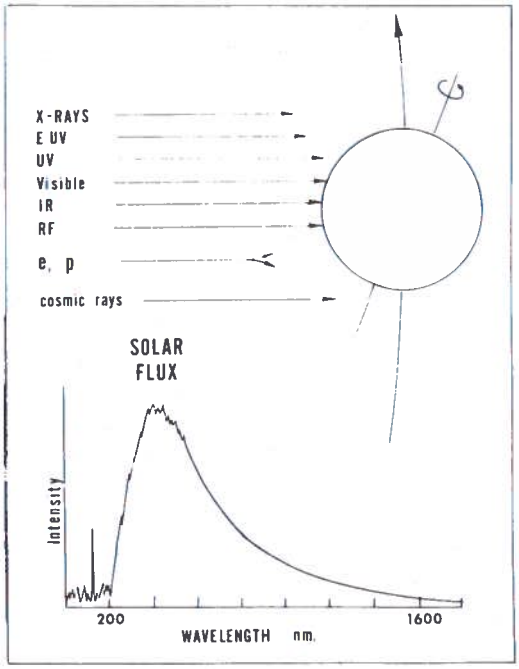

Figure 1. The earth in its solar orbit.

As shown at the left of the figure, the solar flux contains, in addition to the charged particles, an extremely broad spectrum of energy of photons extending from X-rays of about 0.1 nanometers* (nm) to radio-frequencies of many microns' wavelength. Most of the energy is in the blackbody portion of the spectrum at wavelengths longer than 200 nm, as shown in the lower diagram of

*The nanometer (10^{-9} meter) will be used as the unit of wavelength, 1 nm ≡ 10Å ≡ 0.001 micron (micrometer).

Figure 1. The shape of the curve approximates that of a blackbody of about 5700°K temperature, and the energy content of this portion of the solar flux is relatively constant. The very-high-energy portion of the spectrum at the left of the graph is dependent on solar activity, and can vary by orders of magnitude in its intensity, particularly in the range below 1 nm. For present purposes, the blackbody portion is all we need consider. The motions of the earth produce diurnal, seasonal, and latitudinal variations in the amount of solar flux received, and all of these must be taken into account in modeling. To maintain thermal balance, an equivalent amount of energy must be radiated away from the earth. The energy has been degraded through a multiplicity of processes so that this re-radiation occurs at a blackbody temperature of about 250°K.

Figure 2 reviews a few characteristics of the atmosphere upon which this energy impinges. It lies in a very thin layer around the earth, and its density decreases approximately exponentially with altitude. Half of the total atmospheric gas lies below 6 kilometers (about 20,000 feet) altitude; all but 1% lies below 30 kilometers (about 100,000 feet), and 99.9% is below 50 kilometers. Below 100 km altitude, the atmosphere is composed almost entirely of three species: nitrogen molecules, oxygen molecules, and the inert gas argon, in the percentages shown. It is in the other 0.04%, however, the minor constituents, that the great complexity of atmospheric particle processes lies. A few of these species are shown at the left. Of these, the charged particles (important above about 60 km altitude), the O, O_3, OH, and NO (oxygen atoms, ozone, hydroxyl radicals and nitric oxide respectively) are produced directly or indirectly through solar flux action. As mentioned by Professor Friend, the water, nitrous oxide N_2O, and carbon monoxide CO, can have a terrestrial origin and diffuse upward to take part in the interactions.

The primary event in the atmosphere is the interaction of the photons of Figure 1 with the particles of Figure 2. Each species has its own characteristic absorption spectrum, and the amount of solar energy of a given wavelength at a selected altitude is a function of both the input at the top of the atmosphere, and the amount that has been selectively absorbed during passage through the atmosphere to the altitude being considered.

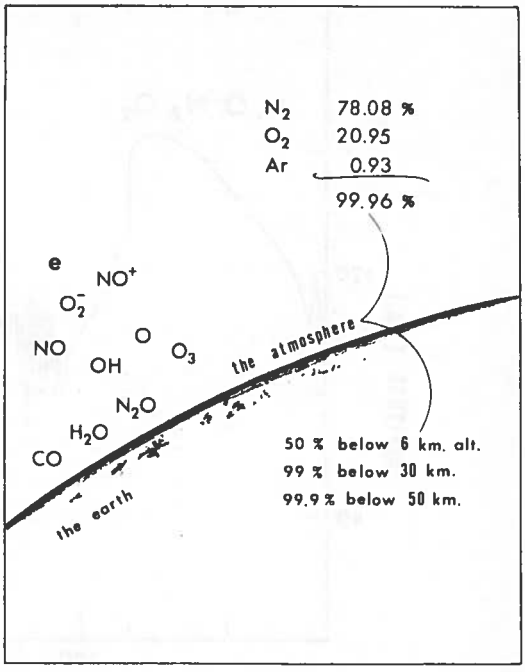

Figure 2. The earth's atmosphere.

A method of showing this for the more energetic part of the solar spectrum is given in Figure 3. The curve indicates the altitude at which the intensity at a given wavelength has been decreased to 1/e (about 37%) of its original value by absorption above that altitude, principally by the species indicated. The very high energies are absorbed high in the atmosphere. Oxygen molecules are the principal absorber in the ultraviolet range from 100-200 nm, while the right-hand side of the figure is the area of one of the principal concerns of this conference – the absorption of light in the near-ultraviolet range by ozone.

Figure 4 demonstrates in a different manner the absorption of solar energy by the atmosphere. The upper curve represents the flux at each wavelength that arrives at the top of the atmosphere, while the lower curve represents the amount that is transmitted through the entire atmosphere to the earth's surface. The portion between the curves is the energy absorbed by the individual species, in a characteristic way, producing electrons, ions, atoms, free radicals, species excited electronically, vibrationally, and rotationally, and translational motion (kinetic energy) of the species. These are the source materials for the chemical kinetic modeling.

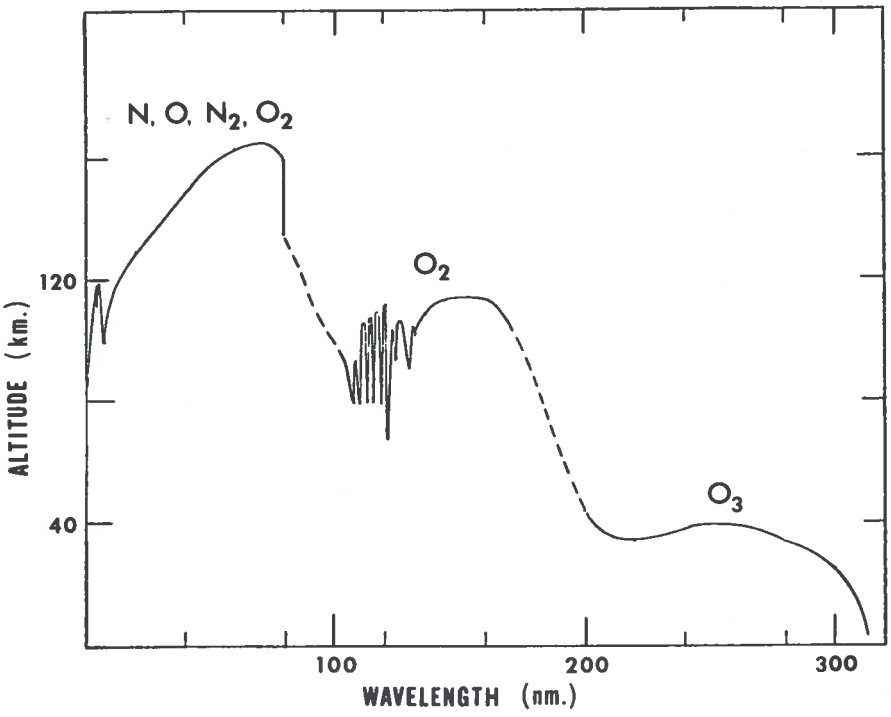

Figure 3. Absorption of solar energy by atmospheric species, as shown by the altitude at which the intensity of solar X-ray and ultraviolet radiation has been reduced to 1/e ($\simeq$37%) of its value outside the earth's atmosphere. The species shown are the principal absorbers in the indicated spectral region. After H. Friedman in *Physics of the Upper Atmosphere*, 1960, ed. J. Ratcliffe, Academic Press.

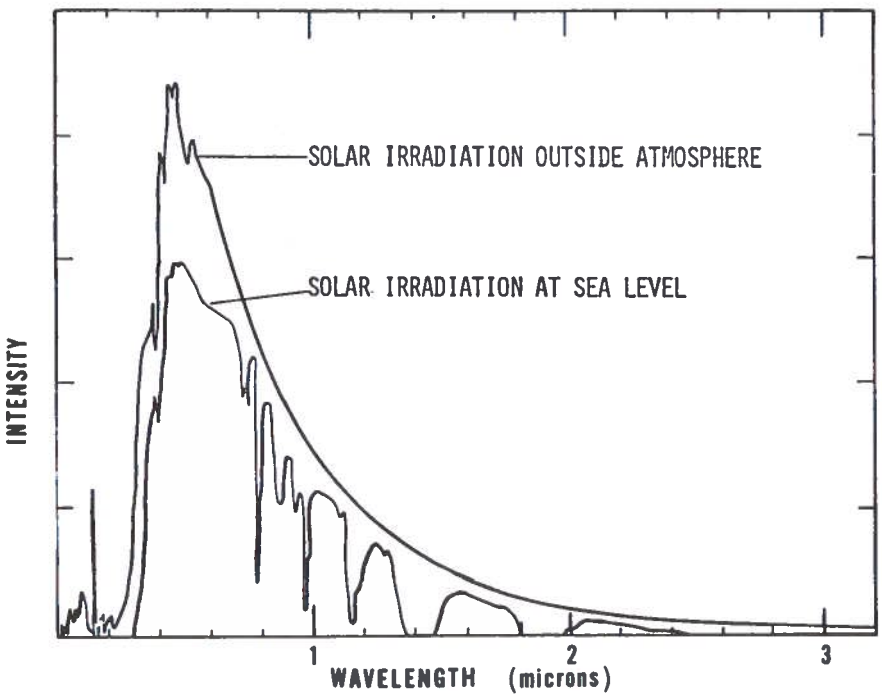

Figure 4. Absorption and transmission of solar energy in the atmosphere. From p. 16-2 of *Handbook of Geophysics and Space Environments*, 1965, ed. S. Valley, McGraw-Hill.

ENERGY STATES OF A MOLECULE

A very effective method for displaying the energy states of a molecule, and the transitions that can result from absorption or emission of energy, is consideration of the molecule's potential energy diagram. Figure 5 is a simplification of one of the diagrams developed by Forrest Gilmore. The separation of the two oxygen atoms of the molecule is represented by the abscissa, and the energy content of the system relative to the ground state of the molecule forms the ordinate. The quantum mechanical and spectroscopic designation of the ground state is $(X^3\Sigma_g^-)$. The lowest curve shown is that for the oxygen negative ion O_2^-, indicating that the ion is more stable than the neutral molecular ground state by almost half an electron volt (eV).

On the curve for the ground state you will note small marks along the right-hand side. These represent the allowable vibrational states. Since the energy separation is small, it requires little transfer of energy to change the vibrational state of the molecule.

Directly above the ground state curve is one labeled $(a^1\Delta_g)$. This is the first electronically excited state of the oxygen molecule. The energy difference is slightly less than one electron volt, equivalent to a photon of wavelength 1.27 microns (1270 nm). The $O_2(a^1\Delta_g)$ molecule is a very important atmospheric species, and because of its greater energy content and different configuration of electron spins, its chemical behavior is different from that of the ground state. It is not easily formed from the ground state by absorption of a photon, however. Because of the differences in electron spin configuration (triplet in the ground state, singlet in the excited state), the transition is "forbidden", i.e., of low probability. In addition, the change of the angular momentum states of the electrons by two (from Σ to Δ) is also "forbidden." Direct production of the singlet-delta state of oxygen by photoexcitation from the oxygen ground state is therefore extremely rare in the atmosphere; however, production through photodissociation of ozone by photons of energy greater than 310 nm is quite rapid in the stratosphere, so it must be considered in the chemistry related to CIAP.

Transitions among the electronic states of a molecule take place very rapidly compared with the times required for movement of the atoms, so the distance between the atoms can be considered as remaining unchanged during the change of electronic states (the Born-Oppenheimer approximation). In terms of the potential energy diagram, this means that transitions are along a direct vertical line between the initial state and possible final states (the Franck-Condon principle). This eliminates many energetically possible transitions, and helps produce the distinctive characteristics of the absorption spectrum of each type of molecule. One such vertical line has been drawn on the graph between the ground state of the molecule, and the third vibrational state of the ground state of the positive molecular ion. This transition would come about quite readily if the requisite 12.8 eV of energy ($\simeq$ 97 nm) were absorbed.

Intermediate in energy between the excited states, such as $(^1\Delta_g)$ and the $(^1\Sigma_g)$, and the ionized states, such as O_2^+ $(X^2\Pi_g)$, are the transitions leading to dissociation into atoms. Note on the vertical line the two crossings of the dotted potential energy curves that have been circled. Neither of these curves has a potential well to stabilize the molecule, and absorption of this amount of energy (about 5.8 eV; 210 nm) will lead to separation of the atoms by movement to the right along the curve, producing two ground-state atoms, $O(^3P)$. The energy in excess of the level shown for the two atoms (5.12 eV) will appear as kinetic energy of the atoms. Light of wavelength less than 175.9 nm (energy greater than 7.05 eV) is required to enter the complexity of curves that result in the next higher set of atoms – one in the ground state $O(^3P)$ and one in the first electronically excited state $O(^1D)$.

The results of the few absorption processes we have considered are the new species O_2 $(^1\Delta_g)$, O_2 $(^1\Delta_g)$, O_2^+, e, $O(^3P)$, $O(^1D)$, vibrational excitation, and kinetic energy. All of these must now be considered in the chemical kinetics of the stratosphere.

Study of the equivalent diagram for nitrogen molecules would show greater energy separations between states, and very poor vertical alignment of equivalent transitions. The N_2 molecules are thus of far less importance as a reactive species, and as producers of reactive species, than are the oxygen molecules. Thus 78% of the stratosphere is chemically a relatively inert matrix, but it still must be considered in thermal, transport, and collision processes.

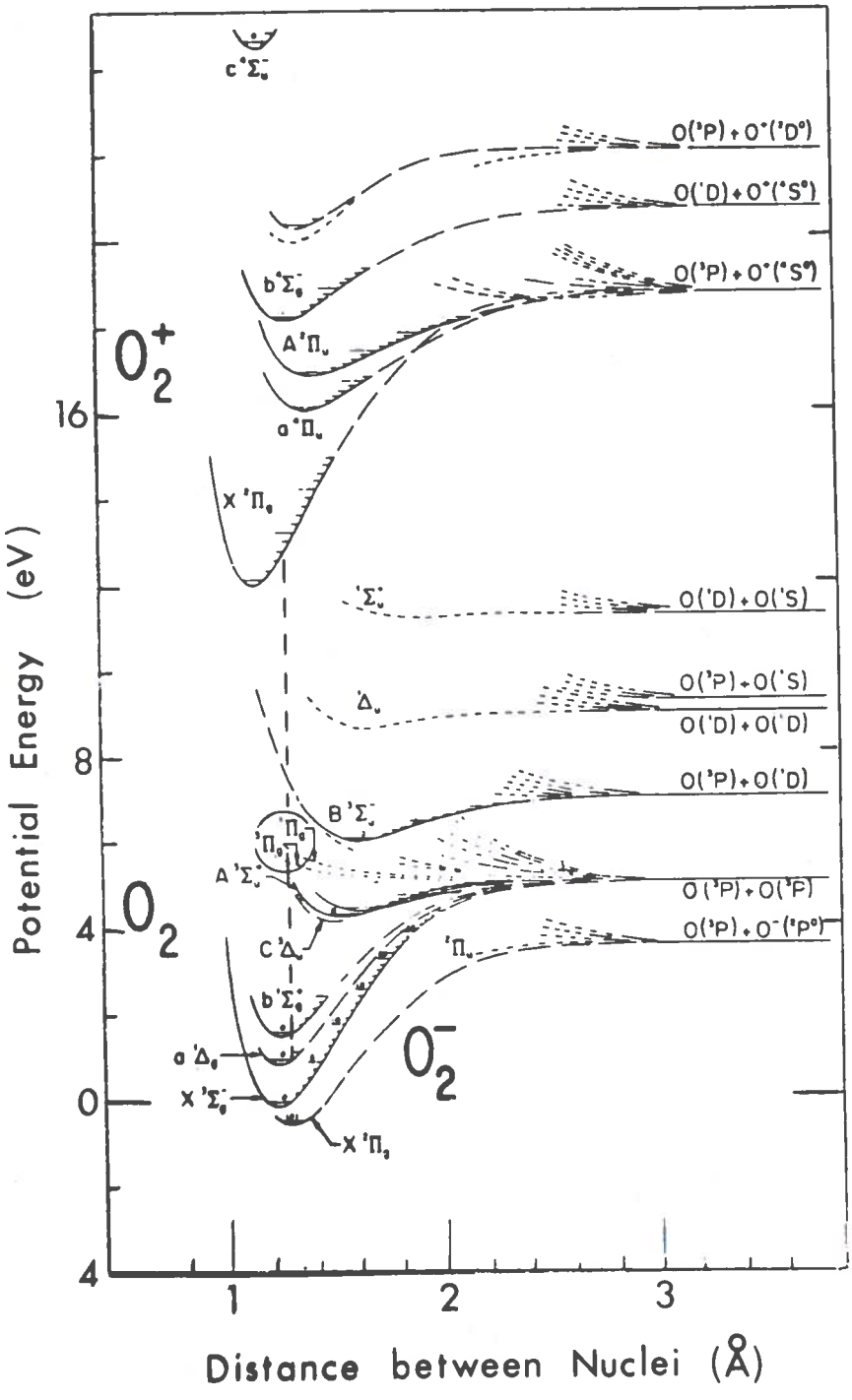

Figure 5. Potential energy diagram for the neutral oxygen molecule and its ions. From the work of Forrest Gilmore.

CHEMICAL REACTIONS

We will now use just one of these physical processes, photodissociation

$$O_2 + h\upsilon\ (\lambda > 175.9\,\text{nm}) \rightarrow O(^3P) + O(^1D) \quad (1)$$

as the start for a step-by-step construction of a fairly complex atmosphere.

Figure 6a shows the two major constituents, N_2 and O_2, and the photo-process (1). This first step has added two very reactive minor constituents which can now react with the basic molecules and with each other. For example:

$$O + O_2 + M \rightarrow O_3 + M \quad (2)$$

$$O(^1D) + N_2^* \rightarrow N + NO \quad (3)$$

$$O + O(^1D) + M \rightarrow O_2 + M \quad (4)$$

The first two of these reactions have been added to the model as shown in Figure 6b. Reaction (3) is speculative. It is included as a categorical representation of any available state of either the oxygen atom or the nitrogen molecule. As stated previously, nitrogen is quite unreactive, but most collisions are with nitrogen molecules (about 78%) and the possibility of a very reactive oxygen atom and/or an excited nitrogen molecule being involved, with greater chance of reaction, is an open question. The symbol M is any third atom or molecule which does not participate in the reaction, but is close enough to the reactants at the time of their encounter that it can carry off the excess energy, so as to stabilize the product. (On the diagrams, the designation fof the ground states, and the third-body M, are omitted.) The model at this second step of development has three reactions and seven species.

Figure 6c adds the photodissociation of ozone, which will produce the O_2 ($^1\Delta g$) discussed previously if the photon energy is greater than 4 eV (310 nm). Also shown (in two places, at top and bottom) is the reaction that Professor Johnston has shown is so critical to the CIAP consideration of the SST aircraft:

$$O_3 + NO \rightarrow O_2 + NO_2 \quad (5)$$

The reaction of the new species nitrogen dioxide NO_2 with atomic oxygen, one of the restoring mechanisms for nitric oxide NO, in his catalytic scheme for destruction of ozone, is shown at the top.

Figure 6d introduces some of the earth-originated species Professor Friend discussed: water, nitrous oxide, carbon monoxide, and methane. The reaction of two of these with the excited oxygen atoms is shown:

$$H_2O + O(^1D) \rightarrow OH + OH \quad (6)$$

$$N_2O + O(^1D) \rightarrow NO + NO \quad (7)$$

The first introduces the highly reactive hydroxyl radical OH, and the second is the natural source of nitric oxide suggested by McElroy and McConnell. The very important photodissociation of NO_2 is also added.

Finally, Figure 6e adds the reactions of hydroxyl radicals with carbon monoxide and methane CH_4, producing carbon dioxide and hydrogen atoms, and methyl radicals CH_3 and water, respectively. The reaction of ozone and OH adds the hydroperoxyl radical HO_2, and two of these react in turn to produce hydrogen peroxide H_2O_2. A member of a new category of species, nitric acid HNO_3, is introduced through the interaction of NO and HO_2.

This development by steps has considered only three photodissociation processes and ten chemical reactions, but there are now 19 chemical species that can enter into reactions or absorb solar energy. They are: O_2, N_2, $O_2(^1\Delta)$, O, O(1D), O_3, NO, NO_2, N_2O, HNO_3, H_2O, OH, HO_2, H_2O_2, CO, CO_2, CH_4, CH_3 and H.

The high reactivity of most of these indicates that many other reactions will occur. To simplify the presentation of these, some of the possible reactions have been grouped diagramatically in the next three figures.

Figure 7 includes only reactions among species made up of nitrogen and oxygen atoms: N_2, O_2, N, O, NO, NO_2, N_2O. In the diagram the reactant at the tail of an arrow reacts with the reactant written on the shaft to give the product at the

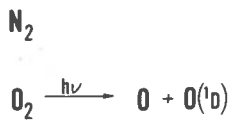

Figure 6a. First step in constructing a multi-species stratosphere by photodissociation and chemical reaction. Photodissociation of oxygen produces two new reactive species – ground and excited oxygen atoms.

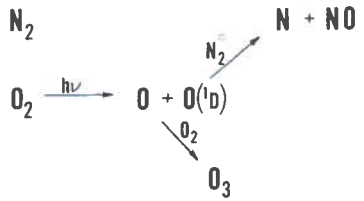

Figure 6b. Step two: the new species interact with the N_2, O_2 matrix producing three more new species – ozone, nitric oxide and nitrogen atoms.

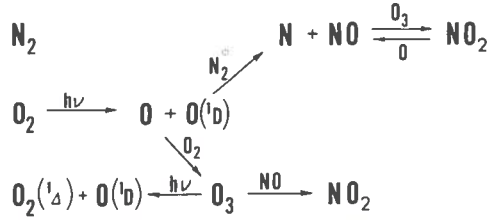

Figure 6c. In step three, photolysis of ozone and the ozone/nitric oxide reaction produce O_2 (1Δ) and NO_2.

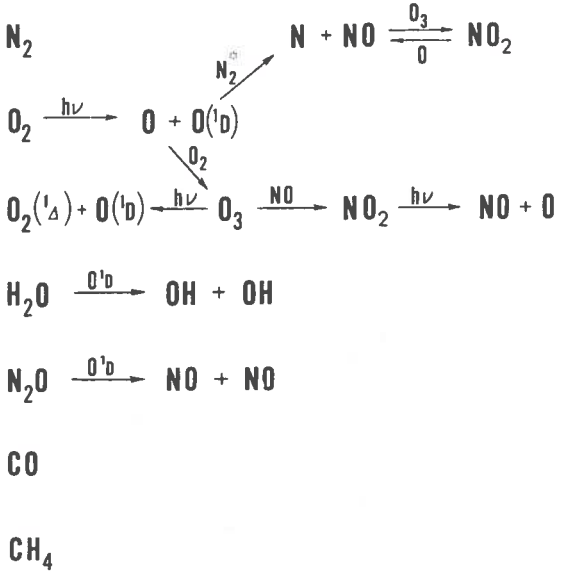

Figure 6d. Four earth-originated species, H_2O, N_2O, CO, and CH_4, diffuse into the stratosphere; the first two react with excited oxygen atoms. The reactive hydroxyl radical is added.

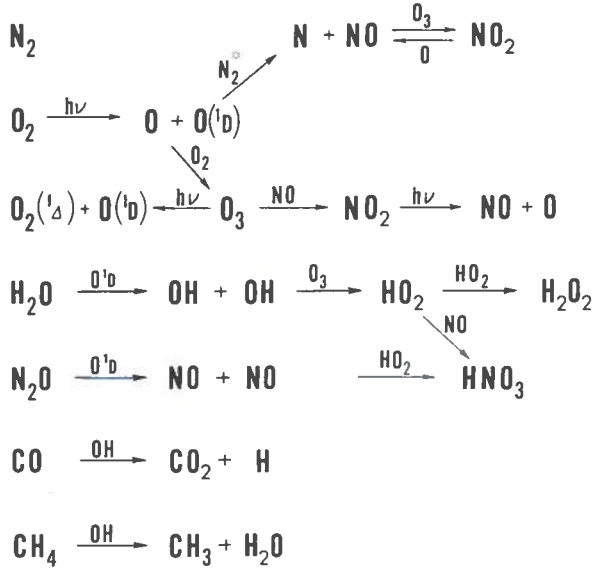

Figure 6e. Five additional reactions produce six new species – H, CO_2, CH_3, HO_2, H_2O_2, and HNO^3 in this fifth step.

head. Other products and third bodies are omitted, and excited states are not separately designated. The principal lesson to be learned from this "busy" diagram is the potential complexity of even a two-atom-based atmosphere. Any detailed discussion of this would be something of a duplication of the talks by Professors Nicolet, Crutzen, Johnston, and Friend.

Increasing this seeming complexity is an equivalent scheme for reactions of species derived from only oxygen and hydrogen atoms: H_2O, OH, HO_2 and H_2O_2. These reactions are shown in Figure 8. In these two diagrams and the next, the relative importance of the reactions shown can vary by many orders of magnitude, and in addition the relative importance may vary with altitude, time of day, season, location, or disturbance introduced.

The last of this series, Figure 9, is for species formed from the three atoms oxygen, hydrogen, and carbon: CO, CO_2, CH_4, CH_3, CH_2, formaldehyde HCHO, the formyl radical CHO, methoxyl radical CH_3O, and methylperoxyl radical CH_3O_2. In this chart there is a flow apparent from methane to carbon dioxide. This, combined with the methane-hydroxyl radical reaction, provides the mechanism behind the statement that methane CH_4, which diffuses upward from the troposphere, ultimately ends up as CO_2 and H_2O in the stratosphere and mesosphere.

This separation of reactions into three families is convenient and instructive, but it is artificial. The families are strongly interlinked by other reactions and must be considered together. The diagrams are also not complete; they do contain most of the reactions significant in the stratosphere, but omit the important interlinking reactions.

MATHEMATICAL FORMULATION

There now remains the problem of expressing this very complex, interrelated set of reactions in a mathematical formulation so that calculations relating to normal or disturbed atmospheric composition can be made. The most fundamental physical principles – conservation of energy and of mass – form the foundation. In this case, the latter could be modified to read "conservation of atoms", since none are created or destroyed. The mathematical expression of a conservation principle is a continuity equation, which for this latter conservation can be written

$$\frac{\partial}{\partial t} n_i = Q(n_j \ldots) - L(n_i, n_j \ldots) - \nabla \cdot pv. \qquad (8)$$

That is, the time dependence of the concentration n of a species i is equal to the rate Q at which it is being formed through reactions, less the rate L at which it is being removed by reaction, and less the rate of addition or loss, from the volume considered, by transport processes.

As an example we will write a very simple equation for ozone, using only three reactions:

$$O + O_2 + M \xrightarrow{k_2} O_3 + M \qquad (2)$$

$$O_3 + NO \xrightarrow{k_5} O_2 + NO_2 \qquad (5)$$

$$O_3 + h\nu \xrightarrow{J_3} O + O_2 \qquad (9)$$

The corresponding continuity equation is:

$$\frac{\partial}{\partial t}[O_3] = k_1 [O] [O_2] [M] - k_2 [NO] [O_3] - J_3 [O_3] \pm \mathcal{T} \qquad (10)$$

The square brackets symbolize particle densities of the species enclosed; k_2 and k_5 are the rates at which the designated reactions proceed; J_3 is the photodissociation rate of ozone; and $\mathcal{T}$ is the net rate of ozone transport into or out of the volume.

The reaction rate constants k_i are complex functions of collision frequencies, collision configurations, and energy requirements for the reactions. They are expressed by the Arrhenius equation:

$$k = AT^B e^{-C/T} \qquad (11)$$

A is related to the collision frequency and the probability of a reaction's occurring during a collision. B is related to the temperature (T) dependence of the collision frequency, and C is proportional to the energy necessary to bring about a reaction. In practice, the rate constants

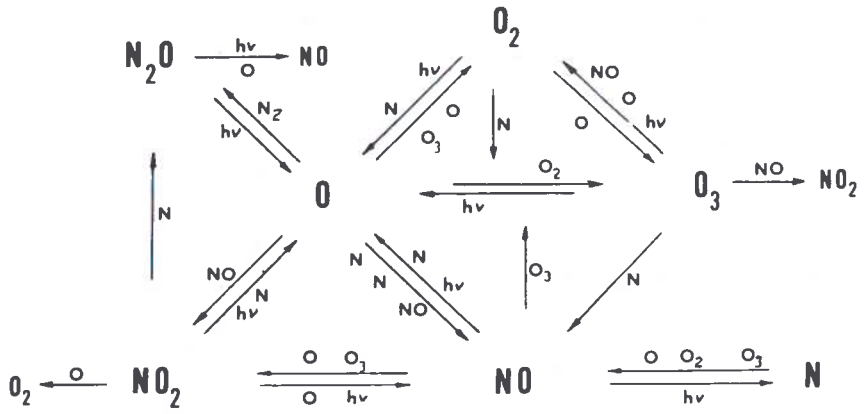

Figure 7. Principal reactions among atmospheric species composed only of oxygen and nitrogen.

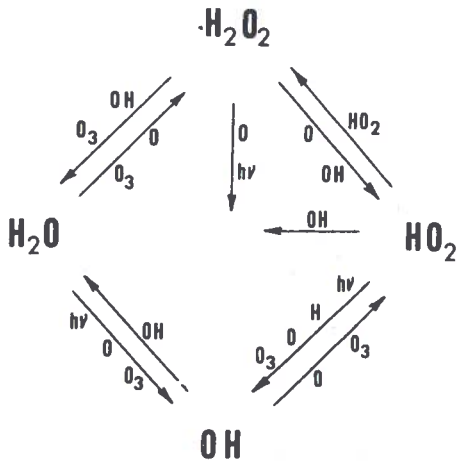

Figure 8. Principal reactions among atmospheric species composed only of oxygen and hydrogen.

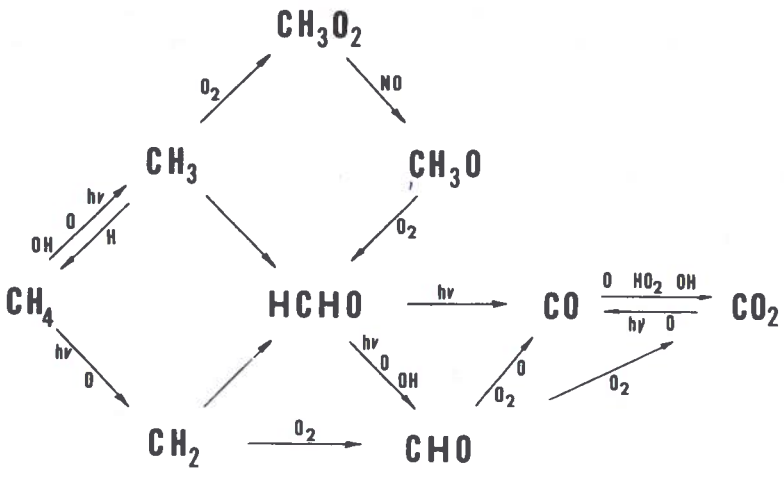

Figure 9. Reactions among atmospheric species composed of carbon, oxygen, and hydrogen.

must come from experiment, and the B and C are found by empirical matching with data. Since two-parameter matching is sometimes ambiguous, frequently only one of the parameters B or C is used.

In equation (10), it will be noted that the ozone particle density depends on the densities of O, NO, and O_2, which in turn have a reciprocal dependence on the ozone particle density and also on other particle densities. A continuity equation must be written for each species whose particle density is time-dependent. The entire set of equations is coupled through all the interlinking chemical reactions that occur. The equations must be solved simultaneously because of the coupling to follow time development of particle concentrations or to find equilibrium densities. For equilibrium conditions, the derivative is, zero, and relationships between various species' densities can be worked out. This has been beautifully demonstrated for a number of situations in the previous papers.

EXAMPLES

This completes the discussion of the physics, the chemical kinetics (which is more physics), and the mathematical formulation of the rather massive problem. The final graphs show some simple examples of the kinds of results that can be obtained by computer solution of the large set of coupled differential equations. The computational method used is based on that developed by T. Keneshea of the Air Force Cambridge Research Laboratories.

In these calculations 33 species, and therefore 33 differential equations, were considered. The species are listed in Table 1. There are about 170 chemical reactions in the model.* These include all the reactions shown previously, either explicitly or diagramatically, plus additional photo-processes, and reactions linking the families shown, as well as reactions of the species listed in Figure 10 but not discussed.

The calculations from which the following results are taken are not necessarily typical. They are part of a study of certain limiting conditions. For example, downward transport of NO and O from the mesosphere is not included. Minimal upward transport of CO, CO_2, CH_4, H_2O, and N_2O is incorporated, but ozone transport is not. Some of the photodissociation rates are poorly known, and approximations have been made. Upper limits as defined by Professor Kaufman have been taken for a number of unmeasured reaction-rate constants. The results presented are selected to show examples of the kinds of information obtainable. Interpretation would be very lengthy and repetitive of the earlier lectures, so only a few remarks will be given.

Table 1. Atmospheric molecules, atoms, and free radicals used in the 33/170 chemical kinetics model described in the text

O	N	H	CO
$O(^1D)$	$N(^2D)$	H_2	CO_2
$O(^1S)$	N_2	OH	CH_4
O_2	NO	H_2O	CH_3
$O_2(^1\Delta)$	NO_2	HO_2	CH_2
$O_2(^1\Sigma)$	N_2O	H_2O_2	CHO
O_3	NO_3	HNO_2	HCHO
	N_2O_5	HNO_3	CH_3O
			CH_3O_2
			CH_3OH

Figure 10 is the computed particle densities of seven principal species for an overhead sun. To the right of the diagram, the line labeled R indicates the slope for a constant mixing ratio, for reference. SST cruise altitude is approximately 20 kilometers, which is near the peak ozone particle density from atmospheric measurements (and many model calculations). The present calculations indicate a relatively high density of nitrous oxide, and NO and NO_2 densities near 10^{10} particles per cubic centimeter at 20 kilometers.

To show the effect of changing a single rate constant, two curves for hydroxyl radical concentrations are shown. The reaction considered is:

$$O_3 + OH \rightarrow O_2 + HO_2$$

To study the finding of Langley and McGrath that the rate is less than 1.0×10^{-16} cm^3 sec^{-1}, computations were made setting the rate above and below this upper limit. Two examples are shown:

For curve (a), $k = 1.0 \times 10^{-15}$ cm^3 sec^{-1}
For curve (b), $k = 1.0 \times 10^{-18}$ cm^3 sec^{-1}.

*Full details of the model, as well as additional results, are available from the author.

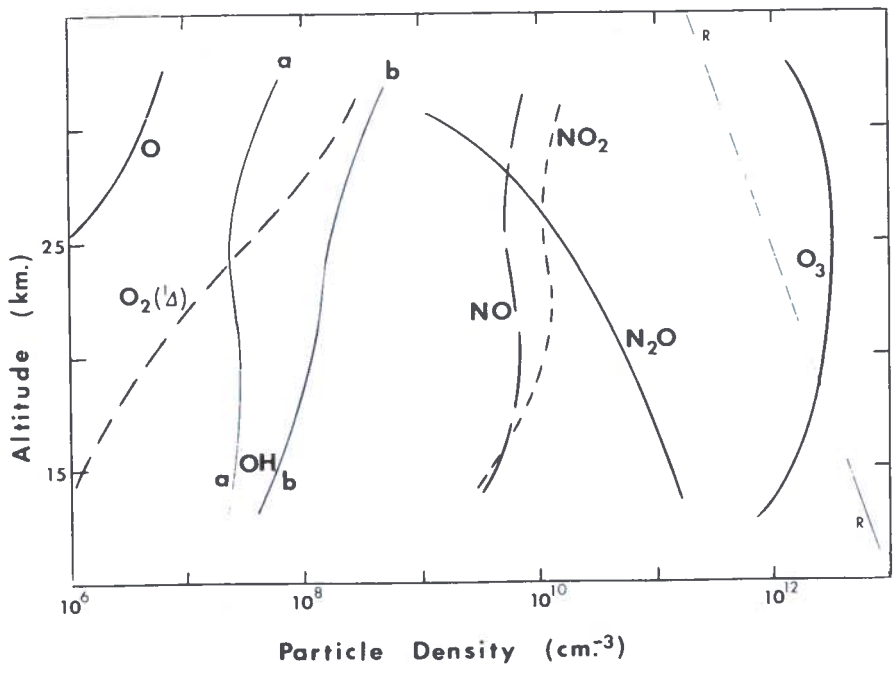

Figure 10. Altitude dependence of calculated daytime particle densities of some oxygen species and the nitrogen oxides, using the 33/170 model. The line R is the approximate slope for a constant mixing ratio. See the text for explanation of the two curves for the hydroxyl radical OH.

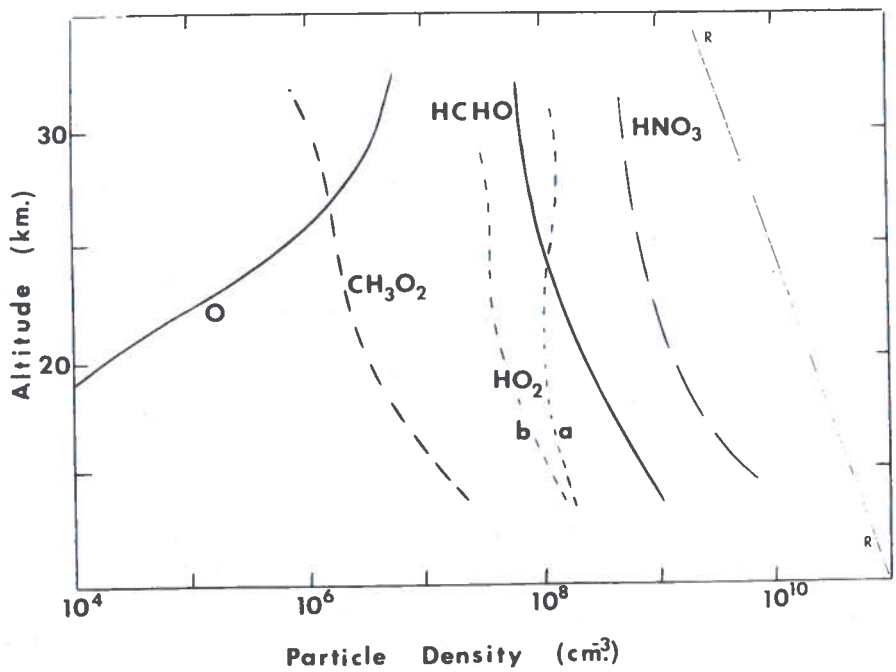

Figure 11. Altitude dependence of calculated daytime particle densities of some unusual atmospheric species and atomic oxygen, using the 33/170 model. The two HO_2 curves are explained in the text.

The increase in OH density for the lower rate is approximately an order of magnitude at 25 to 30 kilometers.

The reduction in HO_2 density for this decrease in reaction rate is shown in Figure 11, which gives the calculated particle densities of four less common but important species: nitric acid, formaldehyde, methylperoxyl radicals, and the two results for the hydroperoxyl radical. The oxygen atom density is also shown.

The effects of changing single parameters, such as the above rate constant, or groups of parameters, can be studied quickly and effectively using models of this type. In terms of the CIAP interests, the effect on species densities or reaction rates brought about by change in density or rate of introduction of one or more species can be followed. In addition, the relative importance of the interactions producing changes, or those tending to restore the normal equilibrium, can be determined.

The final diagram, Figure 12, shows the calculated rates of several very important reactions, under equilibrium conditions, at altitudes from 15 to 30 kilometers. The reactions designated are

A. $O + O_2 + M \rightarrow O_3 + M$

B. $O_3 + h\nu \rightarrow O + O_2$

C. $O_3 + NO \rightarrow O_2 + NO_2$

C. $NO_2 + h\nu \rightarrow O + NO$

D. $NO_2^* \rightarrow NO_2 + h\nu$

E. $O_2 + h\nu \rightarrow O + O$

F. $O + NO_2 \rightarrow O_2 + NO$

G. $CH_4 + OH \rightarrow CH_3 + H_2O$

The approximate equilibrium between three-body formation of ozone and its photodissociation is shown, as is the equilibrium between NO_2 formation in the ozone reaction and its photolysis. The ozone-nitric oxide reaction produces a small percentage of NO_2 molecules in excited states which decay immediately, emitting photons over a fairly broad range of the spectrum with a peak intensity at about 1.1 microns. This rate of photon emission is shown by curve D.

Equivalent information is available for the other 22 species and 162 reactions, for the conditions chosen, or for others that might be specified. Other types of information, and as much detail as desired, can be derived.

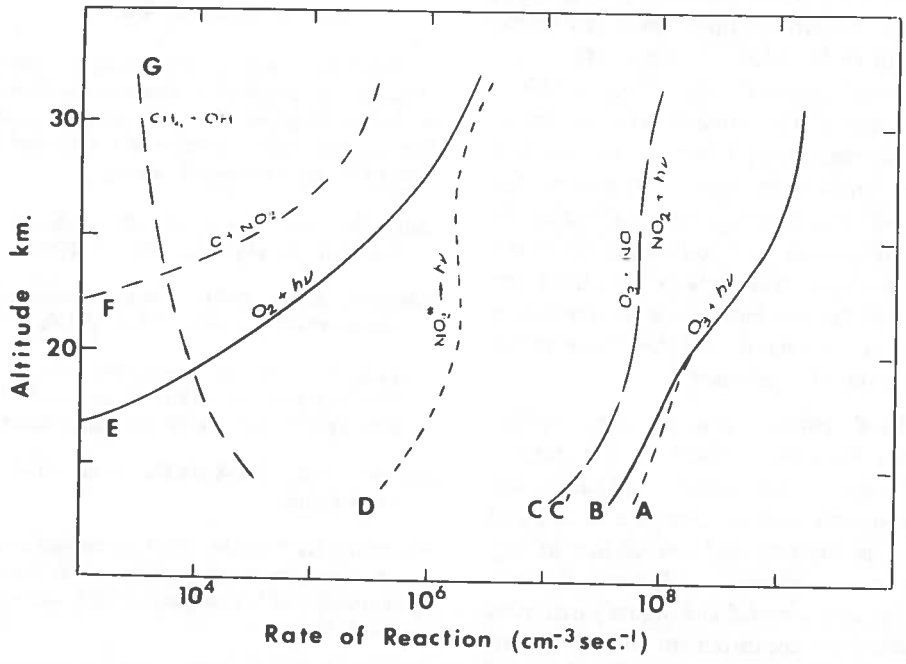

Figure 12. Altitude dependence of calculated daytime rates of eight important stratospheric reactions, using the 33/170 chemical kinetics model.

SUMMARY

A model, such as the one described, is built on:

1. knowledge that a certain species exists in the atmosphere, and
2. knowledge of how each of these species is affected by the solar flux available, and how each interacts with other species present.

Experiment is therefore the basis for the model; it is only as sound as the experimental data it uses, and it is only as valid as its demonstrated ability to match actual measurements of atmospheric parameters.

A time-dependent chemical kinetics model of stratospheric composition and behavior can be built up from the great amount of data that has been obtained through field measurements of atmospheric parameters, and through laboratory measurements of reaction rates and energy absorption cross-sections of atmospheric species. There is enough experimental data available to form a meaningful foundation for such a mathematical model, but more extensive and more accurate data are needed.

Many of the unmeasured rate constants used are based on approximate calculations, thermodynamic and steric considerations, and comparison with rates of similar reactions. In a few cases, for what seem to be relatively unimportant reactions, "informed guesses" by some excellent intuitions represent the present state of knowledge. The accuracy with which a rate constant needs to be known depends of course on the importance of the reaction in establishing or modifying atmospheric composition. Most of the rates of important stratospheric reactions are reasonably well known. More accurate determination of some rate constants, and their temperature dependence, would be very useful.

In the altitude range of concern here, very few measurements have been made of the particle densities of most of the minor constituents discussed. The opportunity to compare model and measurement is limited, and confidence in any model must be correspondingly limited. It is not difficult to develop a model and adjust parameters to match data from measurement of one or two species concentrations under a restricted set of conditions. A model must be able to match data from simultaneous measurement of a number of species densities under a full range of atmospheric conditions.

The most effective approach is to use model and experiment together. Preliminary models can indicate the most important species and processes for the situation to be studied, and thus guide the choice of experiment and experimental parameters. Results of these experiments can modify and greatly improve the model, and the iteration can be continued. Once confidence is established in a high level of validity of the model, a wealth of detailed information can be obtained by computation. One can interpolate and extrapolate on time and space scales, show fine detail of particle interactions, calculate results for situations that it is not feasible to study experimentally, determine the processes that produce the results measured, and obtain some knowledge of unmeasurable parameters. Finally, a very simple equivalent chemical kinetics model can be derived from, and validated by, the complex type of model presented. This is necessary for use in the extensive fluid dynamics calculations that show the global climatological result of the interaction of solar flux with the atmosphere for either normal or disturbed conditions.

REFERENCES

These references are given only for the few papers cited, or as representative papers for authors mentioned. A full bibliography on the subject would be very lengthy; the reader is referred to the detailed atmospheric chemistry papers presented earlier.

Bates, D.R., and Nicolet, M., "Photochemistry of water vapor". J. Geophys. Res., *55*, 301 (1950).

Chapman, S., "A theory of supper atmospheric ozone". Memoirs Roy. Met. Soc., *3*, 103 (1930).

Crutzen, P.J., "Ozone production rates in an oxygen-hydrogen-nitrogen oxide atmosphere". J. Geophys. Res., *76*, 7311 (1971). (See also this volume.)

Gilmore, F.R., RM-4034-PR, June 1964, The Rand Corporation.

Hesstvedt, E., "On the effect of vertical eddy transport on atmospheric composition in the mesosphere and thermosphere". Geofysiske Publikasjoner, *27* (1968), No. 4, 1.

Hunt, B.G., "Photochemistry of ozone in a moist atmosphere". J. Geophys. Res., *71*, 1385 (1966).

Johnston, H., "Reduction of stratospheric ozone by nitrogen oxide catalysts from SST exhaust". Science, *173*, 517 (1971). (See also this volume.)

Langley, K.F., and McGrath, W.D., "The ultraviolet photolysis of ozone in the presence of water vapor". Planet. Space Sci., *19*, 413 (1971).

McElroy, M.B., and McConnell, J.C., "Nitrous oxide: a natural source of stratospheric NO". J. Atmos. Sci., *28*, 1095 (1971).

Nicolet, M., "Nitrogen oxides in the chemosphere". J. Geophys. Res., *70*, 679 (1965). (See also this volume.)

DISCUSSION

I. Alber asked why the model had no relationships for turbulent eddy diffusion. He mentioned a current experiment at TRW on dissociation of N_2O_4 in a turbulent shear field; even with the best available rate constants, they had been unable to calculate the measured concentration of NO_2. They found that they were time-averaging the rate equation to come up with an effective diffusivity and effective production rate – which is also an average. This in effect neglects fluctuations in a species; if the concentrations of two species are correlated, the fluctuation products $\overline{C_1' C_2'}$ are non-zero. He felt that these turbulent phenomena might be almost as important as the kinetic rates in chemical reactions, at least in the lower stratosphere. Hudson agreed.

T. Taylor asked whether Hudson's model used eddy diffusivity. Hudson said no, but added that it would be needed on one with a larger time scale.

R. Cvetanović asked the source of the reaction of O with CH_4 to give CH_2, as shown in Hudson's Figure 9. Hudson replied that it was included just to see what effect it would have, and was inconsequential.

A. Goldburg asked whether Hudson intended to tackle the full aerothermal-coupled problem, and asked about the curves of Figures 11 - 13 and their time scales. Hudson said yes to the first, and explained that the curves were the result of trying different values for photo-dissociation rates, under an assumption of steady-state solar radiation, to see their effects on the concentration and the reaction rates.

COMPOSITION OF THE STRATOSPHERIC "SULFATE LAYER"

RICHARD D. CADLE
*National Center for Atmospheric Research**
Boulder, Colorado 80302

ABSTRACT: A highly structured layer of particles, several kilometers thick, exists world-wide in the stratosphere. The history of the study of this layer, which consists predominantly of sulfate particles in the 0.1 to 1.0μ radius size range, is briefly reviewed. During the last 2-1/2 years NCAR scientists have been determining the nature and concentration of particles collected from this layer by means of filters and impactors flown on Air Weather Service aircraft and on balloons. The results of these NCAR studies are summarized. Most of the particulate material consisted of sulfuric acid droplets. Amounts of nitrate (which apparently was absorbed nitric acid vapor), at times as great as those of sulfate, were collected on one type of filter.

INTRODUCTION

A highly structured layer of particles, several kilometers in thickness, exists world-wide in the stratosphere a few kilometers above the tropopause. The history of the study of this layer was recently reviewed by Rosen (1969), who states that twilight effects believed to be produced by the presence of particles in the stratosphere have been reported in the literature for more than eighty years. Measurements of light scattered from the twilight sky have been made relatively recently by Bigg (1956, 1964), Volz and Goody (1962), and Volz (1964, 1965). Meinel and Meinel (1963) studied the late twilight glow produced by the airborne particles from the Mt. Agung eruption in Bali in 1963. They observed two glows on at least one occasion and, from the times of transit, estimated the heights to be 22.3 km for the boundary of the brighter glow and 52.6 for the boundary of the fainter.

Other remote sensing techniques have involved measurement of daytime sky brightness, direct measurement of extinction, searchlight techniques, and the use of lidar (laser radar). The latter method has proved to be especially useful for studying the stratospheric particle layer (Fiocco and Grams, 1964; Grams and Fiocco, 1967; Clemesha et al., 1966; Lazrus, Gandrud and Cadle, 1971).

Rosen (1964, 1968, 1969) used photoelectric particle counters carried by balloons to obtain altitude vs. number concentration graphs (vertical profiles). His results demonstrated that the variation in concentration with altitude was very irregular. Junge (1961) determined vertical profiles of Aitken nuclei (particles smaller than 0.1μ radius) with a balloon-borne recording nuclei counter. The particle concentrations decreased with increasing altitude throughout the troposphere and the lower stratosphere but were nearly constant between 20 and 27 km altitude.

Chagnon and Junge (1961), Junge and Manson (1961), and Junge, Chagnon, and Manson (1961) used impactors carried by balloons and aircraft to determine the composition and concentrations of stratospheric particles greater than 0.1μ radius. They observed maxima in the number concentrations for 0.1 to 1.0μ particles ("large" particles) between about 16 and 23 km altitude. Very few larger particles were collected. The major element in the collected particles was determined by electron microprobe techniques to be sulfur. Friend (1965) also sampled stratospheric particles using impactors carried by aircraft. He concluded that the particles consist largely of ammonium sulfate and persulfate and "may have liquid associated with them."

Manson et al. (1961) suggested that gas-phase reactions are responsible for the formation of the

* The National Center for Atmospheric Research is sponsored by the National Science Foundation.

stratospheric aerosol layer. Cadle and Powers (1966) concluded from laboratory studies of the kinetics of the reaction of atomic oxygen with sulfur dioxide that this reaction, followed by hydration of the product (SO_3) and reaction with ammonia, may be a source of ammonium sulfate in the stratosphere:

$$SO_2 + O + M \rightarrow SO_3 + M \quad (1)$$

$$SO_3 + H_2O \rightarrow H_2SO_4 \quad (2)$$

$$H_2SO_4 + 2NH_3 \rightarrow (NH_4)_2SO_4 \quad (3)$$

Cadle, Wartburg, and Grahek (1971), on the basis of studies at Kilauea Volcano in Hawaii, suggested that extremely explosive eruptions, such as that of Mt. Agung, may inject large amounts of sulfuric acid and various sulfates directly into the stratosphere, as well as volcanic ash. Martell (1966) concluded, on the other hand, that Aitken particles in the troposphere account for most of the sulfate in the atmosphere, and that there is no stratospheric sulfate layer, but only a stratospheric large-particle layer formed by agglomeration of Aitken particles.

Shedlovsky and Paisley (1966) analyzed particles collected on polystyrene fiber filters at 19 to 21 km altitude. They estimated that the chondritic meteorite component was negligible (less than 10% of the collected iron and sodium). They obtained a maximum sulfur mixing ratio of 2.9×10^{-9} g S/g dry air, about sixty times larger than that obtained by Junge et al. (1961). Newkirk and Eddy (1964) also estimated the relative concentration of meteoric debris in aerosols at 20 km and deduced that over the size range 0.1 to 2.0 μ radius it represents less than ten percent. However, they concluded that above 25 km it represents a major part of the particulate matter for particles larger than 0.3 μ radius.

METHOD OF APPROACH

During the last 2-1/2 years, a group at NCAR has been determining the nature and concentration of particles collected from the stratospheric aerosol layer by means of filters and impactors flown on Air Weather Service RB-57F aircraft and on balloons. The aircraft were equipped to carry twelve 42-cm diameter filters and expose them sequentially in flight. The balloon flights utilized a direct-flow sampler (Conlon, 1970) modified for the collection of nonradioactive trace constituents.

Two general types of filters were used. One type consisted of IPC filters, which are cellulose fiber impregnated with the oil diethylbutoxyphthalate. During the early part of this study these filters were used as received, but because they were found to have high background sulfate, an automated precleaning process was used for the more recent work. Flight tests showed that neither the pressure drop nor the aerosol collection efficiency was appreciably altered by this pretreatment. The other type of filter consisted of sub-micron diameter polystyrene fibers. These were usually prepared at NCAR using a modification of the technique of Cadle and Thuman (1960). Commercial polystyrene filters were used during a few flights. The collection efficiencies of these filters are discussed by Lazrus, Gandrud, and Cadle (1971). They are very efficient even for particles in the Aitken size range ($<0.1\mu$ radius) under the conditions of this study.

The polystyrene filters fabricated at NCAR are much freer of contaminants than even the washed IPC filters, but their preparation is quite time-consuming.

The material collected on the filters was analyzed by wet-chemical and neutron activation techniques. For the former technique, filters were extracted with water using the methods described by Cadle et al. (1970) and Lazrus, Gandrud, and Cadle (1971). The other technique is of course non-destructive.

The impactors were similar to those described by Junge and Manson (1961), but equipped with improved O-ring seals to prevent contamination (Figure 1). Shallow holes were drilled in the impactor surfaces to accommodate electron microscope screens. An alternate method of use was to cement platinum foil to the impactor surfaces so that particles collected on the foil could be identified by electron microprobe techniques or analyzed by wet chemical methods.

A few laboratory tests were made to determine whether nitric acid vapor is absorbed from

air by IPC filters but not by polystyrene filters (Lazrus, Gandrud, and Cadle, 1972). The tested IPC filters always absorbed nitric acid vapor but the polystyrene filters never did.

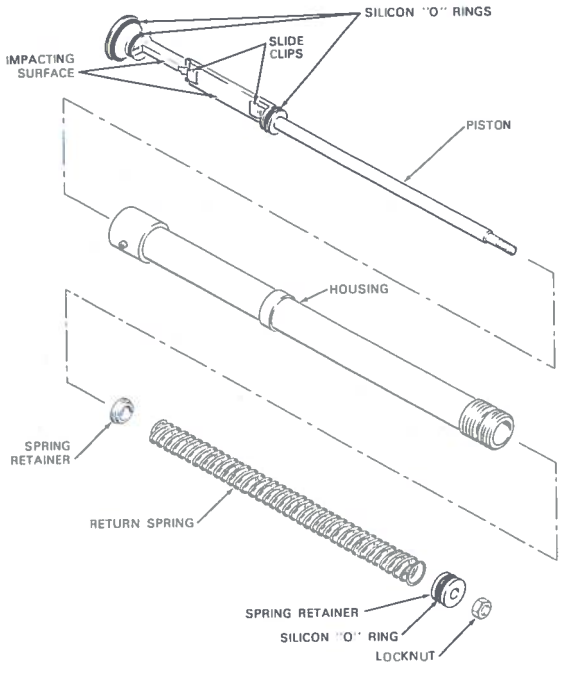

Figure 1. Schematic Drawing of Impactor

RESULTS

Representative sets of results obtained from the stratospheric flights in 1969 with unwashed IPC filters in the tropics are shown in Table 1. The sulfate concentrations varied markedly during each flight but were much higher than those for any other constituent except nitrate, which at times exceeded sulfate.

Ratios of concentrations for pairs of constituents were markedly different from those for sea water. The large variation in concentration found for $SO_4^=$ was also observed for the other constituents, but there was no significant correlation with latitude. No potassium, nitrite, or ammonium ions were detected on any of the filters.

The analyses of particles collected both on IPC and on polystyrene filters in the mid-latitude stratosphere are shown in Table 2. Results obtained with the two types of filters were very similar, with two notable exceptions: namely, that little or no nitrate was found on the polystyrene filters, and that the values for silicon were much higher for the polystyrene than for the IPC filters. Ammonium ion, although absent from the tropical stratospheric samples, was found on the samples collected both by IPC and

Table 1. Analyses of Particles Collected on IPC Filters in the Tropical Stratosphere* above Central America

At start of sampling Latitude (N)	Longitude (W)	Altitude (ft x 10^{-3})	Concentration (μ g/m^3 ambient) $SO_4^=$	Si	Na	Cl	NO_3^-	Mn	Br	Radioactivity (Nb^{95}) (Dpm/m^3 ambient)
31°40′	99°30′	55	0.11	0.052	0.020	0	0.058	0	0.0025	3.09
30°00′	96°05′	55	0.12	0	0	0	0.042	0	0.0014	2.39
28°00′	93°20′	55	0.13	0.022	0.025	0	0	0	0.0026	6.09
25°30′	90°30′	55	0.075	0	0.037	0.038	0	0	0.0020	0.69
23°00′	88°00′	56	0.10	0.058	0.004	0	0.16	0	0.0019	1.49
20°30′	85°20′	56	0.26	0	0.015	0.034	0	0	0.0030	1.73
19°20′	83°30′	57	0.092	0	0	0	0	0	0.0020	1.19
18°30′	80°00′	58	0.30	0.008	0.015	0	3.4	0	0.0068	8.77
11°00′	79°00′	58	0.11	0.015	0.049	0.017	0.20	0.00047	0.0030	4.84
8°00′	80°00′	58	0.20	0.0057	0	0	0.17	0	0.0018	3.18
4°00′	81°20′	58	0.17	0.040	0.053	0.053	0.058	0.00047	0.0015	1.57
2°00′	82°30′	58	0.14	0.025	0	0	0.049	0	0.0009	1.54
1°30′	83°30′	58	0.32	0.010	0	0.002	0.058	0.00002	0.0021	2.19
3°00′ (S)	85°00′	62	0.13	0	0	0	0.021	0	0.0006	1.05
1°00′ (S)	82°00′	62	0.29	0.0062	0.002	0.018	0.015	0.00004	0.0015	1.65

*All samplings were 30 minutes long. Longitudes and latitudes are for start of sampling. No nitrite, potassium or ammonium ion was detected in any of the samples, and the NO_3^- concentration was calculated by the method specific for NO_3^-. The upper set of samples was obtained on 7/10/69 and the lower set on 7/23/69.

Table 2. Analyses of Particles Collected on IPC and Polystyrene Filters in the Mid-latitude Stratosphere.*

Filter Type	Lati-tude (N)	Longi-tude (W)	Alti-tude (ft x 10^{-3})	Concentrations ($\mu g/m^3$ ambient)								Radio-activity (Nb^{95}) (Dpm/m^3 ambient
				$SO_4^=$	Si	Na	Cl	(NO_3^-)**	NH_4	Mn	Br	
PS	34°30′	102°55′	55	0.32	0.18	0.004	0.042	0(0.0012)	0.0034	0.0036	0.0021	28.4
PS	37°20′	102°30′	58	--	0.19	0.003	0.023	--	--	0.0021	0.0019	37.5
IPC	40°20′	102°15′	58	0.21	0.037	0.054	0.071	0.31	0.026	0.0010	0.0028	40.9
IPC	43°25′	101°50′	59	0.37	0.035	0.030	0.052	0.41	0.0089	0.0009	0.0021	29.2
PS	46°30′	101°31′	59	0.24	0.19	0.003	0.041	0(0)	0.017	0.0025	0.0026	42.6
PS	47°48′	101°45′	60	0.22	0.17	0.002	0.030	0(0)	0.012	0.0012	0.0020	43.2
IPC	44°25′	101°45′	61	0.35	0.084	0.050	0.088	0.36	0.0067	0.0009	0.0030	49.3
IPC	41°00′	102°10′	60	0.32	0.031	0.001	0.046	0.35	0.0040	0.0004	0.0020	32.3
PS	37°30′	102°40′	60	0.36	0.17	0.003	0.051	0(0.0036)	0.043	0.0049	0.0024	59.7

*All samplings were 30 minutes long, made on December 4, 1969. Longitudes and latitudes are for start of sampling. No potassium ion or nitrite ion was detected in any of the samples.

**The NO_3 concentration was calculated from the total combined nitrogen less that combined as NH_4^+ (the value in parentheses), and also by the method specific for NO_3^-

polystyrene filters from the mid-latitude stratosphere.

The chlorine concentrations for unwashed control IPC filters were so high that the values calculated for the atmosphere from the results using IPC filters are rather unreliable. Just the opposite was true for the polystyrene filters, and it is noteworthy that the Cl/Br ratios obtained with these filters varied from 12 to 19 compared with about 300 for sea water.

A comparison of Tables 3 and 4 with Table 2 shows that the concentrations of several trace constituents of the mid-latitude stratosphere decreased from their values in 1969 during 1970 and early 1971.

Table 3. Average Chemical Composition of IPC Filter Samples Collected over the Central United States at 17-18 km Altitude*

Date	$SO_4^=$ $\mu g/m^3$	NH_4^+ $\mu g/m^3$	NO_3^- $\mu g/m^3$
5/11/70	0.20	0.0033	0.36
10/17/70	0.10	0.0025	0.12
2/3/71	0.10	0.0000	0.20
2/28/71	0.028	0.0027	0.027

*Data of Lazrus, Gandrud, and Cadle (1971, 1972)

Table 4. Concentrations of Atmospheric Trace Constituents Collected from the Midlatitude Stratosphere in 1970.

Date (1970)	Sample No.	Lati-tude (N)	Longi-tude (W)	Alti-tude (ft x 10^{-3})	Concentration ($\mu g/m^3$)						
					$SO_4^=$	Si	Na	Cl	K	Mn	Br
10/21	C1	33°00′	103°45′	55	0.032	0.030	0.026	0.0086	0.034	1.3×10^{-4}	5.1×10^{-4}
10/21	C2	31°00′	96°50′	55	0.037	0.0095	0.0022	--	0.0068	0.4×10^{-4}	3.9×10^{-4}
10/21	C3	39°15′	95°00′	60	0.032	0.0074	0.0084	0.026	0.0062	1.1×10^{-4}	4.0×10^{-4}
10/29-30	C6	34°15′	105°00′	50	0.024	--	--	--	--	--	2.2×10^{-4}
10/29-30	C7	30°27′	97°15′	50	0.021	--	--	--	--	--	2.8×10^{-4}
10/29-30	C8	25°45′	90°40′	50	0.011	--	0.0017	0.0028	--	--	2.0×10^{-4}
10/29-30	C9	20°30′	86°15′	50	0.022	0.16	0.012	0.012	0.016	5.2×10^{-4}	5.7×10^{-4}
10/30	C11	33°00′	102°00′	60	0.004	--	--	0.011	--	--	0.9×10^{-4}
10/30	C12	29°20′	95°00′	60	0.052	--	--	0.0082	--	--	6.9×10^{-4}
10/30	C13	24°45′	89°25′	60	0.020	--	--	0.0020	--	--	--
10/30	C14	19°20′	85°30′	60	0.040	0.0012	--	--	--	--	3.1×10^{-4}

* Sample time – one hour -- indicates not detectable over blank All polystyrene filters

Table 5. Balloon Sampling Data.*

Date	Altitude (10^3m)	Latitude (N)	Longitude (W)	μ gNO_3^-/m^3	Molar Ratio $[NO_3^-]/[SO_4^=]$	Mixing Ratio 10^{-9}g/g
Feb. 26, 1971	21	8°27′	79°03′	0.318	6.5	6.1
April 7, 1971	21	8°27′	79°03′	0.14	2.2	2.5
April 8, 1971	24	8°27′	79°03′	0.12	3.3	4.0
April 9, 1971	27	8°27′	79°03′	0.085	8.1	5.2
May 13, 1971	21	31°28′	100°22′	0.58	10.7	9.6
May 14, 1971	24	31°28′	100°22′	0.41	7.7	11.0
June 5, 1971	21	64°39′	147°04′	0.67	12.1	9.6
June 8, 1971	24	64°39′	147°04′	0.40	11.4	9.7

*From Lazrus, Gandrud, and Cadle (1972). All filters were IPC.

Balloon sampling data are shown in Table 5. The concentrations of nitrate were higher than those of sulfate, often by more than an order of magnitude. High concentrations of nitrate were found up to the highest altitude sampled, 27 km. Ammonium ion was found at higher concentrations in the tropics at the higher altitudes of the balloon sampling.

As indicated above, immediately after the Agung eruption in 1963 the stratospheric sulfate was largely volcanic. To learn whether the sulfate is still mainly volcanic, samples from the plume of Hekla Volcano were compared isotopically with stratospheric sulfate collected in the mid-latitude northern stratosphere (Lazrus, Gandrud and Cadle, 1971). The $\delta^{34}S$ values were +2.8 and +1.8, respectively. These values are at least consistent with the hypothesis of a volcanic origin for the sulfate.

On June 10 and June 11, 1971, two RB-57F flights were made at 18 km altitude to compare the collection efficiencies of the impactors with those of the washed IPC filters. The impactor on one flight had a platinum foil surface coated with 250,000 centistokes "Silicone 200" fluid to render the results comparable with those of Junge and Manson (1961). The other impactor had an uncoated platinum foil surface. Both flights were of about four hours' duration at sampling altitude. The concentrations of sulfate, estimated from the filter collections, were 0.13 and 0.11 μ g/m^3 ambient, respectively. The amounts collected by the impactors were so small that they could not be reliably distinguished from the traces of sulfate on the "clean" platinum surfaces, coated or uncoated. The amounts of sulfate collected by the impactors could not have exceeded those corresponding to 20% of the concentrations determined by the filters and were probably much less. On the other hand, the concentrations of ammonium ion estimated from the filter collections were about 1×10^{-3} μg/m^3 and those estimated from the impactor collections equaled or exceeded this value. These results must be considered to be tentative until confirmed by additional similar flights.

Electron micrographs of particles collected by impaction from stratospheric air at about 18 km are shown in Figures 2 through 4. The particles in Figure 2 were droplets that produced a pattern characteristic of dilute sulfuric acid droplets. Crystals of unknown composition, such as those shown in Figure 3, were often collected. Particles collected on another flight a few weeks after extensive brush fires in California (Figure 4) included chainlike agglomerates of particles resembling those produced by burning wood. Such particles have been collected from the stratosphere by other investigators and were considered to have an extraterrestrial origin.

Two large-scale investigations of stratospheric trace constituents were conducted in 1971, one in spring and one in autumn. The sampling was conducted using RB-57F aircraft at four altitudes between the tropopause and 19 km and from 75°N to 51°S (Lazrus and Gandrud, 1971). A manuscript by these authors describing the results is in preparation and will probably be submitted to the *Journal of Geophysical Research*. There was a lack of any significant

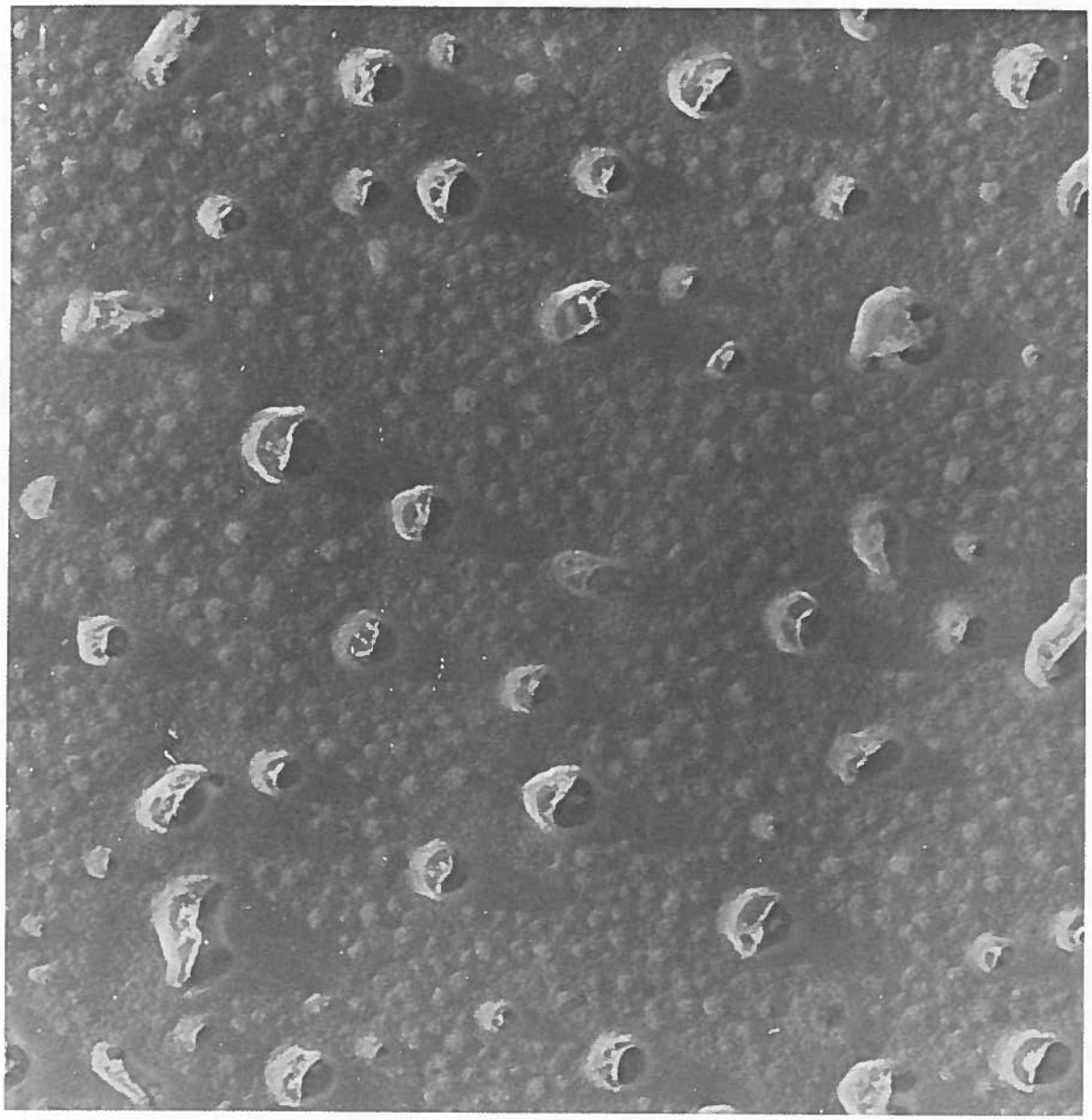

Figure 2. Electron micrograph of droplets collected by impaction from the midlatitude stratosphere at 18 km altitude. The unshadowed regions apparently were destroyed by the electron beam. Distance across the micrograph = 2μ.

gradient in sulfate concentration between the tropical and temperate stratosphere. If one were at constant altitude, there would be a $SO_4^=$ concentration gradient from low to high latitudes. But along the slope of the layer, no large gradient occurred.

NCAR lidar measurements in 1969 exhibited strong scattering from the stratospheric sulfate layer. The scattering dropped to zero during 1970 and at the time of writing (February 1972) has only partially returned toward the 1969 values.

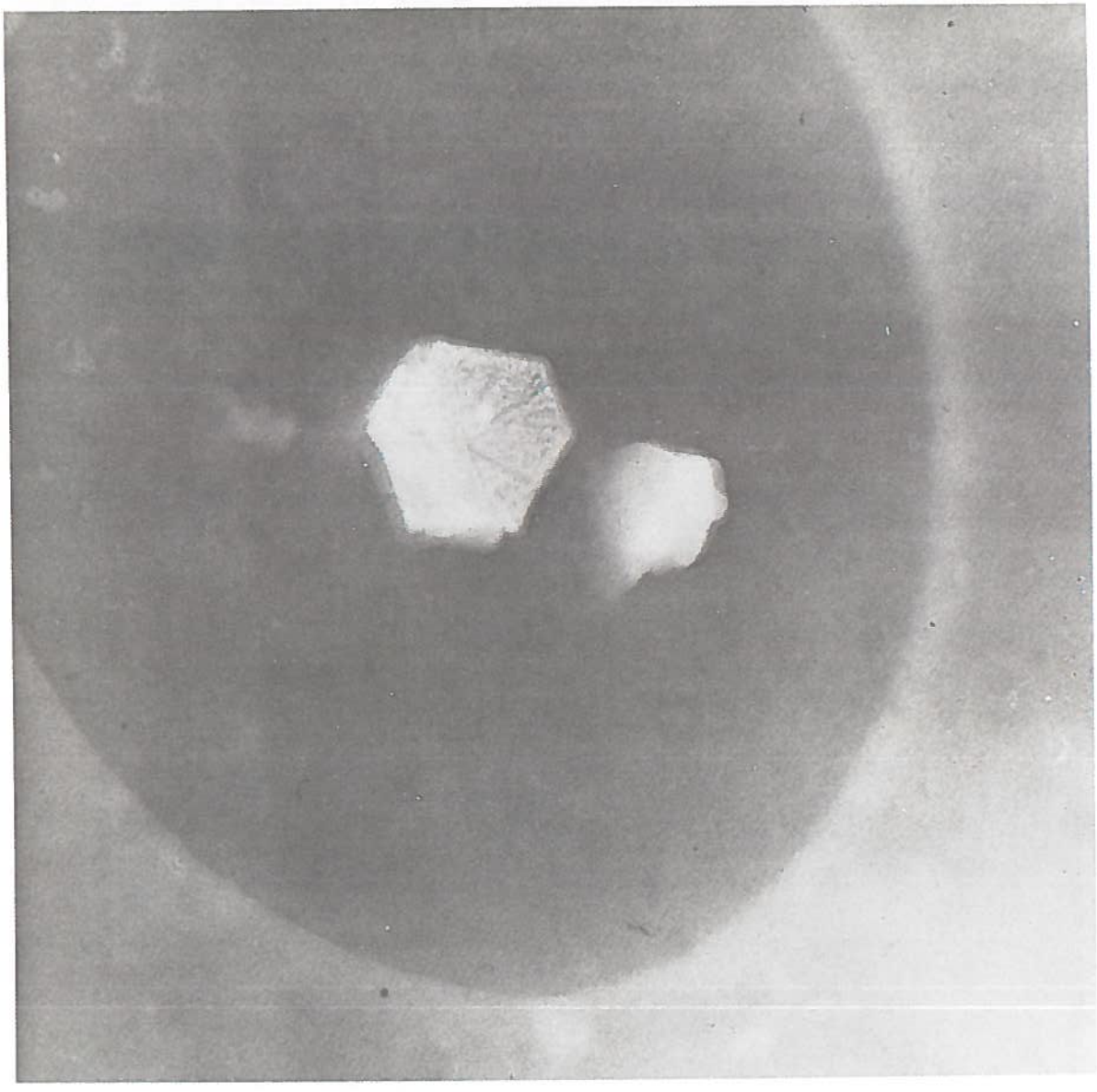

Figure 3. Typical crystal of unknown composition collected by impaction from midlatitude stratosphere at 18 km altitude. Distance across the micrograph = 2.3 μ.

DISCUSSION

There can be little doubt that the marked increase in the concentration of stratospheric aerosols following the Agung eruption was the result of that eruption. However, recent changes in these concentrations are not so obviously related to variations in volcanic activity, although that possibility cannot be ruled out. The disappearance of a lidar signal from the sulfate layer during 1970, the lack of collection of measurable amounts of sulfate particles on the impactors in 1971, and the continued collection of particles on the filters during 1970 and 1971 (although in amounts corresponding to decreased stratospheric concentrations compared with 1969) suggest that the decrease was largely for particles about 0.1 μ radius and larger. Unlike the

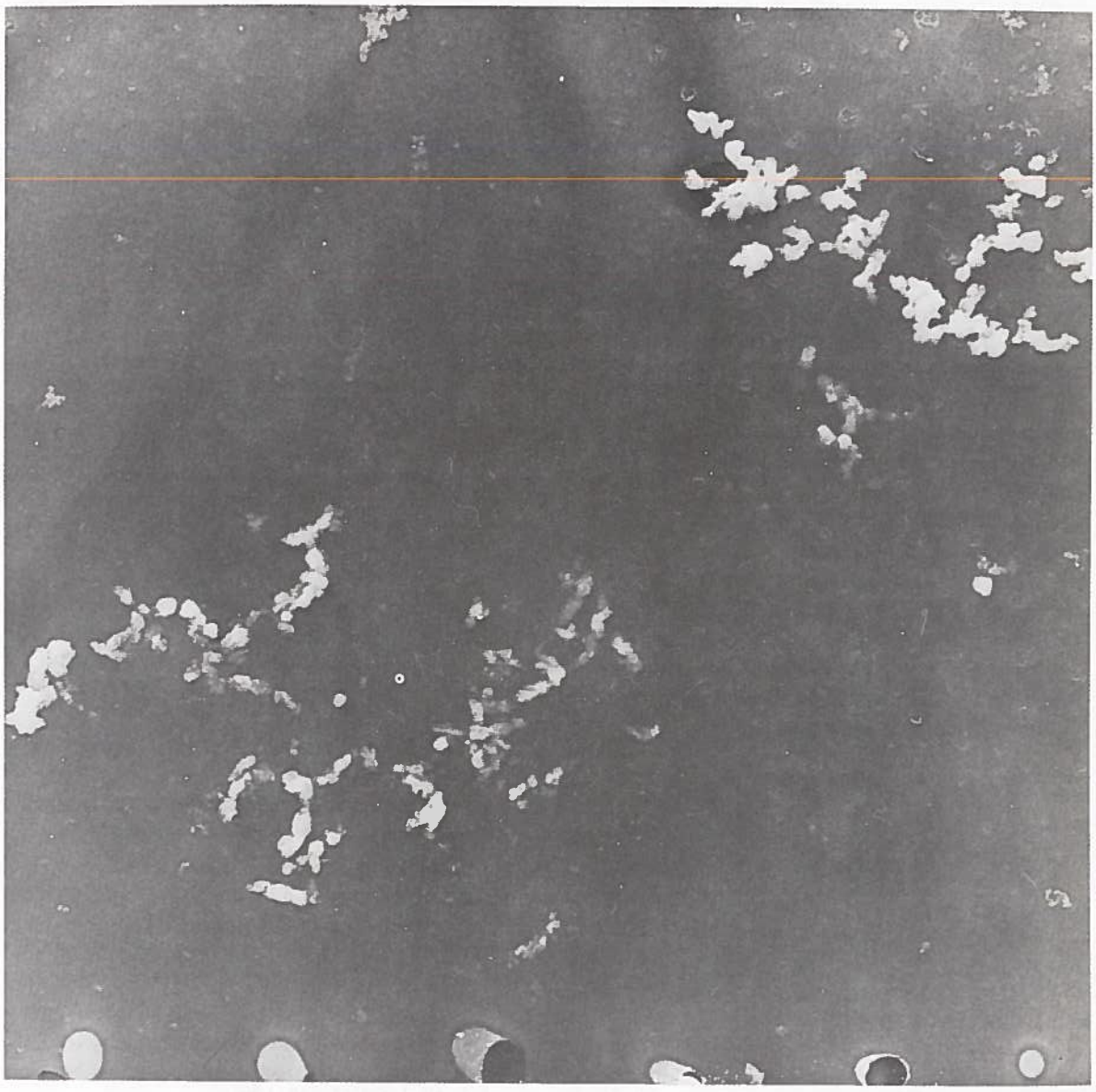

Figure 4. Particles collected by impaction from the midlatitude stratosphere at 18 km altitude on October 21, 1970. Distance across the micrograph = 6μ.

filters, the impactors are very inefficient for collecting particles in the Aitken size range; also, the lidar is quite insensitive to Aitken particles.

The fact that the stratospheric ammonium ion concentrations estimated from the impactor samples were comparable to those obtained by filtration suggests that the ammonium sulfate particles were larger than the sulfuric acid droplets.

The source of the silicon as well as that of the sulfate may be volcanic (volcanic "ash"), but it also may be ordinary soil. The nitrate is almost certainly nitric acid vapor absorbed on the IPC filters. One would not expect to find oxides of nitrogen and nitric acid vapor among magmatic gases. Small amounts of nitric oxide may be formed by nitrogen fixation resulting from the contact of air with hot erupting lava, but this

process can hardly account for the nitric acid vapor found in the stratosphere. Several suggestions have been made as to the source of such compounds in the stratosphere, for example:

$$O(^1D) + N_2O \rightarrow 2NO \quad (4)$$

$$NO + O_3 \rightarrow NO_2 + O_2 \quad (5)$$

$$NO + OH \rightarrow HNO_3 \quad (6)$$

Our finding relatively high concentrations of HNO_3 at altitudes as high as 27 km is consistent with recent laboratory results demonstrating that the reaction of $O(^3P)$ with HNO_3 is very slow.

The Cl/Br ratios are much lower than those found by Duce et al. (1965) for the aerosol particles close to the sea surface near Hawaii. They reported values of about 1000 for the particles over water and about 100 for those over land. They emphasized that the atmospheric chemistry of the halogens is very complex, but that the difference may result from bromine compounds in automobile exhaust gases. The low ratios we found may be a result of worldwide air pollution from automobiles.

REFERENCES

Bigg, E. K., "The Detection of Atmospheric Dust and Temperature Inversions by Twilight Scattering". J. Meteorol. *13*, 262 (1956).

Bigg, E. K., "Atmospheric Stratification Revealed by Twilight Scattering". Tellus *16*, 76 (1964).

Cadle, R. D. and Thuman, W. C., "Filters from Submicron-Diameter Organic Fibers". Ind. Eng. Chem. *52*, 315 (1960).

Cadle, R. D., and Powers, J. W., "Some Aspects of Atmospheric Chemical Reactions of Atomic Oxygen". Tellus *18*, 176 (1966).

Cadle, R. D., Lazrus, A. K., Pollock, W. H., and Shedlovsky, J. P., "The Chemical Composition of Aerosol Particles in the Tropical Stratosphere". In Proceedings of the Symposium on Tropical Meteorology, Honolulu, Hawaii, June 1970.

Cadle, R. D., Wartburg, A. F., and Grahek, F. E., "The Proportion of Sulfate to Sulfur Dioxide in Kilauea Volcano Fume", Geochimica et Cosmochimica Acta *35*, 503 (1971).

Chagnon, C. W., and Junge, C. E., "The Vertical Distribution of Sub-Micron Particles in the Stratosphere". J. Meteorol. *18*, 746 (1961).

Clemesha, B. B., Kent, G. S., and Wright, R. W. H., "Laser Probing the Lower Atmosphere". Nature *209*, 184 (1966).

Conlon, R. P., Upper Air Sampling and Monitoring Program. Tech. Rep. 3430, contract AT (11-1)-401, U.S.A.E.C., Litton Systems, Inc., Minneapolis, Minn., 1970.

Duce, R. A., Winchester, J. W., and Van Nahl, T. W., "Iodine, Bromine, and Chlorine in the Hawaiian Marine Atmosphere". J. Geophys. Res. *70*, 1775 (1965).

Fiocco, G., and Grams, G., "Observations of the Aerosol Layer at 20 km by Optical Radar". J. Atmos. Sci. *21*, 323 (1964).

Friend, J. P., "Properties of the Stratospheric Aerosol". Tellus *18*, 465 (1966).

Grams, G. W., and Fiocco, G., "Stratospheric Aerosol Layer During 1964 and 1965". J. Geophys. Res. *72*, 3523 (1967).

Junge, C.E., "Vertical Profiles of Condensation Nuclei in the Stratosphere". J. Meteorol. *18*, 501 (1961).

Junge, C.E., and Manson, J. E., "Stratosphere Aerosols Studies". J. Geophys. Res. *66*, 2163 (1961).

Junge, C.E., Chagnon, C. W., and Manson, J. E., "Stratospheric Aerosols." J. Meteorol. *18*, 81 (1961).

Lazrus, A. L., Gandrud, B., and Cadle, R. D., "Chemical Composition of Air Filtration Samples of the Stratospheric Sulfate Layer". J. Geophys. Res. *76*, 8083 (1971).

Lazrus, A. L., and Gandrud, B. W., "Stratospheric Trace Constituents." EOS *52*, 928 (1971).

Lazrus, A. L., Gandrud, B. W., and Cadle, R. D., "Nitric Acid Vapor in the Stratosphere". J. Appl. Meteorol. *11*, 389 (1972).

Manson, J. E., Junge, C. E., and Chagnon, C. W., "The Possible Role of Gas Reactions in the Formation of the Stratospheric Aerosol Layer". In *Chemical Reactions in the Lower and Upper Atmosphere*, R. D. Cadle, ed., Interscience Publishers, New York, 1961, p. 139.

Martell, E. A., "The Size Distribution and Interaction of Radioactive and Natural Aerosols in the Stratosphere". Tellus *18*, 486 (1966).

Meinel, M. P., and Meinel, A. B., "Late Twilight Glow of the Ash Stratum from the Eruption of Agung Volcano". Science *142*, 582 (1963).

Newkirk, G., Jr., and Eddy, J. A., "Light Scattering by Particles in the Upper Atmosphere". J. Atmos. Sci. *21*, 35 (1964).

Rosen, J. M., "The Vertical Distribution of Dust to 30 Kilometers". J. Geophys. Res. *69*, 4673 (1964).

Rosen, J. M., "Simultaneous Dust and Ozone Soundings over North and Central America", J. Geophys. Res. *73*, 479 (1968).

Rosen, J. M., "Stratospheric Dust and Its Relationship to the Meteoric Influx". Space Sci. Rev. *9*, 58 (1969).

Shedlovsky, J. P., and Paisley, S., "On the Meteoritic Component of Stratospheric Aerosols". Tellus *18*, 499 (1966).

Volz, F. E., "Twilight Phenomena Caused by the Eruption of Mt. Agung Volcano". Science *144*, 1121 (1964).

Volz, F. E., "Note on the Global Variation of Stratospheric Turbidity Since the Eruption of Agung Volcano". Tellus *17*, 513 (1965).

Volz, F. E., and Goody, R. M., "Intensity of the Twilight and Upper Atmospheric Dust". J. Atmos. Sci. *19*, 385 (1962).

Because of Dr. Sekera's poor health, the following paper was presented by Dr. Venkateswaran.

RADIATION SCATTERING IN THE STRATOSPHERE

Z. SEKERA
Institute of Geophysics and Planetary Physics
University of California
Los Angeles, California 90024

ABSTRACT: Scattering, like absorption and emission, is one of the main physical processes that produce and modify the radiation field in the stratosphere. In the scattering process the energy received by a scattering medium (air molecules and particulates) is reradiated in all directions, causing phenomena like twilight glow. This diffuse, reflected, and transmitted radiation is an important secondary radiation source in stratospheric photochemistry and radiation dynamics.

Radiation scattered by aerosol particles becomes polarized and produces the polarization of the skylight, which has been measured and studied extensively since 1809. The correlation of this polarization with atmospheric turbidity is so strong that the skylight polarization measurements represent the most efficient and accurate estimate of turbidity. This has been documented by measurements before and after volcanic eruptions. Moreover, these measurements provide a means of distinguishing between low-level and stratospheric turbidity. They should be given highest priority in monitoring turbidity changes due to stratospheric flights.

Recent advances in radiative transfer theory make it possible to assess radiational effects due to turbidity changes; more reliable data will be available, though, when the overall variability of the low-level turbidity changes is better understood.

As in the lower atmosphere, the radiation field in the stratosphere is produced and modified by three basic physical processes: absorption, emission, and scattering. At the beginning of this century it was believed that these processes could be studied separately, and several fundamental properties were deduced under this assumption. However, more recent studies have indicated that these three processes are not independent, and that it is necessary to consider also their interaction and mutual involvement. This, indeed, complicates the matter considerably and requires considerable sophistication of most recent radiation theories.

The fundamental properties of absorption and emission, as they affect the stratospheric circulation by heating and cooling, are dealt with in other papers given at this conference. This paper will concentrate on the third process, scattering, especially with respect to its utilization in detecting the changes in stratospheric turbidity, and in estimating the effects of an increased concentration of particulates in the stratosphere.

Scattering of radiation is the physical process by which the radiation received by a scattering center, a particulate, is reradiated in all directions. The intensity and other properties of the scattered radiation depend on the size, shape, and optical characteristics of the scattering center in a rather complicated way, in some cases too complex to define by a simple mathematical analysis. Determining the scattering properties of a unit volume of air containing particulate matter is therefore rather difficult. The task is generally simplified by making two assumptions, namely that all scattering centers in that volume scatter the radiation independently (i.e., incoherently), and that all centers have a spherical shape. Surprisingly enough, such theoretical estimates agree remarkably well with the actual conditions in the atmosphere, suggesting that these hypotheses are not far from the reality.

In the scattering process the radiation from a source is reradiated in all directions; hence, so-called diffuse radiation appears even in the space which is not directly illuminated by the source. For example, the twilight illumination of the sky after sunset occurs because particulate matter in the upper atmospheric layers scatters the direct sun's illumination down to the atmospheric layers in the Earth's shadow. Spectacular twilight sky illuminations have been observed after strong volcanic eruptions, like the one visible in southern

California after the last eruption of Mt. Agung* which was so intense in the fall of 1963 that it prolonged the twilight by an hour. The spectacular coloring was the combined effect of the attenuation of the sun's rays due to the ozone absorption in the Chappuis band and of atmospheric scattering by molecules and small particles. The lower layers of the volcanic dust, illuminated by the sun's rays passing through maximum ozone concentration, had a dark violet hue, while the upper layers, illuminated by the sun's rays passing above the ozone maximum, had an intense golden glow, which persisted much longer.

As the scattered radiation appears all around the scattering volume and is almost always symmetrical with respect to the direction of illumination, approximately equal amounts of radiation are scattered downwards and upwards. Hence, an intense twilight glow caused by vast amounts of particulates in the stratosphere will be visible from outer space as well as on Earth. In fact, the glow will be seen as even more brilliant there, since its intensity will not be decreased by attenuation within the lower dense atmosphere. To an observer in outer space, or in a satellite picture, this glow will produce a shift of the terminator, i.e., the line dividing the illuminated part of the planet from that in the shadow. The study of the intensity gradient across the terminator in an ATS-type satellite picture, suggested first by Deirmendjian (1962) for the detection of noctilucent clouds, can be thus applied with considerable success in the determination of aerosol content in the stratosphere.

The existence of a twilight glow points out one quite important feature of atmospheric scattering. Since scattering redistributes some portion of radiant energy in all directions, the observed intensity of the source is diminished by the amount of radiation scattered in other directions by the scattering medium. In the case of a dense medium, like a stratus or fog, the source may even become invisible. The scattering volume represents a secondary source of radiation, usually called "diffuse" radiation. (It is "diffuse transmission" when directed downward, "diffuse reflection" if directed upward.)

*See also Deirmendjian (1971).

The magnitude of this diffuse radiation can be appreciated from Figure 1, which shows the dependence of the quantity S/H on the solar zenith distance, S and H being respectively the solar and the diffuse sky radiation, measured as received by unit horizontal area. The upper two solid lines give the values of this ratio for a pure, particulate-free atmosphere for two ground reflectivities (of 0 and .25). The dashed curves represent the values measured by the Smithsonian Institute in 1917, on Hump Mountain (1460 meters a.b.l.); they correspond to the case of a very clear atmosphere with a low turbidity. The heavy dashed curve, included for comparison, is based on data in Nicolet and Dagniaux's 1951 article in Mem. Inst. Roy. Meteor. Belgique, XLVII. The lowest curve gives values observed at Mt. Wilson at the elevation of 1737 meters in two days in September 1913, when volcanic dust from Katmai eruption in June 1912 was apparently present in the upper atmosphere. This diagram clearly indicates that the magnitude of the direct illumination and that of the diffuse radiation may under some conditions be comparable.

While Figure 1 gives values integrated over all wavelengths, Figure 2 gives values for one particular wavelength. Here the radiant flux of the direct sun's radiation, S, emerging from the bottom of a pure, aerosol-free atmosphere of a given optical thickness, is compared with the flux of the diffuse radiation, emerging both downwards, H_d (sky radiation) and upwards, H_u (diffuse reflection). From this diagram one can easily see that the sun's radiation after transmission through a thin layer such as that above the ozone layer is comparable in magnitude to the diffuse upward flux from the dense underlying atmosphere. This is even more valid for UV radiation, for which the optical thickness of the lower atmosphere is close to unity. This upward flux should be considered as an additional radiation source in quantitative evaluation of the photochemistry or radiative heating and cooling in stratospheric layers.

One characteristic of the light scattering is particularly germane to the topic of this conference. The process of scattering gives rise to the polarization of the scattered radiation. If the scattering particle is very small, of a size negligible with respect to the wavelength of the incident radiation, then the law of scattering is very simple: the

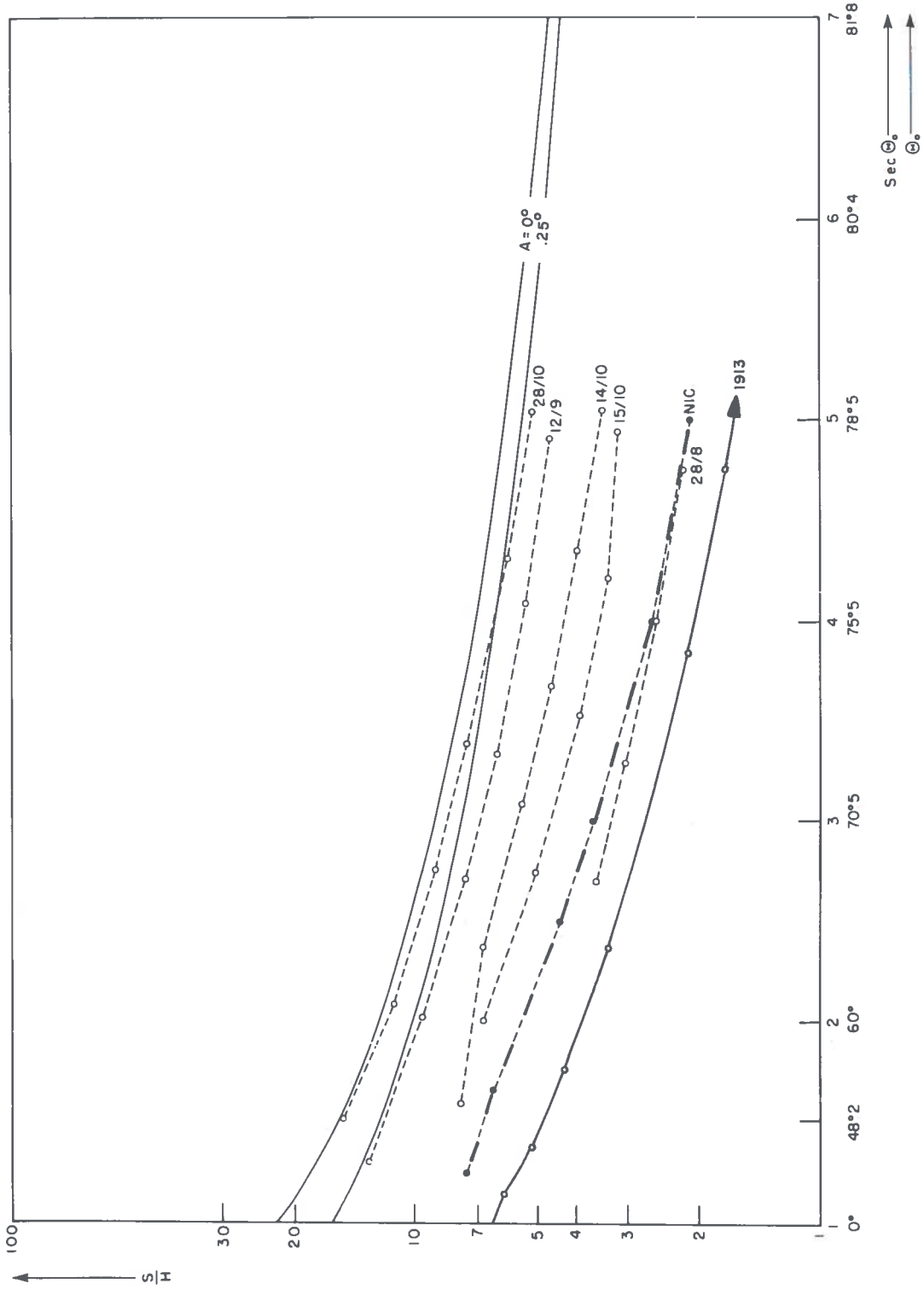

Figure 1. Ratio of solar radiation (S) and of diffuse sky radiation (H) received by a unit horizontal area for different sun elevations. Full curves marked A = 0 and .25 represent theoretical values for a pure, particulate-free atmosphere with reflectivity A. (After Deirmendjian and Sekera, 1954.)

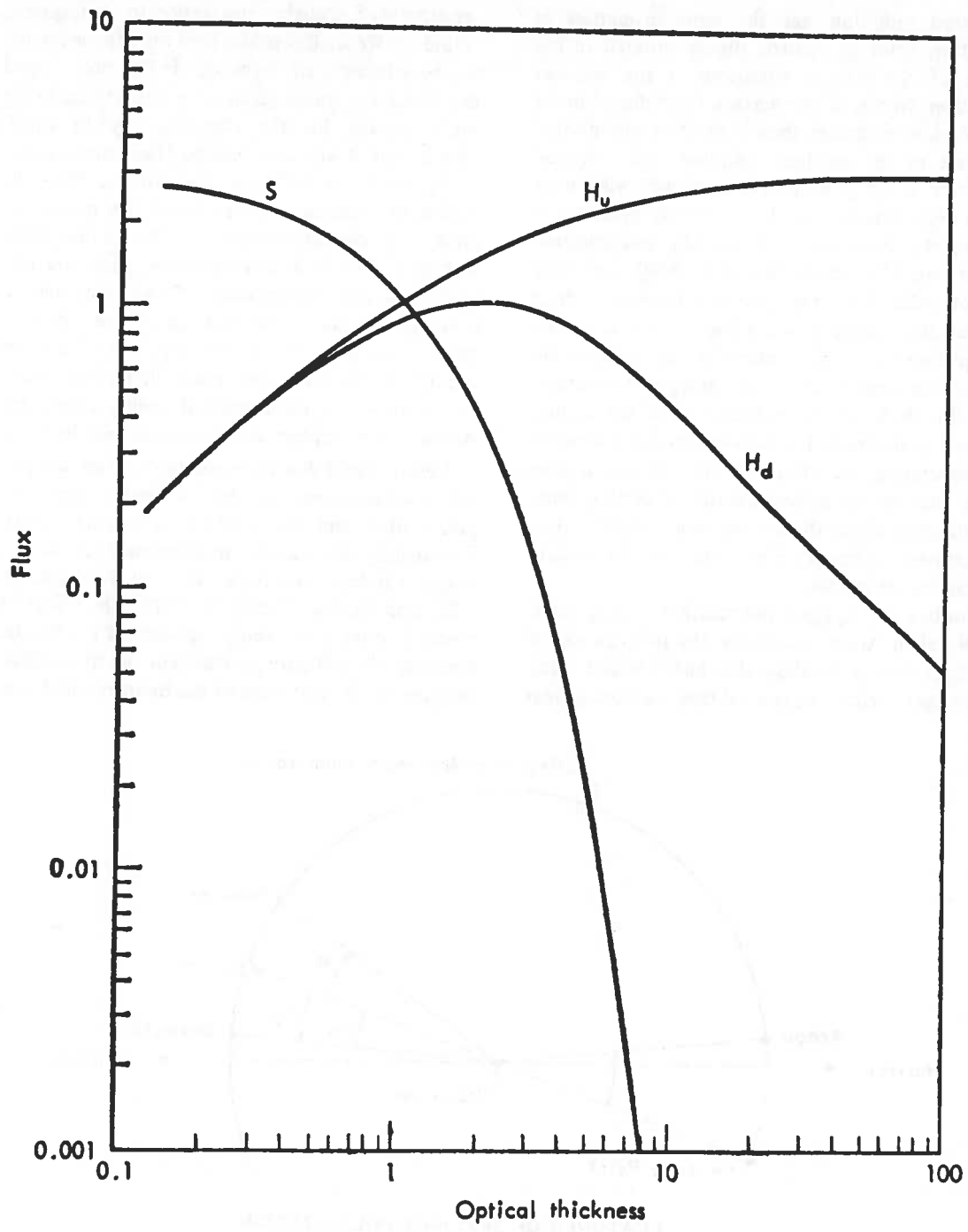

Figure 2. Direct solar radiation (S) and downward (H_d) and upward (H_u) diffuse sky radiation received by a unit area on the top or bottom of a pure molecular atmosphere with reflectivity A = 0 as a function of the optical thickness (for sun in the zenith). (After Kahle, 1967.)

scattered radiation has the same properties as radiation from an electric dipole situated in the plane of the electric vibrations of the incident radiation. Hence, if the particle is irradiated by an unpolarized radiation, then in the direction normal to that of the incident radiation, the scattered radiation is completely polarized, with vibrations only perpendicular to the scattering plane (containing the directions of the incident and scattered radiation). This simple law of Rayleigh scattering is not valid for large particles, however; these scatter the radiation according to a much more complicated law. Consequently the particulates in the atmosphere scatter the sunlight differently, and the study of the polarization of the diffuse upward or downward radiation provides the means for separating the effect of the aerosol particles from that of the molecules and of getting some information about the atmospheric turbidity, i.e., the contamination of a pure molecular atmosphere by particulate matter.

Studies of skylight polarization dating from 1809, when Arago discovered the polarization of the light from a cloudless sky, have yielded many interesting results. In general they indicate a great sensitivity of skylight polarization to atmospheric turbidity. We shall consider here only those related to the stratospheric turbidity. It has been found that there are four regions of major interest in the sun's vertical for the cloudless sky in which polarization should be measured.These are indicated in Figure 3. At 90° from the sun one finds the region of maximum polarization, its magnitude giving an overall measure of the atmospheric turbidity. For high sun elevation, there are two regions of zero polarization (the so-called neutral points), one above the sun, called the "Babinet point," another below the sun, the "Brewster point". When this latter point disappears under the horizon, a third neutral point, called the Arago point, appears above the antisolar horizon.

Before World War II considerable effort was put into measurements of the maximum degree of polarization and the position of neutral points. Fortunately the available measurements cover two major volcanic eruptions, that of Krakatoa in 1883 and that of Katmai in 1912. The effect of volcanic dust was clearly apparent in a drastic decrease of maximum polarization and in a sudden increase of the distances of the Babinet and Arago

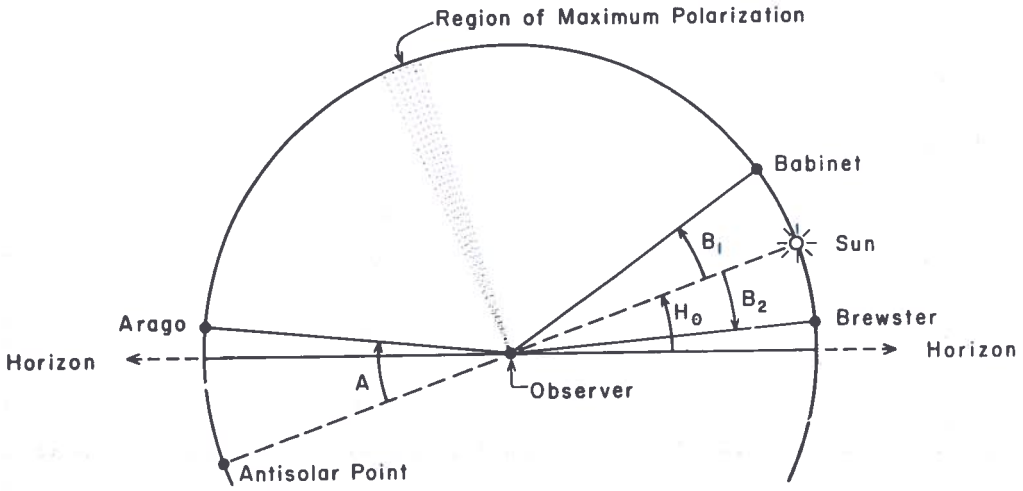

FEATURES OF SKYLIGHT POLARIZATION IN THE SUN'S VERTICAL

A = Antisolar distance of the Arago Point
B_1 = Solar distance of the Babinet Point
B_2 = Solar distance of the Brewster Point
H_θ = Elevation of Sun

Figure 3. Schematic illustration of the location of the maximum degree of polarization and of the neutral points in the sun's vertical. (After Holzworth and Rao, 1965.)

neutral points from the sun and the antisolar point, respectively. Cornu (1884) noticed, for example, that after the Krakatoa eruption the maximum polarization never reached a value larger than $P_{max} = 0.48$, while before the eruption values of $P_{max} = 0.75$ had been measured. The neutral points also shifted by 10^{o} to 15^{o} from their normal positions. The same effects were observed after the Katmai eruption; Figure 4 indicates the change in the position of neutral points before and after that eruption.

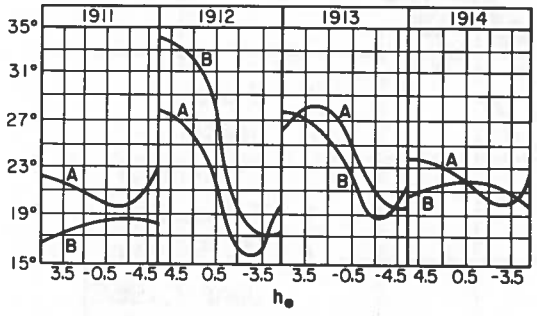

Figure 4. Positions of the Arago and Babinet points as observed before and after Katmai volcanic eruption. $H_{\odot}$ is solar elevation in degrees. (After Ch. Jensen, 1928.)

Shortly before World War II, when photoelectric detectors were slowly introduced into the photometric method, the comparison of the previous visual and of the new photoelectric measurements gave rise to the question of the dispersion of the skylight polarization, i.e., its dependence on wavelength. The analysis of a limited number of observations of skylight polarization in the narrow spectral ranges available at that time revealed two interesting results: a strong correlation of the maximum polarization in red with atmospheric turbidity, and a dependence of the difference P_{red}-P_{blue} on the turbidity or on the value of polarization (Sekera, 1957). This is indicated in Figure 5, where the difference P_{red}-P_{blue} is plotted against the polarization P_{red}. For larger turbidity, the points have a tendency to group around two distinct curves, one parallel to the zero line, the other curved in the region of the negative values of this difference. When the turbidity conditions of each observation are closely investigated, it becomes clear that the upper branch corresponds to a low-level turbidity as measured at UCLA, and the lower branch to turbidity at the upper-atmospheric level (like that measured by Dietze (1951) during the period of blue sun observed in Europe in 1950 when the clouds of ashes from Canadian forest fires drifted over Europe).

Recent photoelectric measurements of skylight polarization performed by a UCLA research group (Sekera, 1956) have confirmed all the above-mentioned results of previous visual measurements, and showed that the low-level turbidity produces shifts of neutral points in the opposite direction from those observed after volcanic eruption and connected with stratospheric turbidity. These recent studies of atmospheric scattering, and especially of its state of polarization, permit us not only to distinguish between low- and high-level turbidity, but also to make a quantitative estimate of the particulate concentration from the magnitude of the difference of measured and theoretical values for a pure molecular atmosphere.

From what has been said so far, it follows that properly designed polarization measurement of the diffuse atmospheric radiation is the most suitable and efficient method of monitoring stratospheric contamination such as that produced by supersonic transports. Its greatest advantage over other methods, such as those based on the use of optical lasers, follows from the fact that, due to multiple scattering, the observed polarization represents some kind of average of conditions of a volume of air up to 100 miles in radius. Such averaging is necessary because the particulates are always grouped in patches or clouds, and this inhomogeneity in horizontal distribution introduces uncontrollable uncertainties and errors in any particle concentration estimate derived from a narrow-beam observation or a direct *in situ* particle count in a small volume of air.

Present theories of radiative transfer for various atmospheric conditions should make it possible to compute the quantities needed to estimate the overall heating and cooling on the atmosphere, and their effect on circulation. At present, however, this is true only for a pure, particulate-free atmosphere with the scattering according to Rayleigh's law and with the surface reflection according to Lambert's law. In the very near future the theories could be extended to a general law of reflection covering different types of soil and terrain, since we are hindered only by

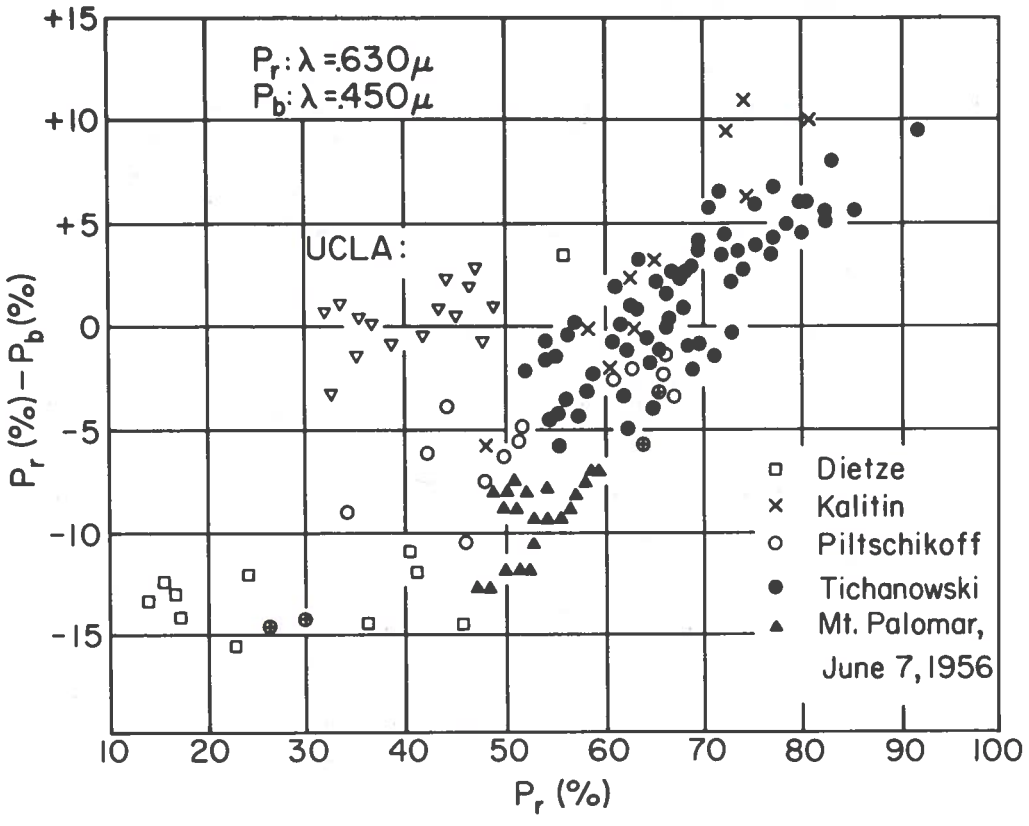

Figure 5. Dispersion of skylight polarization, showing the dependence of (P_{red} - P_{blue}) on P_{red}.

the inherent mathematical difficulties in the theory of radiative transfer in a turbid atmosphere, most of which will probably be overcome shortly. One difficulty will remain serious, however, namely, the lack of proper input data related to the great variability of the atmospheric turbidity in the lower part of the atmosphere. For the stratosphere, several theories on the photochemical reactions which produce and destroy aerosol particles can provide the input for different models of stratospheric turbidity, and the computed radiation parameters can be compared with the observational data mentioned before. However, no data are currently available to form a basis for realistic modeling of low-level turbidity.

The greatest obstacle to this endeavor is the great dependence of the turbidity on the weather, i.e., local ventilation, cloudiness, etc. Strong pollution in an area can be cleared by the passage of a front with strong winds rather quickly, and smog can be formed just as quickly in an area of calm air with the proper amount of contamination and strong irradiation under clear, cloudless skies. These difficulties become more serious because the radiation field in upper atmospheric layers depends critically on the diffuse reflection from the dense lower atmosphere. For this reason it seems almost imperative to build a network of properly equipped ground-based radiation stations to monitor low-level turbidity. In a rather short time such a network could provide data which would characterize its variability and provide some information about the expected extremes. Only then will it be possible to predict factors like global distribution of the intensity of ultraviolet radiation and its variations due to the changes in stratospheric contamination, and to assess realistically its physiological effects. Without a knowledge of low-level turbidity and its local and temporal variations, theoretical estimates based on models may deviate considerably from the reality of actual atmospheric conditions.

REFERENCES

Cornu, A., "Observations Relatives á la Couronne Visible Actuellement autour du Soleil". C.R. Acad. Sci., Paris, *99* (1884), p. 488-493.

Deirmendjian, D., "Detection of Mesospheric Clouds from a Satellite". *Proc. First Intern. Symp. on Rocket and Satellite Meteorology* (1962), p. 406-444.

Deirmendjian, D., "Global Turbidity Studies I. Volcanic Dust Effects – A critical survey." RAND Report R-886-ARPA (October 1971).

Deirmendjian, D., and Sekera, Z., "Global Radiation Resulting from Multiple Scattering in a Rayleigh Atmosphere". Tellus, *6*, No. 4 (1954), p. 382-398.

Dietze, G., "Die anormale Trübung der Atmosphäre September/Oktober 1950". Z. f. Met., *5* (1951), p. 86.

Holzworth, G.C., and Rao, C.R.N., "Studies of Skylight Polarization". J. Opt. Soc. Am., *55* (1965), p. 403-408.

Jensen, Ch., "Die Himmelstrahlung" in *Hdb. d. Physik* (Springer Verlag, Berlin), Vol. 19 (1928), p. 70-152.

Kahle, A.B., "Global Radiation Emerging from a Rayleigh Scattering Atmosphere of Large Optical Thickness". RAND Memorandum RM-5343-PR (May 1967).

Sekera, Z., "Polarization of Skylight" in *Encyclopedia of Physics* (Springer Verlag, Berlin), Vol. 48 (1957), p. 288-328.

Sekera, Z., "Recent Developments in the Study of Skylight Polarization" in *Advances in Geophysics* (Academic Press, Inc., New York) Vol. 3 (1956), p. 45-104.

MOTIONS IN THE STRATOSPHERE

ROBERT E. DICKINSON
*National Center for Atmospheric Research**
Boulder, Colorado 80302

ABSTRACT: Motions in the stratosphere occur on different space and time scales. Before their transport of trace constituents can be quantitatively evaluated, we need a theoretical understanding of these motions which will permit us to construct numerical models which can be tested against actual observations.

We can classify those stratospheric motions which are significant for transport into the following categories: zonal-wind/meridional-circulation systems, planetary waves, and synoptic-scale and mesoscale motions. Stratospheric zonal-wind systems include the winter westerly and summer easterly mid-latitude vortices and the tropical quasi-biennial oscillation, as well as a semiannual component. Planetary waves include quasistationary waves with phase locked at some longitude, e.g., the Aleutian High; traveling waves with slowly varying amplitude; and large sporadic variations, e.g., midwinter sudden warmings.

Synoptic-scale potential vorticity-conserving motions are of importance in the lower stratosphere. Gravity waves and clear-air turbulence act to mix and dissipate synoptic-scale motions.

INTRODUCTION

Dynamic meteorologists are concerned with stratospheric motions largely as a subject of intrinsic scientific interest. On the other hand, chemists are interested in stratospheric motions largely as a mechanism for transport of various trace substances.

These two points of view are complementary. Motions cannot be immediately parameterized in some simple fashion, such as by eddy mixing coefficients, if a reliable description of atmospheric transport is to be obtained. The different stratospheric motion processes and their variability in space and time must be understood. This understanding must be based on observation [1] but have enough theoretical depth to permit quantitative modeling of the more important features of these motions. In other words, the dynamicists' basic understanding is needed for the evaluation of the motions as a tool for transport. Conversely, the chemist's observations of transport processes can provide further insight into stratospheric dynamics [2, 3].

The production and loss of ozone is an especially interesting example of the relationship between motions and stratospheric trace substances. It has long been recognized that stratospheric ozone located below 30 km is not in photochemical equilibrium [1-11]. Its concentration is generally insensitive to chemical loss processes, and depends instead on the manner in which it is transported downward into the troposphere. The concentration of ozone is transport-controlled even in the photochemical equilibrum region above 30 km, if ozone loss processes are dominated by substances such as water-vapor products or odd-nitrogen molecules which have been transported into the stratosphere from other parts of the atmosphere [12-24].

The transport of odd nitrogen either upward from the troposphere or downward from the ionosphere would be quite sporadic. Consequently, if ozone loss rates are linearly proportional to NO concentration, rather large transport-controlled fluctuations of ozone above 30 km become possible.

*The National Center for Atmospheric Research is sponsored by the National Science Foundation.

STRATOSPHERIC MOTIONS: ZONAL WINDS AND PLANETARY WAVES

First we shall consider planetary-scale stratospheric zonal winds, that is, the eastward component of wind. Figure 1 [15] shows somewhat schematically the longitudinally averaged stratospheric vortices in winter and summer. The zonal-mean stratospheric winds blow mostly from the west in winter and from the east in summer, with maximum values in middle latitudes near the stratopause. The 'topsides of the tropospheric westerly cores give secondary maxima in the lower stratosphere. The jet cores as shown here are much weaker, because of averaging, than the cores seen instantaneously at one longitude.

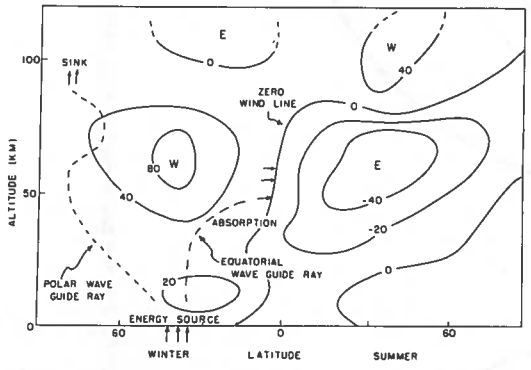

Figure 1. Schematic sketch of stratospheric zonal winds and planetary-wave ray paths according to Dickinson [15].

In addition to the reversal of sign from summer to winter, there is much greater departure from zonality in winter than in summer. This departure is a consequence of the upward propagation of planetary waves from the troposphere in the winter hemisphere [15-17]. Vertical propagation of stationary planetary waves is shown schematically as rays on the figure.

Figure 2 [18] shows examples of the distribution of geopotential heights on a 30-mb (24-km) pressure-level map during summer and winter. Geostrophic winds flow parallel to these contours, with low values to the left of the direction of motion. The westward flow around the summer polar high is nearly circular on a monthly mean basis. The eastward flow around the winter low, on the other hand, is quite asymmetric. We see this asymmetry is planetary in scale, consisting largely of longitudinal Fourier wave components one and two. These components reinforce each other to give a large high-pressure ridge in the Gulf of Alaska, the "Aleutian High". During stratospheric sudden warmings [19-22], the zonal component of the circulation nearly disappears and the ridges and troughs become individual high and low cells.

Figure 3 [23] shows a longitude-height section of the contribution of wave number one to the geopotential heights averaged over January 1958. The bottom frame shows the height amplitude increasing with altitude to values as large as 900 m at 10 mb (30 km). Maximum values may occur at levels of 40-50 km or higher, but hemispheric wind data for Fourier analysis in longitude are generally not available much above 30 km. There are factor-of-two variations in monthly mean January amplitudes of wave number one from one year to the next.

The top frame shows the variation of wave phase with latitude and height. The wave tilts westward with increasing height, with a more than 180° phase shift from the lower troposphere to 30 mb. There is also considerable westward tilt with decreasing latitude, reflecting the propagation of wave energy towards the zero-wind-line critical layer in the tropics. The vertical phase progression indicates a northward eddy transport of heat by the wave, and the latitudinal phase progression indicates a poleward eddy momentum transport.

Figure 4 [24] shows the corresponding wave number one component for the Southern Hemisphere for a long-term July average. The amplitude of this wave in the stratosphere is comparable to that of its counterpart in the Northern Hemisphere. In contrast to the latter, however, the stationary wave number one does not increase in phase in the troposphere with increasing altitude; this presumably reflects a difference in the distribution of forcing. The other notable difference between hemispheres is the near-absence of a time-mean wave number two in the Southern Hemisphere; in the Northern Hemisphere this wave is comparable in amplitude to wave number one.

Several observational and numerical studies have been made of the dynamics and energetics of the breakdown of the winter stratospheric zonal flow, known as a sudden warming [25-29]. Matsuno's theoretical explanation of sudden warming is the most satisfactory [30]. Matsuno

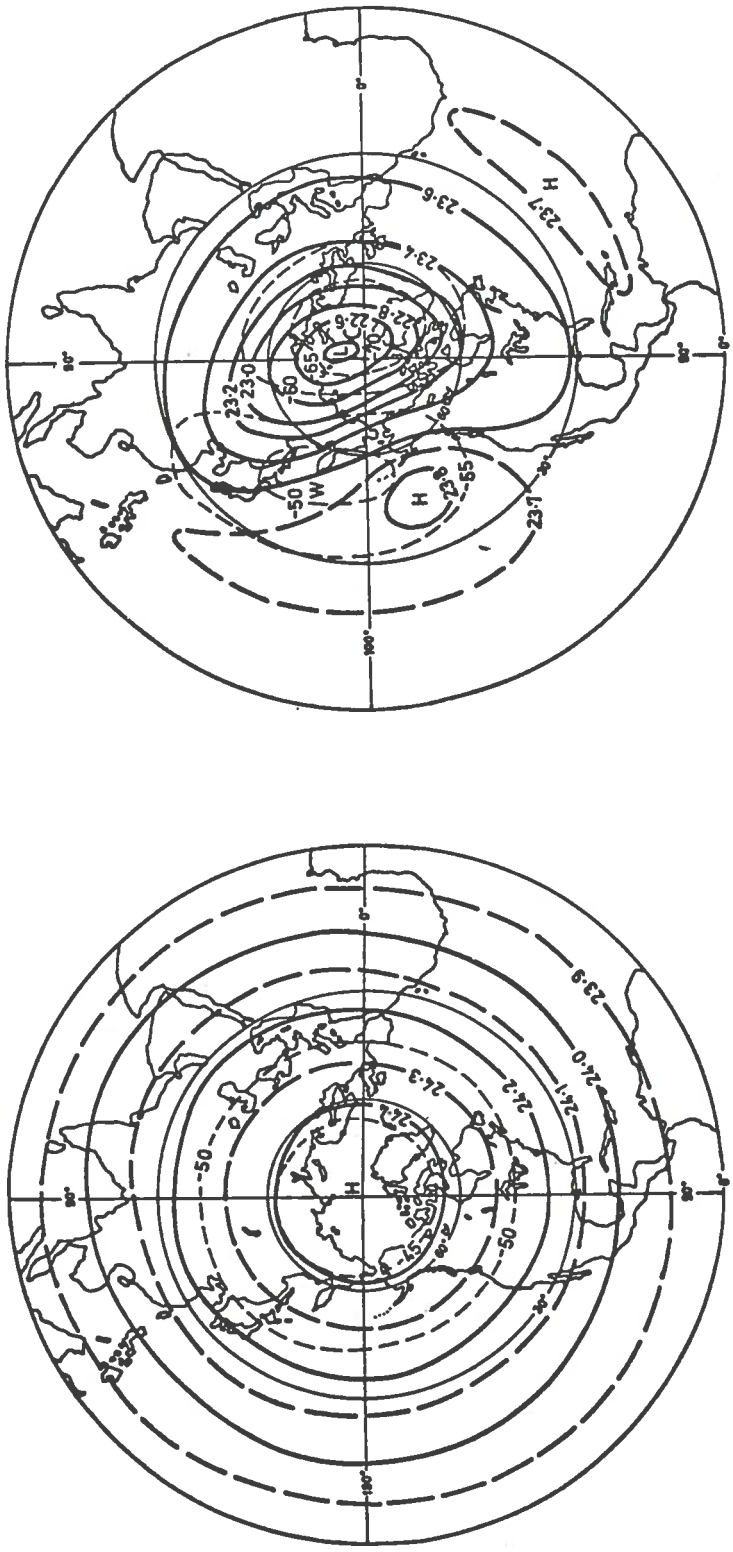

Figure 2. Mean 30-mb topography (24 km) for summer and winter seasons 1958-61 according to Hare [18].

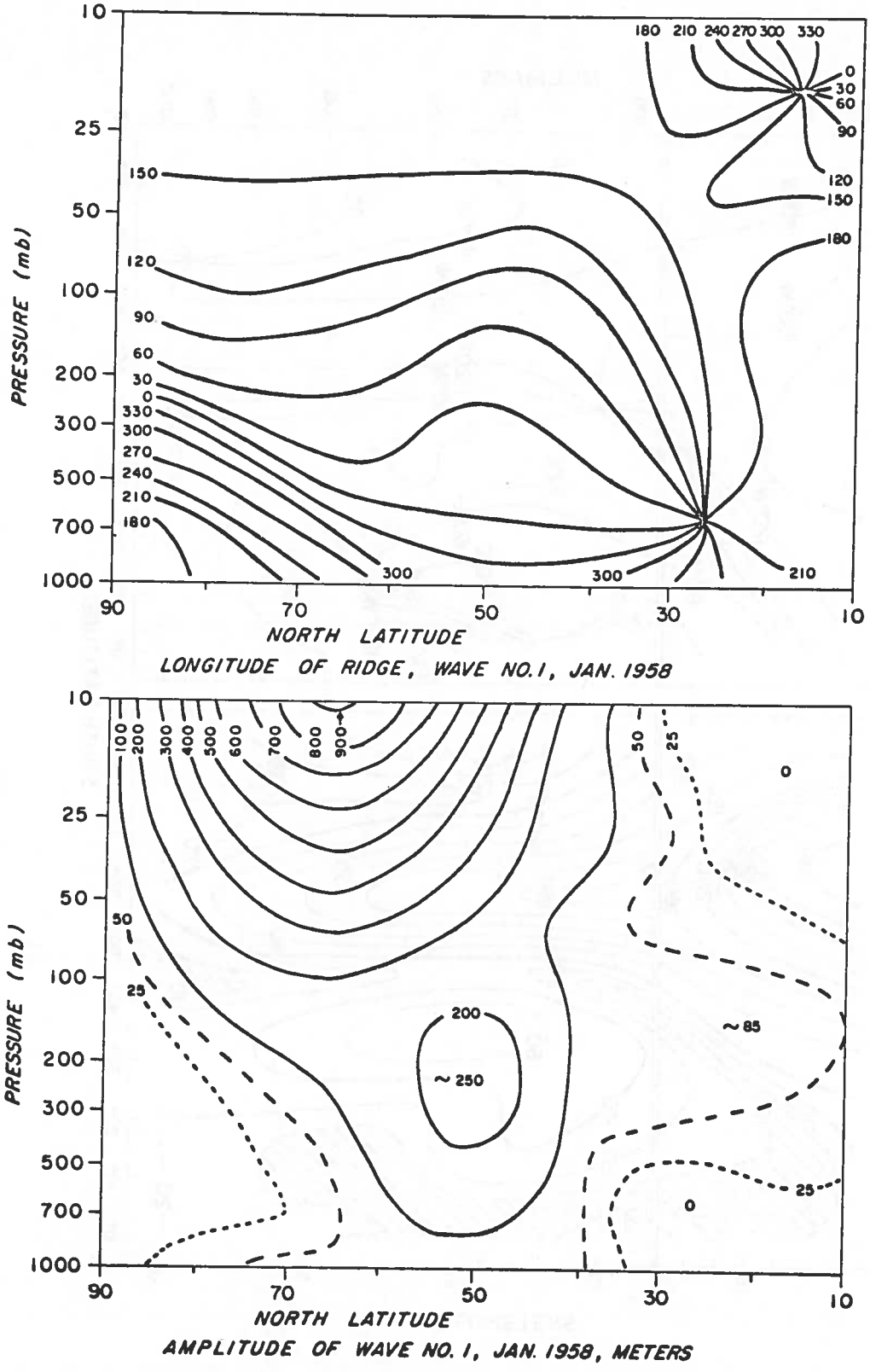

Figure 3. Monthly mean amplitude and phase of wave number one for January 1958 from Muench [23].

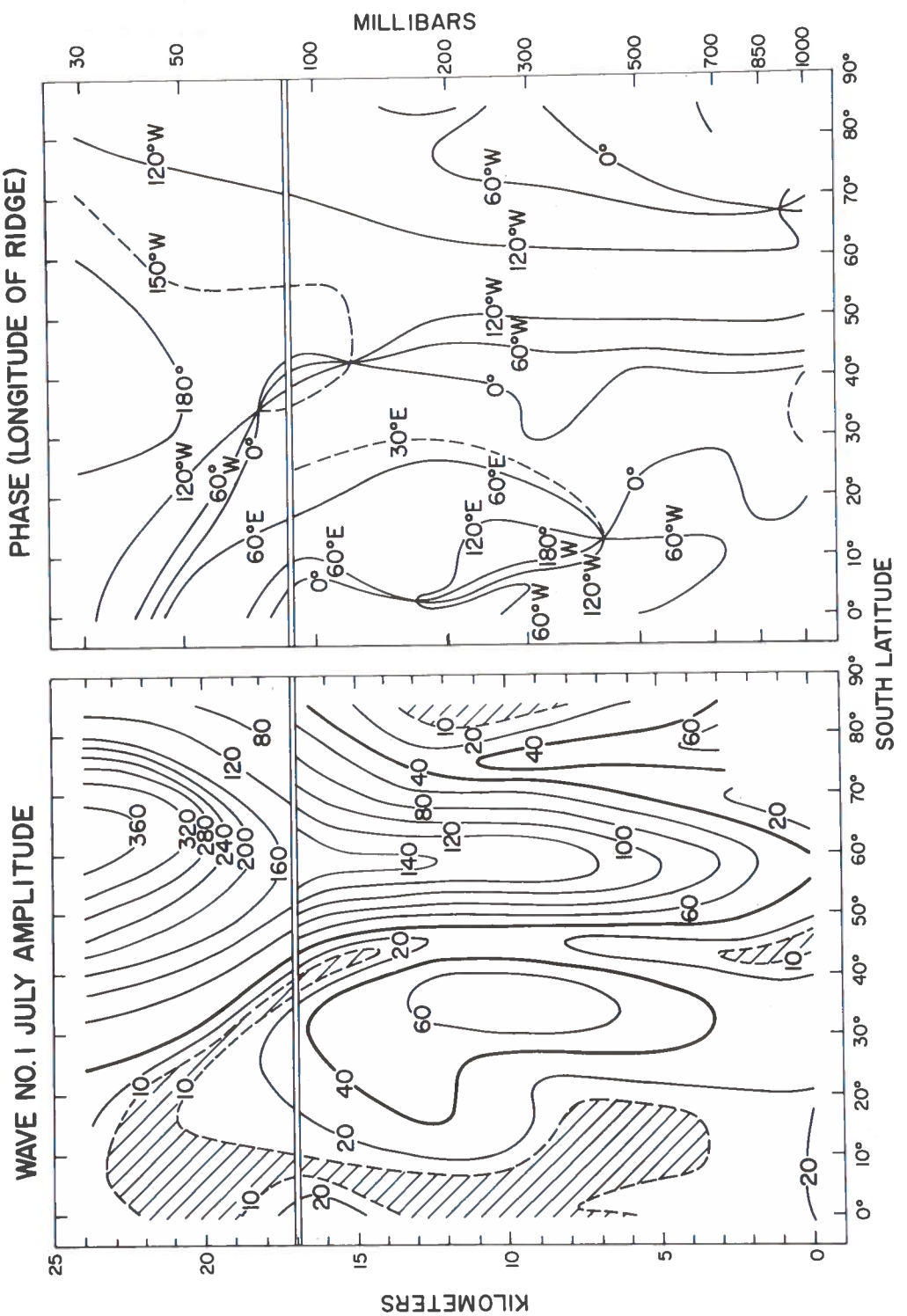

Figure 4. July mean wave number one amplitude and phase from van Loon and Jenne [24].

shows how a sudden increase of wave number one or two in the troposphere can produce a transient, vertically propagating planetary wave, which by transporting potential vorticity southward destroys the stratospheric westerlies and warms polar latitude. Figure 5 [30] shows an example of the breakdown of the zonal westerlies at 30 km according to Matsuno's calculations. Momentum is extracted from the zonal wind by the planetary wave, both in middle latitudes by the upward-propagating transients and in the tropics by the quasistationary part of the wave. This quasistationary component produces a divergence of horizontal eddy momentum transport in the tropics in the vicinity of the zero-wind critical layer, pulling the zero-wind line northward.

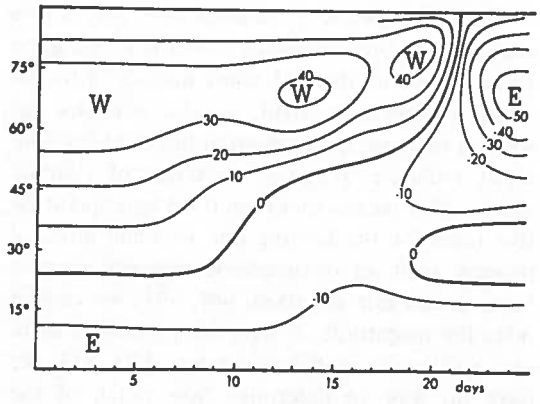

Figure 5. Zonal westerlies at 30 km versus time according to theoretical calculations by Matsuno [30].

This extraction of zonal westerly momentum from the tropics by planetary waves must be occurring on a mean basis throughout the winter [15, 31]. Since no comparable process occurs during the summer, this wintertime loss of westerly momentum from low latitudes would be expected to produce a semiannual component in the zonal wind such as that indicated by observations [32] shown in Figure 6. Even averaging over a winter, the eddy momentum transport fluctuates considerably from year to year, as shown at 20 km in Figure 7 [33]. The "transient eddy" component is largely due to amplitude and phase fluctuations of the quasistationary planetary waves, rather than actual traveling waves. Free Rossby planetary waves propagating westward as global modes are best found in summer wind data, where the quasistationary waves are absent. Figure 8 [34] shows 5- to 10-day oscillations in the zonal wind at 30 km, indicating the possible presence of these free modes. These motions, along with diurnal and semi-diurnal tides, have little relevance to transport problems in the stratosphere, but these waves may also increase in amplitude with height like tides, to become important at higher levels.

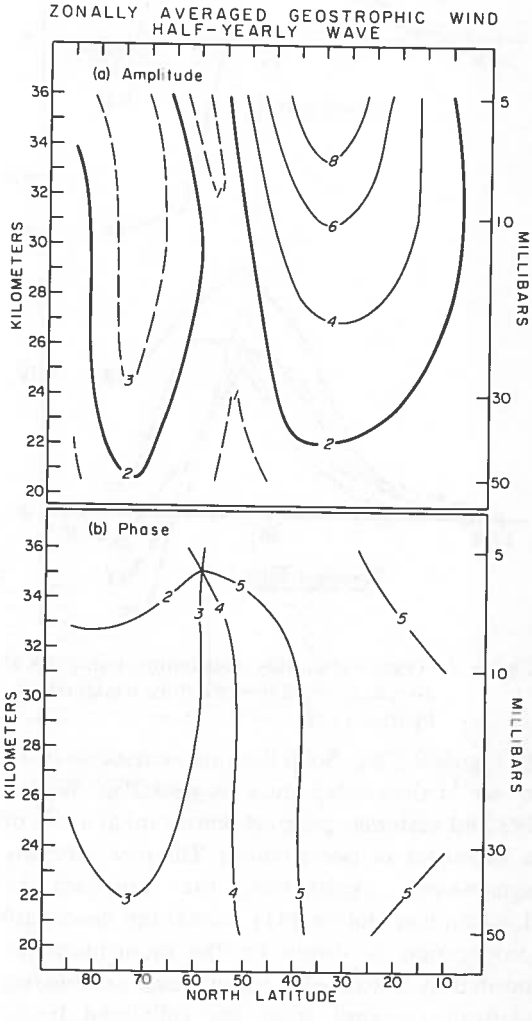

Figure 6. Semiannual component of zonal wind according to van Loon *et al.* [32].

There is a significant biennial component [35-39] to the year-to-year variability of mid-latitude winter stratospheric circulation, presumably reflecting the interaction of the quasi-stationary planetary waves with the biennial zonal-wind oscillation over the equator as shown

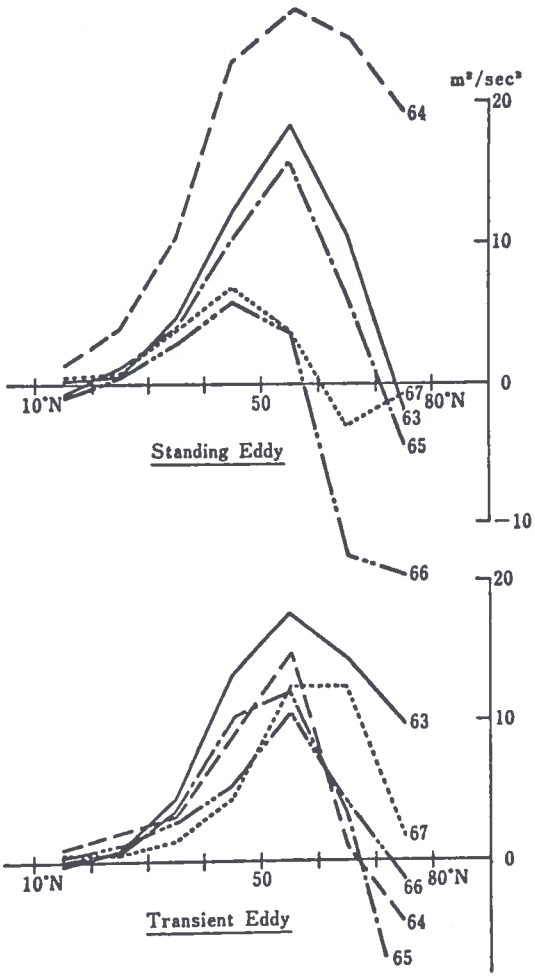

Figure 7. Year-to-year eddy momentum transports at 30 mb, averaged over the three winter months by Hirota [33].

in Figure 9 [40]. Solid lines are increments of 10 m sec^{-1}; the shaded areas are westerlies. Westerlies and easterlies progress downward at a rate of a kilometer or two a month. The now generally agreed-upon explanation, first proposed by Lindzen and Holton [41], is that this downward propagation is driven by the momentum deposited by 5- to 10-day period waves propagating vertically upward from the equatorial troposphere [42, 43]. The biennial zonal winds are largely confined to within 15° of the equator. Winds at 20° latitude, as seen in the lowest frame, are dominated by the semiannual component.

MEAN MERIDIONAL CIRCULATIONS

Mean meridional circulation, that is, zonal-mean north-south and vertical motions, are very difficult to observe directly. They are generally inferred from balance requirements in the dynamic and thermodynamic equations [44-47], like the circulation shown in Figure 10 derived by Vincent [47] from momentum balance. A much more vigorous stratospheric meridional circulation is produced in the winter hemisphere by eddy momentum transports than could occur in the nearly zonally-symmetric summer hemisphere. The winter meridional circulation in the stratosphere generally consists of two cells, with rising motion over the equator and pole and sinking motion in middle latitudes, which connect smoothly to the tropospheric Hadley and Ferrel cells. The tropical cell in the lower stratosphere is much weaker than the tropospheric Hadley cell.

The stratospheric meridional cells play a role analogous to the tropospheric cells in keeping the zonal winds in thermal wind balance with the zonal temperature field in the presence of sources of zonal momentum or heat and frictional or radiative damping. In terms of climatic impact, this means that even if we have quantitative rates for the heating due to some physical process such as stratospheric aerosols emitted from a volcanic eruption [48, 49], we cannot infer the magnitude of temperature change without a dynamic model calculation [50, 51]—we have no way to determine how much of the heating will be balanced by adiabatic cooling through vertical motions. The dynamic constraints in equatorial latitudes require production of zonal available potential energy in the thermal field to be accompanied by a much greater generation of zonal kinetic energy [52]. Simply put, it may be easier to produce a temperature perturbation with a momentum source than with a thermal source.

EDDIES IN THE LOWER STRATOSPHERE

In the lower stratosphere, i.e., below 15 km or the 100-mb level, the topside of synoptic-scale tropospheric eddies becomes greater in amplitude than the planetary-scale waves. (Synoptic scale refers to horizontal scales of a few hundred to a few thousand kilometers. Motions on this scale are controlled largely by the properties of nonlinear hydrodynamic flow, and wave aspects are rather insignificant.) The concept of potential

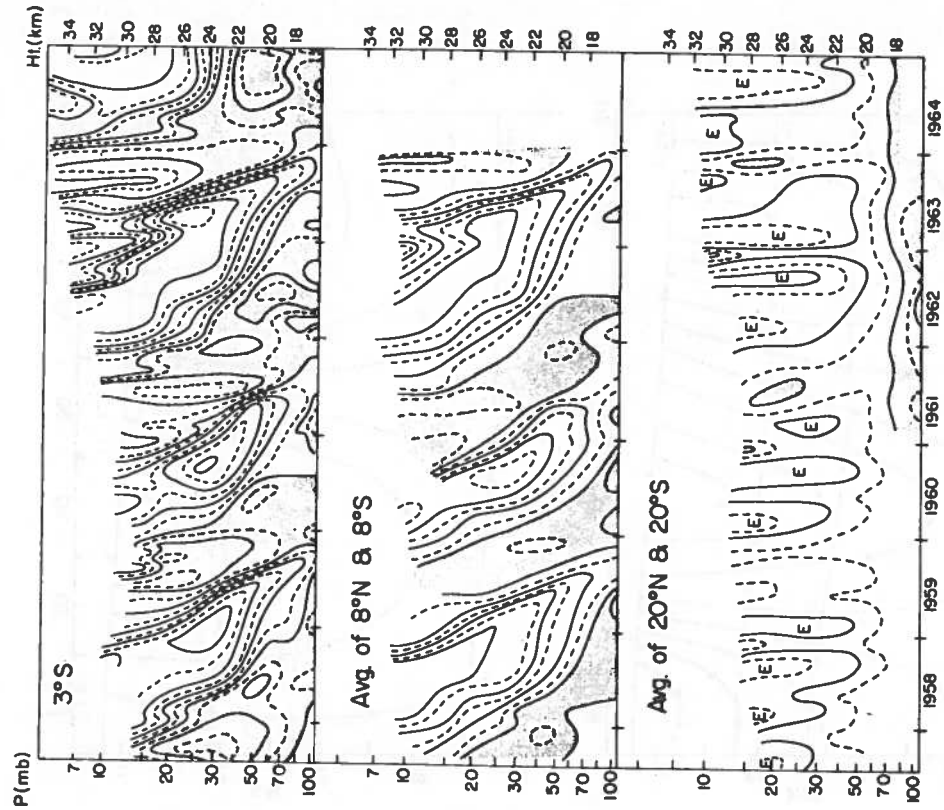

Figure 9. Biennial wind oscillation from Wallace [40] at selected latitudes, averaged between hemispheres.

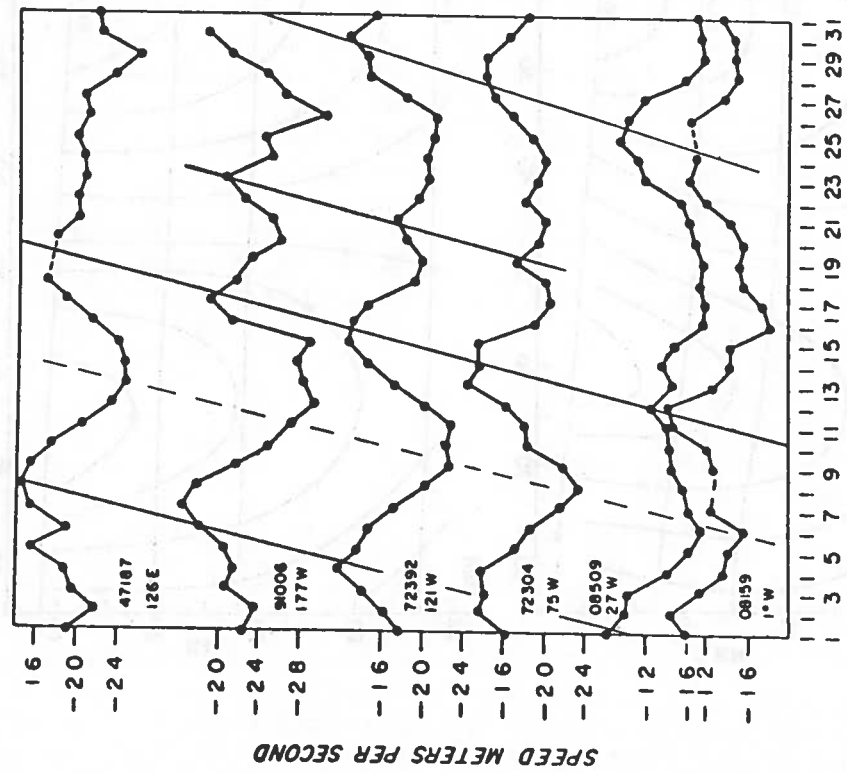

Figure 8. Zonal wind versus time at 10 mb for stations near 35°N during July 1963 by Muench [34].

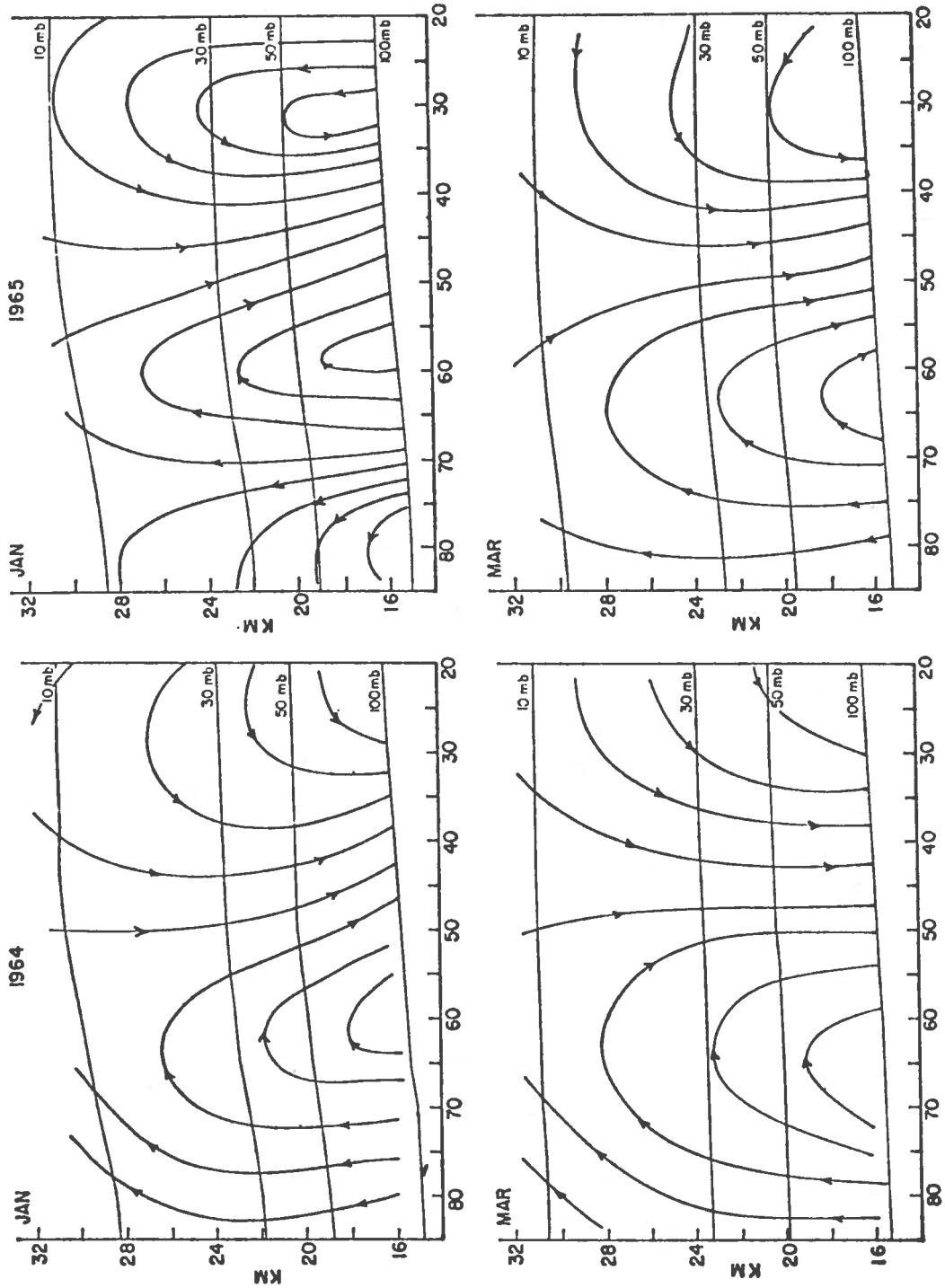

Figure 10. January and March mean meridional circulations according to Vincent [47].

vorticity becomes very useful for interpreting the synoptic-scale motions of the lower stratosphere. It not only serves as a tracer of motions, but also generates the time evolution of the flow. Synoptic-scale eddies in the lower stratosphere serve the very important role of regulating total ozone content by transporting ozone poleward and downward, ultimately across the tropopause to destruction in the troposphere [54, 55].

The earlier-mentioned downward vertical motion between the Hadley and Ferrel cells, viewed on the synoptic scale without averaging in longitude and time, reveals itself as a much narrower and stronger circulation in the vicinity of the poleward edge of the local zonal jet core. This circulation folds the tropopause, pulling downward tongues of stratospheric air to eventual mixing in the troposphere. Danielsen [54] has shown how this process can be followed, using potential vorticity, ozone, and radioactivity as tracers of stratospheric air as shown in Figure 11 [56].

On the mesoscale, orographically induced gravity waves [57] and clear-air turbulence [58] are of frequent occurrence in the lower stratosphere. The importance of motions on this scale for transport processes lies in their irreversible mixing of air and consequent destruction of potential vorticity.

RECOMMENDATIONS

For studies of global transport problems, it seems desirable to seek parameterization of mesoscale and synoptic-scale motions in terms of the statistics required for turbulent transport theory [59, 60]. It is clear, however, that planetary-scale motion systems in the stratosphere are either too sporadic (such as sudden warming), or too nonrandom (such as the mean meridional circulation and the quasistationary planetary waves) for statistical transport-theory methodology to be very applicable. Consequently, numerical models of these motions in the stratosphere are an essential tool for determining transport. Properly formulated numerical simulation is also a desirable test of our present understanding of stratospheric motions.

Finally, there are two areas in which better understanding of the chemistry and distribution of ozone may further improve our knowledge of stratospheric motions. First, we need a quantitatively reliable description of the enhancement of radiative damping through the temperature dependence of ozone photochemistry [61, 62]. The vertical propagation of stationary planetary waves is rather sensitive to radiative damping processes [63], and even when longitudinal variation of ozone heating is not taken into account, radiation has been observed to destroy a significant amount of the eddy available potential energy of stratospheric planetary waves [64, 65].

Second, we would benefit from satellite measurements of total ozone [66, 67]. If properly interpreted, they would provide a wealth of information on the horizontal variation of vertical motions in the lower stratosphere, especially in the tropics, where it is very difficult to derive vertical motions by conventional techniques.

REFERENCES

1. Newell, R.E., 1963: "The general circulation of the atmosphere and its effects on the movement of trace substances." J. Geophys. Res., *68*, 3949-3962.
2. List, R.J., and Telegadas, K., 1969: "Using radioactive tracers to develop a model of the circulation of the stratosphere." J. Atmos. Sci., *26*, 1128-1136.
3. Martell, E.A., 1968: "Tungsten radioisotope distribution and stratospheric transport processes." J. Atmos. Sci., *25*, 113-125.
4. Brewer, A.W., and Wilson, A.W., 1968: "The regions of formation of atmospheric ozone." Quart. J. Roy. Met. Soc., *94*, 249-265.
5. Dutsch, H.U., 1970: "Atmospheric ozone—a short review." J. Geophys. Res., *75*, 1707-1712.
6. Gebhart, R., 1971: "On the equatorial ozone profile." Ann. Geophys., *27*, 242-254.
7. Gebhart, R., Bojkov, R., and London, J., 1970: "Stratospheric ozone: a comparison of observed and computed models." Beiträge zur Physik der Atmosphäre, *43*, 209-227.
8. Hering, W.S., 1966: "Ozone and atmospheric transport processes." Tellus, *18*, 329-330.
9. Kulkarni, R.N., 1968: "Ozone fluctuations in relation to upper air perturbations in the middle latitudes of the southern hemisphere." Tellus, *20*, 305-313.
10. Newell, R.E., 1961: "The transport of trace substances in the atmosphere and their implications for the general circulation of the stratosphere." Geofisica Pura e Applicata, *49*, 137-159.

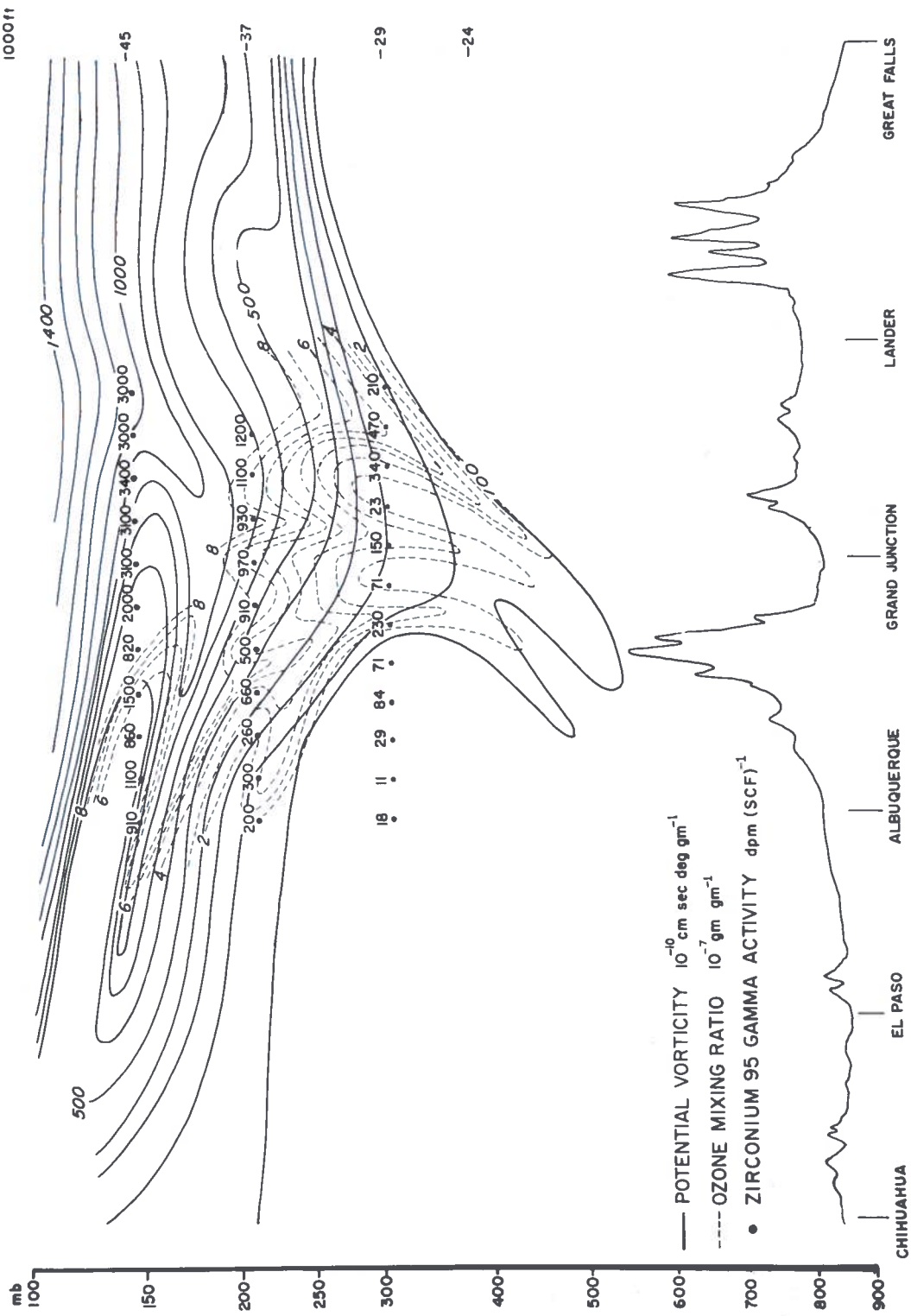

Figure 11. Vertical cross-section showing stratospheric extension of potential vorticity (solid lines), ozone (dashed lines), and Zirconium 95 activities (plotted numbers) from Danielsen et al. [56].

11. Pittock, A.B., 1970: "Ozone behaviour associated with the middle stratospheric circulation during the southern spring of 1967." Quart. J. Roy. Met. Soc., *96*, 214-225.

12. Crutzen, P.J., 1971: "Ozone production rates in an oxygen-hydrogen-nitrogen oxide atmosphere." J. Geophys. Res., *76*, 7311-7327.

13. McElroy, M.B., and McConnell, J.C., 1971: "Nitrous oxide: a natural source of stratospheric NO." J. Atmos. Sci., *28*, 1095-1098.

14. Strobel, D.F., 1971: "Odd nitrogen in the mesosphere." J. Geophys. Res., *76*, 8384-8393.

15. Dickinson, R.E., 1968: "Planetary Rossby waves propagating vertically through weak westerly wind wave guides." J. Atmos. Sci., *25*, 984-1002.

16. Charney, J.G., and Drazin, P.G., 1961: "Propagation of planetary-scale disturbances from the lower into the upper atmosphere." J. Geophys. Res., *66*, 83-109.

17. Matsuno, T., 1970: "Vertical propagation of stationary planetary waves in the northern hemisphere." J. Atmos. Sci., *27*, 871-833.

18. Hare, F.K., 1968: "The Arctic." Quart. J. Roy. Met. Soc., *94*, 439-459.

19. Finger, F.G., and Teweles, S., 1964: "The midwinter 1963 atmospheric warming and circulation change." J. Appl. Meteor., *3*, 1-15.

20. Johnson, K., 1969: "A preliminary study of the stratospheric warming of December 1967 - January 1968." Mon. Wea. Rev., *97*, 553-564.

21. Labitzke, K., 1968: "Midwinter warming in the upper stratosphere in 1966." Quart. J. Roy. Met. Soc., *94*, 279-192.

22. Quiroz, R.S., 1969: "The warming of the upper stratosphere in February 1966 and the associated structure of the mesosphere." Mon. Wea. Rev., *97*, 541-552.

23. Muench, H.S., 1965: "On the dynamics of the wintertime stratospheric circulation." J. Atmos. Sci., *22*, 349-360.

24. van Loon, H., and Jenne, R.L., 1972: "The zonal harmonic standing waves in the southern hemisphere." J. Geophys. Res., *77*, 992-1003.

25. Clark, J.A., 1970: "A quasi-geostrophic model of the winter stratospheric circulation." Mon. Wea. Rev., *97*, 443-461.

26. Julian, P.R., and Labitzke, K.B., 1965: "A study of atmospheric energetics during the January-February 1963 stratospheric warming." J. Atmos. Sci., *22*, 597-610.

27. Mahlman, J.D., 1970: "Eddy transfer processes in the stratosphere during major and minor breakdowns of polar night vortex." J. Geophys. Res., *75*, 1701-1706.

28. Miyakoda, K., Strickler, R.F., and Hembree, G.D., 1970: "Numerical simulation of the breakdown of the polar night vortex in the stratosphere." J. Atmos. Sci., *27*, 139-154.

29. Perry, J.S., 1967: "Long-wave energy processes in the 1963 sudden stratospheric warming." J. Atmos. Sci., *24*, 539-550.

30. Matsuno, T., 1971: "A dynamical model of the stratospheric sudden warming." J. Atmos. Sci., *28*, 1479-1493.

31. Dickinson, R.E., 1969: "Theory of planetary wave - zonal flow interaction." J. Atmos. Sci. *26*, 73-81.

32. van Loon, H., Labitzke, K., and Jenne, R.I., 1972: "The half-yearly wave in the stratosphere." J. Geophys. Res., *77*, in press.

33. Hirota, I., and Sato, Y., 1970: "Year to year variation of horizontal eddy flux of momentum in the winter stratosphere." J. Met. Soc. Japan, *48*, 61-68.

34. Muench, H.S., 1968: "Large-scale disturbances in the summertime stratosphere." J. Atmos. Sci., *25*, 1108-1115.

35. Labitzke, K., 1965: "On the mutual relation between stratosphere and troposphere during periods of stratospheric warmings in winter." J. Appl. Meteor., *4*, 91-99.

36. Angell, J.K., and Korshover, J. 1967: "Biennial variation in springtime temperature and total ozone in extratropical latitudes." Mon. Wea. Rev., *95*, 757-762.

37. Dart, D.B., and Belmont, A.D., 1970: "A global analysis of the variability of the quasi-biennial oscillation." Quart. J. Roy. Met. Soc., *96*, 186-194.

38. Miller, A.J., 1971: "Kinetic energy and the quasi-biennial oscillation." Mon. Wea. Rev., *99*, 912-918.

39. Wallace, J.M., and Newell, R.E., 1966: "Eddy fluxes and the biennial stratospheric oscillation." Quart J. Roy. Met. Soc., *92*, 481-489.

40. Wallace, J.M., 1966: "Long period wind fluctuations in the tropical stratosphere." Report No. 19, Planetary Circulations Project, Dept. of Meteorology, MIT.

41. Lindzen, R.S., and Holton, J.R., 1968: "A theory of the quasi-biennial oscillation." J. Atmos. Sci., *25*, 1095-1107.

42. Kousky, V.E., and Wallace, J.M., 1971: "On the interaction between Kelvin waves and mean zonal flow." J. Atmos. Sci., *28*, 162-169.

43. Lindzen, R.S., 1971: "Equatorial planetary waves in shear: Part I." J. Atmos. Sci., *28*, 609-622.

44. Dickinson, R.E., 1962: "Momentum balance of the stratosphere during the IGY." Final Report, Dept. of Meteorology, MIT. Planetary Circulations Project AF 19(604)-5223.

45. Mahlman, J.H., 1969: "Heat balance and mean meridional circulations in the polar stratosphere during the sudden warming of January 1968." Mon. Wea. Rev., *97*, 534-540.

46. Murgatroyd, R.J., 1969: "A note on the contributions of mean and eddy terms to the momentum and heat balances of the troposphere and lower stratosphere." Quart. J. Roy. Met. Soc., *95*, 194-202.

47. Vincent, D.G., 1968: "Mean meridional circulation in the Northern Hemisphere lower stratosphere during 1964 and 1965." Quart. J. Roy. Met. Soc., *94*, 333-349.

48. Newell, R.E., 1970: "Stratospheric temperature change from the Mt. Agung volcanic eruption of 1963." J. Atmos. Sci., *27*, 977-978.

49. McInturff, R.M., Miller, A.S., Angell, J.K., and Korshover, J., 1971: "Possible effects on the stratosphere of the 1963 Mt. Agung volcanic eruption." J. Atmos. Sci., *28*, 1304-1307.

50. Wallace, J.M., and Holton, J.R., 1968: "A diagnostic numerical model of the quasi-biennial oscillation." J. Atmos. Sci., *25*, 280-292.

51. Meyer, W.D., 1970: "A diagnostic numerical study of the semiannual variation of the zonal wind in the tropical stratosphere and mesosphere." J. Atmos. Sci., *27*, 820-830.

52. Wallace, J.M., 1967: "A note on the role of radiation in the biennial oscillation." J. Atmos. Sci., *24*, 598-599.

53. Berggren, R., and Labitzke, K., 1968: "The distribution of ozone on pressure surfaces." Tellus, *20*, 88-97.

54. Danielsen, E.F., 1968: "Stratospheric-tropospheric exchange based on radioactivity, ozone, and potential vorticity." J. Atmos. Sci., *25*, 501-518.

55. Newell, R.E., 1963: "Transfer through the tropopause and within the stratosphere." Quart J. Roy. Met. Soc., *89* 167-204.

56. Danielsen, E., Bleck, R., Shedlovsky, J., Wartburg, A., Haagenson, P., and Pollock, W., 1970: "Observed distribution of radioactivity, ozone, and potential vorticity associated with tropopause folding." J. Geophys. Res., *75*, 2353-2362.

57. Danielsen, E., and Bleck, R., 1970: "Tropospheric and stratospheric ducting of stationary mountain lee waves." J. Atmos. Sci., *27*, 758-772.

58. Kao, S.-K., and Gebhard, J.B., 1971: "An analysis of heat-momentum-transports and spectra for clear air turbulence in mid-stratosphere." Pure Appl. Geophys., *88*, 180-185.

59. Kao, S.-K., and Powell, D.C., 1969: "Large-scale dispersion of clusters of particles in the atmosphere: II. Stratosphere." J. Atmos. Sci., *26*, 734-740.

60. Murgatroyd, R.J., 1969: "Estimations from geostrophic trajectories of horizontal diffusivity in the mid-latitude troposphere and lower stratosphere." Quart. J. Roy. Met. Soc., *95*, 40-62.

61. Lindzen, R., and Goody, R., 1965: "Radiative and photochemical processes in mesospheric dynamics: Part I, models for radiative and photochemical processes." J. Atmos. Sci., *22*, 341-348.

62. Leovy, C., 1964: "Radiative equilibrium of the mesosphere." J. Atmos. Sci., *21*, 238-248.

63. Dickinson, R.E., 1968: "Vertical propagation of planetary Rossby waves through an atmosphere with Newtonian cooling." J. Geophys. Res., *74*, 929-938.

64. Dopplick, T.G., 1971: "The energetics of the lower stratosphere including radiative effects." Quart. J. Roy. Met. Soc., *97*, 209-237.

65. Paulin, G., 1969: "A simplified method of computing stratospheric heating rates and associated generation of available potential energy." Mon. Wea. Rev., *97*, 359-370.

66. Mateer, C., Heath, D.F., and Krueger, A.J., 1971: "Estimation of total ozone from satellite measurements of backscattered ultraviolet earth radiance." J. Atmos. Sci., *28*, 1307-1311.

67. Prabhakara, C., Salomonson, V.V., Conrath, B.J., Steranka, J., and Allison, L.J., 1971: "Nimbus 3 IRIS ozone measurements over southeast Asia and Africa during June and July 1969." J. Atmos. Sci., *28*, 828-831.

DISCUSSION

H. Johnston said that if the stratosphere is regarded as a box, and one integrates the rate of dissociation of O_2 over its volume, and integrates how much O_3 leaks out over its edges, the second number is at most 2% of the first. Dickinson replied that this production of 2% of the ozone might be responsible for maintaining 90% of the total ozone content. J. Lauermann asked whether Dickinson could elaborate on the physical mechanisms responsible for the different classes of motions and their interactions. Dickinson said the hydrodynamic mechanisms were too complex to go into, and to please take them on faith for the moment.

There was a question from the floor as to whether anything was known about the mesoscale effects of the chemical inhomogeneities which SST's would introduce into the stratosphere; would they give rise to vertical

motions because of differential heating and cooling, and how would they affect vertical and horizontal transport. Dickinson replied that present information was based on a few case studies, not enough to infer global behavior. He cited E. Danielson as having cases in which mesoscale motions seemed to significantly affect the jetstream, which is synoptic-scale, suggesting transport of momentum and heat. He noted that motions on this scale cannot be observed by conventional techniques; expensive platforms such as airplanes are needed.

S. Zimmerman asked about the effects of the small-scale structure observed in sounding data and chemical releases, particularly over the region shown in his ozone profile, on vertical and horizontal transport. He noted that these smaller-scale motions add up to a spectrum when averaged over the total altitude range that might make a considerable contribution. Dickinson responded that he felt the larger-scale (both time and space) motions were more important for transport, at least in the middle stratosphere, than Rossby-wave mesoscale motions, because they carried material over much larger areas. Zimmerman suggested that the mesoscale motions might act as viscous damping on the larger ones. Dickinson said that there were several open questions at present, such as the role of orographically-induced Rossby waves, and flow over surface topography transporting momentum up into the stratosphere, which might need to be taken into account in calculating zonal winds. Zimmerman then asked about the large fluctuations in wind and temperature observed in northern latitudes, particularly 60^{o} N, which were not apparent in Dickinson's representations of large-scale circulation. Dickinson explained that all but his last example were very much averaged-out; he felt it more important to concentrate on the mean structure and ignore the short-term fluctuations for the moment. R. Lindzen offered a clarification on the role of the mesoscale motion: that if it were parameterized, and an eddy coefficient made up, the resulting mixing link would require a bigger coefficient.

Because of the particular applicability of some very recent work done at the Max Planck-Institut, the following unscheduled paper was presented.

BEHAVIOR OF CO-MIXING RATIO NEAR THE TROPOPAUSE AND IN THE LOWER STRATOSPHERE

PETER WARNECK
Max Planck-Institüt für Chemic
Mainz, Germany

Repeatedly during this conference reference has been made to new data from our group at Mainz concerning the CO distribution in the vicinity of the tropopause and in the lower stratosphere. I therefore wish to take just a few minutes to present some slides showing the data that Dr. W. Seiler in our group has obtained.

Measurements were made on board a chartered Hawker Siddeley 125 twin-jet-engine plane; sampling of air was performed through the ventilation system, with outside air entering this system via the air intake in front of the engine and spending not more than 0.5 seconds in the compressor and air duct regions. CO mixing ratios were measured with the instrumentation developed by Dr. Seiler [1]. Ozone was measured, along with CO, with a Mast recorder, mainly to obtain an indication for the tropopause level. Temperature soundings from the nearest weather stations were also used to locate the tropopause level.

On each flight mission several ascents and descents were made, starting at altitude levels just below the tropopause and going up as high as the aircraft would allow (the ceiling was about 13 km). All flights were performed in Western Europe in the late winter of 1971. In addition, weather situations were selected for which the tropopause sank to a low level of about 9 km, corresponding to a trough over the British Isles.

Figure 1 shows our first data, obtained on January 21, 1971 about 9:00 pm. Three ascents and descents were flown; the data are lumped together. Note that as the ozone concentration (given in $\mu g/m^3$ at cabin pressure of

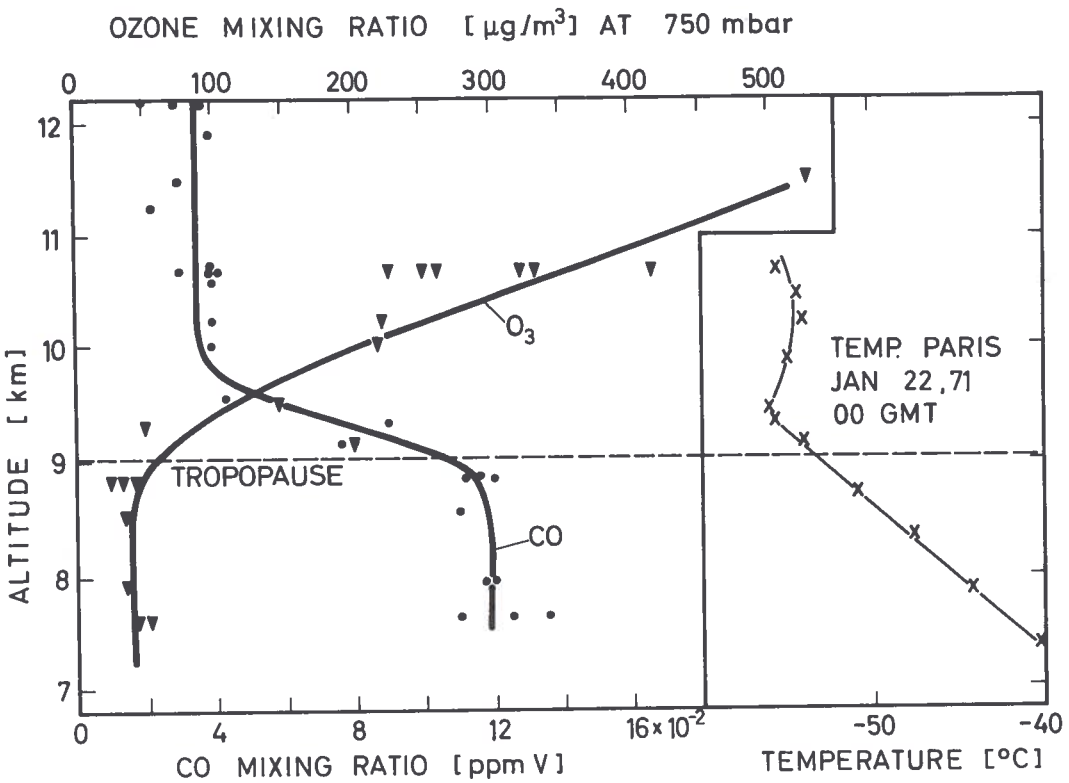

Figure 1. Summed data, West France, January 21/22, 1971

750 mb) rises, indicating that the stratosphere has been entered, the CO mixing ratio goes down, reaching a new constant level about a kilometer above the tropopause.

Figure 2 gives more data points with essentially similar results for a flight made on March 19, 1971, again in the late evening. All the data from four ascents and descents are presented. A third flight mission was performed on March 10, 1971 during the noon hours and again gave results similar to those presented above. Figure 3 shows only a single ascent and descent profile.

Inspection of the data reveals that on all three flights the same constant stratospheric CO mixing ratio is present, approximately 40 ppbv. The strong decline of CO concentration levels immediately above the tropopause makes it obvious that CO is consumed in the stratosphere, and we have previously argued that this consumption is due to OH radicals [2, 3]. Since the CO mixing ratio does not decrease indefinitely, however, but reaches a new constant level, it appears that there also exists in the stratosphere a source for CO. At the present time, having considered various possibilities, we believe that this CO results from the oxidation of methane, initiated by attack of OH radicals. The details of the arguments that led us to this conclusion will be available in a paper [4] submitted to the Journal of Geophysical Research.

REFERENCES

1. Seiler, W. and Junge, C., "Carbon monoxide in the atmosphere", J. Geo. Res. *75* (1970), 2217-2226.
2. Seiler, W. and Junge, C., "Decrease of carbon monoxide mixing ratio above polar tropopause", Tellus *21* (1969), 447-449.
3. Pressman, J. and Warneck, P., "The stratosphere as a chemical sink for carbon monoxide", J. Atm. Sci. *27* (1970), 155-163.
4. Seiler, W. and Warneck, P., "Decrease of CO-mixing ratio at the tropopause", to be published in J. Geo. Res.

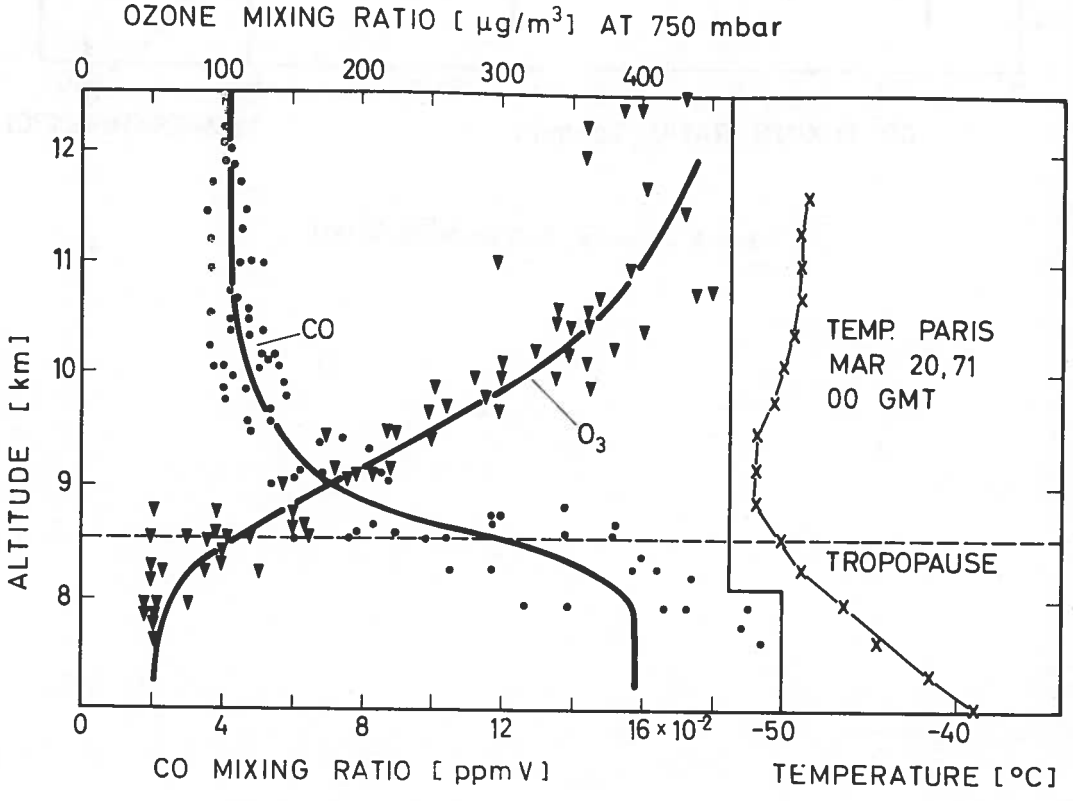

Figure 2. Summed data, West France, March 19, 1971

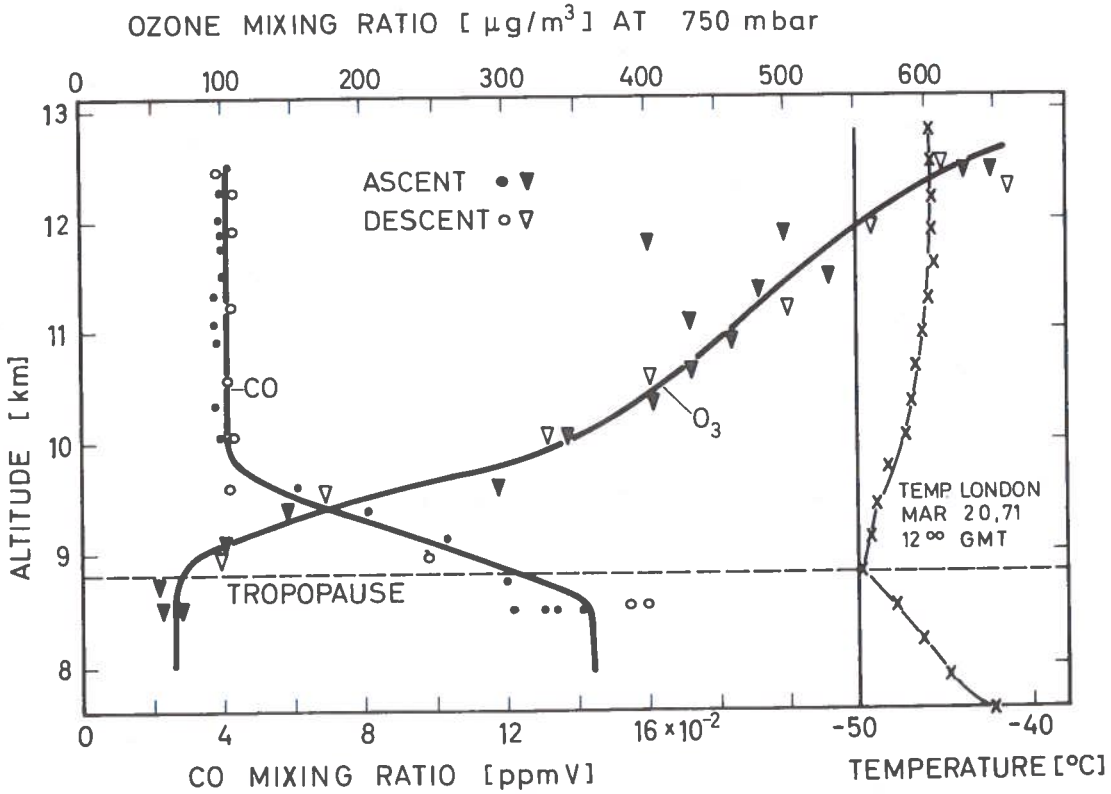

Figure 3. One ascent, North Sea, March 20, 1971

CLIMATOLOGY OF THE STRATOSPHERE FROM OBSERVATIONS

REGINALD E. NEWELL
Department of Meteorology, MIT
Cambridge, Massachusetts 02139

ABSTRACT: Some results from studies at MIT of the general circulation of the stratosphere and tropical atmosphere are briefly reviewed. The interaction between radiative effects and atmospheric motions in governing stratospheric temperature is discussed. The energy budget of the stratosphere and its relation to that of the troposphere is outlined. Some aspects of the global ozone budget are discussed and new values of the contribution of mean meridional motions are presented. The influence of volcanic eruptions on temperature and stratospheric ozone content are also discussed, with particular reference to the Mt. Agung eruption in March 1963.

INTRODUCTION

For the past twelve years we have performed diagnostic studies of the general circulation of the stratosphere, with the aim of understanding its momentum, energy, and mass budgets. Initially, data from the IGY-IGC were used and vertical motion was computed from the adiabatic approximation. It was found that the lower stratosphere at middle and high latitudes receives its energy from the troposphere. The studies were extended to 60 km using the Meteorological Rocket Network data (though without vertical motion computations); even at these heights there is a large response to energy transmitted upwards through 30 km. Spring maxima in surface fallout, stratospheric ozone concentrations, and sudden warming in the lower stratosphere were found to be related to variations in the vertical energy flux. A numerical model was developed by Peng (1965) which reproduced the temperature increase with latitude in the lower stratosphere.

Next we developed a series of programs to compute radiative heating and applied them to compute vertical motion from temperature and geopotential data for the International Quiet Sun Year in the 200 - 10 mb layer. We found a very large variability in the vertical energy flux into the stratosphere, associated closely with the spring maximum in ozone. The energy is ultimately lost by differential radiative cooling around latitude circles; we call this radiative destruction of eddy available potential energy.

The close association between stratospheric and tropospheric events led us to suggest that the biennial oscillation in the stratosphere was similarly forced from below, and in 1963 we expanded our studies to include the general circulation of the tropics at all levels. The first stage of this study has been completed and is being published by the MIT Press as a two-volume monograph.

A host of items relevant to tropospheric-stratospheric interactions have become evident from these studies. Temperature in the tropical lower stratosphere varies with an annual cycle which is apparently due to a modulation in the Hadley cell strength; this modulation in turn occurs because middle-latitude baroclinic eddies reach their overall (global) maximum in January. In July, heating over land in the northern hemisphere diminishes the meridional temperature gradient, hence the baroclinic eddy activity there, and consequently the total eddy activity. This differs from the situation in the southern hemisphere, where the oceanic temperature variation with latitude holds the atmospheric temperature gradient high throughout the year. Thus, if we consider the Hadley cell as driven by middle-latitude eddies of both hemispheres, then the peak forcing occurs in January.

There is a further biennial modulation of the temperature in the tropical lower stratosphere which is associated with a biennial modulation of the tropospheric baroclinic eddy activity. Decreased energy flux into the middle-latitude lower stratosphere and decreased eddy activity there accompany the maximum tropospheric eddy activity. Stratospheric ozone at both low and middle latitudes is modulated by this circulation oscillation.

A further modulation of temperature and ozone in the lower stratosphere occurs due to the presence of volcanic aerosols, and consequent heating effects. The biennial oscillation is temporarily interrupted, dilution of the ozone formation region at low latitudes seems to decrease, and ozone content therefore increases. Noctilucent clouds also increase, indicating that more tropospheric water vapor is admitted into the stratosphere, with a weaker mean circulation and higher temperatures near the tropical tropopause. The tropospheric circulation itself may be changed by a feedback from these changes in the stratosphere; the validity of this hypothesis is presently unknown, however, as is the time mode of the possible changes. Oceanic influences are again obviously of importance here.

This tutorial discussion will take up three points: factors involved in the modulation of temperature, the stratospheric energy budget, and the ozone budget, with particular reference to the role of observed circulations.

MODULATION OF STRATOSPHERIC TEMPERATURE

The first question is: What are the factors which govern the temperature at any point in the atmosphere?

Figure 1 shows an example of the temperature variation obtained from the zonal mean observations. The observations are of monthly mean temperature for tropical stations between 5° and 15° north, for the 50 mb (about 21 km) level; this graph simply traces the temperature variation as a function of time. We ask what it is that governs this temperature variation.

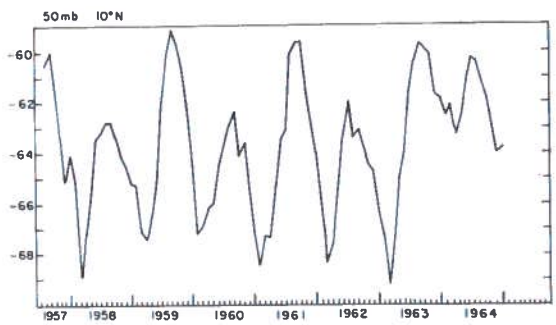

Figure 1. Monthly mean temperature $\overline{[T]}$ (°C). (Newell et al., 1969)

The figure shows three features. First of all, there is an obvious recurring annual variation with a minimum temperature in February and a maximum temperature towards the end of August. The same phase holds at about 10° south; the effect is not hemispheric but global.

Second, we see that the summer temperatures peak at different values in alternate years; warmer values were reached towards the end of odd-numbered years. R.E. Dickinson discussed this biennial oscillation earlier at this conference.

The third feature is that towards the end of the data sample the regular biennial cycle was broken.

The equation below governs the factors that go into determining local change of the mean zonal temperatures at a given point in the atmosphere.

$$\frac{\partial}{\partial t}[T] = [Q_{rad}] + [Q_{LH}] + [Q_{BLH}] + [Q_F] + [Q_{cond}] + \Gamma\omega - \frac{[v]}{a}\frac{\partial [T]}{\partial \phi} - \frac{1}{a\cos\phi}\frac{\partial}{\partial \phi}[\bar{v}^*\bar{T}^* + \overline{v'T'}]\cos\phi - \frac{\partial}{\partial p}[\bar{\omega}^*\bar{T}^* + \overline{\omega'T'}] + \frac{R}{c_p p}[\bar{\omega}^*\bar{T}^* + \overline{\omega'T'}]$$

where $$\Gamma = \frac{R}{c_p}\frac{[T]}{p} - \frac{\partial [T]}{\partial_p}$$

The governing factors are: radiative factors Q_{rad}, those involving CO_2, H_2O, ozone, and aerosols; latent heat liberation; boundary-layer heating, which is the conduction of sensible heat from the bottom boundary (not a direct influence in the stratosphere); frictional heating, which occurs if there is internal energy dissipation (this is a small factor. in the total heating compared to the radiative effects); heat conduction down the temperature gradient; and the adiabatic effect (perhaps best described as the bicycle-pump effect: if air is pressed down, it contracts and gets warmer; if it is pushed up, it expands adiabatically and cools off). The magnitude of the heating or cooling is obtained from the mean pressure change (here in millibars per second) multiplied by the stability factor, which is about 2° per millibar at 30 millibars, for example. So we can calculate rates of

individual pressure change which we can translate into vertical motion, or we can translate them into temperature change at a point.

The next term represents advection of the heat in the horizontal direction, and is simply the temperature gradient times the mean north-south velocity, for which I am using v. The next term is the sensible heat convergence due to a change with latitude in the transfer of heat by the large-scale motions. If more sensible heat is transferred across 30° than across 40°, there is convergence in between, which gives a net heating rate.

The last two terms involve the vertical motion; the first is convergence of the vertical eddy flux, which is analogous to its counterpart for the horizontal eddy flux, and the second is more or less analogous to $\Gamma\,\bar{\omega}$. These two terms are very difficult to determine; fortunately, they usually turn out to be somewhat smaller than the other terms.

Figure 2 shows the terms we can measure as a function of latitude at 50 millibars for December-February. The various terms in the equation were determined from actual data using vertical motion computations on a daily basis, and then averaging them together. The vertical motion was computed using radiation, horizontal advection, and local temperature change. At high latitudes there is a convergence of the eddy flux of heat which contributes to heating. More sensible heat comes across 50° north and then goes across 70° north, so there is a tendency for the temperature to increase. Advection by the mean motion is not very important there. The heavy solid curve is the residual after we add the known terms. Its existence means there are some other factors which we haven't caught completely (as the local temperature change observed is small), which is not surprising. The dashed curve is the radiative effect computed from the zonal mean radiation; the radiation varies with longitude as well as the vertical motion and the temperature, of course, as will be seen later.

The thin solid curve is the effect of the vertical motion which produces cooling at high latitudes and heating at middle latitudes. This is the meridional overturning which has already been discussed. At low latitudes, this effect also contributes to cooling, and at this height there is an offsetting between radiative heating and cooling due to the vertical motion. Our *Nature* paper (Newell et al., 1969) showed that we could balance these two

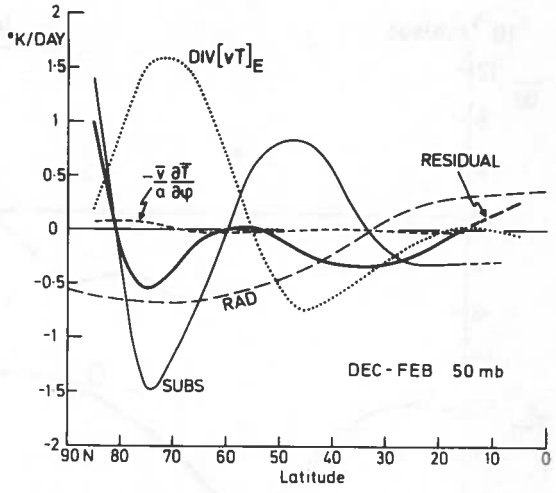

Figure 2. Heat budget components (°K/day). (Newell et al., in press)

terms at the tropical tropopause and so derive a value for the mean vertical motion.

The key question is, how are the changes observed in Figure 1 produced? Since radiation does not have the right annual variation, vertical motion must, and therefore one modulates the Hadley cell penetration into the lower stratosphere. As noted in the summary, one can argue that the modulation of the Hadley cell itself is forced by the middle latitude eddies, as discussed previously by Dickinson.

The regular changes on Figure 1 are probably the effect of this vertical motion modulation. The recent change in the pattern is a combination of the radiative effect through aerosols and the vertical motion effect, as will be seen later.

Figure 3 shows the variation with longitude of the vertical motion and the temperature, at 70°N in January 1964. Again this is an actual-derived vertical motion, computed from 30 individual daily maps and then averaged on an individual grid-point basis for 30 days. What we see here is one way of expressing the vertical motion, the rates of change of pressure on an air parcel as it goes up and down. The peak sinking motion is about 2 centimeters per second.

Imagine that an air parcel is streaming from west to east through this pattern; what is happening is that in the left-hand side of the pattern it is rising, moving towards lower pressure and therefore cooling adiabatically, so the temperature goes from -50° over Alaska down to -80° or so over Iceland. This is the region in which one can expect to see mother-of-pearl clouds, over Iceland in the

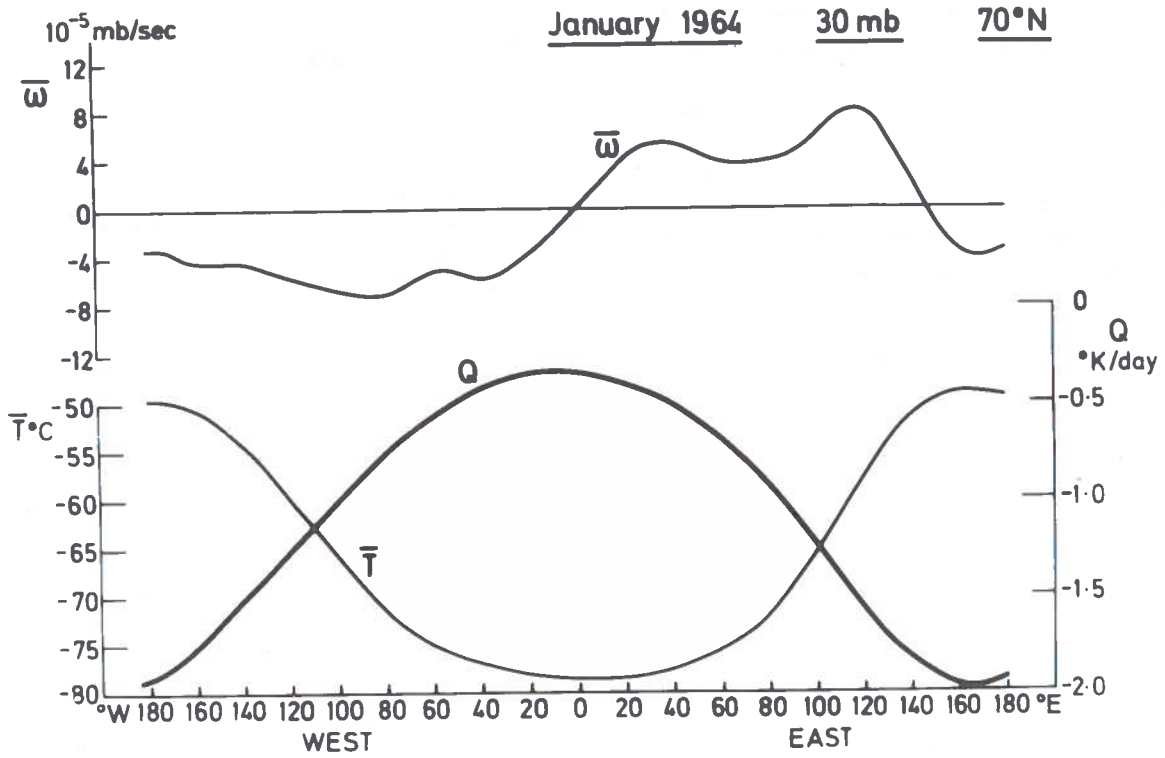

Figure 3. The longitudinal distribution of the vertical motion ω, the net radiative heating rate Q, and temperature. (Newell et al., in press)

winter, where a boost on the vertical velocity is provided, we think, by the mountains of Norway. Here is where additional clouds would appear if additional water vapor were present, for the air is already close to saturation.

What is happening, then, is that when the air parcel reaches somewhere about Iceland in the trajectory, the temperature is at a minimum; from then on it starts descending into the hole over Russia in the pressure field which is on top of the high below. The parcel slides down, and there is adiabatic heating on the right-hand side of the pattern, so the temperature gradually begins to increase again.

At the same time that this is going on, the radiative effect on the parcel is given by the "Q" curve. This is calculated as before along 70°N. We see that the largest radiative cooling occurs when the parcel is warmest, as you might expect, and the smallest when it is coldest, also as you might expect. There is a difference in the radiative cooling of more than 1.5° C/day. With a stability factor of about 2°C per millibar and a rising motion corresponding to 5 x 10^{-5} mb sec^{-1} the adiabatic cooling is about 10°C per day; this is larger than the radiative effect, of course, and shows the importance of vertical motions. (This example is very simplified; the variations with latitude are ignored.)

Figures 4 through 8 are examples of components of the radiative heating rates. Figure 4 shows heating due to ozone absorption of solar radiation. (Since we don't have good measurements of the vertical distribution of ozone in the Southern Hemisphere, we have used known total amounts in the Southern Hemisphere and the observed Northern-Hemisphere vertical distribution corresponding to the same total amounts.) Figure 5 shows the heating rate due to the 9.6 μ band of ozone, Figure 6 that due to the 15 μ band of CO_2, and Figure 7 that for all wavelengths absorbed by H_2O. Figure 8 is the total for all trace substances.

The point here is that from radiative effects alone in the tropical lower stratosphere, one would have net radiative heating when adding up the contribution from all of the constituents;

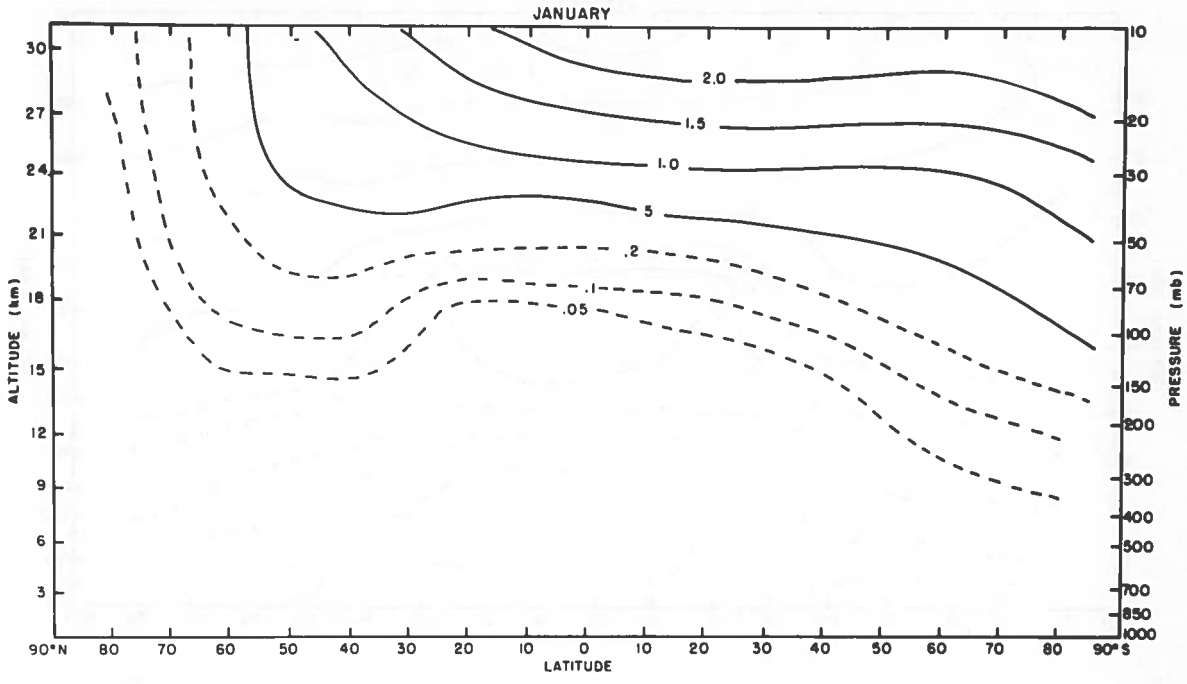

Figure 4. Radiative heating rate due to absorption of solar radiation by O_3 (°C/day). (Newell et al., in press)

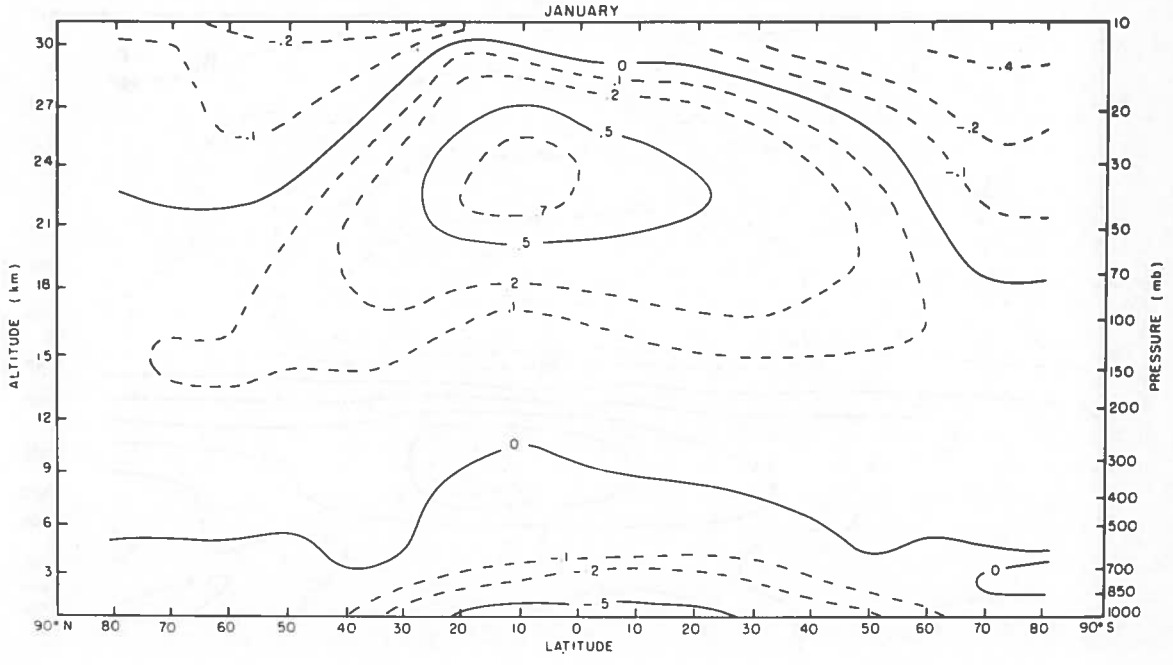

Figure 5. Radiative heating rate associated with IR bands of O_3 (°C/day). (Newell et al., in press)

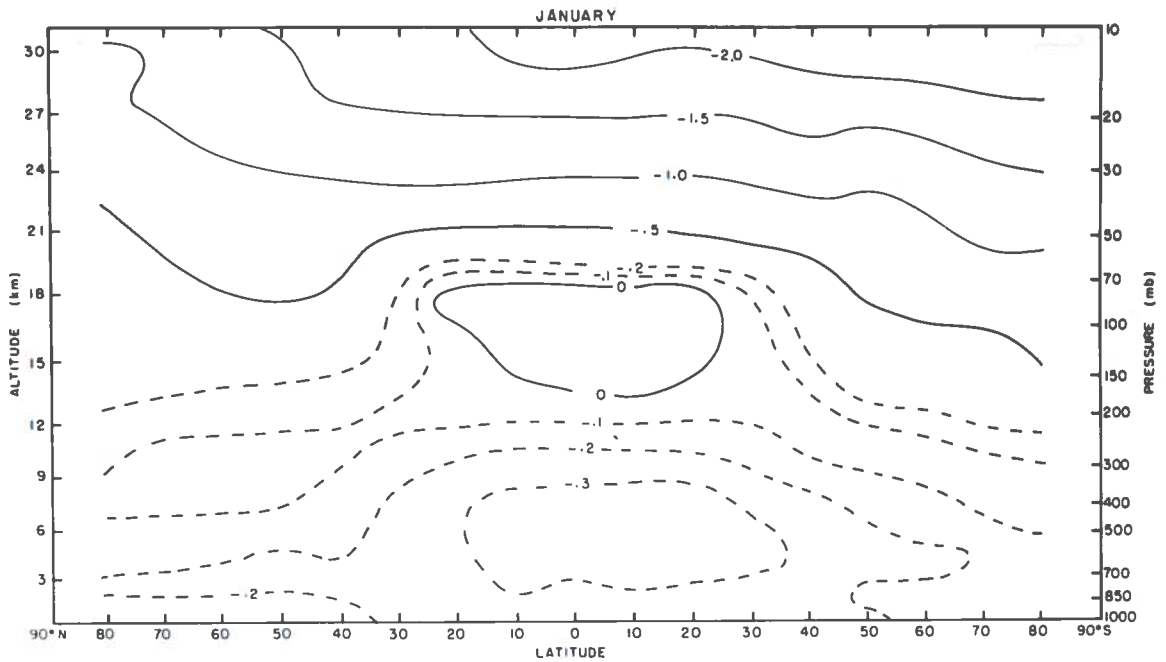

Figure 6. Radiative heating rate associated with IR bands of CO_2 (°C/day). (Newell et al., in press)

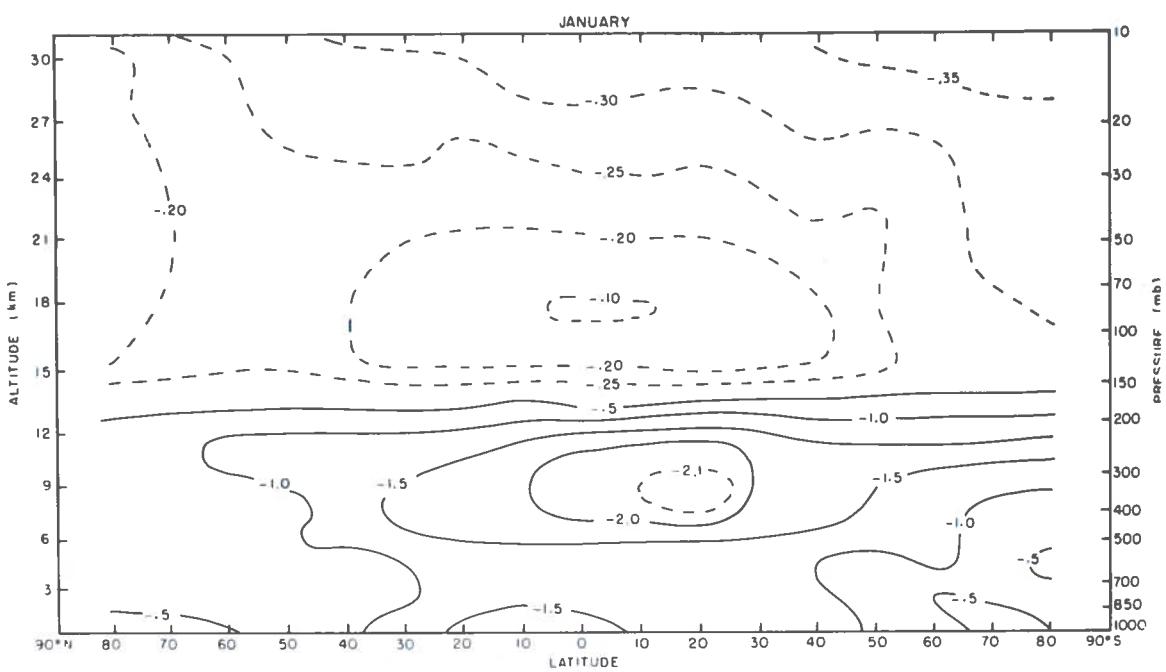

Figure 7. Radiative heating rate associated with IR bands of H_2O (°C/day). (Newell et al., in press)

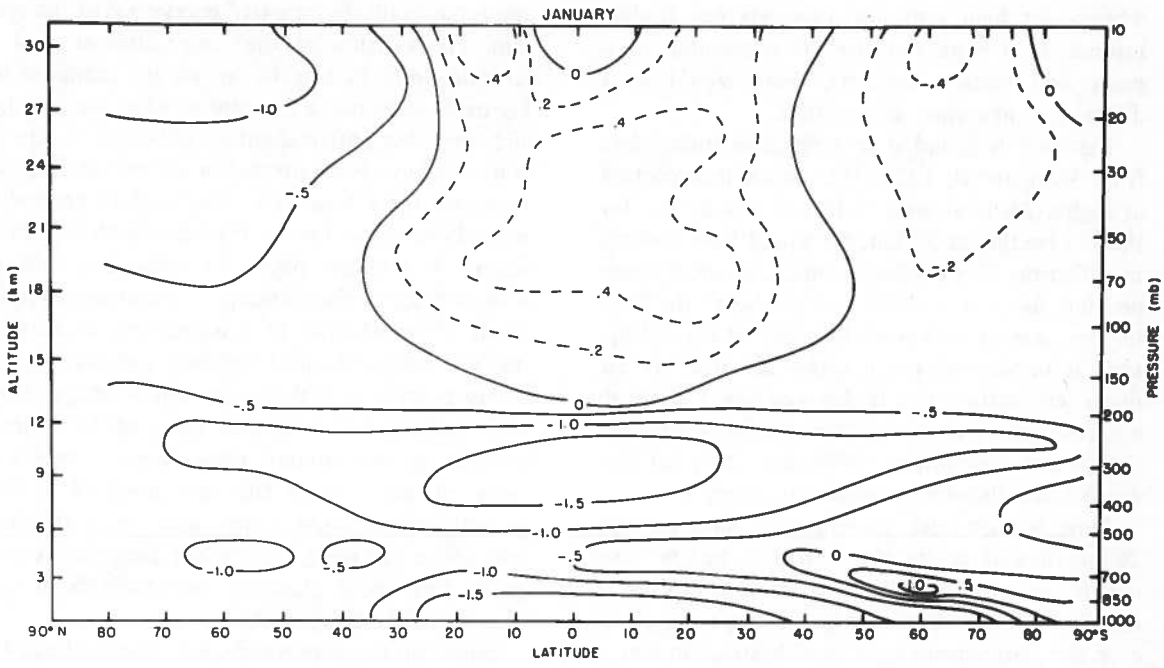

Figure 8. Total radiative heating (°C/day). (Newell et al., in press)

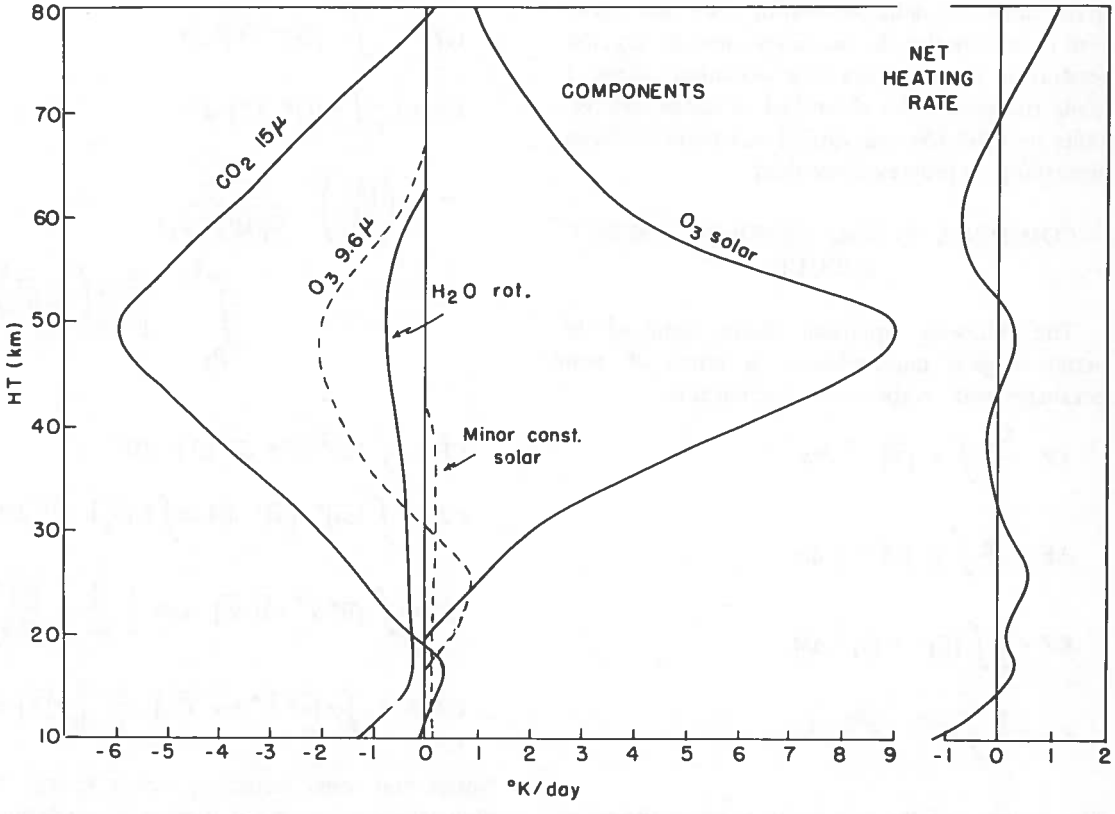

Figure 9. Vertical distribution of the components of the net radiative heating rate. (Newell and Gray, 1972)

whereas at high latitudes, one gets net cooling instead. If it were not for the horizontal transports and vertical motions, there would be a different temperature distribution.

Figure 9 is included to emphasize (using data from Murgatroyd, 1958) that ozone is important at higher levels as well; in fact, if it were not for the O_3 heating at 50 km, we would have nothing to offset the CO_2 cooling. Lindemann and Dobson pointed this out in 1921 and predicted the peak temperature at 50 km on the basis of O_3 absorption; it turned out to be within about 2° of the mean temperature that is observed now – quite an achievement. (There was a period in between when theory and observations differed by 20°, but that was because the observations were wrong.)

Now we are back to where we have perhaps 20 profiles of ozone above 30 km, but nothing else to go on to calculate the radiative heating in the 30 - 80 km layer except assumptions; however, the photochemistry is "well known" in that it will predict ozone up in these regions over the globe at all times. Earlier discussions at this conference have cast doubt on the reliability of these predictions for radiative heating rates and therefore for computing the necessary input to, say, the generation of zonal available potential energy. I made the same point about lack of ozone observations in 1963 (Newell 1963a) and there has been essentially no progress since then.

COMMENTS ON STRATOSPHERIC ENERGY BUDGET

The following equations define some of the meteorological nomenclature in terms of temperatures and temperature distribution.

$$AZ = \frac{C_p}{2} \int \gamma \, [\bar{T}]''^{\,2} \, dM$$

$$AE = \frac{C_p}{2} \int \gamma \, [\bar{T}^{*2}] \, dM$$

$$KZ = \frac{1}{2} \int [\bar{u}]^2 + [\bar{v}]^2 \, dM$$

$$KE = \frac{1}{2} \int [\bar{u}^{*2} + \bar{v}^{*2}] \, dM$$

The variance of the temperature across the meridional cross-section (term 1) gives one a measure of the zonal available potential energy AZ of the system. The variance of the temperature around a latitude circle, such as the one we just examined in Figure 3, gives one a measure of what we call the eddy available potential energy AE (term 2). These concepts have been present in the meteorological literature for a long time; they evolved gradually until 1955 when Lorenz crystallized them into a theory in a classic paper for *Tellus* and told us how to describe the workings of the atmosphere in terms of variabilities of temperature, wind, momentum transports, heat transports, and so on.

My point here is that variations of temperature with latitude and longitude must be taken into account in determining these terms. These are some of the factors that are involved in the general circulation, and one must be careful not only about changing the absolute temperature at a point, but about changing the gradients or the variance of the temperature.

Some of the conversions just discussed can be shown formally as

$$GZ = \int [\bar{Q}] \, [\bar{N}] \, dM$$

$$GZ = C_p \int \gamma \, [\bar{Q}]'' \, [\bar{T}]'' dM$$

$$GE = C_p \int \gamma \, [\bar{Q}^* \, \bar{T}^*] \, dM$$

$$\gamma = -\left(\frac{[\bar{\theta}]}{[\bar{T}]}\right)^2 \frac{R_d}{C_p (p_2 - p_1)} \int_{p_1}^{p_2} \frac{[\bar{T}]}{[\bar{\theta}]} \frac{1}{p} \left(\frac{d}{dp} [\tilde{\bar{\theta}}]\right)^{-1} dp$$

$$CE = -\int [\bar{\omega}^* \, \bar{a}^* + \overline{\omega' a'}] \, dM$$

$$CZ = -\int [\bar{\omega}]'' \, [\bar{a}]'' \, dM \simeq \int f \, [\bar{u}_g] \, [\bar{v}] \, dM$$

$$CK = -\int [\bar{u}^* \bar{v}^* + \overline{u' v'}] \cos\phi \, \frac{1}{a} \frac{d}{d\phi} \left(\frac{[\bar{u}]}{\cos\phi}\right) dM$$

$$CA = -c_p \int \gamma \, [\bar{v}^* \bar{T}^* + \overline{v' T'}] \, \frac{1}{a} \frac{d}{d\phi} [\bar{T}] \, dM$$

Notice that zonal available potential energy in the atmosphere is created if there is a correlation between Q and T. Q is the net radiative heating in

the stratosphere; T is the temperature. The primes represent perturbations from the average. From the previous papers the reader probably noted that the temperature increased with latitude. I have just shown in Figure 8 that the radiative heating rate decreases with latitude, so GZ is negative for the stratosphere. There is a bleeding off of the energy in the temperature field. It is always trying to smooth itself out by radiative processes. One has to keep boosting AZ and AE, thus maintaining the temperature gradients, by actual motions which derive their energy from below, from the upper troposphere. A more comprehensive discussion of these equations, together with current values of the conversions for the globe, can be found in our recent summary (Newell et al., 1970).

Table 1 shows the energy contents at various altitudes in summer.

Table 1. Summer Energy Contents by Altitude

Layer	GZ	AZ	KZ
km	ergs cm^{-2} sec^{-1}	10^5 ergs cm^{-2}	10^5 ergs cm^{-2}
77.5-67.5	-0.20	0.4	4.7
67.5-57.5	0.06	0.5	20.9
57.5-47.5	0.31	0.4	38
47.5-37.5	0.50	4.8	65
37.5-27.5	0.36	8.4	87
27.5-17.5	-24	393	256
17.5-7.5	-73.6	2993	1352
7.5-2.5	534	7338	637

Figure 10 shows the factors that maintained the zonal available potential energy field and the zonal kinetic energy during 1964. They may not be quite the same in 1965. It seems that AZ was maintained in 1964 by what we call CZ, which is conversion from kinetic to potential energy by mean meridional overturning. KZ is about eight times greater than AZ in late January and February, 1964. This is the opposite of the situation in the troposphere, where the energy in the temperature field, the available potential energy, is greater by a factor of 100 or 200 than the energy in the kinetic energy field. (As was implied by R.E. Dickinson in the paper preceding this one, it is easier to force a temperature change by motions than vice versa in the stratosphere.) AZ was maintained by KZ, except in the month of March 1964 when there was a big ozone boost; what happened then was that eddies moved heat against the mean temperature gradients. The heat flux is up the temperature gradient (CA positive in

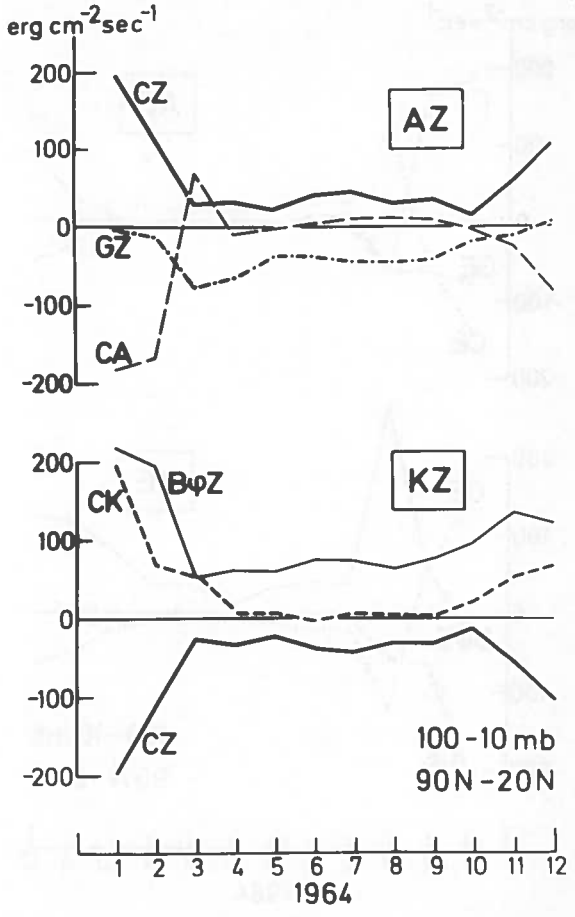

Figure 10. Processes which maintain the zonal available potential energy and the zonal kinetic energy. (See text for definitions.) (Tabulated by Dopplick, 1971)

Figure 10) instead of down the temperature gradient. Therefore the motion obtains its energy from below. That happened in March 1964; the term CA outweighed the meridional overturning CZ. Throughout the period the system lost energy through GZ, which represents radiative losses. The system was radiating away more energy at high middle latitudes in the warm regions than it was gaining at the lower (cold) latitudes. $[\overline{Q}]''$ $[\overline{T}]''$ was negative. BϕZ is the boundary work, which was very uncertain here.

Figure 11 shows the factors maintaining the eddy available potential energy and the eddy kinetic energy. A big source of the energy was the boundary flux on the kinetic energy term. Some of that energy went through the system. Warm air sank and cold air rose, the opposite of what happens in the troposphere in this month,

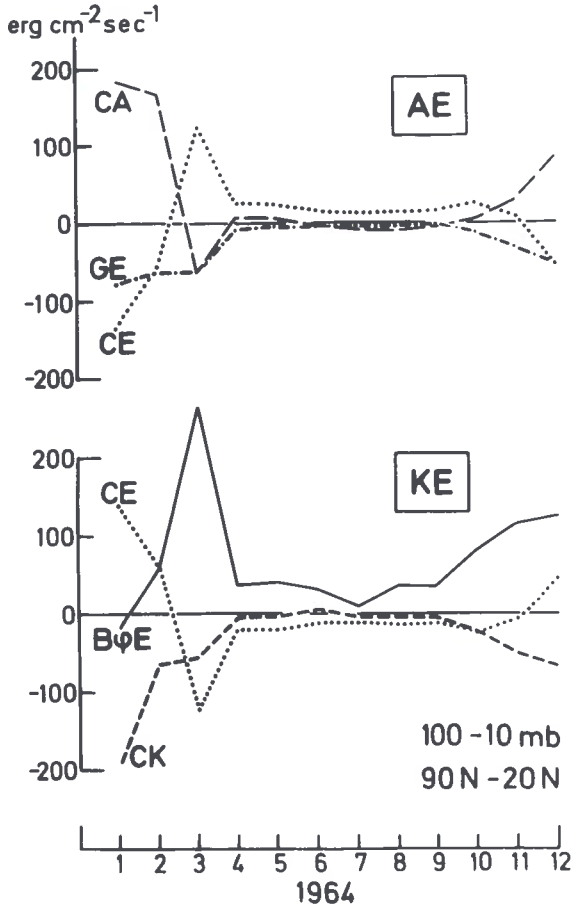

Figure 11. Processes which maintain the eddy available potential energy and the eddy kinetic energy. (See text for definitions.) (Tabulated by Dopplick, 1971)

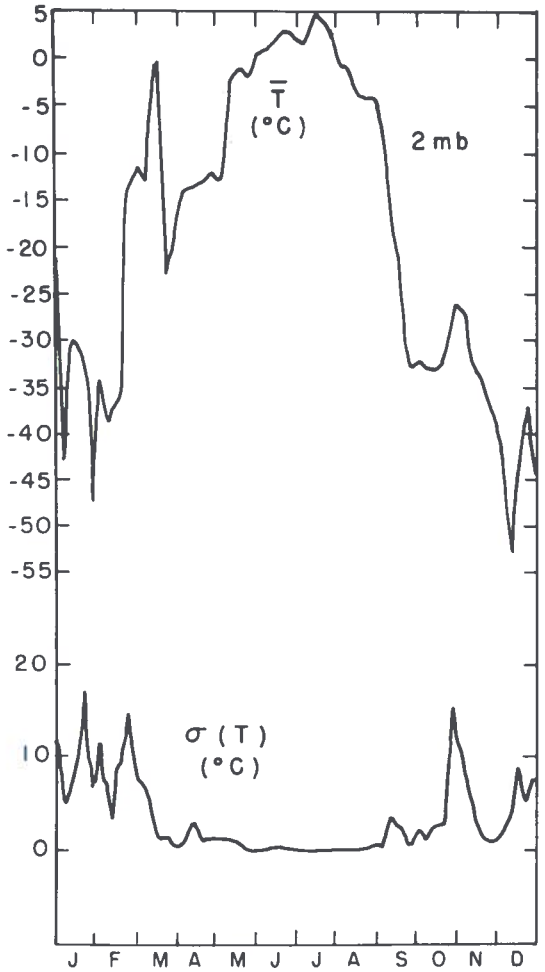

Figure 12. The variation of temperature and a measure of the spatial standard deviation of temperature at 2 mb before 1964.

and eddy potential energy was created from kinetic energy. This was in turn fed through the system to zonal available potential energy, and accounted for the observed increase in the mean zonal temperature gradient. This is the sort of mechanics that operates in the sudden warming; it is quite different from the situation in the summer. The layer considered here is 100 - 10 mb; it is possible to subdivide further and locate the levels at which those conversions occur. It is important, I think, to watch out for possible changes in the temperature gradients as well as for absolute temperature changes. Figure 12 shows temperature variation taken from once-weekly ESSA maps for 1964 for the 2-mb level. In March, corresponding to the energy boost in the 100 - 10mb layer, the temperature was higher at 2 millibars, which was actually due to energy leaking from the troposphere up through the lower and middle stratosphere into the upper stratosphere. It produced that temperature change by forcing some northward-moving parcels to descend. This is the sort of mechanism discussed earlier (Newell, 1961, 1964).

COMMENTS ON OZONE BUDGET

Figure 13 is a meridional cross-section of ozone concentration. Oblique motions or meridional motions can obviously carry ozone down its mixing-ratio gradient, and can increase the ozone at a given point. What seems to happen in the middle latitudes is that air parcels move backward and forward in the planetary waves. The situation is rather like shuffling a pack of cards. The ozone

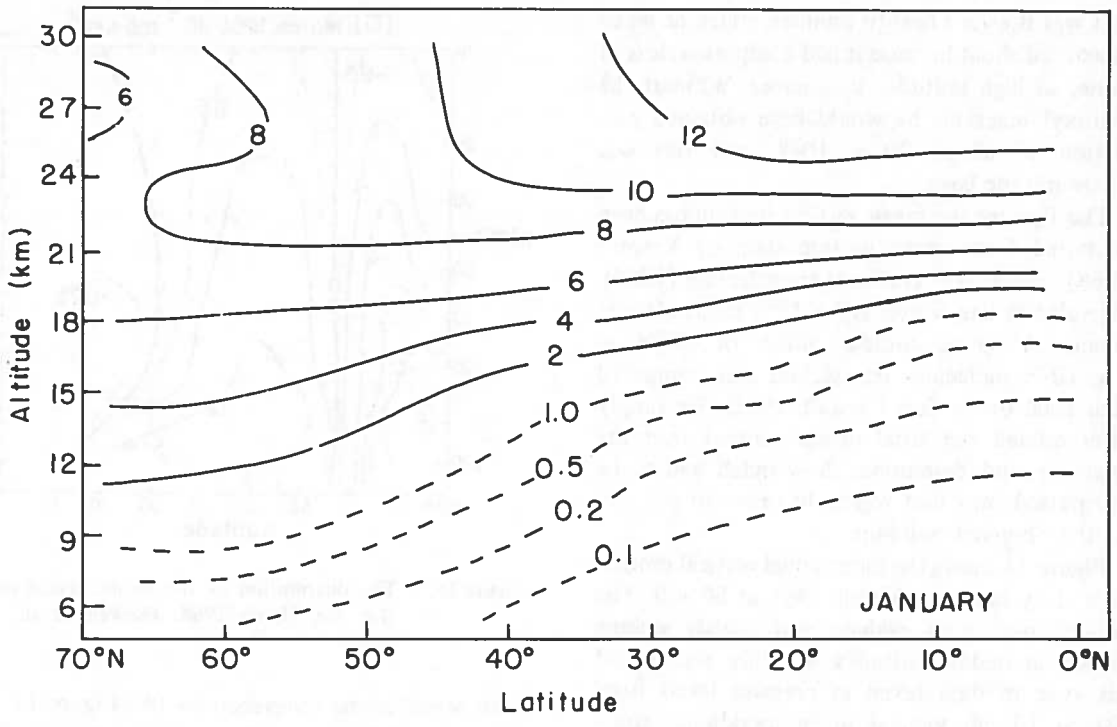

Figure 13. Distribution of ozone (μg/g). (After Hering and Borden)

gradually moves down to the bottom of the "deck" and finally drops out into the troposphere with the exchange mechanism that R.E. Dickinson illustrated from the work of Danielsen. Radiation is continuously contributing to the cooling. On top of that we have this back-and-forth movement of the parcels. The planetary waves carry trace substances backwards and forwards. There is a general transfer downwards, so more ozone can be built up in the middle and high latitudes below the photochemical zone. Ozone is also brought down by the mean meridional circulation. Photochemistry alone predicts very little ozone in this region, since the residence time for air parcels there is much less than the time required to produce a significant quantity of ozone. Thus, it is the motion that is important in this problem. The equation for the rate of change of local ozone concentration is analogous to that discussed earlier for temperature:

$$\frac{\partial \overline{O_3}}{\partial t} = q - \frac{\partial}{\partial y}(\overline{O'_3 v'}) - \overline{v}\frac{\partial \overline{O_3}}{\partial y} - \overline{w}\frac{\partial \overline{O_3}}{\partial z} - \frac{\partial}{\partial z}(\overline{O'_3 w'})$$

Ozone changes depend on: the production factor q by the photochemistry; convergence of the horizontal eddy fluxes; advection by mean motions, both north-south and up and down; and a convergence or divergence of vertical eddy flux. If we include all scales of motion with flux terms, extra K's are not needed. We can dress this equation up in different ways as well. Many years ago we looked at the horizontal eddy flux term very crudely. W. Hering looked at it in a more sophisticated fashion from the much better data which he had from his network (Hering, 1966). We correlated the total ozone in the column with the north-south wind in the stratosphere, the reasoning being that the total ozone in the column was highly correlated with the ozone in the lower stratosphere. Mateer and Godson (1960) found this correlation to be about 0.95. Thus we can use the total ozone, for which there is a lot of data, together with the meridional wind in the stratosphere, and from these quantities compute the ozone flux in the lower stratosphere.

The flux $(\overline{O'_3 v'})$ through 50° north in the spring is about 3×10^{29} molecules per second. Brewer and Wilson quote a production rate for the globe of about 8×10^{29} molecules per second – though that may be out of date as of this conference because it included the hydroxyl reactions.

That was Brewer's best-fit number, which he was a bit worried about because it had dissipation, loss of ozone, at high latitudes in summer. Without the hydroxyl reactions he would have obtained production of about 20 x 10^{29}, and this was apparently too large.

The flux by the mean vertical motion has been computed from mean motion data by Vincent (1968), and ozone gradients from Hering (1966). The value in late winter is 3 x 10^{29} molecules per second. A spring buildup north of 50°N of 2 x 10^{29} molecules per second was computed from total ozone data (Newell, 1961). We simply differentiated the total ozone content over the polar cap and determined how much had to be transported into that region in order to account for the observed build-up.

Figure 14 shows the mean zonal vertical motion on a daily basis for March 1964 at 50 mb. The two-cell pattern is evident, with steady sinking motion in middle latitudes. Monthly averages of this type of data taken at pressure levels from 200 to 10 mb yielded mean meridional cross-sections like Figure 15. These can then be matched

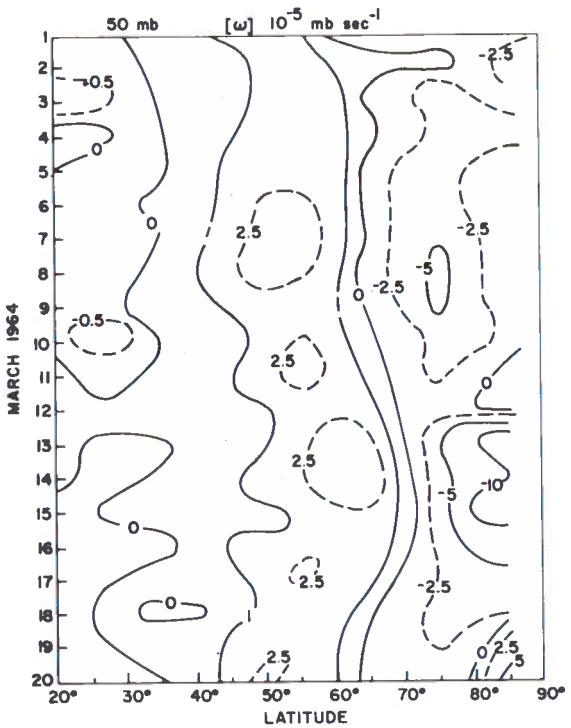

Figure 14. Mean zonal vertical velocity (in pressure coordinates) for March 1964. (Newell et al., in press)

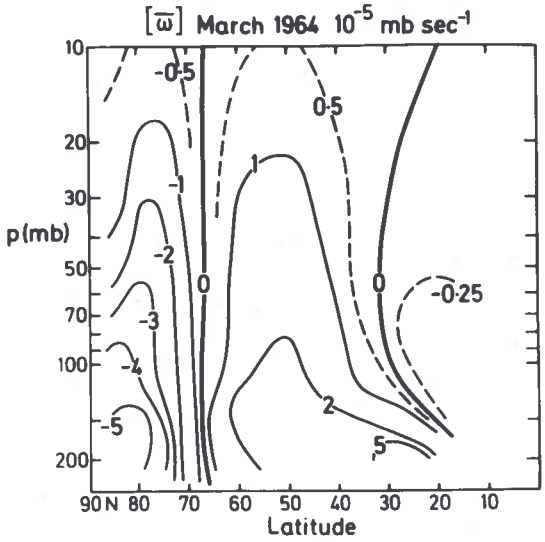

Figure 15. The distribution of the mean vertical motion for March 1964. (Newell et al., in press)

with mean ozone cross-sections like Figure 13 to get the contribution to the local rate of change by advection by the mean vertical motion. Such values appear in the upper part of Figure 16. Evidently this term contributes an increase in local ozone in middle latitudes and a decrease at low and high latitudes.

On the lower half of Figure 16 is the production rate of ozone computed by Brewer and Wilson (1968), with hydroxyl reactions included. At 10 mb at the equator about 4 x 10^5 molecules of ozone cm^{-3} sec^{-1} are being made. Ozone is thus made at the higher levels at low latitudes and is transported poleward and downward, not only by the mean motion shown here but also by eddy motion.

The other terms can also be estimated. For example, $\bar{v}\partial O_3/\partial y$ can be computed. This term contributes a local decrease at low latitudes and an increase at middle latitudes. Again, this pattern arises simply from orientation of the mixing ratio lines and the mean meridional motion pattern. The term $\partial(O_3'v')/\partial y$, the convergence of the flux by horizontal eddies, contributes to depletion of ozone in the 20 - 40°N region and to an increase of ozone in the 60 - 80°N region.

Since there are only about 25 northern-hemisphere stations to base these statistics on, we can't take this approach and produce a full two-dimensional picture even though we have a lot of

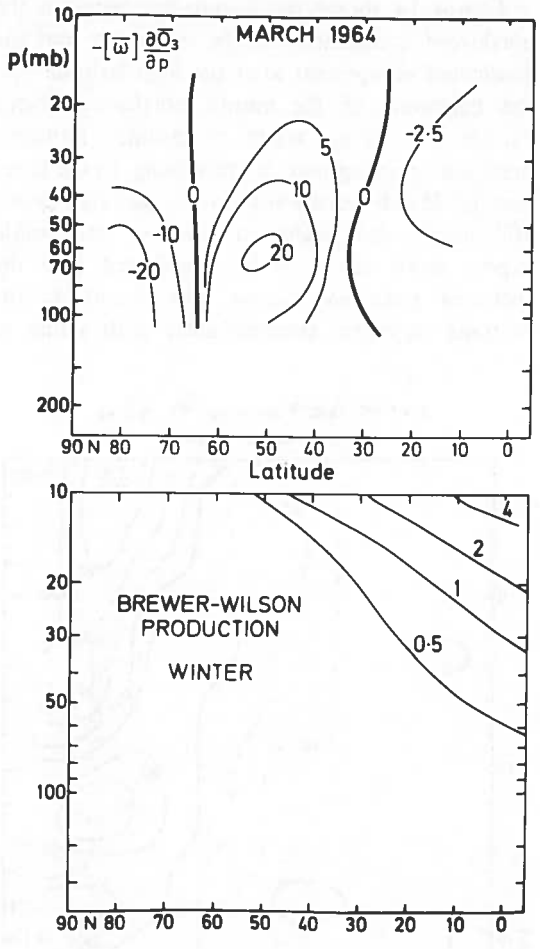

Figure 16. Components of ozone budget (10^5 mols cm^{-3} sec^{-1}). (Newell et al., in press)

observations of total ozone. If we assume the action is confined to a layer about 5 km deep, values are about 5 x 10^5 molecules cm^{-3} sec^{-1} in both of these regions, 5 to 10; these values are comparable to those already discussed.

We also looked at the vertical eddy flux a few years ago, but did not succeed in producing meaningful results. In fact, it is almost impossible to evaluate this term with the present observational network.

Table 2 shows the average of 14,000 observations on the covariance; the final covariance is positive, corresponding to a polewards transport. There is an increase in covariance, or northward flux of ozone, with latitude. Since there are so many observations to go into the value, the results cannot be statistical error. There is a convergence at high latitudes and a divergence at low latitudes caused by the eddies, in addition to all of the other items.

What causes the spring maximum in ozone? We decided at the 1961 AEC meeting from the preliminary observations that there was additional eddy mixing in the lower stratosphere which carried ozone down its mixing ratio gradient in the spring. We attributed it to the fact that additional energy is transferred up into the lower stratosphere from the troposphere in the spring. In turn, the additional energy transfer appears to be due to "blocking", the changes in the cyclone/anti-cyclone configuration in the troposphere. There seems to be a reasonable case for arguing that changes in the ozone in the stratosphere are triggered by changes in the tropospheric circulation, both in the middle latitudes by eddies and at the lower latitudes by the direct circulation through the influx of air into the lower stratosphere from the troposphere. Even the mean indirect circulations in the stratosphere, such as those of Figure 15, are linked to the eddy motions.

Is there evidence of variability in the meridional motions? Figure 17 is the standard deviation of the north-south component of the motion, shown on

Table 2. Average Covariances (cm of O_3 at STP x cm sec^{-1}). (Newell, 1964a)

Latitude	Winter Oct 1957 - March 1958 Oct 1958 - March 1959	Summer Apr 1958 - Sept 1958 Apr 1959 - Sept 1959	Year
0-30°N	+0.74	+0.21	+0.40
50 mb	(324)	(555)	(879)
30-60°N	+2.37	+0.77	+1.49
100mb	(6302)	(7780)	(14082)
60-90°N	+11.16	+2.50	+5.09
100mb	(769)	(1804)	(2573)

a mean monthly basis but calculated from daily observations. Obviously in the spring at high latitudes there is more variability than in the summer. So one would expect more variability of ozone if motions carry ozone down the mixing ratio gradients.

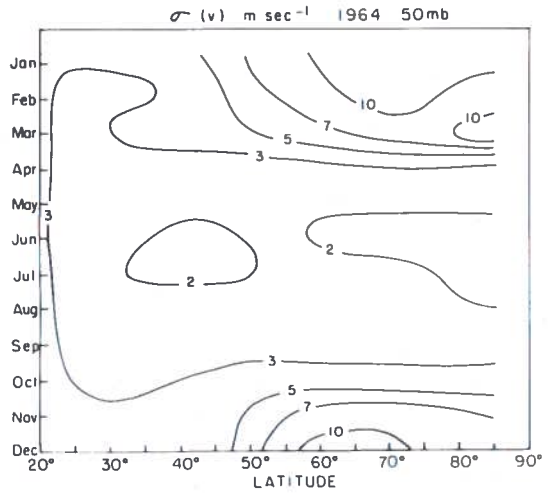

Figure 17. The standard deviation of v at 50 mb during 1964. (Newell et al., in press)

Figure 18 shows the variance of the vertical motion, again taken on a monthly basis but based on daily observations. Much up and down mixing occurs at high latitudes in March and February, when the highest value of the whole year is found.

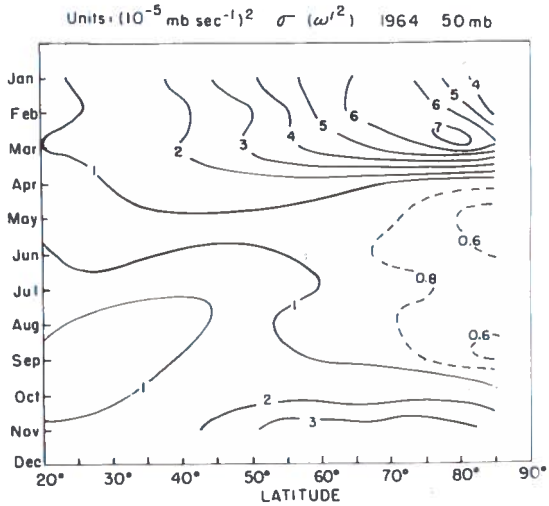

Figure 18. The variance of the vertical motion at 50 mb for 1964. (Newell et al., in press).

Figure 19 shows the correlation between the northward component of the motion v and the downward component ω at the high latitudes. At the beginning of the month northward-moving parcels are rising, while at middle latitudes northward-moving parcels are sinking. In the latter part of March northward-moving parcels beyond 50° north also begin to sink, so one would expect more ozone to be transferred into the sheltered polar cap region. The change in the motions happens concomitantly with a flux of

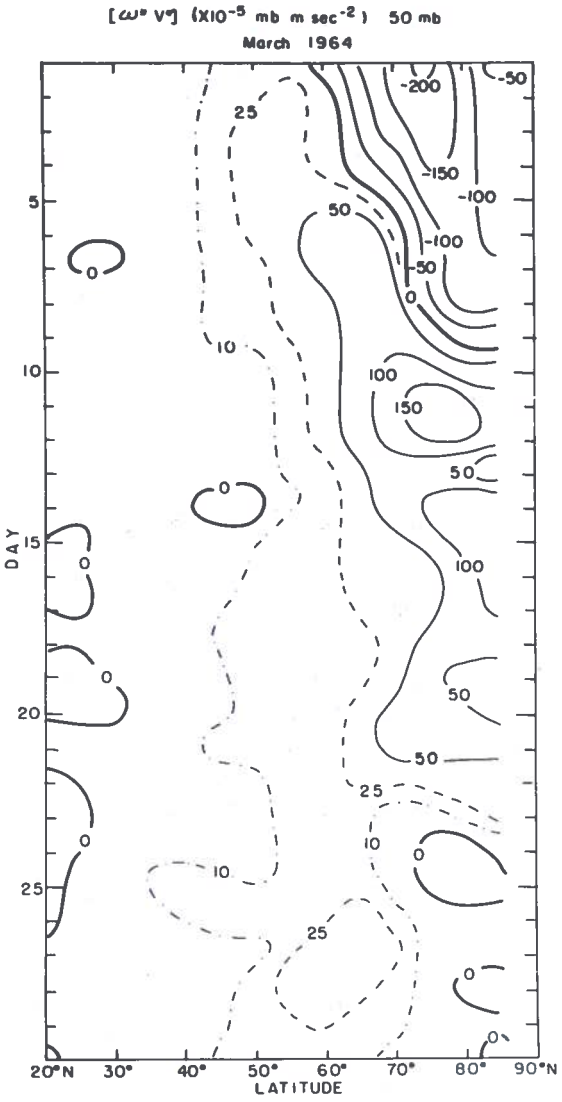

Figure 19. A measure of the correlation between northward and descending motion for March 1964. (Newell et al., in press)

energy up into the lower stratosphere from the troposphere, so we have to look at the troposphere for the source of the change.

Figure 20 is a superposition of total ozone onto the eddy motions at 100 mb. Notice that total ozone went up to 500 m atm-cm. After the northward-moving parcels started sinking, total ozone started to increase, and it was much higher during the rest of the month. We could calculate the downward flux by mean motions on a daily basis to compare it with the observed change if there were sufficient data for good daily ozone maps.

Figure 21 emphasizes Dr. Crutzen's point that there is practically no transport in the summer, as we have seen from Figures 17 and 18.

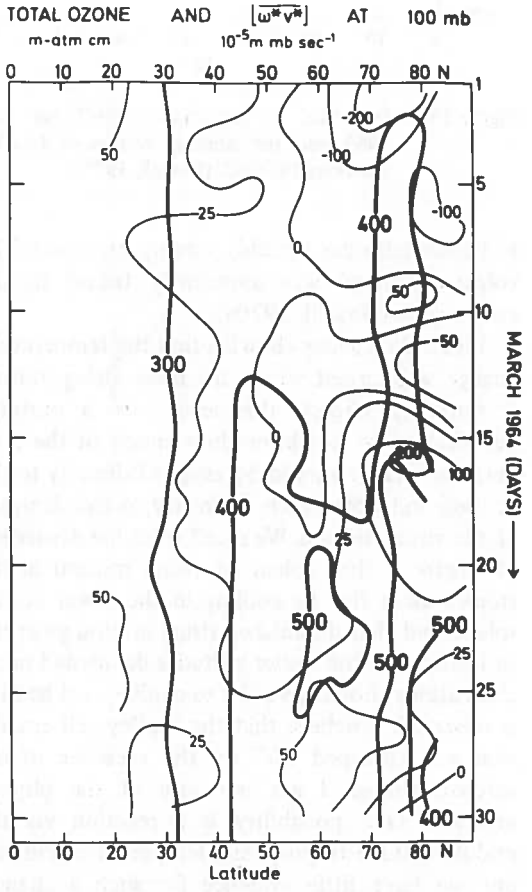

Figure 20. Total ozone (m-atm cm) and correlated northward and descending motion (10^{-5} m mb sec^{-1}) for March 1964. (Newell et al., in press)

Figure 21 represents mean vertical motions in the summer. The observed value of 0.5 x 10^{-5} mb sec^{-1} compares with 5 x 10^{-5} mb sec^{-1} in the winter and it is difficult to be very sure of the sign of the deduced vertical motion.

Ozone, of course, is not the only important absorber in the stratosphere with which we are concerned; aerosols, or particulates, are also important. This brings us to the matter of volcanos.

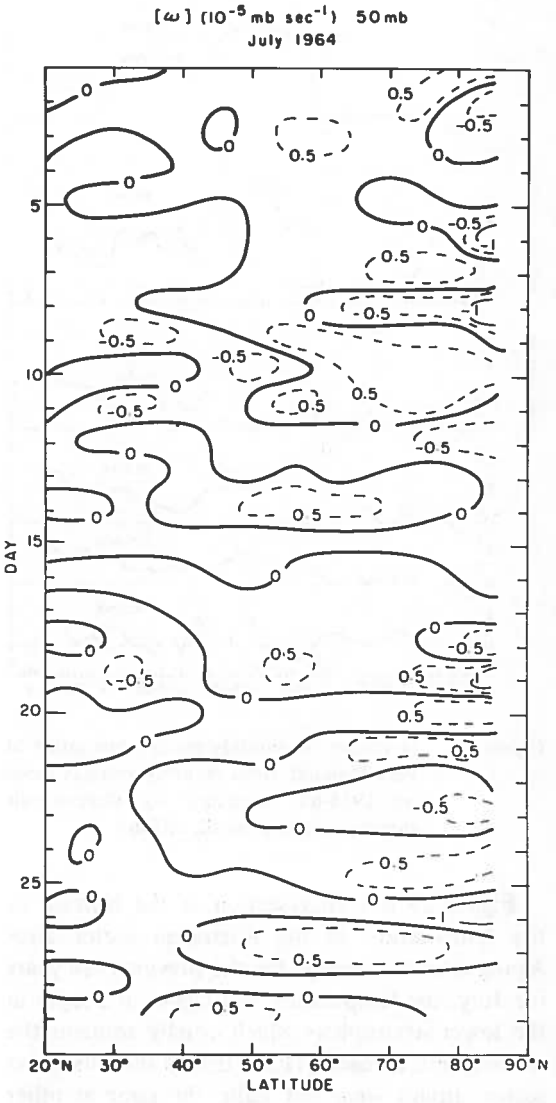

Figure 21. Mean zonal vertical velocity (in pressure coordinates) for July 1964. (Newell et al., in press)

INFLUENCE OF VOLCANIC ERUPTIONS ON TEMPERATURE

Figure 22 shows the temperature change due to the Agung volcano as measured at Port Hedland, Australia (Newell, 1970b, 1971). The values shown are three-month running means; note that temperature increased almost immediately after the eruption of the Mt. Agung volcano in March 1963.

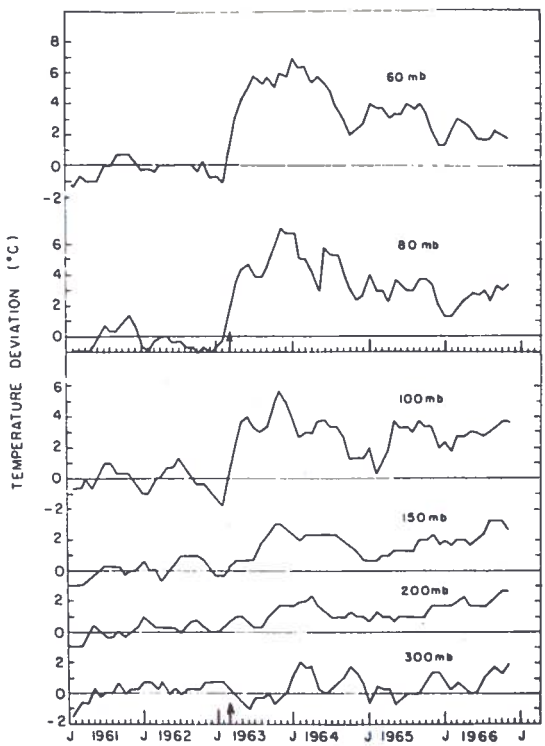

Figure 22. Deviation of monthly mean temperature at Port Hedland, from monthly averages based on 1958-62, smoothed by three-month running means. (Newell, 1970b)

Figure 23 is a cross-section of the increase in the temperature in the Australian sector after Agung over the average for the previous five years for July; the temperature was higher in a layer in the lower stratosphere which usually contains the stratospheric aerosol. (This is true in the Australian sector; things were not quite the same at other longitudes, as will be seen later.)

Figure 24 shows the distribution of Tungsten 185 in the stratosphere in the fall of 1958. Radioactive trace substances such as this showed that debris from low latitudes spread fairly rapidly

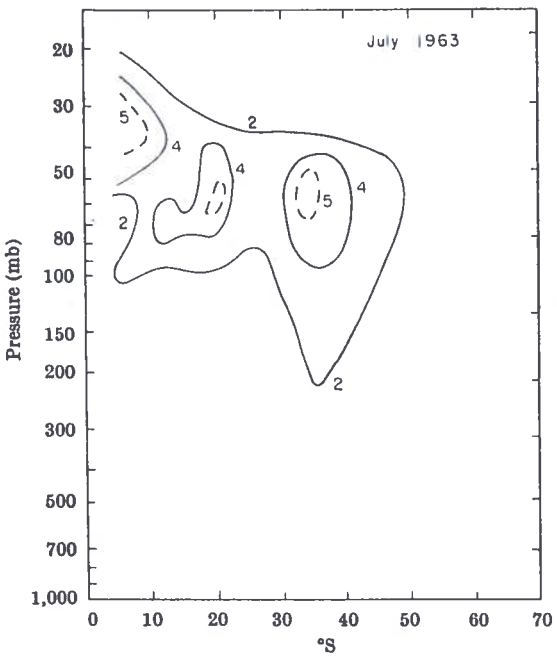

Figure 23. Deviation of temperature (°C) for July 1963 from the monthly average of data for the years 1958-62. (Newell, 1970a)

to higher latitudes by eddy mixing processes. The volcanic aerosol was apparently found in the same region (Newell, 1970a).

Figure 25 is a map showing that the temperature change was largest where the mean rising motion is normally largest; this leads into a problem because we do not know how much of the temperature change should be assigned directly to the heating and how much indirectly to the damping of the rising motion. We recall from the discussion of Figure 1 that enhanced rising motion in the tropics gives rise to cooling in the lower stratosphere and that diminished rising motion gives rise to heating. At the higher latitudes dampened mean circulations should give rise to cooling, yet heating is observed. I believe that the Hadley-cell circulation was "damped off" by the presence of the aerosol, though I am not sure of the physics involved. One possibility is a reaction via the middle-latitude tropospheric temperature gradient, but we have little evidence for such a change. Another possibility is an effect of the stratosphere on the troposphere. This latter would be particularly interesting, since we normally think of such reactions as working in the other direction. The biennial oscillation at this period was stopped

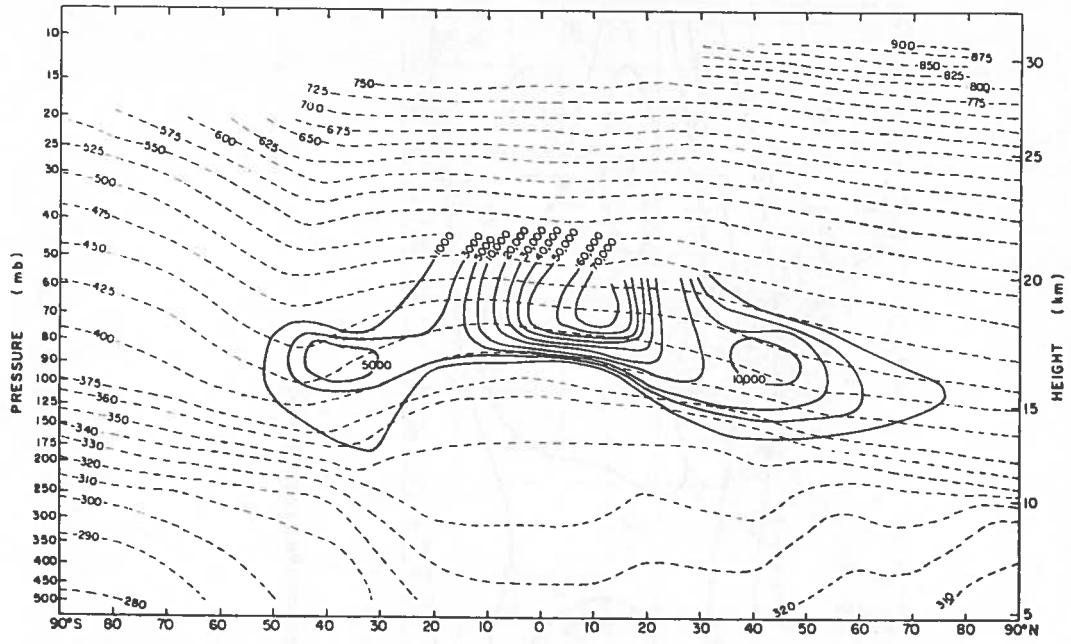

Figure 24. Distribution of tungsten (solid lines) and potential temperature (dotted lines) in the stratosphere. Tungsten values for September-October 1958. Units are disintegrations per minute per 1,000 standard cubic feet of air. Potential temperatures for July 1957 (°K). (Newell, 1963)

suddenly by the eruption of the volcano. Figure 25 contains temperature increases for one year; any other year would show just the biennial oscillation, which is much smaller than this.

Figure 26 represents heating rates due to absorption of visible radiation by the aerosol (2500 - 6500 Å; peak concentration, 10 cm^{-3}; refractive index, 1.4 - 0.04i) from unpublished work by my colleague H. Malchow. We see that particles produce heating, but we do not know what produces the cooling to offset the heating. We have to do some realistic sums on the infrared cooling as well.

Figure 27 represents 12-month running mean values of total ozone. Prior to the volcanic eruption there was a regular biennial oscillation. Enhanced rising motion in the tropics produced low ozone at Kodaikanal; concomitantly enhanced sinking motion at middle latitudes produced high ozone over Australia. We deduced enhanced rising motion as outlined previously from the observed low temperatures. The volcano came along, the aerosol was injected, and the biennial oscillation stopped; it stopped with ozone high in the tropics, which was itself an interesting item. Normally ozone is low in that region because tropospheric air is moving up into it, cutting down the total

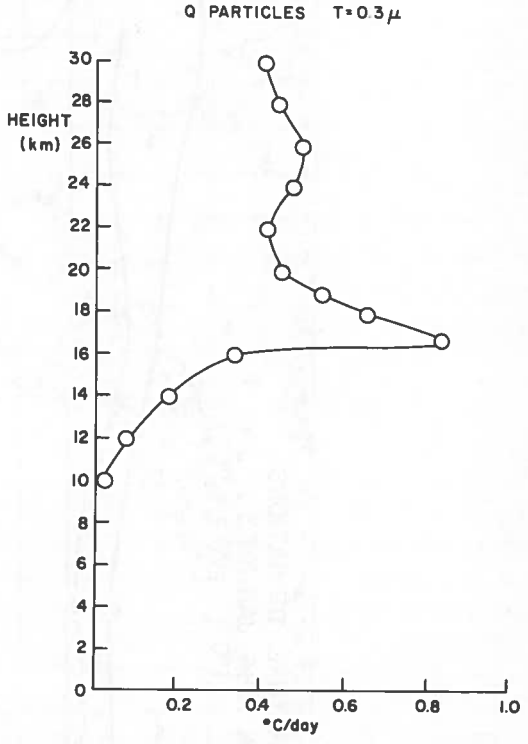

Figure 26. Heating rates due to absorption of visible radiation by the aerosol (see text for details).

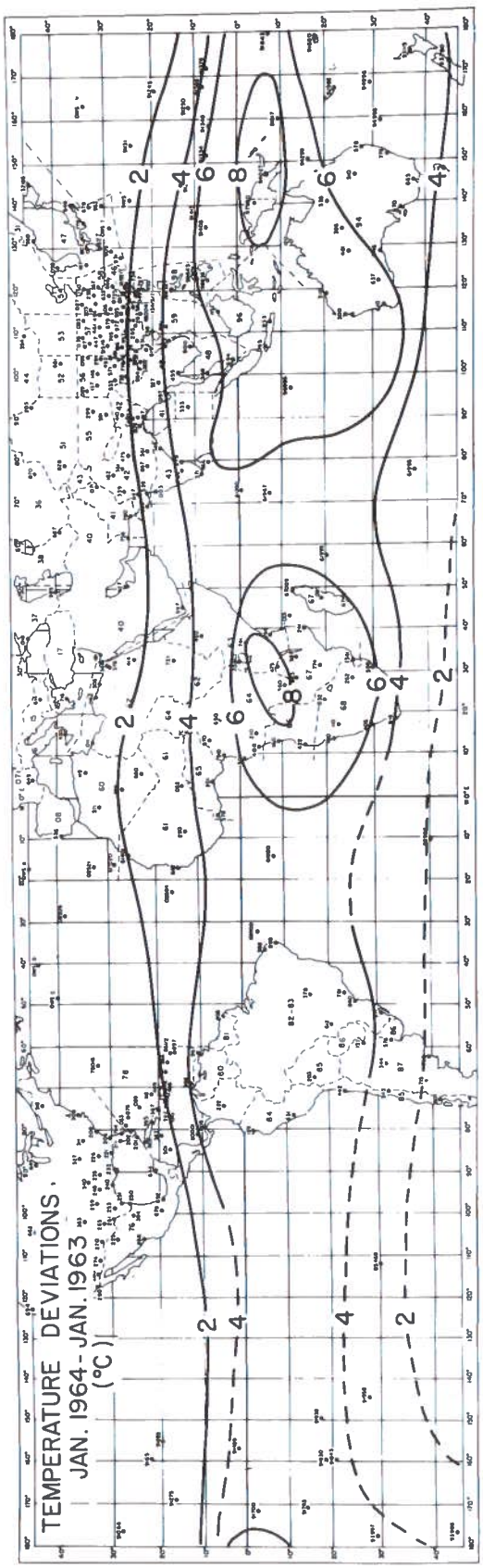

Figure 25. Increase of temperature in January 1964 as compared to January 1963. (Newell, 1971)

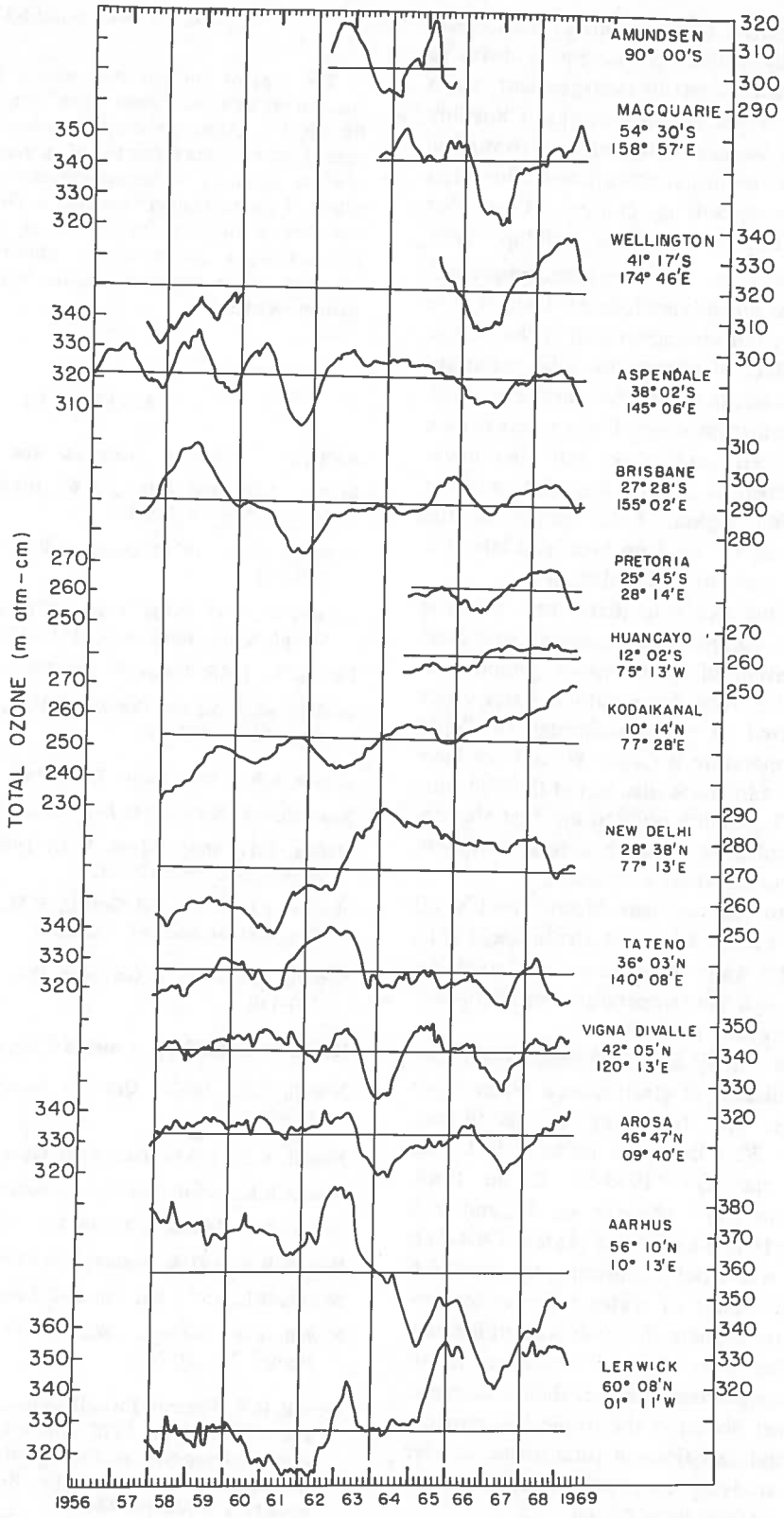

Figure 27. Twelve-month running means of total ozone.

ozone in the column. (Total ozone in the tropical column normally builds up by ozone's diffusing downwards, down the mixing ratio gradient, and is offset by the enhanced rising motion.) Possibly it stopped high because that region of formation of ozone in the tropical stratosphere suffered less dilution by tropospheric air coming up into that region, permitting more ozone buildup there.

In sum: Volcanic gas enters the stratosphere and the stratospheric aerosols are formed. Temperature increases; we are not sure how much of the change is the direct effect of heating by solar radiation, and how much is due to modulated vertical motion. The biennial oscillation stops. There seems to be a weaker Hadley-cell penetration into the lower stratosphere, which would give less dilution of the ozone formation region. Total ozone in the tropics is allowed to build up high, and later the eddies can take more to higher altitudes.

One additional point is that when we first looked at this temperature change it was clear that concentration of water vapor should also change (Newell 1970b). More natural water vapor will be permitted to pass up through the "cold trap" if its temperature is raised. We did not have any observations to check this, but at the Williamstown meeting L. Machta pointed out that Mastenbrook's data did show an increase in stratosphere water vapor concentration with time.

There is also one problem. Mastenbrook's full paper, which I have just seen (Mastenbrook, 1971), shows that the water vapor does not go down again even though the temperature has decreased. This is an interesting anomaly.

Let us look briefly at noctilucent clouds too, as another indicator of stratospheric water-vapor concentrations. The frequency of noctilucent clouds for the West European network is 2 cases per year in the IGY, 1958-59, 23 in 1964, increasing up to 1967, where it was 33, and then diminishing to 18 in the past year (Paten, 1964-71). The network was strictly uniform only for 1964-71. Indirect evidence of water vapor concentrations in the stratosphere thus points to an increase for four or five years after the first boost in the tropical tropopause temperature, then a decrease. There are other boosts in the tropical tropopause temperature and variations of total ozone, and we are presently studying the possibility of influences by volcanic eruptions since Agung.

ACKNOWLEDGMENTS

The support for our stratospheric and tropical circulation studies has come from the Fallout Studies Branch, U.S. Atomic Energy Commission. The work has been done by a large number of students and colleagues over the years, as we learned together about the stratosphere. I am particularly grateful to Dr. George J. Boer and Gerald Herman for their help in preparing this presentation. I should like to emphasize that it was intended as an informal tutorial, not as an in-depth written review.

REFERENCES

Aldaz, L., 1969: J. Geophys. Res. *74*, 6943-6946.

Brewer, A.W., and Wilson, A.W., 1968: Quart. J. Roy. Meteor. Soc. *94*, 249-265.

Dopplick, T.G., 1971: Quart. J. Roy. Meteor. Soc. *97*, 209-237.

Fabian, P., and Junge, C.E., 1970: Archiv. für Met. Geophys. and Biokl. *A19*, 161-172.

Hering, W., 1966: Tellus *18*, 329-336.

Lindemann, F.A., and Dobson, G.M.B., 1921: Proc. Roy. Soc. *A102*, 411-437.

Lorenz, E.N., 1955: Tellus *7*, 157-167.

Mastenbrook, H.J., 1971: J. Atmos. Sci. *28*, 1495-1501.

Mateer, C.L., and Godson, W.L., 1960: Quart. J. Roy. Meteor. Soc. *86*, 512-518.

Murgatroyd, R.M., and Goody, R.M., 1958: Quart. J. Roy. Meteor. Soc. 84, 225-234.

Newell, R.E., 1961: Geofisica Pura e Applicata *49*, 137-158.

Newell, R.E., 1963a: J. Atmos. Sci. *20*, 213-225.

Newell, R.E., 1963b: Quart. J. Roy. Meteor. Soc. *89*, 167-204.

Newell, R.E., 1964a: Pure Appl. Geophys. *59*, 191-206.

Newell, R.E., 1964b: Pure Appl. Geophys. *58*, 145-156.

Newell, R.E., 1970a: J. Atmos. Sci. *27*, 977-978.

Newell, R.E., 1970b: Nature *227*, 697-699.

Newell, R.E., 1971: Sci. Am. *224*, January, 32-42.

Newell, R.E., Kidson, J.W., and Vincent, D.G., 1969: Nature *222*, 76-78.

Newell, R.E., Vincent, D.G., Dopplick, T.G., Ferruzza, D., and Kidson, J.W., 1970: The energy balance of the global atmosphere, in *The Global Circulation of the Atmosphere*, Ed. G.A. Corby, Royal Meteorological Society, London, pp. 42-90.

Newell, R.E., and Gray, C.R., 1972: Meteorological and Ecological Monitoring of the Stratosphere and Mesosphere. NASA Report CR2094.

Paton, J., 1971: Met. Mag. *100*, 179-182 (and previous articles in series).

Peng, L., 1965: Pure Appl. Geophys. *61*, 197-218; *62*, 173-190.

Vincent, D.G., 1968: Quart. J. Roy. Meteor. Soc. *94*, 333-349.

DISCUSSION

H. Dutsch pointed out that a smaller Hadley cell in the tropics should lead to less excess ozone, because there will be a smaller ozone deficit in the production region, and thus in these latitudes the values should decrease with altitude. Newell agreed that the middle latitudes in the Southern Hemisphere have something of an anomaly, in that the changed circulation produces higher values at low latitudes, but the change at higher latitudes also produces higher values. He pointed out that the biennial oscillation seems to be due to the low-altitude increase which results from reduction of the Hadley cell. The production is reduced, but the downward transport would be larger. Dutsch noted that with photochemical equilibrium nothing is produced. However, if air stops going in the gradient will be greater; how it goes out is not yet clear. A. Goldburg expressed doubt that a simple chemical-rate model, based on a simple chemical compound, one-dimensional and steady-state, could explain the richness of the observed phenomena of ozone creation and motion.

W. Libby made the following observations based on his recent work.

W. LIBBY
UCLA

Radioactive fallout data is quite useful in determining circulation in the stratosphere and stratospheric residence time. For example, the first thing we learned from it was that stratospheric residence time is a matter of years.

Explosions of less than a megaton TNT equivalent put their debris in the troposphere, which leads to a deposition in a matter of a few weeks, largely restricted to the latitude of the firing. Explosions of one megaton or larger, however, deposit radioactive debris in the stratosphere, which leads to a worldwide deposition of this over a period of years. In other words, Northern Hemispheric shots which are below a megaton in yield will not contaminate the Southern Hemisphere; shots that are over a megaton contaminate the whole world.

We are still observing radioactive fallout from the Russian shots in 1961. It is coming down in the form of HTO, radio carbon dioxide $C^{14}O_2$, strontium 90 and cesium 137, the long-lived radioisotopes. This is a good opportunity to get more or less quantitative information about the circulation and the residence time. We have quite a few data which should be processed as before to bring us up to date; perhaps we should also make more measurements.

NUMERICAL SIMULATION OF THE STRATOSPHERE: IMPLICATIONS FOR RELATED CLIMATE CHANGE PROBLEMS

J. D. MAHLMAN AND S. MANABE
Geophysical Fluid Dynamics Laboratory
Princeton, New Jersey 08540

ABSTRACT: Current results are presented from an atmospheric simulation model which extends to a height of about 30 km. The model is global and contains 11 vertical levels with a horizontal resolution of about 265 km. Realistic topography, an annual march of radiation, sea surface temperature, and water vapor effects are included.

Zonal-mean cross-sections of temperature and zonal wind are shown and compared with reality. The results indicate close agreement with observations except for a few important exceptions; e.g., the simulated stratospheric polar night vortex is about a factor of two stronger than the observed. Synoptic charts for the 38-millibar pressure level are shown for different seasons of the year. These reveal a satisfactory simulation of the stratospheric winter Aleutian anticyclone and polar vortex, as well as the summertime easterlies.

Special attention is directed toward the problems of using atmospheric simulation models to study mechanisms acting to redistribute trace substances. Numerical and physical problems of modeling tracer advection, sub-grid-scale transfer, sources, and sinks are discussed in relation to the climate change problem. On the basis of current experience, some speculations are offered on efforts toward solving problems in which the distribution of tracers affects, and is affected by, the dynamics of the stratosphere.

INTRODUCTION

Because the goal of the Climatic Impact Assessment Program (CIAP) is the assessment of the effects of a high-altitude fleet on the climate of the earth, this paper outlines some of the authors' current research which has some bearing on that topic. The problem can be conveniently divided into two important questions which must be answered:

1. How is the aircraft effluent of potentially important constituents (e.g., H_2O, NO_x and particulates) spread throughout the stratosphere and removed to the troposphere?
2. How would the resulting change in stratospheric composition actually affect the climate?

A satisfactory answer to the first question is a necessary condition for answering the second. As a result, the proper numerical simulation of three-dimensional transport of tracers in the stratosphere assumes an important position in this kind of climate change problem. Hunt and Manabe (1968) attempted such a model. Their results indicate a quite delicate balance between the transport by large-scale waves (or "eddies") and the axially symmetric (mean meridional) circulations for effecting a net meridional and vertical tracer transport. It is this delicate coupling that makes parameterization of such stratospheric transfer processes by simple one- and two-dimensional "eddy diffusion" hypotheses somewhat dangerous.

To investigate the second basic question, it is necessary that a model be able to simulate not only the present climate, but also the proper sensitivity of climate to various perturbing factors. This appears to impose a more serious barrier than that presented by the first question: the first question might be answered with an explicit dynamical model of the present climate, while the second requires the ability to simulate rather subtle interactions which are not at present well understood. Examples of these are the interactions with the oceans and cryosphere, effects of particulates, and a disturbed ozone photochemistry. Furthermore, the earth's climate exhibits a year-to-year variability which in many cases can be as large as the effect of a given climate-perturbing mechanism.

Highly simplified models are unlikely to provide satisfactory answers to such relatively sophisticated questions. Explicit dynamical models of the climate should produce more reliable results. Attempts to develop such models have been going on for some years now, and have progressed considerably in sophistication and performance since the landmark studies of Phillips (1956) and Smagorinsky (1963). See, for example, Smagorinsky et al. (1965), Manabe and Hunt (1968), Manabe and Bryan (1969), Holloway and Manabe (1971), Mintz (1968), and Washington (1969, 1971). As noted above, a condition which needs to be satisfied before a quantitative climate-change experiment can be carried out is that the model must be able to simulate the important features of the atmospheric general circulation as it exists today. One of the main goals of this paper is to present preliminary results from the general circulation model recently developed at the Geophysical Fluid Dynamics Laboratory (Manabe, Holloway and Hahn, 1972) and show the level of simulation of which such a model is capable.

MODEL DESCRIPTION

The model obtains a numerical solution of the hydrostatic equations of motion, first law of thermodynamics, equation of state, mass continuity equation, and water-vapor continuity equation. The equations are solved on a global grid with 11 vertical levels, the highest at about 30 km. The horizontal grid spacing is about 265 km, with approximately uniform spacing over the entire globe.

An annual march of radiation without diurnal variation is included. Local variations of water vapor and temperature are included in the radiation calculation, but the effects of clouds, carbon dioxide and ozone are incorporated in a simpler fashion. The mixing ratio of carbon dioxide is assumed to be constant in space and time, but cloudiness and ozone are fixed according to their observed, seasonally varying zonal-mean values. No radiative effects of particulates other than the specified clouds are included. The hydrologic cycle includes precipitation, evaporation, storage, and runoff of water at the ground surface.

The sea-surface temperature is fixed according to observed seasonal means. Mountain effects are included through realistic topography smoothed to the scale of the computational grid. Sub-grid-scale diffusion of momentum, heat and moisture is accomplished by using a non-linear deformation-dependent diffusion coefficient (Smagorinsky, 1963.) A more complete description of the essential features of this model is given in Holloway and Manabe (1971).

MODEL RESULTS

The time integration of the model described here has only recently been completed. More detailed analysis is currently under way, and the results presented here should be regarded as preliminary.

Because the model is marching through the various seasons, the output and its interpretation is quite complicated. Monthly averages of zonal means of some of the basic quantities are presented as a way of looking at the results in the form of a simple display.

Figures 1 and 2 give the zonal-mean temperature ($^{\circ}$K) as a function of latitude and altitude for January and April, respectively. The figures show that the mean tropospheric temperatures are simulated quite successfully. The equatorial tropopause is located at the correct altitude, at nearly the correct temperature. The downward slope of the tropopause and the warm region in the mid-latitude lower stratosphere are successfully simulated. In the polar night stratosphere, however, the temperature is too cold by as much as 25-30°K; at present the exact cause of this defect has not been isolated. By April the high-latitude stratosphere has warmed considerably in the Northern Hemisphere and has begun to cool off in the Southern Hemisphere. (For examples of observations for comparison against Figures 1-6, see Newell et al., 1970.)

Figures 3 and 4 give monthly averages of the zonal-mean westerly wind component in meters per second. The January cross-section shows a realistic troposphere, with the possible exception of the equatorial mid-tropospheric region where weak easterlies should be present. Consistent with the temperature field of Figure 1, the circulation in the polar night stratosphere is too strong by about a factor of two. Figure 3 shows weak easterlies for the Southern Hemisphere stratosphere. This is in agreement with observation, except for a weak band of westerlies

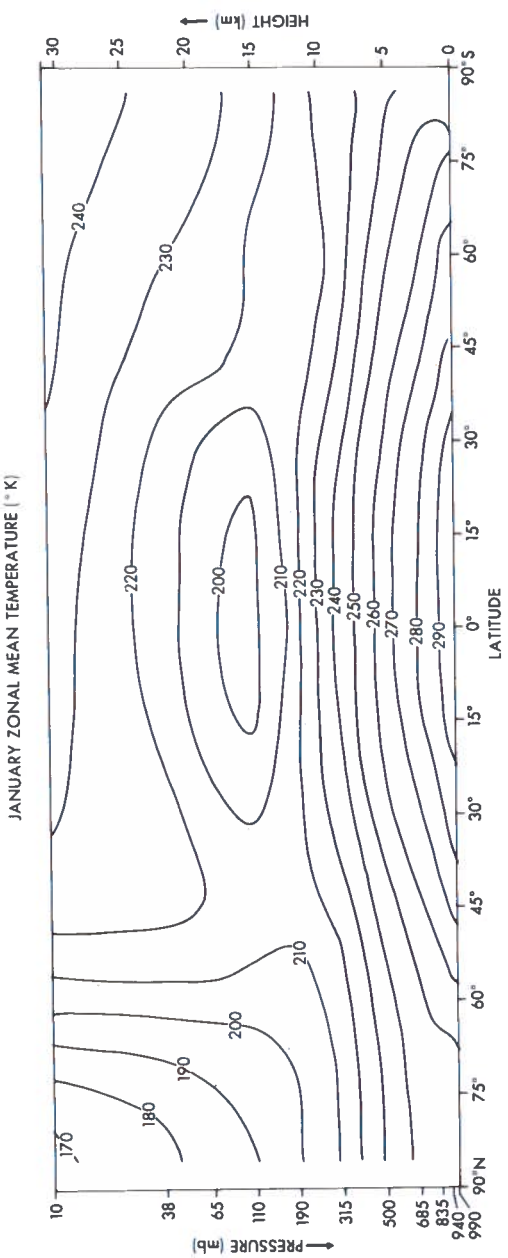

Figure 1. Latitude-height distribution of model-computed zonal-mean temperature (^{o}K) for January.

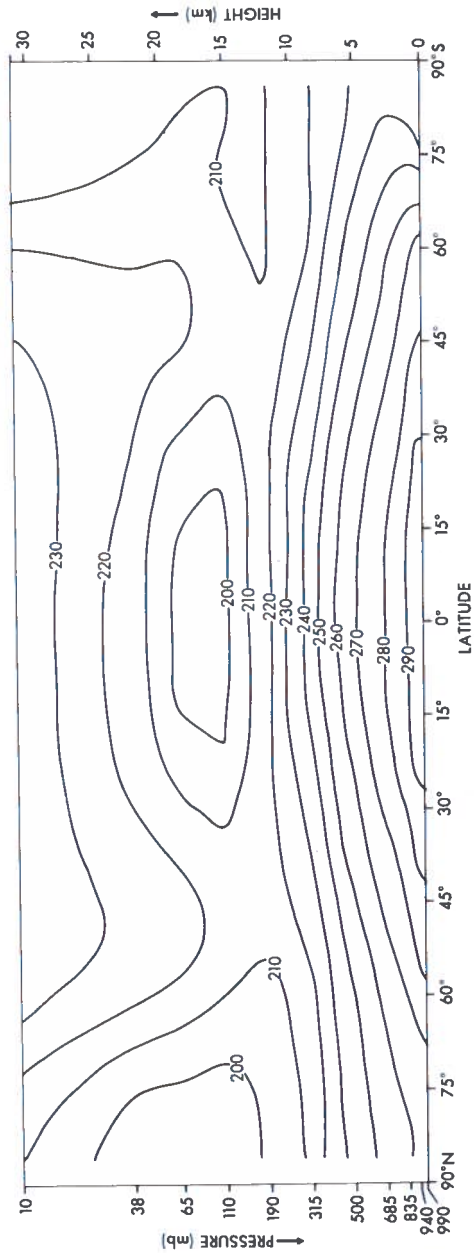

Figure 2. Latitude-height distribution of model-computed zonal-mean temperature (^{o}K) for April.

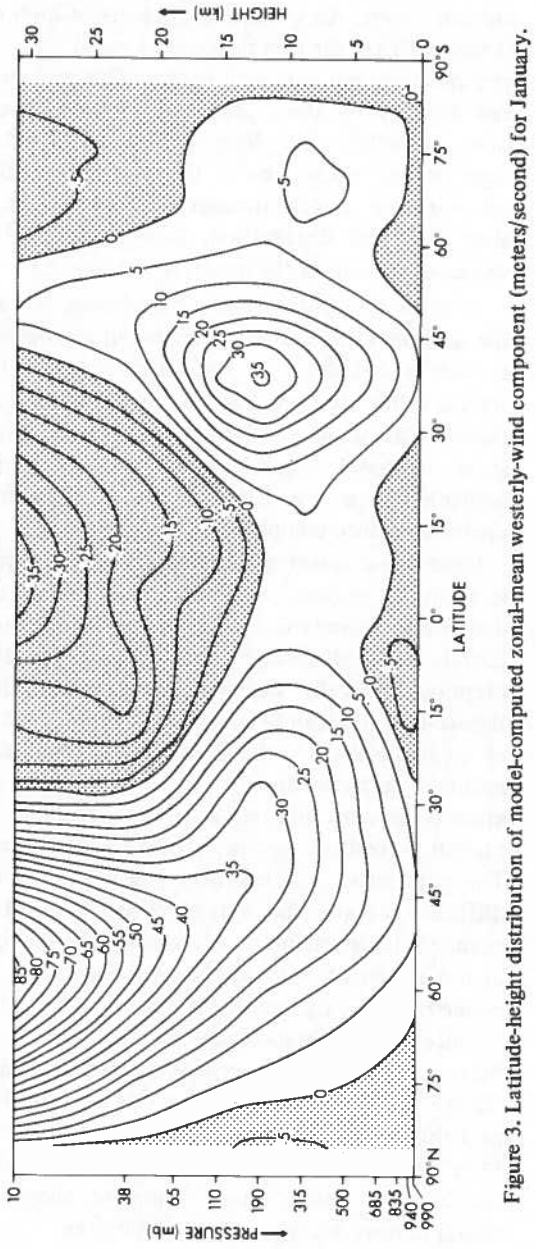

Figure 3. Latitude-height distribution of model-computed zonal-mean westerly-wind component (meters/second) for January.

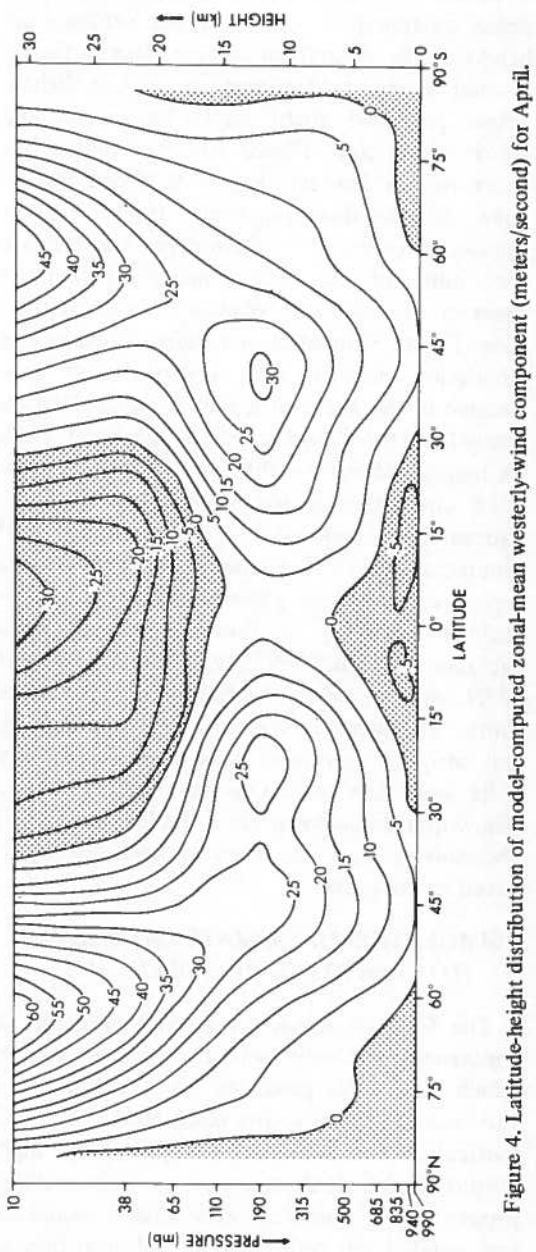

Figure 4. Latitude-height distribution of model-computed zonal-mean westerly-wind component (meters/second) for April.

at about 50°S. The April stratosphere given in Figure 4 shows a weakening Northern Hemispheric westerly circulation and a strong build-up of westerlies in the Southern Hemisphere as the winter season approaches.

Figures 5 and 6 give Northern Hemisphere polar stereographic charts of the geopotential height at the 38-millibar surface. This surface is located at about 22 kilometers, or just slightly above projected flight levels for commercial supersonic aircraft. Figure 5 is an instantaneous chart for 15 January; Figure 6 is one for 15 June. Because these represent "typical" rather than mean charts, the meteorologist can evaluate the ability of the current model to simulate observed stratospheric behavior on a "synoptic" basis. Figure 5 reveals a characteristic mid-winter circulation pattern, with a pronounced anticyclone in the Aleutian region and a cold vortex located on the Eurasian side of the North Pole. As mentioned earlier, the intensity of the simulated circulation is too strong. However, the structure and scale of the circulation are well simulated. The 15 June chart of Figure 6 shows a typical early-summer pattern, with a polar anticyclone beginning to form, a belt of weak cyclones at about 55°N, a belt of anticyclones at 35°N, and the onset of steady easterlies further south. The summer season, and the late-spring and early-fall transition seasons are apparently quite well simulated. On the other hand, the mid-winter breakdown (or "sudden warming") phenomenon has not been successfully reproduced in this model.

SIMULATION OF CLIMATE CHANGE DUE TO STRATOSPHERIC POLLUTANTS

The Climatic Impact Assessment Program is concerned principally with the climatic changes which might be produced by the release of various trace constituents (e.g., H_2O, NO_x, and particulates) into the stratosphere by high-altitude flights. If these effects are to be assessed properly in a numerical atmospheric model, as was pointed out earlier, the model must possess the capability of realistically simulating the dispersion of such pollutants from the source region. The ability of the models to do so may be limited by a number of potential difficulties. First, any defects in the simulated wind field lead to tracer advection which may differ from reality. This problem is becoming less important as the simulation models continue to improve. On the other hand, even if the wind field is quite realistic, the effects of truncation error in computing the spatial derivatives for advection can lead to unrealistic results if proper precautions are not taken. Also, for some tracers of importance to CIAP, the chemical and physical sources and sinks are not very well known. This problem can significantly affect predicted tracer distributions. Finally, over long time periods, the assumptions made about the nature of the sub-grid-scale tracer transfer can significantly alter the final distribution, particularly if the spatial resolution of the model is too coarse.

In order to try to solve these problems, one of the authors (Mahlman) is involved in a program to test the ability of the current model to simulate the observed behavior of stratospheric tracers. This work is still in a comparatively early stage, however. More specific results will be available when the current numerical experiments have been completed.

Once these tracer difficulties have been satisfactorily overcome, it should be possible to design experiments which allow these artificially introduced stratospheric constituents to interact thermodynamically with the model calculation. Before this step can be accomplished, the effects of such tracers on the local and global heat balances must be known. The present level of knowledge does not seem to be adequate to provide a realistic inclusion of such processes. The particulate problem may prove to be very difficult, because the optical properties of airborne particles remain poorly known. Knowledge of the effects of NO_x on the photochemistry of ozone is advancing rapidly, however.

Once the above-indicated barriers have been overcome, it may be possible to run a climate change experiment which possesses a reasonable probability of arriving at a meaningful result. More simplified methods might also obtain valid conclusions, but a more complete approach would remove a large portion of the risks.

ACKNOWLEDGMENT

The authors are grateful to J. L. Holloway and D. G. Hahn for allowing use of preliminary results of the work in which they participated.

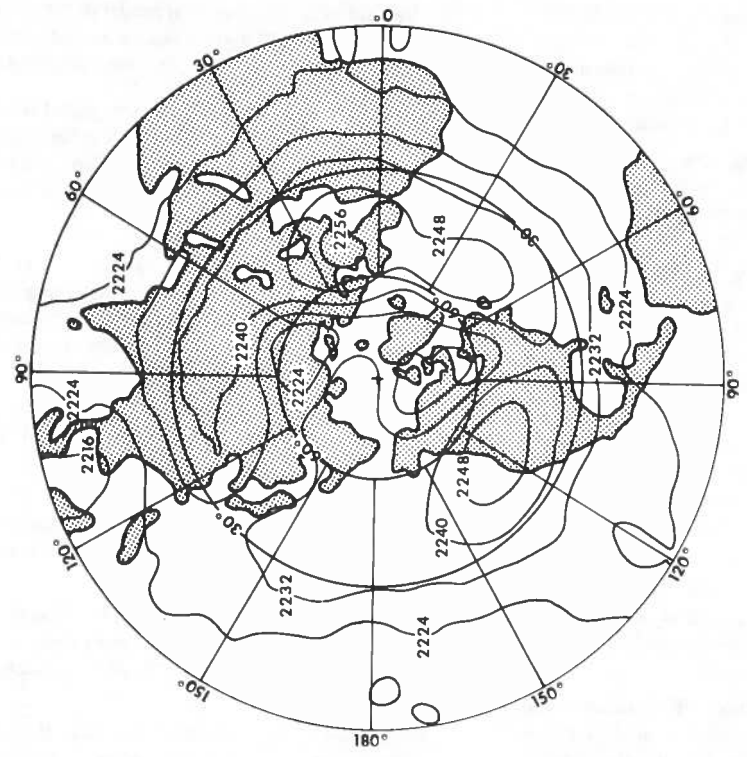

Figure 6. Model-computed Northern Hemisphere polar stereographic chart of geopotential height (decameters) on the 38-millibar surface. This is an instantaneous chart for 15 June. Analysis contour interval is 80 meters.

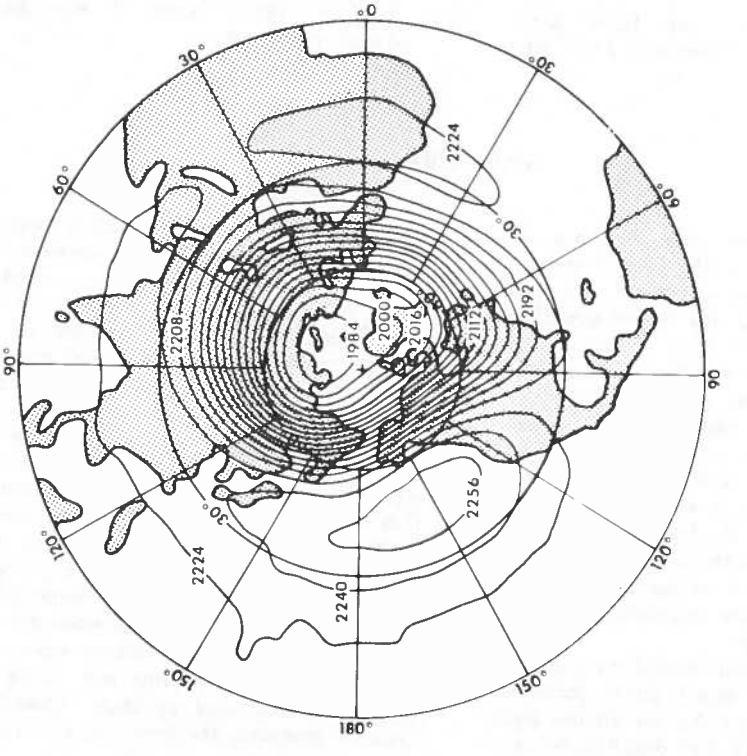

Figure 5. Model-computed Northern Hemisphere polar stereographic chart of geopotential height (decameters) on the 38-millibar surface. This is an instantaneous chart for 15 January. Analysis contour interval is 160 meters.

REFERENCES

Holloway, J.L., and Manabe, S., 1971: "Simulation of climate by a global general circulation model," Monthly Weather Review, *99* (5), 335-370.

Hunt, B.G., and Manabe, S., 1968: "Experiments with a stratospheric general circulation model: II. Large-scale diffusion of tracers in the stratosphere," Monthly Weather Review, *96* (8), 503-539.

Kasahara, A., and Washington, W.M., 1968: "Thermal and dynamical effects of orography on the general circulation of the atmosphere." *Proceedings of the WMO/IUGG Symposium on Numerical Weather Prediction*, Tokyo, Japan, Japan Meteorological Agency, *(IV)*, 47-56.

Kasahara, A., and Washington, W.M., 1971: "General circulation experiments with a six-layer NCAR model, including orography, cloudiness and surface temperature calculations," J. Atmos. Sci., *28* (5), 657-701.

Manabe, S., Smagorinsky, J., and Strickler, R.F., 1965: "Simulated climatology of a general circulation model with a hydrologic cycle," Monthly Weather Review, *93* (12), 769-798.

Manabe, S., and Hunt, B.G., 1968: "Experiments with a stratospheric general circulation model: I. Radiative and dynamic aspects." Monthly Weather Review, *96* (8), 477-502.

Manabe, S., and Bryan, K., 1969: "Climate calculations with a combined ocean-atmosphere model," J. Atmos. Sci. *26* (4), 786-789.

Manabe, S., Holloway, J.L., and Hahn, D.G., 1972: "Seasonal variation of climate in a time-integration of a mathematical model of the atmosphere." *Proceedings of the Symposium of Physical and Dynamical Climatology*, (Leningrad), WMO, Geneva.

Mintz, Y., 1968: "Very long-term global integration of the primitive equations of atmospheric motion: An experiment in climate modification." Meteorological Monographs, American Meteorological Society, Boston, Mass., *8* (30) 20-36.

Newell, R.E., Vincent, D.G., Dopplick, T.G., Ferruzza, D., and Kidson, J.W., 1969: "The energy balance of the global atmosphere." *The Global Circulation of the Atmosphere*, The Royal Meteorological Society, London, 42-90.

Oort, A.H., and Rasmusson, E.M., 1970: "On the annual variation of the monthly mean meridional circulation," Monthly Weather Review, *98* (6), 423-442.

Phillips, N.A., 1956: "The general circulation of the atmosphere: A numerical experiment," Quart. J. Roy. Meteor. Soc. *82* (352), 123-164.

Smagorinsky, J., 1963: "General circulation experiments with the primitive equations: I. The basic experiment," Monthly Weather Review, *91* (3), 99-164.

Smagorinsky, J., Manabe, S., and Holloway, J.L., 1965: "Numerical results from a nine-level general circulation model of the atmosphere," Monthly Weather Review, *93* (12), 727-768.

Vincent, D.G., 1968: "Mean meridional circulations in the Northern Hemisphere lower stratosphere during 1964 and 1965," Quart. J. Roy. Meteor. Soc., *94* (401), 333-349.

DISCUSSION

D. Deirmendjian mentioned some Weather-Bureau observations of solar radiation at the South Pole which suggest that volcanic dust from Agung had been transported to the South Pole at 20 km. He also questioned the remarks reporting the advection of stratospheric tracers. Mahlman replied that real data shows evidence of dramatic meridional transfers resulting from particular kinds of injections, and it might be possible to have two completely unrelated trace substances in one injection within a time scale of a week or two. While the model does simulate the essential wave dynamics of the troposphere and stratosphere (in terms of lower wave numbers at least), and so could theoretically simulate such a situation, the amplitude of disturbances is suppressed to some degree, and such spectacular phenomena might not be correctly simulated.

J. Lauermann asked about the altitude of the horizontal grid lines and what upper outer-boundary conditions were used. Mahlman answered that the altitude levels were 10, 38, 65, 110, 190, 315, 500, 685, 835, 940, and 990 millibars; and the upper boundary condition was that the vertical motion in the sigma system was zero at the half level above 10 mb. N. Sissenwine asked whether the model, with its 10-mb altitude limit, would show explosive warnings, which originate at higher altitudes. Mahlman said probably not, that Matsuno's study showed that the energy "lid" at 10 mb indicates that the model does not have the right conditions to simulate the increased meridional heat flux and induction of the mean meridional circulation. T. Taylor asked what numerical scheme was used in the diffusion model and how truncation was controlled, and whether the model had been checked against laboratory experiments. Mahlman responded that the diffusion scheme had a centered time-stepping leapfrogging with a quadratic-preserving invection calculation included, which made it possible to preserve not only the volume integral and mass of a tracer but also its mean square properties. All the diffusive processes were calculated explicitly. Asked about flow visibility problems, Mahlman said that the system has

non-linear viscosity which is turned on when the horizontal deformation fields get strong and tearing effects occur. As to the question of checking the model against lab data, he said they would like to be free from the assumptions about how the sub-grid-scale transfer processes work, since they did not have complete theoretical confidence in them. He added that resolution in his present model was perilously close to the level at which critical wave numbers are damped.

H. Johnston brought up a point pertinent to Newell's paper and a remark by H. Dutsch. He said that the zero rate of photochemical equilibrium is not zero to a chemist; there are two large rates, one going up and one going down. The difference between the photolysis of oxygen and the processes that destroy odd oxygen, the Brewer-Wilson rate, is what meteorologists think of as rate. For the chemists, there are the gross rates of the formation and the destruction of ozone, with the difference between the two at any point being the transport vector.

Mahlman noted that this was Dickinson's point, that that particular difference was significant in terms of transport, and that chemistry and meteorology were equally important there. S. Zimmerman said that the production and destruction times of ozone produce a time constant so large that nearly any transport motion would destroy the ozone distribution due to photochemical equilibrium, and it is this transport, as witness Hunt's calculation, which is of prime importance.

NUMERICAL SIMULATION OF THE SEASONALLY AND INTER-ANNUALLY VARYING TROPOSPHERIC CIRCULATION

Y. MINTZ, A. KATAYAMA, and A. ARAKAWA
Department of Meteorology, UCLA
Los Angeles, California 90024

ABSTRACT: The tropospheric circulation was numerically simulated for three years of simulated time, during which the underlying sea-surface temperature and the distribution of the sea ice were held constant. Most of the large-scale features of the observed tropospheric circulation were successfully reproduced, including their seasonal variations. The simulated circulation also showed inter-annual variations that are not unlike the year-to-year variations of the real atmosphere.

THE GENERAL CIRCULATION MODEL

A numerical simulation of the tropospheric circulation was made, for three years of simulated time, with a two-level model of the atmosphere. The model has been briefly described by Arakawa, Katayama, and Mintz (1969), and documented in detail by Gates, Batten, Kahle, and Nelson (1971). The basic principles behind the model are given in a report by Arakawa (1972).

The model covers the global domain with grid intervals of 5° of longitude and 4° of latitude. The upper boundary is the 200-mb pressure surface. The lower boundary is the earth's surface, whose height follows the large-scale mountain systems. Thermodynamically, the earth's surface is prescribed as open or ice-covered ocean, and bare, snow-covered, or ice-covered land.

The model atmosphere is divided into two layers of equal mass, and the horizontal velocity components and the temperature are carried as prognostic variables in each layer. Water vapor is carried as a prognostic variable in the lower layer. The surface pressure and the water stored in the ground are the remaining prognostic variables.

In the model there are frictional stresses at the earth's surface and at the interface between the two layers. There is radiative heating, by absorption of solar radiation and by infrared transfers, which depends on the temperature and water vapor, and on a parameterized cloudiness. There is sensible heat transfer at the earth's surface which depends on the temperature difference between the air and the surface. Over all forms of land, and over ice-covered ocean, the surface temperature is calculated from the surface heat flux and the assumption of no heat storage in the land or ice. Over the open ocean, the surface temperature is held constant with time and equal to its observed mean annual distribution. But the declination of the sun, and its distance from the earth, varies with the season of the year. The latitudinal boundary of the land snow cover also varies, in a prescribed way, with the season of the year.

In the model, evaporation from the open ocean, ice, and snow depends on the difference between the vapor pressure of the air and the saturation vapor pressure of the surface. Over bare land, the evaporation depends also on the wetness of the ground (the water stored in the ground), which itself is predicted from the precipitation, runoff, and evaporation. The runoff depends on the rate of precipitation and the ground wetness.

There are two kinds of precipitation in the model. Large-scale precipitation, with release of latent heat in the lower layer, occurs when the relative humidity in the lower layer exceeds the saturation value. Cumulus-scale precipitation, with release of latent heat and a sub-grid scale vertical heat flux, is parameterized as a function of the large-scale variables.

Figure 1 shows the prescribed distributions of bare and ice-covered land and of open and ice-covered ocean, and also the height contours of the land and the temperature of the oceans.

SEASONAL VARIATIONS

Figures 2 through 5 show the January, April, July, and October mean surface pressures reduced to sea level, and the heights of the 400-mb pressure surface, averaged for the three years of

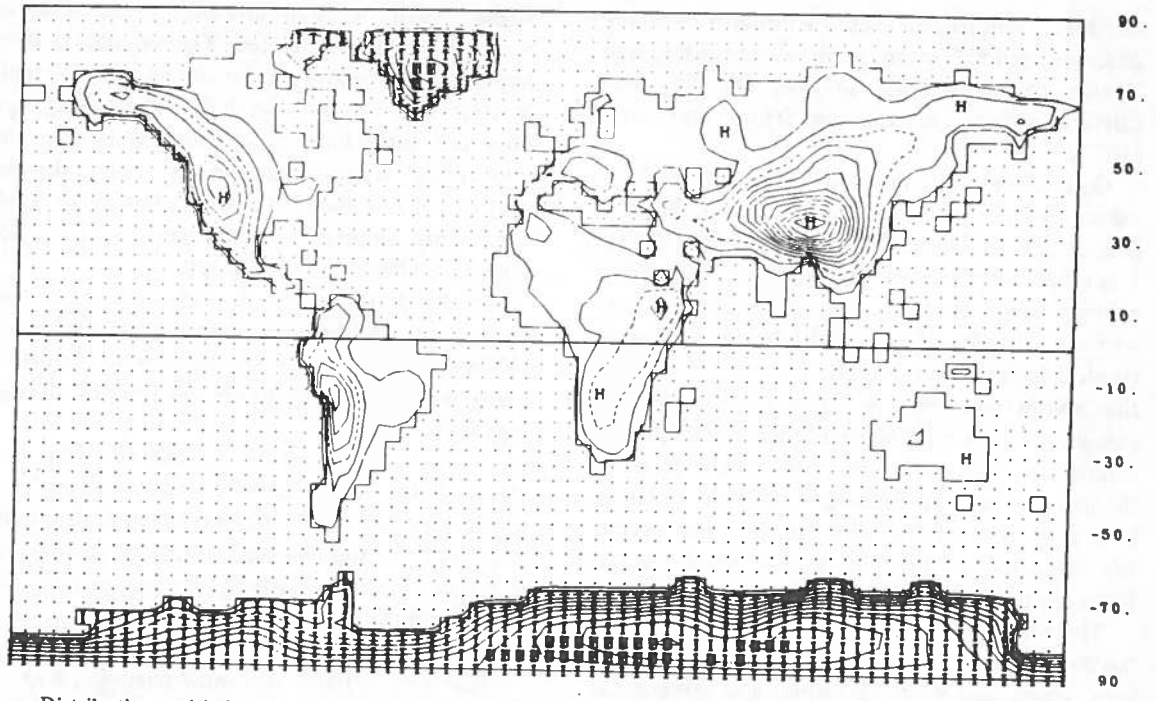

Distribution and height of the land and distribution of land ice. The height contours are at intervals of 1000 ft and the broken line contour is 3000 ft. The letters "I" show ice-covered land.

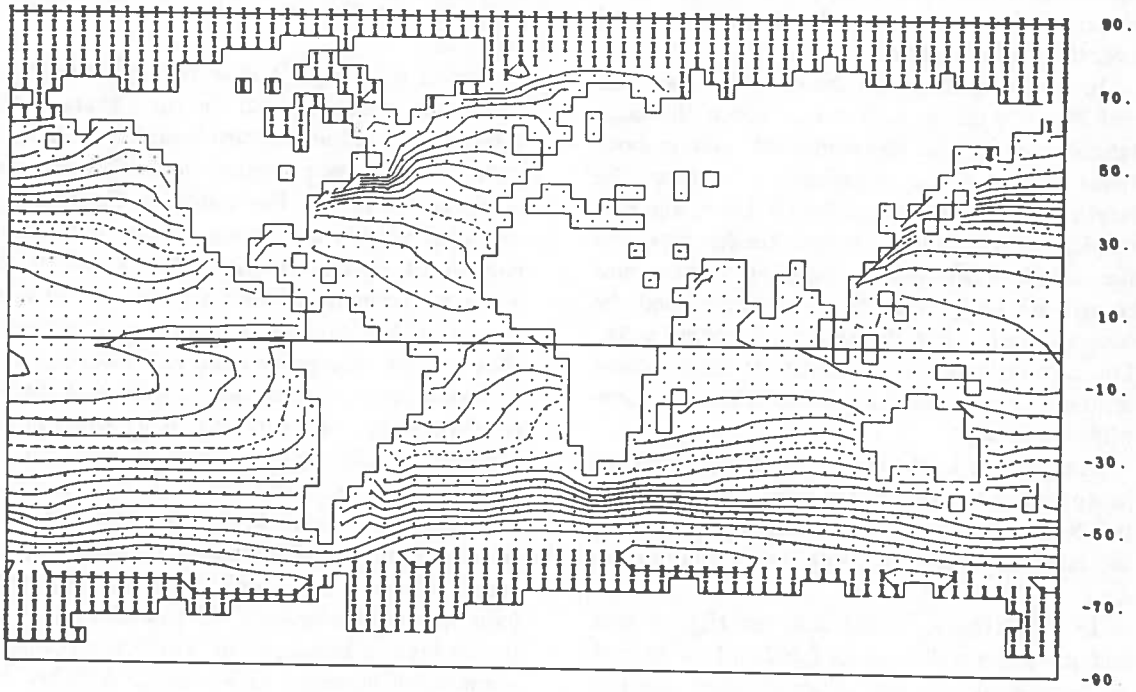

Prescribed ocean surface temperature and distribution of sea ice. The isotherms are at intervals of 2°C and the broken-line isotherm is 20°C. The letters "I" show the sea ice distribution.

Figure 1. Prescribed surface conditions.

numerical simulation. These figures also show the observed normal mean sea-level pressures, and heights of the 400-mb surface, for the same calendar months, as given by Schutz and Gates (1971).

Comparing the simulated with the observed mean sea-level pressures, we see that in January (Figure 2) the North Atlantic and North Pacific Lows, the Siberian High, the northern-hemisphere subtropical high-pressure belt, the equatorial low-pressure trough, the southern-hemisphere subtropical high-pressure belt and its high centers, and the southern-hemisphere subpolar low-pressure trough are fairly well reproduced in the numerical simulation. The only substantial differences are that the simulated Siberian High and North Atlantic Low are somewhat too close to the equator, and the simulated North Atlantic and North Pacific Lows are too intense.

The simulated 400-mb height field, in January, has about the same pattern of northern-hemisphere long waves and southern-hemisphere quasi-zonal mean flow as the observed field. The principal difference is that the simulation has an excessively strong blocking pattern (splitting of the jet stream) over the North Atlantic.

In April (Figure 3) the simulated Siberian High and North Atlantic Low are at about the same latitudes as in the observed field, and in both fields there is a new subtropical Asian Low. The North Atlantic and North Pacific Lows, the subtropical oceanic Highs in both hemispheres, and the southern-hemisphere subpolar low-pressure trough are fairly alike in the simulated and the observed fields. But the simulated North Pacific Low is too intense, and the centers of the simulated southern-hemisphere subtropical Highs are somewhat too far east.

The 400-mb height field is fairly well simulated in April. But the blocking is again too strong over the North Atlantic, and the height gradients are too large at the east coasts of North America and Asia.

In July (Figure 4) the Siberian High is gone and there is a well-developed Indian Low in both the simulated and the observed mean sea-level pressure fields. In both fields there are Lows over the western Sahara and over the southwestern United States, and the North Atlantic and North Pacific Lows have just about disappeared. But the North Atlantic and North Pacific subtropical Highs, which are so pronounced in the observed field, are poorly simulated. The simulation does have a high-pressure center in about the right location in the eastern North Pacific, but this High does not have the correct configuration in the central and western part of the ocean. In the southern hemisphere, the new Australian High is correctly simulated, but the centers of the other subtropical Highs are too far east.

At the 400-mb level, in July, there are only small amplitude waves in the northern-hemisphere observed mean height field, whereas the simulated mean field incorrectly shows short waves of large amplitude.

In October (Figure 5) the Siberian High has returned, the Indian Low is about gone, and the north Australian Low has returned, in both the simulated and the observed fields; for the globe as a whole there is fairly good agreement. The principal difference is that the simulated sea-level pressure is too high over western North America.

The 400-mb fields also show fairly good agreement in October, except again for the excessive blocking over the North Atlantic and too-strong gradients over the east coasts of North America and Asia.

Figures 6 through 9 show the simulated mean vector winds, averaged for the three years, at the 400-mb level and at the earth's surface, as linearly interpolated or extrapolated from the calculated winds of the model. For clarity of presentation, the wind vectors are shown at only half of the number of horizontal grid points at which the winds are computed. The directions of the wind vectors conform to the distortion of the streamlines by the map projection. The magnitudes of the wind vectors are shown in five categories of equal frequency of magnitude, as indicated in the captions to the figures. Thus: at 400 mb in January, magnitudes between 0.1 and 3.8 m/sec are shown by a double-broken line and with one-sided barb; magnitudes between 3.8 and 7.5 m/sec are shown by a single-broken line with one-sided barb; magnitudes between 7.5 and 13.3 m/sec are shown by a continuous line with one arrowhead; magnitudes between 13.3 and 22.5 m/sec are shown by a continuous line with two arrowheads; and magnitudes between 22.5 and 58.0 m/sec (the maximum magnitude on this map) are shown by a continuous line with three arrowheads. The same system is used on the other charts.

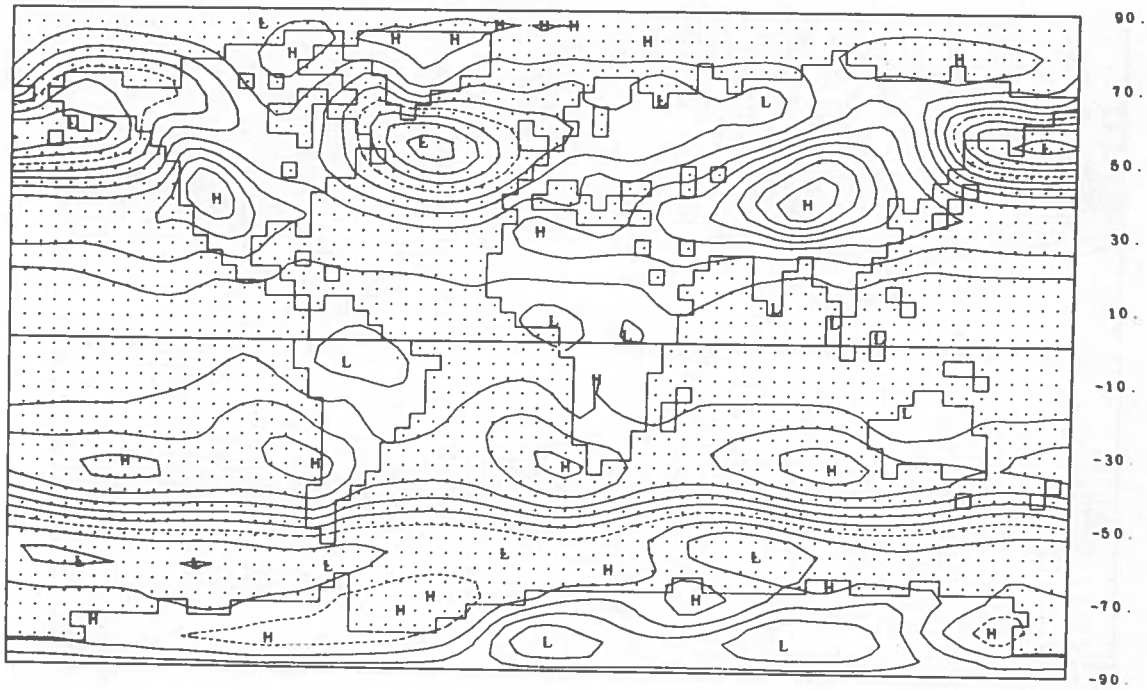

Simulated January mean sea-level pressure, averaged for the three years.

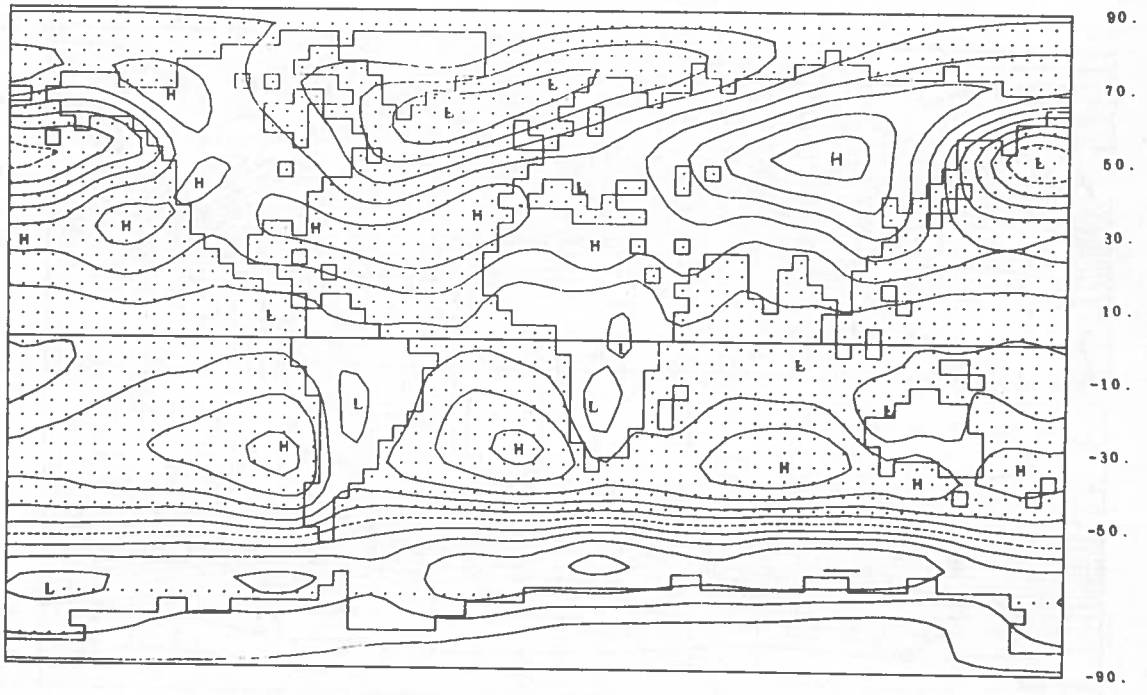

Observed January normal mean sea-level pressure.

Figure 2a. January mean surface pressure reduced to sea level. The isobars are at intervals of 4 mb and the broken-line isobar is 1000 mb.

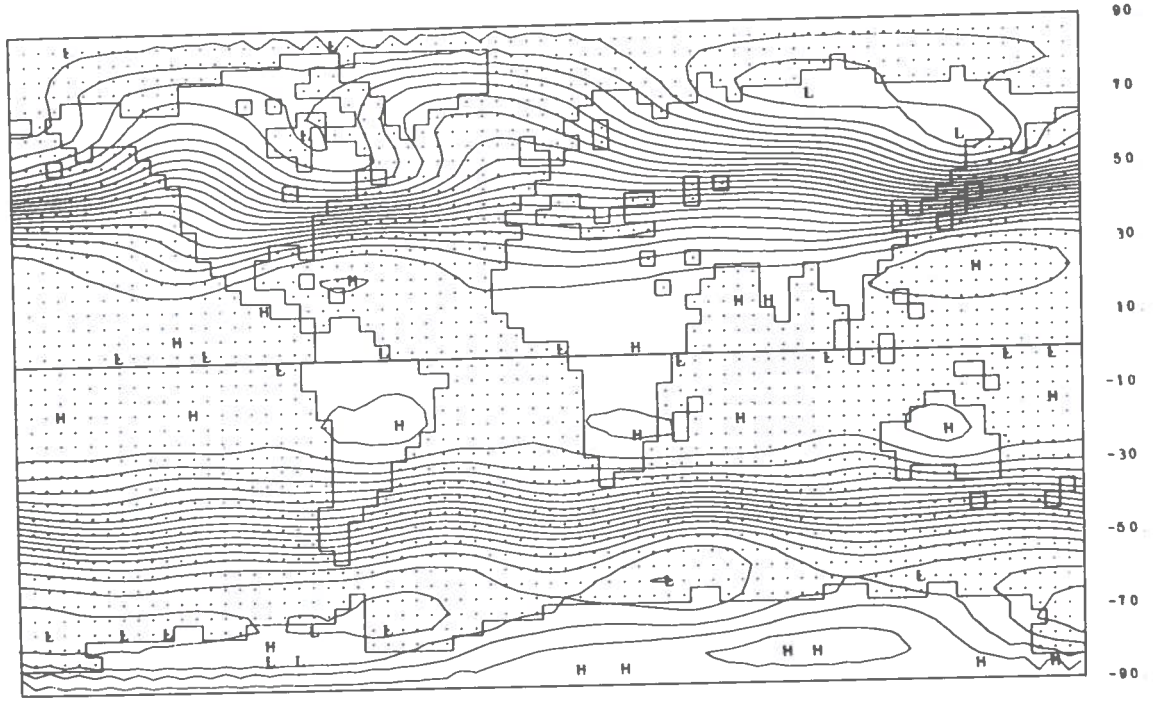

Simulated January mean height, averaged for the three years.

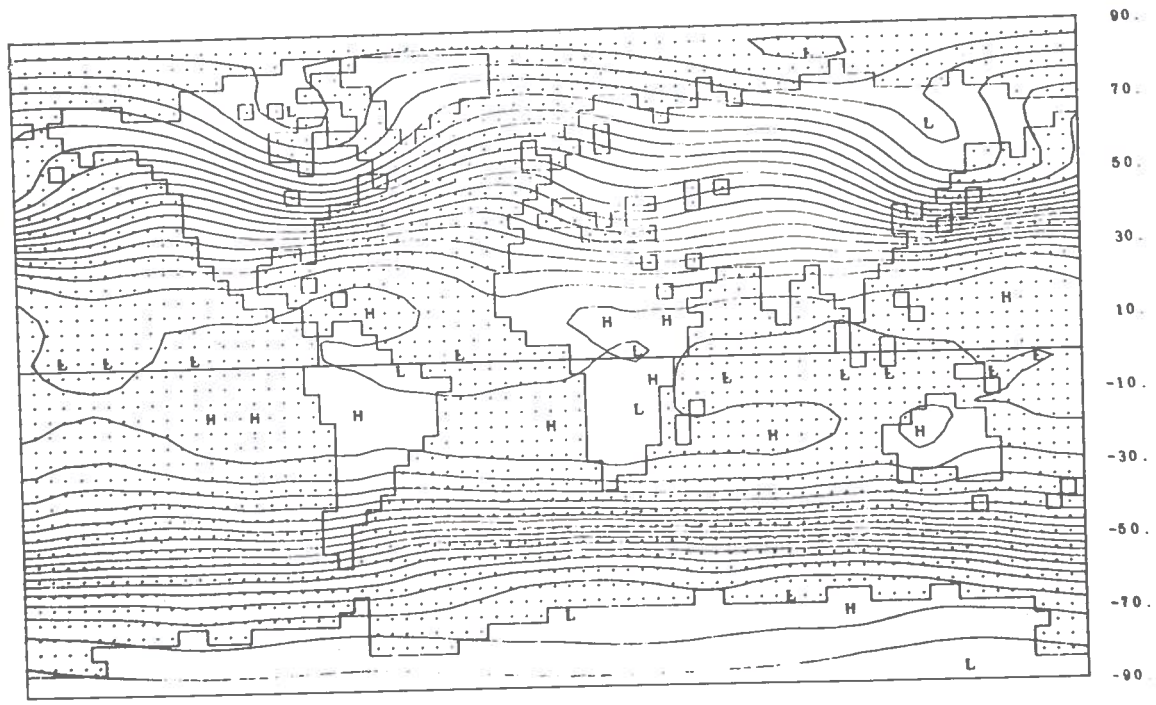

Observed January normal mean height.

Figure 2b. January mean 400-mb height. The height contours are at intervals of 60 meters.

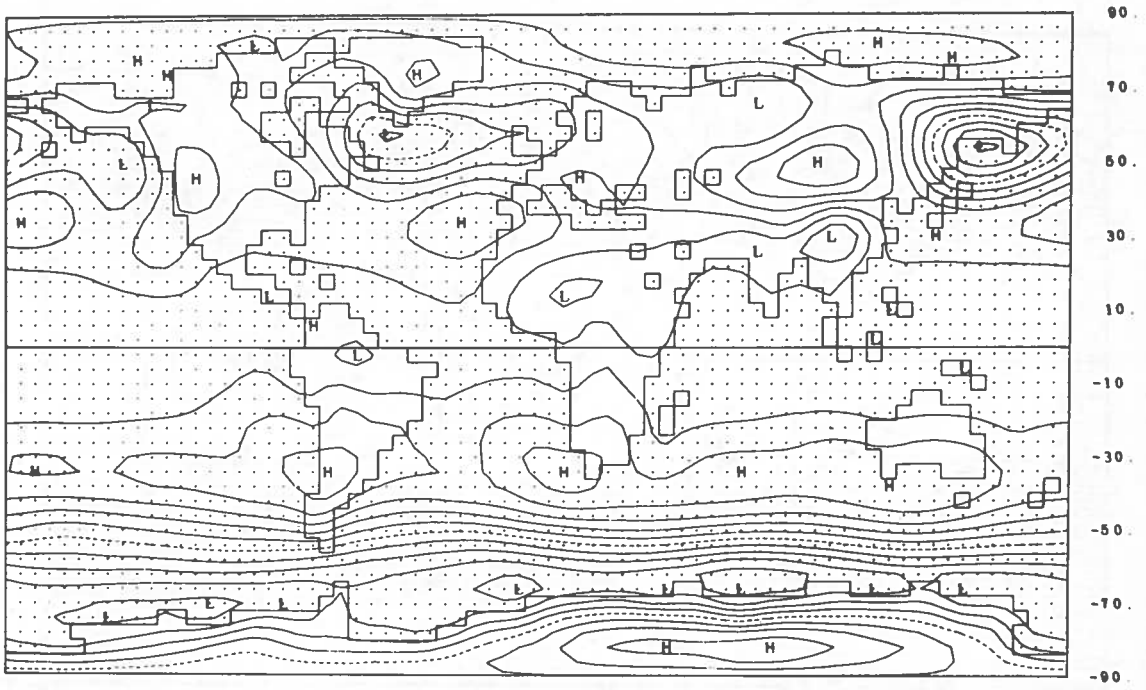

Simulated April mean sea-level pressure, averaged for the three years.

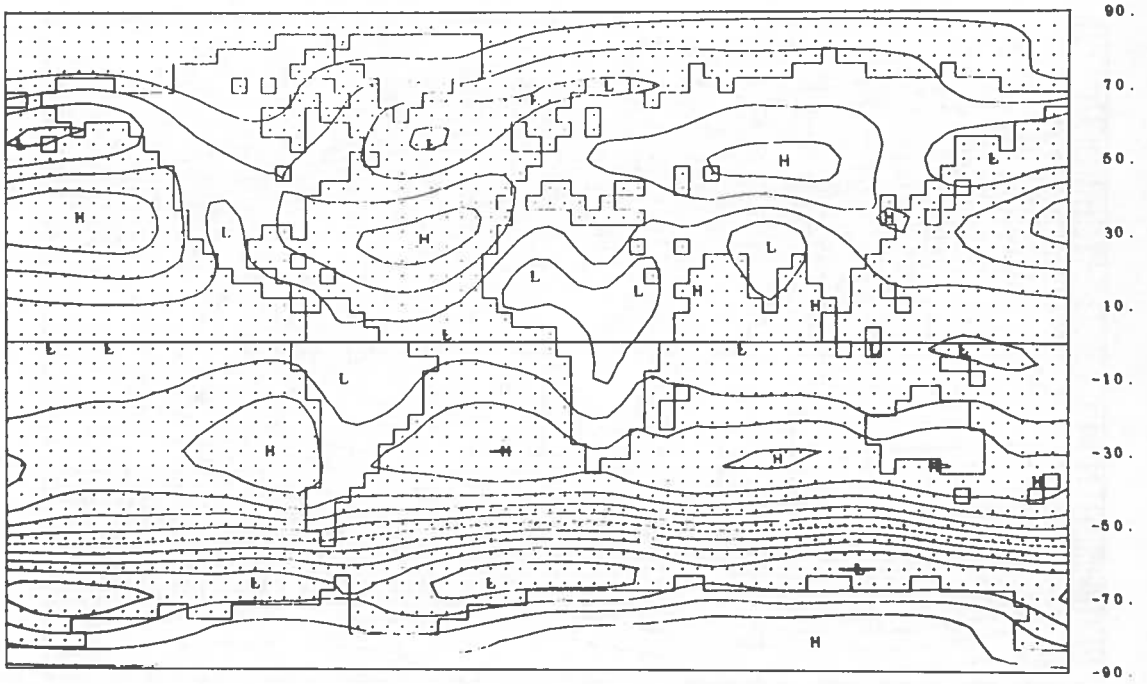

Observed April normal mean sea-level pressure.

Figure 3a. April mean surface pressure reduced to sea level. The isobars are at intervals of 4 mb and the broken-line isobar is 1000 mb.

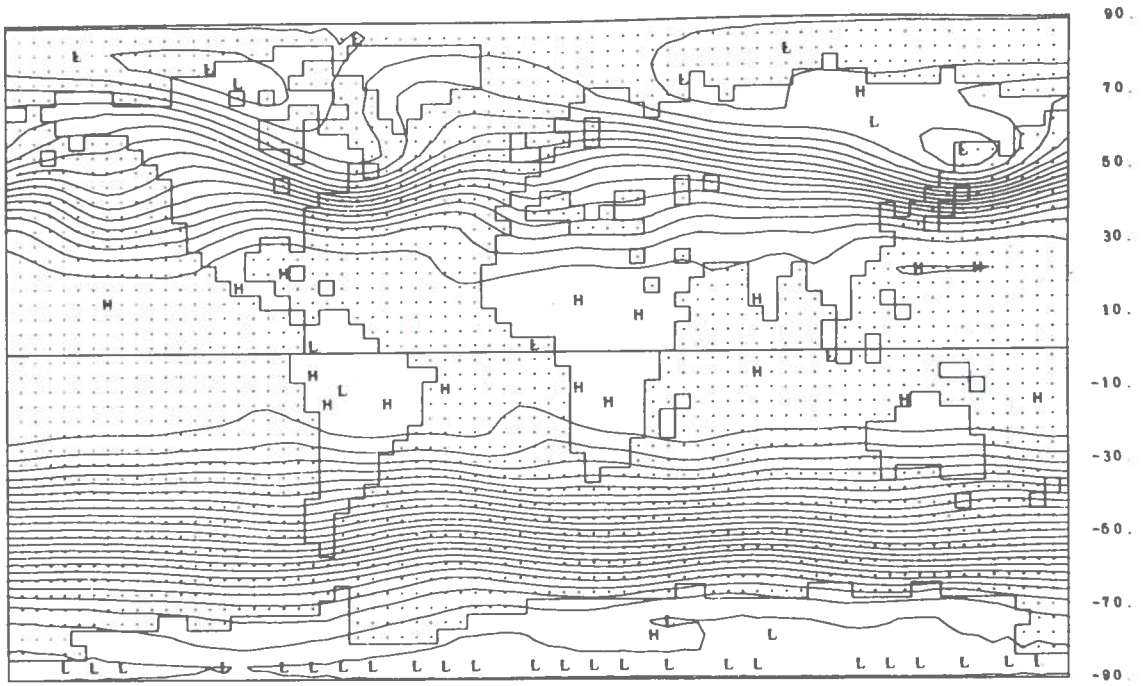

Simulated April mean height, averaged for the three years.

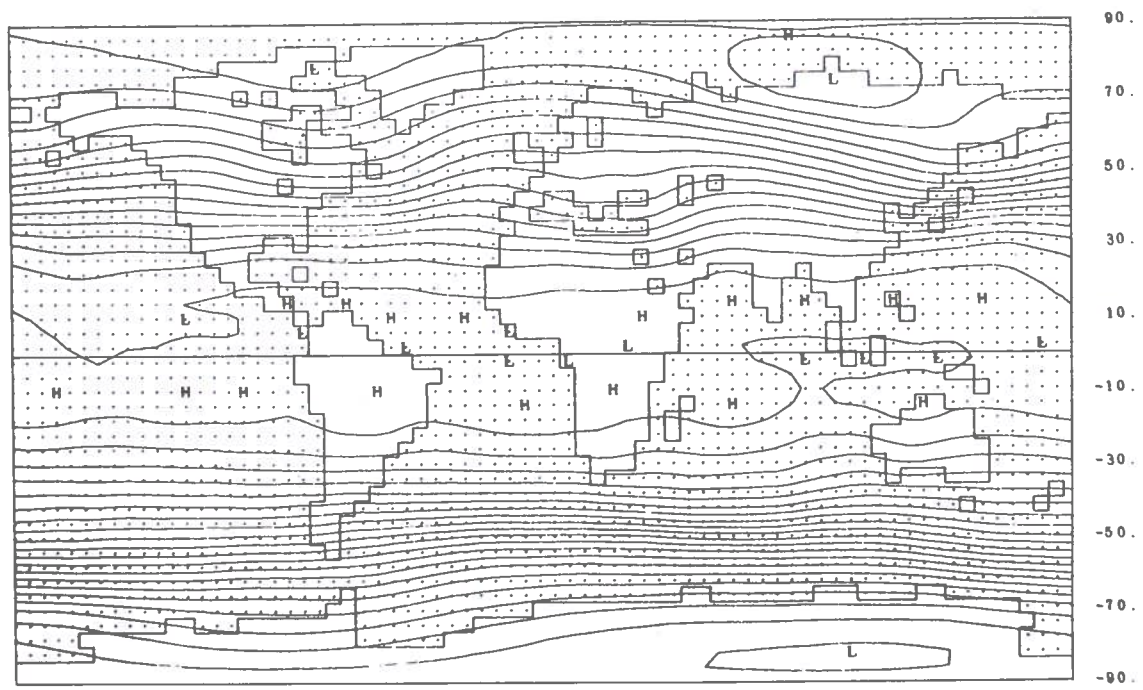

Observed April normal mean height.

Figure 3b. April mean 400-mb height. The height contours are at intervals of 60 meters.

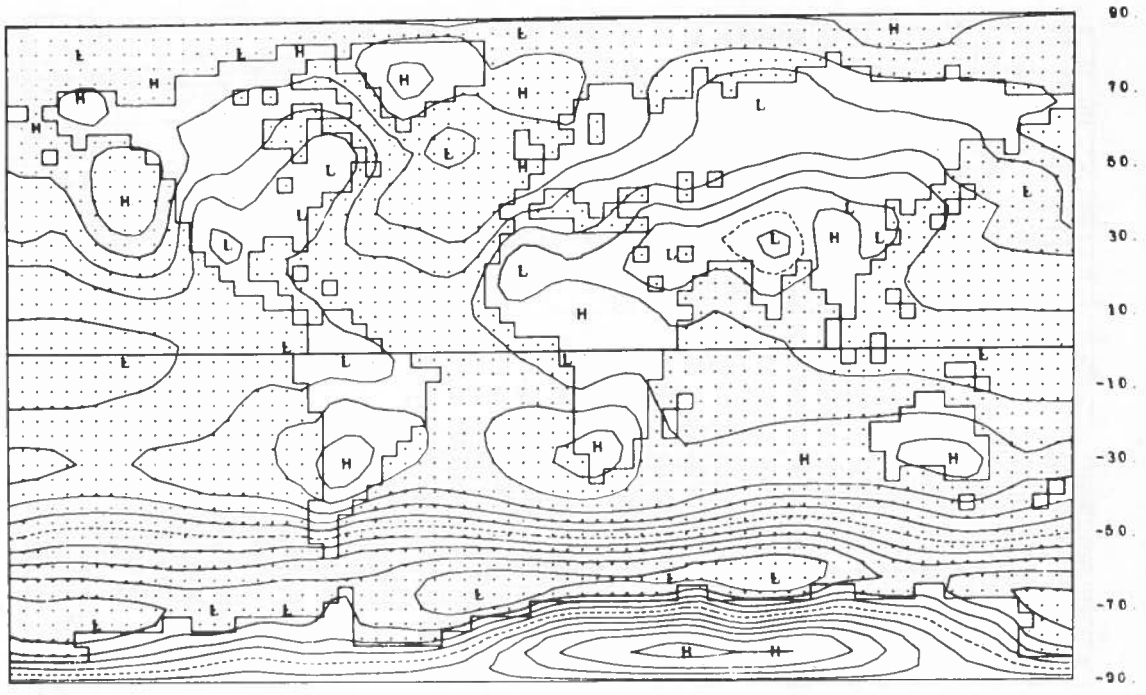

Simulated July mean sea-level pressure, averaged for the three years.

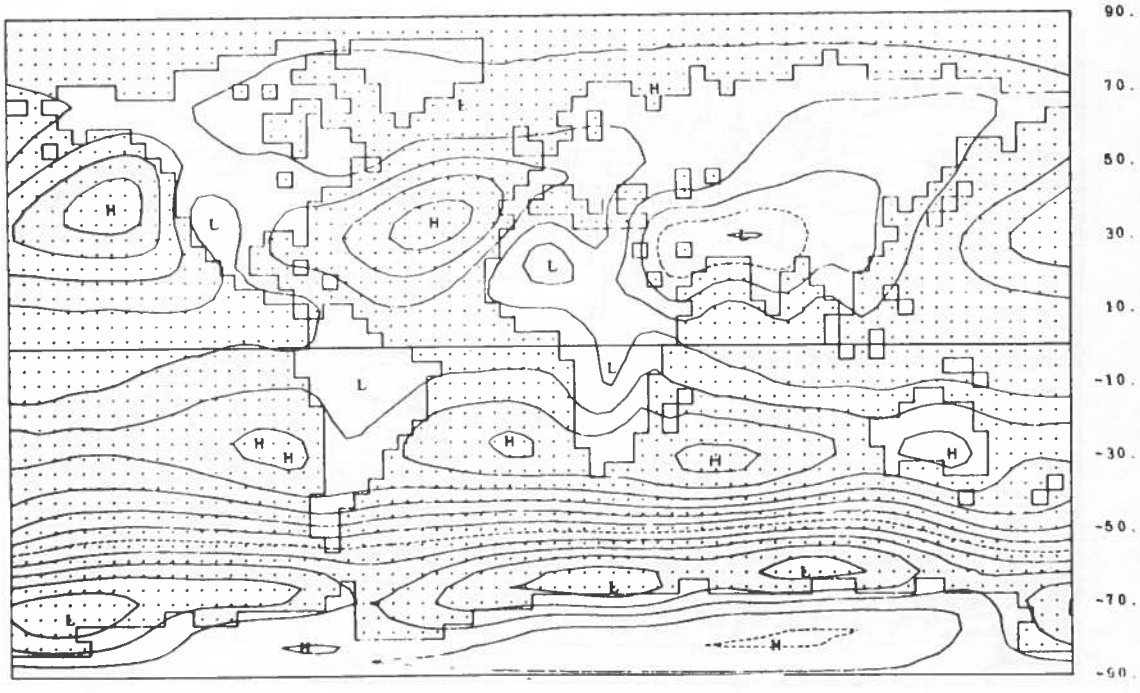

Observed July normal mean sea-level pressure.

Figure 4a. July mean surface pressure reduced to sea level. The isobars are at intervals of 4 mb and the broken-line isobar is 1000 mb.

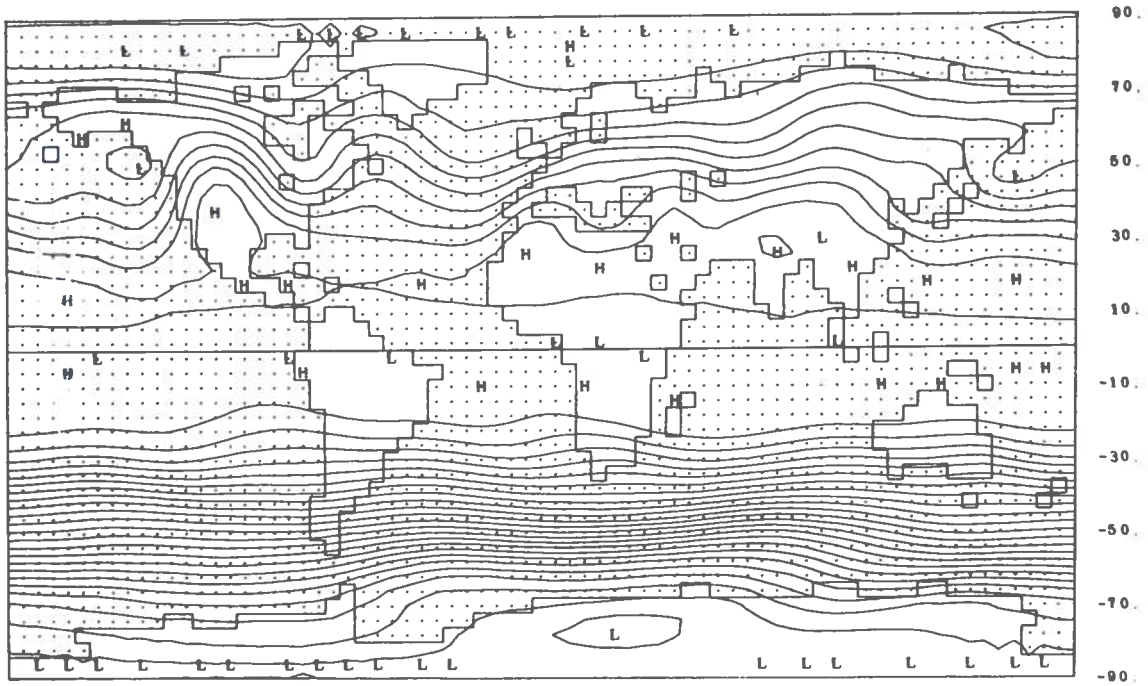

Simulated July mean height, averaged for the three years.

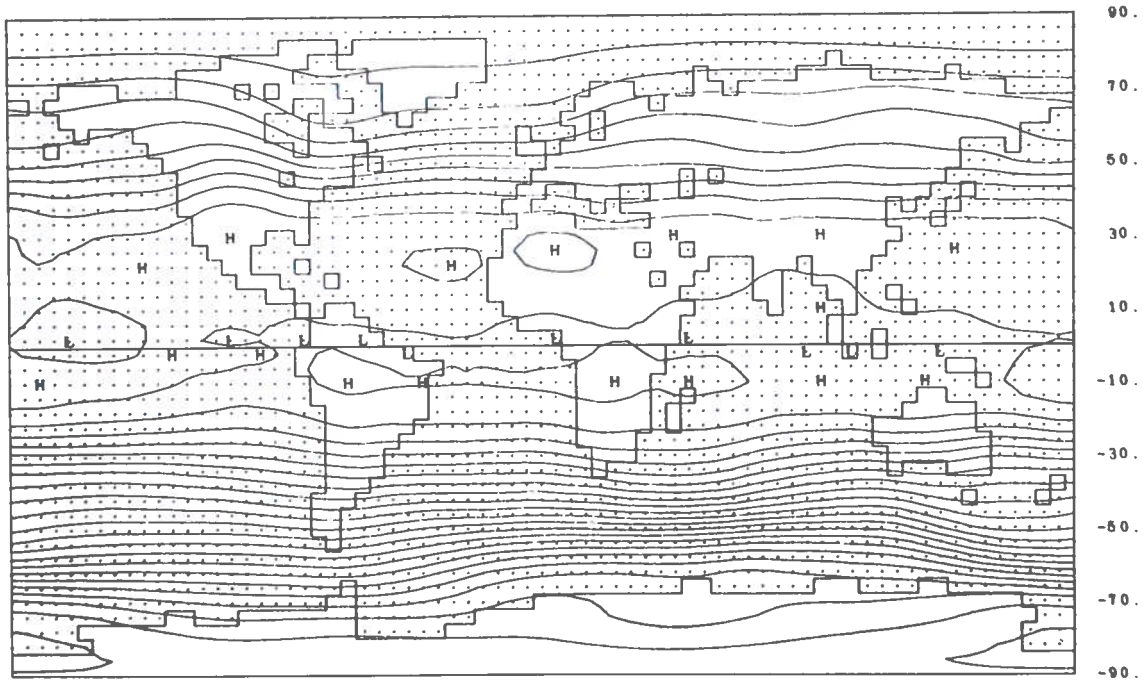

Observed July normal mean height.

Figure 4b. July mean 400-mb height. The height contours are at intervals of 60 meters.

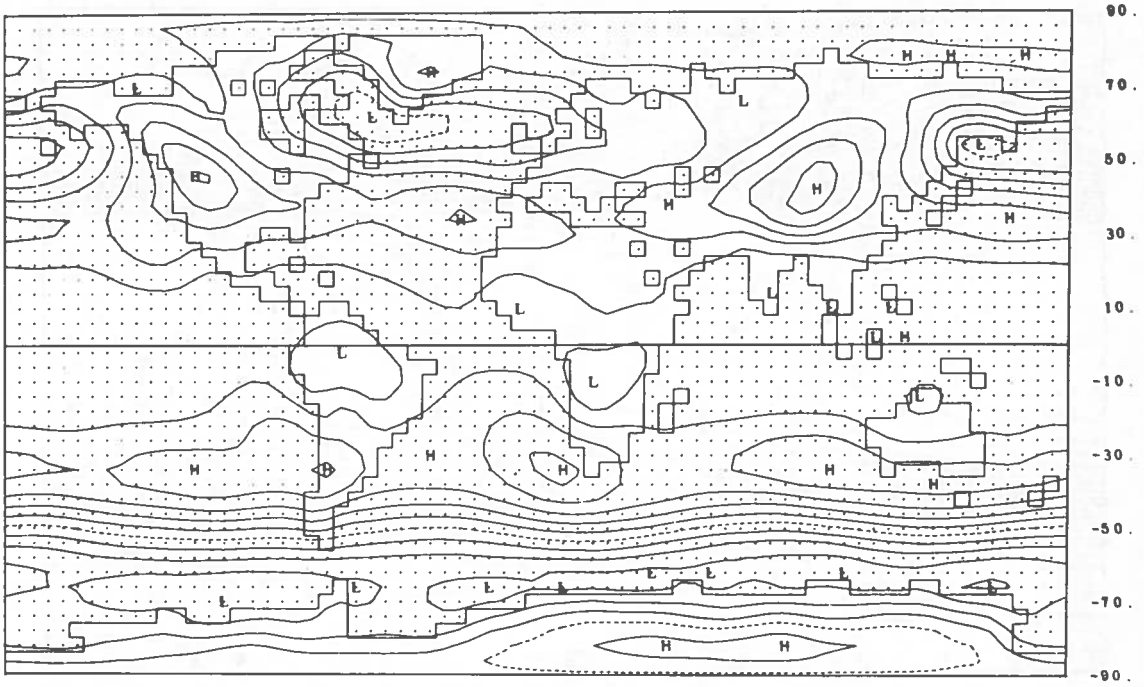

Simulated October mean sea-level pressure, averaged for the three years.

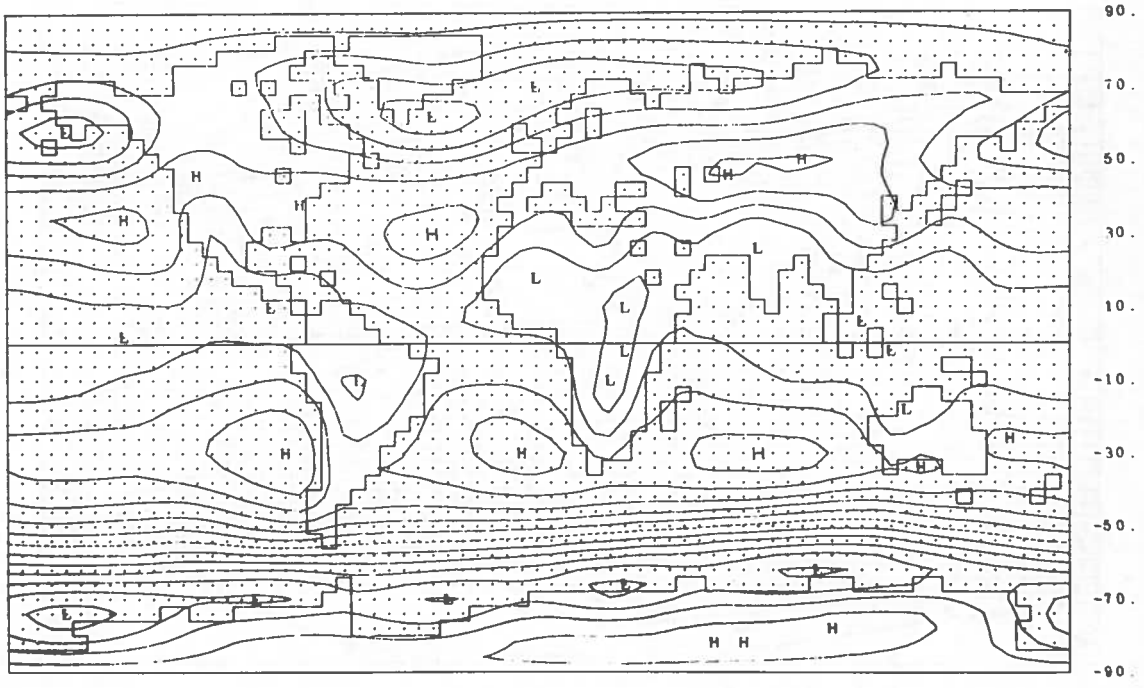

Observed October normal mean sea-level pressure.

Figure 5a. October mean surface pressure reduced to sea level. The isobars are at intervals of 4 mb and the broken-line isobar is 1000 mb.

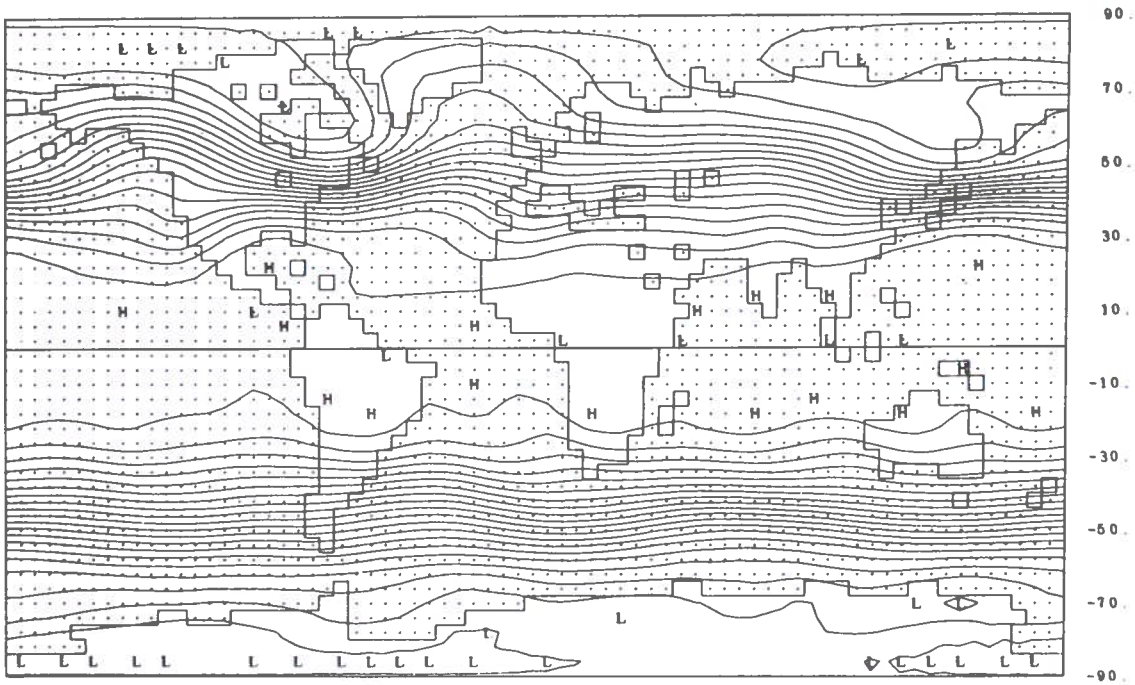

Simulated October mean height, averaged for the three years.

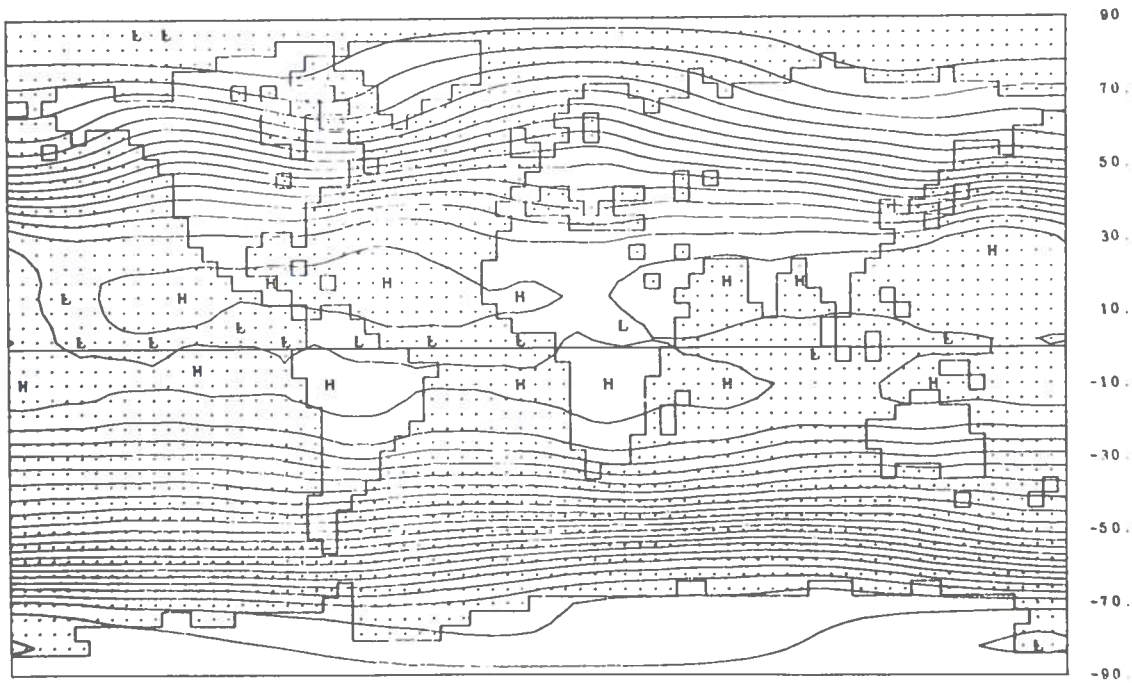

Observed October normal mean height.

Figure 5b. October mean 400-mb height. The height contours are at intervals of 60 meters.

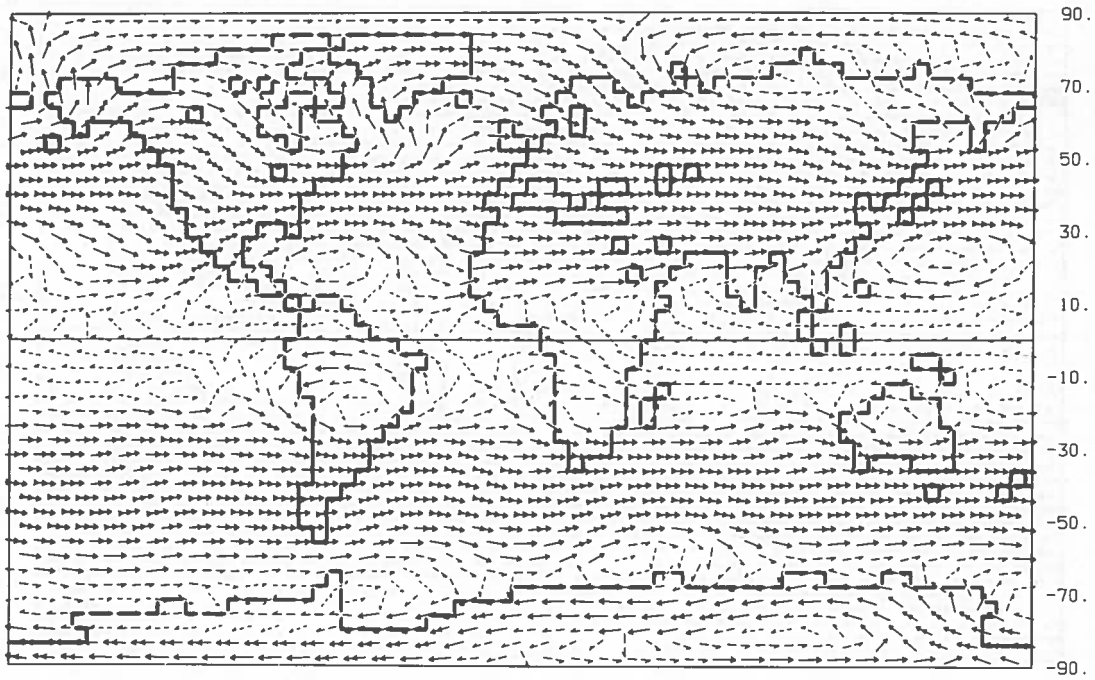

400-mb winds, for the intervals: 0.1 - 3.8 - 7.5 - 13.3 - 22.5 - 58.0 m/sec.

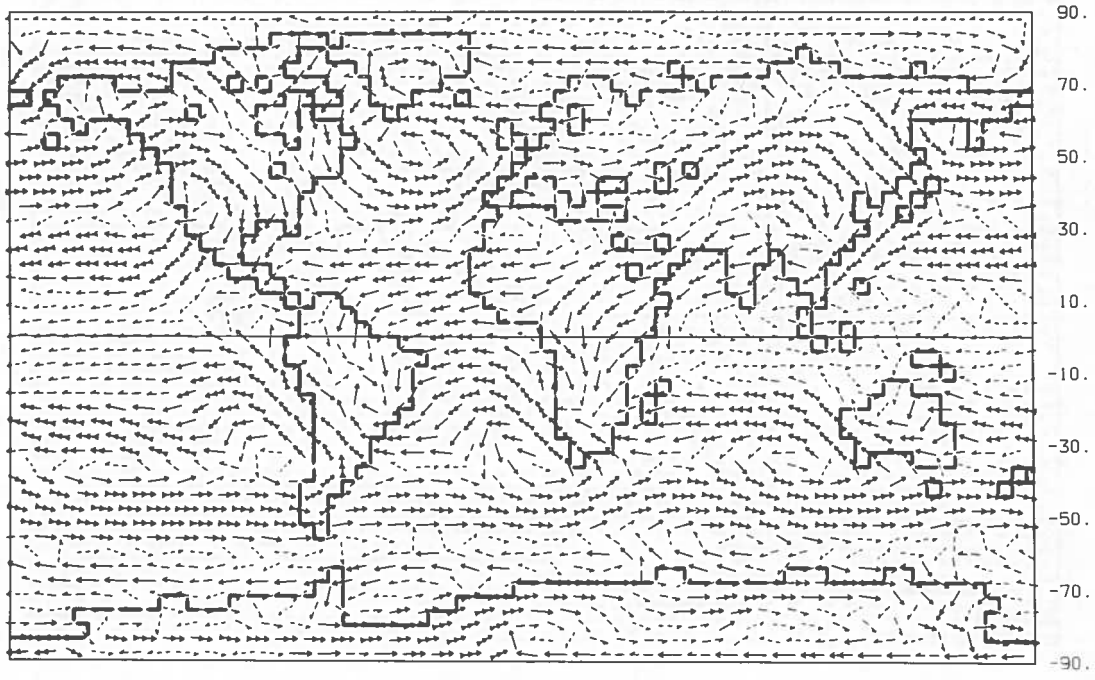

Surface winds, for the intervals: 0.1 - 2.3 - 3.7 - 5.7 - 8.2 - 17.9 m/sec.

Figure 6. Simulated January mean vector winds, averaged for the three years. The directions of the wind vectors conform with the distortion of the streamlines by the map projection. The wind magnitude representation is explained in the text.)

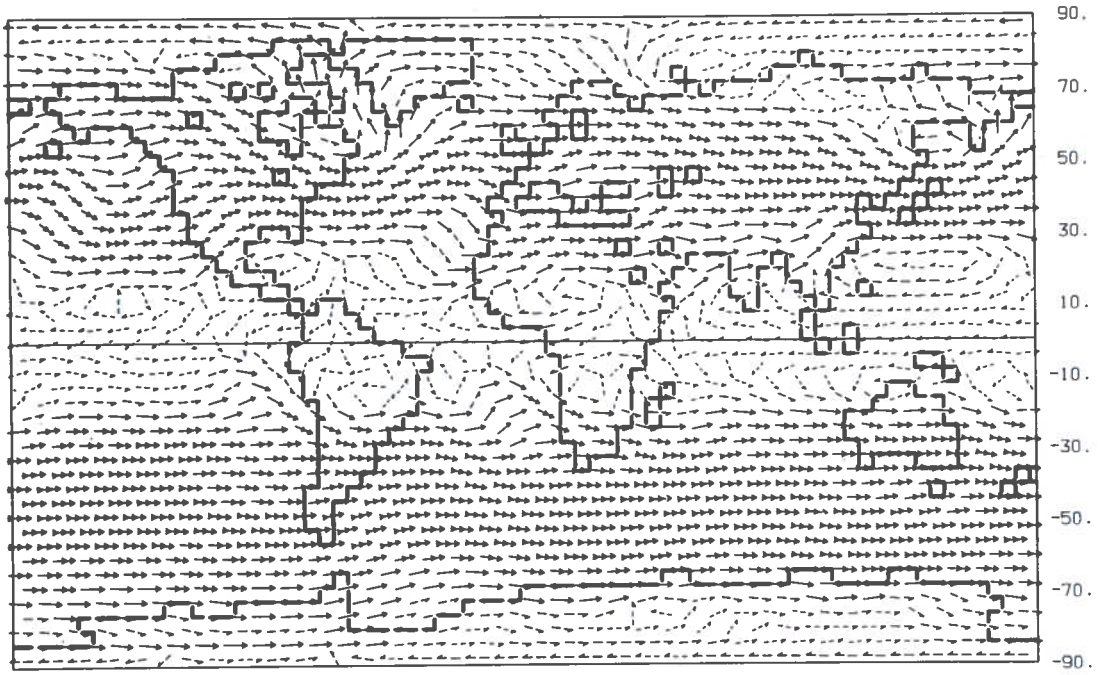

400-mb winds, for the intervals: 0.1 - 2.8 - 6.3 - 13.5 - 22.2 - 46.4 m/sec.

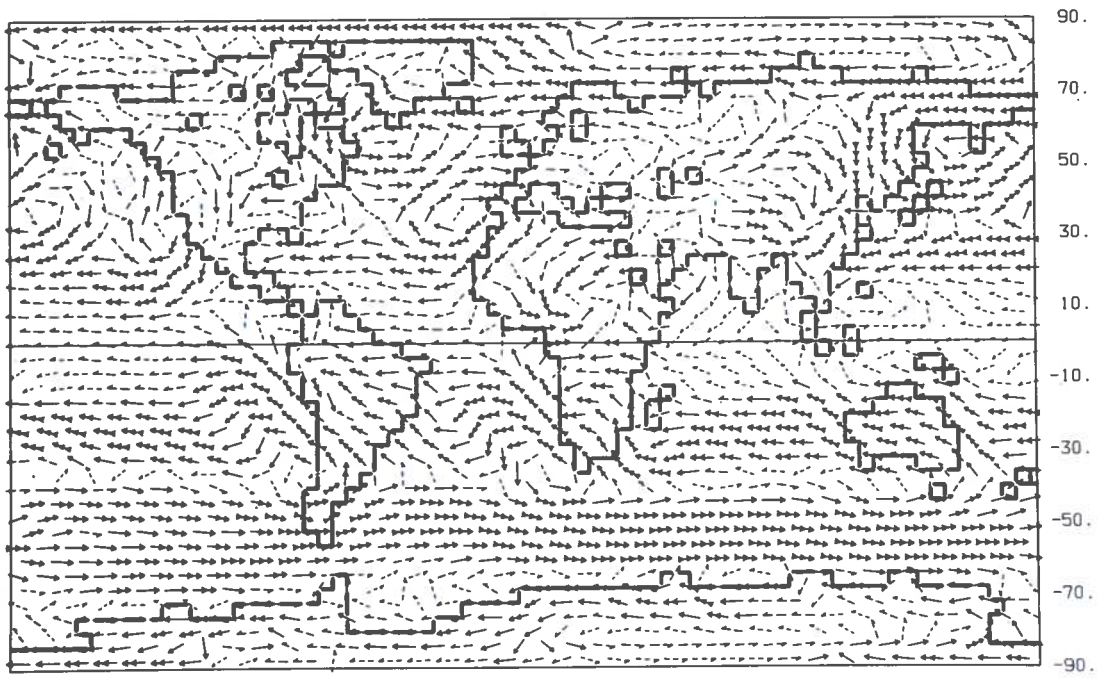

Surface winds, for the intervals: 0.1 - 2.2 - 3.6 - 5.1 - 7.2 - 13.7 m/sec.

Figure 7. Simulated April mean vector winds, averaged for the three years. The directions of the wind vectors conform with the distortion of the streamlines by the map projection. (The wind magnitude representation is explained in the text.)

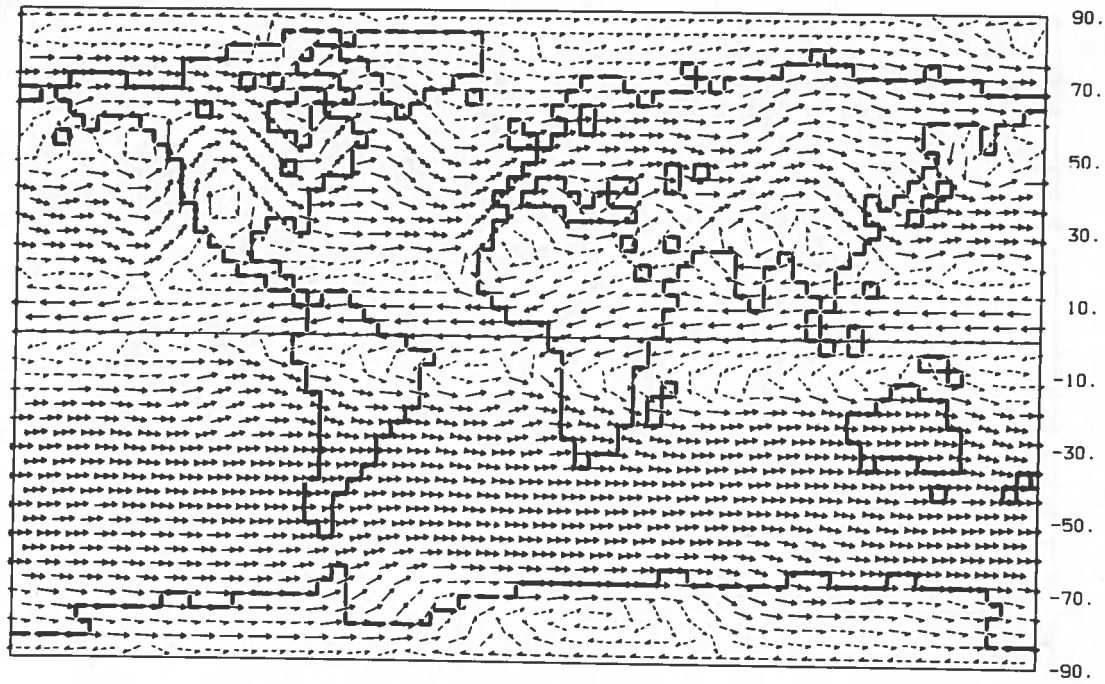

400-mb winds, for the intervals: 0.1 - 4.3 - 7.1 - 10.6 - 19.3 - 34.5 m/sec.

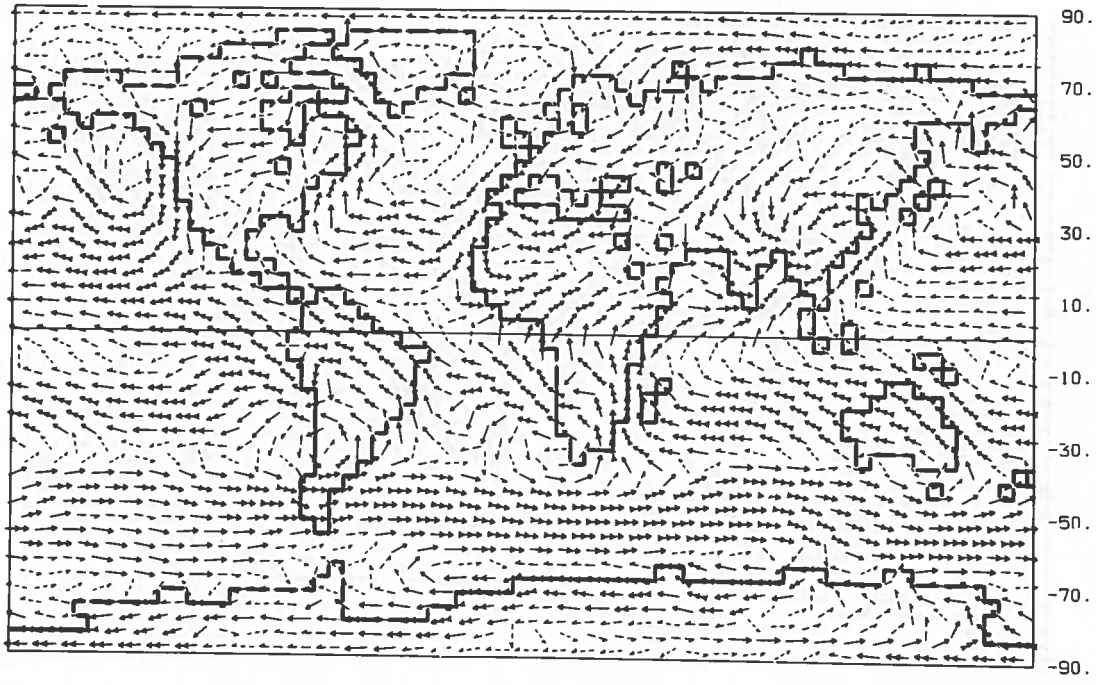

Surface winds, for the intervals: 0.1 - 2.3 - 3.5 - 4.9 - 7.1 - 14.8 m/sec.

Figure 8. Simulated July mean vector winds, averaged for the three years. The directions of the wind vectors conform with the distortion of the streamlines by the map projection. (The wind magnitude representation is explained in the text.)

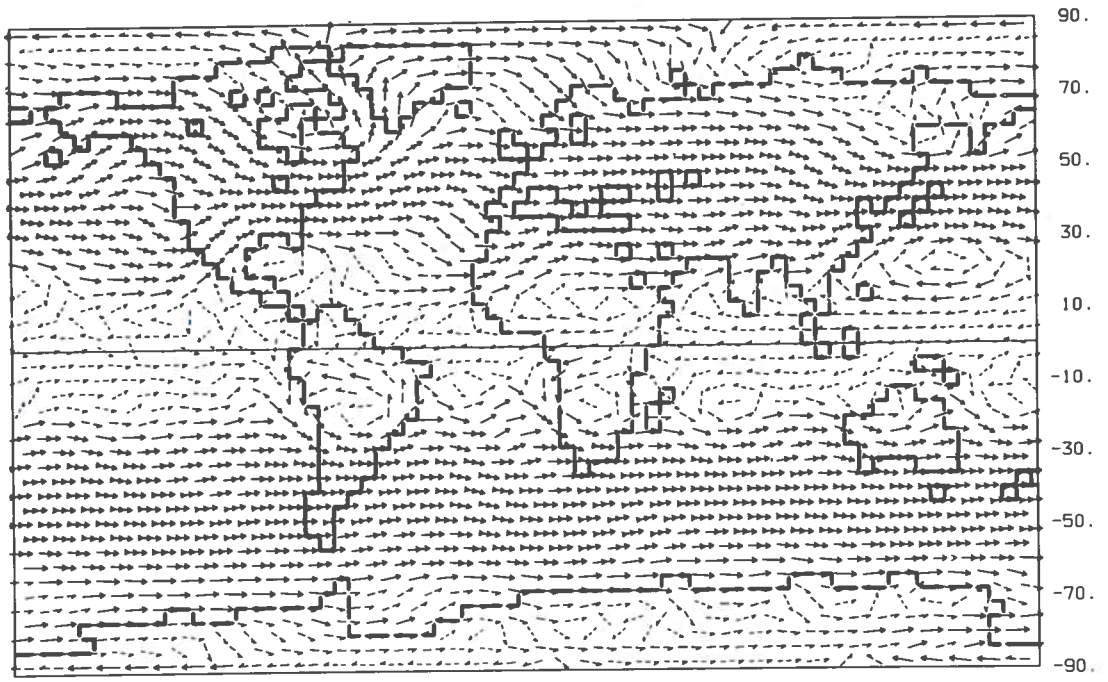

400-mb winds, for the intervals: 0.1 - 3.1 - 6.4 - 12.6 - 21.3 - 49.2 m/sec.

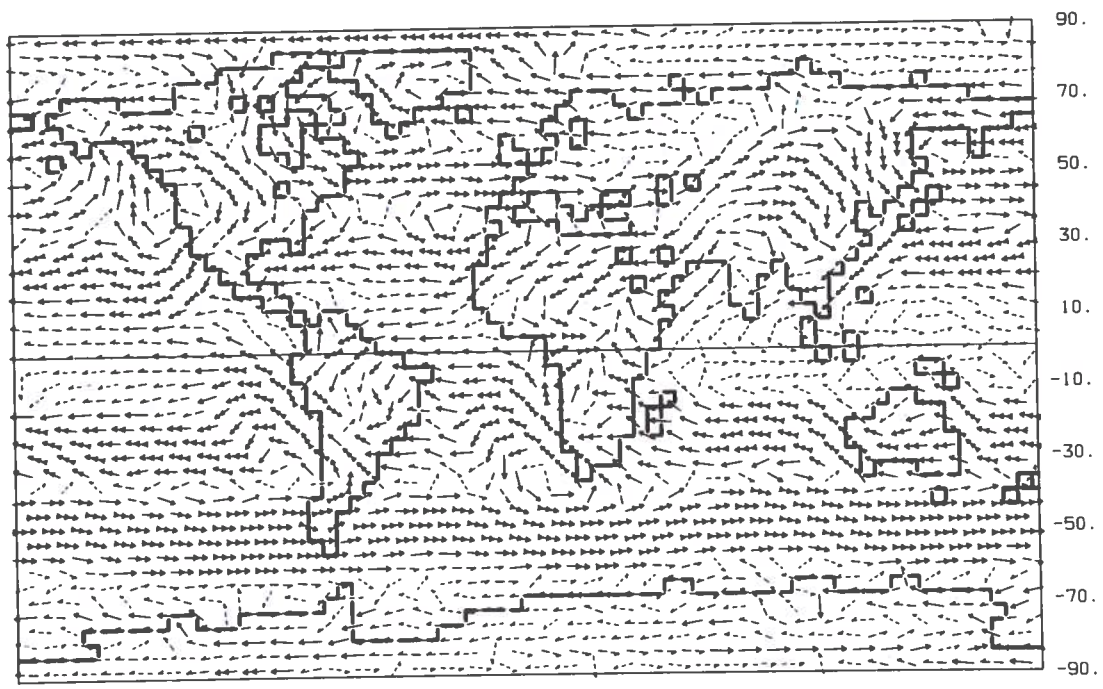

Surface winds, for the intervals: 0.1 - 2.0 - 3.2 - 4.6 - 6.9 - 12.1 m/sec.

Figure 9. Simulated October mean vector winds, averaged for the three years. The directions of the wind vectors conform with the distortion of the streamlines by the map projection. (The wind magnitude representation is explained in the text.)

If we compare these winds with the corresponding 400-mb height and sea-level pressure fields, we see that the winds are quasi-geostrophic (blowing parallel to the height contours or isobars, and with a magnitude proportional to the horizontal pressure gradient), except near the equator (or where there is a large height difference between the surface winds and the sea-level pressure, as over central Greenland in January, where the surface winds are westerly but the sea-level pressure increases from south to north).

Within the tropics, the simulated winds show many circulation features not revealed by the 400-mb height and sea-level pressure fields, either because the analysis intervals of 60 meters and 4 millibars are too large there, or because the winds have large ageostrophic components. When compared with observed climatology, the tropical trade winds and the seasonal African-Asian monsoon winds are fairly well simulated, but the simulated intertropical convergence zone is too broad and diffuse.

INTER-ANNUAL VARIATIONS

Figures 10 through 13 show the individual monthly mean fields of sea-level pressure for the months of January, April, July, and October, in each of the three simulated years.

Although the sea surface temperature and the distribution of the sea ice were held constant, the simulated individual monthly mean fields are not the same in the same calendar month of each year. For example, there is a well developed high-pressure system over Europe and the western Mediterranean in January in year I, but not in years II and III. The North Atlantic Low is displaced to the northwest and the North Atlantic and North Pacific subtropical Highs are better developed in April in year II than in years I and III. The North Atlantic High is better developed in July in years I and III than in year II. In October in year II the principal North Atlantic Low center is north of England; in year III it is west of Greenland. And if we subtract the monthly mean simulated sea-level pressures of one year from those of another year for the same calendar month, we obtain differences of the order of 20 mb and more. On the whole, these simulated inter-annual variations are not unlike the year-to-year variations of the real atmosphere.

CONCLUSIONS

The numerical simulation fairly successfully reproduced most of the principal features of the observed seasonal tropospheric circulation, in spite of the fact that the prescribed sea surface temperature and distribution of the sea ice were held constant throughout the simulation. The major shortcomings of the simulation were excessive blocking of the northern-hemisphere upper-tropospheric flow field, excessively large-amplitude northern-hemisphere stationary waves in summer, and a too broad and diffuse intertropical convergence zone.

The numerical simulation also produced inter-annual variations similar to those of the real atmosphere. Because the external forcing of the model atmosphere was exactly the same from year to year, these inter-annual variations were therefore an internal property of the atmosphere. Whether or not variations of this kind are predictable is an open question. Because of these inter-annual variations, we will need to make numerical integrations over many years of simulated time in order to simulate the normal climate, or to obtain definitive conclusions from numerical climate modification experiments.

We are in the process of improving the model, so as to obtain better simulations of the atmospheric circulation and global climate. One of the major improvements is a better parameterization of the planetary boundary layer and the interacting cumulus convection. We are also extending the domain of the model downward, by coupling it with the multi-level world ocean model of Dr. Kenzo Takano, and making the sea ice a prognostic variable. We plan to extend the domain upward too, by moving the upper boundary from the 200-mb level to the mesopause, with ozone and possibly other photochemically active constituents as additional prognostic variables.

ACKNOWLEDGMENTS

The authors wish to thank Daniel Sabsay, Stephen Schleimer, Donna Hollingworth, and Christopher Kurasch for their considerable assistance in programming the numerical general circulation model; and A.B. Nelson, of the Rand Corporation, for the use of his map analysis contour program. We also thank the Central Computing Network of UCLA for intra-mural computing support. Partial support for the research reported here was also

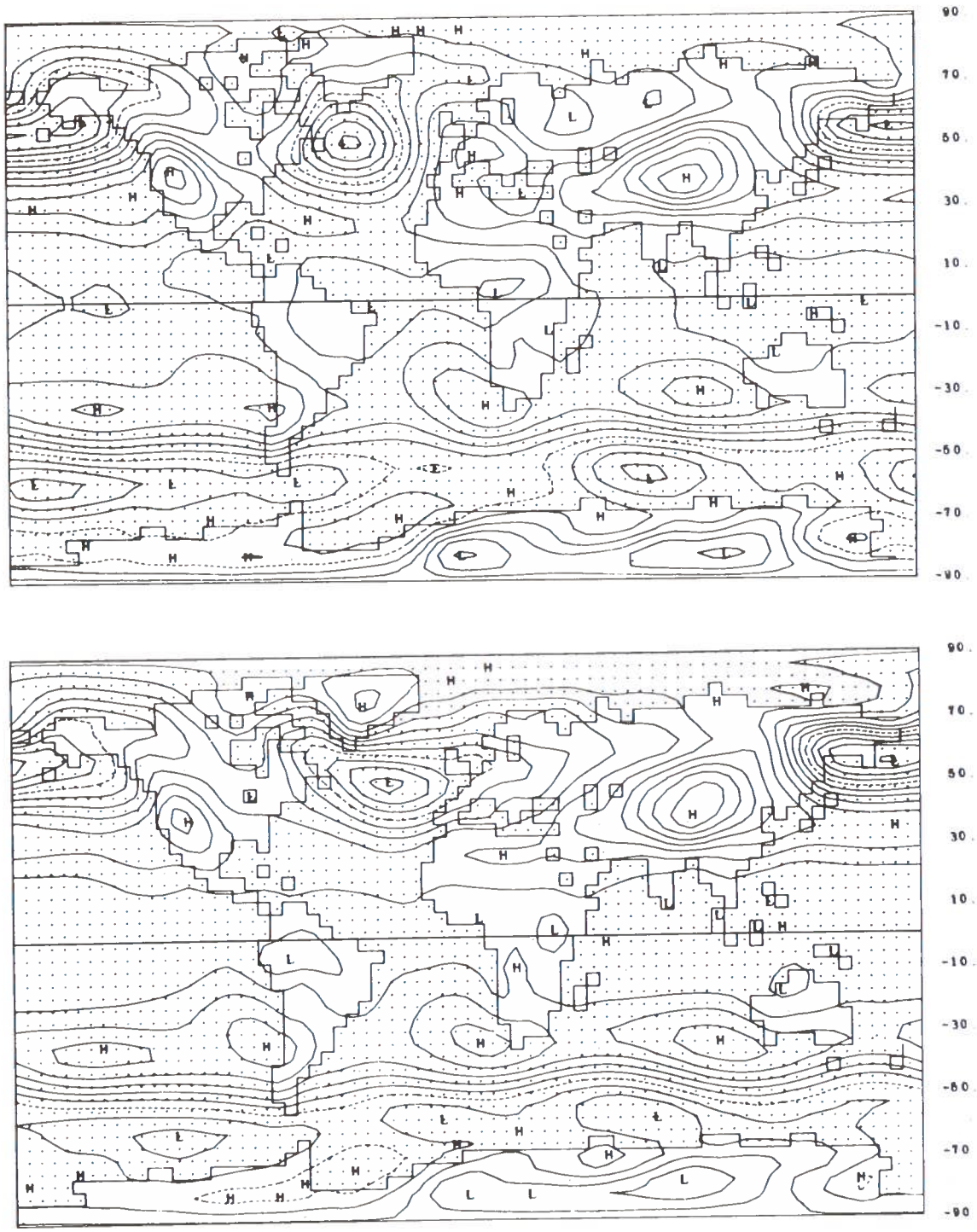

Figure 10a. Simulated January mean sea-level pressure for year I (top) and year II (bottom). The isobars are at intervals of 4 mb and the broken-line isobar is 1000 mb.

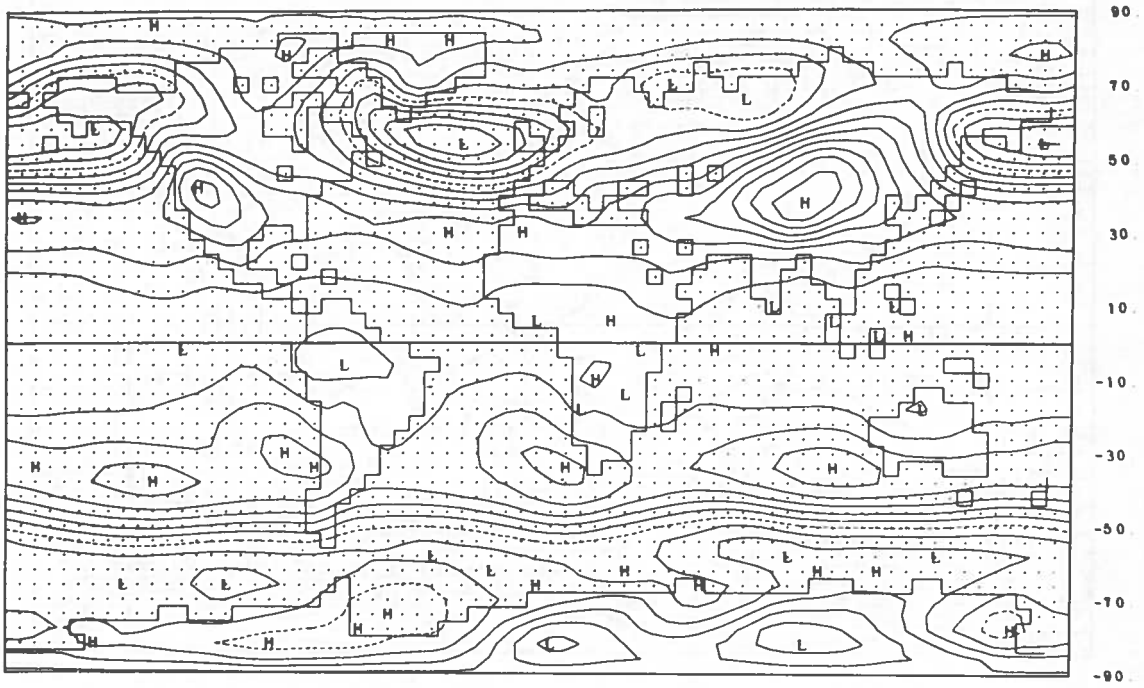

Figure 10b. Simulated January mean sea-level pressure for year III. The isobars are at intervals of 4 mb and the broken-line isobar is 1000 mb.

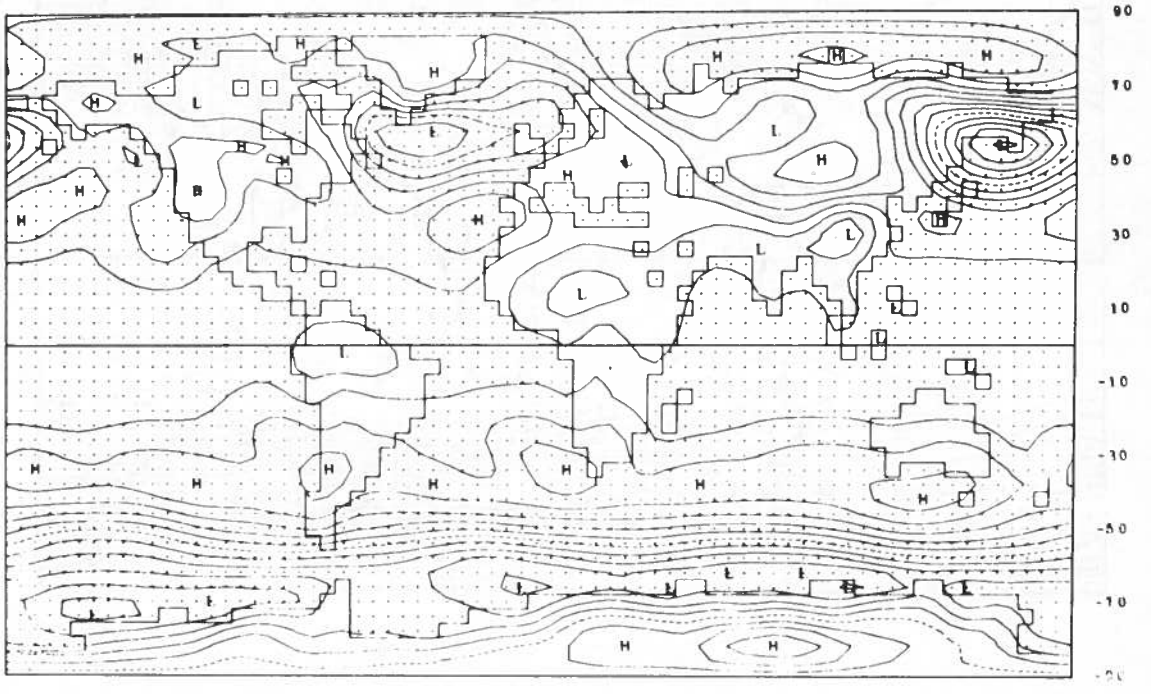

Figure 11b. Simulated April mean sea-level pressure for year III. The isobars are at intervals of 4 mb and the broken-line isobar is 1000 mb.

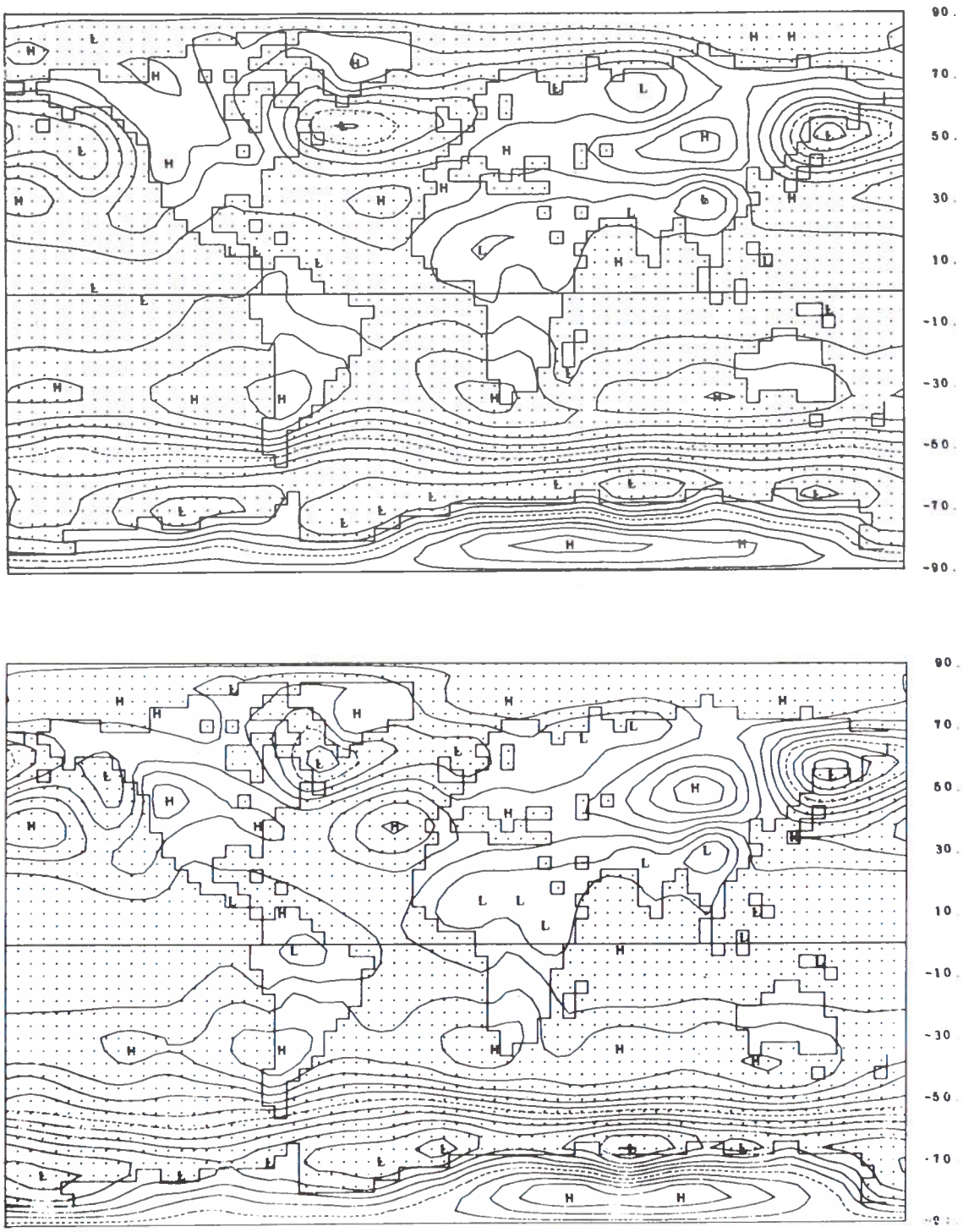

Figure 11a. Simulated April mean sea-level pressure for year I (top) and year II (bottom). The isobars are at intervals of 4 mb and the broken-line isobar is 1000 mb.

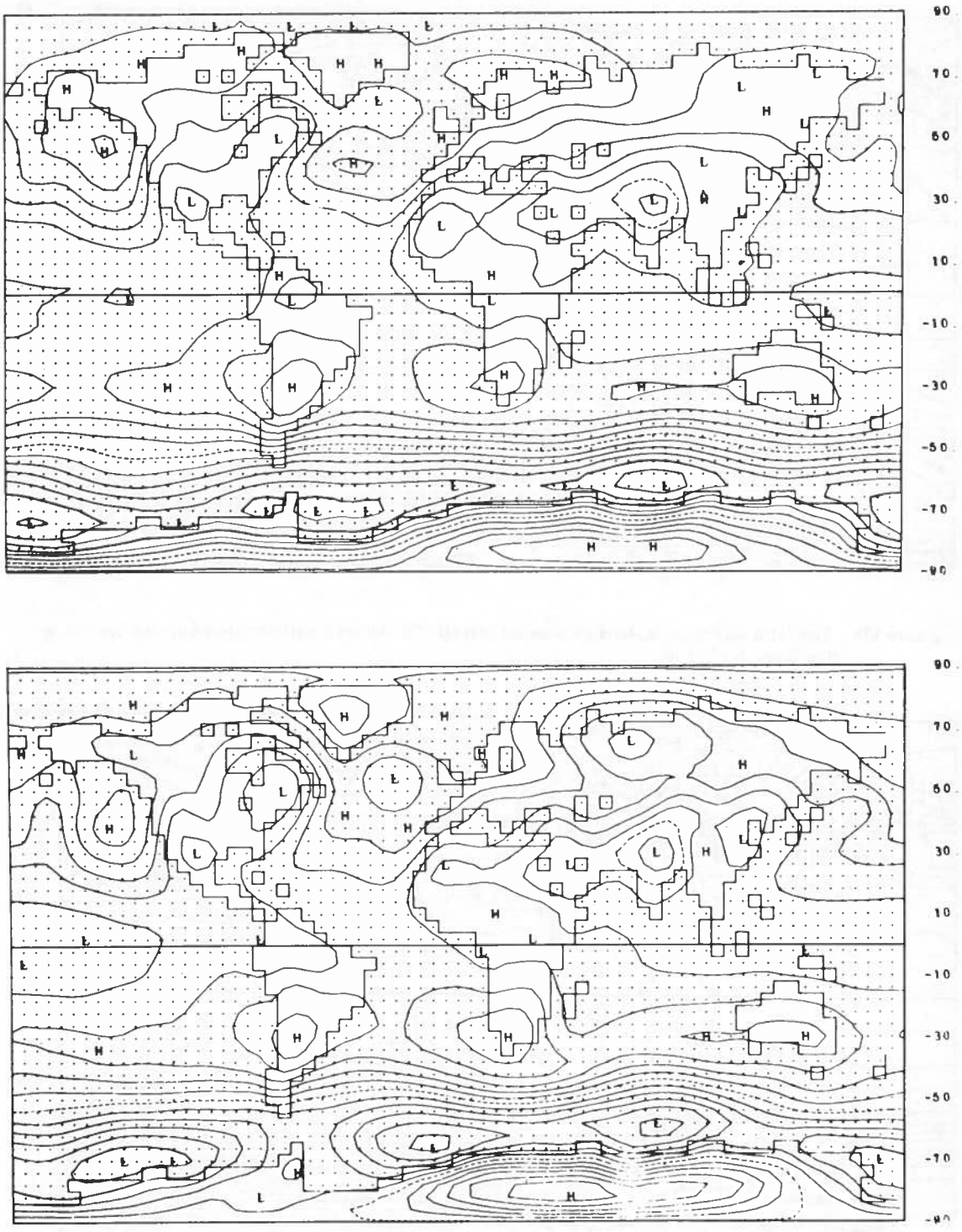

Figure 12a. Simulated July mean sea-level pressure for year I (top) and year II (bottom). The isobars are at intervals of 4 mb and the broken-line isobar is 1000 mb.

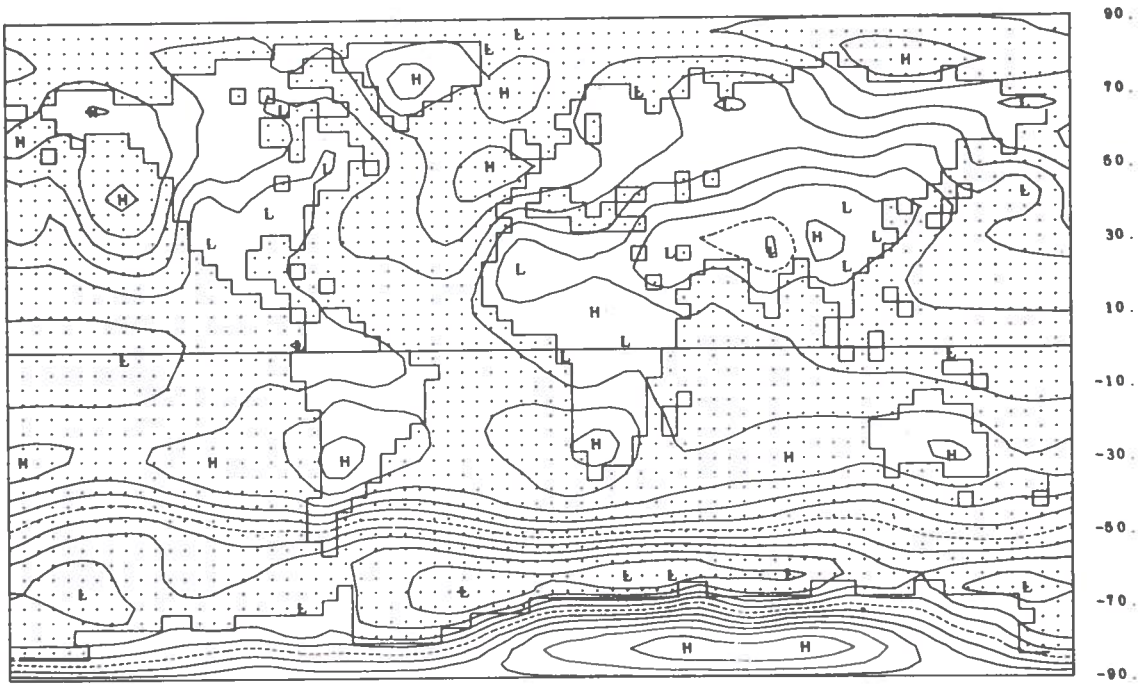

Figure 12b. Simulated July mean sea-level pressure for year III. The isobars are at intervals of 4 mb and the broken-line isobar is 1000 mb.

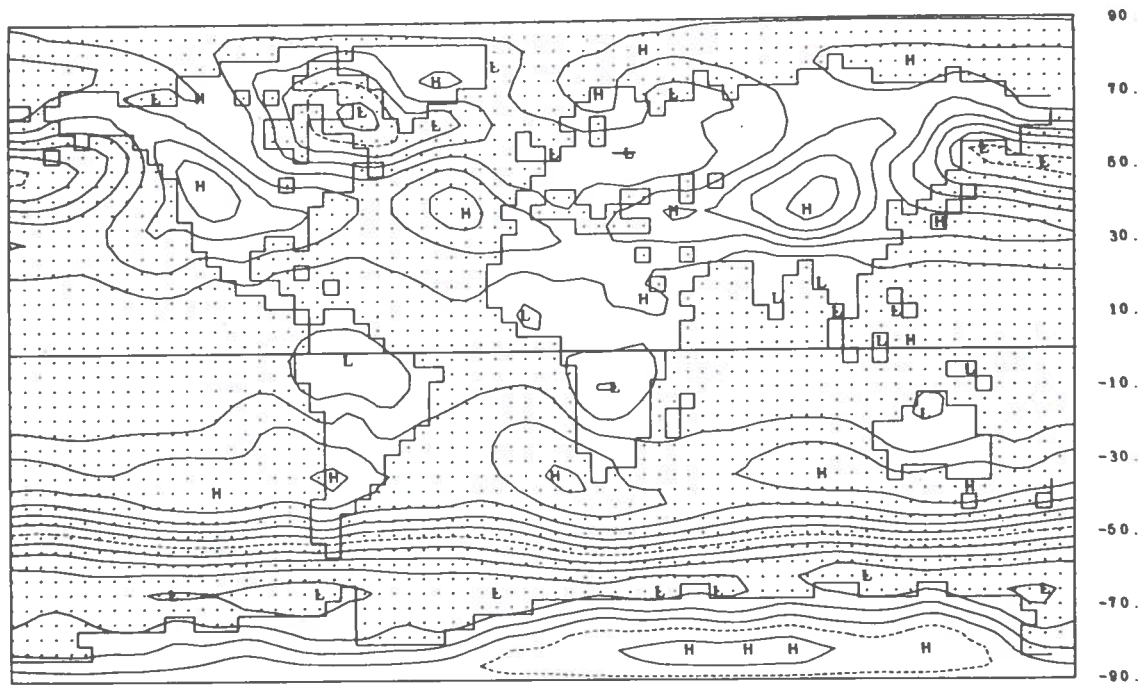

Figure 13b. Simulated October mean sea-level pressure for year III. The isobars are at intervals of 4 mb and the broken-line isobar is 1000 mb.

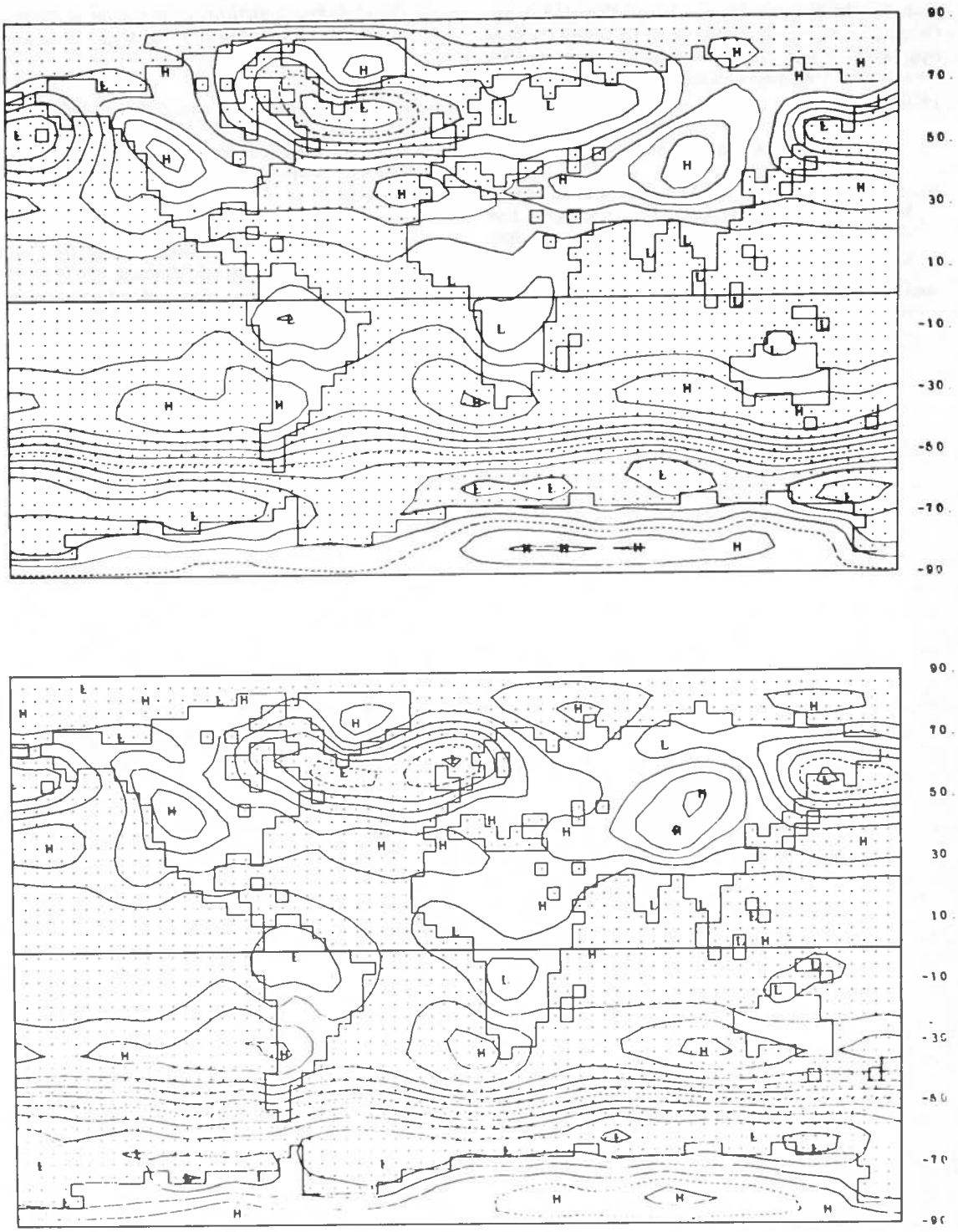

Figure 13a. Simulated October mean sea-level pressure for year I (top) and year II (bottom). The isobars are at intervals of 4 mb and the broken-line isobar is 1000 mb.

given by the National Science Foundation, U.S.-Japan Cooperative Science Program (Grant GF-369). The principal support was provided by the National Science Foundation, Atmospheric Sciences Section (Grant GA-1470).

REFERENCES

Arakawa, A., "Design of the UCLA General Circulation Model". Tech. Report No. 7, *Numerical Simulation of Weather and Climate,* Dept. Meteorology, Univ. California, Los Angeles, 1972, 122 pp.

Arakawa, A., Katayama, A., and Mintz, Y., "Numerical Simulation of the General Circulation of the Atmosphere". In *Proc. WMO/IUGG Symposium on Numerical Weather Prediction, Tokyo, 1968,* Meteor. Soc. Japan, 1969, pp. IV. 7-IV.8.12.

Gates, W.L., Batten, E.S., Kahle, A.B., and Nelson, A.B., *A Documentation of the Mintz-Arakawa Two-Level Atmospheric General Circulation Model,* R-877-ARPA, The Rand Corporation, Santa Monica, Calif., 1971, 408 pp.

Schutz, C., and Gates, W.L., *Global Climatic Data for the Surface, 800 mb, 400 mb: January,* R-915-ARPA, The Rand Corporation, Santa Monica, Calif., 1971, 173 pp.

THE MEASUREMENT OF MINOR STRATOSPHERIC CONSTITUENTS USING HIGH-ALTITUDE AIRCRAFT

I. G. POPPOFF
Earth Science Applications Office
NASA-Ames Research Center
Moffett Field, California

ABSTRACT: The use of aircraft for stratospheric sampling applications is discussed. It is concluded that aircraft fill a specific need that is complementary to the roles of balloons, rockets, and satellites. Aircraft provide the only means for obtaining spatial data with *in situ* sampling techniques. The problems of sampling from aircraft are relatively straightforward and solvable; a large body of experience exists. Limitations, however, are found in the availability of suitable instruments. The problem is that the background minor constituents in the stratosphere exist in number concentrations of 10^{-10} or less. Instruments capable of measuring a wide range of molecular weights and, hence, capable of discovering new data, are not sufficiently sensitive. A few dedicated instruments, each capable of measuring one or two specific constituents to the desired sensitivities, are available, however. It is concluded that a group of dedicated instruments can be packaged for early acquisition of a limited amount of data needed for model development; however, efforts must continue to develop more versatile instruments.

INTRODUCTION

In order to provide input and verification data for stratospheric models, systems must be devised to measure the concentrations and distribution of minor stratospheric constituents. Indirect or remote measuring systems are limited, at present and in the near future, to ozone and aerosols; thus, it is still necessary to resort to *in situ* techniques using balloon, rocket, or aircraft platforms. All three platforms have their advantages and disadvantages; none can replace another because they are generally complementary in their usages. In brief, a rocket platform has the advantage in maximum altitude capability, the balloon has good altitude and payload capabilities, and the airplane has the advantages of mobility, flexibility, large payloads, and, in most cases, man-attendance.

We will discuss some of the problems and benefits of aircraft use in this paper and leave the discussion of rockets, balloons, and remote techniques to others. Making measurements from aircraft in the stratosphere is quite easy in many respects and quite difficult in others. Let's consider the good things first.

AIRCRAFT OPERATIONS

Aircraft are mobile. They can, in principle, be operated from airports all over the world; they are not restricted to a limited number of launch sites. Inasmuch as they can fly over large horizontal distances they provide an opportunity for global coverage second only to satellites. Aircraft are the only available platforms for three-dimensional *in situ* studies of the distribution of atmospheric constituents. With moderately efficient usage, they can also be shown to be very cost-effective; this is a very important consideration in these days of declining budgets and inflating costs.

Laboratory-oriented researchers will find that most aircraft provide a friendly environment for the operation of instruments—at least as compared to rockets, balloons, and spacecraft—and hence the design and cost of instrumentation are not much greater than they would be for comparable laboratory equipment; indeed, laboratory equipment can be used with only minor modifications. This is because most aircraft are heated and pressurized, carry large payloads, and have very generous power supplies. In many

cases, experimenters can accompany their instruments, fiddle with the knobs, check performance and calibration, and make minor repairs. These are significant advantages for most researchers.

There is also a considerable body of experience in conducting research from aircraft; it exists in laboratories operated by DOD, NOAA, NCAR, AEC, NASA, and several universities, and can be tapped simply by asking. Several institutions have groups whose sole mission is to operate research aircraft and to help experimenters use these facilities.

Ames Research Center is one such institution, and two of the Ames aircraft suitable for stratospheric research are illustrated in the following figures. The Ames CV-990 (Figure 1) has been operated as a flying laboratory for 7 years and has carried as many as 15 experiments at one time. Figure 2 shows the interior during one such expedition. Note the modular experiment stations and a central data acquisition system which also serves as a limited in-flight computation facility. This mode of operation can provide the opportunity to make many kinds of measurements simultaneously in the lower stratosphere (the operational ceiling is approximately 14 km) and to compare several kinds of instruments for the measurement of a specific atmospheric constituent. Table 1 lists some of the facilities that are available.

Table 1. Support Facilities in CV-990.

Power

(A)· 400 Hz ±1%; 200/115V ±1.5%; 3-phase
Approximately 40 KVA available

(B) 60 Hz ±0.25%; 115 V ±1%
Approximately 14 KVA available

– Cabin, cargo, and electronics compartments pressurized to 8,000 ft when aircraft is at 40,000 ft.

– Humidity averages 10%

– Temperature range is 65°F to 74°F

– Exterior boundary layer: Thickness grows 1.0 inch per every 100 inches of travel aft from nose

Data Systems

* Astrodata Model 6190 Time Code Generator
* Chrono-Log Model 20,001 Time Code Generator
* Flight instrument and navigation outputs to experiment recorders through Sanborn differential amplifiers

Figure 1. Ames CV-990 Research Aircraft.

For higher-altitude measurements, two U-2 aircraft (Figure 3) can be made available (schedules permitting). The operational ceiling of these aircraft is approximately 20 km, which is comparable to the operating altitudes of the faster supersonic aircraft. Figure 4 is a diagram of the instrument bay of a U-2; Table 2 lists power, payload, and environmental details as guidance for potential experimenters. Unfortunately, experimenters cannot accompany their equipment; hence, the instruments must be capable of safe, reliable operation for the duration of the flight. The pilot can only turn equipment on or off and fly the designated routes.

Figure 3. Ames U-2 Earth Resources Aircraft.

Figure 2. Interior of CV-990, Showing Experiment Stations.

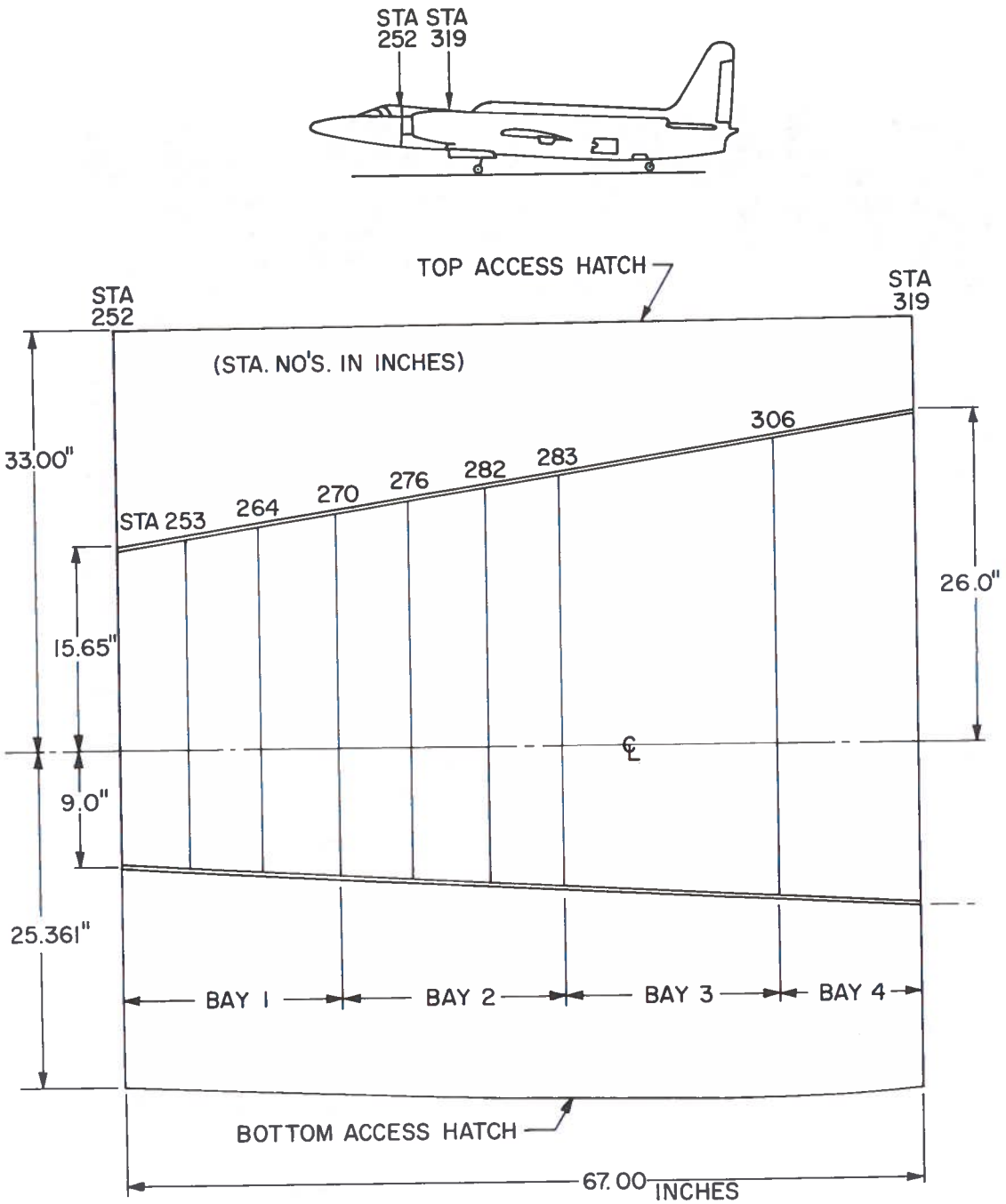

Figure 4. U-2 Equipment Bay Diagram.

Table 2. Support Facilities in U-2

Payload Weight	400 lb
Temperature Range	5° C to 10°C at inlet 15° C to 25°C at outlet
Exterior Boundary Layer Thickness at Equipment Bay	2.0 inches
Pressure	3.88 lb/in^2 outside ambient. (Emergency dump is 4.38 lb/in^2 above ambient).
Electrical Power	A. 320 to 450 Hz, 208/120 ±5 V, 8.0 KVA available. B. 28 ±1.0 V, 100 A available. C. 400 ±10 Hz; 115 ±2-1/2 V, 3-phase, 750 VA available.

Load Factors

		Stress Level
Down	6.0 G	Ultimate
Up	2.5 G	Ultimate
Side	2.5 G	Ultimate
Aft	2.5 G	Ultimate
Fwd.	8.0 G	Ultimate (permanent set permitted)

Consider factors individually, not vector additions.

SAMPLING FROM AIRCRAFT

Sampling the atmosphere from aircraft is reasonably straightforward and uncomplicated, for non-reactive gases. A considerable number of atmospheric sampling programs have been and are being conducted. It is necessary only to provide an inlet that extends through the boundary layer and is forward of the engines and vents. Experience to date indicates that with these precautions, the influence of the aircraft is insignificant. The boundary layer on the CV-990, for example, is on the order of a few cm; it is similar on the U-2. The collection of particulate material requires careful consideration to insure isokinetic flow through the inlet in order not to discriminate against the smaller particles. Reactive gases require individual consideration; in some cases special materials may be required for interior surfaces of the sampling train (e.g., Teflon appears to be suitable for sampling ozone), whereas in other cases very short lines or heated inlets may be required. Obviously, the experimenter must verify the adequacy of his equipment; to a large extent this can be done in the laboratory before flying.

The nature of aircraft operations is such that the ram air flow will vary considerably during a flight. For many experiments, calibration of instrumentation as a function of airflow and pressure is sufficient. Some instrumentation, however, requires regulation; this can be manual for man-attended operation but must be automatic for applications in the higher-flying aircraft, such as the U-2 and RB-57.

LIMITATIONS OF INSTRUMENTS

When we consider the types of instruments available, the picture is not so optimistic. The problem we are addressing is that of obtaining measurements of the natural, background, minor constituents of the stratosphere. In order to put this in perspective, let us consider the concentrations predicted for some of these minor constituents. A partial list is presented in Table 3. Note that these concentrations are not presented with a high degree of confidence; most have not even been detected, much less measured, and with the possible exception of ozone and carbon dioxide, the measurements that have been made are still the subject of some debate. We chose to guesstimate values at 10 and 20 km because this is roughly the range of stratospheric altitudes available to aircraft. The gases CO_2, H_2O, and O_3 have been measured many times and with many instruments, and whether we debate the results or not, we do have order-of-magnitude (or better) values for atmospheric models. The others on this selected list are expected to be found in number concentrations of less than 10^{11} cm^{-3} or in relative abundances of less than 4 ppb at STP; and most are expected to exist in concentrations that are even smaller, by several orders of magnitude.

The ideal airborne measurement system for stratospheric research would have the ability to detect and measure continuously any constituent in any concentration. Of course, it would also be automated and satisfy the payload constraints of a U-2 or RB-57. Such an instrument is necessary because we really don't know what is there and

Table 3. Partial List of Minor Stratospheric Constituents

Constituent	Concentration (particles per cc)		Approx. Ratio of pressure at 20 km to STP
	10 km	20 km	
$O(^3P)$	10^5	3×10^6	10^{-13}
$O(^1D)$	10^{-4}	10^{-2}	3×10^{-22}
* O_3	10^{11}	10^{12}	3×10^{-8}
NO	2×10^{10}	2×10^{10}	6×10^{-10}
NO_2	2×10^{10}	2×10^{10}	6×10^{-10}
* H_2O	2×10^{13}	8×10^{12}	3×10^{-7}
OH	4×10^5	6×10^5	2×10^{-14}
H_2O_2	4×10^7	10^7	3×10^{-13}
* CO_2	10^{16}	4×10^{15}	10^{-4}
CO	3×10^{11}	10^{11}	3×10^{-9}
CH_4	4×10^{11}	10^{11}	3×10^{-9}
CH_3	4×10	10	3×10^{-20}

* measured many times

in what concentration, although we might use certain existing models for guidance and plan our measurements accordingly. We must be able to explore beyond the range of the models if we are to truly understand the stratosphere. Or, in other words, if we only look for certain predicted constituents, we will never discover anything new.

This means that we should look to optical spectroscopy, mass spectrometry, or similar techniques capable of detecting and measuring substances over a wide range of molecular weights.

The state of development of such instruments, however, is not sufficiently advanced to provide us with the capability we need. It's always dangerous to make predictions, but such instruments might be 2-3 years in the future—if indeed there is a clear incentive (i.e., funds) to develop them. At present, measurements with various types of spectrometers are limited to the ppm or possibly the pphm range. These instruments are also limited in their applicability; optical spectroscopy is limited to specific easily resolved lines or bands, and mass spectrometry is limited by some reactive species (e.g., atomic oxygen, water vapor), as well as by resolution (e.g., separation of CO from N_2 or of N_2O from CO_2).

On the other hand, there are instruments capable of the measurement of single specific constituents in the ppb range. Many of these are essentially "off-the-shelf" now; many have actually been used in aircraft for atmospheric sampling; some require a small amount of additional development. For example, water vapor can be measured by frost-point devices or devices that depend on the absorption of water vapor; ozone can be measured through the analysis of surface or gas-phase chemiluminescence or by a liquid-phase reaction with KI; carbon monoxide can be measured by monitoring the mercury vapor released by the reduction of HgO; nitric oxide can be detected by virtue of its very efficient chemiluminescent reaction with ozone; and carbon dioxide can be measured reliably with non-dispersive IR techniques. The overhead burden and some profile information can be obtained for water vapor and ozone by using IR radiometric and UV backscattering techniques, respectively. Instruments based on these kinds of reactions and capable of measuring a single constituent are called dedicated instruments.

Obviously, one is faced with a choice between waiting for the development of wide-ranging detectors suitable for exploratory work or packaging presently available dedicated instruments and obtaining a limited amount of data. The first choice may be more pleasing intellectually, but the second choice is the more practical for obtaining the early data needed to bound theoretical models.

AN EXAMPLE OF A DEDICATED INSTRUMENT PACKAGE

The Ames Research Center has a dedicated instrument package. Designed for use in a U-2 aircraft, it is being tested in a CV-990 until we are satisfied that it can operate reliably and automatically.

Four gas-analysis instruments were selected because they were essentially "off-the-shelf" and had the required sensitivity; three of the instruments had been flown previously, but they all required some modification for stratospheric use. A fifth gas-analysis instrument will be added as soon as its sensitivity is increased. An aerosol collection device will also be flown, but it will be

separated physically from the gas-analysis instruments. Table 4 is a list of the instruments with some notes on their operating principles and sensitivities. Figure 5 schematically shows the automatic flow control system. In practice, not all the instruments will be connected as shown; for example, if it appears that ozone, NO, or water vapor is being lost in the compressor, it will be sampled directly. Figure 6 is a photograph of the package.

A package like this must be dynamic. That is, new and better instruments should be substituted or added as they become available. This example shows a first-generation package that should be ready for U-2 flights within a few months. Already there are plans for modifications.

OTHER APPROACHES

Other laboratories are in the process of developing airborne packages. Some additional ideas will be described in the next paper. The fact that it is possible to make some limited measurements now should not preclude the continued development of more sensitive and more versatile instrumentation; indeed, it is a requirement if we

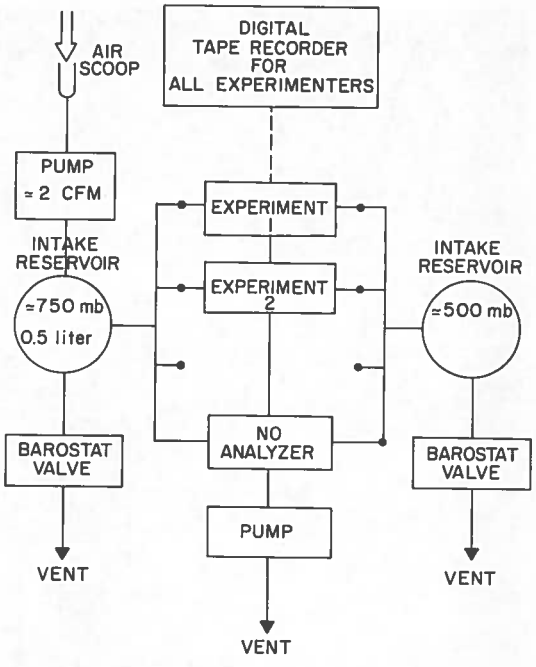

Figure 5. Schematic of Automatic Flow Control System

Table 4. Instruments in Ames Stratospheric Sampling Package

EXPERIMENTER	CONSTITUENT	TECHNIQUE	SENSITIVITY		APPROXIMATE MIXING RATIO AT ALTITUDE	
			ppm STP	Number Density	40,000 ft p = 188mb	70,000 ft p = 45 mb
ARC	CO	Hot Mercuric Acid Reactor		(L_o=3x10^{19}cm^{-3})		
		Hg O + CO	≃10 ppb	≃ 3 x 10^{11}cm^{-3}	≃100 ppb	?
ARC	CO_2	Nondispersive Infrared Abs.	≃ 5 ppm	≃ 1.5 x 10^{14}cm^{-3}	330 ppm	330 ppm
ARC	O_3	Oxidant Meter KI+O_3	≃10 ppb	≃3x10^{11}cm^{-3}	2x10^{12}cm^{-3} 70 ppb	4.5x10^{12} 70 ppb
ARC	H_2O	Crystal Oscill. LiCl Surface	≃ 1 ppm	≃3x10^{13}cm^{-3}	5 ppm	5 ppm
DOT	NO	Chemiluminescent NO + O_3	≃0.5 ppb	≃ 10^{10}cm^{-3}	?	?
NOAA	H_2O	Zenith Radiometer	±0.1μ(3x10^{17})	Total Water Overburden		
		17-23 μ Rotation Band	ΔH_2O ≃ 1x10^{13}		——	——

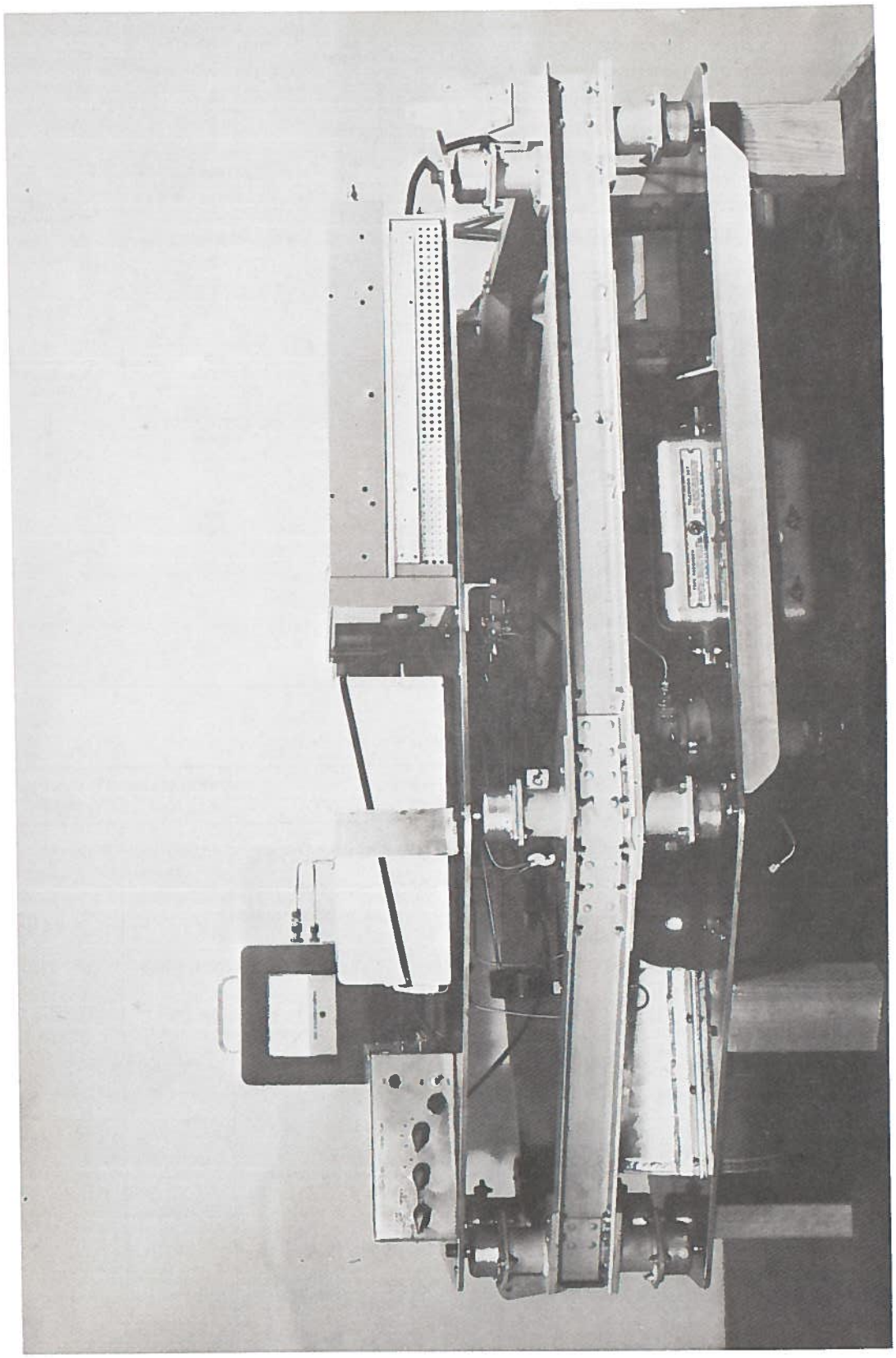

Figure 6. U-2 Stratospheric Analysis Package.

expect to understand the stratosphere well enough to evaluate the impact of future aeronautical operations with confidence.

CONCLUSIONS

The use of aircraft is relatively straightforward and poses no unique or insurmountable difficulties. Spatial distributions of most stratospheric constituents can be studied in no other way.

Instrumentation suitable for stratospheric gas analysis is presently limited to a few dedicated instruments, but these can provide valuable early data while better instruments are being developed.

DISCUSSION

R. Narcisi suggested a design for an air sampler using liquid nitrogen (cryopumping) on the surface or on a sieve. Such a system could be baked out to 10^{-10} to several hundred degrees C, including a viscous leak. A properly designed one-liter volume could sample about 25 atmosphere-liters in about an hour. One could not use it to measure O_3 or OH, but could use it to measure H_2O, CO_2, CH_4, and hydrocarbons. (Oxides of nitrogen or of sulfur could not be reliably measured.) The sample could be taken back to the laboratory for chromatography, mass spectrometry, or chemical analysis under well-controlled conditions. An equivalent real-time instrument might take 3 years to develop; whole-air samplers, however, are both readily fabricated and completely aircraft-transportable; they could even sample SST contrails at the point of emission. He noted that an LN_2 system might cost $3 to 5 K and an LHe system three times that.

N. Sissenwine asked about the size of the area that could be exposed outside the boundary layer on a flat-plate sampling area. B. McCormac asked about putting an IR Fabry-Perot filter on a standard balloon or infrared system for distinguishing ppb constituents. Poppoff said such systems were being developed but were not yet available. C. Gray asked whether the USAF SR-71 would be a useful test bed, since it could fly higher than the U-2. Poppoff said it might, but supersonic sampling was a serious problem. Coroniti noted that the use of the NASA YF-12A was being considered by DOT.

SOME EXPERIMENTAL TECHNIQUES AND PROBLEMS ASSOCIATED WITH STRATOSPHERIC MEASUREMENTS

DONALD F. HEATH
Goddard Space Flight Center
Greenbelt, Maryland 20771

ABSTRACT: Present-day remote sensing technology provides a highly effective means of gathering much of the information required to better understand the structure, composition, and dynamics of the stratosphere. The operational constraints of remote sensors, both satellite and rocket-borne, are considered. Measurement of the variation of solar UV irradiance is discussed and its role in determining the composition of the stratosphere illustrated. A general discussion of the use of stratospheric ozone profiles derived from satellite data to map atmospheric circulation patterns is followed by a brief review of a few recent experiments. The value of simultaneous rocket/satellite measurements is shown and several recent developments in the instrumentation area are reviewed.

INTRODUCTION

The solution of stratospheric problems requires an understanding of the structure, composition, and dynamics of the stratosphere, and its interaction with the troposphere and mesosphere at its boundaries. Essential to this understanding is the acquisition of experimental data, which calls for a diversity of experimental techniques, used from various observational platforms.

The two general methods of observation involve either remote sensing or *in situ* sampling techniques. Currently available observational platforms include satellites, rockets, balloons, high-altitude aircraft, and ground-based stations. Satellite experiments, obviously, can be used only for "remote" sensing of the stratosphere; in the future, we can look forward to the use of the atmospheric science facility presently being considered for the Space Shuttle.

A major problem encountered in performing a satellite experiment is the large time interval which exists between conception of an experiment and the actual launch of the satellite carrying the experiment. Typically, this delay is about four years, and may be more if the satellite fails to achieve orbit and another launch is required. Financial problems also loom large, since experiment costs often are in the one- to two-million-dollar range just for small experiments on the "observatory class" satellites.

Rockets can be used to carry experiments which are capable of either remote or *in situ* observations of the stratosphere. With rockets, the period from experiment conception to launch phase is generally about one year, which represents approximately a four-fold reduction over the satellite case. Costs of rocket experiments are generally measured in hundreds of thousands of dollars.

Balloons and high-altitude aircraft are similarly capable of both remote and *in situ* observations, while ground-based observations, by their very nature, are remote measurements.

The principal advantages of the satellite platform include global coverage (at the expense of vertical resolution), more consistency between successive measurements, and greater economy for a large number of measurements. Rocket-borne instrumentation is much better suited for exploratory investigations: it generally provides better vertical resolution; cost is significantly less when only a single measurement is required; the period required to develop an experiment is shorter; and the experiment is not restricted to a satellite orbit.

The succeeding sections will outline some of the measurement techniques which have recently been used in the acquisition of data on the stratosphere.

REMOTE SENSING – OPERATIONAL CONSIDERATIONS

The ability of a remote sensor to recover data on the distribution of an atmospheric constituent is dependent upon a weighting function which re-

lates the magnitude of the observable to the altitude profile of the constituent. Figure 1 shows an example of the characteristic weighting functions for the 9.6-micron atmospheric emission band of ozone, for both strong- and weak-band absorption. The fact that the true weighting functions for both weak and strong absorption are at a maximum at the same altitude at which the ozone concentration is at a maximum indicates that only one piece of information can be recovered: either the distribution of ozone concentration about the maximum, or the total amount of ozone, may be derived, but not both.

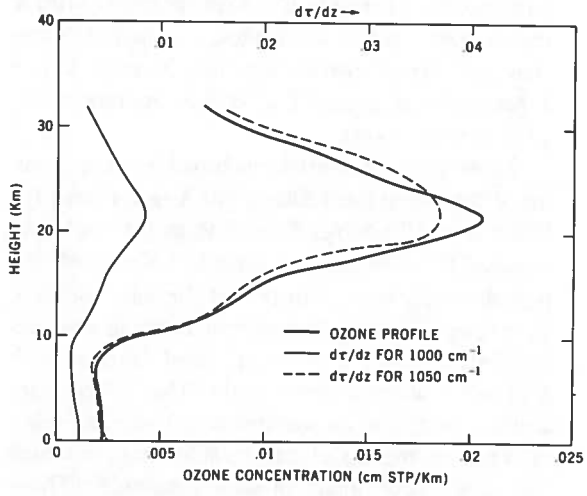

Figure 1. Weighting functions for weak (1000 cm^{-1}) and strong (1050 cm^{-1}) absorption in the 9.6-micron O_3 band, and the corresponding vertical ozone distribution.

In the ultraviolet region of the spectrum, this situation is much improved. Figure 2 shows the weighting functions for scattered UV solar radiation for 8 of the 12 wavelength channels employed in the NASA Backscattered Ultraviolet (BUV) experiment instrument. It is easily seen that the weighting functions are well defined from 30 km to about 55 km. Below 30 km, the problem of reducing this data, by inversion techniques, to obtain an altitude profile of ozone concentration is greatly complicated by the bimodal nature of the weighting functions.

In addition to the requirement for sophisticated data reduction, better radiation standards are needed for absolute optical calibration of atmospheric satellite sensors. As an example, consider the calibration problem associated with the Nimbus

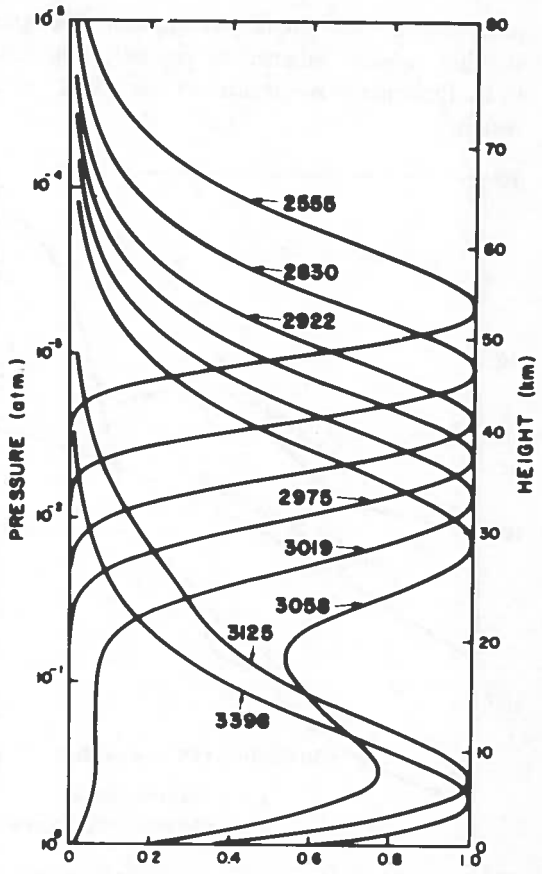

Figure 2. Weighting functions for scattered UV solar radiation; 8 BUV channels centered at wavelength indicated (Å).

4 BUV experiment mentioned earlier. The nature of the problem is illustrated in Figure 3. At 2550 Å, the solar irradiance is about 10^4 greater than the equatorial radiance. Absolute calibration of the instrument must be carried out with the 1000-watt quartz-halogen lamp used as a standard of spectral irradiance. Unfortunately, the spectral irradiance at 2500 Å has an absolute uncertainty of about 8%. Fortunately, only the ratio of earth radiance to solar irradiance, which can be determined more accurately than the absolute value of either, is needed for the derivation of the ozone profile.

Present-day radiometric standards are inadequate by nearly an order of magnitude to permit the interpretation of satellite data in terms of possible long-term climatological effects. A new absolute radiation standard which appears to be more capable of meeting the requirements for investigations of long-term climatological effects is synchrotron-source radiation, which is capable of

providing a high-intensity continuum of great stability whose radiance is precisely calculable from the microwave region to the "soft" x-ray region.

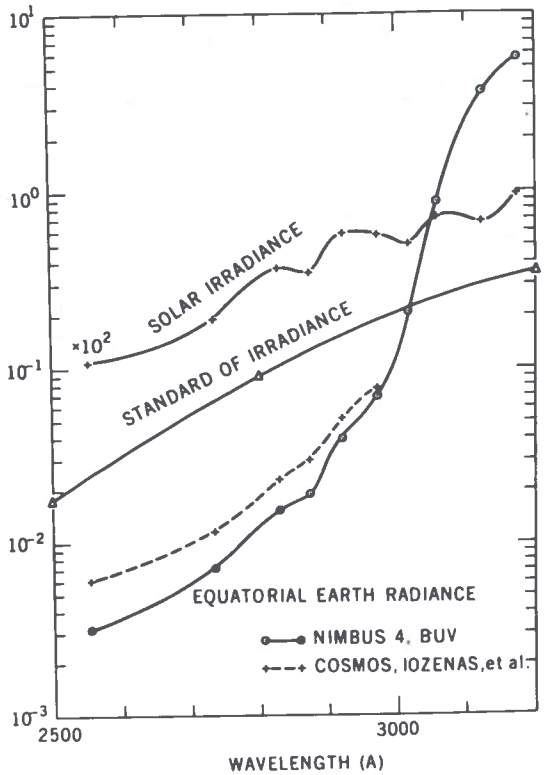

Figure 3. Wavelength dependence of the solar irradiance, laboratory standard of irradiance, and equatorial terrestrial radiance. Units of irradiance are ergs cm^{-2} sec^{-1} $Å^{-1}$; those of radiance, ergs cm^{-2} sec^{-1} $Å^{-1}$ sr.

Other ambiguities may be introduced into the data by degradation in the space environment. In the case of satellite experiments, degradation results principally from contamination due to outgassing of the spacecraft and its associated experiments, the high-energy charged-particle radiation in the Van Allen radiation belts, and the changes induced by the sun in the form of UV degradation and heating of the spacecraft. These all must be minimized and accounted for in order to maintain fidelity of the data.

SOLAR ULTRAVIOLET MEASUREMENTS

An important minor atmospheric constituent is ozone, which reaches its maximum concentration in the stratosphere. Photochemical processes play a major role in the formation and destruction of ozone. Since its presence shields us from biologically lethal ultraviolet solar radiation, we must understand those factors which determine the equilibrium concentration of ozone. We need information on the intrinsic solar-ultraviolet variability and the spectral absorption of solar UV as a function of altitude in the stratosphere.

Recent measurements of ultraviolet solar radiation in the 2500 - 3400 Å region are shown in Figure 4. These observations were made with the Nimbus 4 BUV experiment instrument; determinations of the ultraviolet albedo in the 2500 - 3400 Å region were used to deduce total ozone concentration and vertical distribution from 30 to 55 km on a geographical basis. (The crosses represent the BUV measurements.)

Three years of continuous broad-band monitoring of the sun in the 1200 - 3000 Å region with the Monitor of Ultraviolet Solar Energy (MUSE) have revealed that the sun is a variable UV star, with a period closely related to that of the solar rotation. This variability is at a maximum at the short wavelengths and exhibits an exponential decrease with decreasing wavenumber (cm^{-1}). The 27-day variability is principally associated with two ultraviolet-active solar regions of comparable strength which are about 180° apart in solar longitude. (Those have been observed since the launch of the Nimbus 3 satellite in April, 1969). This means that the fluctuations in atmospheric phenomena which are related to the ultraviolet solar radiative input should exhibit a periodicity of about 13.5 days, instead of the 27-day rotational period. The two long-lived ultraviolet-active regions can be seen in Figure 5, where the longitude of the central meridian is indicated for the day on which a UV maximum was observed. It is assumed that a maximum in the UV irradiance is observed when the active region is at the central meridian. (The non-zero slope indicates that the active region has a different rotation rate from that of the heliographic longitude.)

Another form of solar variability in the UV has been observed in the MUSE channel which includes Lyman alpha. This radiation appears to have reached a broad maximum in the springs of 1969 and 1971 which was several times greater than the annual variation due to the variable sun-earth distance.

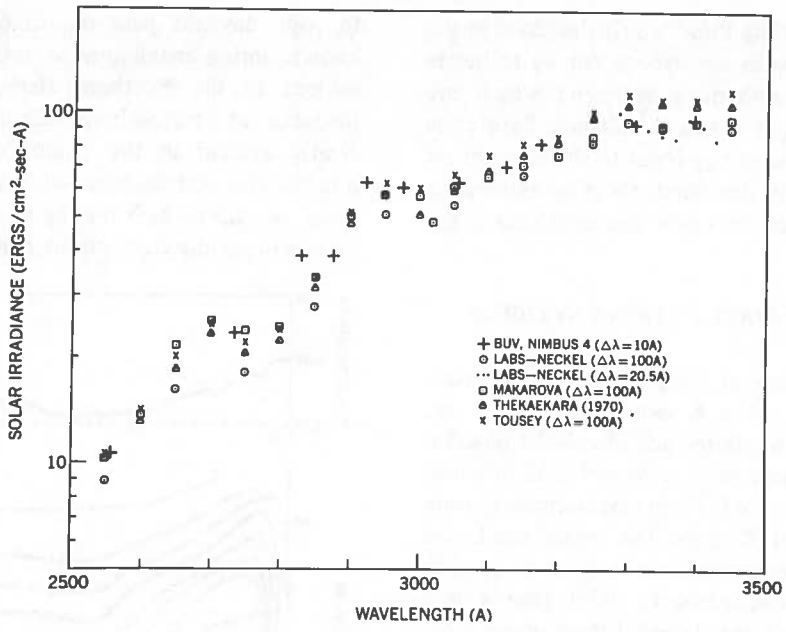

Figure 4. Comparison of solar irradiance from Nimbus 4 with Thekaekara, Labs and Neckel, Makarova and Kharitonov, and Tousey.

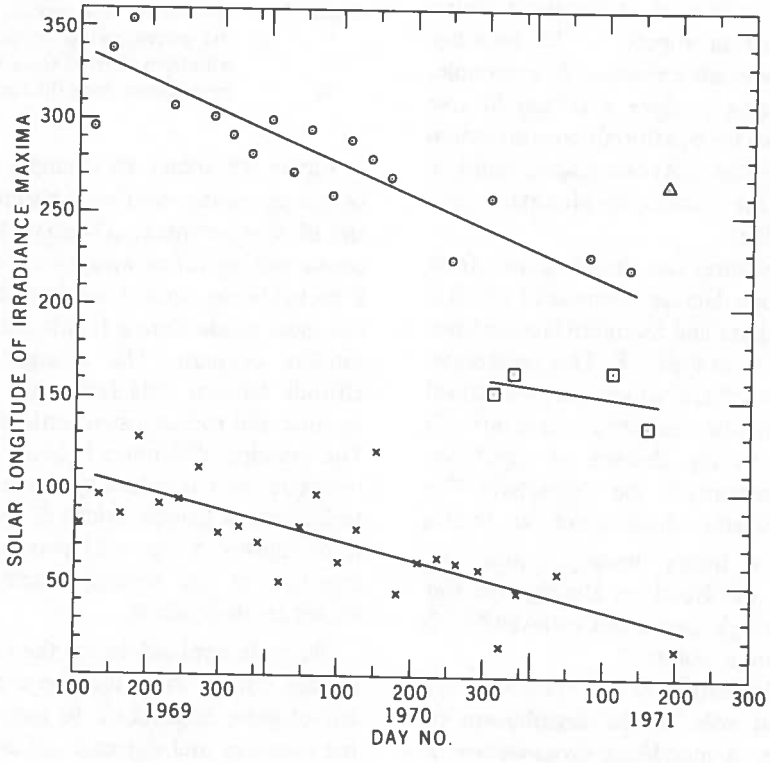

Figure 5. Carrington longitude of the central meridian at the time of observed UV maxima.

Measurements like those briefly discussed in the preceding paragraphs are needed for us to better understand atmospheric phenomena which are sensitive to changes in solar irradiance. Before the mechanism of solar-energy input to the atmosphere can be completely described, these measurements must be extended to cover the complete solar-activity cycle.

ATMOSPHERIC CIRCULATION PATTERNS

The distribution of total ozone along a meridional pass of Nimbus 4, shown in Figure 6, was derived from both infrared and ultraviolet observations. This satellite data was acquired in 52 minutes, whereas the shipboard Dobson measurements, made in 1965, required 52 days. The spatial resolution of the infrared measurements is twice as good as that of the UV measurements, and in general their agreement is excellent. Infrared measurement obviously cannot be used when the atmosphere is nearly isothermal. On the other hand, the UV measurements require a sunlit earth, and the infrared instrument does not have this limitation.

An example of how climatological factors influence the distribution of atmospheric ozone can readily be seen in Figure 7, the monthly average of total ozone concentration. For example, the Rocky Mountains produce a trough of low ozone concentration; the equatorial ozone minimum is easily seen in the figure. Another significant low is observed over the Himalayan Mountains and a high plateau in Tibet.

Similar global pictures can also be drawn from the UV-derived ozone data, an example of which is shown for the Northern and Southern Hemispheres in a polar projection in Figure 8. This representation shows the type of data which can be obtained in the polar regions where infrared data is difficult to interpret due to the absence of significant vertical thermal gradients in the atmosphere. The two significant features which stand out in this figure are the more highly developed planetary wave structure in the Northern Hemisphere and the possible ozone highs associated with the North and South geomagnetic poles.

It was previously mentioned that transport may play an important role in the distribution of atmospheric ozone. A meridional cross-section of total ozone and the mass mixing ratio derived from the BUV experiment is shown in Figure 9 for one daylight pass of Nimbus 4. The well-known spring maximum in total ozone is very evident in the Northern Hemisphere. The importance of stratospheric transport processes is clearly evident in the structure of the vertical mixing-ratio distributions with latitude. The presence of cells of high mixing ratio definitely indicates a departure from photochemical equilibrium.

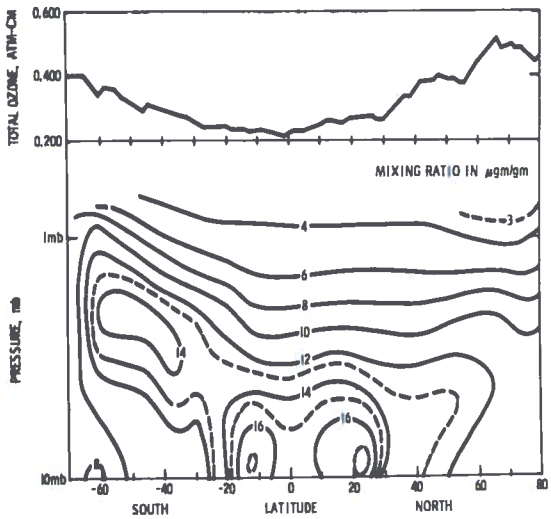

Figure 9. Meridional cross-section of total ozone and the corresponding vertical mixing ratio distributions derived from the Nimbus 4 BUV experiment along the Nimbus 4 orbit.

Figure 10 shows an example of the variation of ozone mixing ratio with altitude, derived from the BUV experiment on Nimbus 4. Also shown are ozone mixing ratios which were determined from a rocket-borne optical sonde and a balloon-borne chemical sonde during flights coincident with the satellite overpass. The divergence of the high-altitude balloon data from that obtained by the satellite and rocket instruments is not unexpected. The principal difference between the mixing-ratio distributions determined by the satellite and rocket techniques is that the width of the weighting functions (shown in Figure 2) smooths the actual fine structure in the vertical distribution which the rocket sonde observes.

Such determinations of the variation of ozone mixing ratio with altitude on a geographical basis are of great importance to our understanding of the structure and dynamics of the stratosphere. In upper levels of the stratosphere, ozone is in photochemical equilibrium; in the middle strato-

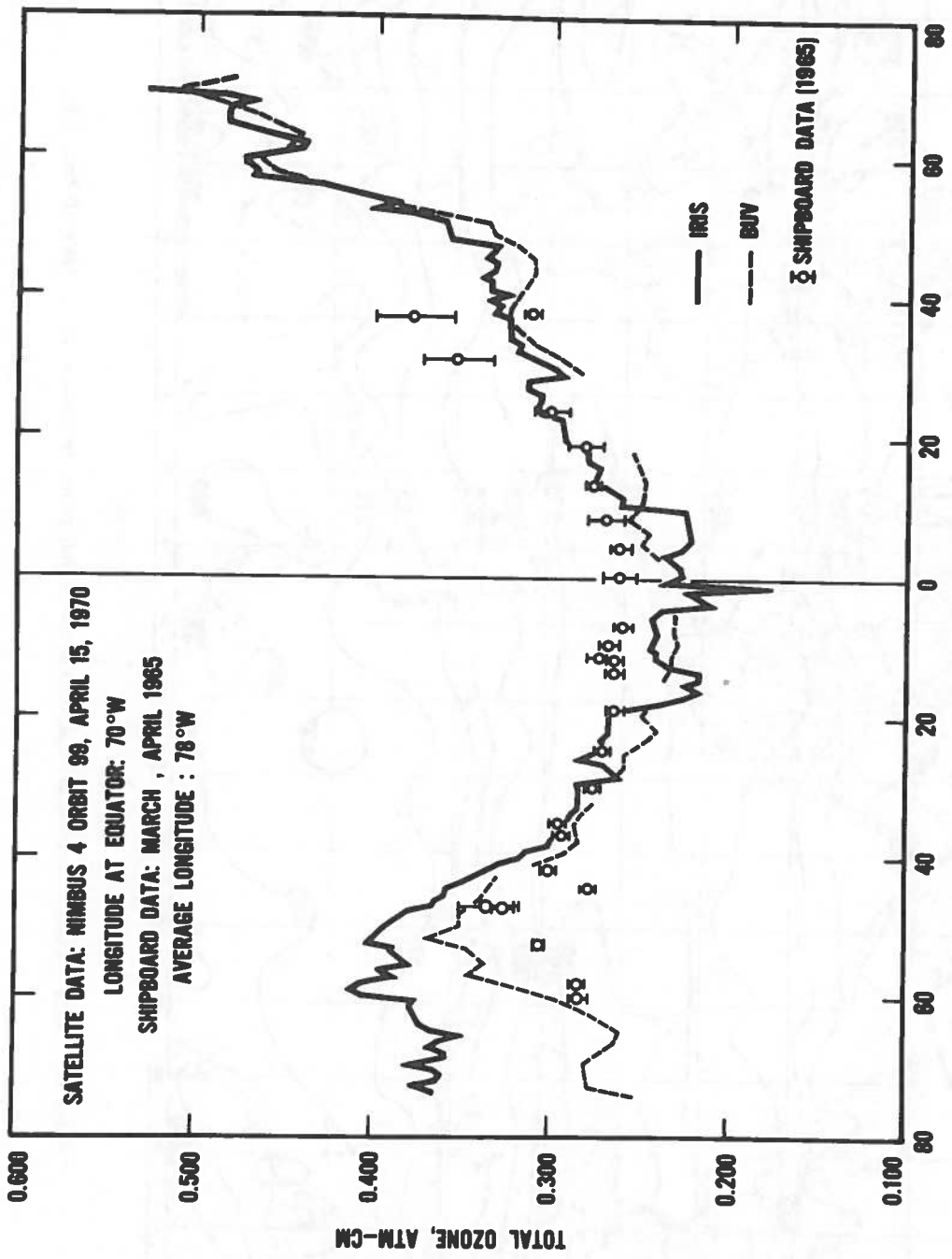

Figure 6. Comparison of total ozone amounts with latitude, from Nimbus 4 ultraviolet and infrared radiances in 1970 and shipboard Dobson measurements in 1965.

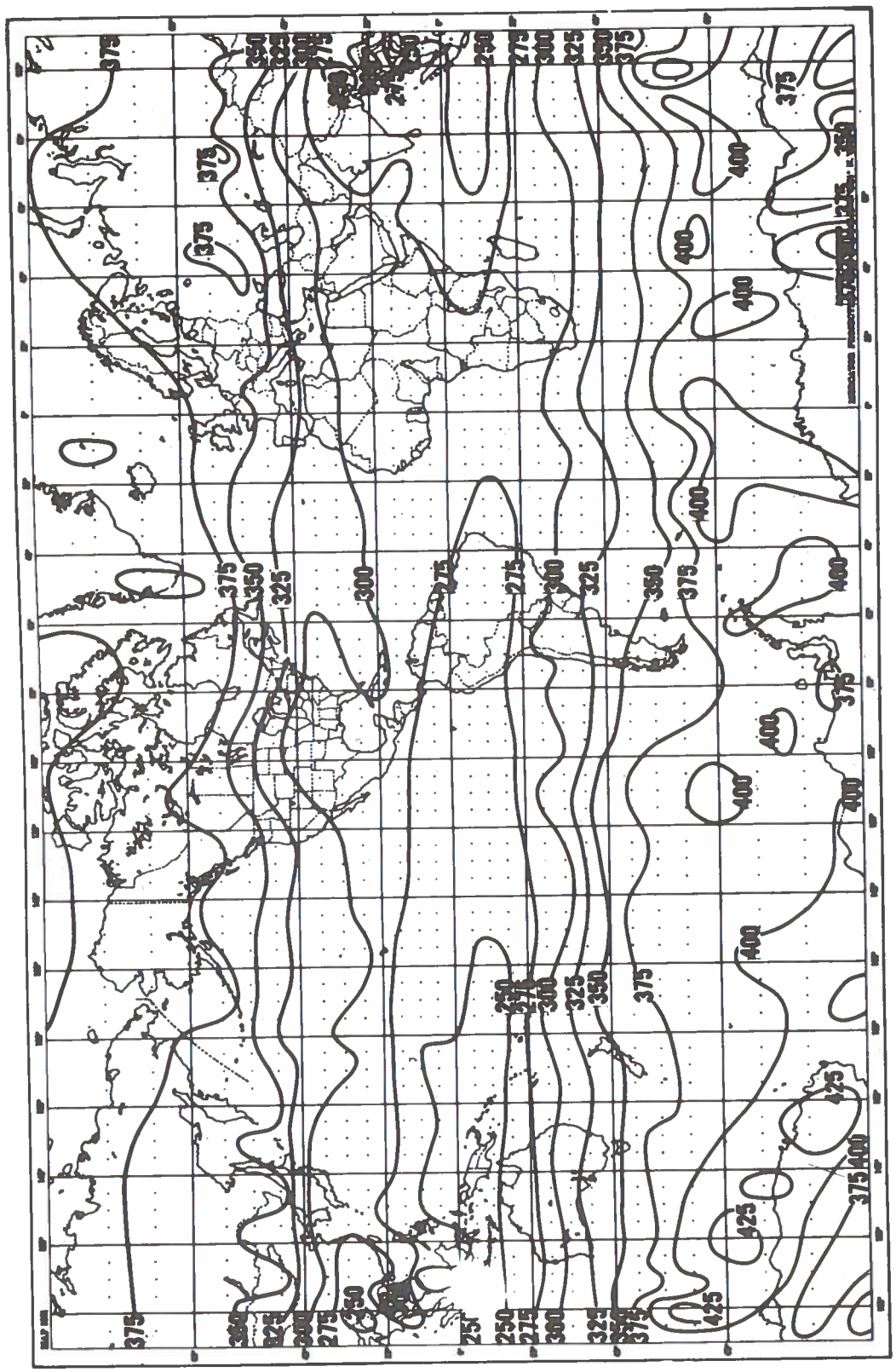

Figure 7. Nimbus 3 IRIS experiment determination of the monthly average total ozone for July 1969 (10^{-3} cm, STP).

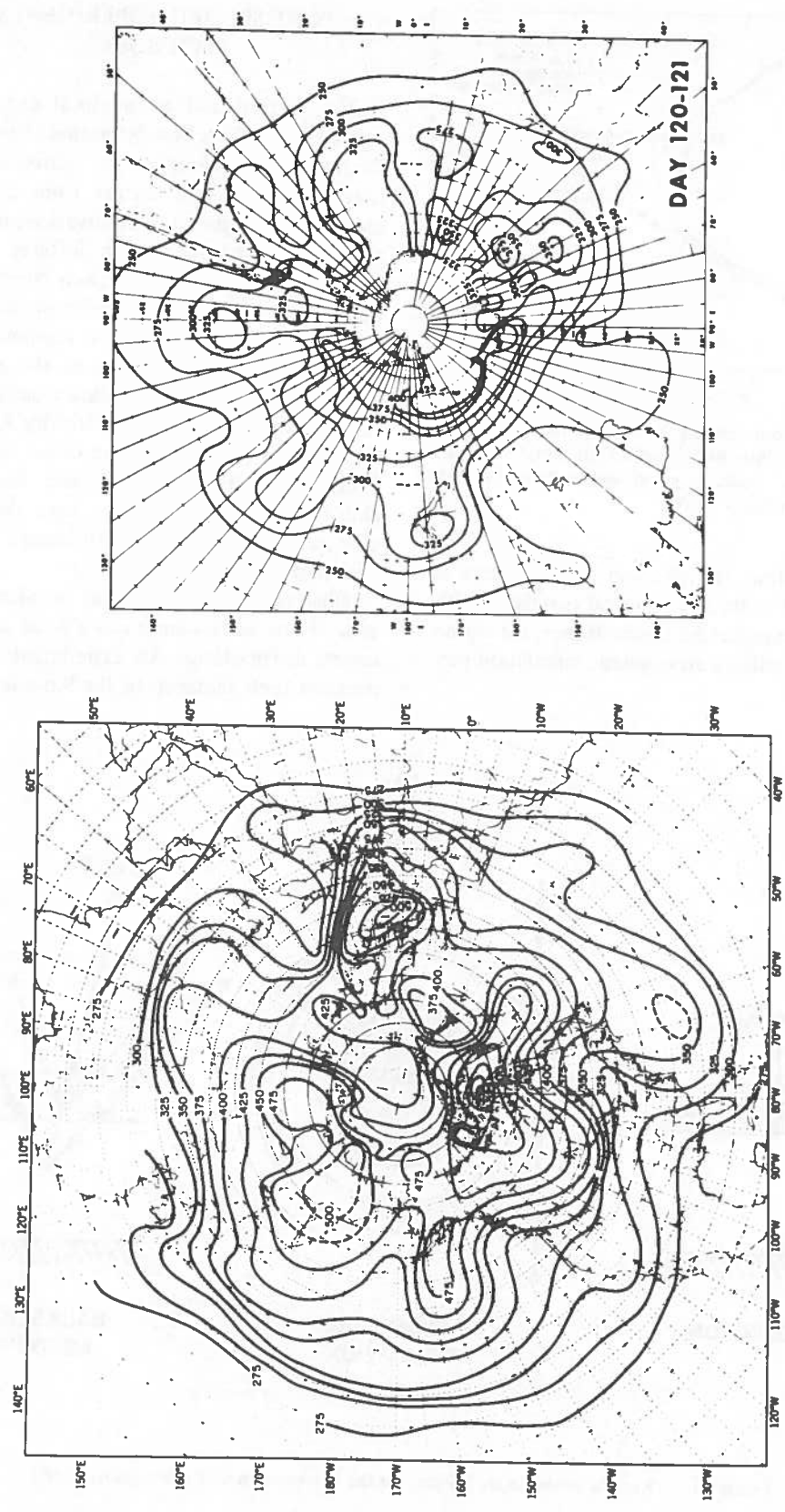

Figure 8. Northern and southern contours of total ozone derived from the Nimbus 4 BUV experiment for April 30 - May 1, 1970 (m-atm cm).

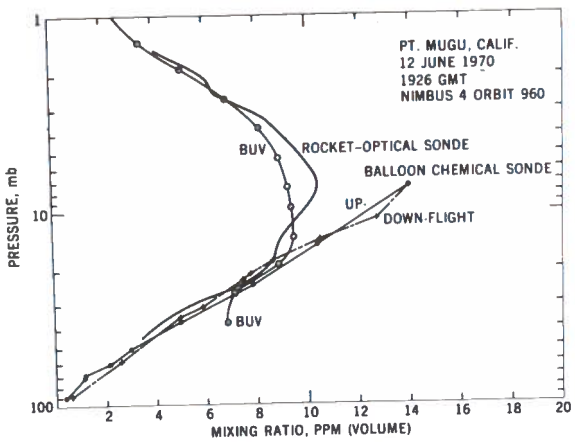

Figure 10. Ozone mixing ratio comparison between satellite BUV experiment during overpass and rocket optical and balloon chemical sondes in 1970.

sphere and below, the photochemical lifetime is long compared to the time interval associated with stratospheric transport processes. Hence, the ozone concentration reflects atmospheric circulation patterns.

SOME SPECIFIC EXPERIMENTAL TECHNIQUES

The vertical and geographical distribution of ozone is, therefore, best determined from satellites. Three general techniques for recovering information on atmospheric ozone from satellites are illustrated in Figure 11. Observations of the earth radiance in the 9.6-micron infrared absorption band of ozone were made from Nimbus 3 and 4 by the Infrared Interferometer Spectrometer (IRIS) experiment, which employs a scanning Michelson interferometer. Observations of the atmospheric absorption of the UV irradiance from an occulting star have been made from the Orbiting Astronomical Observatory (OAO) to derive ozone distributions. (This technique does not lend itself well to global mapping, but it does have the advantage of increased sensitivity due to increased atmospheric path length at the earth's limb.)

Observation of the infrared or microwave emission of the earth's limb can also be used to infer ozone distributions. An experiment designed to measure limb radiance in the 9.6-micron band of

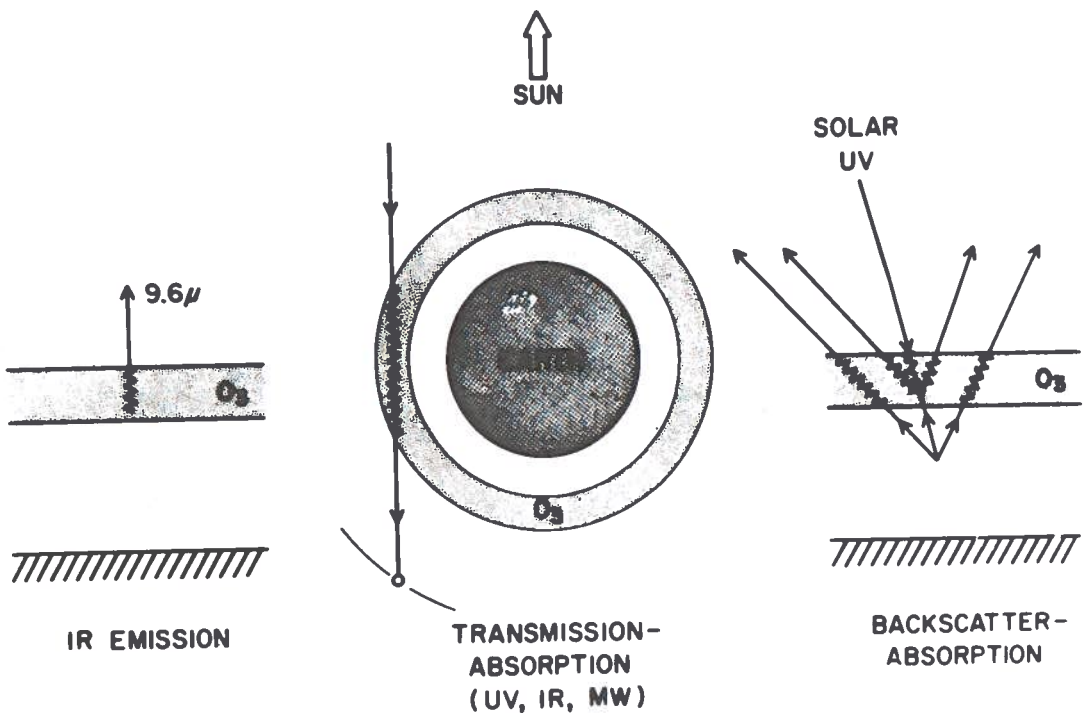

Figure 11. Remote sounding techniques for the determination of atmospheric ozone.

ozone is slated to be flown on the Nimbus F satellite. The distribution of ozone can also be determined from observations of the ultraviolet albedo of the earth in the 2550 - 3400 Å region, since atmospheric ozone reduces the intensity of solar radiation scattered by the atmosphere in wavelength regions where ozone optically absorbs. This reduction was used to measure ozone profiles in the Nimbus 4 BUV experiment.

An example of the type of information which can be recovered from the measurement of the infrared earth radiance is shown in Figure 12. The 15-micron CO_2 band emission is inverted to yield an atmospheric temperature profile up to an altitude of 10 mb pressure. This information is used in conjunction with the 9.6-micron band emission of ozone to give either total amount of ozone, or the distribution of ozone concentrations in the vicinity of the maximum. Finally, the infrared emission in the water-vapor bands has been inverted to obtain the water-vapor mixing ratio up to the 300-mb level.

The typical data record shown in Figure 13 is a measure of the ultraviolet earth radiance along the Nimbus orbit as measured by the BUV experiment system. At the northern terminator, a diffuser plate is deployed to measure solar irradiance at the top of the atmosphere. These two measurements are then combined to yield the ultraviolet terrestrial albedo. From left to right on Figure 13 are shown the upper 13 curves of the terrestrial radiance as measured in the 12 BUV wavelength channels between 2500 and 3400 Å and a photometer channel centered at 3800 Å. As the spacecraft approaches the northern terminator the radiance decreases rapidly with increasing solar zenith angle. The diffuser plate is deployed past the terminator; as the satellite passes into "earth night" a residual signal remains, caused by scattered light from the spacecraft (which is still in "satellite day"). The abrupt transition is then observed as the unit passes into "satellite night". The next increase in signal is due to the passage of the spacecraft through the South Atlantic anomaly. The following large increase in signal comes from the transition from earth night to earth day or the spacecraft's crossing the southern terminator. Wavelengths longer then 3000 Å clearly show the presence of clouds.

Figure 14 shows a typical example of how the variation with wavelength of the terrestrial albedo

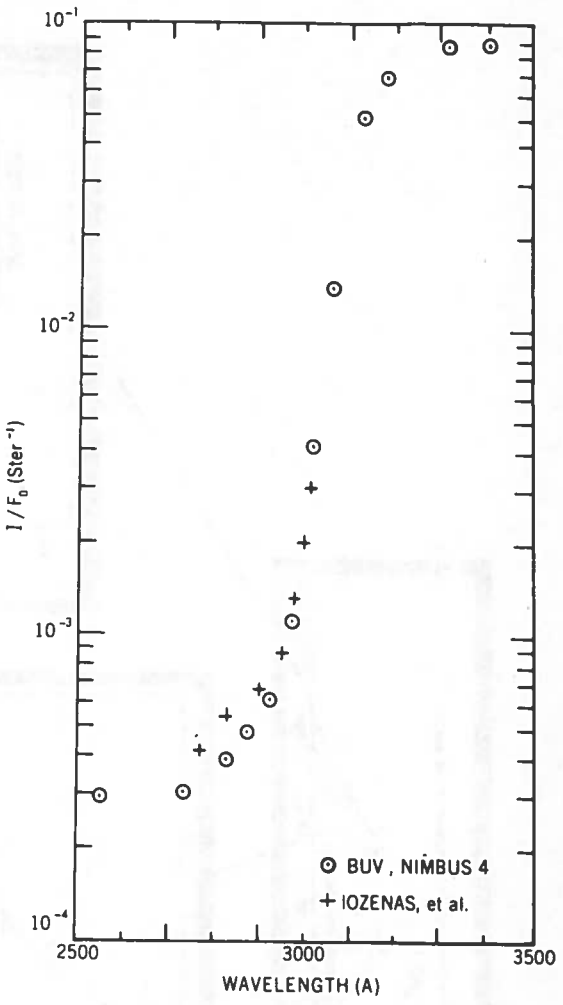

Figure 14. Comparison of the equatorial earth radiance observed from the U.S. Nimbus 4 in 1970 and the USSR Cosmos series in 1965 and 1966.

at the equator may be determined. The albedo changes by nearly four orders of magnitude over about 600 Å, which is why it was necessary to use a double monochromator to eliminate instrumental scattered light. The circles in Figure 14 represent the data recorded by the BUV experiment system on Nimbus 4; the crosses denote measurements during the flight of a double monochromator on a Soviet Cosmos series satellites, in 1965 and 1966, which lasted for about three days in each case. The agreement is excellent in the vicinity of 3000 Å, but the values for the albedo diverge at shorter wavelengths. Two distinct interpretations are possible: either the Soviet

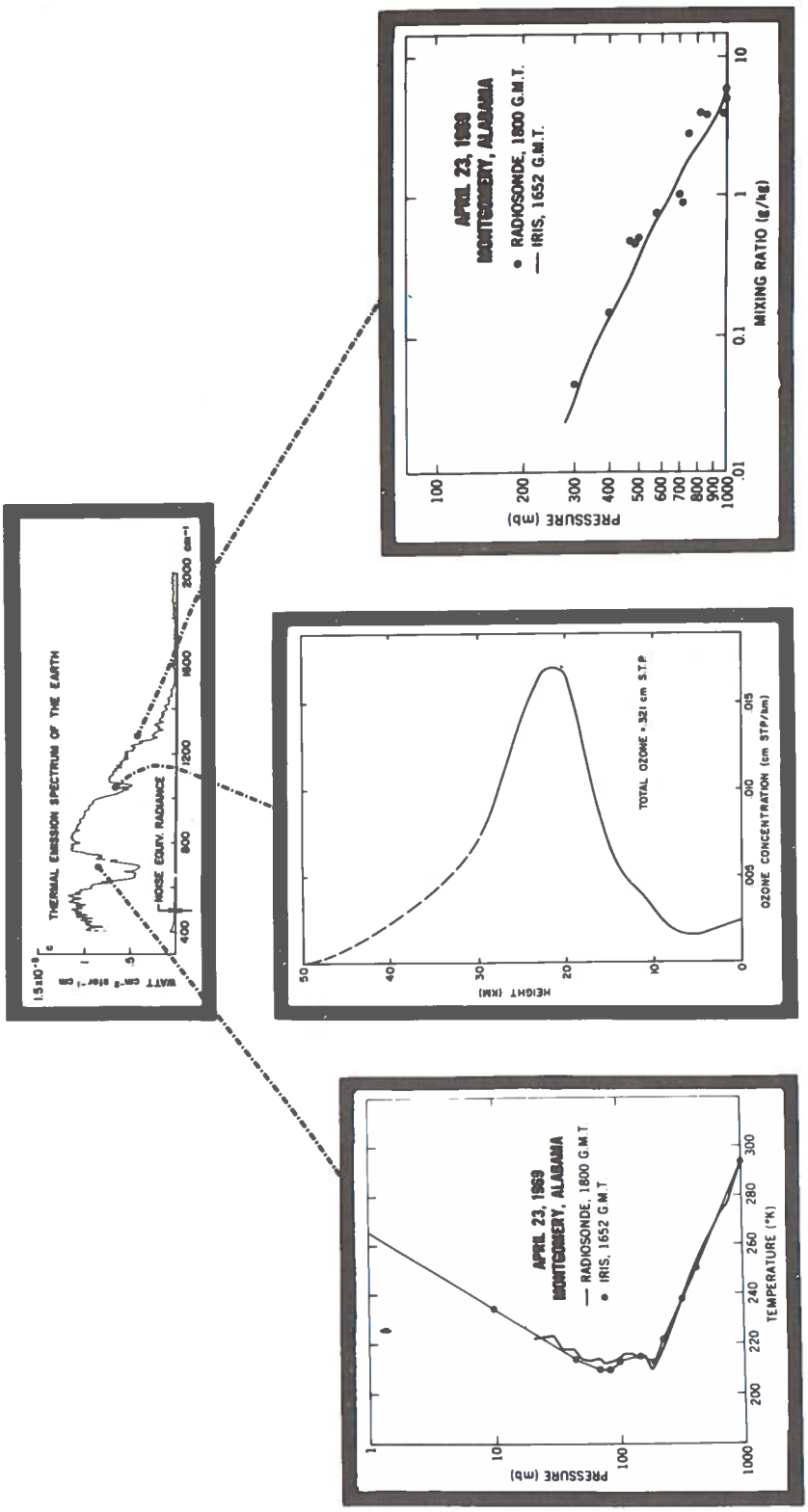

Figure 12. IRIS experiment spectral scan of the terrestrial thermal emission with subsequent inversions to produce vertical profiles of temperature, ozone, and water vapor.

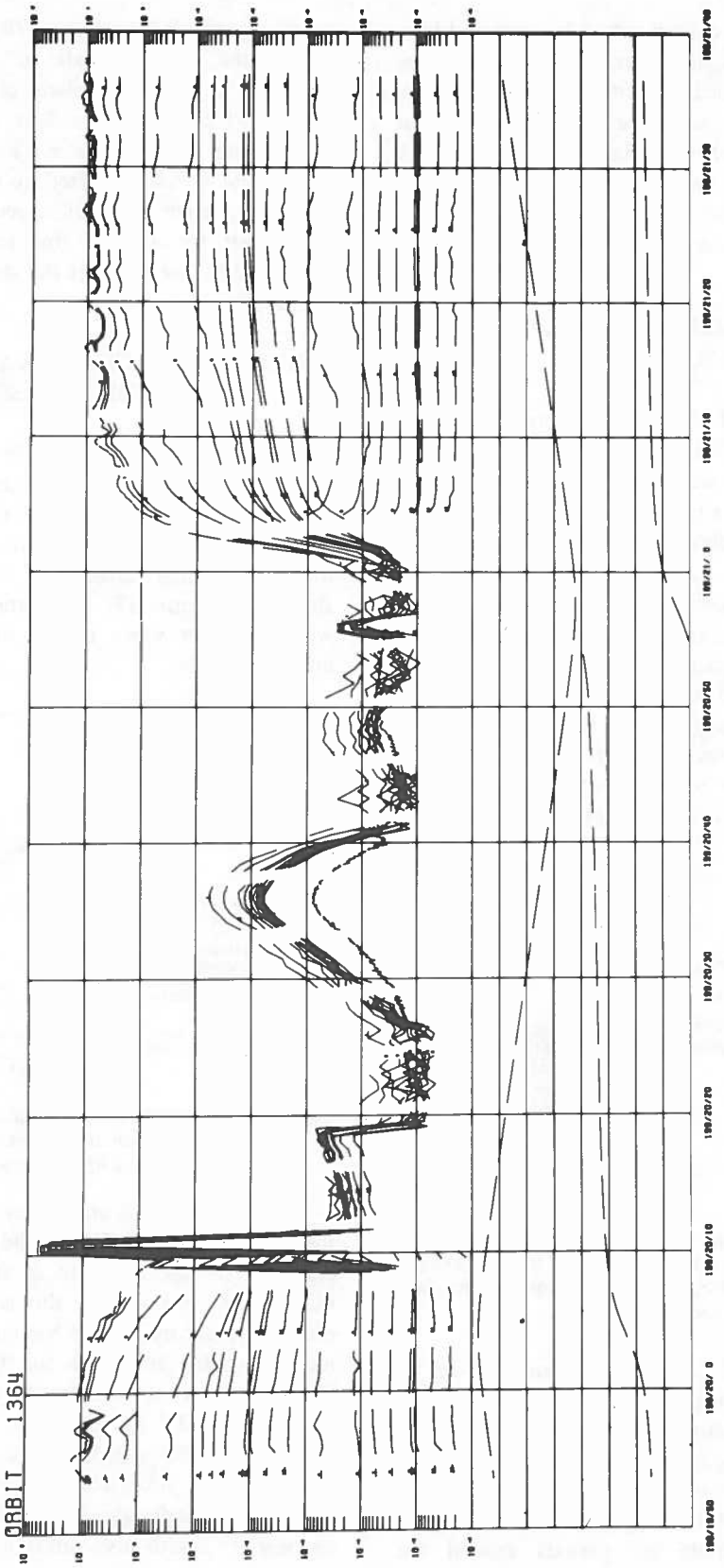

Figure 13. Nimbus BUV experiment observations of solar irradiance and atmospheric radiance for one orbit.

measurements are contaminated by scattered light at shorter wavelengths where the instrument sensitivity was low, or the high-altitude ozone concentrations were lower near solar minimum than near solar maximum, when Nimbus 4 was launched. (A decrease in the ozone content of the upper stratosphere would lead to an increase of the atmospheric radiance at the shorter wavelengths.)

COMPLEMENTARY ROCKET MEASUREMENTS

An example of the complementary nature of satellite and rocket soundings of atmospheric parameters can be seen in the vertical temperature profiles in the stratosphere and mesosphere. Compilations of about 19 winter firings and 10 summer firings of rocket grenade experiments from Point Barrow, Alaska were made to determine the average vertical temperature structure through the upper stratosphere and mesosphere. Figure 15 shows the spread of the actual data and the corresponding average of the summer and winter temperature profiles. The large excursions in the winter profile are real and not noise; they were observed within a 12-hour period on one day.

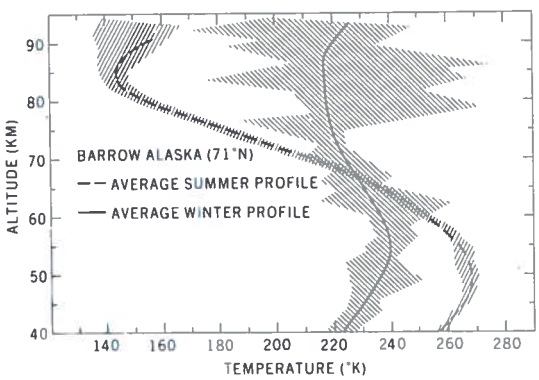

Figure 15. Envelope and mean of stratospheric and mesospheric temperatures from rocket grenade firings from Pt. Barrow, Alaska, for a winter and summer series.

Similar vertical temperature soundings up to 60 km are being made by the Selective Chopper Radiometer (SCR) instrument systems on Nimbus 4 from radiance measurements in the 15-micron CO_2 band. Examples can be seen in the temperature contour plots of Figure 16 as a function of altitude and latitude for periods around the solstices and equinoxes in 1970 and 1971. In the winter the data indicate a nearly isothermal structure in the stratosphere of the North Polar region which is not evident in the Southern Hemisphere, where there is a low of 180°K at the tropopause which is shifted up to the 30-millibar level. Here again the satellite sounding is not able to recover the detailed fine structure, which is smoothed by the width of the atmospheric weighting functions.

RECENT DEVELOPMENTS APPLICABLE TO CLIMATIC IMPACT ASSESSMENT

Currently there is great interest in what role oxides of nitrogen play in determining the distribution of atmospheric ozone. The classical photochemical model cannot account for the rocket-measured diurnal variation of atmospheric ozone shown in Figure 17. The data do not indicate whether water vapor or the oxides of nitrogen are responsible.

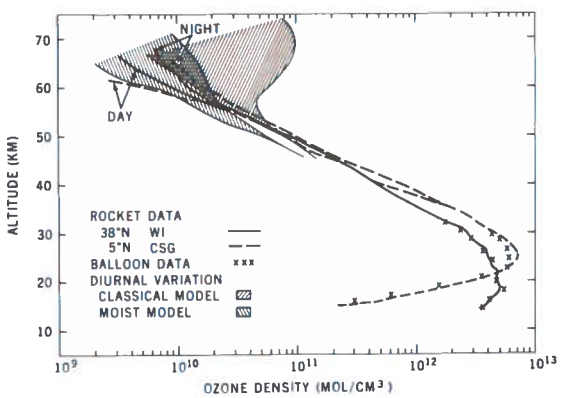

Figure 17. Observed diurnal variation of vertical ozone distribution at mid- and equatorial latitudes compared with photochemical models.

Currently work is under way to adapt satellite instrumentation to balloons and stratospheric aircraft for the measurement of stratospheric parameters. One example of this is that part of the residual inventory of the Nimbus 4 BUV experiment is being modified for flight aboard the WB-57F aircraft to measure the *in situ* deposition of the solar UV energy in the stratosphere as a function of wavelength and altitude. These observations will also yield data on the overburden of ozone. If the double monochromator is oriented to view the zenith sky, atmospheric radiance data

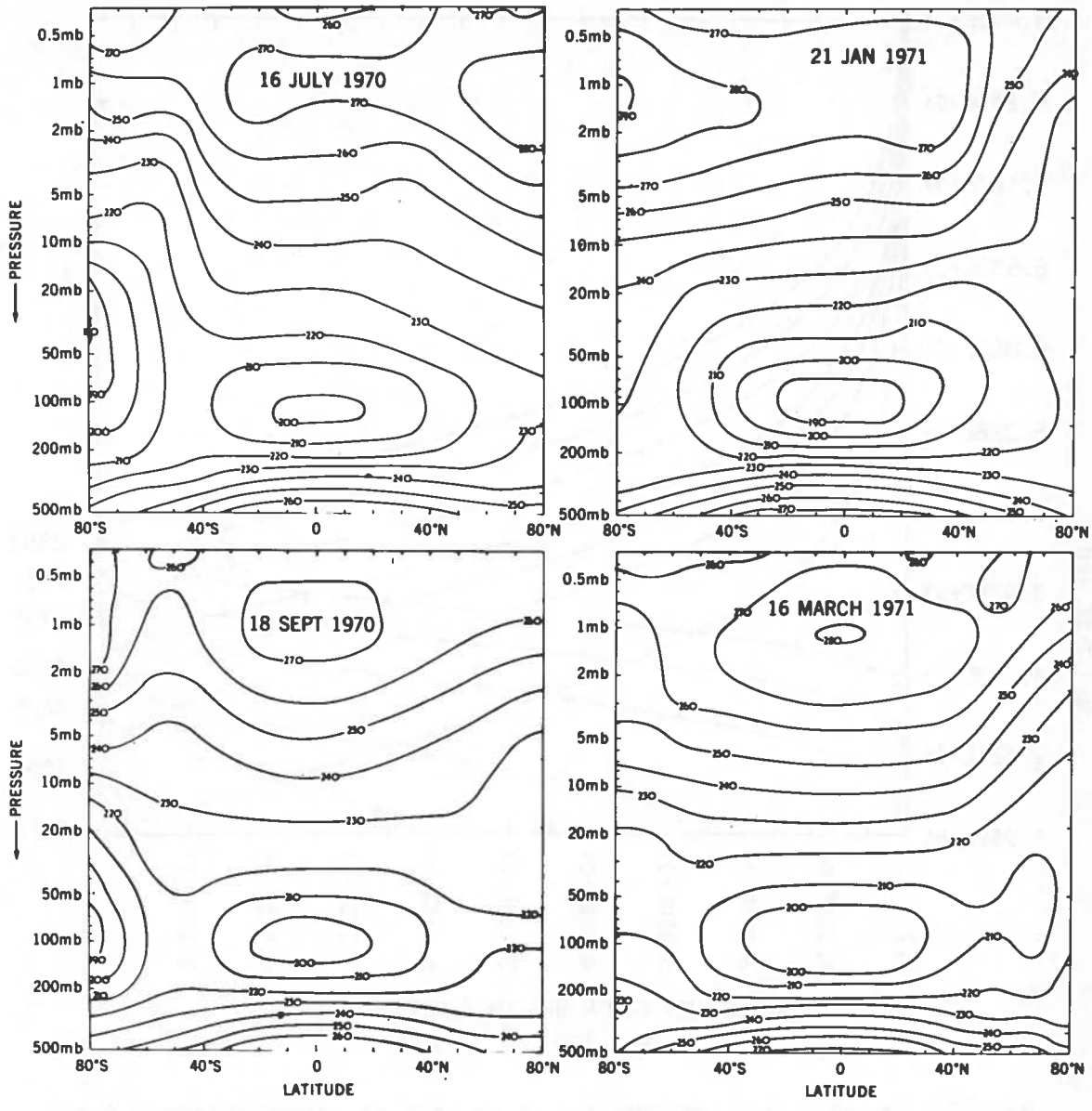

Figure 16. Vertical distributions of stratospheric temperature derived from the SCR experiment on Nimbus 4.

can be inverted to give the vertical ozone distribution up to about 40 km, for large solar zenith angles. An example of the weighting functions applicable to this inversion is shown in Figure 18.

A new sensor being developed for stratospheric water-vapor measurements is the aluminum oxide hygrometer, which has already been flown aboard the NASA CV990. As an example of the performance of the sensor, Figure 19 shows the measured water-vapor mixing ratios for a flight from Fairbanks, Alaska to Moffet Field, California at the 240-mb level. The mixing ratios shown along the flight path are superimposed on the Nimbus 4 THIR scan of the earth in the water-vapor channel recorded in coincidence with the flight. The dark areas indicate cloud-free regions of low moisture content. The aluminum-oxide hygrometer is currently being developed for sounding rockets. Unfortunately, the escaping water vapor outgassing from the rocket presents a serious problem to the *in situ* measurement in the relatively dry stratosphere.

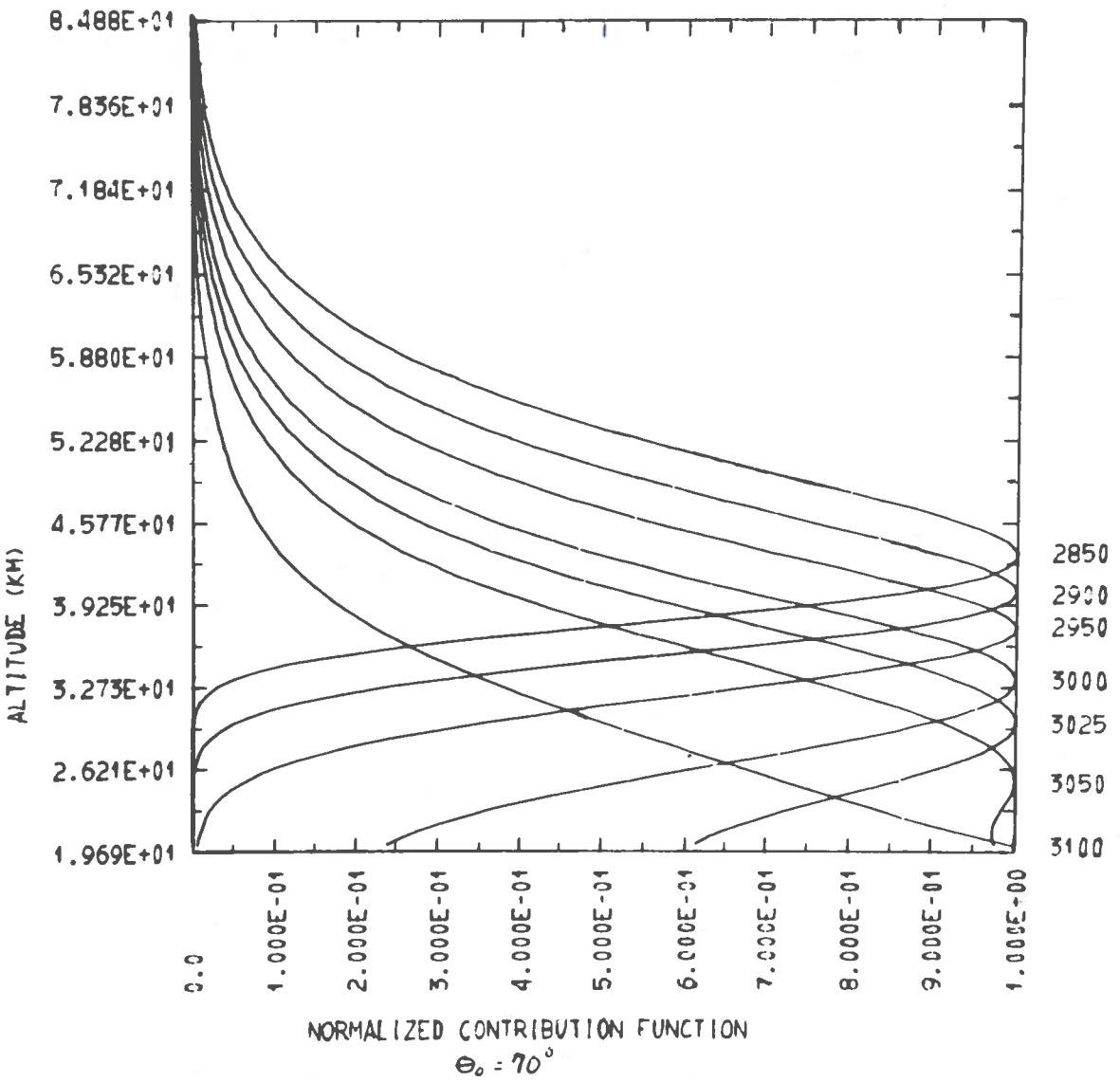

Figure 18. Atmospheric ozone contribution functions for zenith sky radiance measurements from a stratospheric aircraft.

Another remote sensing technique which shows great promise for determining the distribution of trace constituents through the stratosphere is the tunable UV laser which might be used to excite resonance scattering and fluorescence. The fundamental limitation on the resonance scattering technique is that the optical depth of the strongest absorption line should be comparable to or greater than the Rayleigh scattering optical depth. Observation of fluorescence could free one from this latter limitation if the normal radiative background were sufficiently low.

Such developments in instrumentation show great promise. Application of this technology, with continued use of complementary rocket, balloon, and satellite measurements, will permit a much better understanding of the dynamics of the atmosphere and those factors which are important in climate modification.

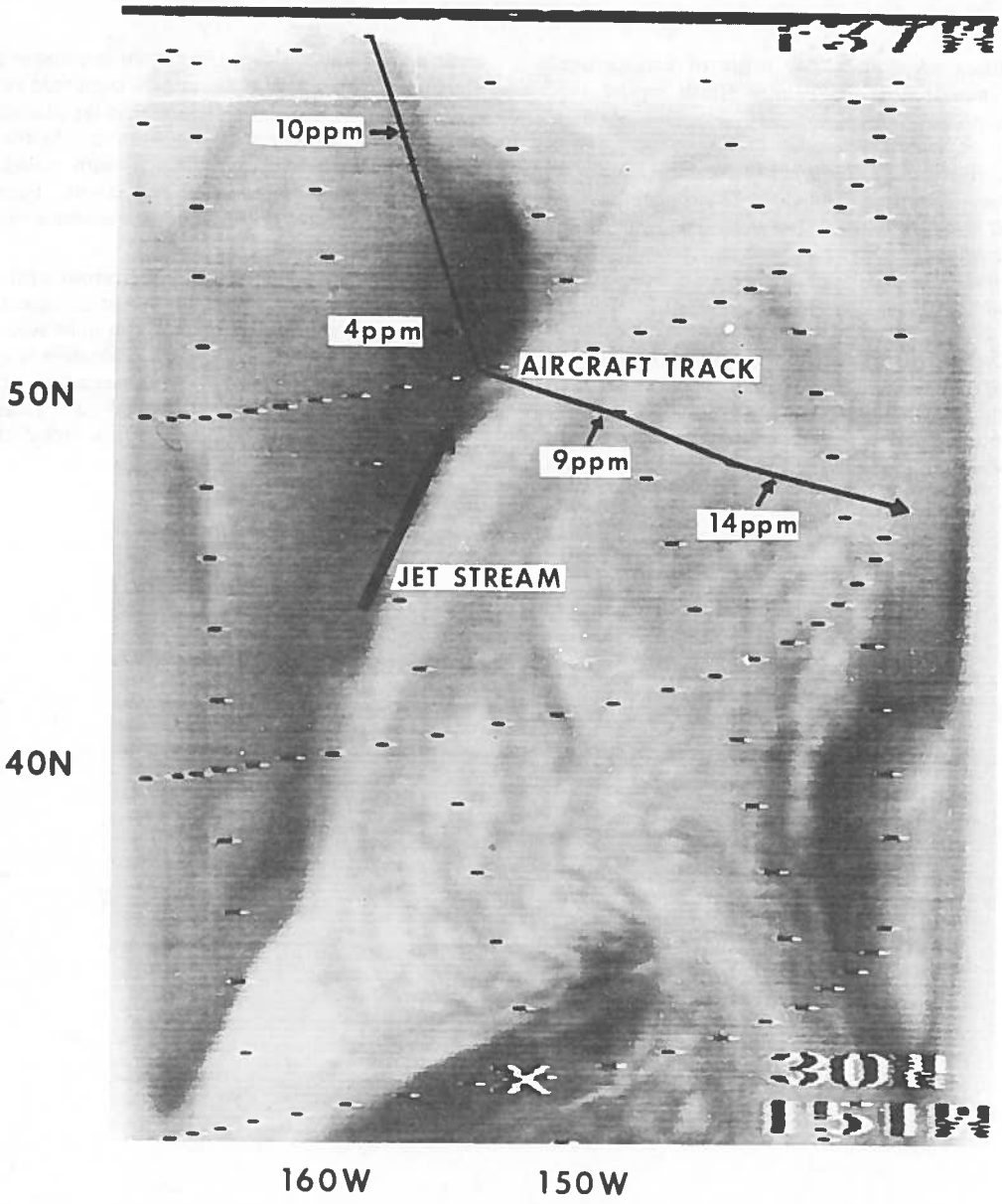

Figure 19. $A1_2O_3$ hygrometer determinations of water-vapor mixing ratio along the flight path of the NASA CV990 from Fairbanks, Alaska to Moffett Field, California against the water-vapor channel background observed with the Nimbus 4 THIR experiment.

REFERENCES

The general references for this work are:

"Observations of the global structure of the stratosphere and mesosphere with sounding rockets and with remote sensing techniques from satellites." Heath, D.R., Hilsenrath, E., Krueger, A.J., Nordberg, W., Prabhakara, C., and Theon, J.S. Presented at the International School of Atmospheric Physics, ETTORE MAJORANA Center for Scientific Culture, Erice, Italy, 13-27 June 1971 (in press, Gordon Breach).

Nimbus 3 and 4 Users Guide, 1969, 1970; Nimbus 3 and 4 Data Catalogs. Nimbus Project, Goddard Space Flight Center, Greenbelt, Md.

"The Best of Nimbus". Allied Research Associates, Inc., Concord, Mass. Report 9G45-80, March 1971.

DISCUSSION

F. Urbach asked about the origin of backscattered radiation measured at 2500 Å. Heath replied that measurements were made from 1100 km looking down, and that the radiation originated at about the 50-km level. L. Hale mentioned some of his recent measurements, reported at the 1971 Fall AGU meeting. His data have been extended down to the stratosphere and in the higher altitudes generally agree with the (revised) mixing ratio of 4×10^{-8} reported by the Arago people. They found that the mixing ratio was not constant from 30 km down to 22 km, but that there was a vertical profile of either NO or NO_2 (they could not be distinguished by the photoionization technique being used).

J. Gille offered further comments on the weighting functions in the limb scanning experiments. He said that for temperature, a vertical wavelength as small as 4 km could be distinguished, depending on the instrument parameters. For ozone, 5 or 6 km at 20% amplitude variation might be picked up, and he hoped that the diurnal variations at about 50 km could be resolved. As for water vapor, he said it looked as though, with variations in the wavelength, 6 km could be picked out. Heath said he felt Gille's experiment was a great advance in stratospheric knowledge.

J. McNesby noted that people concerned with tropospheric pollution were measuring NO at a concentration of 10 ppm. Present measurements seem to be accurate to only within a factor of 3 to 5, and calibration is a problem. He said that when it came to measuring 1 ppb of NO, as EPA is expected to, it would be optimistic to expect an accuracy much better than a factor of 5 to 10 with present calibration techniques.

THE BIOLOGICAL EFFECTS OF ULTRAVIOLET RADIATION ON MAN, ANIMALS AND PLANTS *

KENDRIC C. SMITH
Department of Radiology
Stanford University School of Medicine
Stanford, California 94305

ABSTRACT: Solar radiation is probably the most important element in our environment, yet, perhaps because of its ubiquity, the great scope of its chemical and biological effects is often not fully appreciated. Although the sun is necessary for life, many of the effects of solar radiation are detrimental. It is the ultraviolet (UV) portion of the solar spectrum that is most detrimental to plant and animal cells. Although atmospheric ozone filters out much of this harmful radiation, a biologically significant amount of UV radiation does reach the surface of the earth. Most cells have a remarkable ability to repair UV damage to their genetic material. Whether a cell can survive exposure to solar radiation depends in large part upon its ability to repair the damage produced. ***Living things are therefore in a delicate balance between the photochemical destruction of cellular components by solar radiation and their biochemical repair.*** When this balance is upset by exposure to increased amounts of UV radiation or by interference with repair (by chemical or genetic means) the organism will be injured and may die, or mutations may appear in offspring.

In addition to skin cancer, sunlight produces a variety of detrimental effects in man, of which the most common are sunburn and chronic skin changes leading to wrinkling, discoloration and thinning of the skin. A variety of chemicals, some medicinal, some environmental, sensitize human skin and increase the effectiveness of solar radiation in producing phototoxic and photoallergic reactions.

In spite of these detrimental effects on man, the more serious question to be considered is what effect an increased flux of UV radiation might have on plants and animals. For example, if plants (including plankton) were killed by an increased solar flux, or the behaviour of insects (who see with UV radiation) altered such that they no longer pollinated plants, the ecological consequences would be much more severe than even the production of thousands of extra cases of skin cancer in humans.

INTRODUCTION

Solar radiation is a very important element in our environment, yet, perhaps because of its ubiquity, the great scope of its chemical and biological effects is often not fully appreciated. The sun is necessary for life. We are warmed by its rays, and we are able to see because our eyes respond to a portion of the solar spectrum known as visible light. More important, visible light is required for photosynthesis—the process by which plants obtain the energy needed for their growth and man's sustenance.

Nevertheless, many of the effects of solar radiation are detrimental. Most people are aware that a painful sunburn can be caused by excessive exposure to the sun, and colors fade and materials age in the sun. Skin cancer is also produced by excessive exposure to sunlight. There are many other effects of sunlight on cells, including the production of chemical changes (mutations) in their hereditary (genetic) material. Recent work has shown that plant and animal cells are able to repair radiation-induced genetic damage. Evidently plants and animals have evolved in such a way as to be able to protect themselves from the detrimental radiations of the sun, while at the same time allowing themselves to receive the benefit of other portions of the solar spectrum. The situation is one of balance. Sunlight is necessary for life, yet in excess it is harmful.

It is the ultraviolet portion of the solar spectrum that is most detrimental to plant and animal cells. A small amount of ozone in the earth's stratosphere filters out these harmful wavelengths of ultraviolet light and thus prevents

*Based upon the report of Reference 6.

most such radiation from reaching the surface of the earth. The formation of this ozone shield in geologic time was most likely a prerequisite for the evolution of terrestrial life. However, even in the presence of this ozone layer, a biologically significant amount of ultraviolet radiation does reach the surface of the earth.

Because the current terrestrial intensity levels of solar UV radiation are known to have adverse effects on living cells, it is important to explore the consequences to man and other living organisms of changes in the intensity or character of the UV radiation reaching the earth's surface. This report attempts to:

1. Review some of the known effects of UV radiation on man and other living organisms;
2. Assess as far as possible the consequences to man and other living organisms if the amount of solar UV radiation reaching the surface of the earth were to be increased; and
3. Identify those areas where knowledge is inadequate and further research is urgently needed.

BASIC CONCEPTS IN PHOTOCHEMISTRY AND PHOTOBIOLOGY

The biological effects of light are the consequences of the absorption of specific wavelengths of light by specific chemical molecules in cells, and their resultant photochemical alteration. If the molecules absorbing the radiation are present in multiple copies in a cell and only a small proportion is altered, little biological effect will be noted. If the number of absorbing molecules is few and their biological significance is great, the effects of the radiation on a cell can be profound.

In all cells there is one compound, deoxyribonucleic acid (DNA), which is present in only one or a relatively few copies and which carries the genetic information of the cell. The electronic structure of DNA is such that it absorbs UV radiation but not visible light. (This is the principal reason why UV radiation is so detrimental to cells and why visible light is much less harmful unless photosensitizing compounds are present.) If one of these DNA molecules is altered by radiation, the functioning of the cell is markedly affected, resulting in mutations and/or death.

Principles of Photochemistry [1-3]. For radiation to have an effect it must first be absorbed. The unique electronic structure of each type of molecule determines which wavelengths of radiation will be selectively absorbed. Once energy has been absorbed, photochemical alterations can occur.

Molecules are normally in a stable (low-energy) ground state. When molecules absorb radiation, they are raised to a higher-energy (excited) state which has a high chemical reactivity. Such absorbed energy cannot be stored, but must be quickly dissipated. While excited molecules may release their energy by undergoing chemical alteration, they can also return to the ground state by releasing their absorbed energy harmlessly in the form of heat or of light (fluorescence, phosphorescence).

The direct absorption of light is not always required to cause photochemical change. A molecule that has been raised to its excited state by the direct absorption of radiation can transfer its energy by a collisional process to a molecule of a different chemical type, thereby inducing a photochemical change in the second molecule. In another indirect mechanism, called photodynamic action, the excited molecule (photosensitizer) transfers its energy to oxygen, and the excited oxygen then oxidizes some target molecule. These reactions exemplify how cells, in the presence of photosensitizing compounds, can be damaged by radiation at wavelengths which normally would have little effect upon them (e.g., phototoxicity and photoallergy in man).

Repair of Radiation Damage to DNA [3,4]. Some cells and organisms are protected from the damaging effects of UV radiation by external shields such as shells, feathers, or pigments. For cells that are actually exposed to radiation, their sensitivity (measured in terms of lethality) depends mainly upon their ability to repair radiation damage to their DNA. This point is dramatically illustrated in Figure 1, where the ease with which bacterial strains genetically deficient in repair capacity are killed by UV radiation is compared with the resistance to UV radiation of a repair-proficient strain.

We currently know of three major enzymatic pathways under different genetic control for the repair of UV-induced damage to DNA.

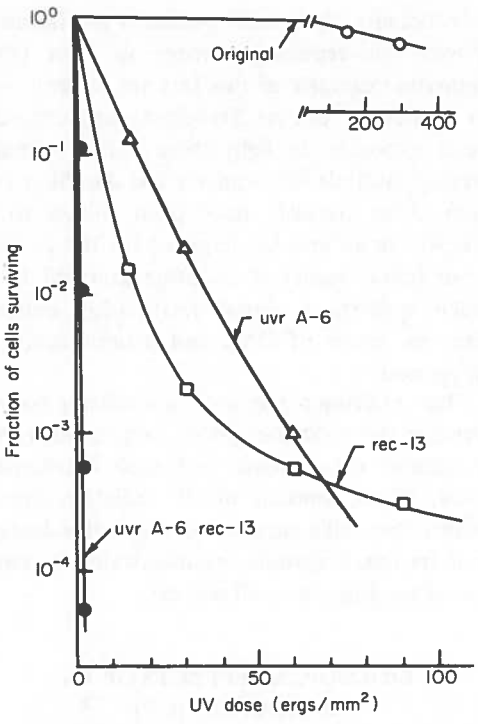

Figure 1. The sensitivity of different strains of *Escherichia coli* K-12 to UV radiation (254 nm). The survival curve marked "original" is the "wild type" parent strain from which the other strains were derived. The *uvr-A6* mutant is deficient in the excision repair of radiation damage. The *rec-13* mutant is defective in the postreplication repair of radiation damage. The double mutant *uvr-A6 rec-13* is deficient in both repair systems and is much more UV-sensitive than either of the single mutants, which in turn are more sensitive than the "wild type" strain (adapted from ref. 5).

1. *The damaged part of the DNA molecule is restored to its functional state in place.* For example, a large percentage of a culture of bacterial cells that have been killed by UV radiation (254 nm) can be brought back to life by a second irradiation with visible light around 400 nm. This process is called *photoreactivation.* It is due to the action of a single enzyme (photoreactivating enzyme) that is widely distributed throughout nature—except in placental mammals. Photoreactivation is a striking example of a situation in which radiation of a considerably different wavelength can modify (in this case beneficially) the effects of the first radiation.

2. *The damaged section of a DNA strand is excised and replaced with undamaged nucleotides to restore the normal function of the DNA.* This system requires several enzymatic steps which proceed in the absence of light. This "dark repair" system (so called to distinguish it from photoreactivation) has been shown to repair a variety of structural defects in DNA induced by radiation and chemicals (Figure 2).

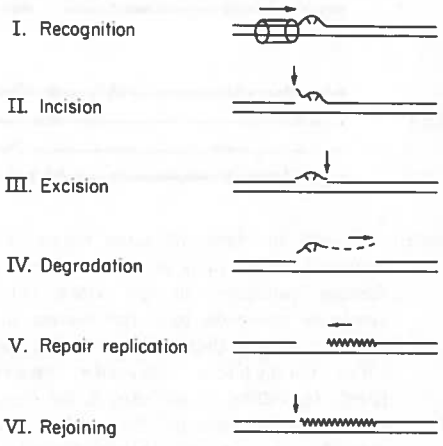

Figure 2. Schematic representation of the postulated steps in the excision repair of damaged DNA. The first steps in this repair system are the recognition of damage and the introduction of a break in the DNA chain near the lesion. This is followed by the complete removal of the lesion from the DNA and possibly a further widening of the excised region. After the excision step, the gap may be filled with undamaged bases by the action of the enzyme DNA polymerase, using the undamaged opposite strand of DNA as the template. When the excised region is completely filled, the single-strand interruption is then closed enzymatically, yielding repaired DNA (from ref. 3).

3. *The damaged section of DNA is not directly repaired but is bypassed during replication.* When the damage in the parental strands of DNA is bypassed during normal replication, gaps are produced in the newly synthesized daughter strands of DNA. These gaps are subsequently repaired, yielding normal DNA, by enzymatic processes that are still not well understood. This postreplication repair process is also a dark repair system (Figure 3).

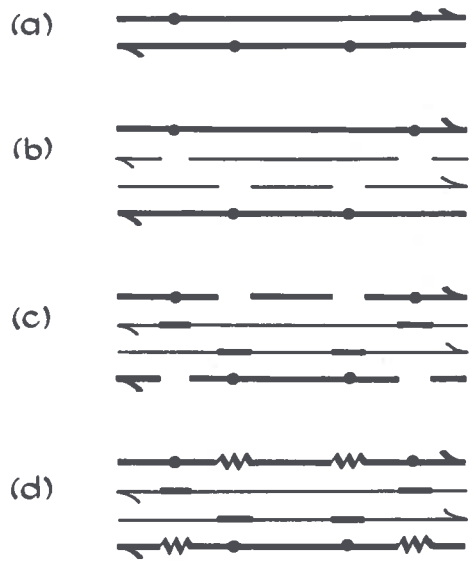

Figure 3. A model for postreplication repair of UV-damaged DNA. (a) The dots indicate base damage produced in the DNA. (b) DNA synthesis proceeds past the lesions in the parental strands (heavy lines) leaving gaps in the daughter strands (narrow lines). (c) Filling of the gaps in the daughter strands with material from the parental strands by a recombinational process. (d) Repair of the gaps in the parental strands by repair replication. Thus, the original UV-induced lesions are not repaired but are bypassed (from ref. 4).

X-radiation and certain types of sensitized reactions mediated by near-UV and visible light produce damage in DNA that differs chemically from that produced by UV-radiation. We presently have evidence that at least three separate processes for the repair of this type of damage (chain breaks) exist in bacteria. These repair systems are not as well understood at the molecular level as the systems for the repair of UV-induced damage to DNA.

Thus, we currently know of six distinct repair systems by which cells can repair radiation damage to their genetic material. This multiplicity of repair systems suggests that the repair of radiation-damaged DNA is of critical importance to the survival of cells.

Conclusions. Since the absorption of UV radiation means that photochemical change will probably occur, plants and animals can survive the onslaught of solar (and man-made) radiation only because their cells possess a multitude of systems for repairing damage to their DNA. Dramatic examples of this fact are patients with the hereditary disease Xeroderma pigmentosum. Upon exposure to light these patients usually develop multiple skin cancers and die. Skin cells from these patients have been shown to be deficient in an enzyme required for the excision repair (dark repair) of radiation-damaged DNA, which suggests a causal relationship between defective repair of DNA and light-induced carcinogenesis.

Thus, in living things there is a delicate balance between the continual photochemical alteration of cellular components and their biochemical repair. If the amount of UV radiation damage exceeds the cell's capacity to repair this damage, or if its repair systems are inactivated by mutation or by drugs, the cell will die.

BIOLOGICAL EFFECTS OF UV RADIATION [6,7]

For thousands of years sunlight was believed to have prophylactic, healing, and healthful powers—witness the millions of people who flock to beaches. Although the physiological, biochemical, and psychological mechanisms remain largely unstudied and unknown, two beneficial effects are indeed supported by evidence. First, UV radiation kills bacteria and viruses, and prior to the discovery of antibiotics, UV radiation was used for the treatment of skin infected with *tubercle bacilli* and streptococci. Second, in man and all other animals with calcified internal skeletons, UV radiation converts provitamin D in the skin to vitamin D. Vitamin D is necessary to prevent rickets; an excessive amount of vitamin D can be toxic, however. Whether man and other animals could successfully adapt to increased vitamin D synthesis from increased UV radiation cannot be predicted from available information.

The sunlight is transmitted through the skin of man and produces a variety of effects detrimental to living cells absorbing it. The most common effects are sunburn and chronic skin changes leading to wrinkling, discoloration, and thinning of the skin. These injuries, which are interpreted as aging, are primarily the result of exposure to UV radiation, and are slowed by the

presence of melanin, the brown pigment in skin. Tanning, the production of new melanin, is considered a protective response to radiation injury of the skin. However, many light-skinned people, genetically incapable of tanning adequately, are liable to repeated injury and consequent premature development of skin changes. While some features of the processes leading to skin damage by UV radiation are reasonably well understood, the molecular bases for these effects are not adequately known. Inasmuch as a significant portion of our population is currently overexposing itself to sunlight, any additional UV radiation load from increased UV radiation in sunlight would lead to an even greater number of people with serious irreversible changes in their skin.

A variety of chemicals, some medicinal, some environmental, sensitize human skin and increase the effectiveness of solar radiation in producing phototoxic and photoallergic reactions. As more and more such chemical agents are introduced into our environment, either deliberately or accidentally, the number of patients with such disorders will continue to increase, particularly if solar UV radiation intensities are increased.

The induction of the three most common malignant tumors of human skin—basal-cell and squamous-cell carcinomas, and malignant melanomas—is correlated with exposure to sunlight. The incidence of each shows a marked increase with the lack of skin pigmentation, with the inability to tan, with increasing time spent out-of-doors, and with decreasing latitudes of residence. (N.B: The ozone layer becomes thinner with decreasing latitudes.)

From the relationship between the concentration of ozone in the upper atmosphere and its transmission of ultraviolet radiation, and the relationship between current levels of solar UV radiation and neoplastic changes in human skin, it is possible to estimate conservatively that a 5% decline in ozone would produce an additional 8,000 skin carcinomas and melanomas in a population the size of the white population of the U.S. living at 40^{o} N latitude. Even with contemporary methods of treatment, these would produce 300 extra deaths a year.

UV radiation of the wavelengths which reach the surface of the earth is transmitted through pure water. Because of the great amount of life in the world's oceans, increased UV radiation in this environment could have serious ecological consequences. Present information on the depth to which UV radiation penetrates natural bodies of water, as well as the effect it has on the organisms therein, is fragmentary, however.

Unlike man and other vertebrates, most insects see in the near-ultraviolet (300-400 nm) as well as in the visible portion of the solar spectrum. Moreover, near-UV light is a distinct color for many species and has special significance in influencing the behavior of members of this large and ecologically important group of animals. For example, because near-UV is the most effective spectral region in attracting insects, light traps are fitted with UV lamps. Conversely, because lamps that are poor in blue and UV light offer much less stimulation to insects, yellow bulbs are frequently used on porches and patios. There are other examples, less obvious but vastly more important ecologically: celestial navigation by insects using the blue and UV polarization pattern of skylight; recognition of flowers by their distinct patterns and colors generated by UV reflectance; and sex recognition in butterflies based on UV reflectance patterns from the wings.

An increase in the intensity of UV radiation at wavelengths shorter than 320 nm would increase the relative brightness of objects reflecting in this spectral region, but neither the effects on insect behavior nor possible deleterious consequences of increased chronic exposure of the receptor cells can be accurately predicted from available data.

Under laboratory conditions, UV radiation is clearly detrimental to a wide variety of plant species, from bacteria to higher plants. Agricultural species are among the plants most sensitive to UV radiation. Although it is not possible to predict the exact biological consequences of increased UV radiation at the earth's surface, sensitive plant species may well be endangered. Natural defenses against UV radiation and efficient repair systems exist in plants, but these may not be sufficient to keep pace with higher intensities of UV radiation.

In addition to these effects on living organisms, it should be remembered that solar UV radiation is harmful to many widely-used materials. These include plastics, paints, dyes, and both natural and synthetic fibers. Industry already

expends a significant effort to design additives to combat the effects of solar radiation on materials; an increase in the intensity of solar UV radiation would thus have important economic consequences.

CONCLUSIONS

When considering the biological effects of solar UV radiation we must not be led astray by mathematical and graphical manipulations. The amount of solar energy reaching the earth is most often plotted on a linear scale as energy per wavelength as a percent of the total energy. At 300 nm the percentage is about 1%, which effectively becomes zero because the artist's pen is not sufficiently fine to draw a line distinguishable from zero, but it is not zero [8]. Although in many considerations 1% of a total can be safely ignored, it certainly cannot be ignored in terms of the biological effectiveness of solar radiation. As shown in Figure 4, radiation at 290 nm is about 100 times more effective than that at 325 nm in killing bacteria, and about 4 orders of magnitude more effective than that at 550 nm. Thus the UV radiation making up this 1% of the total solar energy spectrum is orders of magnitude more effective in killing cells than is the remaining 99% of the solar spectrum.

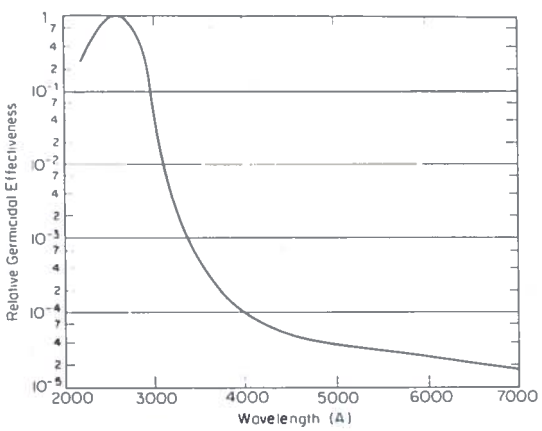

Figure 4. An action spectrum (the relative efficiency of different wavelengths of light) for the killing of the bacterial strain *Escherichia coli*. The shape of this curve would be different for cells unable to repair radiation damage or for cells irradiated in the presence of photosensitizing compounds (from ref. 9).

It is fortunate that plants and animals have evolved remarkably effective systems for the repair of radiation damage to their genetic material. Thus in large measure they are able to withstand the detrimental effects of certain wavelengths of solar radiation while benefiting from other wavelengths. It is important to emphasize again that living things exposed to solar radiation are in a delicate balance between the continual photochemical alteration of their cellular components and their enzymatic repair. If the amount of UV radiation damage exceeds the cell's capacity to repair this damage, or if its repair systems are inactivated by mutation or by drugs, then the cell will die. The genetic loss of repair capacity can also lead to the induction of fatal skin cancer, as mentioned earlier for patients with the heritable disease Xeroderma pigmentosum.

Because light, depending upon its wavelength, intensity and cyclicity, has such profound and variable effects on living cells, we should be very cautious before embarking on national or international ventures that may permanently alter the quality and quantity of the solar radiation that reaches the earth, until we have a much better appreciation of the biological effects of the different wavelengths of light on man and other living things.

RECOMMENDATIONS

In consideration of the mission of the Climatic Impact Assessment Program (CIAP) and the time allotted to this program, the following projects are essential for assessing and quantifying the possible ecological effects of increasing the amount of UV radiation between 280 and 320 nm reaching the surface of the earth.

1. A network of monitoring stations should be established in order to determine the spectral distribution and intensity of natural ultraviolet radiation reaching the surface of the earth. These stations should be located at various latitudes and altitudes and be capable of extended operation so that short-term and long-term changes in the intensity and spectral quality of solar UV radiation can be adequately documented. This information is needed not only as a baseline for monitoring possible

environmental changes (e.g., from SST's), but is also critically necessary in order to evaluate numerous biological effects of sunlight that currently are correlated only with changes in latitude or altitude (e.g., skin cancer incidence in man).

It is important that these measurements provide narrow-band spectral data rather than mean values of intensity for wide wavelength intervals.

2. The ability of selected plants of agricultural importance to grow and produce in the field when exposed to additional amounts of UV radiation over the region of 280-320 nm should be determined.

   Similar studies on natural plant communities should be undertaken. This might be done in cooperation with the Analysis of Ecosystems Program of the International Biological Program (IBP).

3. Because of the unique importance of plankton in the ecological chain, their sensitivity to solar UV radiation should be studied systematically.

4. Laboratory experiments using animals are urgently needed to gain more insight into the molecular bases and dose response characteristics of UV-induced skin cancer.

REFERENCES

1. Calvert, J.G., and Pitts, J.N., Jr., *Photochemistry*, John Wiley, New York (1966).
2. Lamola, A.A., and Turro, N.J., *Energy Transfer and Organic Photochemistry*, Interscience (John Wiley). New York (1969).
3. Smith, K.C., and Hanawalt, P.C., *Molecular Photobiology: Inactivation and Recovery*, Academic Press, New York (1969).
4. Smith, K.C., "The Roles of Genetic Recombination and DNA Polymerase in the Repair of Damaged DNA," in *Photophysiology: Current Topics in Photobiology and Photochemistry*, Vol. 6, pp. 209-278 (A.C. Giese, ed.), Academic Press, New York (1971).
5. Howard-Flanders, P., and Boyce, R.P., "DNA repair and genetic recombination: studies on mutants of *Escherichia coli* defective in these processes." Radiat. Res., Suppl. 6, 156 (1966).
6. *Effects of Ultraviolet Radiation on Man and Other Living Organisms.* A report prepared for the Environmental Studies Board (NAS/NAE) by *ad hoc* committee (Kendric C. Smith, Chairman) at a meeting in Philadelphia on November 10-12, 1971. Publication is expected in early 1973.
7. *The Biologic Effects of Ultraviolet Radiation with Emphasis on the Skin* (F. Urbach, ed.), Pergamon Press, Oxford (1969).
8. Barker, R.E., Jr., "The availability of solar radiation below 290 nm and its importance in photomodification of polymers," Photochem. Photobiol., 7, 275 (1968).
9. Jagger, J., *Introduction to Research in Ultraviolet Photobiology*, Prentice-Hall, Inc., Englewood Cliffs, New Jersey, (1967).

DISCUSSION

D. Hausknecht commented that the nuclear reactor industry was focusing on radiation as a cause of cancer or mutation, but that conventional chemical pollutants should be considered too. Smith agreed, but noted that it was not within the scope of this meeting. He re-emphasized his concern with the effects of increased UV on the entire ecosystem, not just man's skin. H. Levine pointed out that information is needed in the range below 2900 A, since that is where the greatest intensity change would occur if the ozone shield were reduced. Smith amplified that by saying that reduction of the ozone shield would permit the penetration of shorter wavelengths, which are biologically more detrimental, as well as increased penetration of those wavelengths presently reaching the earth.

A. Goldburg asked for comments on an *increase* in the ozone, pointing out that the effects of a fleet of SST's are uncertain at present. Smith said that since the present terrestrial UV level is detrimental to all living things, presumably a decrease in UV due to an increase in ozone would be an improvement; the difference it would make to the number of skin-cancer patients could not be assessed without better UV measurements and correlations. B. McCormac took issue with Smith. F. Urbach gave a brief review of past efforts to establish beneficial effects of UV. They came up with two: production of vitamin D at the surface of the skin, and killing skin TB. Except in very underdeveloped countries we are presently oversupplied with vitamin D, however; and the lamps Finson used for killing TB turn out to be opaque to wave-

lengths shorter than 4000 Å, and probably worked not by UV but by a phototoxic effect (the TB bacillus contains a bright yellow pigment which absorbs at about 4200 Å).

R. Oliver asked how much the natural UV background varied among Los Angeles, Denver, and the tropics. Goldburg said he thought the Smithsonian had found it to be at least a factor of 2. H. Levy of the Smithsonian said those were broad-band measurements; however, if the total ozone could vary by a factor of 2, the amount of UV flux reaching the ground could vary by a factor of 10 or 100 near 2900 Å, depending on the exact wavelength. Urbach presented the results of some measurements of sunburn radiation, integrated from 2920 to 3200 Å over a year, made in Brisbane (27.5° S), Philadelphia (about 40° N), and Galway (53.3° N). Four times as much sunburn UV was found in Brisbane as in Galway, and Galway and Philadelphia differed by about 15%. The ratios of skin cancer in these areas correlate with these UV levels, even though they vary as to time of maximum UV and to the dose on any given day. It is the continuous exposure that counts.

RISK/BENEFIT CONSIDERATIONS OF STRATOSPHERIC FLIGHT

R. C. ERDMANN AND CHAUNCEY STARR
School of Engineering and Applied Science
University of California
Los Angeles, California 90024

ABSTRACT: This paper discusses risk/benefit considerations for application to the Climatic Impact Assessment Program. Several risk/benefit studies are reviewed, including a noise abatement study on subsonic aircraft by the National Academy of Engineering and an underground gas-storage project. General risk/benefit concepts are then developed. Most of the present-day risk/benefit work has been concerned with nuclear siting. The application of such risk analyses to supersonic transports is discussed next. It is found that risks can be arranged in several categories, and that such a breakdown can be quantified to provide the risk level per person per year due to flights in the stratosphere. A modest benefit analysis is then discussed.

If quantitative analyses are made for the risk and the benefit sides of the Climatic Impact Assessment Program, the resulting risk/benefit comparison can be reduced to a dollar figure. Specific techniques to be used in the SST risk/benefit analysis are described and a program suggested.

HISTORICAL RISK/BENEFIT CONSIDERATIONS

Historically, the development and implementation of a new technology was stimulated by the obvious benefit to be derived from its use. Associated safety problems or adverse effects on the environment were corrected when accidents or other unpleasant experiences required the reduction of the risks to an acceptable level. Thus the development of safety practices and attempts to reduce the environmental impact lagged considerably behind the initial introduction of these new technologies.

An example of this sequence can be found in the development of boilers for steamboats that plied U.S. rivers in the middle of the nineteenth century. There was, of course, a great deal of benefit and profit in having steamships on our inland waterways. The steamboat manufacturers and owners initially ignored the risks to life—explosions and sinking—which resulted from faulty boiler manufacture. Not until the loss of life became unacceptable to the public did Congress enact legislation which specified what constituted safe boiler construction. This, the first such legislation passed by Congress, not only led to present-day boiler codes but established the concept of federal regulation of private industry.

The explosives manufacturing industry had a similar history. Several serious accidents in the early nineteen-hundreds finally led to the restricted location of these manufacturing plants. Here again consideration of the benefits of the technology preceded assessment or quantification of the risks.

Thus, in past times new products and technologies were offered to the public long before their adverse impacts were quantified and taken into account. (How these innovations might affect the environment was usually completely neglected.) However, several relatively new technologies have been required to take into account both the risk level to which they are exposing the public and the associated environmental impact. For example, the airplane industry and the nuclear power industry have been carefully controlled by our government so that they provide a valuable commodity with a minimum of risk. Any new technology which affects a major portion of our population is expected to have both benefit and risk analyses done on it, to ensure that risks are examined at least as carefully as the benefits which might be derived from it. Sometimes the risk issue may even decide whether or not the new product is acceptable.

PRESENT-DAY RISK/BENEFIT STUDIES

Three technological assessments carried out by the National Accademy of Engineering are described in Reference 1. The three assessments were of (a) the technology of teaching aids, (b) subsonic aircraft noise, and (c) multiphasic health screening. For each of the three studies a specified methodology was used. This methodology consisted, in part, of the following steps:

1. Identify and define the subject to be assessed.
2. Delineate the scope of the assessment and develop a data base.
3. Identify alternative strategies to solve selected problems with the technology under assessment.
4. Identify parties affected by the selected problems and the technology.
5. Identify the impact on the affected parties.
6. Evaluate or measure the impacts.
7. Compare the pros and cons of alternative strategies.

A distinction was made in the NEA work between problem-initiated and technology-initiated assessments. In problem-initiated assessments, existing technologies were used in seeking the best possible solution to a given problem. In technology-initiated assessments, the goals were either to identify the effects of some developing technology, or to pick specific applications that matched the technology to several existing or potential problems, thus converting the assessment to a problem-initiated study. The teaching-aid study began as a technology-initiated study, while the subsonic aircraft noise project began as (and remained) a problem-oriented assessment.

Let us examine the procedure used in evaluating the alternatives for reducing subsonic aircraft noise. Here an ad hoc task force was assembled which was knowledgeable in research, economics, airport management, noise engineering, airline operations, law, air frame manufacture, and sociology. The DOT's Federal Aviation Administration and the Department of Housing and Urban Development were included in the task force.

The first segment of the project determined what factors should be included in an assessment. In the social considerations section, for example, individual rights, group rights, environment, recreation, and safety were each examined. Economic considerations included the impact of the noise abatement procedures on the gross national product and on local or regional finances, payment to those "damaged" (in a legal sense) because of inadequate noise reduction, and the cost to operators of noise abatement equipment. Under technological considerations, the noise reduction required by people's tolerance levels was studied; also, technologically feasible noise-reduction techniques were examined. In addition, certain political considerations were raised.

A data base was gathered (it appears as Appendix B of Reference 1) from which conclusions such as the following could be drawn:

- For civil aviation to grow at the rate now predicted, appropriate action must be initiated to reduce the subsonic aircraft noise problem.
- An increasing number of communities are organizing efforts and starting suits to achieve relief from aircraft noise.

Next, strategies to reduce subsonic aircraft noise levels were formulated and studied:

1. Continue the methods used in previous years.
2. Relocate airports.
3. Create a buffer zone around airports.
4. Soundproof the residences affected.
5. Modify aircraft hardware and flight profiles.
6. Rearrange flight operations.
7. Use V/STOL operations to connect to large-plane airports.
8. Use land control, including zoning, around new airports.
9. Require more transportation on the surface.
10. Reduce transportation in favor of added communication.

Next, those affected by these strategies were identified. These included airlines passengers, aircraft operators, aircraft manufacturers, taxpayers, local residents, the local business community, and local and regional governments. The impact of the various strategies was then determined. It was found that modification of aircraft

hardware and flight profiles (strategy 5) had the greatest chance of success. This conclusion was based primarily on non-economic considerations; taking the cost of such modifications into account might change this conclusion.

It was suggested, however, that a "best" solution to such problems might be a combination of two or more alternate strategies. For example, here one might simultaneously modify structures around existing airports (strategy 4), locate new airports away from congested areas (strategy 2), and design quieter engines for the new aircraft (strategy 5).

Certain procedural methods were adopted in the technological assessments carried out by the National Academy of Engineering. It was learned, for example, that no single task force could be employed to carry out a variety of technological assessments. It was better to form ad hoc task forces that were disbanded upon completion of a specific technological assessment. The NAE also learned that cause/effect chains were very useful in problem-initiated analyses, since the future course of events would be a converging one. (The cause/effect approach was suggested by Emilio Q. Daddario; it can be found in Reference 2.)

The NAE study noted that intuitive contributions were important. Individual minority reports were encouraged as part of the study teams' total deliberation, since it was felt that the judgment of creative individuals would provide a key element in the technologically initiated assessment. Even in the problem-initiated analysis the intuition of experts is to be valued.

In summary it was concluded that a technological assessment consists of a mixture of warning signals and glimpses of opportunity. On the one hand, the analysis can predict probable adverse consequences of present trends; on the other, it can point to areas that give promise of improvement in the quality of life. It is important that the technological-assessment participants pursue both ends vigorously. Indeed, preoccupation with emerging problem areas can easily stifle innovative contribution. This assessment process, it was concluded, could provide a forum for both public and private interests for initiating mutually beneficial courses of action.

A final point which appeared in the NAE study is that unpredictable events and discoveries limit the value of long-term forecasts or assessments (where by "long-term" one means over 25 years). A predictive forecast can be expected to last about five years, after which it should be revised to include up-to-date information.

A risk/benefit analysis, described in Reference 3, was carried out for a plowshare project. The authors explore the possible benefits of using plowshare-type atomic explosions to provide for underground natural-gas storage. They quantify the risks by relating them to the amount of time lost by the surrounding population during the explosion. They then relate this risk value to the benefits to be derived by these three groups: the industrial sponsor, the communities within the range of physical awareness of ground shock, and society as a whole.

While this work is preliminary, it does attempt to place dollar values on the risks and benefits to be derived from a technological innovation. Of further interest in this paper are two statements which indicate that risks are not necessarily perceived by people in relation to their everyday existence. First, the local population surrounding an atomic blast may perceive the risks as larger than those estimated by accident statistics from previous shots. Second, the local population (according to the authors) is not *a priori* against any project affecting them; people tend to make their own evaluations of the advantages and disadvantages of the project, and have their own unique conceptions of the benefit/risk ratio. Therefore, one should attempt to get the local residents involved in all possible decisions related to the project.

The approaches of these two studies provide some ideas on how a risk/benefit study of SST flights in the stratosphere might be made. The next section of this paper presents general concepts for use in such an analysis.

GENERAL CONCEPTS TO BE USED IN RISK/BENEFIT ANALYSIS

C. Starr's paper (Reference 4), "Social Benefit Versus Technological Risk," considers the concepts of risk and associated benefits in detail. Starr suggests an approach for establishing a measure of benefit relative to cost for accidental death arising from technological developments and their public use. The analysis is based on two assumptions: first, that the historical national

accident record is adequate for revealing consistent patterns of risk acceptance in the public use of technology, and second, that such historically revealed social preferences are enduring.

Starr found that individuals view social activities as having two different risk levels, depending upon whether their participations are voluntary or involuntary. While it was not always easy to differentiate between these two divisions, his analysis resulted in the curves of Figure 1. In examining this figure, it appears that the risk of death from disease (about 10^{-6} per person per hour of exposure) is a yardstick for determining the acceptability of risk on a voluntary basis. The public seems willing to accept voluntary risks 1,000 times greater than involuntary risks. In addition, the risks are found to be roughly proportional to the third power of the benefits when Starr's calculational procedure is used. In the case of voluntary activity, the amount of money spent on an activity by the average participant was assumed to be proportional to its benefit to him. One last noteworthy conclusion is that the social acceptance of risk is directly influenced by public awareness of the benefits which can be derived, and that the awareness level can be shifted by advertising.

Table 1 presents risks to population on a more quantitative basis. These are the accidental death statistics for 1967, which incidentally, do not change from year to year in any noticeable way. Indeed, in looking over past years, one finds that variations are generally within a factor of ten. For example, lightning caused about 100 fatalities in 1966 and 88 in 1967. (This is a rather low number; usually it is somewhat larger.)

Not all people are equally exposed to each of these hazards, and some are not exposed to certain hazards at all. For example, not everyone will be exposed to death by aircraft, since some never travel by air. Others may live in an area with indigenous poisonous snakes or insects and so assume a larger risk from this cause than urban dwellers. In spite of this unevenness of individual exposure implicit in Table 1's statistics, we feel they have meaning in two respects. First, many of the accident exposures listed are common enough in our society that the statistics do represent the risk for the average person with average exposure. Second, these statistics may represent the bases on which people form their subjective feelings about certain hazards.

Accidents which provide a hazard on the order of 10^{-3} per person per year are difficult to find. When the risk approaches this level, immediate action is taken to reduce the hazard, so this level of risk can be considered unacceptable to everyone. At an accident risk level of 10^{-4} per person per year, people are willing to spend money both privately and publicly to prevent the hazard. Money is spent for traffic signs and control, fire departments are maintained with public money, and fences are built to prevent falls. It is for accidents in this category that this slogan applies: "The life you save may be your own." The magnitude of this risk is apparent to each of us upon entering a car.

Risks at the level of 10^{-5} per person per year are those which people still might recognize. Mothers generally warn their children about the hazard of drowning, and firearm deaths make the news during hunting season. The safety slogans "never swim alone," or "never point a gun" correspond to these accident types. Another factor of 10 down (to 10^{-6} per person per year), it seems that accidents with this risk are not of great concern to the average person. He may be aware of them, but feels that they are not likely to happen to him. We hear such phrases as "lightning never strikes twice" or "an act of God." People seem to have an intuitive yardstick for determining the risk of certain classes of activities.

Another important factor in risk analysis is the number of people dying in a particular accident. For example, an accident which causes the death of 100 people receives more attention than 100 separate accidents that each cause the death of one person, and people are likely to view it as a greater hazard.

The risk level which a population may be willing to assume is, of course, related to the benefit to be derived from a given activity. Involuntary risk seems to have an upper bound not greater than the risk of death from disease, no matter what benefits may result from the activity. Conversely, people seem to accept many natural hazards having risk levels less than or equal to the risk of death from lightning, independently of any corresponding benefit. The curve shown in Figure 2 indicates how our population might respond to involuntary risks,

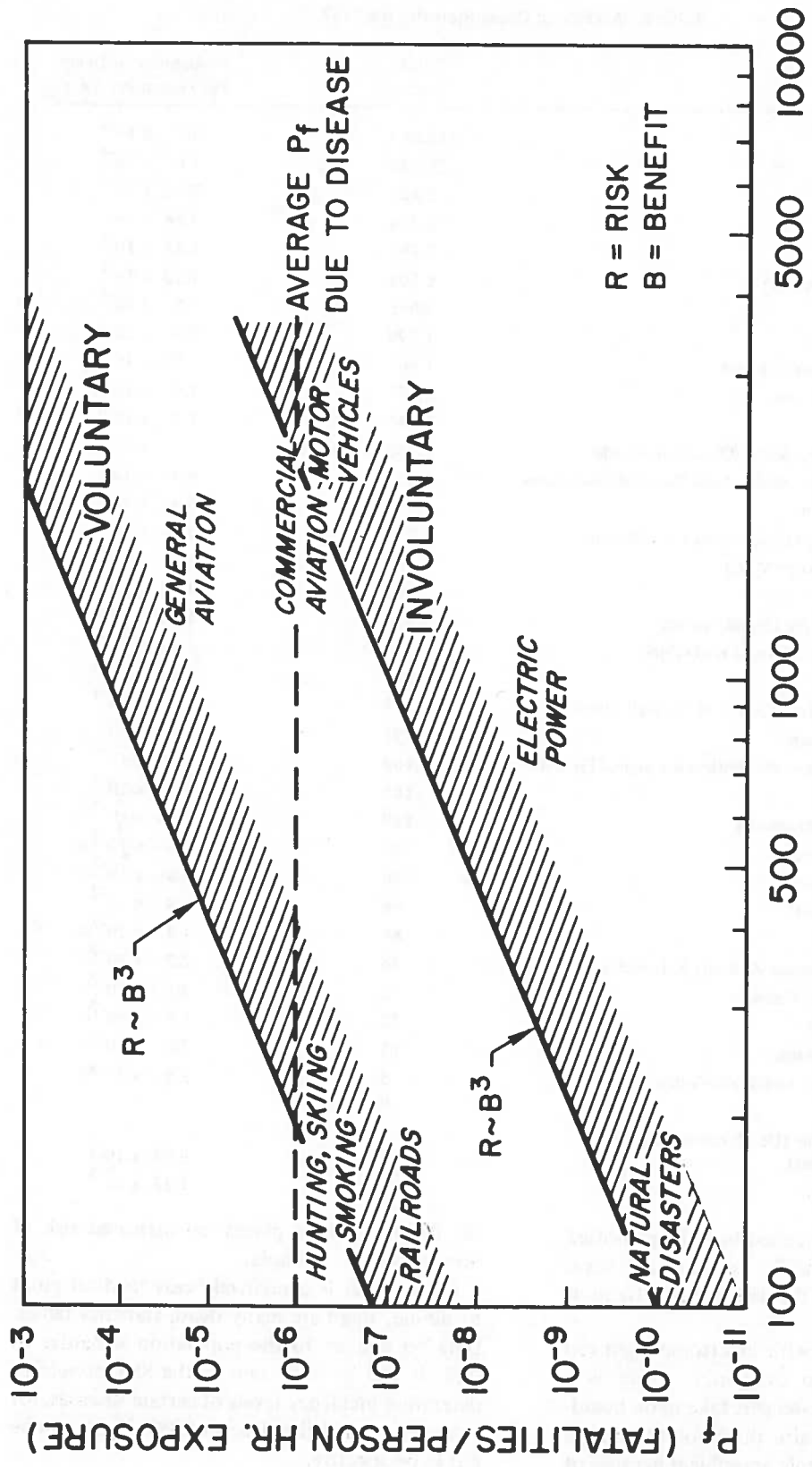

Figure 1. Risk vs. Benefit for Voluntary and Involuntary Exposure

Table 1. Accidental Death Statistics for 1967

Type of Accident	Total Deaths	Probability of Death Per Person Per Year
Motor Vehicle	113,563	5.7×10^{-4}
Falls	20,120	1.0×10^{-4}
Fire and Explosion	7,423	3.72×10^{-5}
Drowning	5,724	2.86×10^{-5}
Firearms	2,896	1.45×10^{-5}
Poisoning (Solids & Liquids)	2,506	1.25×10^{-5}
Machinery	2,055	1.0×10^{-5}
Aircraft	1,799	9.0×10^{-6}
Inhalation and Ingestion of Food	1,607	8.0×10^{-6}
Poisoning (Gases & Vapors)	1,574	1.0×10^{-5}
Water Transport	1,545	7.7×10^{-6}
Blow from Falling or Projected Object or Missile	1,435	7.2×10^{-6}
Accident in Therapeutic Medical and Surgical Procedures	1,262	6.31×10^{-6}
Mechanical Suffocation	1,182	5.9×10^{-6}
Foreign Body Entering Orifice other than Mouth	1,117	5.59×10^{-6}
Railway Accident (Except M.V.)	997	5.0×10^{-6}
Electric Current	992	4.97×10^{-6}
Hot Substance, Corrosive Liquid, Steam	376	1.88×10^{-6}
Inhalation & Ingestion of Non-Food Object	373	1.81×10^{-6}
Excessive Cold	327	1.63×10^{-6}
Road Transport Accident Except M.V., Rail Streetcar	283	1.4×10^{-6}
Hunger, Thirst, Exposure	193	9.7×10^{-7}
Accident in Non-Therapeutic Medical & Surgical Procedures	169	8.5×10^{-7}
Cataclysm	165	8.3×10^{-7}
Cutting & Piercing Instruments	149	7.47×10^{-7}
Animals (Non-Venomous)	125	6.3×10^{-7}
Excessive Heat & Isolation	96	4.8×10^{-7}
Vehicle (Non-Transport)	96	4.8×10^{-7}
Lightning	88	4.4×10^{-7}
Bites & Stings (Venomous Animals & Insects)	44	2.7×10^{-7}
Explosion of Pressure Vessel	42	2.1×10^{-7}
Lack of Care of Infants	22	1.1×10^{-7}
High and Low Air Pressure	13	7.0×10^{-8}
Streetcar (Except M.V. and Train Collision)	5	2.5×10^{-8}
Radiation	0	0
Late Effect of Accident (Death more than one year after accident)	789	3.95×10^{-6}
Other and Unspecified	2,656	1.33×10^{-5}

consistent with the associated benefit quantified as shown. Below the line lies an acceptable area, while above the line the risk/benefit trend is unacceptable.

The risks connected with supersonic flight can be separated into two categories. There is a voluntary risk which passengers take upon boarding a plane. There are also the involuntary risks to which non-flying people are subject because of the flights of these planes—an increased risk of skin cancer, for example.

Since death is a relatively easy medical point to define, there are many death-statistics tables. Data on injuries to the population is harder to find. It will be important to the SST project to determine incidence levels of certain diseases, for example, so that the effects of SST flights can be put in perspective.

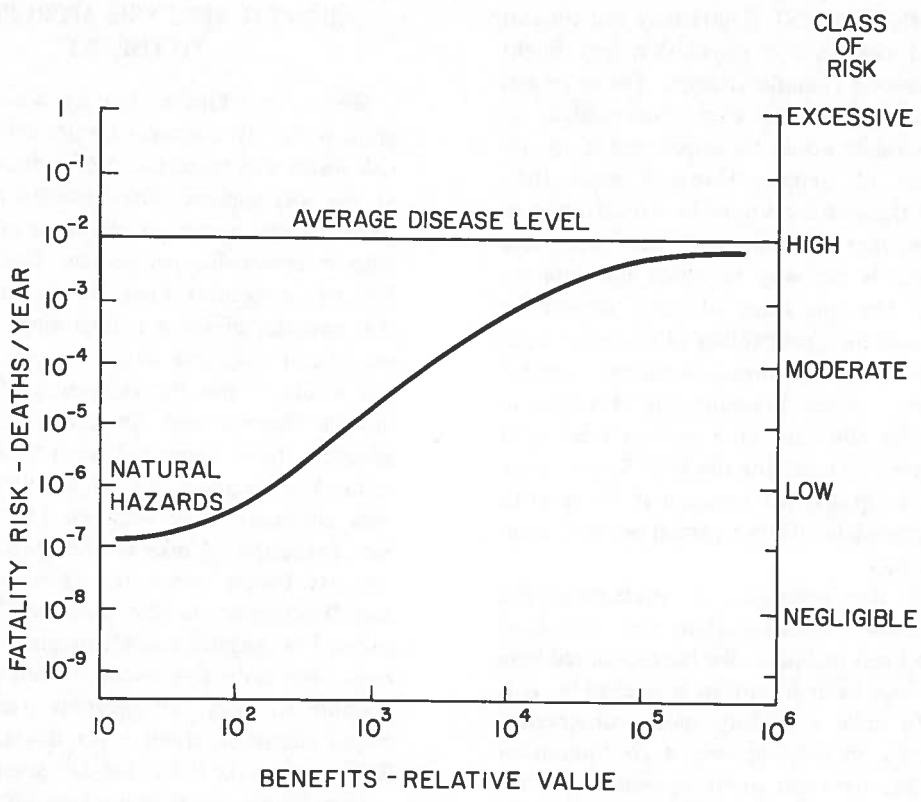

Figure 2. Benefit-Risk Pattern, Involuntary Exposure

Note that within the involuntary risk category we are concerned with two types of risk levels: the absolute risk level and the relative risk level. The absolute risk level is, for example, that which occurs because the planes are flying and carrying passengers. The relative risk level is that which occurs because we are using these planes rather than subsonic planes flying at lower altitudes. Both of these risk estimates are important and relevant to this study.

For the Climatic Impact Assessment Program, it will be necessary to establish what level of risk due to SST flights is acceptable to the population. In Table 1 we see that the probability of death from an aircraft crash is approximately 10^{-5} per person per year. If this risk level were calculated on a per-hour-of-exposure basis, it would increase somewhat. However, present flights have little impact on the ground population. The higher-altitude flights of the SST will not only expose the flying population to a voluntary risk, but expose the ground population to an involuntary risk. This involuntary risk should be made as low as possible—preferably in the natural-disaster range, 10^{-7} per person per year.

RISK ANALYSIS APPROPRIATE TO THE SST

On the basis of our previous discussion, let us divide the risk attendant on SST flights into two categories: voluntary and involuntary. In the voluntary risk section are those that the passengers assume, such as the risk of crash and the risk of irradiation from high-altitude flights. The involuntary risks, those that are imposed on the entire population, include the effects of ozone depletion, general stratospheric contamination at certain levels, and the climatic impact. In addition, the comparable impacts upon our plant and animal life must be estimated.

These risk estimates should be carried out both absolutely and comparatively, as described above, contrasted with the risks of other means of transportation.

Other effects of SST flights may not present any actual risk to the population but might produce adverse climatic changes. For example, optical variations in the stratosphere might be increased, which would be unacceptable to certain groups of people. However small their likelihood, these changes must be considered too.

As important as gathering data on these various risks is the way in which the data are combined. The spectrum of risks should be weighted with their probability of occurrence per year per person, and summed. A sample curve for risk severity versus frequency is sketched in Figure 3, for the case of a nuclear reactor. A similar curve will exist for the SST. Such a curve would be integrated (or summed if discrete) to yield the complete risk per person per year from the SST flights.

One of the problems in evaluating and summing discrete risks is making sure that all of them have been included. We have assumed here that what has been forgotten is negligible. It is possible to take a slightly more conservative viewpoint by integrating over a continuum of points, rather than just summing over those risks that come to mind. Such integration was performed for Figure 3, resulting in meaningful data.

BENEFIT ANALYSIS APPROPRIATE TO THE SST

While the Climatic Impact Assessment Program is mainly concerned with determining the risk levels due to certain SST-induced variations in the stratosphere, the benefits due to SST traffic should also be examined so as to place the risks in reasonable perspective. The benefits fall into two categories. First, there is the benefit to the national business community. Such flights would not only save businessmen precious time, but would permit the expansion of territory to include Europe and Australia. Past air travel advances have permitted such business expansions. For example, we on the West Coast can now commute daily between Los Angeles and San Francisco, thanks to the speed of present-day jets. People commute to Boston, New York, and Washington in the same way. Flights between Los Angeles and Washington or New York now take only five hours, which has made it possible to carry out business transactions between coasts on about a two-day schedule. The SST would make this a one-day operation.

Benefits to society include possible help in our balance of payments if such planes are manufactured in this country, or even if the SST merely

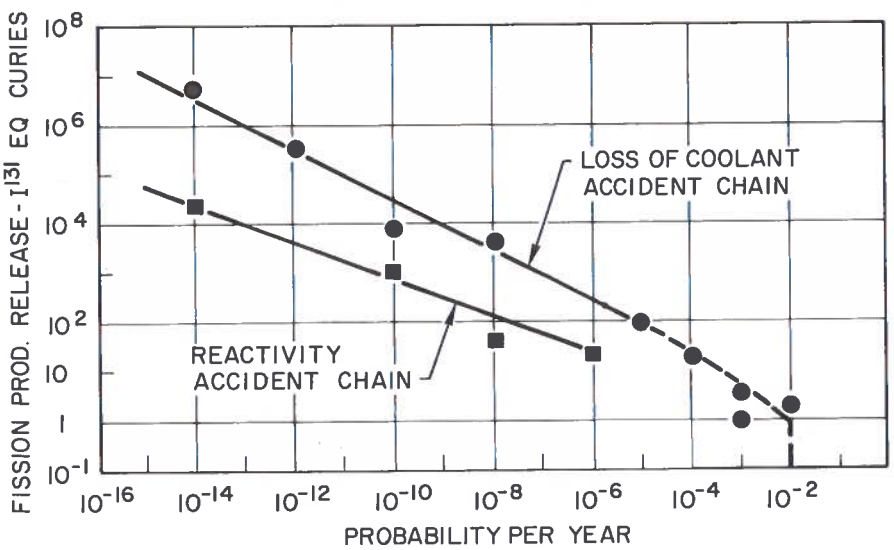

Figure 3. Fission Product Release vs. Probability

improves our business climate. In addition, technology will be transferred from this industry to others, just as we now use at home a number of materials and products which are the results of technological advances due to our aerospace program.

A SUGGESTED PROGRAM FOR CARRYING OUT THE RISK/BENEFIT ANALYSIS

The following program, which utilizes the ideas discussed previously, could be used to carry out an SST risk/benefit analysis. It should begin at a modest level while the fact basis for such a study is being defined and gathered. (This groundwork should take about six months.) The initial program work would include interviews with a series of experts in many professions to obtain their views on risks and benefits from the SST. This initial field work should rapidly delineate the areas that need assessing.

On the risk side, relevant phenomena should be discussed with medical personnel, agricultural experts, demographers, geophysicists, meteorologists, and others. On the benefit side, economists, business forecasters, political scientists, transportation experts, and others should be interviewed. Finally, a group of people (not necessarily different from the above sample) who can predict or envisage the social impacts of a technological change such as the SST should be consulted. This initial phase would provide the Department of Transportation with a preliminary picture of the direction the assessment is taking. The second and more thorough phase of the project, including increased consultations, is expected to validate these preliminary conclusions.

Several main themes emerge from this program recommendation. First, although the Climatic Impact Assessment Program is concerned with the risks of SST flights, the benefits must also be determined to permit a useful, balanced judgment. Second, while the SST is indeed a new mode of air travel, it is also an extension of present air transport, an upgrading of existing technology. A comparative study as well as an absolute one is needed. Third, the experience and intuition of as many professionals as possible should be brought to bear on an SST assessment. The broader the spectrum of inputs, and the more informed the opinions, the greater will be the value of the risk/benefit analysis.

REFERENCES

1. *A Study of Technology Assessment,* Report of the Committee on Public Engineering Policy, National Academy of Engineering, July 1969.
2. Daddario, Emilio Q., *Technology Assessment,* Statement to the Committee on Science and Astronautics, U. S. House of Representatives, July 3, 1967.
3. Otway, H., VanderHarst, L., and Higgins, G., *Socio-Economic Aspects of a Plowshare Project,* Los Alamos Report LA-DC-12796, 1971.
4. Starr, C., "Social Benefit Versus Technological Risk," *Science, 165,* 1232-38, Sept. 1969.

DISCUSSION

P. Lebouc suggested that airplane travel be evaluated in terms of seat miles rather than hours of exposure, which would make it possible to compare different modes of transport fairly. He also felt that risks decreased sharply in the 60's, and pre-1960 data reflected prop-jet risks. Erdmann agreed on the first point, but said his data to 1970 did not suggest much change in risks in the 60's. J. Kassner pointed out the difference between SST passenger-mile risks (voluntary) and those to Earth's population and ecology (involuntary). L. Anderson agreed with time as a parameter, and asked about criteria for predictions – for example, whether controlled experiments or accident statistics were used in the nuclear case. Erdmann said they were system failure data based on component data. The voluntary and involuntary risks associated with automobiles were lightly touched on.

INTRODUCTION TO CONFERENCE SUMMARY

Alan J. Grobecker

At this conference we have talked about a great many things in passing, but the relevance of each to the others has not always been brought out. Professor Erdmann's presentation of risks versus benefits voiced some interesting ideas which help to keep things in perspective. We must recognize that CIAP is not concerned with justifying a particular mode of travel. If our assessment reveals only harmful environmental effects, it is for the proponents of supersonic transport or whatever to show whether the economics balance or outweigh the other factors. We should be careful to keep this an objective scientific study, and raise issues rather than espouse causes.

CONFERENCE SUMMARY

MICHAEL B. McELROY
Harvard University
Cambridge, Massachsetts 02138

I have the unenviable task of trying to show how all the material presented in the last two days is applicable to the Climatic Impact Assessment Program, and leading the discussion of what recommendations we should or can make at the moment. I must say I am staggered by the magnitude of the task. Never before have I been deluged with so much concentrated information in two days, or covered such an enormous range. We have gone all the way from significant minor species like CH_3O_2, present only in traces, to obviously major questions, such as what an increase in ultraviolet radiation could do to mankind or the ecological balance.

I did have some help in trying to pull this all together. The two people mentioned in the program, Dr. McConnell and Dr. Wofsy, were very helpful. Dr. McConnell unfortunately is in the hospital today, though I don't think it was a reaction to the first day's talks. I have also had a great deal of help from Dr. Donahue and Dr. Blamont, but they shouldn't be held accountable for anything I say.

As I see it, the problem can be divided into several fairly distinct areas, though there is a considerable overlap. Let's start with the chemistry and dynamics of the normal atmosphere. I think this is worth a good deal of thought. What is the chemistry of the normal atmosphere? What are the relative roles of the chemistry, dynamics and other physical processes? Obviously we must understand the normal atmosphere before we can make any detailed predictions of what will happen when we add gases or particulates to a region of the atmosphere.

Second, we must define what we mean by the "polluted" atmosphere. How do we model the effects of the aircraft we discussed today? What are their effluents? How are they distributed with height and geographic position?

The third topic is the chemistry of the polluted atmosphere. Given this magic figure of 500 aircraft flying in the stratosphere, how serious a problem are we faced with? Can we say right now that it is very serious? On the other hand, can we say that it is *not* very serious? There are people here who feel strongly both ways, and I should like to address the question later.

We must certainly address the ecological effects of stratospheric flights. To some extent this is a separate issue, but it is obviously extremely important. And last, there are the economic tradeoff factors. Those I don't feel competent to comment on; you've just heard an expert's commentary.

Let me start with the chemistry. What is it that controls the natural level of ozone? Can we define the relative importance of water and oxides of nitrogen? We heard the excellent discussions of the chemistry from Nicolet, Johnston, and Crutzen. Indeed, this subject in a large measure belongs to Professor Nicolet; together with Chapman and Bates, he is responsible for much of what we now know. For many of the problems discussed at the

conference, we are still trying to put details into papers written 20 or 30 years ago.

One large change which was clearly emphasized at this conference concerns the role of hydrogen compounds in ozone chemistry. It now looks as though the effect of hydrogen on the ozone reaction scheme has been somewhat overplayed recently. That happened because it was very difficult to account for the observed ozone using the simple Chapman chemistry, the classic pure-oxygen model. Something else was needed, and the obvious thing was to look at the water system. The laboratory data were not good enough to define the rates for some important ozone reactions, notably the OH and HO_2 reactions. Aeronomical modelers had a lot of fun playing games adjusting those parameters to fit the data. Having two adjustable parameters helps a lot in fitting one profile, especially if you can blame the rest of the problem on dynamics.

Let me remind you of the two hydrogen reactions which formed the keystone of the wet-oxygen chemistry: $OH + O_3 \rightarrow HO_2 + O_2$ and $HO_2 + O_3 \rightarrow OH + 2O_2$. The subject owes a great debt to Professor Kaufman, who publicized the upper limits of the rate coefficients, and a much smaller one to the people who later turned those limits into actual rate coefficients and in some cases even attached activation energies to them.

What has happened to change this state of affairs? A recent paper by Langley and McGrath reduced the upper limit on the $OH + O_3$ reaction by three orders of magnitude: their new upper limit is 10^{-16}. As several speakers at the conference have pointed out, this finding effectively eliminates the wet chemistry as a significant catalyst in the removal of atmospheric ozone.

I think that's a fair summary of where the subject is now, but I feel a word of caution is appropriate. Much depends on a single measurement of the $OH + O_3$ reaction by Langley and McGrath, and there aren't many details in their paper. The study is probably valid, but the reaction is so central to the entire ozone problem that it merits further laboratory study. I understand that Kaufman and Anderson have one such experiment in progress.

The most recent innovation in ozone chemistry concerns the role of oxides of nitrogen. It seems beyond dispute that odd nitrogen plays an important catalytic role, as discussed by Crutzen and Johnston. Unfortunately, we don't know what the NO_x concentrations in the ambient atmosphere are, a point which I want to stress. We have no reliable measurements of NO_x in the regions of the stratosphere in which the ozone catalysis must occur. I don't mean to minimize the importance of NO; I consider it essentially established that NO plays a very important role in determining the ambient ozone concentration.

Let me say a few words about the physics and chemistry of atmospheric NO. The NO problem involves a complicated distribution of sources and sinks. There is one source of NO in the ionosphere above about 100 kilometers which supplies a flux of the order of 10^8 molecules per square centimeter per second to the mesosphere. This source is formed by chemical reactions involving charged particles. There is also a source at ground level: pollution. Presumably automobiles and the like are major contributors. Some fraction of the ground NO_x source can reach the stratosphere by upward diffusion. The dominant sink for NO_x is in the troposphere; it involves the rainout of NO_2 and HNO_3.

A third source is particularly interesting because it represents the only known natural mechanism for the production of NO in precisely the region of the atmosphere in which the aircraft would be flying. This source involves the reaction $N_2O + O(^1D) \rightarrow 2NO$. The N_2O, as we heard at this meeting, is largely produced by bacteria at the surface of the earth. It diffuses upward and is photolyzed, mostly to give nitrogen molecules and oxygen atoms, but some fraction of the events leads to production of NO in the stratosphere at a rate which we can calculate with a fair degree of confidence, since we have actual measurements of N_2O in the troposphere and the lower stratosphere.

Figure 1 shows calculations of the mixing ratio of N_2O as a function of height in the atmosphere, and offers a comparison of those calculations with observations which exist for the upper troposphere and lower stratosphere. Part of this calculation tries to infer the magnitude of the source of NO associated with N_2O. The calculation makes the serious assumption that transport can be modeled by eddy diffusion.

If we consider the various estimates for NO_x production by 500 planes, we must conclude that the SST would be comparable to, or even larger than, the natural source, if the numbers are right.

It follows that stratospheric flight is at least a potentially serious disturbance to ambient conditions in the stratosphere.

What McConnell, Wofsy, and I did was to see to what extent we could model the chemistry of the nitrogen-carbon-oxygen-hydrogen system. We tried to do as complete a job as possible on the chemistry, while also recognizing the importance of dynamics. Figures 2 through 6 show the results of these calculations.*

Figures 2 and 3 show the vertical distribution of CH_4 and CO. For the details I refer you to our article "Atmospheric CH_4, CO, and CO_2," which should appear in the *Journal of Geophysical Research* this year. Figure 4 shows theoretical curves for HNO_3, calculated under various assumptions. Let me remark on these assumptions. I mentioned the importance of the ionosphere as a source of nitric oxide for the stratosphere. Professor Nicolet commented on the probable importance of very slow loss processes for NO because of the very long time constants involved in the downward diffusion of material. If we assume no destruction at all of NO in the stratosphere, that it simply flows down until it reaches the rain-out sink in the troposphere, this model should define an upper bound to the amount of HNO_3 as indicated in Figure 4.

In another model we made the very drastic assumption that there is some slow release of atomic nitrogen associated with the photolysis of NO_2. No experimental data suggests that this might be so, and I think it chemically unlikely, but suppose you take the measured absorption cross-sections of NO_2 and, where energetically possible, consider a possible source of N. I think we adopted a quantum yield for N of 10% in this study. Atomic nitrogen can react with NO, making molecular nitrogen with consequent removal of odd nitrogen. Again, remember that there is no observational evidence that NO_2 photolysis actually leads to any significant source of N. But laboratory measurements in this area would be interesting and might be important.

Another study considers the production of N by predissociation of NO in the delta bands. There is strong observational evidence that this process does indeed occur. The aeronomical uncertainty involves the transmission of the radiation near 1900 Å, which is limited by the Schumann-Runge bands of molecular oxygen. This is a very difficult problem. The transmission in the Schumann-Runge bands must be very carefully analyzed in order to make any precise estimates of the magnitude of the odd nitrogen sink.

One might then guess that the preferred theoretical curve would be curve A. The observations (the points with horizontal error bars), on the other hand, appear to show rather more HNO_3 than this calculation. I believe that there is important loss of odd nitrogen in the flow region. I don't feel very confident about NO_2 as a source of N, but I feel that the NO predissociation is fairly well established.

Figure 5 shows the computed profiles for NO_2; again the no-loss situation gives us a rather large amount of NO_2. The other calculations, which explore other uncertainties in the model, show somewhat smaller amounts of NO_2. The NO_2, NO, and HNO_3 in these calculations are all essentially equally abundant. HNO_3 is most abundant in the lower stratosphere, next NO_2, then NO.

The two points with vertical error bars represent a preliminary attempt to see how much NO_2 might be present. These results are derived from spectroscopic observations made by Murcray and his associates. Dr. Wofsy has been considering this problem. The two points reflect two assumptions about the curve of growth of the NO_2 lines. In one case it was assumed that the absorption would lie on the linear part of the curve of growth. In the other case it was assumed that the absorption would lie on the square-root part of the curve. These are the spectroscopic extremes for the possible range of NO_2 implied by those data. Again, note that there seems to be a tendency to calculate less NO_2 than what may be observed.

Figure 6 shows something which I think was not adequately aired at this conference. Professor Hale spoke only briefly after Dr. Heath about his NO or NO_2 measurements in the stratosphere and mesosphere. The point is that if he is correct, there is quite a large amount of NO or some unidentified ionizable constituent in the stratosphere. Hale's experiment was very direct, at least in principle. He was measuring the production of electrons due to the ionization of the ambient air by a Lyman α source carried on a rocket. Judging from the standard chemical tables, it is very

*This work was supported by NSF Atmospheric Sciences Division under Grant GP-13982 to Harvard University.

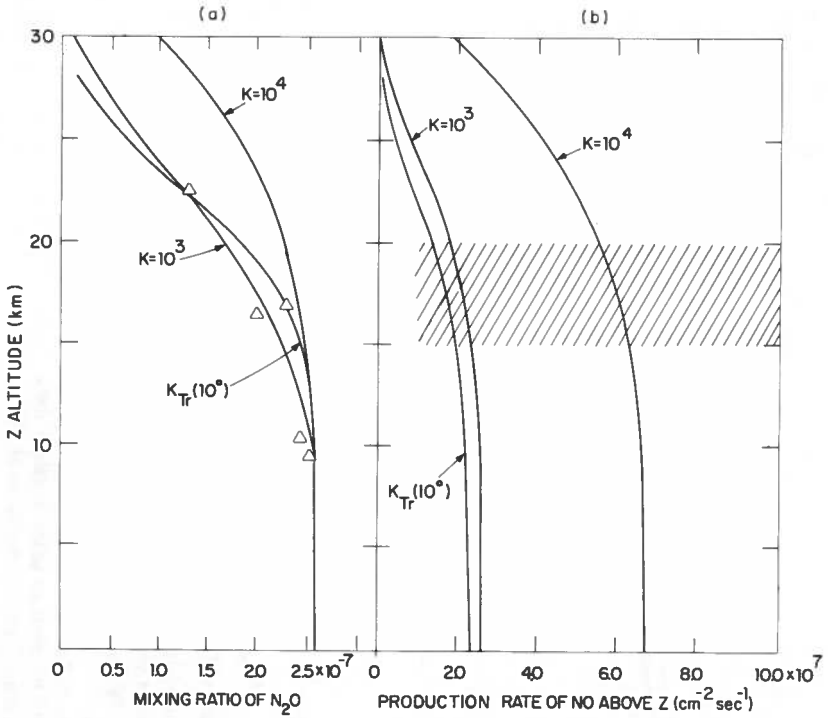

Figure 1. Part (a) shows the mixing ratios of N_2O computed for three different values of the eddy coefficient in the stratosphere. The curve marked $K_{Tr}(10^o)$ was calculated using the 10^o latitude (Oct. - Dec.) vertical eddy coefficients of Gudiksen et al. (1968) obtained from tracer studies. The triangles are the observations taken from Figure 8 of Schütz et al. (1970). The calculations were constrained to give an N_2O mixing ratio of 2.6×10^{-7} at the surface with the tropopause at 10 km. Part (b) gives the production rate of NO above the altitude Z from the reaction $N_2O + O(^1D) \rightarrow 2NO$ for various values of the stratospheric eddy coefficient. The total amount of NO production (cm^{-2} sec^{-1}) from photodissociation (assuming a 1% NO yield where energetically possible) is 15 and 30% of that from the above reaction for $K = 10^3$ and 10^4 cm^2 sec^{-1} respectively.

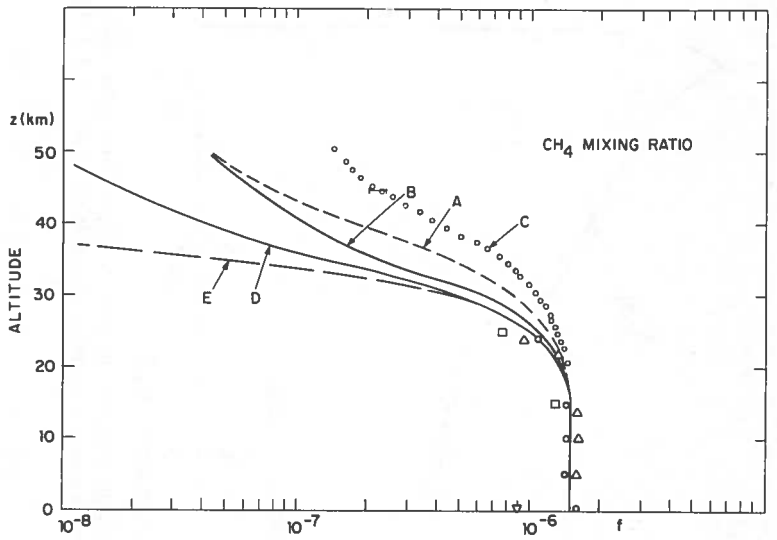

Figure 2. Calculated mixing ratios for CH_4: A, Model 3; B, Model 1 with rate coefficient of Hochanadel et al. (1972) for reaction $OH + HO_2 \rightarrow H_2O + O_2$; C, Model 3, with the same rate coefficient; D, Model 1; E, Model 2. Data of Bainbridge and Heidt (1966) are indicated by △ and ○, data of Kyle et al. (1969) by □, and data of Ehhalt et al. (1972) by ⊢⊣.

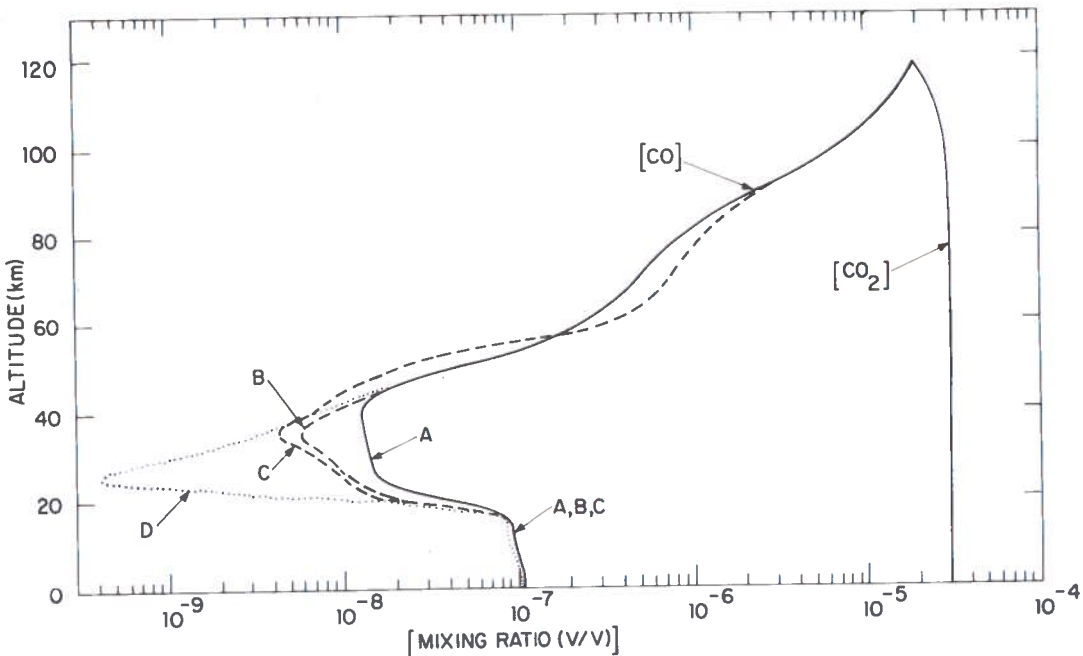

Figure 3. Mixing-ratio profiles of CO and CO_2. Curves A, B, and C correspond to various assumed eddy diffusion coefficients. Curve D uses the same eddy diffusion coefficient as B, without CO production from CH_4 oxidation.

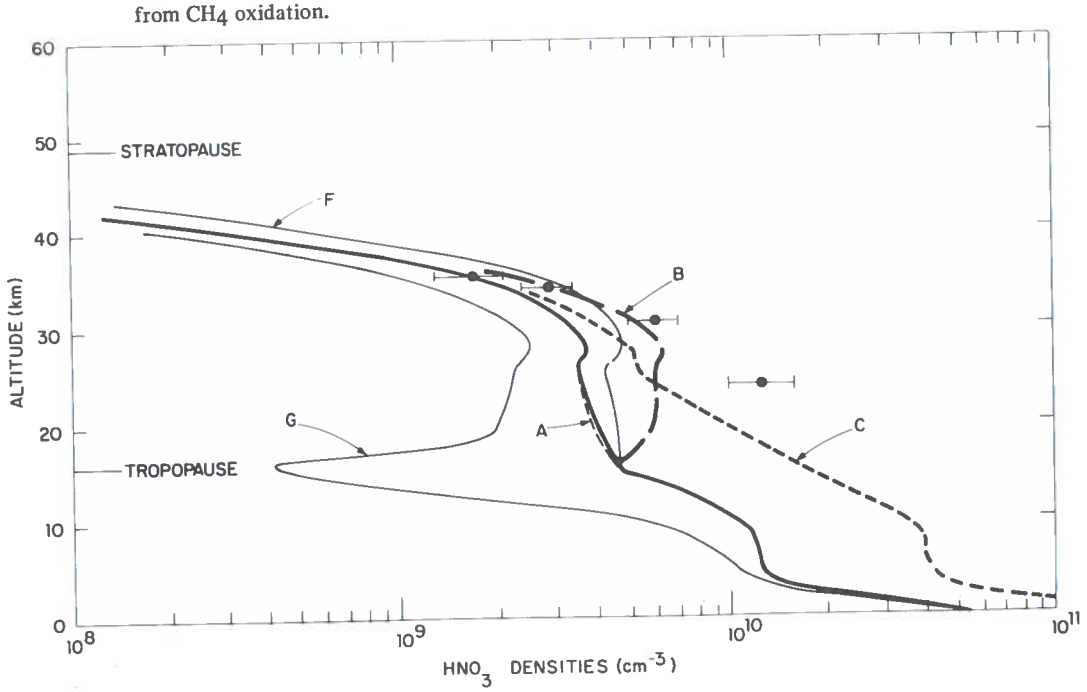

Figure 4. Density of HNO_3 (cm^{-3}). The notation in this and subsequent figures is as follows:

A: Standard model, using best estimates for uncertain rate constants.
B: Uses $O(^1D)$ quantum yields measured by DeMore and Raper for O_3.
C: Assumes a high value for surface mixing ratio of NO_x, 1.0×10^{-8}.
D: Neglects ionospheric source of NO.
E: Assumes an enhanced ionospheric source of NO, 1.5×10^8 cm^{-2} sec^{-1} at 80 km.
F: Neglects loss of NO by predissociation in delta bands.
G: Assumes unit quantum yield for photolysis of HNO_3.
H: CH_4 and CO chemistry included in calculations.

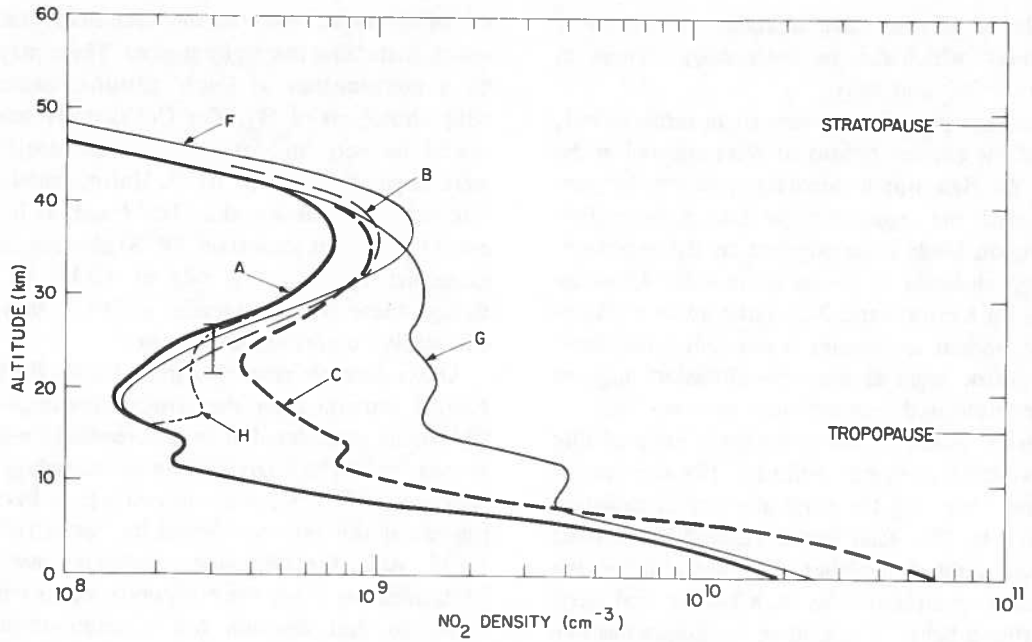

Figure 5. Density of NO_2 (cm^{-3}).

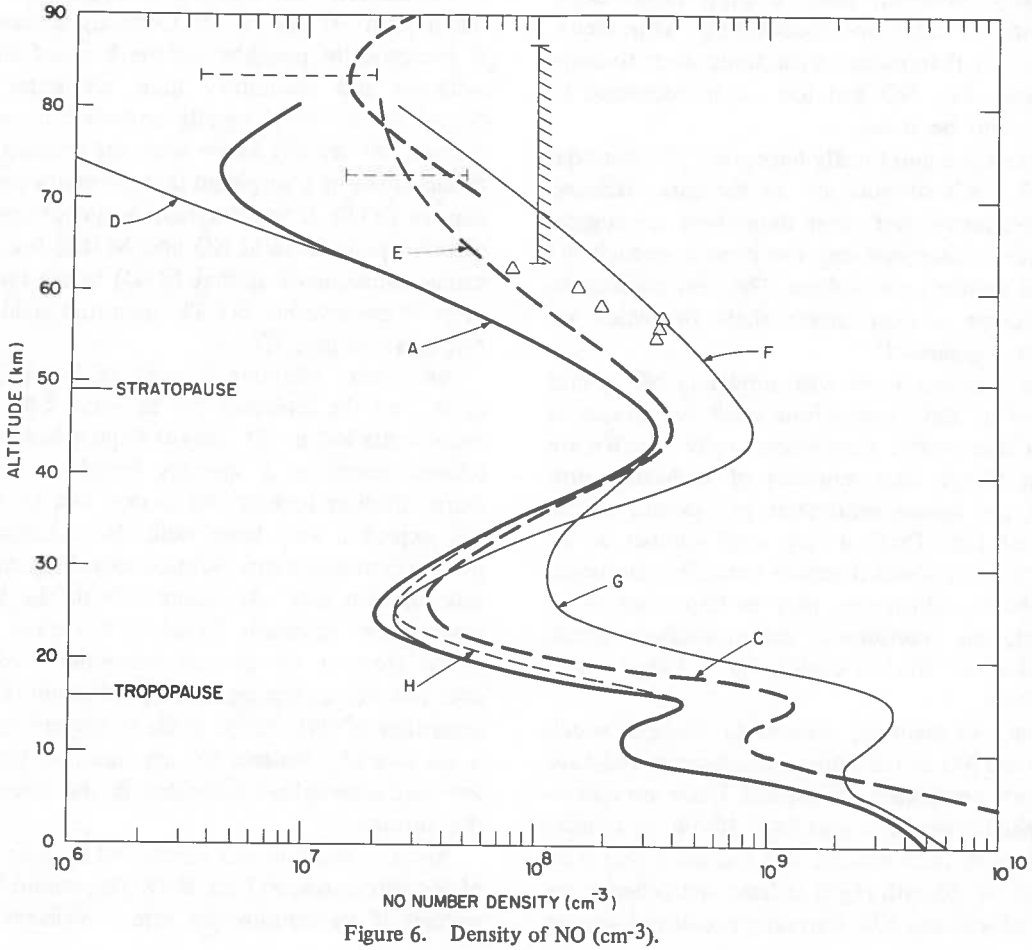

Figure 6. Density of NO (cm^{-3}).

difficult to identify any abundant atmospheric constituent which can be ionized by Lyman α, other than NO and NO_2.

If we interpret the experiment in terms of NO, we find the concentrations of NO indicated in the figure. As Hale noted, his data appear to be consistent with the higher-altitude data of Meira. This comparison lends some support to the approach, although all kinds of caveats are in order. Obviously data on stratospheric NO, gathered by a variety of independent techniques, are urgently required. Hale's work suggests that the situation may be more complicated than any of us now realize.

Meira's results, on the other hand, are probably quite reliable at higher altitudes. His experiment involved observing the total amount of radiation scattered by NO. That signal is then differentiated to derive ambient densities. At lower altitudes the problem is complicated by high background levels of scattered light. The airglow technique has limited use below 80 km. Recent studies of D-region chemistry, however, seem to imply rather larger amounts of NO, not inconsistent with Meira. Again, our theoretical calculations seem to compute too little NO, not too much, compared to what might be there.

In sum, we don't really have good observational data. I don't consider any of the data discussed here definitive. But what data there are suggest that our calculations may not provide enough NO for the ambient atmosphere. The next question is, what other sources might there be which we haven't considered?

The problem I see with modeling NO is that most of us don't realize how small the sources of NO in the normal atmosphere really are. We are talking about total numbers of molecules produced per square centimeter per second of the order of 10^8. That's a very small number, so we have to worry about reactions normally considered improbable, which may play an important role — in fact, any reactions in the atmosphere which have the net effect of cycling N_2 and O_2 to yield some NO.

Now, are there any reasonable reactions which can make NO in the normal atmosphere and have not been considered previously? There are quite a few which merit a serious look. If you start thinking of metastable species, you recognize that reaction of $O(^1S)$ with N_2 is at least energetically capable of yielding NO. Certainly non-trivial sources of $O(^1S)$ exist, such as the Chapman reaction, which maintains the night airglow. There may also be a contribution at lower altitudes associated with photolysis of O_3. The $O(^1S) + N_2$ reaction would be very important if its rate coefficient were larger than about 10^{-16}. Unfortunately, the rate coefficient is less than 10^{-19} and, as it turns out, $O(^1S)$ is not important. $O(^1S)$ also reacts with molecular oxygen at a rate of 10^{-13}, so even though there are large supplies of $O(^1S)$, they play essentially no part in NO chemistry.

Other possible schemes can be found. Professor Nicolet remarked on the possible importance of $O(^1D)$; he considered it in a three-body reaction to give N_2O which would then by secondary reactions give NO. That reaction could have been important if the rate coefficient had been 10^{-32} or 10^{-33}. Alas, the laboratory chemists have again been uncooperative; the rate coefficient is trivially small, so that reaction too is unimportant for atmospheric NO.

Conceivably, the reaction of $N_2(A^3\Sigma)$ with O might yield NO and $N(^2D)$. Certainly the reaction is energetically possible. On the basis of airglow evidence and laboratory data, we know that $N_2(A^3\Sigma)$ is indeed rapidly quenched by atomic oxygen. We do not know what the products are, though there is a suspicion that the major product may be $O(^1S)$. If we entertain the possibility of a reaction path to yield NO and $N(^2D)$, the interesting consequence is that $N(^2D)$ reacts immediately to give another NO. The quantum yield from $N_2(A)$ would be 2NO.

Are there adequate sources of $N_2(A)$? Not many, but the molecule can be excited by ultraviolet radiation in the Vegard-Kaplan bands. The relevant transition is optically forbidden. The radiative lifetime is about one second, and we would not expect a very large yield. Nonetheless, the process certainly merits further study. Incidentally, this reaction may play some role in the higher atmosphere; Professor Donahue has some fascinating ideas on the auroral atmosphere and possible instabilities leading to the production of great quantities of NO. Nitric oxide in the atmosphere poses lots of problems for mankind, particularly for that elite subset interested in the physics of the aurora!

Another reaction was mentioned by Bates, that of N_2 with ozone to form N_2O. This would be important if its bimolecular rate coefficient were

about 10^{-27}; unfortunately, according to Goody and Wallshaw, the rate coefficient at room temperature is less than 10^{-30} cm^6 sec^{-1}.

A more likely process leading to NO involves the reaction of N_2 with O to form N_2O in the presence of a third body. That reaction is chemically very similar to $CO + O + M \rightarrow CO_2 + M$. The CO_2 reaction is slow, less than 10^{-36} cm^6 sec^{-1}, but as we remarked earlier, even slow processes may play an important role for NO. From the work of Dondes and Harteck one can infer an activation energy for the N_2 + O reaction. Their analysis implies a three-body rate coefficient of about 10^{-42} cm^6 sec^{-1} at room temperature, and one is tempted to dismiss the process as an unimportant source of N_2O. One is normally conditioned to think of thermal distributions of atoms in the atmosphere; however, we must recognize that the atoms are produced with kinetic energy. For example, O atoms are produced by the quenching of O(^{1}D), and their initial translational energies may be as large as 1 eV. If so, then O(^{3}P)* may have enough energy to overcome the activation barrier to form the N_2O complex. Normally the complex is unstable, and returns to the initial reactants; however, roughly one in 10^5 collisions may give the stable N_2O form. Considering O(^{3}P)* to be the main product of the quenching of O(^{1}D), which in turn is roughly equal to the photolysis rate of ozone, we have a source of hot atoms of the order of 10^{14} cm^{-2} sec^{-1}. A source of NO of the order of 10^8 cm^{-2} sec^{-1} is significant. Hence an efficiency of 10^{-6} for $N_2 + O + M \rightarrow N_2O + M$ would become interesting. Some branching is associated with the N_2O + O(^{1}D) reaction required to form NO. The N_2 + O mechanism is certainly speculative, but should be studied in view of its potential importance.

Now, what about the SST? Despite our hosts' admonitions, we spent very little time talking about aircraft other than the SST. The major question is, how much is the natural NO level in the atmosphere increased by stratospheric flight, and how much does this affect the ozone level? Johnston put the case very succinctly: you can simplify matters greatly if you first calculate the integrated source of NO in the stratosphere; if the present amount is important for the current atmosphere, and if an SST will deposit 10 times that, the addition will lead to some reduction in ozone. That statement ought to be free from controversy, and should apply irrespective of the role of dynamics.

There is, however, one caveat: If the natural level of NO is somehow determined by ozone, then reducing ozone cuts down the natural source, and the SST might simply be acting as a restoring force. The N_2 - hot O reaction chain has the interesting feature that production of NO at a given total atmospheric density varies as the square of the ozone density, because O(^{1}D) is used twice to make NO. If NO production depends on the square of the ozone concentration, there may indeed be a restoring process.

We should at least consider the possibility that the natural level of NO is somehow directly controlled by ozone itself. If that is so, then the nonlinearities are going to be very important, and any predictions about what the SST does chemically need careful study. Again, let me caution you that these ideas are highly speculative; they are intended merely to indicate that significant gaps remain in our knowledge of atmospheric chemistry.

The debate about the roles of dynamics and chemistry struck me as overstated on both sides and unproductive – though perhaps I just didn't understand it. As I see it, dynamics clearly plays the dominant role in determining the actual geographic distribution of ozone. The ozone at high latitudes is there because it was transported from low latitudes. Again, there is the question which Johnston raised: If you integrate the continuity equation over height, and integrate it over latitude using the tropopause as a base, Johnston would say that the total amount of ozone produced in the stratosphere, minus the total amount lost, obviously has to be equal to the flux into the troposphere, since that's the only place it has to go.

I don't see what conclusion can be drawn on the basis of that statement. There are two terms, production and loss, which may be of roughly equal magnitudes, but we can't reliably estimate the loss term because right now we don't know what the NO level is. It seems to me the debate is proceeding in a vacuum. Dynamics and chemistry both play parts, but we need a lot more work before we know exactly how much of each is involved in controlling what.

As to recommendations, I see a prime need for atmospheric measurements. We are talking about the chemistry and dynamics of the atmosphere from the point of view of ozone with grossly inadequate data. We need good measurements of NO, NO_2,

and HNO_3, as well as reliable measurements of OH if possible. Can Anderson's measurements be extended to lower altitudes? Are there possible schemes for measurement of HO_2? In fact, we really need an extensive set of measurements of all the active chemical constituents.

There is one important point which I forgot to mention. Now that odd hydrogen has been demoted to a subsidiary role, and methane and nitric oxide have been promoted to more important roles, let's recognize that it's gotten harder to model the chemistry of the atmosphere. In my opinion, the OH concentration is greatly influenced by the concentration of CO, and by the concentration of methane near the ground as well. CO plays a very important role in determining the balance of OH versus HO_2.

Second only to the need for good field measurements is the need for good laboratory work, which is my second recommendation. A lot of the chemical rate coefficients are not well enough known. Blamont has spoken of one technique he is studying: the possibility of using a resonant cell to measure the airglow of NO, which would get rid of the scattering background problem which the Boulder group has. That experiment may have the potential for detecting very small amounts of NO. Schiff expects to be able to measure as few as 10^8 NO molecules per cubic centimeter in the stratosphere by the chemiluminescent reaction of NO with O_3. Again, the point is that we now seem to have the ability to make these critical measurements; since the stratosphere has become very important to many people, we must make them. I won't enumerate all those processes which should be studied, but two of them are the yield of $O(^1D)$ from O_3 as a function of wavelength, and Langley and McGrath's measurement of the rate of $OH + O_3 \rightarrow HO_2 + O_2$ which must be confirmed or invalidated.

Another recommendation is that we try to clarify the role of dynamics. One way to go about it, which we heard described here, is to use computer simulation to solve the primitive dynamic equations. Valuable though that is, it can't tell the whole story. Computer simulations run into certain difficulties, which I'm not sure were brought out at this conference. One difficulty is that atmospheric chemistry involves a very large range of time constants, and an equally impressive range is associated with the dynamics. For example, data on the fallout of radioactive debris suggest residence times of as much as five years at 35 kilometers. To me that means that the computer programs must function reliably – i.e., without the sub-grid-scale noise – for a model time of at least five years. That's a long time compared to current simulations.

In other words, the stratosphere poses problems for dynamic meteorologists which are intermediate between weather prediction and climatology, which predicts the dynamics over a very large time scale. Dynamic climatology programs are expensive to run, even without the chemistry. At present, the only economical way we have for grappling with the problem of putting the chemistry into the dynamics and vice versa is to use simplistic concepts like eddy diffusion. Do they even establish the direction of the flow? Are the flows contragradient rather than along the gradient? These are the kinds of information which dynamic modeling can usefully feed back into aeronomy. In any event, a proper marriage of dynamics and chemistry must precede any satisfactory solution of the stratospheric problem.

As for engine effluents, we clearly need to resolve the variety of NO_x emission estimates for the Concorde, the GE engine, and so on, by means of reliable laboratory or field measurements.

We undoubtedly need more work on the biological implications. Physical scientists tend to be a little offhand about them, but the skin cancer issue is really serious, to say nothing of all the ecological effects.

DISCUSSION

H. Levine pointed out that even if Langley and McGrath were wrong by about two orders of magnitude, odd hydrogen still cannot account for the ozone deficit. He noted that there had been very little mention of the possible role of subsonic jets, even though about 10 or 15 per cent of the total air traffic enters the stratosphere, and that percentage will grow. Both this traffic and all that just below the tropopause contribute NO_x to the stratosphere, and it is very important to estimate those contributions. First, we must determine whether the amount already put in is significant compared to what we conjecture for the unpolluted strato-

sphere; second, we must calculate how large the subsonic traffic contribution to stratospheric NO_x will be 20 years from now. It might be significant in comparison with the projected SST input. In fact, if we assume for the sake of argument that the NO_x output of the SST turns out to be a very serious problem, we may find that the subsonic NO_x problem is equally severe, and all have to go back to traveling by train.

McElroy agreed that subsonic aircraft do indeed fly in the stratosphere at high latitudes. Aeronomists used to think the tropopause an impermeable membrane, but to dynamicists it is not. Does the stratosphere really have integrity over the entire globe? Does an exhaust injection make its way into the region in which it can destroy ozone, or does it pass through the tropopause gaps and eventually rain out to the surface? 500 SST's are equivalent to about 10^{11} passenger miles a year, considerably more than the present traffic.

K. Forney called attention to one part of the SCEP report which had been overlooked at the conference, except for McElroy's mention: the water introduced by subsonic jets at subsonic cruise altitudes. The report said that contrails and clouds might increase at a greater rate if U. S. SST development were discontinued and the increased traffic handled by subsonic planes.

McElroy responded that he was not competent to judge that, but that it was certainly true that the likelihood of contrails' forming in the stratosphere is significantly less than in the troposphere. The extra moisture introduced in the cloudiness might have some long-term effects on the climate, but we don't know how to predict climatology yet. Unless the state of the art in dynamic meteorology can start to handle this, we will have to wait and see whether anything happens, or else go back to the train before it does. McElroy felt that this question was an appropriate one for CIAP to consider. Goldburg suggested that we should be wary of trains, and pointed out that per passenger mile the aviation gas turbine provides one of the cleanest forms of passenger transportation.

A. Barrington commented apropos of Hale's experiment that he believed other components might ionize at Lyman α, such as hydrocarbons. McElroy replied that he could not find anything in the chemical handbook other than NO with an ionization potential of less than 10 volts.

G. Daniels suggested that since the literature was not in agreement about the relationship between average integrated ozone content and sunspot cycles, and the UV radiation was important, further measurements of correlation between minimum ozone content and sunspots might be worthwhile. He said some papers had correlated certain diseases with sunspots. McElroy agreed that the question was an interesting one and pointed out that sunspots could affect the ozone chemistry both directly and through ionospheric production of NO. F. Marmo added that a recent article said that variations in solar cosmic radiation caused up to 15% changes in ozone content. He also corroborated Barrington's statement, saying that residual signals can be observed during ionization experiments, which do not match any of the thresholds listed in the handbook, indicating some unknown background substances.

LIST OF PARTICIPANTS

Dr. Arthur C. Aikin
Goddard Space Flight Center
Greenbelt, Maryland 20771

I. E. Alber
TRW Systems
1 Space Park
Redondo Beach, California 90278

Capt. Hugh Albers, USN (Ret.)
Department of Commerce
Washington, D.C. 20230

Dr. Franklin Aldrich
Environmental Medical Institute
MIT
Cambridge, Mass. 02139

J.M. Anderson
Department of Chemistry
University of Pittsburgh
Pittsburgh, Pa. 15213

Dr. Larry Anderson
Lockheed Missiles & Space Co.
Lockheed Palo Alto Research Laboratory
3251 Hanover St.
Palo Alto, California 94304

Professor Akio Arakawa
Department of Meteorology
UCLA
Los Angeles, California 90024

Walter Baginsky
Meteorological Staff Program
Air Force Cambridge Research Laboratories
Hanscom Field
Bedford, Mass. 01730

Edward J. Bair
Department of Chemistry
Indiana University
Bloomington, Indiana 47401

Dr. Charles E. Baker
NASA Lewis Research Center
21000 Brookpark Road
Cleveland, Ohio 44135

Dr. John Baldeschwieler
Executive Office of the President
Office of Science and Technology
Washington, D.C. 20506

Emmanuel M. Ballenzweig
DOT Federal Aviation Administration
800 Independence Avenue, SW
Washington, D.C. 20591

Dr. Morton L. Barad
Air Force Cambridge Research Laboratories
Hanscom Field
Bedford, Mass. 01730

Professor John L. Barnes
Department of Engineering
UCLA
Los Angeles, California 90024

Dr. Alfred E. Barrington
Environmental Measurements Branch
DOT Transportation Systems Center
55 Broadway
Cambridge, Mass. 02142

Dr. E. Karl Bastress
IKOR, Inc.
Second Avenue
Burlington, Mass. 01803

Dr. R. Bates
The Queen's University of Belfast
Belfast, No. Ireland

Mr. George Bates
DOT Federal Aviation Administration
800 Independence Avenue
Washington, D.C. 20591

Dr. E.S. Batten
Physical Sciences Department
RAND Corporation
1700 Main Street
Santa Monica, California 90406

Dr. Ernest Bauer
Institute for Defense Analysis
400 Army-Navy Drive
Arlington, Va. 22202

Mr. A.D. Belmont
Research Division
Control Data Corp.
Box 1249
Minneapolis, Minnesota 55440

Professor Jacques E. Blamont
CNES – Universite' de Paris
129, Rue de l'Universite'
Paris 7e, France

Dr. H.H. Blau
Environmental Research & Technology
429 Marrett Rd.
Lexington, Mass. 02173

Lt. William Blazowski
Air Force Aero Propulsion Lab.
Wright-Patterson AFB, Ohio 45433

George Boer
Meteorology Department
MIT
Cambridge, Mass. 02139

Dr. M.H. Bortner
General Electric Co. Valley Forge Space Center
P.O. Box 8555
Philadelphia, Pa. 19101

Mr. Stephen Bowling
Department of Space Science
Rice University
Houston, Texas 77001

Professor J. Bricard
Faculté des Aérosols
9, Quai St. Bernard
Paris 5e, France

Anthony J. Broderick
DOT Transportation Systems Center
55 Broadway
Cambridge, Mass. 02142

Mr. Broida
Department of Physics
University of California
Santa Barbara, California 93106

Dr. W. Burroughs
British Embassy
3100 Massachusetts Ave.
Washington, D.C. 20008

Dr. Richard D. Cadle (Conference Speaker)
National Center for Atmospheric Research
P.O. Box 1470
Boulder, Colorado 80302

Capt. Joseph Calo
Air Force Cambridge Research Laboratories
Hanscom Field
Bedford, Mass. 01730

Dr. Robert H. Cannon, Jr.
Office of the Secretary
Department of Transportation
400 7th Street, S.W.
Washington, D.C. 20590

Dr. Kenneth Champion
Air Force Cambridge Research Laboratories
Hanscom Field
Bedford, Mass. 01730

Dr. Seville Chapman
94 Harper Road
Buffalo, New York 14226

M. Chevalier
Aérospatiale
37 Blvd. de Montmorency
Paris 16e, France

Mr. Ronald Collis
Atmospheric Sciences Laboratory
Stanford Research Institute
333 Ravenswood Ave.
Menlo Park, California 94025

Samuel C. Coroniti
Deputy Program Manager, CIAP
Department of Transportation
400 7th Street, S.W.
Washington, D.C. 20590

Eugene S. Cotton
MIT Lincoln Laboratories
Lexington, Mass. 02173

Dr. P.J. Crutzen
Meteorological Institute
University of Stockholm
Tuleg 41, POB 19111, S10432
Stockholm, Sweden

Dr. Derek Cunnold
Department of Meteorology
MIT
Cambridge, Mass. 02139

Dr. Harold Curtis
Harrington, Davenport, and Curtis, Inc.
74 Loomis Street
Bedford, Mass. 01730

Mr. R.J. Cvetanovic'
National Research Council of Canada
Ottawa, Ontario, Canada

Gerald M. Daniels
Avco-Everett Research Laboratory
2385 Revere Beach Parkway
Everett, Mass. 02149

Dr. Edwin Danielson
National Center for Atmospheric Research
P.O. Box 1470
Boulder, Colorado 80302

Eric Davies
Rolls Royce (1971) Ltd.
551 Fifth Ave.
New York, New York 10017

Dr. Douglas Davis
Department of Chemistry
University of Maryland
College Park, Md. 20740

Dr. Paul Davis
Institute for Defense Analysis
400 Army-Navy Drive
Arlington, Va. 22202

James DeHaven
RAND Corporation
1700 Main Street
Santa Monica, California 90406

Dr. D. Deirmendjian
Physical Sciences Department
RAND Corporation
1700 Main Street
Santa Monica, California 90406

Dr. J.J. Deluisi
National Center for Atmospheric Research
P.O. Box 1470
Boulder, Colorado 80302

L. Devries
NASA Marshall Space Flight Center
Huntsville, Alabama 35812

Dr. Robert Dickinson (Conference Speaker)
National Center for Atmospheric Research
Boulder, Colorado 80302

Professor Thomas Donahue
University of Pittsburgh
Pittsburgh, Pa. 15213

Col. C.S. Downie
1007 Priscilla Lane
Alexandria, Va. 22308

Professor Hans U. Dutsch
Lab. for Atmospheric Physics
Eidgenossische Technische Hochschule
Gloriastrasse 35
Zürich, Switzerland 8006

Dr. Frank Eden
Department of Atmospheric Sciences
National Science Foundation
1800 G Street
Washington, D.C. 20550

Dr. David Elliot
Executive Office of the President
National Aeronautics & Space Council
Washington, D.C. 20502

James Elwood
Pratt & Whitney Aircraft Division
United Aircraft Corp.
400 Main St.
E. Hartford, Conn. 06108

Dr. Rudolf Engelman
Atomic Energy Commission
Washington, D.C. 20345

Dr. Morley English
Department of Engineering
UCLA
Los Angeles, California 90024

Professor Robert Erdmann (Conference Speaker)
Department of Energy & Kinetics
UCLA
Los Angeles, California 90024

Ronald P. Espinola
Arthur D. Little, Inc.
Acorn Park
Cambridge, Mass. 02140

Professor James Fay
Department of Mechanical Engineering
MIT
Cambridge, Mass. 02139

Dr. A. Ferri
Advanced Technology Laboratory
400 Jericho Turnpike
Jericho, New York 11753

Professor Robert F. Fleagle
Department of Atmospheric Sciences
University of Washington
Seattle, Washington 98115

A.K. Forney (Chairman of Sessions IA and IB)
DOT Federal Aviation Administration
800 Independence Ave., S.W.
Washington, D.C. 20591

Dr. J.W. Frazer
Lawrence Livermore Laboratory
P.O. Box 808
Livermore, California 94550

Dr. James P. Friend (Conference Speaker)
Department of Meteorology and Oceanography
New York University
Bronx, New York 10453

Dr. David Garvin
Physical Chemistry Division
National Bureau of Standards
Washington, D.C. 20234

Dr. Richard L. Garwin
Watson Scientific Computing Lab.
Columbia University
New York, New York 10027

Dr. Norman E. Gaut
Environmental Research and Technology
429 Marrett Road
Lexington, Massachusetts 02173

Dr. R. Gelinas
Lawrence Livermore Laboratory
P.O. Box 808
Livermore, California 94550

Dr. John Gille
National Center for Atmospheric Research
P.O. Box 1470
Boulder, Colorado 80302

Forrest Gilmore
R & D Associates
P.O. Box 3580
Santa Monica, California 90403

Dr. Arnold Goldburg
4 Carriage Lane
Littleton, Colorado 80121

Peter Goldsmith
Meteorological Center
Bracknell, Berks, England

Dr. H. Goldstein
General Electric Company
Valley Forge Space Center
P.O. Box 8555
Philadelphia, Pa. 19101

R. Earl Good
Air Force Cambridge Research Laboratories
Hanscom Field
Bedford, Mass. 01730

Philip Goodman
Pana-Metrics, Inc.
221 Crescent St.
Waltham, Mass. 02154

Carlton Gray
Draper Laboratory
MIT
Cambridge, Mass. 02139

Dr. Alan J. Grobecker (Chairman)
Program Manager, Climatic Impact Assessment Program
Office of the Secretary
Department of Transportation
400 Seventh Street, S.W.
Washington, D.C. 20590

Mr. Jack Grobman (Conference Speaker)
NASA Lewis Research Center
21000 Brookpark Road
Cleveland, Ohio 44135

Mr. Paul Guthals
Los Alamos Scientific Laboratory
P.O. Box 1663
Los Alamos, New Mexico 87544

J.B. Haberl
Ordnance Systems
General Electric Co.
100 Plastics Ave.
Pittsfield, Mass. 01201

Eugene Hadge
DOT Transportation Systems Center
55 Broadway
Cambridge, Mass. 02142

Dr. Leslie Hale
Department of Electrical Engineering
Penn State University
University Park, Pa. 16802

Dr. Robert Hampson
Physical Chemistry Division
National Bureau of Standards
Gaithersburg, Maryland 20760

Dr. Thomas M. Hard
DOT Transportation Systems Center
55 Broadway
Cambridge, Mass. 02142

Dr. Halstead Harrison
Boeing Scientific Research Labs
P.O. Box 3981
Seattle, Washington 98124

D. Hausknecht
Department of Engineering
UCLA
Los Angeles, California 90024

Dr. Donald Heath (Conference Speaker)
NASA Goddard Space Flight Center
Greenbelt, Maryland 20771

Mr. F. Henriques
Department of Commerce, Room 3877
14th bet. E & Constitution Ave.
Washington, D.C.

Mr. Wayne S. Hering
Meteorology Laboratory
Air Force Cambridge Research Laboratories
Hanscom Field
Bedford, Mass. 01730

Mr. Benjamin M. Herman
Institute of Atmospheric Physics
University of Arizona
Tucson, Arizona 85721

John Herron
National Bureau of Standards
Gaithersburg, Md. 20760

Professor John Heywood
Department of Mechanical Engineering
MIT
Cambridge, Mass. 02139

Mr. Henry Hidalgo
Institute for Defense Analysis
400 Army-Navy Drive
Arlington, Va. 22202

Dr. E. Hilsenrath
NASA Goddard Space Flight Center
Greenbelt, Maryland 20771

Dr. Glenn R. Hilst
Aero Research Associates of Princeton
Princeton, N.J. 08540

Dr. Adolf Hochstim
Research Institute for Engineering Sciences
College of Engineering
Wayne State University
Detroit, Michigan 48202

Professor D.J. Hofman
Physics Department
University of Wyoming
Laramie, Wyoming 82070

Dr. David Holtz
National Academy of Sciences
2101 Constitution Ave.
Washington, D.C. 20418

Mr. Jack Hope
Executive Office of the President
Office of Science and Technology
Washington, D.C. 20506

Dr. Hiroshi Hoshizaki
Lockheed Missile & Space Co.
Lockheed Palo Alto Research Lab
Palo Alto , California 94304

Joseph W. Howell
Department of Transportation
400 7th Street S.W.
Washington, D.C. 20590

Dr. Frank P. Hudson (Conference Speaker)
Sandia Laboratories
Albuquerque, New Mexico 87115

James Hughes
Office of Naval Research
Arlington, Va. 22217

Mr. B.G. Hunt
Commonwealth Meteorological Research Ctr.
Box 5089 AA
Melbourne, Australia 3001

Mr. Richard W. Hurn
U.S. Bureau of Mines Energy Research Center
Bartlesville, Oklahoma 74003

M.R. Joatton
Aerospatiale
37 Blvd. de Montmorency
Paris 16 France

Professor H.S. Johnston (Conference Speaker)
Department of Chemistry
University of California
Berkeley, California 94720

Dr. S.K. Kao
Department of Atmospheric Sciences
University of Utah
Salt Lake City, Utah 84112

Mr. J. Kaplan
Department of Physics
UCLA
Los Angeles, California 90024

Professor James Kassner
Cloud Physics Department
University of Missouri
Rolla, Mo. 65401

Dr. Sidney Katz
Illinois Institute of Technology Research Institute
10 W. 35th Street
Chicago, Illinois 60606

Professor Frederick Kaufman
Department of Chemistry
University of Pittsburgh
Pittsburgh, Pa. 15213

A.S. Kesten
United Aircraft Corp. Research Laboratories
400 Main Street
E. Hartford, Conn. 06108

Dr. Joseph B. Knox
Lawrence Livermore Laboratory
P.O. Box 808
Livermore, California 94550

Mr. Philip W. Krey
Environmental Studies Division
Health and Safety Laboratory
U.S. Atomic Energy Commission
376 Hudson Street
New York, New York 10014

Professor John Kroening
Physics Department
University of Minnesota
Duluth, Minnesota 55812

Dr. Allen Krueger
NASA Goddard Space Flight Center
Greenbelt, Maryland 20771

Dr. Peter Kuhn
Atmospheric Physics and Chemistry Laboratory
NOAA Environmental Research Laboratory
Boulder, Colorado 80302

Dr. R.H. Kummler
Research Institute for Engineering Sciences
College of Engineering
Wayne State University
Detroit, Michigan 48202

Dr. Michael J. Kurylo
National Bureau of Standards
Gaithersburg, Maryland 20760

Mr. Glenn Larson
DOT Transportation Systems Center
55 Broadway
Cambridge, Mass. 02142

Dr. Laufer
National Bureau of Standards
Gaithersburg, Md. 20760

J.A. Lauermann
National Academy of Sciences
Washington, D.C. 20418

Dr. James D. Lawrence
NASA Langley Research Center
Hampton, Va. 23365

Dr. J.F. Leach
British Aircraft Corp.
Box 77
Filton, Bristol, England

Mr. Philippe Lebouc
European Aerospace Corp.
605 3rd Avenue
New York, New York 10016

Dr. Richard L. Lehman
National Oceanic & Atmospheric Administration
Department of Commerce
Washington, D.C. 20230

Dr. Howard B. Levine
Department of Chemical Engineering
Virginia Polytechnical Institute
Blacksburg, Virginia 24061

Dr. Hiram Levy II
Smithsonian Astrophysical Observatory
60 Garden Street
Cambridge, Mass. 02138

Dr. Leona Libby
UCLA
Los Angeles, California 90024

Dr. W.F. Libby
Institute of Geophysics and Planetary Physics
UCLA
Los Angeles, California 90024

Mr. Charles Lieder
Department of Chemistry
Stanford University
Stanford, California 94025

Mr. Newton Lieurance
National Oceanic and Atmospheric Administration
Department of Commerce
Rockville, Md. 20852

Marshall M. Lih
Chemical Engineering Department
Catholic University
Pangborn Building
Washington, D.C. 20017

Lt. Lawrence H. Linden
HQ USAF PREV
Washington, D.C. 20330

Mr. Harold Lindenhofen
Aeronautical Engine Department
U.S. Navy Air Propulsion Test Center
Philadelphia Naval Base
Philadelphia, Pa. 19112

Dr. Richard Lindzen
Department of Geophysical Sciences
University of Chicago
Chicago, Illinois 60637

Dr. Alan Lloyd
Statewide Air Pollution Research Center
University of California
Riverside, California 92501

Dr. Ernest V. Loewenstein
Air Force Cambridge Research Laboratories
Hanscom Field
Bedford, Mass. 01730

Dr. Robert McClatchey
Air Force Cambridge Research Laboratories
Hanscom Field
Bedford, Mass. 01730

Dr. John McConnell
Center for Earth & Planetary Physics
Harvard University
Cambridge, Mass. 02138

Dr. Billy M. McCormac
Lockheed Missiles & Space Co.
Lockheed Palo Alto Research Laboratory
3251 Hanover Street
Palo Alto, California 94304

Professor R.E. McCrosky
Smithsonian Astrophysical Observatory
60 Garden St.
Cambridge, Mass. 02138

Dr. Michael B. McElroy (Conference Speaker)
Center for Earth and Planetary Physics
Harvard University
Cambridge, Mass. 02138

Dr. James R. McNesby
National Bureau of Standards
Washington, D.C. 20234

Dr. M. MacCracken
Lawrence Livermore Laboratory
P.O. Box 808
Livermore, California 94550

Dr. Paul P. MacCready, Jr.
Aerovironment Inc.
P.O. Box 4525
Pasadena, California 91106

Dr. Lester Machta
Air Resources Laboratory
NOAA Environmental Research Laboratories
Silver Spring, Maryland 20910

Harvey L. Malchow
9 Alaska Avenue
Bedford, Mass. 01730

Mr. Jerry D. Mahlman (Conference Speaker)
NOAA ERL Geophysical Fluid Dynamics Laboratory
Princeton University
P.O. Box 308
Princeton, New Jersey 08540

Mr. Donald W. Male
Arnold Engineering Development Center
Arnold Air Force Station
Tullahoma, Tenn. 37389

Dr. Phillip Mange
Naval Research Laboratory
4555 Overlook Avenue, SW
Washington, D.C. 20390

Mr. Carroll Maninger
Lawrence Livermore Laboratory
P.O. Box 808
Livermore, California 94550

Dr. Gene Mannella
School of Engineering and Architecture
Catholic University
620 Michigan Avenue, NE
Washington, D.C. 20017

Mr. Bernard Manowitz
Radiation Division
Brookhaven National Laboratory
Upton, L.I., New York 11973

Mr. Howard Margolis
Institute for Defense Analysis
400 Army-Navy Drive
Arlington, Va. 22202

Dr. Fred F. Marmo
GCA Technology Division
Burlington Road
Bedford, Mass. 01730

Mr. John Mastenbrook
Naval Research Laboratory
1555 Overlook Avenue, SW
Washington, D.C. 20390

Dr. L.R. Megill
Center for Research in Aeronomy
Utah State University
Logan, Utah 84321

Dr. R. Miller
Department of Aeronautics
MIT
Cambridge, Mass. 02139

Professor Yale Mintz (Conference Speaker)
Department of Meteorology
UCLA
Los Angeles, California 90024

O.K. Moe
McDonnell-Douglas Corp.
Huntington Beach, California 92647

Mr. Robert Mognard
Secretary-General of Civil Aviation
93 Boulevard du Montparnasse
Paris, France

Professor Volker Mohnen
Aerosol Sciences Research Center
State University of New York
1400 Washington Ave.
Albany, New York 12222

Dr. Roger Molander
Institute for Defense Analysis
400 Army-Navy Drive
Arlington, Virginia 22202

James Morris
DOT Transportation Systems Center
55 Broadway
Cambridge, Mass. 02142

Professor David G. Murcray
Department of Physics
University of Denver
Denver, Colorado 80210

Dr. R. Murgatroyd
Meteorological Office
London Road
Bracknell, Berks, England

Dr. Rocco Narcisi
Air Force Cambridge Research Laboratories
Hanscom Field
Bedford, Mass. 01730

Capt. Dennis F. Naugle
Air Force Weapons Laboratory
Kirtland AFB, New Mexico 87116

James E. Neely
Arnold Engineering Development Center
Tullahoma, Tenn. 37389

Arthur W. Nelson
Pratt & Whitney Aircraft Division
United Aircraft Corp.
400 Main Street
E. Hartford, Conn. 06108

Professor Reginald E. Newell (Conference Speaker)
Department of Meteorology
MIT
Cambridge, Mass. 02138

Professor M. Nicolet (Conference Speaker)
Institut d' Aeronomie Spatiale de Belgique
Avenue Circulaire, 3
Brussels, Belgium 1180

Hiromi Niki
Scientific Research Laboratory
Ford Motor Company
P.O. Box 2053
Dearborn, Michigan 48121

Richard Norton
NOAA Environmental Research Laboratory
Boulder, Colorado 80302

Dr. John Noxon
NOAA Environmental Research Laboratory
Boulder, Colorado 80302

Mr. Arthur E. O'Brien
DOT Transportation Systems Center
55 Broadway
Cambridge, Mass. 02142

Dr. Robert Oliver
Institute for Defense Analysis
400 Army-Navy Drive
Arlington, Va. 22202

Dr. Richard Orville
Physics Department
State University of New York
1400 Washington Ave.
Albany, New York 12222

Dr. J. Gote Östlund
Institute of Marine & Atmospheric Sciences
University of Miami, Virginia Key
Miami, Florida 33149

T. Overcamp
Department of Mechanical Engineering
MIT
Cambridge, Mass. 02138

Professor Hans Karl Paetzold
Institute of Geophysics & Meteorology
University of Köln
Köln, W. Germany

Mr. L. Palcza
Naval Air Propulsion Test Center
Trenton, New Jersey

J.C. Paree
French Embassy
French Scientific Mission
1033 Massachusetts Avenue
Cambridge, Mass. 02138

J.H. Park
Astro-Geophysics Department
University of Colorado
Boulder, Colorado 80302

Professor T.J. Pepin
Physics Department
University of Wyoming
Laramie, Wyoming 82070

P.J. Perkins
NASA Lewis Research Center
21000 Brookpark Rd.
Cleveland, Ohio 44135

Dr. Robert Peterson
Los Alamos Scientific Lab.
Los Alamos, New Mexico 87544

Norman Phillips
Meteorology Department
MIT
Cambridge, Mass. 02139

Dr. E.T. Pierce
Stanford Research Institute
Menlo Park, California 94025

Robert W. Pinnes
Office of the Secretary
Department of Transportation
400 7th Street SW
Washington, D.C. 20590

Walter Planet
NOAA National Environmental Satellite Service
Federal Office Bldg. 4
Suitland, Maryland 20233

Dr. Josef Podzimek
Cloud Physics Research Center
University of Missouri
Rolla, Missouri 65401

Dr. Martin A. Pomerantz
Bartol Research Foundation
The Franklin Institute
Swarthmore, Pa. 19081

Dr. I.G. Poppoff (Conference Speaker)
NASA Ames Research Center
Moffett Field, California 90035

Mr. Jerome Pressman
4 Fessenden Way
Lexington, Mass. 02173

Mr. Martin Prochnik
Offiee of the Science Advisor
Department of the Interior
Washington, D.C. 20240

Alan Quilleverre
SNECMA
Villaroche
77 Moissy, France

Dr. R.R. Rapp
Physical Sciences Dept.
RAND Corp.
1700 Main Street
Santa Monica, California 90406

Dr. Elmar R. Reiter
Department of Atmospheric Sciences
Colorado State University
Ft. Collins, Colorado 80521

Dr. Herbert Richardson
Department of Transportation
400 7th Street, SW
Washington, D.C. 20590

Mr. Louis W. Roberts
Director of Technology
DOT Transportation Systems Center
55 Broadway
Cambridge, Mass. 02142

Dr. G.D. Robinson
The Center for Environment and Man, Inc.
275 Windsor Street
Hartford, Conn. 06120

Professor James M. Rosen
Physics Dept.
University of Wyoming
Laramie, Wyoming 82070

Dr. N.W. Rosenberg
Air Force Cambridge Research Laboratories
Hanscom Field
Bedford, Mass. 01730

Dr. William H. Roudebush
National Aeronautics and Space Administration
600 Independence Ave.
Washington, D.C. 20015

Professor Malcolm A. Ruderman
Department of Physics
Columbia University
New York, New York 10027

Richard A. Rudey
NASA Lewis Research Center
21000 Brookpark Rd.
Cleveland, Ohio 44135

Lothar H. Ruhnke
National Oceanic and Atmospheric Administration
Boulder, Colorado 80302

Mr. Robert W. Rummel (Conference Speaker)
Vice President, Trans World Airlines
605 Third Avenue
New York, New York 10016

Professor Robert F. Sawyer
Department of Mechanical Engineering
University of California
Berkeley, California 94720

Dr. Milton Scheer
National Bureau of Standards
Connecticut Avenue
Washington, D.C. 20234

Dean Harold Schiff
University of York
Toronto, Ontario, Canada

Dr. Richard Schoen
National Sciences Foundation
1800 G Street, NW
Washington, D.C. 20550

Dr. Burton Schuster
National Center for Atmospheric Research
Boulder, Colorado 80302

Donald F. Schutz
Teledyne Isotopes
50 Van Buren Ave.
Westwood, N.J. 07675

Dr. Michael J. Scotto
DOT Transportation Systems Center
55 Broadway
Cambridge, Mass. 02142

Dr. Donald Sheldon
Institute for Defense Analysis
400 Army-Navy Drive
Arlington, Va. 22202

Dr. T. Shimazaki
NOAA Environmental Research Laboratory
Boulder, Colorado 80302

Dr. R. Simonaitis
Penn State University
University Park, Pa. 16802

Dr. S. Fred Singer
Department of Environmental Sciences
Brooks Museum
University of Virginia
Charlottsville, Va. 22903

Professor G. Siscoe
Department of Meteorology
UCLA
Los Angeles, California 90024

Mr. Norman Sissenwine
Aeronomy Laboratory
Air Force Cambridge Research Laboratories
Hanscom Field
Bedford, Mass. 01730

Dr. Joseph Smagorinsky
NOAA ERL Geophysical Fluid Dynamics Laboratory
P.O. Box 308
Princeton University
Princeton, New Jersey 08540

H.L. Smith
Los Alamos Scientific Laboratory
Los Alamos, New Mexico 87544

Professor Kendric C. Smith (Conference Speaker)
Department of Radiology
Stanford University School of Medicine
Palo Alto, California 94305

Dr. A. Snelson
Illinois Institute of Technology Research Institute
10 W. 35th Street
Chicago, Illinois 60657

Dr. Donald Snider
Ballistic Research Laboratory
Aberdeen Proving Ground
Aberdeen, Md. 21005

Anthony Souza
Scott Research Laboratories
P.O. Box D-11
Plumsteadville, Pa. 18949

Mr. Kenneth C. Spengler
American Meteorological Society
45 Beacon Street
Boston, Mass. 02108

Mr. William Steber
Offiee of the Secretary of Transportation
Department of Transportation
400 Seventh St. SW
Washington, D.C. 20590

Mr. R. Steinberg
NASA Lewis Research Center
21000 Brookpark Road
Cleveland, Ohio 44135

Dr. C. Stergis
Air Force Cambridge Research Laboratories
Hanscom Field
Bedford, Mass. 01730

Dr. Richard L. Strombotne (Program Chairman)
Office of the Secretary
Department of Transportation
400 Seventh St., SW
Washington, D.C. 20590

Mr. Joseph Sturm
DOT Transportation Systems Center
55 Broadway
Cambridge, Mass. 02142

William Swider
Air Force Cambridge Research Laboratories
Hanscom Field
Bedford, Mass. 01730

Dr. Lee M. Talbot
Council on Environmental Quality
622 Jackson Place, NW
Washington, D.C. 20006

Dr. Thomas Taylor
The Aerospace Corporation
1111 Mill Street
San Bernadino, California 92401

Dr. C.M. Tchen
City College of New York
New York, New York 10031

R. Thorne
UCLA
Los Angeles, California 90024

Dr. Shelby Tilford
Naval Research Laboratories
4555 Overlook Avenue, SW
Washington, D.C. 20390

Dr. Richard B. Timmons
Department of Chemistry
Catholic University
Washington, D.C. 20017

Dr. Edward Todd
National Science Foundation
1800 G Street, NW
Washington, D.C. 20006

Dr. Robert Toth
Jet Propulsion Laboratory
4800 Oak Grove Drive
Pasadena, California 91103

Dr. R. Tousey
Naval Research Laboratories
4555 Overlook Ave., SW
Washington, D.C. 20390

Robert L. Underwood (Chairman of Sessions II C and D)
Office of the Secretary
Department of Transportation
400 7th Street, SW
Washington, D.C. 20590

Dr. Frederick Urbach
Skin and Cancer Hospital
Temple University
3322 N. Broad Street
Philadelphia, Pa. 19140

Dr. Vaglio-Laurin
Advanced Technology Lab.
400 Jericho Turnpike
Jericho, New York 11753

Charles C. Van Valin
National Oceanic and Atmospheric Administration
Environmental Research Labs.
Boulder, Colorado 80302

Dr. S.V. Venkateswaran (Conference Speaker)
Department of Meteorology
UCLA
Los Angeles, California 90024

Herbert Viebrock
EPA National Environment Research Center
Research Triangle Park, North Carolina 27711

Dr. Martin Walt
Lockheed Missiles & Space Co.
Lockheed Palo Alto Research Lab.
3251 Hanover Street
Palo Alto, California 94304

R.C. Wanta
28 Hayden Lane
Bedford, Mass. 01730

Dr. Peter Wardman
British Aircraft Corporation Ltd.
Filton, Bristol, England

Dr. Peter Warneck
Max Planck-Institut für Chemie
Saarstrasse 23
Postfach 3060
Mainz 65, Germany

Dr. Hugh Webster
Australian Embassy
1601 Massachusetts Ave. NW
Washington, D.C. 20036

Dr. Helmut Weickmann
NOAA Environmental Research Lab.
Boulder, Colorado 80302

Professor James Weinman
Department of Meteorology
University of Wisconsin
Madison, Wisconsin 53706

Dr. Michael P. Weinreb
NOAA National Environmental Satellite Service
Suitland, Md. 20233

Mr. George A. Welford
Health and Safety Laboratory
U.S. Atomic Energy Commission
376 Hudson Street
New York, New York 10014

Dr. A.A. Westenberg
Applied Physics Lab.
John Hopkins University
8621 Georgia Ave.
Silver Spring, Md. 20910

Dr. Ray Wexler
NASA Goddard Space Flight Center
Greenbelt, Md. 20771

Eldon Whipple
National Oceanic and Atmospheric Administration
Boulder, Colorado 80302

Dr. R.C. Whitten
NASA Ames Research Center
Moffett Field, California 95014

M.R. Williams
Bristol Engine Division
Rolls Royce (1971) Ltd.
P.O. Box 3
Filton, Bristol, England

Mr. J. Wirsching
3364 Marina Ave.
Livermore, California 94550

Dr. Stephen Wofsy
Center for Earth & Planetary Physics
Harvard University
Cambridge, Mass. 02138

Robert O. Woods
Sandia Laboratories
Albuquerque, New Mexico 87115

David Wu
MIT
Cambridge, Mass. 02139

Morton Wurtele
UCLA
Los Angeles, California 90024

Dr. Alex S. Zachor
Honeywell Radiation Center
2 Forbes Road
Lexington, Mass. 02173

Dr. S. Zimmerman
Air Force Cambridge Research Laboratories
Hanscom Field
Bedford, Mass. 01730

☆ U.S. GOVERNMENT PRINTING OFFICE: 1973—701—161/34